Pergamon Materials Series 14

Self-Diffusion and Impurity Diffusion in Pure Metals

Handbook of Experimental Data

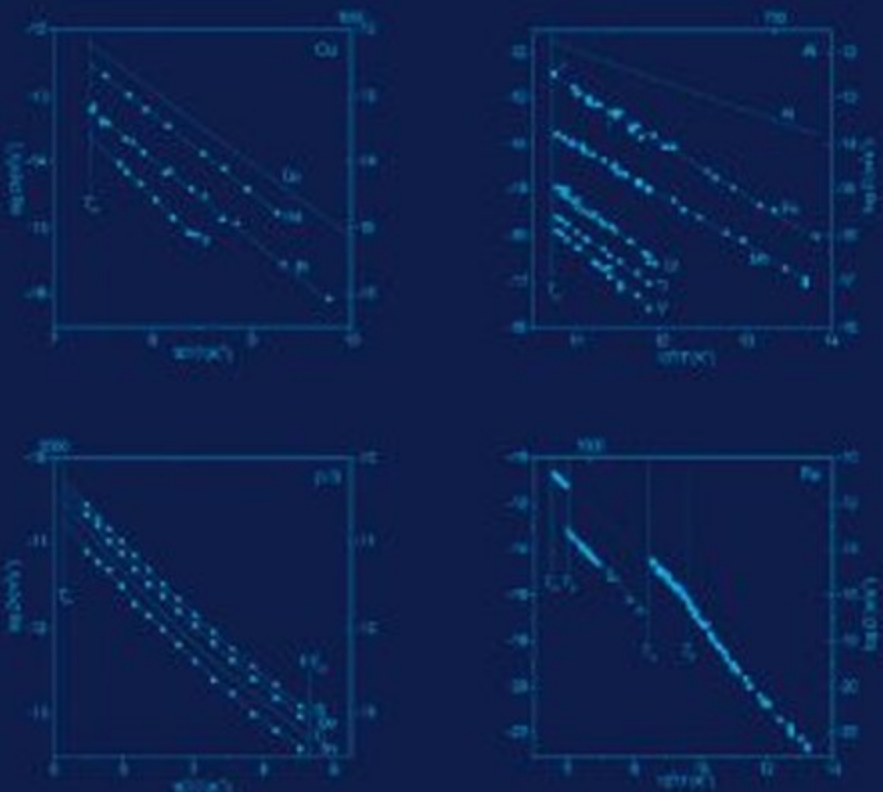

Gerhard Neumann and
Cornelis Tuijn

SELF-DIFFUSION AND IMPURITY DIFFUSION IN PURE METALS: HANDBOOK OF EXPERIMENTAL DATA

By

GERHARD NEUMANN
Institut für Physikalische Chemie
Freie Universität Berlin

CORNELIS TUIJN
Department of Physics
Universiteit van Amsterdam

ELSEVIER

Amsterdam • Boston • Heidelberg • London • New York • Oxford
Paris • San Diego • San Francisco • Singapore • Sydney • Tokyo
Pergamon is an imprint of Elsevier

Pergamon is an imprint of Elsevier
Linacre House, Jordan Hill, Oxford OX2 8DP, UK
Radarweg 29, PO Box 211, 1000 AE Amsterdam, The Netherlands
525 B Street, Suite 1900, San Diego, CA 92101-4495, USA

First edition 2009

British Library Cataloguing in Publication Data
A catalogue record for this book is available from the British Library

Library of Congress Cataloging-in-Publication Data
A catalog record for this book is available from the Library of Congress

ISBN: 978-1-85617-511-1

For information on all Pergamon publications
visit our website at books.elsevier.com

Printed and bound in Great Britain

09 10 11 12 13 10 9 8 7 6 5 4 3 2 1

PREFACE

The most recent comprehensive data collection on diffusion in metals was published in 1990 (Landolt-Börnstein NS III 26). In the meantime numerous new results on self-diffusion and impurity diffusion in solid metals have been published. Especially, impurity diffusion coefficients measured by means of electron probe microanalysis (EPMA), Rutherford backscattering (RBS) and heavy ion backscattering (HIRBS) have been reported. Moreover, a number of earlier results had to be reassessed.

The present comprehensive data collection is based on a critical valuation of the hitherto published data and and aims at being the most complete data collection on this subject at this moment.

The authors wish to thank the employees of the libraries of the Hahn-Meitner Institute in Berlin and of the Library of Science of the University of Amsterdam, for the supply of many earlier articles, and in particular Mrs. Marijke Duyvendak, for searching in libraries all over the world.

The authors are also grateful to Professor Denis Ablitzer (Nancy), Professor Dieter Bergner (Freiberg), Professor Yoshiaki Iijima (Sendai) and Professor Jean Philibert (Orsay) for providing reprints and copies of a number of publications.

Gerhard Neumann
Cornelis Tuijn
January 2008

CHAPTER 0

Introduction

The first diffusion investigation in metals was that of Au in lead by Roberts-Austen in 1896. Between 1930 and 1935 further impurity and self-diffusion investigations in lead had been performed by Hevesy, Seith and coworkers (for references see Chapter 4). Later on, when the first artificial radioisotopes became available, self-diffusion in gold [00.01, 00.02], copper [00.03, 00.04], silver [00.05] and zinc [00.06] was measured. Systematic investigations on self-diffusion and impurity diffusion in solid metals started with the availability of numerous artificial radioisotopes after the Second World War. Results of non-radioactive investigations represented a minority in that period. In the last two decades, however, the fraction of non-radioactive measurements has markedly increased.

The last comprehensive data collection in metals and alloys was published in 1990 [00.07], including self-diffusion [00.08] and impurity diffusion [00.09] in metals. Since then numerous further investigations have been performed, especially in aluminum, α- and β-titanium, α-zirconium and α-iron. Moreover, a large number of earlier investigations had to be reassessed.

The present collection contains data of self-diffusion and impurity diffusion in metals. Diffusion in silicon, germanium, selenium and tellurium is not topic of the present collection. Diffusion of C, N and O in metals is also not included in the present data collection. Data of these impurities are compiled in Ref. [00.10].

0.1. EXPERIMENTAL TECHNIQUES

Numerous methods have been developed for the measurement of self-diffusion and impurity diffusion coefficients in metals. The most reliable experimental data can be obtained with the aid of tracer sectioning techniques by means of radioactive isotopes. Also a number of non-radioactive investigation methods permits the determination of impurity diffusion coefficients. Furthermore, some non-destructive techniques, especially scattering experiments, were used for diffusion investigations. The methods for measuring diffusion coefficients have been described in detail in a number of reviews [01.01–01.04]. In the present chapter the most frequently applied measuring methods are briefly described.

Diffusion investigations are performed in a concentration gradient. The temporal and local change of the tracer concentration $c(x,y,z,t)$ is described by Fick's second law

$$\frac{\mathrm{d}c}{\mathrm{d}t} = D\Delta c \tag{01.01}$$

The serial sectioning technique consists of measuring the activity of thin sections removed from the sample parallel to the surface, i.e. normal to the diffusion direction. This simplifies Eq. (01.01) to the one-dimensional form

$$\frac{\mathrm{d}c}{\mathrm{d}t} = D\frac{\mathrm{d}^2c}{\mathrm{d}x^2} \tag{01.02}$$

The solutions of Eqs. (01.01) and (01.02) depend on the initial and boundary conditions, respectively, and are collected in Refs. [01.05, 01.06].

0.1.1 Radiotracer techniques

The experimental details of the measurement of tracer diffusion coefficients are extensively reviewed by Rothman [01.02]: sample preparation, tracer deposition, annealing, temperature measurement, determination of the effective annealing time, sectioning and counting (for further reviews see Refs. [01.07, 01.08]).

In the present chapter the different sectioning techniques and the respective range of measured diffusion coefficients are compared. Especially the penetration plots give informations concerning the accuracy of D. A number of possible sources in the determination of D has to be taken into consideration:

- Falsification of the penetration profile owing to surface diffusion contributions can be avoided by removing a layer of some $\sqrt{Dt}$ thickness from the side faces of the samples.
- Temperature measurements by use of thermocouples (mainly Pt/Pt(Rh), Ni(Cr)/Ni) may lead to errors of ± 1.5 K, which corresponds to an uncertainty of $\pm 3\%$ in D. Temperature measurements using optical pyrometry lead to distinctly larger uncertainties. An error of about 30 K in T at 3,000 K corresponds to an uncertainty of about 20% in D.
- For the determination of the accurate diffusion time a correction for the heating and cooling period has to be performed [01.09].

Macrosectioning techniques

Direct profile measurements. The most accurate methods for the measurement of diffusion coefficients are sectioning techniques using precision lathe and microtome, which permits the removal of sections of only a few microns thick. The section thickness is determined by weighing. Microtome and lathe sectioning is suited for ductile but not too soft materials.

If an infinitesimally thin layer ($\ll \sqrt{Dt}$) of radiotracers is deposited on the flat surface of the sample, the initial and boundary conditions for the semi-infinite

diffusion couple are

$$\begin{aligned}&\lim_{\delta\to 0} c(x,0) = \frac{M}{2\delta} \text{ for } |x| \le \delta, \text{ i.e. } \infty \text{ for } x = 0\\ &\lim_{\delta\to 0} c(x,0) = 0 \text{ for } |x| > \delta, \text{ i.e. } 0 \text{ for } x \neq 0\end{aligned} \tag{01.03}$$

where M is the deposited amount in g/m^2 and δ the layer thickness. The so-called *thin film solution* of Eq. (01.02) yields [01.05]:

$$c(x,t) = \frac{M}{2\sqrt{\pi D t}} \exp\left(-\frac{x^2}{4Dt}\right) \tag{01.04}$$

which is linear in ln c against x^2 (see Figure 01.01). The slope of this plot yields D.

Deviations from linearity and the respective error sources are treated in a special section (see below). Diffusion coefficients with an uncertainty of only a few percent can be obtained with the aid of microtome and lathe sectioning.

Grinding or lapping is the standard method of sectioning brittle materials. Emery or abrasive SiC papers as well as diamond paste are used for 3–100 µm sections. The section thickness is determined by weighing the sample after each section that has been removed. Equation (01.04) describes the penetration plot.

Lathe, microtome and grinder sectioning permit the measurement of diffusion coefficients larger than $10^{-16}\,m^2\,s^{-1}$ or temperatures higher than about $0.7\,T_m$ (T_m is melting temperature), grinding with SiC papers diffusion coefficients as small as $10^{-17}\,m^2\,s^{-1}$.

Residual activity method. An alternative method for the determination of D using grinding was proposed by Gruzin [01.11]. Instead of measuring the activity of the sections the residual activity of the sample after removing the sections is measured. Then the activity of the n-th section is the difference of the residual activities after removing $n-1$ and n sections. The solution of Eq. (01.02) yields [01.05]

$$\frac{A_n}{2A_0} = \frac{1}{\sqrt{Dt}} \operatorname{erfc}\left(\frac{x}{2\sqrt{Dt}}\right) \tag{01.05}$$

where A_0 is the initial counting rate and A_n the remaining activity after the removal of n sections. erfc(z) is the complementary error function

$$\operatorname{erfc}(z) = 1 - \operatorname{erf}(z)$$

see Figure 01.02. D can also be derived from the Gaussian plot

$$\ln \frac{\partial A}{\partial x} = \text{const} - \frac{x^2}{4Dt} \tag{01.06}$$

The plot of the inverse function of erfc(z) $= A_n/2A_0$, i.e. $\operatorname{erfc}_{(-1)}(A_n/2A_0)$ against x is linear if the initial and boundary conditions are properly fulfilled (see Figure 01.02).

The Gruzin method is considered as less precise than the before-mentioned sectioning techniques. Only if the tracer is a hard γ radiator the absorption is

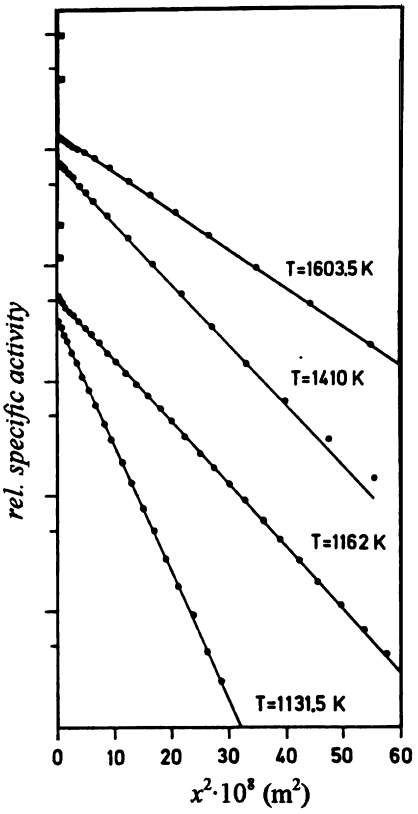

Fig. 01.01 Impurity diffusion of ^{95}Nb in α- and γ-iron. Microtome sectioning (2–5 μm sections) (from Ref. [01.10]).

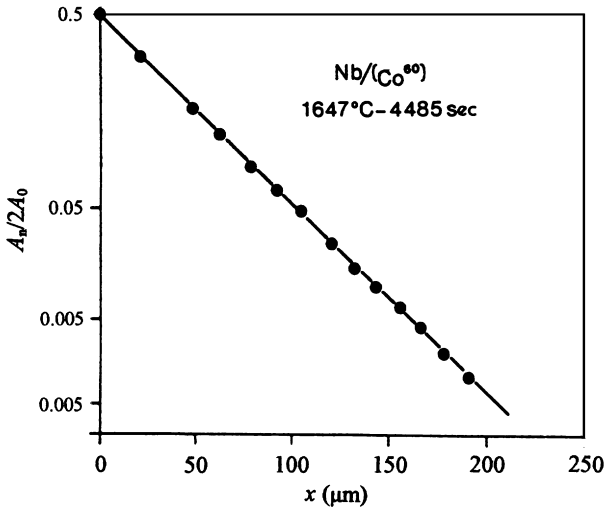

Fig. 01.02 Impurity diffusion of ^{60}Co in niobium. Residual-activity measurement. Profile fitted to Eq. (01.05) (from Ref. [01.12]).

negligible. Otherwise the linear absorption coefficient of the radiation has to be measured accurately. The method is mainly used in grinder sectioning investigations on polycrystalline materials.

Surface activity decrease method. The measurement of the decrease of the surface activity (or simple absorption method) before and after the diffusion anneal can also be used for the determination of D [01.13, 01.14]. This method is based on the surface activity decrease during the anneal which is caused by the absorption of the radiation of the tracer material diffused into the bulk. As in the Gruzin technique the absorption coefficient of the radiation has to be known. The method is regarded as less reliable than the sectioning techniques because it needs assumptions about the concentration profile. Particularly, errors can arise from tracer loss, oxide hold-up and short-circuiting contributions (grain boundary and dislocation contributions).

A variant of the simple absorption method is the Kryukov absorption method [01.15]. The radioactivity from both front face and back face of a very thin sample is counted after the diffusion anneal. So, D can be evaluated without the knowledge of the absorption coefficient.

Autoradiography. Autoradiography has also been used for the measurement of diffusion coefficients [01.16, 01.17]. The tracer penetration is derived from an autoradiograph taken from a flat cut at a small angle to the plane where the tracer was deposited. Although this cannot be considered a highly precise technique, for Sb diffusion in copper at least at high temperatures good agreement with the lathe sectioning data was observed [01.18].

Microsectioning techniques

Diffusion coefficients smaller than $10^{-17}\,m^2\,s^{-1}$ can be measured with the aid of chemical and electrochemical techniques. Sectioning by chemical dissolution permits the removal of 100 nm thick layers [01.19]. Sections between 10 and 100 nm can be obtained by mechanically stripping of electrochemically anodized layers [01.20]. This enables the measurement of diffusion coefficients as small as $10^{-22}\,m^2\,s^{-1}$ at temperatures of about 0.5 T_m [01.21]. Lundy and coworkers have used this method for the investigation of self-diffusion and impurity diffusion in β-Ti, β-Zr, Nb, Ta and W.

Diffusion coefficients as small as $10^{-23}\,m^2\,s^{-1}$ at $T \approx 0.4\,T_m$ can be obtained by application of sputtering methods. Sections smaller than 1 nm can be removed by ion bombardment (ion-beam sputtering, IBS). A concentration-depth profile can be measured by collecting the sputtered-off radiotracer material [01.22, 01.23] or by selecting and counting the sputtered-off material in a mass spectrometer (secondary-ion mass spectroscopy, SIMS) [01.24]. The depth of the profile (total crater depth) is measured by optical interference methods after sectioning has been completed. The thickness of the sections is determined under the assumption that the material is removed uniformly as a function of time. To avoid short-circuiting contributions single crystals with small dislocation densities have to be

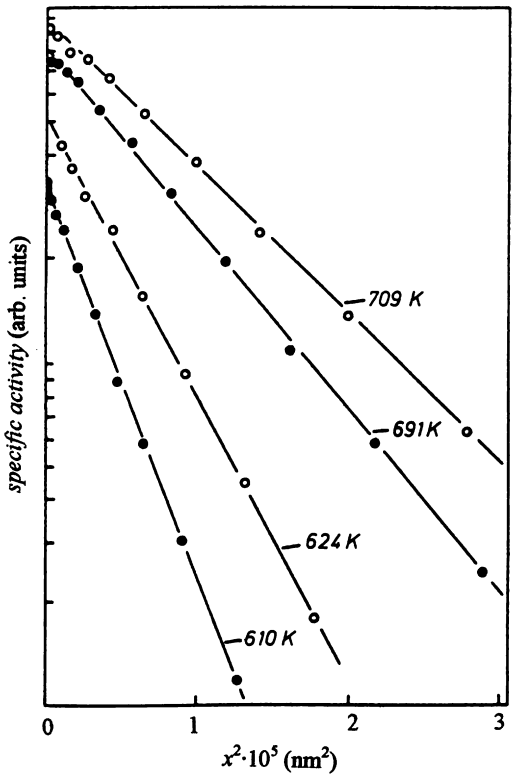

Fig. 01.03 Impurity diffusion of ^{114m}In in silver. Ion-beam sputtering (from Ref. [01.25]).

used. The depth resolution of the sputter sectioning technique is limited which results from roughening and atomic mixing [01.24]. Roughening reduces the depth resolution because atoms are sputtered simultaneously from different depths with different concentrations of tracers. Mixing of atoms from different depths is a consequence of the lattice damage caused by the sputter ions. Roughening increases with depth. The accuracy of diffusion coefficients measured by means of sputtering techniques is within 10–20%.

In Figures 01.03 and 01.04 the penetration profiles for In diffusion in silver [01.25] and Ni diffusion in copper [01.24] are shown. For ^{114m}In in silver Ar^+ ions with an energy of about 0.5 keV were used for sputtering. The penetration profiles are ranging from about 100–500 nm (see Figure 01.03). For Ni in copper single crystalline samples with inserted thin Ni layers are used. The sputter deposited Ni (monoatomic layer with initial distribution with a half-width of 11 nm) is covered by an epitaxial, almost monocrystalline layer of copper of about 100 nm. O_2^+ ions of 4 keV were used for sputtering. The penetration plots are smaller than 100 nm (see Figure 01.04).

IBS plus radiotracer counting permits the measurement of self-diffusion as well as impurity diffusion coefficients in the temperature range between about 0.4 and 0.6 T_m. Especially for self-diffusion in fcc metals the low-temperature

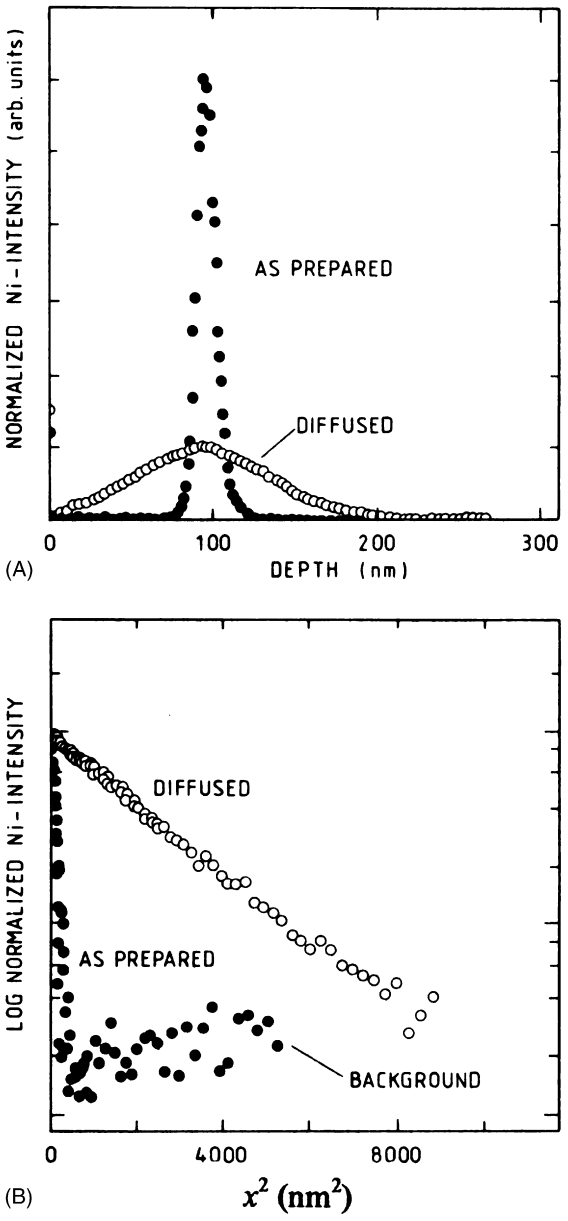

Fig. 01.04 Impurity diffusion of Ni in copper. Ion-beam sputtering and SIMS analysis (initial distribution with a half-width of 11 nm) (from Ref. [01.24]).

data detect the slight curvature of the Arrhenius plot of D and enables the evaluation of $D(T)$ in form of two-exponential fits (see Chapter 0.2). IBS plus SIMS analysis permits the measurement of impurity diffusion coefficients of elements which have no suitable radioisotopes.

Non-Gaussian diffusion profiles

Deviations from linearity of the ln c vs. x^2 plot, i.e. non-Gaussian profiles, are observed if the boundary conditions are not properly fulfilled or if other mechanisms like short-circuiting diffusion overlap the lattice diffusion. Non-Gaussian profiles are obtained, if

1) Grain boundaries or dislocations contribute to D (this contribution increases with decreasing temperature and decreasing grain diameter).
2) Oxide layers at the surface hinder the penetration of the tracer atoms.
3) Reduced solubility of impurities changes the boundary conditions.
4) Tracer atoms evaporate from the surface, which also changes the boundary conditions.

Short-circuiting contributions lead to an upward deviation from the Gaussian plot at deeper penetrations (see Figure 01.05). Grain-boundary diffusion results in a proportionality between ln c and $x^{6/5}$ [01.27, 01.28]. The short-circuiting contribution can be eliminated mathematically if the penetration plot is fitted to [01.29]

$$c(x,t) = \frac{M}{2\sqrt{\pi D t}} \exp\left(-\frac{x^2}{4Dt}\right) + A\exp(-Bx^{6/5}) \qquad (01.07)$$

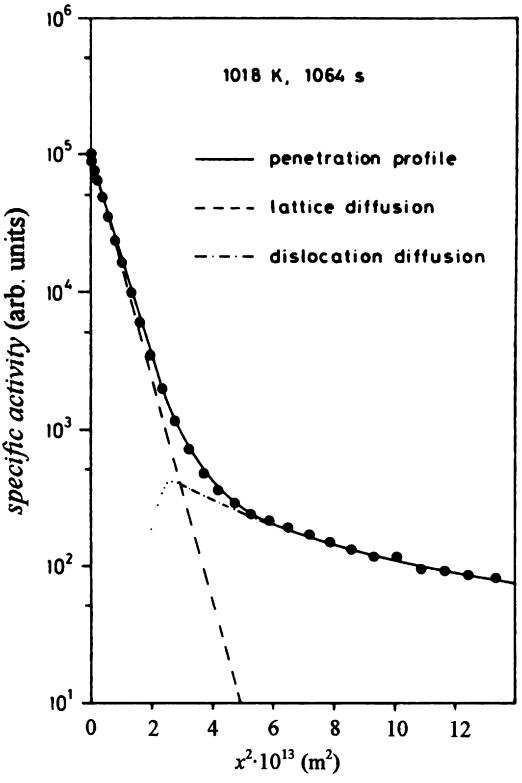

Fig. 01.05 Self-diffusion of ^{59}Fe in α-iron. Penetration profile with dislocation tail (from Ref. [01.26]).

where A and B are fitting parameters. A disregard of the correction term in Eq. (01.07) results in enhanced diffusion coefficients and in a diffusion energy smaller than the vacancy diffusion energy Q_{1V}.

An oxide layer on the sample surface can act as a barrier to the tracer. Depending on the chosen boundary conditions different solutions for $c(x,t)$ result [01.02, 01.06, 01.30, 01.31]. Simply, the profile can be expressed by

$$\frac{\mathrm{d}\ln c}{\mathrm{d}x^2} = -\frac{A}{x} - \frac{1}{4Dt} \tag{01.08}$$

where A is a fitting parameter which includes the diffusivity in the oxide layer and its thickness. The ln c vs. x^2 plot shows an upward curvature near the sample surface (near-surface effect, NSE). With rising x the profile approaches a straight line.

Figure 01.06 shows a surface hold-up for Fe diffusion in aluminum owing to a stable Fe_4Al_{13} layer formed at the surface, which decomposes very slowly. Note that the extent of hold-up increases with decreasing temperature. Figure 01.07 shows profiles of Al and Mn diffusion in aluminum at 844 K. The profiles become straight lines at penetrations larger than about 150 µm. While the evaluated D_{Al} is within the range of values obtained by different methods, D_{Mn}, however, is about one order of magnitude larger than that obtained in more recent investigations (see Table 3.4).

The hold-up due to an oxide layer can be avoided if the tracer is implanted by ion bombardment, as for the first time done by Hood [01.33] (for a review of modern implantation techniques see Ref. [01.34]). This type of tracer deposition is particularly applied in the more recent diffusion investigations of transition metals in aluminum (see Table 3.4).

Non-Gaussian profiles can appear in impurity diffusion investigations if the deposited metal has only a small solubility in the host. Only if the surface concentration drops below the solubility limit c_s in a period which is short compared to the total annealing time ($t_s \ll t$), the profile is described by Eq. (01.04).

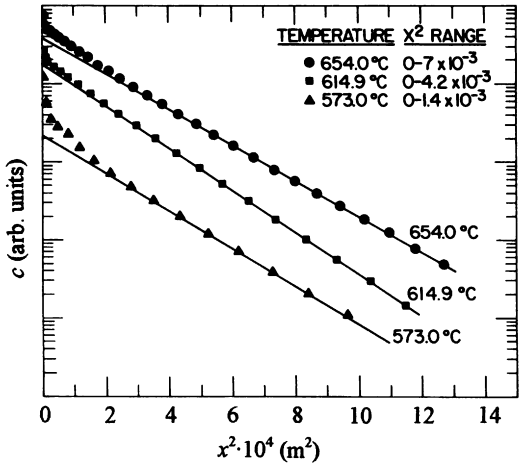

Fig. 01.06 Impurity diffusion of ^{59}Fe in aluminum. Surface hold-up due to slow dissolution of the tracer (from Ref. [01.02]).

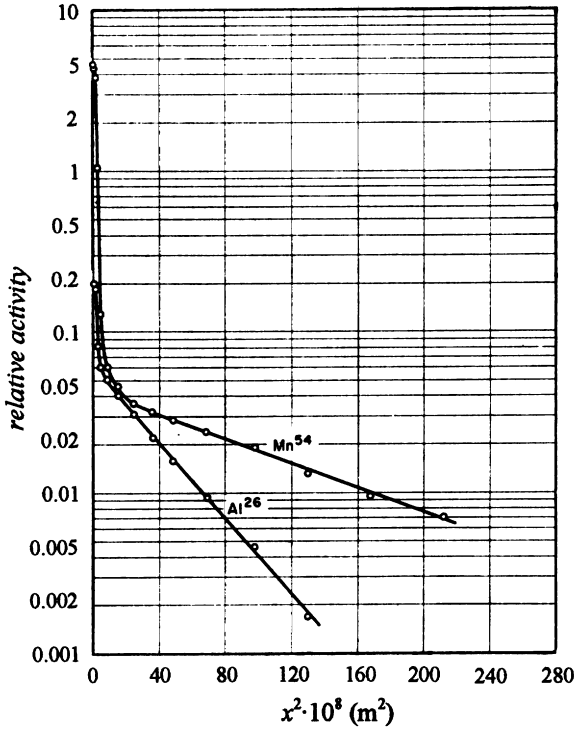

Fig. 01.07 Diffusion of ^{26}Al and ^{54}Mn in aluminum. Pronounced near-surface effect due to oxide hold-up. ($T = 844$ K, $D_{Al} = 2.5 \times 10^{-13}\,m^2\,s^{-1}$, $D_{Mn} = 8.3 \times 10^{-13}\,m^2\,s^{-1}$, evaluated from deeper penetrations) (from Ref. [01.32]).

However, for $t < t_s$, which corresponds to a constant boundary concentration $c(0,t) = c_s$ during the entire diffusion run, the diffusion profile is described by an error function [01.05]

$$c(x,t) = c_s \mathrm{erfc}\left(\frac{x}{2\sqrt{Dt}}\right) \tag{01.09}$$

where $c(x,t)$ is linear in the inverse complementary error function $\mathrm{erfc}_{(-1)}\, c$ against x (see e.g. Figure 01.08). The validity ranges of Eqs. (01.04) and (01.09) depend on t_s/t and thus on c_s and δ [01.36]. For $t \geqslant t_s$ an intermediate solution of Eq. (01.02) was derived by Malkovich [01.37]

$$c(x,t) = c_s \frac{2}{\sqrt{\pi}} \int_z^\infty \exp(-y^2)\mathrm{erf}y\left(\frac{t_s}{t - t_s}\right)^{1/2} \mathrm{d}y \tag{01.10}$$

with

$$z = x/2(Dt)^{1/2} \quad \text{and} \quad t_s = \pi M^2/4Dc_s^2$$

For $t < t_s$ the evaluation of $c(x,t)$ according to Eq. (01.04) instead of Eq. (01.09) leads to a value of D which is smaller than the correct one (see e.g. Figure 01.09).

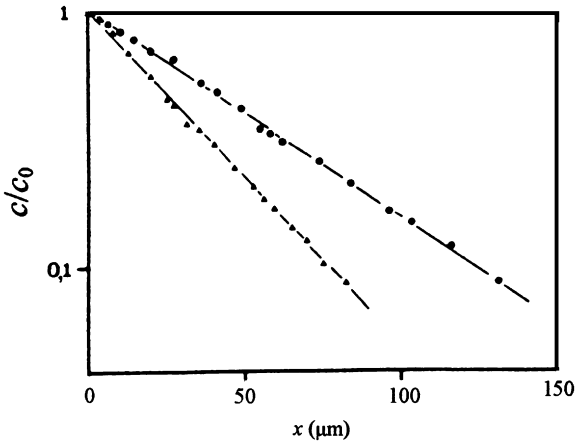

Fig. 01.08 Impurity diffusion of ^{63}Ni in silver (●, $T = 1{,}006$ K; ▲, $T = 1{,}081$ K). Profile fitted to Eq. (01.09) (from Ref. [01.35]).

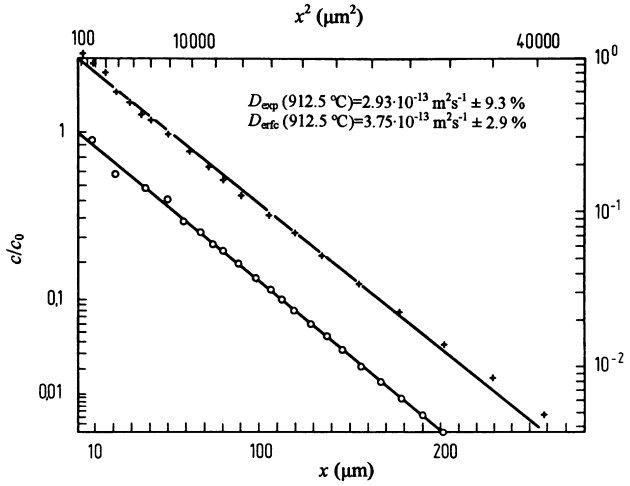

Fig. 01.09 Impurity diffusion of ^{51}Cr in silver. Evaluations according to Eqs. (01.04) (+) and (01.09) (○) (from Ref. [01.38]).

Similar results are obtained for Fe diffusion in silver (see Figure 01.10). For $T = 797.3°C$, as an example, the evaluation of the penetration profile results in $D(\text{erfc}) = 2.8 \times 10^{-14}\,\text{m}^2\,\text{s}^{-1}$, compared to $D(\text{exp}) = 2.25 \times 10^{-14}\,\text{m}^2\,\text{s}^{-1}$ as tabulated in Ref. [01.39].

The frequently steep decrease of $c(x,t)$ in $\ln c - x^2$ was sometimes associated with an NSE. Lundy and Padgett [01.40] have proposed to divide the penetration plot into three regions (see Figure 01.11). Region I is the result of an NSE, region II represents lattice diffusion and region III stems from extrinsic

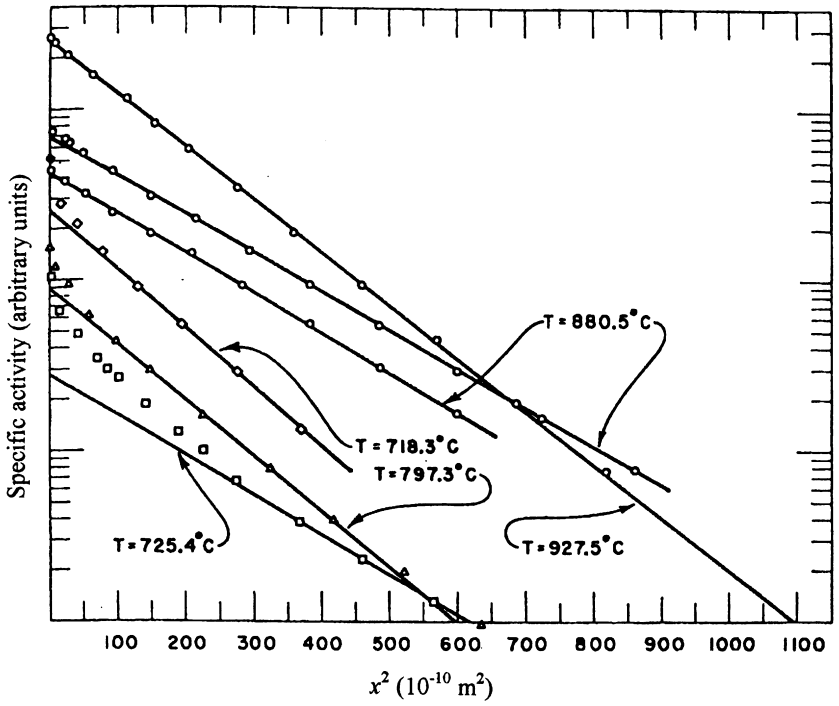

Fig. 01.10 Diffusion of ^{59}Fe in silver. Evaluation according to Eq. (01.04) (from Ref. [01.39]).

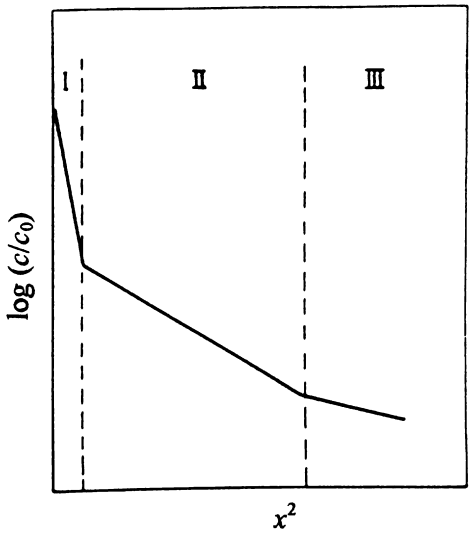

Fig. 01.11 Schematic penetration plot. Region I: near-surface effect (NSE); Region II: lattice diffusion; Region III: short-circuiting contributions (according to Ref. [01.40]).

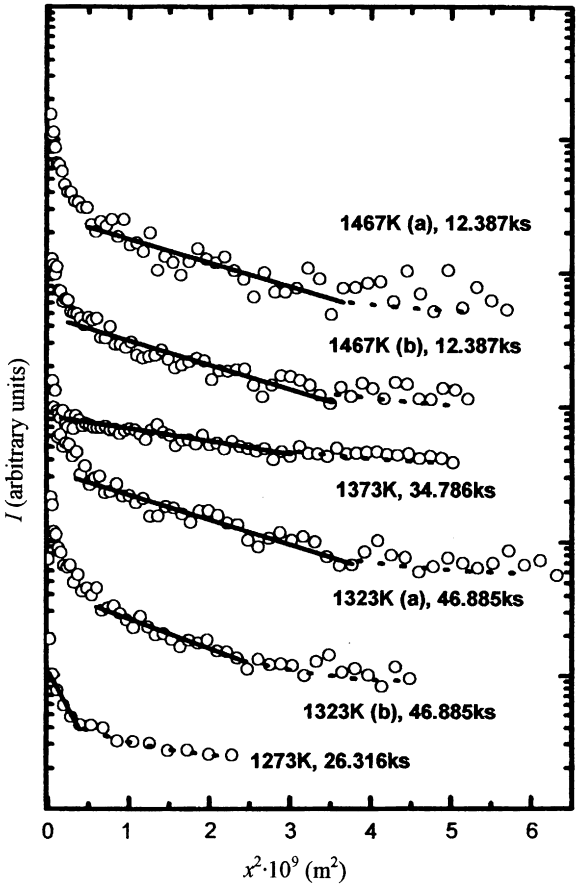

Fig. 01.12 Diffusion of Al in nickel. Determination of D from region II according to Eq. (01.04) (from Ref. [01.41]).

effects (short-circuiting contributions). In the case of an oxide hold-up the slope of region II could in principle yield the lattice diffusion coefficient, obviously with large uncertainty. For $t < t_s$, however, because of the continuous curvature of the $\ln c - x^2$ plot, the averaged slope of region II leads to an erroneous value of D (see Figures 01.09 and 01.10). The determination of D from region II is highly questionable, as this can lead to erroneous results (see Figure 01.12).

If the deposited metal has a high vapour pressure, the tracer will simultaneously evaporate and diffuse into the bulk. The resulting penetration profile then exhibits a peak near the surface in the $\ln c - x^2$ plot (see e.g. Figure 01.13). Solutions of Fick's second law for different boundary conditions are given in the literature [01.02, 01.06, 01.42–01.44].

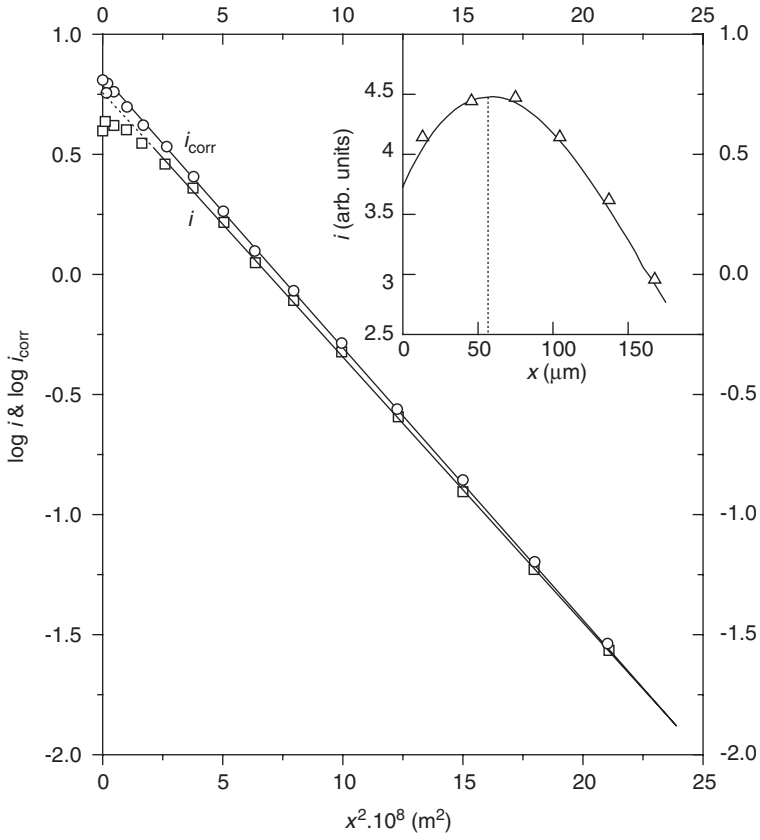

Fig. 01.13 Impurity diffusion of ^{67}Ga in copper. Penetration plot with tracer loss due to evaporation (from Ref. [01.43]).

Further radioactive methods

Out-diffusion of spallation and fission products. Metal foils (Nb, Ta, Mo, W) are irradiated with high-energetic protons [01.45]. This generates spallation and fission products, which are homogeneously distributed in the sample. The out-diffusion of these reaction products is measured by means of γ spectroscopy. Because of the irradiation damage of the samples, short-circuit contributions should dominate the diffusivity.

Fissiography. After the diffusion run of natural uranium in a solvent metal, the sample is irradiated with thermal neutrons [01.46]. The activity of the generated fission products is measured radiographically.

0.1.2 Non-radioactive methods

In addition to SIMS investigations further non-radioactive techniques have been developed, which permit the determination of impurity diffusion coefficients.

Methods with and without profile measurement have to be distinguished. As in the second group of these methods only the integral concentration changes are measured, deviations from Gaussian profiles like surface hold-up or short-circuiting contributions cannot be detected. If these error sources can be avoided, the resulting diffusion coefficients are close to those obtained by tracer sectioning methods.

Rutherford backscattering

In the Rutherford backscattering method (RBS) or heavy ion RBS (HIRBS), a high-energy ion beam (^{4}He or ^{19}F) bombards the sample along the diffusion direction. From the energy spectrum of the elastically backscattered ions the profile can be determined. Diffusion coefficients between 10^{-16} and $10^{-23}\,m^2\,s^{-1}$ can be measured with an uncertainty of about 20%. RBS and HIRBS are mainly applied to heavy impurities in a light solvent, especially α-Ti (for a review see Ref. [01.47]).

Nuclear reaction analysis

In the nuclear reaction analysis (NRA) the sample is bombarded in the diffusion direction with a proton beam. This leads to reactions like ^{27}Al(p, γ)^{28}Si or ^{30}Si(p, γ)^{31}P. The concentration profiles are determined by measuring the broadening of the resonance energy of the nuclear reaction.

Diffusion coefficients between 10^{-16} and $10^{-23}\,m^2\,s^{-1}$ can be measured. The NRA technique was applied to Al and Si diffusion mainly in group IVa metals.

X-ray diffraction investigations

Fogelson [01.48, 01.49] has developed an X-ray diffraction method for the measurement of impurity diffusion coefficients. The principle of this method is similar to the absorption method [01.14], i.e. it is based on the measurement of the surface concentration decrease of the solute. X-ray diffraction measurements of the change in the lattice parameters of the resulting solid solution can be used for the determination of the surface concentration of the deposited impurity. A polycrystalline foil of the solvent, about 200 μm thick, is covered by a 0.05–1 μm thick film of the solute. The surface concentration after the diffusion anneal is determined by analysing the diffraction line profile. The diffraction profile depends on the lattice parameter of the alloy (assuming that the metals form a solid solution), and consequently on the concentration of the element diffusing in the layer. The shift of the edge line, which changes by about 1–3%, is used to determine the concentration.

Diffusion coefficients between 10^{-11} and $10^{-16}\,m^2\,s^{-1}$ can be measured with an accuracy of about 10–15%. The method is mainly applied to impurity diffusion in noble metals.

Resistometric investigations

Ceresara et al. [01.50] have developed a method for the determination of diffusion coefficients in dilute alloys by measuring the electrical resistivity of a sample as a function of time. A wire, about 1 mm in diameter, is covered with a

layer of the dopant, about 1 μm thick. The resistivity of the wire is measured during the whole diffusion run. The change of the resistivity, which results from the in-diffusion of the dopant, can be recalculated to a concentration change. The solution of Eq. (01.01), where the Δ-operator is transformed to cylindrical coordinates, is a Bessel function [01.05, 01.50].

As in the X-ray diffraction investigations, diffusion coefficients derived from resistivity mesurements deviate from the most reliable tracer sectioning by not more than 10–15%.

Nuclear methods

Examples for non-destructive nuclear methods are nuclear magnetic resonance (NMR), quasi-elastic Mößbauer spectroscopy (QMS) and quasi-elastic neutron scattering (QNS). Limited availability of suitable isotopes restricts the applicability of these methods to a small number of systems.

Nuclear magnetic resonance

Various methods have been used for the investigation of atomic motion in metals by means of NMR: linewidth measurements, measurement of the spin-lattice relaxation time (SLRT) T_1 and $T_{1\rho}$ (for reviews see Refs. [01.51, 01.52]) or measurement of the SLRT using the more recent β-NMR technique (see e.g. [01.53, 01.54]). Compared to the T_1-technique, the $T_{1\rho}$-technique (SLRT in a rotating frame) allows the extension of the measurement to lower temperatures, so that diffusion coefficients as small as $10^{-19}\,m^2\,s^{-1}$ can be measured (compared to the $10^{-15}\,m^2\,s^{-1}$ deduced from T_1 measurements). In the β-NMR technique (β-radiation detected NMR) the spin polarization of the β-active nucleus is measured. Special models are required to recalculate the relaxation rates $1/T_1$ and $1/T_{1\rho}$ into diffusivities, which involves the assumption of a definite diffusion mechanism (see e.g. [01.55]).

There are only a few applications of NMR to diffusion, particularly to self-diffusion in metals. Self-diffusion studies have been carried out on Al, Li and Na, Cu and V. In particular for Li and Al NMR is an alternative to tracer studies, as no suitable radioactive isotopes of these metals exist. Self-diffusion coefficients ranging from 10^{-17} to $10^{-10}\,m^2\,s^{-1}$ and from 10^{-17} to $10^{-12}\,m^2\,s^{-1}$ are measured for Li and Al, respectively.

Quasi-elastic Mößbauer spectroscopy and quasi-elastic neutron scattering

The linewidths in QMS as well as in QNS have a contribution which results from the diffusional motion of the atoms (line broadening). Both, jump frequencies and broadening increase exponentially with temperature. From the diffusional broadening the diffusion coefficient can be determined. Furthermore, the jump vector can be obtained, which enables conclusions with respect to the diffusion mechanism. As the line broadening must be comparable to or exceed the natural linewidth in QMS and the energy resolution in QNS, the diffusivities must be larger than $10^{-14}\,m^2\,s^{-1}$ in QMS and larger than $10^{-13}\,m^2\,s^{-1}$ in QNS investigations. For reviews on diffusion investigations with QMS see Refs. [01.56, 01.57] and with QNS see Refs. [01.57–01.59].

There is only a small number of nuclei suitable for QMS investigations. The most frequently applied Mößbauer atom is ^{57}Fe. This was used for the investigation of self-diffusion in γ- and δ-iron and for impurity diffusion of Fe in Cu, Au, Al, V, β-Sn, β-Ti and β-Zr (see Refs. [01.56, 01.57]). The results of the self-diffusion measurements on iron are in agreement with tracer diffusion data only near to the transition temperature $T_{\gamma\delta}$ [01.60]. For Fe diffusion in copper the D values are strongly scattering around the tracer data [01.61]. For Fe in β-Zr [01.62] the measured diffusion coefficients are one order of magnitude smaller than those obtained from tracer measurements. This suggests the existence of a second diffusion mechanism which is too fast to be seen in the time window of the QMS method.

QNS is applicable to a few fast-diffusion elements with a large enough quasi-elastic scattering cross-section for neutrons. A number of moderate scatterers exists, however, as yet mainly Na, Ti and Co were applied to diffusion investigations with QNS. Self-diffusion investigations on Na and β-Ti led to the conclusion that the monovacancy mechanism dominates. For Co diffusion in β-Zr [01.63] the result is analogous to that of Fe diffusion in β-Zr, using QMS, i.e. the measured diffusion coefficients are one order of magnitude smaller than those obtained from tracer diffusion measurements.

0.1.3 Interdiffusion measurements

The measurement of the concentration profile of a diffusion couple consisting of two pure metals A and B or a pure metal and an alloy, A/A(B), yields the interdiffusion coefficient $\tilde{D}$.

According to Darken [01.64] $\tilde{D}$ can be expressed by

$$\tilde{D}(c) = D_A X_B + D_B X_A \tag{01.11}$$

where D_A and D_B are the concentration-dependent intrinsic diffusion coefficients of the components A and B in the alloy; X_A and X_B are the respective mole fractions.

D_A and D_B are in general not equal which leads to a net flux of atoms across the interface and to a shift of lattice planes with respect to the sample-fixed axes (Kirkendall effect [01.65, 01.66]).

According to Manning [01.67] $\tilde{D}$ can be connected with the tracer diffusion coefficient by

$$\tilde{D}(c) = (D_A^T X_B + D_B^T X_A)\Phi S \tag{01.12}$$

where Φ is the thermodynamic factor and S the so-called vacancy-wind factor [01.67]. Φ is

$$\Phi = \frac{\mathrm{d}\ln a}{\mathrm{d}\ln X} = 1 + \frac{\mathrm{d}\ln f}{\mathrm{d}\ln X} \tag{01.13}$$

where a is the thermodynamic activity and f the activity coefficient.

The extrapolation of $\tilde{D}$ to $X_B = 0$ yields the impurity diffusion coefficient D^T.

$\tilde{D}$ can be determined from the concentration profile by means of the Boltzmann–Matano method [01.68, 01.69]. For an A/B or A/A(B) couple $\tilde{D}$ can be

calculated from

$$\tilde{D}(c') = -\int_0^{c'} \frac{(x - x_0)\mathrm{d}x}{2t(\mathrm{d}c/\mathrm{d}x)_{c=c'}} \tag{01.14}$$

where x_0 is the position of the Matano interface (not identical with that of the welding interface). x_0 describes the position at which the material flux in one direction equals that to the opposite direction. x_0 can be determined from

$$\int_0^{c_{\max}} (x - x_0)\mathrm{d}c = 0 \tag{01.15}$$

where $c_{\max}$ is the maximum concentration of B in a couple A/A(B).

A method which does not require the knowledge of the Matano interface was developed by Sauer and Freise [01.70], Wagner [01.71] and den Broeder [01.72]. Accordingly, the following expression holds for $\tilde{D}$

$$\tilde{D}(c') = \frac{1}{2t(\mathrm{d}y/\mathrm{d}x)_{x'}} \left((1 - y') \int_{-\infty}^{x'} y\mathrm{d}x + y' \int_{x'}^{\infty} (1 - y)\mathrm{d}x \right) \tag{01.16}$$

with

$$y = \frac{c - c_{\min}}{c_{\max} - c_{\min}}$$

where $c_{\min}$ and $c_{\max}$ represent the terminal concentrations of the couple, x' and y' refer to the values of x and y, respectively, when $c = c'$.

The evaluation according to Eq. (01.16) leads to $\tilde{D}$ values very close to D^{T} if A/A(B) couples with $x_{\mathrm{B}} \leqslant 0.01$ are used.

The evaluation of the concentration profiles according to Refs. [01.70–01.72] yields credible diffusion coefficients $\tilde{D}$ in the middle part of the profile. At the limiting values of c ($c = 0$ and $c = c^B_{\max}$for a A/A(B) couple), the diffusion coefficients calculated in this way are of considerable uncertainty.

Hall [01.73] has developed a method which permits the determination of $\tilde{D}$ at the limiting concentrations. $\tilde{D}$ can be calculated from

$$\tilde{D} = \frac{1}{4h^2} + \frac{k\pi^{1/2}}{2h^2} \exp(u^2)\mathrm{erfc}u \tag{01.17}$$

with

$$\frac{c}{c_{\max}} = \mathrm{erf}u,\ u = h\frac{x}{t^{1/2}} + k$$

where h is the slope and k the intercept of the linear portion of the concentration ratio curve. $c_{\max}$ is the maximum concentration of B in a couple A/A(B). The Hall method permits the determination of $\tilde{D}$ values close to D^{T}.

For concentration-independent interdiffusion coefficients $\tilde{D}$ can be determined according to [01.74]:

$$\frac{c - c_1}{c_2 - c_1} = \frac{1}{2}\mathrm{erfc}\frac{x}{2(Dt)^{1/2}} \tag{01.18}$$

valid for the concentration range between c_2 and c_1. For concentration-independent $\tilde{D}$ Eq. (01.18) can be used instead of Eqs. (01.14) and (01.16).

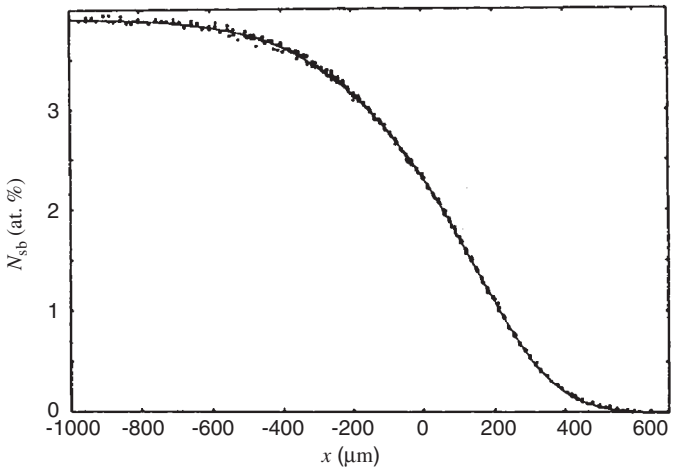

Fig. 01.14 EPMA diffusion profile for a Ag/Ag (3.93% Sb) couple at 1,048 K (from Ref. [01.75]).

Electron probe microanalysis (EPMA)

The diffusion profile of a diffusion couple A/B or A/A(B) after annealing can be measured by means of an electron probe microanalyser. A thin electron beam (diameter 1 μm) stimulates the X-ray emission of the elements in the alloy. The profile can be obtained by analysing the characteristic radiation from the sample along the diffusion direction. Figure 01.14 shows a typical EPMA diffusion profile. The interdiffusion coefficient $\tilde{D}$ can be determined by application of the methods described before. The method is restricted to diffusion coefficients larger than $10^{-15}\,m^2s^{-1}$ since the depth resolution is limited by the size of the volume excited by the electron beam.

The extrapolation of $\tilde{D}$ to $x_B = 0$ yields the impurity diffusion coefficient of B in A (see e.g. Figure 01.15). Impurity diffusion coefficients deduced from EPMA investigation are in acceptable agreement with those obtained from serial sectioning measurements.

0.1.4 Comparison of the experimental methods

In Table 01.01 the different experimental methods for the measurement of diffusion coefficients are compared. The measuring ranges of D are listed as well as a rough estimation of the attainable accuracy. For sectioning techniques the usual section thicknesses are added.

The most reliable methods are the tracer sectioning techniques. The macrosectioning techniques are applicable to temperatures larger than about $0.7\,T_m$. In combination with microsectioning techniques more than 10 orders of magnitude in D can be measured between $0.4\,T_m$ and T_m.

The less accurate non-radiative methods are important especially if no reliable tracer data are available.

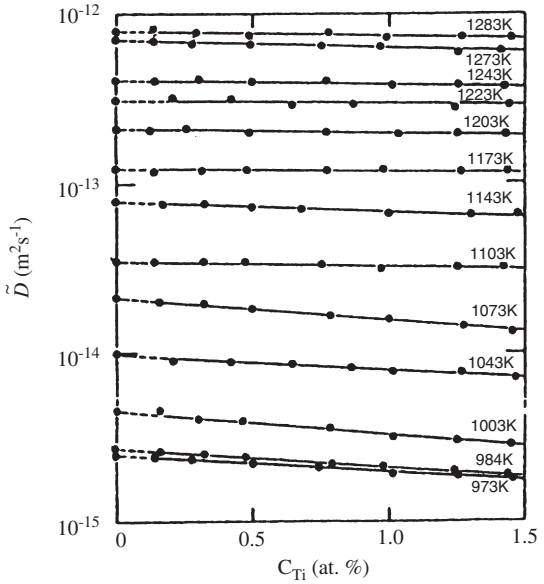

Fig. 01.15 Concentration dependence of the interdiffusion coefficient $\tilde{D}$ in copper–titanium alloys (from Ref. [01.76]).

Table 01.01 Comparison of the experimental techniques for the measurement of diffusion coefficients

Technique	D-range [$m^2 s^{-1}$]	Section thickness	Attainable accuracy[a] (uncertainty in %)
Macrosectioning			
Lathe	10^{-16}–10^{-11}	5–100 μm	<5
Microtome[b]	10^{-16}–10^{-11}	1–100 μm	<5
Grinding	10^{-17}–10^{-11}	3–100 μm	5–10
Residual activity	10^{-16}–10^{-12}	10–100 μm	>10
Microsectioning			
Chemical	10^{-18}–10^{-12}	50–200 nm	5–10
Anodizing	10^{-21}–10^{-15}	10–100 nm	5–10
Sputtering	10^{-23}–10^{-15}	1–20 nm	10–20
Non-radioactive methods			
RBS, HIRBS, NRA	10^{-23}–10^{-16}		10–20
X-ray diffraction	10^{-16}–10^{-11}		10–15
Resistometry	10^{-14}–10^{-12}		10–20
EPMA	10^{-16}–10^{-11}		10–15
Nuclear methods			
NMR	10^{-17}–10^{-13}		10–15
β-NMR	10^{-17}–10^{-11}		10–15
QMS	10^{-14}–10^{-11}		–
QNS	10^{-13}–10^{-11}		–

[a]The uncertainty arising from the temperature measurement has to be added. For high-temperature measurements using optical pyrometers errors of up to 20% in D have to be taken into account at $T > 3{,}000$ K.
[b]For impurity diffusion in lead, D values up to $10^{-9} m^2 s^{-1}$ were measured by means of microtome sectioning (see Table 4.5).

Nuclear methods are applicable to only a few systems. The results of NMR self-diffusion investigations on Li, Na and particularly Al, where no suited radio isotope exists, are of considerable importance. QMS and QNS investigations are unsuited for the measurement of absolute values of D. The value of these methods is the possibility of a direct observation of the atomic jump process.

0.2. INTERPRETATION OF THE DIFFUSION INVESTIGATIONS

The temperature dependence of the diffusivity can be expressed by the diffusion coefficient D

$$D = D^0 \exp\left(\frac{-Q}{kT}\right) \tag{02.01}$$

where D^0 is the pre-exponential factor, Q the diffusion energy, k the Boltzmann constant and T the absolute temperature. Equation (02.01) corresponds to a linear plot of ln D vs. $1/T$ (Arrhenius plot).

In solid metals self-diffusion is dominated by monovacancy (1V) migration. The diffusion coefficient D_{1V} is given by

$$D_{1V} = g a^2 f_{1V} c_{1V} w_{1V} \tag{02.02}$$

where g is a geometrical factor ($g = 1$ holds for face-centred, fcc, and body-centred, bcc, cubic metals). a is the lattice constant, f_{1V} the correlation factor ($f_{1V} = 0.781$ for fcc metals and $f_{1V} = 0.727$ for bcc metals). c_{1V} is the relative monovacancy concentration and w_{1V} the jump frequency of monovacancies.

c_{1V} and w_{1V} can be expressed by

$$c_{1V} = \exp\left(\frac{-G^{F}_{1V}}{kT}\right) \tag{02.03}$$

and

$$w_{1V} = \nu_{1V} \exp\left(\frac{-G^{M}_{1V}}{kT}\right) \tag{02.04}$$

where G^F_{1V} and G^M_{1V} are the free enthalpy of monovacancy formation and migration, respectively. ν_{1V} is a lattice frequency associated with the monovacancy jump. Because of $G = H - TS$ it follows for D^0_{1V} and Q_{1V}

$$D^0_{1V} = g a^2 \nu_{1V} f_{1V} \exp\left(\frac{S^{F}_{1V} + S^{M}_{1V}}{k}\right) \tag{02.05}$$

and

$$Q_{1V} = H^F_{1V} + H^M_{1V} \tag{02.06}$$

where H^F_{1V}, H^M_{1V} and S^F_{1V}, S^M_{1V} are the vacancy formation and migration enthalpy and entropy, respectively.

In general ln $D - 1/T$ is non-linear. If grain boundary or dislocation contributions to D can be excluded, the non-linearity can be caused by the

contribution of two diffusion mechanisms with different activation energies (two-defect models) or by temperature-dependent enthalpies and entropies (one-defect models), respectively.

In fcc metals the weak curvature of ln $D-1/T$ can only be verified if low-temperature measurements down to 0.4 T_m (T_m is the melting temperature) could be performed. The reason for the curvature of the Arrhenius plot of D is the contribution of divacancies (2V) at higher temperatures [02.01]. D is then given by

$$D(T) = D_{1V}^0 \exp\left(\frac{-Q_{1V}}{kT}\right) + D_2^0 \exp\left(\frac{-Q_2}{kT}\right) \tag{02.07}$$

with

$$D_2^0 = D_{2V}^0 \text{ and } Q_2 = Q_{2V}$$

A forced fit to the high-temperature data (0.7 T_m–T_m) leads to averages for D^0 and Q valid for $\bar{T} = 0.85T_m$

$$D(T) = D_{85}^0 \exp\left(\frac{-Q_{85}}{kT}\right) \tag{02.08}$$

where Q_{85}/T_m is almost constant [02.02] (see Figure 02.01)

$$\frac{Q_{85}}{T_m} \approx 1.5 \times 10^{-3}\text{eV K}^{-1} \tag{02.09a}$$

whereas the pre-exponential factor varies in the limits

$$0.05 \leq D_{85}^0(10^{-4}\text{m}^2\text{s}^{-1}) \leq 5 \tag{02.09b}$$

The curvature of the Arrhenius plot of self-diffusion in bcc metals is much more pronounced than that of fcc metals (see Figure 02.02). The refractory metals of group V and VI show a more or less ''normal'' behaviour, whereas the group IVa metals reveal strongly enhanced diffusivity, especially in the low-temperature range of the bcc phase. The alkaline metals represent an intermediate group. In contrast to the refractory metals the group IVa metals undergo a martensitic phase transition to a close-packed structure at $T_{\alpha\beta} \approx 0.5$ T_m. At very low temperatures ($\leqslant 0.15$ T_m) also Li and Na exhibit a martensitic phase transition.

There is no doubt that monovacancies also dominate the diffusion in bcc metals. Up to now, however, the operating diffusion mechanisms are controversially discussed. Two-defect as well as one-defect models are considered.

In refractory metals divacancies [02.03], self-interstitials [02.04] or next-nearest neighbour jumps [02.05] are assumed to contribute to D at higher temperatures. These two-defect models also obey Eq. (02.07). A fit of the experimental data to Eq. (02.07) leads to the approximation [02.06]

$$Q_{1V}/T_m = 1.5 \times 10^{-3}\text{eVK}^{-1}; \quad Q_{2V}/T_m = 2.0 \times 10^{-3}\text{eVK}^{-1} \tag{02.10}$$

The curvature of the Arrhenius plot can also be described by temperature-dependent enthalpies and entropies. The most simple approximation is a linear

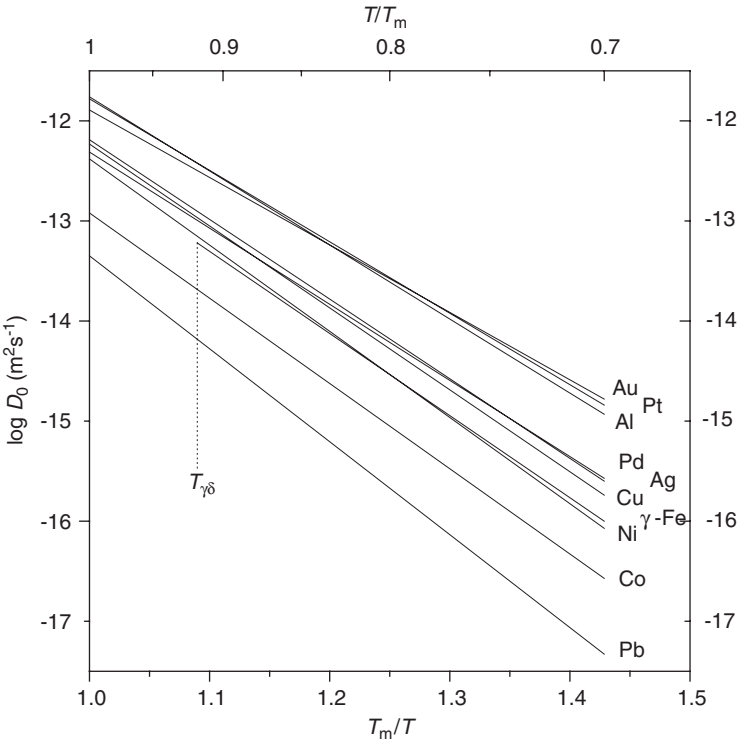

Fig. 02.01 Self-diffusion in fcc metals.

temperature dependence of the enthalpy [02.01]

$$H(T) = H(T_0) + \alpha k(T - T_0) \tag{02.11}$$

where α is an empirical constant and T_0 a suitably chosen reference temperature. Based on Eq. (02.11) this results in the following expression for the temperature dependence of D [02.01]:

$$D(T) = D_\alpha^0(T_0) \exp\left(-\frac{Q_\alpha(T_0)}{kT}\right) \exp\left(2\alpha\left(\ln\frac{T}{T_0} - \frac{T - T_0}{T}\right)\right) \tag{02.12}$$

Self-diffusion in group IVa metals is anomalously high and the Arrhenius plot of D is strongly curved (see Figure 02.02). Q_1 and Q_2 do not obey Eq. (02.10). The reason for the enhanced diffusivity is that at the martensitic phase transition at $T = T_{\alpha\beta}$ the elastic constants c_{11}–c_{12} and a consequence H_{1V}^M approach zero [02.07]. The first saddle point for an (unrelaxed) vacancy jump in the bcc structure forms a configuration identical to the basal plane of the trigonally bonded ω phase. In this position the $L_{\frac{2}{3}}^{\frac{2}{3}}$ (111) phonon is very soft. The softness of the $L_{\frac{2}{3}}^{\frac{2}{3}}$ (111) phonon and the temperature dependence of the T_1(½)(110) phonon frequency are responsible for the enhanced diffusivity and the temperature dependence of Q [02.08, 02.09].

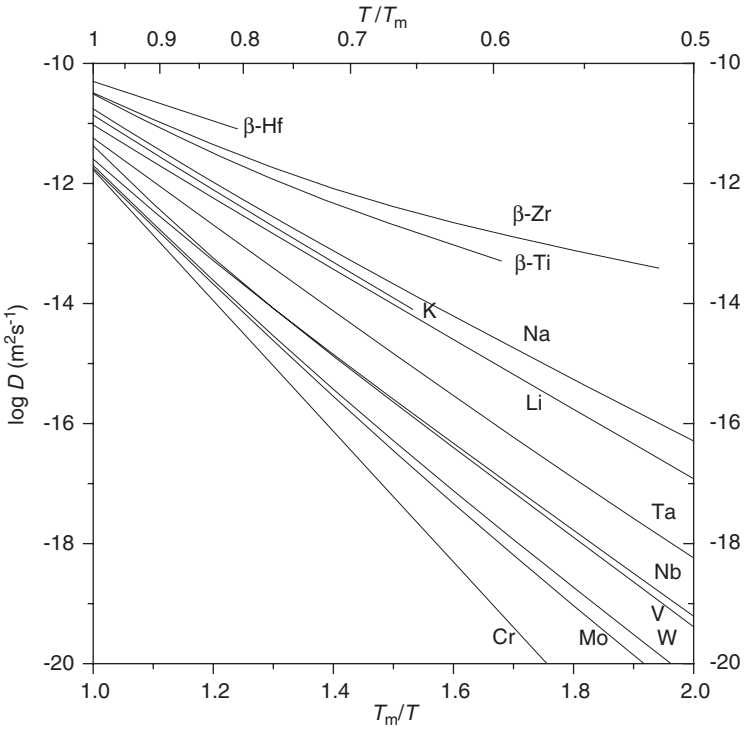

Fig. 02.02 Self-diffusion in bcc metals.

Sanchez and de Fontaine [02.10] related the Gibbs free energy of ω-embryo formation to that of vacancy migration by

$$G_\omega = G_{1V}^M \left(1 - \frac{T_0}{T}\right) \tag{02.13}$$

with $T_0 < T_\omega < T_{\alpha\beta}$, where T_ω is the temperature of the β–ω phase transition and $T_{\alpha\beta}$ that of the α–β phase transition. With the aid of Eq. (02.13) the temperature dependence of D can be expressed by

$$D(T) = D_\omega^0 \exp\left(\frac{-Q_\omega}{kT}\right) \exp\left(\Omega \frac{T_m^2}{T^2}\right) \tag{02.14}$$

where

$$\Omega = \frac{H_{1V}^M T_0}{kT_m^2} \tag{02.14a}$$

In most cases the experimental $D(T)$ is fitted to Eq. (02.14) (see Chapter 4.1), although there is some doubt that only H_{1V}^M decreases with decreasing temperature [02.11]. Köhler and Herzig [02.12] assume that for all bcc metals D can be described by Eq. (02.14).

It may be mentioned that the fits according to Eqs. (02.07), (02.12) and (02.14) in nearly all cases lead to standard deviations σ which do not differ by more than 10% [02.06, 02.13]. The extrapolated values of D at $T = T_m$, however, can differ by up to $> 25\%$ (see e.g. Hf in β-Zr [02.13]).

Diffusion investigations by use of NMR techniques measure the uncorrelated vacancy motion. The resulting D^{NMR} differs from the tracer diffusion coefficient D^T by the correlation factor f, i.e. [02.03]

$$D^T = fD^{NMR} \tag{02.15}$$

If more than one diffusion mechanism is operating

$$D^{NMR} = D_1^{NMR} + D_2^{NMR} \tag{02.16}$$

can be recalculated to D^T according to

$$D^T = f_1 D_1^{NMR} + f_2 D_2^{NMR} \tag{02.17}$$

Presuming that a two-exponential fit of $D_{NMR}(T)$ to Eq. (02.16) is possible, D^T can be calculated if f_1 and f_2 are known. Because of the controversially discussed high-temperature mechanism in bcc metals, the calculated D_2^T and thus D^T is uncertain.

In cubic metals the diffusivity is isotrope. In non-cubic metals (e.g. hexagonal or body-centred tetragonal, bct) the diffusion coefficients perpendicular and parallel to the c-axis, $D_\perp$ and $D_{//}$, respectively, differ. The difference between $D_\perp$ and $D_{//}$ increases with increasing deviation from the closed-packed lattice structure. For the hexagonal close-packed structure (hcp), e.g., the c/a ratio is $\sqrt{(8/3)} \approx 1.633$.

If no single crystals with orientations exactly parallel to the c- and a-axis are available, $D_\perp$ and $D_{//}$ can be calculated from measurements using crystals with orientations deviating by an angle θ from the crystal axis according to

$$D(\theta) = D_\perp \cos^2\theta + D_{//} \sin^2\theta \tag{02.18}$$

In ferromagnetic metals the diffusivity below the Curie temperature T_C is reduced. For $T < T_C$ the diffusivity D can be described by [02.14]

$$D(T) = D_p^0 \exp(-Q_p(1 + \alpha M^2(T))/kT) \tag{02.19}$$

where D_p^0 and Q_p are the pre-exponential factor and diffusion energy, respectively, for the paramagnetic temperature range for the bcc α_p phase above T_C. $M(T)$ is the ratio of the spontaneous magnetization at T to that at $T = 0$. For Fe $M(T)$ was experimentally determined [02.15, 02.16] (see Figure 02.03). Theoretical expressions for α could be derived [02.14]. Experimentally, α can be determined according to Eq. (02.19) [02.17], i.e.

$$\alpha = \frac{1}{M^2(T)} \left(\frac{kT}{Q_p} \ln \frac{D_p^0}{D} - 1 \right) \tag{02.20}$$

or

$$T \ln \frac{D(T)}{D_p^0} = -\frac{Q_p}{k} - \frac{\alpha Q_p}{k} M^2(T) \tag{02.21}$$

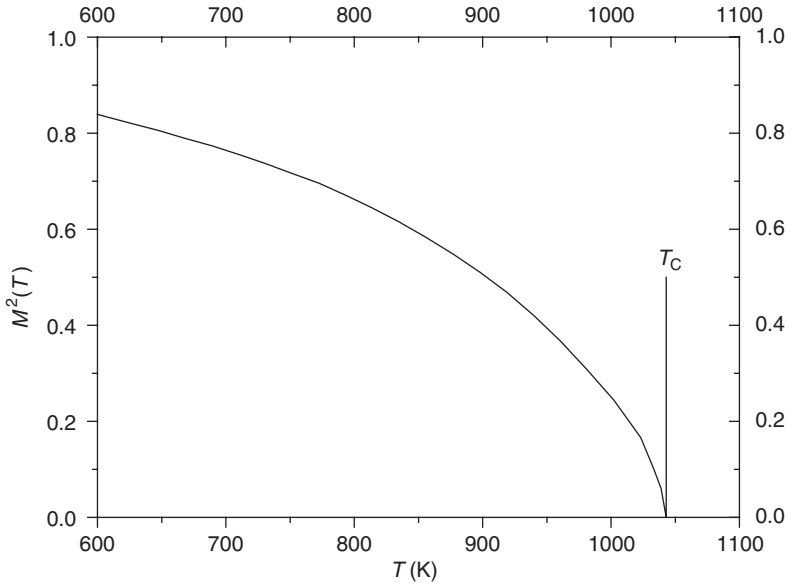

Fig. 02.03 Ratio of the spontaneous magnetization $M(T)$ for α-Fe. $M^2(T)$ in dependence of T (according to Ref. [02.16]).

The plot of $T \ln[D(T)/D_p^0]$ vs. $M^2(T)$ permits the determination of α and Q_p from slope and intercept of the linear function (see Figure 02.04). For self-diffusion in iron α is almost temperature independent [02.14], varies, however, from solute to solute [02.17, 02.18].

Further models for the interpretation of the diffusion anomaly around T_C are referred to in Chapter 8.

Self-diffusion in metals is comprehensively treated in numerous textbooks, e.g. [02.19–02.22] and review papers [02.01, 02.03, 02.24, 02.25].

Substitutionally dissolved impurities diffuse via the same mechanisms as the respective host atoms. The difference between the diffusivity of impurities and host atoms can be described by the electrostatic model (E-model) [02.26] and the thermodynamic model (T_m-model) [02.27]. In the E-model the difference of the activation energy of impurity diffusion and self-diffusion is proportional to the charge difference ΔZ of the atoms:

$$\Delta Q \sim -\Delta Z$$

whereas in the T_m-model ΔQ is described by the proportionality

$$\Delta Q \sim \left(\frac{T_{m2}}{T_{m0}} - 1\right)$$

where T_{m2} and T_{m0} are the melting temperatures of solute and solvent, respectively.

The E-model was applied to noble metals, Fe, Co, Ni, Zn and Cd. The T_m-model was applied to noble metals, Zn, substitutionally dissolved impurities

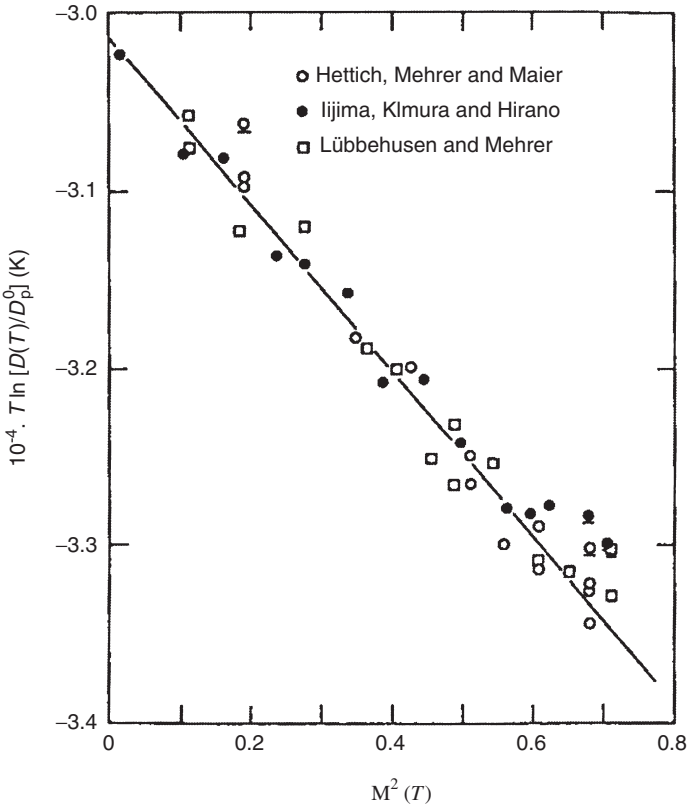

Fig. 02.04 Plot of $T \ln[D(T)/D_p^0]$ vs. $M^2(T)$ for self-diffusion in α_f-iron (from Ref. [02.17]).

in Pb and to refractory bcc metals. Impurity diffusion was comprehensively reviewed in Ref. [02.23].

In a number of host metals part of the impurities is interstitially dissolved. The diffusivity can be described by the "dissociative diffusion mechanism" [02.28], according to which D is given by

$$D = q_0 D_I + (1 - q_0 D_{1V}) \tag{02.22}$$

where q_0 is the fraction of interstitially dissolved solute atoms I

$$q_0 = \frac{c_I}{c_1 + c_I} \tag{02.23}$$

c_1 is the concentration of substitutionally dissolved solute atoms. The tendency to interstitial dissolution increases with decreasing radius of the solute atom [02.29] and decreasing solubility [02.30]. Accordingly, q_0 increases with decreasing solubility [02.31].

Interstitially dissolved impurities diffuse via a direct interstitial mechanism, which results in ultrafast diffusivities with small values of D^0 and Q. Especially 3d group solutes in Na, K, In, Tl, Sn, Pb, Sb (sp solvents), but also

in d group metals such as Nb, α-Ti, α-Zr, β-Zr diffuse via the interstitial mechanism.

Pressure and mass dependence of D, solubility and diffusion in dilute alloys permit conclusions with respect to the operating diffusion mechanisms.

Neglecting a small correction term, the pressure dependence of D is given by

$$\frac{\partial \ln D}{\partial p} \approx -\frac{\Delta V}{kT} \tag{02.24}$$

where ΔV is the activation volume of diffusion (in general expressed in fractions of the molar volume V_0) and p the hydrostatic pressure. In case of two mechanisms contributing to D, $\Delta V(T)$ results in

$$\Delta V(T) = \Delta V_1 \frac{D_1}{D} + \Delta V_2 \frac{D_2}{D} \tag{02.25}$$

The mass dependence of D (isotope effect E) is defined by [02.32]

$$E = \frac{(D_\alpha/D_\beta) - 1}{(m_\beta/m_\alpha)^{1/2} - 1} = f\Delta K \tag{02.26}$$

m_α and m_β are isotope masses and ΔK is the so-called kinetic energy factor. For two contributing diffusion mechanisms, E takes the form [02.33]

$$E(T) = f_1 \Delta K_1 \frac{D_1}{D} + f_2 \Delta K_2 \frac{D_2}{D} \tag{02.27}$$

For fcc metals ΔK is close to unity. $\Delta K_{1V} \approx \Delta K_{2V} \approx 1$ was obtained for noble metals [02.34].

In column 10 of the tables in Chapters 1–10 (''also studied'') the results of E, $\Delta V/V_0$ and solubility c_s are mentioned, also diffusion in alloys is referred to.

0.3. INSTRUCTIONS FOR THE USE OF THE TABLES

All credible self-diffusion and impurity diffusion data are listed in the tables, the most reliable of them are shown in figures. If for a special system no credible data are available, the existing data are tabulated with D^0 and Q in brackets.

The specification ''most reliable data'' differs from host to host. In noble metals diffusion coefficients with uncertainties less than 5% can be obtained by use of macrosectioning techniques. In most of the other metals different reasons lead to less accurate diffusion coefficients. The accuracy of D depends on the applied measuring technique (see Chapter 0.1) or on the attainable purity of the host. Oxygen impurities in V or Fe impurities in α-Zr and α-Ti, for example, strongly influence the diffusivity. Temperature measurements with the aid of optical pyrometry can lead to errors in D up to 20%. In high-melting refractory bcc metals errors up to a factor of two are observed (see Ref. [63.03]).

To present an almost complete data collection, further results (part of which is frequently cited in the literature and in earlier data collections) are listed in a

reference appendix. If not otherwise stated, radiotracer sectioning techniques were used in these measurements.

Not considered in the data collection are results of QMS (exception Fe in Sn), QNS and thermotransport investigations. QMS and QNS results are mentioned in the reference appendix. Also not considered are results where grain-boundary diffusion dominates nearly the entire temperature range under investigation. Furthermore, not considered are results of EPMA investigations, if D strongly depends on the alloy concentration X, so that a proper extrapolation to $X = 0$ is not possible. And, finally, volume diffusion coefficients derived from sintering or creeping investigations are not taken into consideration.

Abbreviations are listed at the end of this chapter.

The contents of the tables

Each table contains 13 columns, numbered 1–12 with column 2 splitted into 2a and 2b. The contents of the columns are as follows:

(1) Investigated solute X, starting with self-diffusion and followed by impurity diffusion in alphabetic order of the chemical sign of the solutes. If two or more phases of the solvent exist, the tabulated data start with the high-temperature phase, e.g. β-Ti, α-Ti or δ-Fe, γ-Fe, α-Fe

(2) D^0 in $10^{-4}\,m^2\,s^{-1}$ (a) and Q in eV and kJ (in brackets) (b)
Questionable results are put into brackets
[+]recalculated data
The evaluation of a curved Arrhenius plot is characterized by
[21]Two-exponential fit according to Eq. (02.07)
[22]Ω-fit according to Eq. (02.14), the fitting parameter Ω is listed in column 9
[23]α-fit according to Eq. (02.12), T_0 and the fitting parameter α are listed in column 9
[24]Fit according to Eq. (02.19), the fitting parameter α (value for $T < T_C$) is listed in column 9

(3) $D(T_m)$ in $10^{-12}\,m^2\,s^{-1}$ is extrapolated
Note that for the same data set $D(T_m)$ calculated from a two-exponential fit is larger than extrapolated from $D^0(\bar{T})$ and $Q(\bar{T})$
For low-temperature investigations or in the case of pronounced data scatter $D(T_m)$ is not extrapolated

(4) Investigated temperature range in K and $\bar{T}/T_m$ (in brackets)
As the Arrhenius plot is generally curved, in a forced fit D^0 and Q depend on the investigated temperature range, i.e. on $\bar{T}/T_m$

(5) The number of measured diffusion coefficients; in brackets the number of investigated temperatures, if more than one measurement per temperature was performed
[51]Diffusion coefficients not tabulated
[52]Diffusion coefficients not tabulated and not shown in a figure

(6) Material: single crystals (sc), polycrystals (pc), in brackets the average grain diameter if measured
Purity: e.g. 4N8 = 99.998%
[61]Purity not specified

(7) Measuring method
Radiotracer methods:

- radio isotope (e.g. ^{64}Cu)
- method of deposition: electroplated, vapor or sputter deposition, implanted, dried-on from a salt solution, chemical deposition (of noble metals)
- sectioning method: lathe, microtome, grinder, chemical and electrochemical sectioning, anodizing and stripping, ion beam sputtering (IBS), serial sectioning (if not exactly specified)

Further radiotracer methods:

- residual activity (in general grinder sectioning), absorption, autoradiography

Non-radioactive methods:

- deposited natural element
- electron probe microanalysis (EPMA)
  composition of the sample (e.g. Cu/Cu (X % Al), X % means X at %)
  method of evaluation, e.g. Boltzmann–Matano
- X-ray diffraction method
- resistometric measurement
- RBS or HIRBS
- SIMS analysis
- NMR, measurement of the relaxation times T_1, T_2, $T_{1\rho}$

Note that NMR measurements result in the uncorrelated diffusion coefficients (see Eq. (02.15))
[71]Radio isotope not specified
[72]Method of deposition not specified
[73]Sandwich samples

(8) As the penetration profiles (pp) permit important conclusions with respect to the quality of the measurements, the presented pp are described in some detail
Number of depicted pp: all, numerous, several, n examples, no
If not otherwise stated, the pp are Gaussian, i.e. linear in ln $c - x^2$
Non-Gaussian diffusion profiles and the respective evaluation are characterized in the following manner:
[81]erfc-solution according to Eq. (01.09)
[82]D evaluated from the middle part of the pp
[83]Short-circuit contributions eliminated according to Eq. (01.07)
[84]Marked NSE
[85]"negative" NSE (tracer loss due to evaporation)

[86]Malkovich solution
[87]"thick-film" solution

(9) Remarks on the quality of the measurements, e.g.:

- The Arrhenius plot exhibits marked scatter
- Grain-boundary or dislocation contributions at lower temperatures
- Erroneous thermal expansion corrections (see below)

Remarks on the evaluation of curved Arrhenius plots:

- two-exponential fit evaluated together with the data of the listed reference numbers
- fitting parameters Ω, α and T_0, α for the evaluations according to Eqs. (02.14), (02.12) and (02.19) respectively

Further general and individual remarks, e.g.
[+]Present reassessment of measured data
In a number of papers an erroneous expansion correction of D has been performed. D is proportional to a^2 (see Eq. (02.02)). The lattice constant increases with rising temperature. In the respective papers D evaluated at room temperature with $a(298\,\mathrm{K})$ was recalculated to $a(T)$. This "correction", however, is erroneous. D is proportional to the square of the average diffusion distance $<d>$

$$D \sim \frac{<d>^2}{t} = \frac{<n>^2 a^2}{t}$$

In a crystal lattice $<d>$ is proportional to the average number $<n>$ of nearest neighbour distances r_1 and lattice distances a passed during the annealing. This means that $<n(T)>$ is responsible for the amount of $D(T)$. $<n(T)>$ is measured at room temperature, where a is $a(298\,\mathrm{K})$. Thus, $D(T) \sim <n(T)>^2 a^2(298\,\mathrm{K})/t$ holds for $D(T)$.
The error introduced by this "correction" can be roughly estimated with the aid of the Grüneisen rule [03.01] according to which the volume of a metal increases by about 7% from absolute zero to T_m. Simply assuming a linear temperature dependence of a, then a^2 is $\sim$3.2% larger then a_0^2 at $T = 0.7\ T_\mathrm{m}$ and about 4.6% at $T = T_\mathrm{m}$. A recorrection of the erroneously calculated D_{85}^0 and Q_{85} shows that D_{85}^0 must be reduced by about 7% and Q_{85} by about 0.2%.
Note that the individual temperature dependence of a for a special solvent can somewhat differ from the rough approximation (see for example self-diffusion in Cu, Ref. [14.14]).

(10) Results of further investigations in the respective paper

- diffusion of further solutes in the same or another host metal
- isotope effect E (for a data collection, see Ref. [03.02])
- pressure dependence of D (reported is $\Delta V/V_0$, for a data collection, see Ref. [03.02])
- solubility c_s

Furthermore, it is referred to investigations on:

- diffusion in alloys (for a data collection, see Ref. [03.03])
- grain-boundary diffusion
- electrotransport, if the results are identical with D^0 and Q in columns 2a and 2b

(11) The most reliable data for the respective host are shown in a figure
(12) Reference: first author, year of appearance, reference number

LIST OF ABBREVIATIONS

bcc	body-centred cubic
dhcp	double hcp
E	isotope effect
EPMA	electron probe micro analysis
fcc	face-centred cubic
fct	face-centred tetragonal
gb	grain boundary
hcp	hexagonal close packed
HIRBS	heavy ion Rutherford backscattering
IBS	ion-beam sputtering
NMR	nuclear magnetic resonance
NRA	nuclear reaction analysis
NSE	near-surface effect
pc	polycrystals
PFG	pulsed magnetic field gradient
pp	penetration profile
QMS	quasi-elastic Mößbauer spectroscopy
QNS	quasi-elastic neutron scattering
RBS	Rutherford backscattering
sc	single crystals
SIMS	secondary-ion mass spectroscopy
SLRT	spin-lattice relaxation time
TEM	transmission electron microscopy
UHV	ultra-high vacuum

REFERENCES

References to Chapter 0

[00.01] A.M. Sagrubskij, Physikal. Z. Sowjetunion **12** (1937) 118.
[00.02] H.A. McKay, Trans. Faraday Soc. **34** (1938) 845.
[00.03] B.V. Rollin, Phys. Rev. **55** (1939) 231.

[00.04] J. Steigman, W. Shockley, F.C. Nix, Phys. Rev. **56** (1939) 13.
[00.05] W.A. Johnson, Trans. AIME **143** (1941) 107.
[00.06] P.H. Miller, R.R. Banks, Phys. Rev. **61** (1942) 648.
[00.07] *Diffusion in Solid Metals and Alloys*, Ed. H. Mehrer, Landolt-Börnstein, New Series III, Vol. **26**, Springer, Berlin (1990).
[00.08] H. Mehrer, N. Stolica, N.A. Stolwijk, Chapter 2, p. 32 in Ref. [00.07].
[00.09] A.D. Le Claire, G. Neumann, Chapter 3, p. 85 in Ref. [00.07].
[00.10] A.D. Le Claire, Chapter 8, p. 471 in Ref. [00.07].

References to Chapter 0.1

[01.01] *Methods of Experimental Physics* **21**, Solid State: Nuclear Methods, Eds. J.N. Mundy, S.J. Rothman, M.J. Fluss, L.C. Smedskjaer, Academic Press, Orlando (1983).
[01.02] S.J. Rothman, in: *Diffusion in Crystalline Solids*, Eds. G.E. Murch, A.S. Nowick, Academic Press, Orlando (1984), p. 1.
[01.03] *Nontraditional Methods in Diffusion*, Eds. G.E. Murch, H.K. Birnbaum, J.R. Cost, The Metallurgical Society of AIME, Warrendale (1984).
[01.04] H. Mehrer, in: *Diffusion in Solid Metals and Alloys*, Landolt-Börnstein, New Series III, Vol. **26**, Ed. H. Mehrer, Springer, Berlin (1990), Chapter 1, p. 1.
[01.05] J. Crank, *The Mathematics of Diffusion*, Oxford University Press (Clarendon), Oxford (1975).
[01.06] H.S. Carslaw, J.C. Jaeger, *Conduction of Heat in Solids*, Oxford University Press (Clarendon), Oxford (1959).
[01.07] C.T. Tomizuka, in: *Methods of Experimental Physics*, Vol. 6A, Eds. K. Lark-Horovitz, V.A. Johnson, Academic Press, New York (1959), p. 364.
[01.08] T.S. Lundy, in: *Techniques of Metals Research*, Vol. 4 (2), Ed. R.A. Rapp, Wiley, New York (1970), p. 379.
[01.09] P.G. Shewmon, *Diffusion in Solids*, McGraw-Hill, New York (1963), p. 31.
[01.10] J. Geise, Ch. Herzig, Z. Metallk. **76** (1985) 622.
[01.11] P.L. Gruzin, Dokl. Akad. Nauk SSSR **86** (1952) 289.
[01.12] D. Ablitzer, Phil. Mag. **35** (1977) 1239.
[01.13] J. Steigman, W. Shockley, F.C. Nix, Phys. Rev. **55** (1939) 605.
[01.14] A.A. Zhukhovitskii, V.A. Geodyakin, Zh. Fiz. Khim. **29** (1955) 1334.
[01.15] S.N. Kryukov, A.A. Zhukhovitskii, Dokl. Akad. Nauk SSSR **90** (1953) 379.
[01.16] H.C. Gatos, A. Azzam, Trans. AIME **191** (1952) 407.
[01.17] H.C. Gatos, A.D. Kurtz, Trans. AIME **200** (1954) 616; **203** (1955) 698.
[01.18] T.J. Renouf, Phil. Mag. **9** (1964) 781.
[01.19] D.L. Styris, C.T. Tomizuka, J. Appl. Phys. **34** (1963) 1001.
[01.20] R.E. Pawel, Rev. Sci. Instr. **35** (1964) 1066.
[01.21] R.E. Pawel, T.S. Lundy, J. Appl. Phys. **35** (1964) 435; J. Elektrochem. Soc. **115** (1968) 233.
[01.22] K. Maier, W. Schüle, Euratom Report EUR 5234d (1974).
[01.23] H. Mehrer, K. Maier, G. Hettich, H.J. Mayer, G. Rein, J. Nucl. Mater. **69/70** (1978) 545.
[01.24] M.P. Macht, V. Naundorf, J. Appl. Phys. **53** (1982) 7551.
[01.25] H. Mehrer, D. Weiler, Z. Metallk. **75** (1984) 203.
[01.26] M. Lübbehusen, H. Mehrer, Acta Metall. Mater. **38** (1990) 283.
[01.27] H.S. Levine, C.J. MacCallum, J. Appl. Phys. **31** (1960) 595.
[01.28] T. Suzuoka, Trans. Jpn. Inst. Met. **2** (1961) 25.
[01.29] N.Q. Lam, S.J. Rothman, H. Mehrer, J.L. Nowicki, Phys. Stat. Sol. (b) **57** (1973) 225.
[01.30] R. Hales, J. Phys. Chem. Sol. **32** (1971) 1417.
[01.31] D.L. Beke, I. Gödény, F.J. Kedves, Z. Metallk. **65** (1974) 382.
[01.32] T.S. Lundy, J.F. Murdock, J. Appl. Phys. **33** (1962) 1671.
[01.33] G.M. Hood, Phil. Mag. **21** (1970) 305.
[01.34] H. Mehrer, Phys. Stat. Sol. (a) **104** (1987) 247.
[01.35] J. Ladet, J. Bernardini, F. Cabané-Brouty, Scr. Metall. **10** (1976) 195.
[01.36] G. Neumann, M. Pfundstein, P. Reimers, Z. Phys. Chem. N.F. **106** (1977) 131.

[01.37] R.Sh. Malkovich, Fiz. Met. Metalloved. **15** (1963) 880.
[01.38] G. Neumann, M. Pfundstein, P. Reimers, Phys. Stat. Sol. (a) **64** (1981) 225.
[01.39] J.G. Mullen, Phys. Rev. **121** (1961) 1649.
[01.40] T.S. Lundy, R.A. Padgett, Trans. AIME **242** (1968) 1897.
[01.41] C.G. Lee, K.T. Youn, H.H. Cho, Y.I. Lee, D.S. Yoo, T. Shimozaki, Defect and Diffusion Forum **194–199** (2001) 109.
[01.42] P. Reimers, Phys. Stat. Sol. **22** (1967) K27.
[01.43] I.Sh. Trakhtenberg, Fiz. Met. Metalloved. **37** (1974) 348.
[01.44] W.E. Evenson, D.L. Decker, Phys. Rev. B **17** (1978) 583.
[01.45] G.J. Beyer, W.D. Fromm, A.F. Novgorodov, Nucl. Instrum. Met. **146** (1977) 419.
[01.46] F. de Keroulas, J. Mory, Y. Quéré, J. Nucl. Mater. **22** (1967) 276.
[01.47] S.M. Myers, in Ref. [01.03], p. 137.
[01.48] R.L. Fogelson, Fiz. Met. Metalloved. **25** (1968) 492.
[01.49] R.L. Fogelson, Ya.A. Ugay, A.V. Pokoyev, Fiz. Tverd. Tela **13** (1971) 1028.
[01.50] S. Ceresara, T. Federighi, F. Pieragostini, Phys. Stat. Sol. **16** (1966) 439.
[01.51] O. Kanert, Physics Reports **91** (1982) 183.
[01.52] H.T. Stokes, in Ref. [01.03], p. 39.
[01.53] P. Heitjans, A. Körblein, H. Ackermann, D. Dubbers, F. Fujara, H.J. Stöckmann, J. Phys. F: Met. Phys. **15** (1985) 41.
[01.54] A. Schirmer, P. Heitjans, G. Majer, A. Seeger, Defect and Diffusion Forum **143–147** (1997) 1317.
[01.55] H. Mehrer, J. Nucl. Mater. **69/70** (1978) 38.
[01.56] J.G. Mullen, in Ref. [01.03], p. 59.
[01.57] W. Petry, G. Vogl, Mater. Sci. Forum **15–18** (1987) 323.
[01.58] T. Springer, *Quasi-elastic Neutron Scattering for the Investigation of Diffusive Motions in Solids and Liquids*, Springer Tracts of Modern Physics, Vol. **64**, Springer, Berlin (1972).
[01.59] H. Zabel, in Ref. [01.03], p. 1.
[01.60] A. Heiming, K.H. Steinmetz, G. Vogl, Y. Yoshida, J. Phys. F: Met. Phys. **18** (1988) 1491.
[01.61] K.H. Steinmetz, G. Vogl, W. Petry, K. Schroeder, Phys. Rev. B **34** (1986) 107.
[01.62] Y. Yoshida, W. Miekeley, W. Petry, R. Stehr, K.H. Steinmetz, G. Vogl, Mater. Sci. Forum **15–18** (1987) 487.
[01.63] W. Petry, G. Vogl, A. Heidemann, K.H. Steinmetz, Phil. Mag. A **55** (1987) 183.
[01.64] L.S. Darken, Trans. AIME **175** (1948) 184.
[01.65] E.O. Kirkendall, Trans. AIME **147** (1942) 104.
[01.66] A.D. Smigelskas, E.O. Kirkendall, Trans. AIME **171** (1947) 130.
[01.67] J.R. Manning, *Diffusion Kinetics for Atoms in Crystals*, Van Nostrand, Princeton (1968).
[01.68] L. Boltzmann, Ann. der Physik und Chemie (NF) **53** (1894) 959.
[01.69] C. Matano, Jpn. J. Phys. **8** (1933) 109.
[01.70] F. Sauer, V. Freise, Z. Elektrochemie **66** (1962) 353.
[01.71] C. Wagner, Acta Metall. **17** (1969) 99.
[01.72] F.J.A. den Broeder, Scr. Metall. **3** (1969) 321.
[01.73] L.D. Hall, J. Chem. Phys. **21** (1953) 87.
[01.74] G. Grube, Z. Metallk. **19** (1927) 11, 438.
[01.75] H. Hagenschulte, Th. Heumann, J. Phys.: Cond. Matter **1** (1989) 3601.
[01.76] Y. Iijima, K. Hoshino, K. Hirano, Metall. Trans. **8A** (1977) 997.

References to Chapter 0.2

[02.01] A. Seeger, H. Mehrer, in: *Vacancies and Interstitials in Metals*, Eds. A. Seeger, D. Schumacher, W. Schilling, J. Diehl, North-Holland, Amsterdam (1970), p. 1.
[02.02] A.D. Le Claire, in: *Diffusion in Body-Centred Cubic Metals*, Eds. J.A. Wheeler, F.R. Winslow, American Society for Metals, Metals Park (1965), p. 3.
[02.03] H. Mehrer, J. Nucl. Mater. **69/70** (1978) 38.
[02.04] R.W. Siegel, J.N. Mundy, L.C. Smedskjaer, Mater. Sci. Forum **15–18** (1987) 451.
[02.05] G. Neumann, C. Tuijn, G. de Vries, H. Bakker, Phys. Stat. Sol. (b) **149** (1988) 483.

[02.06] G. Neumann, V. Tölle, Phil. Mag. A **61** (1990) 563.
[02.07] H.I. Aaronson, P.G. Shewmon, Acta Metall. **15** (1967) 385.
[02.08] Ch. Herzig, in: DIMETA 82, *Diffusion in Metals and Alloys*, Eds. F.J. Kedves, D.L. Beke, Trans. Tech. Publ., Aedermannsdorf, Switzerland (1983), p. 23.
[02.09] W. Petry, A. Heiming, Ch. Herzig, J. Trampenau, Defect and Diffusion Forum **75** (1991) 211.
[02.10] J.M. Sanchez, D. de Fontaine, Phys. Rev. Lett. **35** (1975) 227.
[02.11] G. Neumann, V. Tölle, C. Tuijn, Physica B **296** (2001) 334.
[02.12] U. Köhler, Ch. Herzig, Phil. Mag. A **58** (1988) 769.
[02.13] G. Neumann, V. Tölle, Z. Metallk. **82** (1991) 741.
[02.14] L. Ruch, D.R. Sain, H.L. Yeh, L.A. Girifalco, J. Phys. Chem. Sol. **37** (1976) 649.
[02.15] H.H. Potter, Proc. Roy. Soc. Lond. A **146** (1934) 362.
[02.16] J. Crangle, G.M. Goodman, Proc. Roy. Soc. Lond. A **321** (1971) 477.
[02.17] Y. Iijima, J. Phase Equilibria Diffusion **26** (2005) 466.
[02.18] H. Nitta, Y. Iijima, Phil. Mag. Lett. **85** (2005) 543.
[02.19] C.P. Flynn, *Point Defects and Diffusion*, Clarendon, Oxford (1972).
[02.20] P.G. Shewmon, *Diffusion in Solids*, 2nd ed., The Minerals, Metals and Materials Society, Warrendale (1989).
[02.21] J. Philibert, *Atom Movements, Diffusion and Mass Transport in Solids*, Les Editions de Physique North America, Cambridge (1991).
[02.22] Th. Heumann, H. Mehrer, *Diffusion in Metallen*, Springer, Berlin (1992).
[02.23] G. Neumann, C. Tuijn, *Impurity Diffusion in Metals*, Solid State Phenomena, Vol. **88**, Scitec Publ. Zürich, Switzerland (2002).
[02.24] N.L. Peterson, Sol. Stat. Phys. **22** (1968) 409.
[02.25] N.L. Peterson, J. Nucl. Mater. **69/70** (1978) 3.
[02.26] A.D. Le Claire, Phil. Mag. **7** (1962) 141; ibid. **10** (1964) 641.
[02.27] G. Neumann, W. Hirschwald, Phys. Stat. Sol. (b) **55** (1973) 99; Z. Phys. Chem. N.F. **89** (1974) 309.
[02.28] F.C. Frank, D. Turnbull, Phys. Rev. **104** (1956) 617.
[02.29] G. Hägg, Z. Phys. Chem. B **6** (1929) 221.
[02.30] G. Neumann, C. Tuijn, Physica B **315** (2002) 164.
[02.31] H.B. Vanfleet, Phys. Rev. B **21** (1980) 4340.
[02.32] J.G. Mullen, Phys. Rev. **121** (1961) 1649.
[02.33] H. Bakker, Phys. Stat. Sol. **34** (1969) K153.
[02.34] G. Neumann, V. Tölle, Phil. Mag. A **54** (1986) 619.

References to Chapter 0.3

[03.01] E. Grüneisen, Ann. Phys. 4. F. **33** (1910); 33, 65.
[03.02] H. Mehrer, N. Stolica, Chapter 10, p. 574 in Ref. [00.07].
[03.03] H. Bakker, Chapter 4, p. 213 in Ref. [00.07].

CHAPTER 1

Self-Diffusion and Impurity Diffusion in Group I Metals

Contents

Tables
1.1. Lithium (Li) 38
1.2. Sodium (Na) 42
1.3. Potassium (K) 44
1.4. Copper (Cu) 45
1.5. Silver (Ag) 54
1.6. Gold (Au) 60
Figures
Lithium 64
Sodium 68
Potassium 71
Copper 72
Silver 81
Gold 87
References 91

For **cesium** (Cs) and **francium** (Fr) no data are available. For **rubidium** (Rb) only self-diffusion was investigated by use of NMR (see Ref. [11.01]).

NMR measurements yield the D-values of uncorrelated diffusion. Because of the uncertainty of the high-temperature mechanism of self-diffusion in alkaline metals, D^0 is not corrected according to Eqs. (02.15) and (02.17).

Li and Na pass a martensitic phase transition at about 70 K, which leads to enhanced diffusivities at low temperatures (see Refs. [11.11, 12.06]).

Natural Li consists of 92.5% ^{7}Li and 7.5% ^{6}Li. No suitable radioisotopes are available. Self-diffusion in Li is mainly investigated by use of NMR techniques.

In Table 1.0 lattice structure, lattice constant and melting temperature of the group I metals are listed.

Table 1.0 Lattice structure, lattice constant a and melting temperature T_m

	Li	Na	K	Rb	Cu	Ag	Au
Structure	bcc	bcc	bcc	bcc	fcc	fcc	fcc
a (nm)	0.3510	0.4291	0.5225	0.5585	0.3615	0.4086	0.4078
T_m (K)	454	371	337	312	1,358	1,234	1,336

Table 1.1 Diffusion in lithium

(References, see page 91)

(1)	(2a)	(2b)	(3)	(4)	(5)	(6)	(7)	(8)	(9)	(10)	(11)	(12)
X	D^0 (10^{-4} m^2 s^{-1})	Q(eV) and (kJ mole^{-1})	$D(T_m)$ (10^{-12} m^2 s^{-1})	T-range (K) ($\overline{T}/T_m$)	No. of datapoints	Material, purity	Experimental method	Remarks on the pp	Further remarks	Also studied	Figure	Reference
Self-diffusion												
Li	0.24	0.572 (55.3)	10.6	300–453 (0.83)	[52]	pc (12 μm)	^{7}Li (stable isotope); NMR (SLRT T_1 and T_2)	–		Na, Rb (NMR), D^0(Rb) ≈ 0.23 × 10^{-4} m^2 s^{-1}, Q = 0.41 eV	–	Holcomb (1955) [11.01]
Li	0.39	0.585 (56.5)	12.5	343–443 (0.87)	19 (9T)	pc 2N8	^{6}Li, diffusion couple; microtome (200 μm sections)	1 example[81] (c–x)			–	Naumov (1959) [11.02]
Li	–	0.519 (50.1)		190–240 (0.47)	24[51]	pc (30 μm) 3N8	^{7}Li (stable isotope); NMR (SLRT $T_{1\rho}$)	–			11.01	Ailion (1965) [11.03]
Li	0.120*	0.548* (52.9)	9.9	309–451 (0.84)	19	pc[61]	^{7}Li in nearly pure ^{6}Li and ^{6}Li in nearly pure ^{7}Li; microtome, mass spectroscopy	4 examples	* ^{7}Li in ^{6}Li 0 ^{6}Li in ^{7}Li × ^{7}Li in ^{7}Li (calculated)		11.02	Lodding (1970) [11.04]
	0.123^0	0.557^0 (53.8)	8.0	309–449 (0.84)	12							
	0.14^x	0.558^x (53.9)	8.9									
Li	–	0.489 (47.2)		223–273 (0.56)	(14)[51]	pc (15 μm) 3N8	^{7}Li (stable isotope); NMR (SLRT $T_{1\rho}$)	–			11.01	Weithase (1973) [11.05]
Li	0.133	0.546 (52.8)	11.4	310–453 (0.84)	26[51]	pc[61]	^{7}Li (stable isotope); NMR (SLRT T_1)	–			11.01	Messer (1975) [11.06]
	0.038^{21}	0.520^{21} (50.2)	25	190–453	(64)				Two-exponential fit together with the data of [11.03,11.05]			
	9.5^{21}	0.694^{21} (67.0)										
Li	0.06^{21}	0.520^{21} (50.2)	39	195–450 (0.71)			^{7}Li (stable isotope); NMR (SLRT T_1 and $T_{1\rho}$)	–	See Ref. [11.06]		–	Messer (1976) [11.07]
	28.8^{21}	0.720^{21} (69.5)										

Li	0.32 0.19[21] 95[21]	0.57 (55) 0.556[21] (53.7) 0.796[21] (76.9)	15 26	225–454 (0.75)	~80[51]	pc[61]	^{8}Li; β-NMR, spin-lattice relaxation of polarized ^{8}Li, using asymmetric β-decay	–			–	Heitjans (1985) [11.08]
Li	0.161[(a)] 0.168[(b)] 0.151[(c)] 0.180[(d)] 0.154[(e)]	0.561* (54.2)	9.5 9.9 8.9 10.6 9.1	350–454 (0.89)	~50[51]	pc 3N	^{7}Li, ^{6}Li (stable isotopes) in natural Li and enriched ^{7}Li and ^{6}Li; NMR (PFG)	–	*Average [(a)] ^{7}Li, [(c)] ^{6}Li in natural Li, [(b)] ^{7}Li, [(d)] ^{6}Li in Li (95.5% ^{6}Li), [(e)] ^{7}Li in ^{7}Li		–	Mali (1988) [11.09]
Li	0.31 0.31^{+} (0.036)[21] 0.042^{+} 0.648[21]	(0.58) (56.0) 0.584^{+} (56.4) 0.52[21] (50.2) 0.67[21] (64.7)	10.2^{+} 9.4^{+}	360–450 (0.89)	13[51]	pc[61] (15 μm foil)	^{7}Li (stable isotope); NMR (PFG)	–	$^{+}$Present fit to the experimental data		11.02	Messer (1989) [11.10]
Li	–	–		90–300 (0.43)	14[51]	pc[61] (>5 μm)	^{7}Li, ^{6}Li (stable isotopes) in ^{6}Li and ^{7}Li, vapour deposition; elastic recoil detection analysis	No[83]	Enhanced low-temperature diffusivity, possibly caused by the martensitic phase transition near 70 K		–	Wieland (2001) [11.11]
Impurity diffusion												
Ag	0.37	0.556 (53.7)	25	340–433 (0.85)	7	pc (5 mm)3N8	^{110}Ag, vapour deposition of ^{110}AgCl; microtome	No	Probably curved ln c–x^{2} plots (see [11.13])		–	Ott (1968) [11.12]
Ag	0.54	0.556 (53.7)	36	323–423 (0.82)	5 (3T)	pc 3N8	^{110}Ag, ^{105}Ag, electroplated; microtome	2 examples		E(423 K) = 0.26; Na in Li	11.03	Mundy (1973) [11.13]
Au	0.141* 0.100[x] 0.085* 0.24*	0.465* (44.9) 0.448[x] (43.2) 0.444* (42.8) 0.482* (46.5)	97 106 107	301–450[(1)] (0.83) 301–441[(1)] (0.82) 301–363[(2)] (0.73) 363–450[(2)] (0.90)	29 (20T)	pc 3N8	^{195}Au, vapour deposition; microtome	No	* Au in natural Li [x]Au in Li (95% ^{6}Li) [(1)]Forced fit [(2)]Two linear branches		11.03	Ott (1971) [11.14]

Table 1.1 *(Continued)*

(1)	(2a)	(2b)	(3)	(4)	(5)	(6)	(7)	(8)	(9)	(10)	(11)	(12)
X	D^0 (10^{-4} m^2 s^{-1})	Q(eV) and (kJ mole^{-1})	$D(T_m)$ (10^{-12} m^2 s^{-1})	T-range (K) ($\overline{T}/T_m$)	No. of datapoints	Material, purity	Experimental method	Remarks on the pp	Further remarks	Also studied	Figure	Reference
Bi	5.3×10^{14}*	2.051 (198.0)	0.89	414–450 (0.95)	6	pc 3N5	Bi^{71}, vapour deposition; microtome (100 μm sections)	No (linear in ln c–x^2)	*Corrected value	Pb, Sb, Sn in Li	11.04	Ott (1969) [11.15]
Cd	(0.62)	(0.650) (62.8)	(3.7)	355–449 (0.89)	12 (11T)	pc 3N8	^{115}Cd, vapour deposition; microtome	No	Numerous data in the table are erroneous	Ga, Hg, in Li	11.05	Ott (1970) [11.16]
	2.6$^+$	0.702$^+$ (67.8)	4.2$^+$						$^+$Present fit to the experimental data			
Cu	(0.3) 0.23$^+$	0.434 (41.9)	350$^+$	363–421 (0.86)	5	pc 3N5	^{64}Cu, ^{67}Cu, vapour deposition; microtome	2 examples[86]	$^+$Present fit to the experimental data	$E(420\,\mathrm{K}) = 0.11$; $c_s < 5 \times 10^{-5}$	11.03	Mundy (1973) [11.17]
Ga	(0.21)	(0.560) (54.1)		390–446 (0.92)	5	pc 3N8	^{72}Ga, vapour deposition; microtome	No	$^+$Present fit to the experimental data	Cd, Hg in Li	11.06	Ott (1970) [11.16]
	0.53$^+$	0.593$^+$ (57.3)	13.8$^+$									
Hg	(1.04)	(0.615) (59.4)		331–447 (0.86)	10	pc 3N8	^{203}Hg, vapour deposition; microtome	No	$^+$Present fit to the experimental data	Cd, Ga, in Li	11.07	Ott (1970) [11.16]
	1.43$^+$	0.624$^+$ (60.2)	16.8$^+$									
In	0.39	0.688 (66.4)	0.89	349–445 (0.87)	7	pc 3N5	^{114}In, vapour deposition; microtome	No			11.04	Ott (1968) [11.18]

Na	0.41	0.547 (52.8)	35	326–449 (0.85)	7	pc (5 mm) 3N8	^{22}Na, isotope exchange with ^{22}NaCl; microtome	No			11.07	Mundy (1967) [11.19]
Na	–	–		423	3	pc 3N8	^{22}Na, ^{24}Na, vapour deposition; microtome	2 examples		E(423 K) = 0.19; Ag in Li	11.07	Mundy (1973) [11.13]
Pb	1.6×10^{4}*	1.093 (105.5)	1.2	402–442 (0.93)	7	pc 3N5	Pb^{71}, vapour deposition; microtome (100 μm sections)	No (linear in ln c–x^2)	*Corrected value	Bi, Sb, Sn in Li	11.04	Ott (1969) [11.15]
Sb	1.6×10^{12}*	1.80 (173.8)	1.7	414–449 (0.95)	4	pc 3N5	Sb^{71}, vapour deposition; microtome (100 μm sections)	No (linear in ln c–x^2)	*Corrected value	Bi, Pb, Sn in Li	–	Ott (1969) [11.15]
Sn	(0.62) 0.85^{+}	(0.650) (62.8) 0.694^{+} (67.0)	1.7^{+}	381–447 (0.91)	7	pc 3N5	^{113}Sn, vapour deposition; microtome (100 μm sections)	No (linear in ln c–x^2)	$^{+}$Present approximation	Bi, Pb, Sb in Li	11.05	Ott (1969) [11.15]
Zn	0.57	0.563 (54.3)	32	331–445 (0.85)	10	pc 3N8	^{65}Zn, vapour deposition; microtome (20–100 μm sections)	3 examples			11.06	Mundy (1969) [11.20]

Table 1.2 Diffusion in sodium (References, see page 92)

(1)	(2a)	(2b)	(3)	(4)	(5)	(6)	(7)	(8)	(9)	(10)	(11)	(12)
X	D^0 (10^{-4} m^2 s^{-1})	Q(eV) and (kJ mole^{-1})	$D(T_m)$ (10^{-12} m^2 s^{-1})	T-range (K) ($\overline{T}/T_m$)	No. of data points	Material, purity	Experimental method	Remarks on the pp	Further remarks	Also studied	Figure	Reference
Self-diffusion												
Na	0.242	0.453 (43.8)	16.8	274–367 (0.86)	6 (5T)	pc[61]	^{22}Na, isotope exchange with ^{22}NaCl; microtome (50 μm sections)	2 examples (c–x)	Sharp increase of D close to T_m		12.01	Nachtrieb (1952) [12.01]
Na	0.20	0.434 (41.9)	25.6	~220–370 (0.80)	[52]	pc (12 μm) 3N5	^{23}Na (stable isotope); NMR (SLRT T_1 and T_2)	–		Li, Rb (NMR), D^0(Rb) ≈ 0.23 10^{-4} m^2 s^{-1} Q ≈ 0.41 eV	–	Holcomb (1955) [12.02]
Na	0.145*	0.438* (42.2)	16.4*	273–370* (0.87)	15 (14T)	pc 5N5	^{22}Na, ^{24}Na isotope exchange with ^{22}NaCl and $^{24}Na_2CO_3$; microtome (100 μm sections)	1 example (3 examples in [12.14])	*Results given in the precursor [12.14] ^{x}Number of considered data in the two-exponential fit	E = 0.39–0.24 (248–370 K); $\Delta V/V_0$ = 0.4–0.5	12.01	Mundy (1971) [12.03]
	0.0057[21]	0.370[21] (35.7)	17.4	195–370 (0.76)	29 (27T)							
	0.72[21]	0.499[21] (48.1)			26[x]							
Na	0.004[21]	0.372[21] (35.9)	(79)	150–280 (0.60)	[52]	pc ultrapure	^{23}Na (stable isotope); NMR (SLRT T_1 and $T_{1\rho}$)	–			–	Brünger (1980) [12.04]
	(2.6[21])	0.481[21] (46.4)										
Na	0.0064[21]	0.372[21] (35.9)	17.5	(195–370)	(26)				Two-exponential fit of the data of [12.03]		12.01	Neumann (1990) [12.05]
	0.81[21]	0.503[21] (48.6)										
Na	0.02	0.391 (37.7)	17.5	115–205 (0.43)	10	pc 5N5	^{24}Na, implanted; IBS	No	Enhanced low-temperature diffusivity, possibly caused by the martensitic phase transition at 70 K. Three-exponential fit together with the data of [12.03]		12.01	Neumann (1997) [12.06]
	8.4	0.591 (57.0)										
	1.2×10^{-15}	0.086 (8.3)										

Impurity diffusion												
Ag	0.02	0.22 (21.2)		297–351 (0.87)	5^{51}	pc 3N5	$^{110}Ag^{72}$; microtome	No	$^{+}$Present fit to the depicted data	Cd, In, Li, Sn, Tl in Na	12.02	Barr (1983) [12.07]
	0.04^{+}	0.25^{+} (24.1)	$1{,}600^{+}$	313–351 (0.89)	4							
Au	3.34×10^{-4}	0.096 (9.25)	1,670	274–350 (0.84)	8	pc 3N5	^{198}Au, vapour deposition; microtome	1 example[81] (c–x)		$c_s = 540 \cdot \exp(-0.49\,\text{eV}/kT)$	12.02	Barr (1969) [12.08]
Cd	(0.369) 0.32^{+}	0.42 (40.6)	63^{+}	273–364 (0.86)	6^{51}	pc 3N5	$^{115}Cd^{72}$; microtome	No	$^{+}$Present fit to the depicted data	Ag, In, Li, Sn, Tl in Na	12.03	Barr (1983) [12.07]
In	(1.79) 2.12^{+}	0.51 (49.2)	25^{+}	293–362 (0.88)	8^{51}	pc 3N5	$^{114}In^{72}$; microtome	No	$^{+}$Present fit to the depicted data	Ag, Cd, Li, Sn, Tl in Na	12.04	Barr (1983) [12.07]
K	0.08	0.366 (35.3)	86	273–364 (0.86)	6	pc 3N5	^{42}K, isotope exchange with ^{42}KCl; microtome (100 µm sections)	1 example		Rb in Na, Na in K	12.05	Barr (1967) [12.09]
Li	1.8	0.507 (49.0)	23	291–358 (0.87)	7^{51}	pc[61]	^{6}Li, enriched to 90%, diffusion couple; mass spectrometry	No[81]		Solubility of Li in Na	12.05	Naumov (1964) [12.10]
Rb	0.15	0.368 (35.5)	150	272–358 (0.85)	9	pc 3N5	^{86}Rb, isotope exchange with ^{86}RbCl; microtome (100 µm sections)	1 example		K in Na, Na in K	12.05	Barr (1967) [12.09]
Sn	(0.54) 0.68^{+}	0.46 (44.4)	38^{+}	316–363 (0.92)	6	pc 3N5	$^{113}Sn^{72}$; microtome	No	$^{+}$Present fit to the experimental data	Ag, Cd, In, Li, Tl in Na	12.03	Barr (1983) [12.07]
Tl	0.52	0.44 (42.5)	55	297–356 (0.88)	5	pc 3N5	$^{204}Tl^{72}$; microtome	No		Ag, Cd, In, Li, Sn in Na	12.04	Barr (1983) [12.07]

Table 1.3 Self-diffusion and impurity diffusion in potassium (References see page 92)

(1)	(2a)	(2b)	(3)	(4)	(5)	(6)	(7)	(8)	(9)	(10)	(11)	(12)
X	$D^0(10^{-4}\,m^2\,s^{-1})$	Q(eV) and (kJ mole^{-1})	$D(T_m)$ ($10^{-12}\,m^2\,s^{-1}$)	T-range (K) ($\overline{T}/T_m$)	No. of data points	Material, purity	Experimental method	Remarks on the pp	Further remarks	Also studied	Figure	Reference
K	0.31	0.423 (40.8)	14.7	273–333 (0.90)	6	pc 3N5	^{42}K, vapour deposition of ^{42}KCl; microtome (~150 µm sections)	3 examples			13.01	Mundy (1967) [13.01]
K	0.16	0.406 (39.2)	13.6	221–335 (0.82)	13 (12T)	pc 3N7	^{42}K, vapour deposition of ^{42}KCl; microtome (50–100 µm sections)	3 examples			13.01	Mundy (1971) [13.02]
	0.05[21]	0.386[21] (37.2)	13.7									
	1.0[21]	0.487[21] (47.0)										
Au	1.29×10^{-3}	0.14 (13.5)	1,040	279–326 (0.90)	5	pc 3N5	^{198}Au, vapour deposition; microtome	No (erfc-solutions)		$c_s = 22 \cdot \exp(-0.338\,eV/kT)$	13.02	Smith (1970) [13.03]
Na	0.058	0.323 (31.2)	85	273–335 (0.90)	7	pc 3N5	^{22}Na, vapour deposition of ^{22}NaCl; microtome (100 µm sections)	1 example		K, Rb in Na	13.02	Barr (1967) [13.04]
Rb	0.090	0.381 (36.8)	18	273–333 (0.90)	6	pc 3N5	^{86}Rb, vapour deposition of ^{86}RbCl; microtome	No			13.02	Smith (1969) [13.05]

Table 1.4 Diffusion in copper

(References see page 93)

(1)	(2a)	(2b)	(3)	(4)	(5)	(6)	(7)	(8)	(9)	(10)	(11)	(12)
X	D^0 (10^{-4} m^2 s^{-1})	Q(eV) and (kJ mole^{-1})	$D(T_m)$ (10^{-12} m^2 s^{-1})	T-range (K) ($\overline{T}/T_m$)	No. of data points	Material, purity	Experimental method	Remarks on the pp	Further remarks	Also studied	Figure	Reference
Self-diffusion												
Cu	0.20	2.043 (197.3)	0.52	993–1,336 (0.86)	8	sc 4N	^{64}Cu, electroplated; lathe and grinder	All[85] scattering pp for grinder sectioning			–	Kuper (1954) [14.01]
Cu	0.33	2.090 (201.8)	0.57	1,136–1,330 (0.91)	6	pc (1–4 mm) >4N	^{64}Cu; lathe (40 μm sections)	1 example		Ni in Cu, Cu in Ni; Cu in Cu(Ni)	–	Monma (1964) [14.02]
Cu	0.19	2.034 (196.4)	0.53	973–1,263 (0.82)	7	sc[61]	^{64}Cu, vapour deposition; grinder (abrasive paper)	1 example		Au in Au, Al in Al; $\Delta V/V_0 = 0.91$	–	Beyeler (1968) [14.03]
Cu	0.78	2.190 (211.4)	0.58	971–1,334 (0.85)	18 (14T)	sc 5N	^{64}Cu, ^{67}Cu, electroplated; lathe	Numerous examples		$E = 0.68$ (1,168–1,334 K)	14.01	Rothman (1969) [14.04]
Cu	0.11	1.966 (190.1)	0.54	1,003–1,163 (0.80)		pc powder (<8 μm) 5N	^{63}Cu, ^{65}Cu (stable isotopes) NMR (SLRT T_1 and T_2)	–			–	El-Hanany (1969) [14.05]
	0.15	1.999 (193.0)	0.57	1,003–1,123 (0.78)								
Cu	0.31	2.082 (201.0)		663–833 (0.55)	5	pc (foil) 5N	Cu; void shrinkage (TEM)	–			–	Bowden (1969) [14.06]
Cu	0.43	2.103 (203.1)	0.67	1,073–1,313 (0.88)	23 (11T)	pc (2–3 mm) 4N	^{64}Cu, electroplated; residual activity; grinder (abrasive paper)	Some examples (c/c_0–x)		Cu in Cu(Ni)	–	Kučera (1970) [14.07]
Cu	0.30	2.095 (202.2)	0.50	1,013–1,318 (0.86)	8	pc 5N	^{67}Cu, electroplated; lathe	Several examples (for alloy diffusion)		Ni, Zn in Cu; Cu, Ni, Zn in Cu(Ni), Cu(Zn)	–	Anusavice (1972) [14.08]
Cu	–	–		614–654 (0.47)	3	sc 5N	^{67}Cu, electroplated; anodizing and stripping	All [83]			14.01	Lam (1974) [14.09]

Table 1.4 *(Continued)*

(1)	(2a)	(2b)	(3)	(4)	(5)	(6)	(7)	(8)	(9)	(10)	(11)	(12)
X	D^0 (10^{-4} m^2 s^{-1})	Q(eV) and (kJ mole^{-1})	$D(T_m)$ (10^{-12} m^2 s^{-1})	T-range (K) ($\overline{T}/T_m$)	No. of data points	Material, purity	Experimental method	Remarks on the pp	Further remarks	Also studied	Figure	Reference
Cu	(1.05)* 0.81	2.18 (210.5)	0.65	845–1,111 (0.72)	11	pc powder (3–30 μm) 4N	^{63}Cu(stable isotope) NMR (SLRT $T_{1\rho}$)	–	*D^0 holds for uncorrelated diffusion (see Eq. (02.15))		–	Weithase (1974) [14.10]
Cu	– 0.10[21] 2.0[21]	2.08 (200.8) 2.04[21] (197.0) 2.42[21] (233.7)	 0.48	574–905 (0.54) (632–1,334)	19 (33)	sc 5N	^{64}Cu, sputter deposition; IBS	All	Two-exponential fit together with the data of [14.04] (omitting 4 D at $T<630$ K)		14.01	Maier (1977) [14.11]
Cu	– 0.13[21] 4.6[21]	– 2.054[21] (198.3) 2.472[21] (238.7)	 0.63	1,010–1.352 (0.87) (614–1,352)	16 (9T) (51)	sc 4N7	^{64}Cu, electroplated; microtome	All	Two-exponential fit together with the data of [14.04,14.09, 14.11]		14.01	Bartdorff (1978) [14.12]
Cu	0.68 0.15[21] 4.8[21]	2.17 (209.5) 2.06[21] (198.9) 2.48[21] (239.5)	0.60 0.64	1,078–1,348 (0.89) (632–1,348)	15 (14T) (30)	pc (>2 mm) 5N	^{64}Cu, electroplated; microtome	All	Erroneous thermal expansion correction; two-exponential fit together with the data of [14.11]		–	Krautheim (1979) [14.13]
Cu	(0.877) 0.748*	(2.19) (211.4) 2.18* (210.5)	(0.65) 0.60*	992–1,355 (0.86) 992–1,353 (0.86)	67 (24T) 66 (23T)	pc (5 mm) 5N7	^{67}Cu, electroplated; microtome	All	Erroneous thermal expansion correction *Recalculated after revoking the erroneous thermal expansion corrections		14.01	Fujikawa (1982) [14.14]

Cu	– (0.28)$^{+}$	– (2.08)$^{+}$ (200.8)	(0.53)$^{+}$	980–1,351 (0.86)	15	sc 6N	^{61}Cu, ^{64}Cu, ^{67}Cu, electroplated; microtome	Several examples	$^{+}$Present approximation	$E = 0.54-0.74$ (1,351–1,220 K)	–	Ushino (1989) [14.15]
Impurity diffusion												
Ag	0.63	2.016 (194.7)	2.1	(1,053–1,353) (0.89)	[52]	sc specpure	^{110}Ag; electroplated; lathe	No		Ag, Au, Cd, Ga, Hg in Cu	–	Nachtrieb (1960) [14.16]
Ag	0.61	2.016 (194.7)	2.0	(823–1,273) (0.77)	17[51]	pc, sc 4N	^{110}Ag; electroplated; residual activity	No			–	Barreau (1970) [14.17]
Ag	0.574	2.020 (195.0)	1.8	1,049–1,352 (0.88)	13	sc, pc 4N	^{110}Ag; electroplated; lathe and residual activity	All		Cd, In in Cu	14.02	Gorbachev (1972) [14.18]
Ag	1.25	2.095 (202.3)	2.1	1,033–1,355 (0.88)	13	pc (>2 mm) 5N	^{110}Ag, electroplated; microtome	Several examples	Erroneous thermal expansion correction		14.02	Krautheim (1978) [14.19]
Al	0.131	1.918 (185.2)	1.0	(986–1,270) (0.83)	10[51]	pc 4N	Al; EPMA Cu/Cu (14.7 at% Al), (Boltzmann–Matano)	No	$\tilde{D}$ extrapolated to $c_{Al} = 0$		14.02	Oikawa (1970) [14.20]
Al	0.08	1.878 (181.3)	0.86	973–1,348 (0.85)	7	pc[61]	Al; X-ray diffraction method	–			14.02	Fogelson (1973) [14.21]
As	0.12	1.821 (175.8)	2.1	(1,053-1,353) (0.89)	[52]	sc specpure	^{76}As, electroplated; lathe	No		Ag, Au, Cd, Ga, Hg in Cu	–	Nachtrieb (1960) [14.16]
As	0.202	1.827 (176.4)	3.3	1,086–1,348 (0.90)	7	pc 4N	^{76}As, dried-on from salt solution; lathe and residual activity	All			14.02	Klotsman (1970) [14.22]
Au	0.104	1.984 (191.6)		625–776 (0.52)	7 (6T)	pc 5N	Au, electroplated; RBS	No			14.04	Sippel (1959) [14.23]
Au	0.69	2.181 (210.6)	0.55	(1,053–1,353) (0.89)	[52]	sc specpure	^{198}Au, electroplated; lathe	No		Ag, As, Cd, Ga, Hg in Cu	–	Nachtrieb (1960) [14.16]
Au	0.897	2.201 (212.5)	0.61	1,085–1,342 (0.89)	8	sc 4N	^{195}Au, dried-on from salt solution; lathe	All		Bi, Pb in Cu	14.04	Gorbachev (1977) [14.24]
Au	0.537	2.13 (205.7)	0.67	933–1,350 (0.84)	34 (22T)	sc 5N	^{196}Au, electroplated; microtome	Numerous examples			14.04	Fujikawa (1987) [14.25, 14.26]
Au	0.0803	1.98 (191.2)		633–982 (0.59)	29 (22T)	sc 5N	^{196}Au, vapour deposition; IBS	Numerous examples			14.04	Fujikawa (1987, 1988) [14.26, 14.27]

Table 1.4 *(Continued)*

(1)	(2a)	(2b)	(3)	(4)	(5)	(6)	(7)	(8)	(9)	(10)	(11)	(12)
X	D^0 (10^{-4} m^2 s^{-1})	Q(eV) and (kJ mole^{-1})	$D(T_m)$ (10^{-12} m^2 s^{-1})	T-range (K) ($\overline{T}/T_m$)	No. of data points	Material, purity	Experimental method	Remarks on the pp	Further remarks	Also studied	Figure	Reference
Be	0.66	2.029 (195.9)	1.9	973–1,348 (0.85)	9	pc[61]	Au; X-ray diffraction method	–		Si in Cu	14.04	Fogelson (1973) [14.28]
Be	0.28	1.97 (190.2)		583–800 (0.51)	19 (18T)	sc 5N	Be, sputter deposition; IBS, SIMS analysis	All	Two-exponential fit together with the data of [14.28]		14.04	Almazouzi (1992) [14.29]
	0.164[21]	1.94[21] (187.3)	2.1	(583–1,348)	(28)							
	7.1[21]	2.38[21] (229.8)										
Bi	0.766	1.844 (178.1)	10.9	1,074–1,349 (0.89)	8	sc 5N	^{207}Bi, dried-on from salt solution; lathe	All		Au, Pb in Cu	14.03	Gorbachev (1977) [14.24]
Cd	0.935	1.982 (191.3)	4.1	998–1,223 (0.82)	8	sc 3N8	^{115}Cd[72]; lathe (20 μm sections)	All			14.03	Hirone (1958) [14.30]
Cd	0.73	1.956 (188.8)	4.0	(1,053–1,353) (0.89)	[52]	sc specpure	^{115}Cd; lathe	No		Ag, As, Au, Ga, Hg in Cu	–	Nachtrieb (1960) [14.16]
Cd	1.27	2.016 (194.6)	4.2	1,032–1,346 (0.88)	8	sc 4N	^{109}Cd, electroplated; lathe	All		Ag, In in Cu	14.03	Gorbachev (1972) [14.18]
Cd	1.2	2.009 (194)	4.2	983–1,309 (0.84)	8	pc (2–4 mm) 4N8	^{109}Cd, ^{115}Cd, dried-on from salt solution; grinder	Several examples		$E = 0.13–0.33$ (983–1,309 K); Cu in Cu(Cd) at 1,076 K	14.03	Hoshino (1982) [14.31]
Co	1.3$^+$	2.302$^+$ (222.3)	0.37$^+$	974–1,351 (0.86)	8 (7T)	sc 4N8	^{60}Co, electroplated; lathe	1 example	$^+$Present recalculation	Fe, Ni in Cu, Mn in Cu at $T = 1,342$ K	14.05	Mackliet (1958) [14.32]
	1.93	2.436 (235.2)	0.38	1,177–1,351 (0.93)	4 (3T)							
Co	0.43	2.22 (214.4)		640–848 (0.55)	17 (15 T)	sc 5N	^{60}Co, ^{59}Co, sputter deposition; IBS, γ-counting and SIMS analysis	Several examples			14.05	Döhl (1984) [14.33]
Co	0.74[21]	2.250[21] (217.2)	0.40	(640–1,351)	(24)				Two-exponential fit of the data of [14.32, 14.33]		14.05	Neumann (1988) [14.34]
	736[21]	3.240[21] (312.8)										
Cr	0.337	2.020 (195)	1.1	999–1,338 (0.86)	16 (15T)	pc 4N8	^{51}Cr, dried-on from salt solution; residual activity	2 examples, (anomalous pp[82])		Mn, V in Cu	14.05	Hoshino (1977) [14.35]

Cr	–	–		1,195–1,202 (0.88)	4	sc 5N	^{51}Cr; microtome	All	Simultaneous measurement of Cr, Mn, Zn in a multichannel analyzer; $D(1{,}200\,\mathrm{K}) = 1.4 \times 10^{-13}\,\mathrm{m^2\,s^{-1}}$	Mn, Zn in Cu	14.05	Rockosch (1983) [14.36]
Cr	0.26	1.99 (192.1)		639–829 (0.54)	15 (12T)	sc 5N	Cr, sputter deposition[73]; IBS, SIMS analysis	All (ln c–x)[81]		Mn, Ti in Cu	14.05	Almazouzi (1998) [14.37]
Fe	–	–		992–1,347	8 (6T)	sc 4N8	^{59}Fe, electroplated; lathe	2 examples		Co, Ni in Cu, Mn in Cu at $T = 1{,}342\,\mathrm{K}$	14.08	Mackliet (1958) [14.32]
	1.4	2.246 (216.9)	0.64	1,168–1,347 (0.93)	4 (3T)							
Fe	1.01	2.209 (213.3)	0.63	990–1,329 (0.85)	6 (4T)	sc 4N8	^{59}Fe, ^{55}Fe, electroplated; lathe	All		$E = 0.59$–0.74 (990–1,329 K)	14.08	Mullen (1961) [14.38]
Fe	1.36	2.255 (217.7)	0.58	923–1,343 (0.83)	9	sc, pc 4N5	^{59}Fe, electroplated; residual activity	No		Cr in Cu	–	Barreau (1971) [14.39]
Fe	1.3	2.233 (215.6)	0.67	1,005–1,297 (0.85)	6[51]	sc 5N	^{59}Fe, electroplated; electrolytical sectioning	1 example (slight NSE)		Ru in Cu, Fe, Co in Ag	–	Bernardini (1973) [14.40]
Fe	1.13	2.217 (214.1)	0.66	1,063–1,274 (0.86)	11	sc specpure	Fe, electroplated; resistometric method	–		Ni in Ag	–	Sen (1978) [14.41]
Fe	0.10	2.04 (197.0)		651–870 (0.56)	15 (14T)	sc 5N	Fe, sputter deposition; IBS, SIMS analysis	All (ln c–x)[81]		Ni in Cu	14.08	Almazouzi (1996) [14.42]
Ga	0.78	2.034 (196.4)	2.2	(1,053–1,353) (0.89)	[52]	sc specpure	^{72}Ga; lathe	No		Ag, As, Au, Cd, Hg in Cu	–	Nachtrieb (1960) [14.16]
Ga	0.523	1.996 (192.7)	2.0	1,153–1,351 (0.92)	6	pc 4N	^{67}Ga, electroplated; lathe	All		Ge in Cu	14.06	Klotsman (1971) [14.43]
Ga	0.58	2.008 (193.8)	2.0	973–1,323 (0.85)	5	pc[61]	Ga, vapour deposition; X-ray diffraction method	–		Ga in Ag	14.06	Fogelson (1977) [14.44]
Ge	0.397	1.941 (187.4)	2.5	975–1,289 (0.83)	11	sc 4N8	^{68}Ge, electroplated; lathe	3 examples			14.07	Reinke (1970) [14.45]
Ge	0.315	1.922 (185.5)	2.3	1,111–1,326 (0.90)	6	pc 4N	^{68}Ge, electroplated; lathe	All		Ga in Cu	14.07	Klotsman (1971) [14.43]
Hg	0.35	1.908 (184.2)	2.9	(1,053–1,353) (0.89)	[52]	sc specpure	^{203}Hg; lathe	No		Ag, As, Au, Cd, Ga in Cu	–	Nachtrieb (1960) [14.16]
In	1.30	2.005 (193.6)	4.7	1,051–1,351 (0.88)	14	sc, pc 4N	^{114}In, sputter deposition; lathe	All		Ag, Cd in Cu	14.07	Gorbachev (1972) [14.18]

Table 1.4 *(Continued)*

(1)	(2a)	(2b)	(3)	(4)	(5)	(6)	(7)	(8)	(9)	(10)	(11)	(12)
X	D^0 (10^{-4} m^2 s^{-1})	Q(eV) and (kJ mole^{-1})	$D(T_m)$ (10^{-12} m^2 s^{-1})	T-range (K) ($\overline{T}/T_m$)	No. of data points	Material, purity	Experimental method	Remarks on the pp	Further remarks	Also studied	Figure	Reference
In	1.87	2.034 (196.4)	5.3	1,071–1,354 (0.89)	11	pc 5N	^{114}In, electroplated; microtome	Several examples	Erroneous thermal expansion correction		14.07	Krautheim (1978) [14.46]
In	0.31 (0.22)	1.864 (180) (1.844) (178)		602–1,351 (0.72) (602–873)	24 (16T) (9)	sc 5N8	In, vapour deposition; IBS, SIMS analysis ($^{115}In^+$ signal)	2 examples	Pronounced data scatter		–	Gust (1983) [14.47]
In	0.29[21] 3,110[21]	1.86[21] (179.6) 3.06[21] (295.5)	5.0	(602–1,354)	(49)				Two-exponential fit of the data of [14.18, 14.46, 14.47]		14.07	Neumann (1988) [14.34]
Ir	10.6	2.863 (276.4)	0.025	1,185–1,303 (0.92)	7	sc 4N	^{192}Ir, sputter deposition; lathe	All			14.10	Klotsman (1978) [14.48]
Mn	0.74	2.025 (195.5)	2.2	973–1,348 (0.85)	9	pc[61]	Mn; X-ray diffraction method	–			14.08	Fogelson (1973) [14.49]
Mn	1.02	2.072 (200)	2.1	873–1,323 (0.81)	17	pc 4N5	^{54}Mn, electroplated; residual activity	No (pp as for Cr in Cu)	Marked gb contribution at $T < 971$ K	Cr, V in Cu	14.08	Hoshino (1977) [14.35]
Mn	1.42	2.116 (204.3)	2.0	776–976 (0.64)	4[51]	sc 4N8	^{54}Mn, vapour deposition of $MnCl_2$; electrochemical sectioning	1 example			14.08	Maier (1979) [14.50]
Mn	–	–		1,195–1,202 (0.88)	4	sc 5N	^{52}Mn, ^{54}Mn, electroplated; microtome	All[85]	See Cr in Cu; D(1,195 K) = 2.0, D(1,202 K) = 2.3 (in 10^{-13} m^2 s^{-1})	$E = 0.31$; Cr, Zn in Cu	14.08	Rockosch (1983) [14.36]
Mn	0.43	2.01 (194.1)		582–800 (0.51)	17 (16T)	sc 5N	Mn, sputter deposition; IBS, SIMS analysis	Numerous examples		Cr, Ti in Cu	14.08	Almazouzi (1998) [14.37]
Nb	(2.04)	(2.63) (253.9)	(0.036)	1,080–1,179 (0.83)	5	pc (1–3 mm) 5N	^{95}Nb, dried-on from oxalate solution; residual activity	1 example (flat 15 μm pp)[84]			–	Saxena (1970) [14.51]

Ni	2.7	2.450 (236.6)	0.22	1,016–1,349 (0.87)	7 (6T)	sc 4N8	^{63}Ni, electroplated; lathe	2 examples		Co, Fe in Cu, Mn in Cu at $T = 1{,}342$ K	14.09	Mackliet (1958) [14.32]
Ni	3.8	2.463 (237.8)	0.27	968–1,334 (0.85)	7	sc 4N	^{63}Ni, electroplated; lathe	All			–	Ikushima (1959) [14.52]
Ni	1.7	2.398 (231.5)	0.21	1,172–1,340 (0.92)	7	pc (1–4 mm) > 4N	^{63}Ni; lathe	1 example		Cu in Cu, Cu in Ni	14.09	Monma (1964) [14.02]
Ni	2.3	2.437 (235.3)	0.21	973–1,323 (0.85)	8	pc[61]	Ni, vapour deposition; X-ray diffraction method	–			–	Fogelson (1971) [14.53]
Ni	1.94	2.411 (232.8)	0.22	1,128–1,328 (0.90)	5	pc (1–3 mm) 4N, 5N	^{66}Ni, electroplated; lathe	Several examples (for alloy diffusion)		Cu, Zn in Cu; Cu, Ni, Zn in Cu(Ni) and Cu(Zn)	14.09	Anusavice (1972) [14.08]
Ni	0.62	2.32 (224.0)		613–949 (0.58)	20 (17T)	sc 5N	Ni, sputter deposition; IBS, SIMS analysis	Several examples	Two-exponential fit together with the data of [14.02, 14.08, 14.32]	Fe in Cu	14.09	Almazouzi (1996) [14.42]
	0.56[21]	2.32[21] (224.0)	0.22	(613–1,349)	(38)						14.09	
	48[21]	2.90[21] (280.0)										
P	(3.05×10^{-3})	(1.41) (136.1)		847–1,319 (0.80)	19	sc 5N	^{32}P, dried-on from H_3PO_4; microtome	2 examples (anomalous pp at lower T)	[+]Present approximation		–	Spindler (1976) [14.54]
	(0.026)[+]	(1.65)[+] (159.3)	(1.9)[+]	1,225–1,319 (0.94)	6							
Pb	0.862	1.889 (182.4)	8.4	1,007–1,225 (0.82)	8	sc 5N	^{210}Pb, dried-on from salt solution; lathe	All		Au, Bi in Cu	14.11	Gorbachev (1977) [14.24]
Pd	1.71	2.358 (227.6)	0.30	1,080–1,329 (0.89)	16 (8T)	sc 5N	^{103}Pd, electroplated[73]; lathe	All		Pd in Ag	14.10	Peterson (1963) [14.55]
Pt	0.67	2.416 (233.3)	0.072	1,023–1,348 (0.87)	8	pc[61]	Pt, vapour deposition; X-ray diffraction method	–			14.10	Fogelson (1972) [14.56]
Pt	0.56	2.413 (233)	0.062	1,149–1,352 (0.92)	9 (7T)	sc 5N	^{191}Pt, ^{195}Pt, ^{197}Pt, vapour deposition; microtome	No		Pt in Ag	14.10	Neumann (1982) [14.57]
Rh	3.3	2.515 (242.8)	0.15	1,023–1,348 (0.87)	8	pc[61]	Rh, vapour deposition; X-ray diffraction method	–			14.12	Fogelson (1972) [14.58]
Ru	–	–		1,073-1,335	16[51]	sc	^{103}Ru, electroplated; electrolytical sectioning	3 examples[81]	Dislocation enhanced diffusivity at lower T	Fe in Cu, Fe, Co in Ag; $c_s(\mathrm{Ru}) = 183 \cdot \exp(-2.04\ \mathrm{eV/kT})$ at%	14.12	Bernardini (1973) [14.40]
	8.5	2.667 (257.5)	0.11	1,221–1,335 (0.94)	9[51]	5N						

Table 1.4 *(Continued)*

(1)	(2a)	(2b)	(3)	(4)	(5)	(6)	(7)	(8)	(9)	(10)	(11)	(12)
X	D^0 (10^{-4} m^2 s^{-1})	Q(eV) and (kJ mole^{-1})	$D(T_m)$ (10^{-12} m^2 s^{-1})	T-range (K) ($\overline{T}/T_m$)	No. of data points	Material, purity	Experimental method	Remarks on the pp	Further remarks	Also studied	Figure	Reference
S	–	–		823-1,273	18 (15 T)	sc 5N	^{35}S, H_2/H_2S gas mixture; electrolytical sectioning	2 examples[81] (c/c_0–x)	$D(1{,}223\,K) = 3.5 \times 10^{-12}$ m^2 s^{-1} agrees with [14.60]		–	Moya (1969) [14.59]
	(23)	(2.14) (206.6)	(26)	(1,023–1,273) (0.85)	9 (8 T)							
S	(0.6)	(1.70) (164.1)		1,173–1,273 (0.90)	5	pc[61]	H_2/H_2S gas mixture; resistivity change	–	$^+$Present approximation; $D(1{,}223\,K) = 3.5 \times 10^{-12}$ m^2 s^{-1} agrees with [14.59]	S in Ag, Fe, Ni	–	Wang (1970) [14.60]
	$(0.2)^+$	$(1.64)^+$ (158.4)	$(16)^+$									
Sb	0.34	1.812 (175.8)	5.9	873–1,275 (0.79)	18 (9T)	sc 4N	^{124}Sb, vapour deposition; lathe (50 μm sections)	1 example			14.13	Inman (1960) [14.61]
Sb	0.616	1.893 (182.7)	5.8	994–1,288 (0.84)	6	sc 4N	^{124}Sb, vapour deposition; lathe	All		Sn in Cu	14.13	Gorbachev (1973) [14.62]
Sb	0.48	1.86 (179.6)	6.0	1,049–1,349 (0.88)	8	pc (>2 mm) 5N	^{124}Sb, electroplated; microtome	Several examples	Erroneous thermal expansion correction	Sn in Cu	14.13	Krautheim (1979) [14.63]
Se	1.0	1.87 (180.5)	11.4	878–1,150 (0.75)	8	sc 5N	^{75}Se, implanted; microtome	All		Te in Cu, Se in Ag, Te in Au	14.14	Rummel (1989) [14.64]
Si	0.07	1.778 (171.7)	1.8	973–1,323 (0.85)	8	pc[61]	Si, sputter deposition; X-ray diffraction method	–		Be in Cu	–	Fogelson (1973) [14.28]
Si	0.21	1.937 (187)	1.4	998–1,173 (0.80)	8[51]	pc 4N4	Si; EPMA Cu/Cu (X% Si) (Hall)	No	$X = 6.54$; 9.76		14.13	Minamino (1988) [14.65]
Si	0.19	1.947 (188)	1.1	900–1,150 (0.75)	7[51]	pc (2–4 mm) 4N	Si; EPMA Cu/Cu (X% Si) (Matano, Darken)	No	$X = 6$; 8	Cu in Cu(Si)	14.13	Iijima (1991) [14.66]
Sn	0.842	1.949 (188.2)	4.9	1,011–1,321 (0.86)	9	sc 4N	^{113}Sn, vapour deposition; lathe	All		Sb in Cu	14.11	Gorbachev (1973) [14.62]
Sn	0.82	1.943 (187.6)	5.0	973–1,348 (0.85)	8	pc[61]	Sn, sputter deposition; X-ray diffraction method	–			14.11	Fogelson (1974) [14.67]

Sn	0.67	1.91 (184.4)	5.5	1,018–1,355 (0.87)	12	pc (>2 mm) 5N	^{113}Sn, electroplated; microtome	Several examples	Erroneous thermal expansion correction	Sb in Cu	14.11	Krautheim (1979) [14.63]
Te	0.97	1.87 (180.5)	11	822–1,214 (0.75)	10	sc 6N	^{121}Te, implanted; microtome	All		Se in Ag, Se in Cu, Te in Au	14.15	Rummel (1989) [14.64]
Ti	0.693	2.030 (196)	2.0	973–1,283 (0.83)	13	sc 4N8	Ti; EPMA Cu/Cu(2–3%Ti) (Boltzmann–Matano)	1 example			14.09	Iijima (1977) [14.68]
Ti	0.37	1.99 (192.1)		621–747 (0.50)	15 (14T)	sc 5N	Ti, sputter deposition; IBS; SIMS analysis	All		Cr, Mn in Cu	14.09	Almazouzi (1998) [14.37]
Tl	0.71	1.878 (181.3)	7.6	1,058–1,269 (0.86)	9	sc 5N	^{204}Tl, electroplated; lathe	All	Marked data scatter		14.15	Komura (1963) [14.69]
V	2.48	2.227 (215)	1.3	995–1,342 (0.86)	13	pc 4N5	^{48}V, dried-on from $VOCl_2$ solution; residual activity	No (pp as for Cr in Cu)		Cr, Mn in Cu	–	Hoshino (1977) [14.35]
Zn	0.34	1.977 (190.9)	1.6	878-1,322 (0.81)	5	sc specpure	^{65}Zn, electroplated; lathe	No		Cu, Zn in α-CuZn	14.14	Hino (1957) [14.70]
Zn	0.41^{+}	1.997^{+} (192.8)	1.6^{+}	1,165, 1,220	2	sc 5N	^{65}Zn, ^{69}Zn, electroplated; lathe	1 example	$^{+}$Present calculation	$E = 0.41$; Zn in CuZn	14.14	Peterson (1967) [14.71]
Zn	0.73	2.060 (198.9)	1.6	1,165–1,348 (0.93)	5	pc 5N	^{65}Zn, vapour deposition or electroplated; lathe	Several examples		gb diffusion	14.14	Klotsman (1969) [14.72]
Zn	0.24	1.956 (188.8)	1.3	1,073–1,313 (0.88)	6	pc 4N	^{65}Zn, electroplated; lathe	Several examples (for alloy diffusion)		Cu, Ni in Cu; Cu, Ni, Zn in Cu(Ni) and Cu(Zn)	–	Anusavice (1972) [14.08]
Zn	0.28	1.961 (189.3)	1.5	993–1,193 (0.80)	11[51]	pc specpure	Zn, electroplated; resistometric method			Zn in Ag	–	Dutt (1979) [14.73]

Table 1.5 Diffusion in silver (References see page 95)

(1)	(2a)	(2b)	(3)	(4)	(5)	(6)	(7)	(8)	(9)	(10)	(11)	(12)
X	D^0 (10^{-4} $m^2 s^{-1}$)	Q(eV) and (kJ $mole^{-1}$)	$D(T_m)$ (10^{-12} $m^2 s^{-1}$)	T-range (K) ($\overline{T}/T_m$)	No. of data points	Material, purity	Experimental method	Remarks on the pp	Further remarks	Also studied	Figure	Reference
Self-diffusion												
Ag	0.395	1.912 (184.6)	0.61	903–1,208 (0.86)	7	Sc 4N	^{110}Ag, electroplated; lathe	3 examples			15.01	Tomizuka (1956) [15.01]
Ag	0.278	1.882 (181.7)	0.57	1,039–1,219 (0.91)	8 (6T)	pc[61] 5N	^{110}Ag, vapour deposition; chemical sectioning and residual activity	Several examples		gb diffusion	–	Kaygorodov (1968) [15.02]
Ag	0.67	1.960 (189.2)	0.66	914–1,228 (0.87)	13	sc 5N	^{110}Ag, ^{105}Ag, electroplated; lathe	Numerous examples		$E = 0.72–0.64$ (914–1,228 K)	15.01	Rothman (1970) [15.03]
Ag	–	–		946–1,227 (0.88)	6	sc 5N	^{110}Ag, ^{105}Ag, electroplated; microtome	All		$E = 0.72–0.58$ (946–1,227 K)	15.01	Reimers (1972) [15.04]
Ag	0.041	1.76 (170.0)		547–777 (0.54)	13	sc 5N	^{110}Ag, electroplated; anodizing and stripping	All[83] (non-linear in ln $c–x^2$)			15.01	Lam (1973) [15.05]
Ag	–	–		631–854 (0.60)	12 (9T)	sc 4N	^{110}Ag, electroplated; chemical sectioning (iodine in alcohol)	2 examples	Two-exponential fit together with the data of [15.03, 15.05]		15.01	Backus (1974) [15.06]
	0.046[21]	1.76[21] (170.0)	0.72									
	6[21]	2.24[21] (216.3)										
Ag	0.043	1.76 (170.0)		581–835 (0.57)	11	sc 5N5	^{110}Ag, ^{105}Ag, vapour deposition; IBS	Several examples			15.01	Bihr (1978) [15.07]
Ag	–	–		594–994 (0.64)	5	sc 5N	^{110}Ag, vapour deposition; IBS	1 example (several examples for high pressure measurements)	Two-exponential fit together with the data of [15.03, 15.05]	$\Delta V/V_0 =$ 0.66–0.86 (594–994 K), $\Delta V/V_0$ for Au in Au	15.01	Rein (1982) [15.08]
	0.046[21]	1.76[21] (170.0)	0.46									
	3.3[21]	2.28[21] (220.1)										

Ag	–	–		626–880 (0.61)	7	sc 5N	^{110}Ag, ^{105}Ag, vapour deposition; IBS	2 examples		$E = 0.86–0.68$ (626–880 K)	15.01	Mehrer (1982) [15.09]
Ag	0.055[21]	1.773[21] (171.1)	0.69	(573–1,228)	(54)				Two-exponential fit of the data of [15.03, 15.05 to 15.08]		15.01	Neumann (1986) [15.10]
	15.1[21]	2.35[21] (226.9)										
Impurity diffusion												
Al	0.13	1.652 (159.5)	2.3	873–1,223 (0.85)	8	pc[61]	Al, vapour deposition; X-ray diffraction method	–			15.02	Fogelson (1975) [15.11]
As	0.042	1.549 (149.6)	2.0	915–1,213 (0.86)	10	pc 5N	As, vapour deposited thin film (0.1 μm); EPMA	1 example (intensity vs. x plot)			–	Hehenkamp (1975) [15.12]
Au	0.262	1.973 (190.5)	0.23	923–1,217 (0.87)	16[51] (8T)	sc 4N	^{198}Au, electroplated[73]; lathe	All			15.03	Jaumot (1956) [15.13]
Au	0.41	2.012 (194.3)	0.25	929–1,178 (0.85)	5	pc 4N	^{198}Au, electroplated; microtome	1 example		Au in Au; Au in Ag(Au)	15.03	Mead (1957) [15.14]
Au	0.85	2.094 (202.1)	0.24	991–1,198 (0.89)	6	sc 4N	^{198}Au, chemical replacement; lathe	No		Ag in Au; Ag in Au(Ag) Au in Ag(Au)	15.03	Mallard (1963) [15.15]
Au	0.62	2.061 (199.0)	0.24	923–1,217 (0.87)					Best fit to data of [15.13–15.15]		15.03	
Cd	0.44	1.808 (174.6)	1.8	865–1,210 (0.84)	6	sc 4N	^{115}Cd, electroplated; lathe (40–80 μm sections)	All		In, Sn in Ag	15.02	Tomizuka (1954) [15.16]
Cd	0.504	1.831 (176.8)	1.7	1,042–1,226 (0.92)	9 (7T)	pc 5N	^{109}Cd, vapour deposition of $CdCl_2$ or electroplated; chemical sectioning and residual activity	Numerous examples		gb diffusion	15.02	Kaygorodov (1969)[15.17]
Co	–	–		1,200*	1	sc 5N	^{60}Co, ^{58}Co, dried-on from salt solution; lapping with SiC paper	For $t = 8$ h the pp was linear in ln c–x^2	Investigation of the diffusion time dependence of the pp *D(1,200 K) = 3×10^{-13} m^2 s^{-1}	Ag in Ag at 1,200 K	15.03	Lundy (1968) [15.18]
Co				912–1,214 (0.86)	15	sc 5N	^{60}Co, electroplated; electrolytical sectioning	No[81]		Ag, Fe in Ag, Fe, Ru in Cu; c_s(909 K) = 3.6×10^{-6}	15.03	Bernardini (1973) [15.19]
	1.9	2.114 (204.1)	0.44	1,013–1,214 (0.90)	12							

Table 1.5 *(Continued)*

(1)	(2a)	(2b)	(3)	(4)	(5)	(6)	(7)	(8)	(9)	(10)	(11)	(12)
X	D^0 (10^{-4} $m^2 s^{-1}$)	Q(eV) and (kJ mole^{-1})	$D(T_m)$ (10^{-12} $m^2 s^{-1}$)	T-range (K) ($\overline{T}/T_m$)	No. of data points	Material, purity	Experimental method	Remarks on the pp	Further remarks	Also studied	Figure	Reference
Cr	3.26	2.175 (210)	0.42	1,023–1,215 (0.91)	14 (13T)	pc 5N	^{51}Cr, dried-on from Na_2CrO_4 solution; residual activity	1 example, non-Gaussian pp	Erroneous thermal expansion corrections	Mn, Ti, V in Ag	–	Makuta (1979) [15.20]
Cr	(1.1) 1.2^+	2.00 (193.1)	0.81^+	976–1,231 (0.89)	13 (11T)	sc 6N	^{51}Cr, vapour deposition; microtome	1 example[81] (see Figure 01.09)	$^+$Present recalculation	$c_s = 1{,}620 \cdot \exp(-1.76$ eV/kT)	15.04	Neumann (1981) [15.21]
Cu	1.23	1.999 (193.0)	0.84	990–1,218 (0.89)	16 (8T)	sc 4N	^{64}Cu, electroplated[73]; lathe	No		Hg in Ag	15.03	Sawatzky (1957) [15.22]
Cu	0.029	1.700 (164.1)		699–897 (0.65)	18 (12T)	sc 4N	Cu, vapour deposition; IBS, SIMS analysis (^{63}Cu signal)	2 examples[85]			–	Dorner (1980) [15.23]
Fe	2.42	2.127 (205.3)	0.50	991–1,201 (0.89)	6 (5T)	sc 4N	^{59}Fe, ^{55}Fe, electroplated; lathe	All, curved pp* (see Figure 01.10)	*Erfc-solution, incorrect ln c–x^2 evaluation	Fe in Cu; $E = 0.62 \pm 0.13$ (999–1,201 K)	–	Mullen (1961) [15.24]
Fe	– (2.6) 3.0^+	– 2.125 (205.2)	0.63^+	915–1,205 1,084–1,205 (0.93)	28[51] 14[51]	sc 5N	^{59}Fe, electroplated; electrolytical sectioning	No[81]	$^+$Present approximation	Co in Ag, Fe, Ru in Cu; $c_s(900\,K) = 3 \times 10^{-6}$	15.04	Bernardini (1973) [15.19]
Fe	1.9	2.141 (206.7)	0.34	1,062–1,213 (0.92)	11 (9T)	sc 5N	^{59}Fe, electroplated; lathe	Several examples[84]			–	Bharati (1977) [15.25]
Ga	0.42	1.687 (162.9)	5.4	873–1,213 (0.85)	8	pc[61]	Ga, vapour deposition; X-ray diffraction method	–		Ga in Cu	15.05	Fogelson (1977) [15.26]
Ge	0.084	1.583 (152.8)	2.9	948–1,124 (0.84)	11[51]	pc[61]	^{71}Ge, vapour deposition; lathe and residual activity	No		Tl in Ag; Ag in Ag(Tl), Ag in Ag(Ge)	15.07	Hoffman (1958) [15.27]
Hg	0.079	1.652 (159.5)	1.4	926–1,221 (0.87)	24 (13T)	sc 4N	^{203}Hg, electroplated[73]; lathe	No		Cu in Ag	15.07	Sawatzky (1957) [15.22]
In	0.41	1.762 (170.1)	2.6	886–1,209 (0.85)	6	sc 4N	^{114}In, electroplated; lathe	All		Cd, Sn in Ag	15.06	Tomizuka (1954) [15.16]

In	0.55	1.812 (175.0)	2.2	1,044–1,215 (0.92)	11	pc 5N	^{114}In, vapour deposition; chemical sectioning and residual activity	Several examples			15.06	Kaygorodov (1967) [15.28]
In	0.36	1.75 (169.0)		553–838 (0.56)	15	sc 5N	^{114}In, vapour deposition; IBS	4 examples (see Figure 01.03)	Marked data scatter at lower temperatures		15.06	Mehrer (1984) [15.29]
In	0.27	1.735 (167.5)	2.2	553–1,234					Present approximation (forced fit)		15.06	
Mn	(0.18) 0.45^{+}	1.860 (179.6)	 1.1^{+}	849–1,206 (0.83)	8	pc 5N	Mn; EPMA Ag/Ag (8% Mn) (Grube)	1 example (probability plot)	$^{+}$Present approximation		15.05	Barclay (1969)[15.30]
Mn	(4.29)	(2.030) (196)	(2.2)	883–1,212 (0.85)	16 (15T)	pc 5N	^{54}Mn, electroplated; residual activity	No (non-Gaussian pp)	Erroneous thermal expansion correction	Cr, Ti, V in Ag	–	Makuta (1979) [15.20]
Ni	(21.9)	(2.376) (229.4)	(0.43)	1,022–1,223 (0.91)	6	sc 4N	^{63}Ni, electroplated; lathe	All (pronounced NSE)			–	Hirone (1961) [15.31]
Ni	(15)	(2.251) (217.3)	(0.96)	904–1,199 (0.85)	16	sc 5N	^{63}Ni, electroplated; electrolytical sectioning	2 examples[81] (see Figure 01.08)		$c_s = 2.0 \cdot \exp(-0.69\ \mathrm{eV}/kT)$	–	Ladet (1976) [15.32]
Ni	(2.8)	(2.386) (230.4)	(0.05)	1,023–1,193 (0.90)	9	pc specpure	Ni, electroplated; resistometric measurements	–		Fe in Cu	–	Sen (1978) [15.33]
Pb	0.22	1.652 (159.5)	3.9	948–1,123 (0.84)	3[51]	pc[61]	^{210}Pb, electroplated; lathe	No		Ag, Pb in Ag(X), X = Pb, Al, Cu, Ge	–	Hoffman (1955) [15.34]
Pd	9.57	2.461 (237.6)	0.085	1,009–1,212 (0.90)	16 (8T)	sc 5N	^{103}Pd, electroplated[73]; lathe	All		Pd in Cu	15.08	Peterson (1963) [15.35]
Pt	6.0	2.467 (238.2)	0.050	923–1,223 (0.87)	7	pc[61] (80 μm)	Pt, vapour deposition; X-ray diffraction method	–			–	Fogelson (1975) [15.36]
Pt	1.9	2.413 (235.7)	0.026	1,094–1,232 (0.94)	8	sc 5N	^{191}Pt, ^{195}Pt, ^{197}Pt, vapour deposition; microtome	2 examples (erfc-solution at lower T)		Pt in Cu	15.08	Neumann (1982) [15.37]
Ru	(180)	(2.853) (275.5)	(0.040)	1,066–1,219 (0.93)	6	sc 4N	^{103}Ru, ^{106}Ru, electroplated; lathe	No (pronounced NSE)	ln c–x^2 evaluation in spite of the extremely small solubility		–	Pierce (1959)[15.38]

Table 1.5 *(Continued)*

(1)	(2a)	(2b)	(3)	(4)	(5)	(6)	(7)	(8)	(9)	(10)	(11)	(12)
X	D^0 (10^{-4} $m^2 s^{-1}$)	Q(eV) and (kJ mole^{-1})	$D(T_m)$ (10^{-12} $m^2 s^{-1}$)	T-range (K) ($\overline{T}/T_m$)	No. of data points	Material, purity	Experimental method	Remarks on the pp	Further remarks	Also studied	Figure	Reference
S	1.65	1.735 (167.5)	13.5	873–1,173 (0.83)	4[51]	pc 5N	^{35}S, direct coating with Ag_2S; residual activity	1 example (c–x)			–	Barbouth (1967) [15.39]
S	(0.7)	(1.648) (159.1)	(13)	(973–1,100) (0.84)	6[51]	pc[61]	H_2/H_2S gas mixture; resistivity change	–		S in Cu, Fe, Ni	–	Wang (1970) [15.40]
Sb	0.169	1.662 (160.4)	2.7	742–1,215 (0.79)	11 (10T)	sc, pc (0.1 mm) 4N	^{124}Sb, electroplated; lathe	No (4 examples in [15.66])			15.09	Sonder (1954) [15.41]
Sb	0.234	1.694 (163.4)	2.8	1,051–1,225 (0.92)	12 (9T)	pc 5N	^{124}Sb, vapour deposition; chemical sectioning and residual activity	All		gb diffusion	15.09	Kaygorodov (1967) [15.42]
Sb	–	–	–	914–1,048 (0.82)	3	pc 5N	Sb; EPMA Ag/Ag(3.9% Sb) (Sauer-Freise)	1 example (c–x) (see Figure 01.14)			15.09	Hagenschulte (1989) [15.43]
Se	0.285	1.63 (157.4)	6.3	759–1,109 (0.76)	8	sc 5N	^{75}Se, implanted; microtome	All*	*pp linear in ln c–x^2 except for $T = 759$ K[81]	Se, Te in Cu, Te in Au	15.09	Rummel (1989) [15.44]
Sn	0.25	1.704 (164.5)	2.7	865–1,210 (0.84)	6	sc 4N	^{113}Sn, electroplated; lathe	All		Cd, In in Ag	15.05	Tomizuka (1954) [15.16]
Sn	0.472	1.771 (171.0)	2.7	1,026–1,227 (0.91)	9 (8T)	pc 5N	^{113}Sn, ^{119}Sn, vapour deposition; chemical sectioning and residual activity	All		gb diffusion; Te in Ag	15.05	Kaygorodov (1969) [15.45]

Te	0.47	1.687 (162.9)	6.0	1,044–1,214 (0.91)	5	pc 5N	^{125}Te*, vapour deposition; chemical sectioning	No	*Simultaneous measurement of ^{119}Sn and ^{125}Te	Sn in Ag	15.06	Kaygorodov (1969) [15.45]
Te	0.21	1.602 (154.7)	6.0	650–1,169 (0.74)	7	sc 5N	^{121}Te, implanted; microtome	All (erfc-solution for 650–793 K)		gb diffusion	15.06	Geise (1987) [15.46]
Ti	1.33	2.051 (198)	0.56	1,051–1,220 (0.92)	14 (12T)	pc (2–7 mm) 5N	Ti; EPMA Ag/Ag(X% Ti), X = 0.23; 0.45 (Grube)	1 example (probability plot)	Erroneous thermal expansion correction	Cr, Mn, V in Ag	15.08	Makuta (1979) [15.20]
Tl	0.15	1.644 (158.7)	2.9	(919–1,072) (0.81)	9[51]	pc[61]	^{204}Tl, electroplated; lathe and residual activity	No		Ge in Ag; Ag in Ag(Tl), Ag in Ag(Ge)	15.10	Hoffman (1958) [15.27]
V	2.72	2.165 (209)	0.39	1,012–1,218 (0.90)	14 (12T)	pc 5N	^{48}V, dried-on from $VOCl_2$ solution; residual activity	No (non-Gaussian pp)	Erroneous thermal expansion correction	Cr, Mn, Ti in Ag	–	Makuta (1979) [15.20]
Zn	0.54	1.808 (174.6)	2.2	916–1,197 (0.86)	12 (6T)	sc 4N	^{65}Zn, electroplated[73]; lathe	All			15.10	Sawatzky (1955) [15.47]
Zn	0.532	1.808 (174.6)	2.2	970–1,225 (0.89)	7	sc 5N	^{65}Zn, ^{69}Zn, electroplated; lathe	3 examples		E = 0.48–0.60 (970–1,225 K); Ag in Ag(Zn)	15.10	Rothman (1967) [15.48]

Table 1.6 Diffusion in gold (References see page 97)

(1)	(2a)	(2b)	(3)	(4)	(5)	(6)	(7)	(8)	(9)	(10)	(11)	(12)
X	$D^0(10^{-4}\,m^2\,s^{-1})$	Q(eV) and (kJ mole^{-1})	$D(T_m)$ $(10^{-12}\,m^2\,s^{-1})$	T-range (K) $(\bar{T}/T_m)$	No. of data points	Material, purity	Experimental method	Remarks on the pp	Further remarks	Also studied	Figure	Reference
Self-diffusion												
Au	(0.091)	(1.808) (174.6)		977–1,321 (0.86)	10	pc (1 mm) 3N5	^{198}Au, electroplated; lathe	1 example	Erroneous thermal expansion correction		16.01	Makin (1957) [16.01]
	0.087*	1.806* (174.4)	1.33*						*Correct data			
Au	0.117	1.826 (176.3)	1.5	975–1,172 (0.80)	5	pc (1.5 mm) 3N3	^{198}Au, electroplated; residual activity	All (NSE at lower temperature)	Erroneous thermal expansion correction	Co, Fe, Ni in Au	16.01	Duhl (1963) [16.02]
Au	0.107	1.833 (176.9)	1.30	1,123–1,323 (0.92)	5[51]	sc 3N7	^{195}Au, electroplated; lathe	2 examples			–	Gilder (1965) [16.03]
Au	0.094$^+$	1.810$^+$ (174.7)		623–733 (0.51)	5[51]	pc[61] (1-2 mm) (3 μm foil)	^{195}Au, electroplated; absorption	3 examples $(c(t)/c_0-\sqrt{t})$	$^+$Present fit to the depicted data		16.01	Gainotti (1965) [16.04]
Au	0.043$^+$	1.735 (167.5)	1.23$^+$	873–1,263 (0.80)	9	sc[61]	^{198}Au, vapour deposition; grinder (abrasive paper)	No	$^+$Present approximation; dislocation enhanced diffusivity at lower T	Cu in Cu, Al in Al; $\Delta V/V_0 = 0.72$	–	Beyeler (1968) [16.05]
Au	0.026	1.73 (167.0)		559–685 (0.47)	6 (5T)	sc 4N	^{198}Au, electroplated; anodizing and stripping, residual activity	All			16.01	Rupp (1969) [16.06]
Au	0.078	1.800 (173.8)	1.26	1,059–1,314 (0.89)	14[51]	pc (1.5 mm) 5N	^{195}Au, electroplated; lathe	No (2 examples in Ref. [16.25])		In in Au; Au in Au(In), Au in Au(Sn)	16.01	Dreyer (1972) [16.07]
Au	0.084	1.804 (174.2)	1.31	1,031–1,333 (0.88)	17	sc 5N	^{195}Au, ^{199}Au, electroplated; microtome	No		Co in Au; $E = 0.71$–0.65 (1,041–1,329 K), E(Co in Au)	16.01	Herzig (1978) [16.08]

Au	–	–		692	1*	sc 5N	^{198}Au, vapour deposition; IBS	1 example (several examples for high pressure measurements)	*$D = 6.46 \times 10^{-19}\,m^2\,s^{-1}$	$\Delta V/V_0 = 0.73$, $\Delta V/V_0$ for Ag in Ag	16.01	Rein (1982) [16.09]
Au	0.072	1.71 (165.1)		603–823 (0.53)	6[51]	sc 5N	^{198}Au, vapour deposition; IBS	1 example (several examples for high pressure measurements)		$\Delta V/V_0 =$ 0.73–0.76	16.01	Werner (1983) [16.10]
Au	0.025[21] 0.83[21]	1.703[21] (164.4) 2.20[21] (212.4)	1.36	(603–1,333)	(23)				Two-exponential fit of the data of [16.08, 16.10]		16.01	Neumann (1986) [16.11]
Impurity diffusion												
Ag	0.072	1.743 (168.3)	1.9	972–1,280 (0.84)	6	sc 4N	^{110}Ag, electroplated; lathe	No		Au in Ag; Au in Ag(Au), Ag in Au(Ag)	16.02	Mallard (1963) [16.12]
Ag	0.080	1.752 (169.2)	2.0	1,046–1,312 (0.88)	9 (5T)	pc 4N	^{110}Ag, vapour deposition[73]; electrochemical sectioning and residual activity	2 examples[85]		gb diffusion	16.02	Klotsman (1965) [16.13]
Ag	0.086	1.754 (169.3)	2.1	1,004–1,323 (0.87)	10 (7T)	sc 5N	^{110}Ag, ^{105}Ag, electroplated; microtome	4 examples		$E = 0.45$–0.51	16.02	Herzig (1974) [16.14]
Al	0.052	1.487 (143.6)	12.7	773-1,223 (0.75)	9	pc[61]	Al, vapour deposition; X-ray diffraction method	–			16.03	Fogelson (1978) [16.15]
Co	0.068	1.804 (174.2)	1.1	975–1,221 (0.82)	6 –	pc (1.5 mm) 3N3	^{60}Co, electroplated; residual activity	2 examples[84]	Erroneous thermal expansion correction	Au, Fe, Ni in Au	–	Duhl (1963) [16.02]
Co	0.22	1.899 (183.4)	1.5	973–1,323 (0.86)	8	pc[61]	Co, vapour deposition; X-ray diffraction method	–		Fe in Au	16.02	Fogelson (1977) [16.16]
Co	0.25	1.918 (185.2)	1.45	1,030–1,325 (0.88)	9	sc 5N	^{60}Co, ^{57}Co, electroplated; microtome	No		Au in Au; $E = 0.71$–0.62 (1,030–1,325 K); E (Au in Au)	16.02	Herzig (1978) [16.08]
Cr	0.507	1.982 (191.4)	1.7	979–1,303 (0.85)	9 (8T)	pc 4N	Cr; EPMA Au/Au (0.5% Cr) (Hall)	2 examples (probability plot)		Fe, Hf, Mn, Ti, V, Zr in Au	–	Richter (1998) [16.17]

Table 1.6 *(Continued)*

(1)	(2a)	(2b)	(3)	(4)	(5)	(6)	(7)	(8)	(9)	(10)	(11)	(12)
X	$D^0(10^{-4}\,m^2\,s^{-1})$	Q(eV) and (kJ mole^{-1})	$D(T_m)$ $(10^{-12}\,m^2\,s^{-1})$	T-range (K) $(\bar{T}/T_m)$	No. of data points	Material, purity	Experimental method	Remarks on the pp	Further remarks	Also studied	Figure	Reference
Cu	(0.105) 0.12$^+$	1.763 (170.2)	2.7$^+$	973–1,179 (0.81)	7	pc 4N	Cu, vapour deposited thin film (<2 μm); EPMA	All	$^+$Present recalculation		16.04	Vignes (1966) [16.18]
Fe	(0.082) 0.089$^+$	1.804 (174.2)	1.4$^+$	974–1,172 (0.80)	6	pc (1.5 mm) 3N3	^{59}Fe, electroplated; residual activity	2 examples[84]	Erroneous thermal expansion correction $^+$Present approximation	Au, Co, Ni in Au	–	Duhl (1963) [16.02]
Fe	0.19	1.787 (172.5)	3.4	973–1,323 (0.86)	8	pc[61]	Fe, vapour deposition; X-ray diffraction method	–		Co in Au	–	Fogelson (1977) [16.16]
Fe	0.0437	1.731 (167.1)	1.3	952–1,308 (0.85)	23 (11T)	pc 4N	Fe; EPMA Au (0.5% Fe)/Au/Au (3% Fe) (Hall)	4 examples (probability plot)	Pronounced data scatter	Cr, Hf, Mn, Ti, V, Zr in Au	–	Richter (1998) [16.17]
Ge	0.073	1.497 (144.5)	16.4	1,010–1,287 (0.86)	5	sc, pc 5N	^{68}Ge, electroplated; microtome	All		Zn in Au	16.03	Cardis (1977) [16.19]
Hf	0.5	2.339 (225.8)	0.075	973–1,303 (0.85)	10 (8T)	pc 4N	Hf; EPMA Au/Au (1%Hf)/ Au (Hall)	2 examples (probability plot)	Pronounced data scatter	Cr, Fe, Mn, Ti, V, Zr in Au	–	Richter (1998) [16.17]
Hg	0.116	1.621 (156.5)	8.9	772–1,300 (0.78)	9	sc 4N4	^{203}Hg, vapour deposition; lathe (20–30 μm sections)	2 examples[81,84]	Pronounced data scatter		–	Mortlock (1965) [16.20]
In	0.075	1.592 (153.7)	7.4	971–1,276 (0.84)	16[51] (13T)	sc, pc 5N	^{114}In; lathe; In, EPMA Au/Au (0.3% In)	No		Au in Au; Au in Au(In), Au in Au(Sn)	16.04	Dreyer (1971) [16.07]
Mn	0.107	1.752 (169.1)	2.6	981–1,294 (0.85)	7	pc 4N	Mn; EPMA Au/ Au(X% Mn)/Au (Hall)	3 examples (probability plot)	$X = 0.5$; 2	Cr, Fe, Hf, Ti, V, Zr in Au	–	Richter (1998) [16.17]

Ni	0.30	1.995 (192.6)	0.89	1,153–1,210 (0.88)	5	pc 3N6	^{63}Ni, vapour deposition; lathe (20–50 μm sections)	No		Ni in Ni; inter-diffusion in Au Ni alloys	16.05	Reynolds (1957) [16.21]
Ni	0.034	1.821 (175.9)	0.46	975–1,261 (0.84)	7	pc (1.5 mm) 3N3	^{63}Ni, electroplated; residual activity	2 examples[84]	Erroneous thermal expansion correction	Au, Co, Fe in Au	–	Duhl (1963) [16.02]
Ni	0.25	1.951 (188.4)	1.1	973–1,323 (0.86)	7	pc[61] (45 μ)	Ni, vapour deposition; X-ray diffraction method	–			16.05	Fogelson (1976) [16.22]
Pd	0.076	2.021 (195.1)	0.18	973–1,273 (0.84)	7	pc[61]	Pd, vapour deposition; X-ray diffraction method	–		Pt in Au	16.06	Fogelson (1978) [16.23]
Pt	0.095	2.086 (201.4)	0.13	973–1,273 (0.84)	7	pc[61]	Pt, vapour deposition; X-ray diffraction method	–		Pd in Au	16.06	Fogelson (1978) [16.23]
Sb				(892–1,278)	(17)	pc	Sb; EPMA Au/Au (0.15–0.4% Sb)/Au	1 example (probability plot)			16.07	Herzig (1972) [16.24]
	0.0144	1.340 (129.4)	10.0	1,007–1,278 (0.86)	14 (11T)	5N						
Sn	0.0399	1.482 (143.1)	10.2	962–1,276 (0.84)	7	pc (1.5 mm)	^{113}Sn, electroplated; lathe; Sn, EPMA Au/Au (0.3% Sn)/Au (Hall)	2 examples		Sn in AuSn, Au in AuSn	16.08	Herzig (1972) [16.25]
	0.0412	1.484 (143.3)	10.4	970–1,268 (0.84)	16 (12T)	5N		1 example (c/c_0–x)				
Te	(0.063)	(1.46) (141.0)		908–1,145 (0.77)	6	sc 5N	^{121}Te, implanted; microtome	All[81]	$^{+}$Present approximation	Se, Te in Cu, Se in Ag	16.07	Rummel (1989) [16.26]
	0.026^{+}	1.382^{+} (133.4)	16.0^{+}									
Ti	(1.2)	(2.301) (222.2)		903–1,293 (0.82)	31 (13T)	pc 4N	Ti; EPMA Au/Au (X% Ti)/Au (Hall)	1 example (probability plot)	$X = (0.5–1.3) \times 10^{-3}$% $^{+}$Present approximation	Cr, Fe, Hf, Mn, V, Zr in Au; c_s(Ti) = 7–30 ppma	16.05	Richter (1998) [16.17]
	4.1^{+}	2.403^{+} (232)	0.35^{+}									
V	2.67	2.285 (220.6)	0.64	949–1,303 (0.84)	19 (10T)	pc 4N	V; EPMA Au (1% V)/Au/Au (3% V) (Hall)	3 examples (probability plot)	Pronounced data scatter	Cr, Fe, Hf, Mn, Ti, Zr in Au	–	Richter (1998) [16.17]
Zn	0.082	1.638 (158.2)	5.4	969–1,287 (0.84)	6	sc, pc 5N	^{65}Zn, electroplated; microtome	All		Ge in Cu	16.08	Cardis (1977) [16.19]
Zr	1.1	2.319 (223.9)	0.20	1,023–1,273 (0.86)	6	pc 4N	Zr; EPMA Au/Au (10^{-3}% Zr)/Au (Hall)	3 examples (probability plot)	Pronounced data scatter	Cr, Fe, Hf, Mn, Ti, V in Au	–	Richter (1998) [16.17]

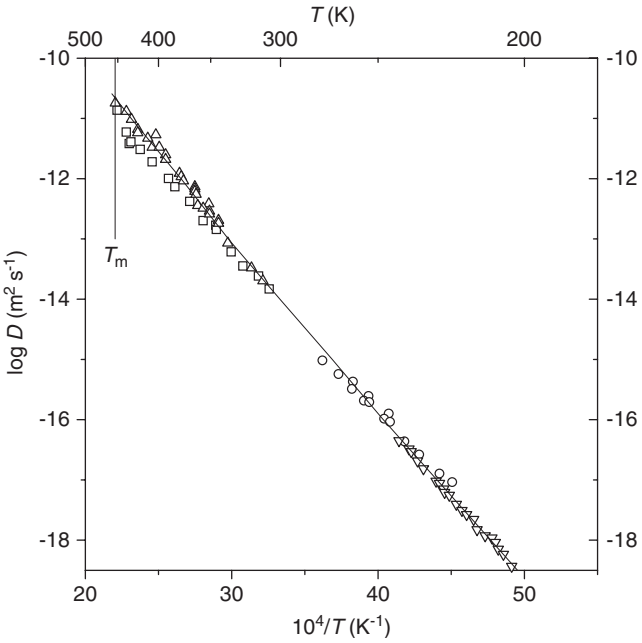

Fig. 11.01 Self-diffusion in lithium. Results of NMR investigations. ∇, Ailion [11.03]; ○, Weithase [11.05]; △, Messer [11.06]; □, Lodding [11.04] (tracer data are shown for comparison). Fitting line according to [11.06].

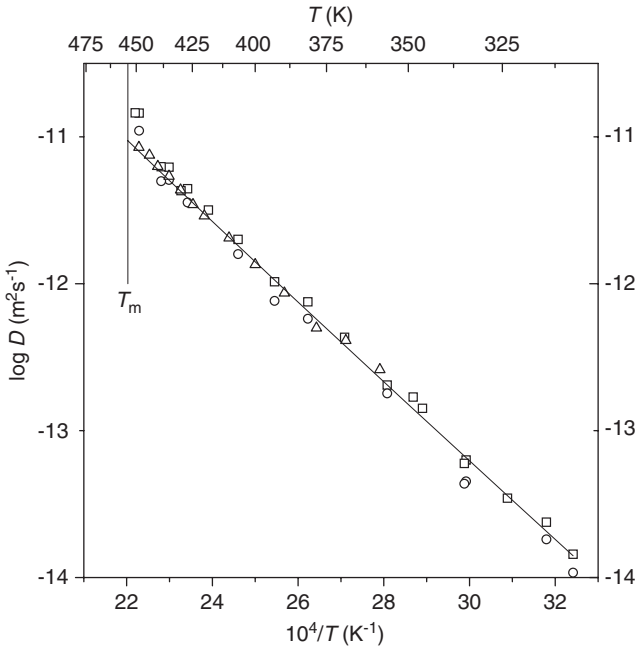

Fig. 11.02 Self-diffusion in lithium. □, ^{7}Li in ^{6}Li and ○, ^{6}Li in ^{7}Li Lodding [11.04]; △, Messer [11.10]. Fitting line: two-exponential fit according to [11.10].

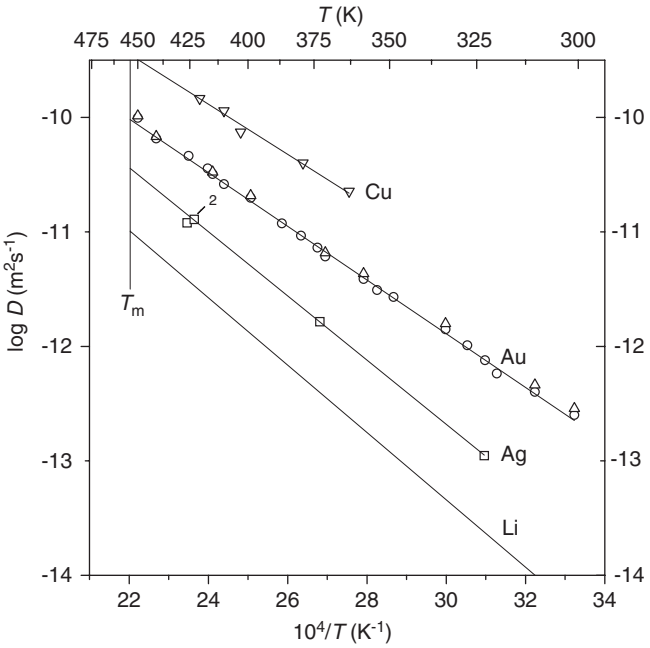

Fig. 11.03 Impurity diffusion in lithium. Ag in Li: □, Mundy [11.13]; Au in Li: ○, Ott [11.14]; Au in ^{6}Li: △, Ott [11.14]. Fitting line determined by the use of $D^0 = 0.141 \times 10^{-4}\,m^2\,s^{-1}$, $Q = 0.465\,eV$. Cu in Li: ∇, Mundy [11.17]; Li in Li according to [11.10] ($D^0 = 0.31 \times 10^{-4}\,m^2\,s^{-1}$, $Q = 0.584\,eV$).

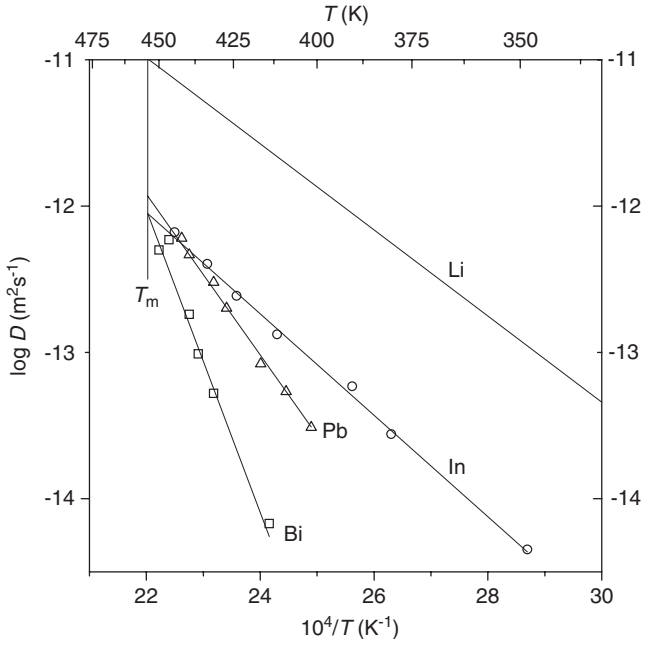

Fig. 11.04 Impurity diffusion in lithium. Bi in Li: □, Ott [11.15]; In in Li: ○, Ott [11.18]; Pb in Li: △, Ott [11.15]; Li in Li according to [11.10] ($D^0 = 0.31 \times 10^{-4}\,m^2\,s^{-1}$, $Q = 0.584\,eV$).

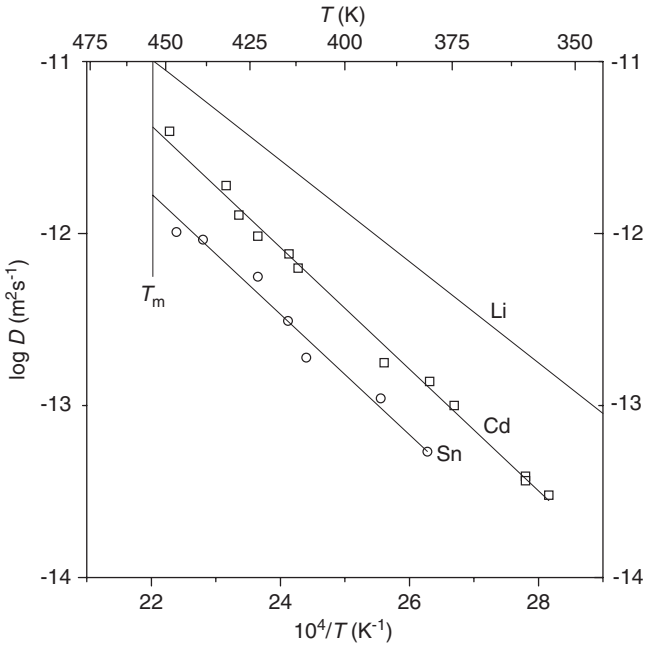

Fig. 11.05 Impurity diffusion in lithium. Cd in Li: □, Ott [11.16]; Sn in Li: ○, Ott [11.15]; Li in Li according to [11.10] ($D^0 = 0.31 \times 10^{-4}\,m^2\,s^{-1}$, $Q = 0.584$ eV).

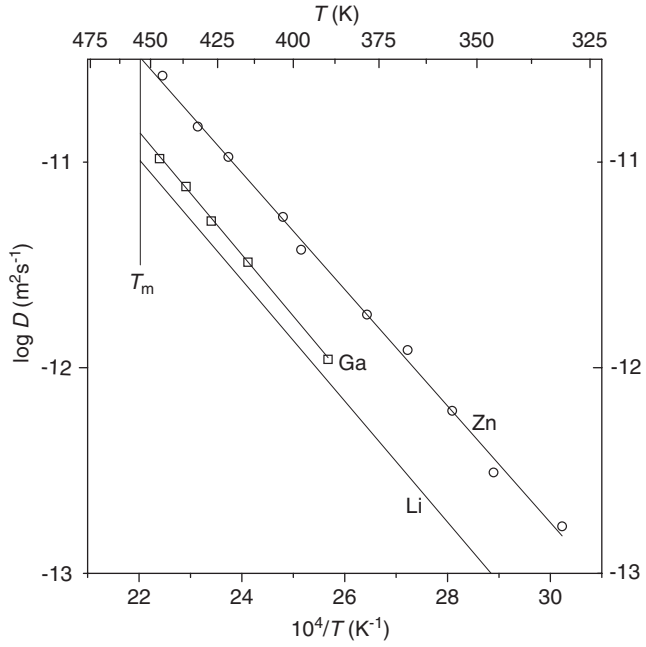

Fig. 11.06 Impurity diffusion in lithium. Ga in Li: □, Ott [11.16]; Zn in Li: ○, Mundy [11.20]; Li in Li according to [11.10] ($D^0 = 0.31 \times 10^{-4}\,m^2\,s^{-1}$, $Q = 0.584$ eV).

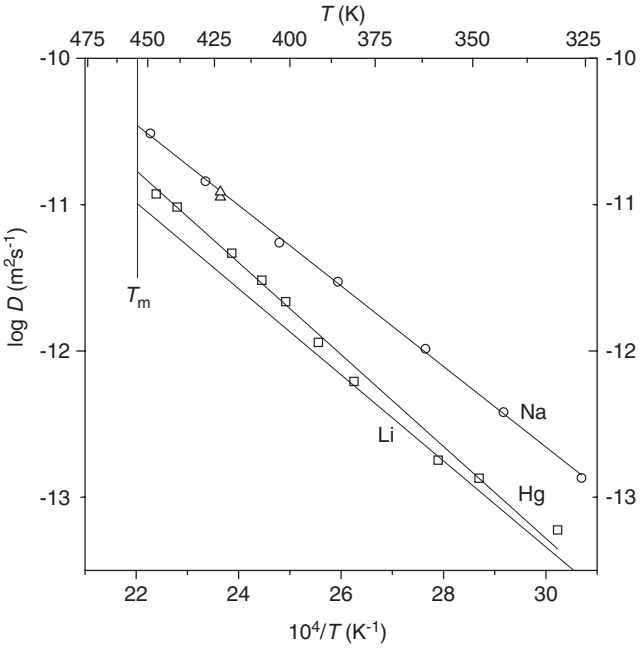

Fig. 11.07 Impurity diffusion in lithium. Hg in Li: □, Ott [11.16]; Na in Li: ○, Mundy [11.19]; △, Mundy [11.13]; Li in Li according to [11.10] ($D^0 = 0.31 \times 10^{-4}\,m^2\,s^{-1}$, $Q = 0.584\,eV$).

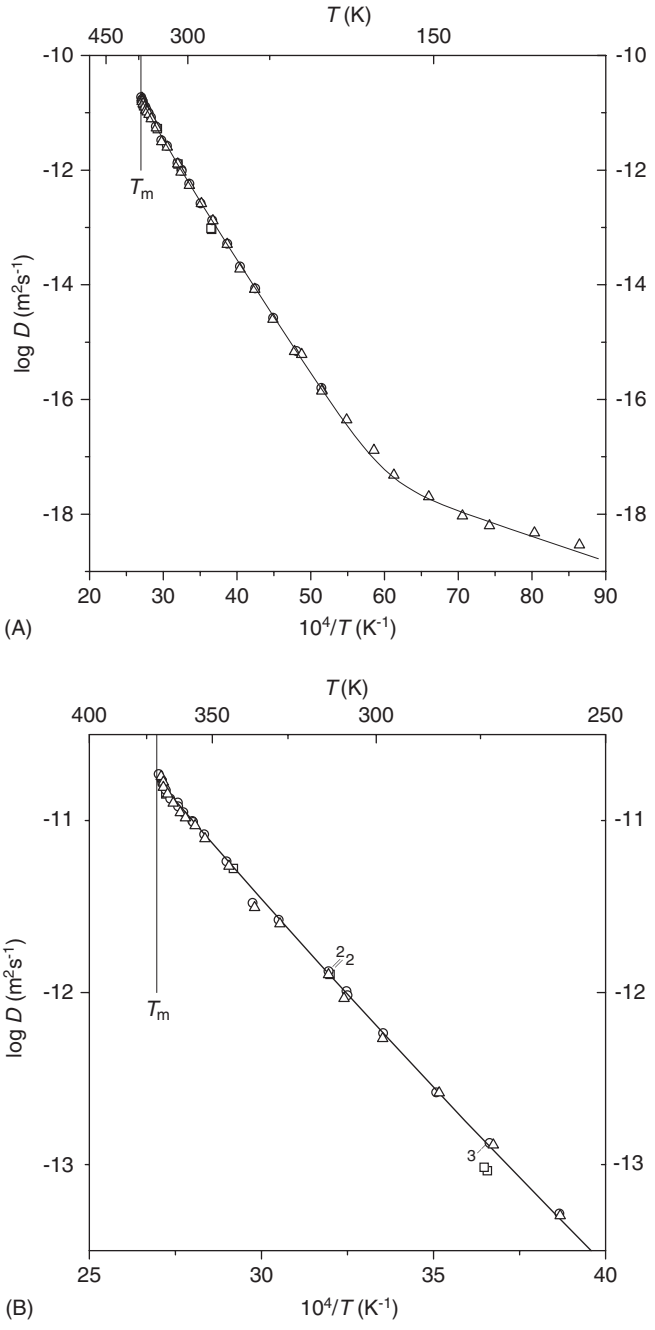

Fig. 12.01 (A) Self-diffusion in sodium. □, Nachtrieb [12.01]; ○, Mundy [12.03]; △, Neumann [12.06]. Three-exponential fit according to Neumann [12.06]. (B) (Detail). Self-diffusion in sodium. □, Nachtrieb [12.01]; ○, Mundy [12.03]; △, Neumann [12.06]. Two-exponential fit according to Neumann [12.05].

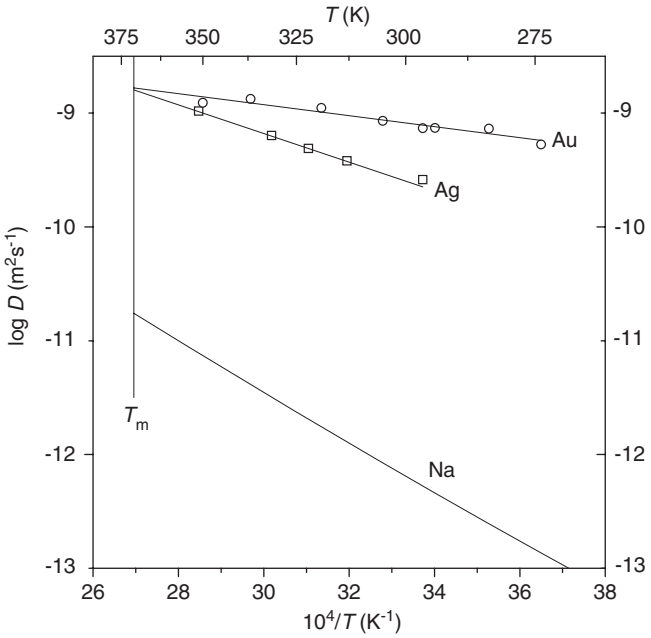

Fig. 12.02 Impurity diffusion in sodium. Ag in Na: □, Barr [12.07]; Au in Na: ○, Barr [12.08].

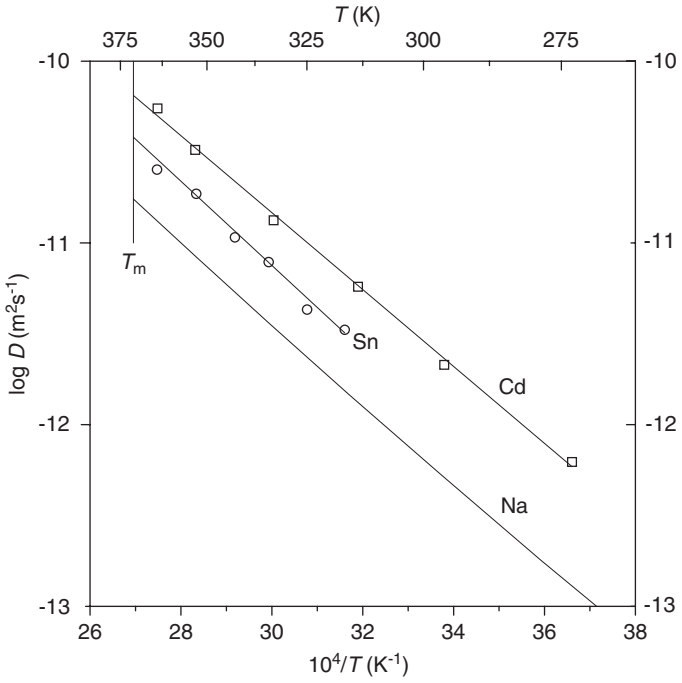

Fig. 12.03 Impurity diffusion in sodium. Cd in Na: □, Barr [12.07]; Sn in Na: ○, Barr [12.07].

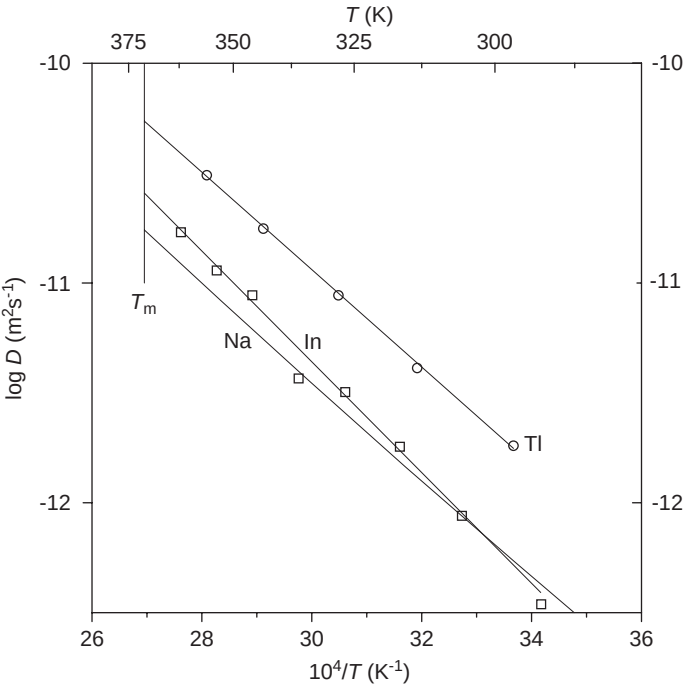

Fig. 12.04 Impurity diffusion in sodium. In in Na: □, Barr [12.07]; Tl in Na: ○, Barr [12.07].

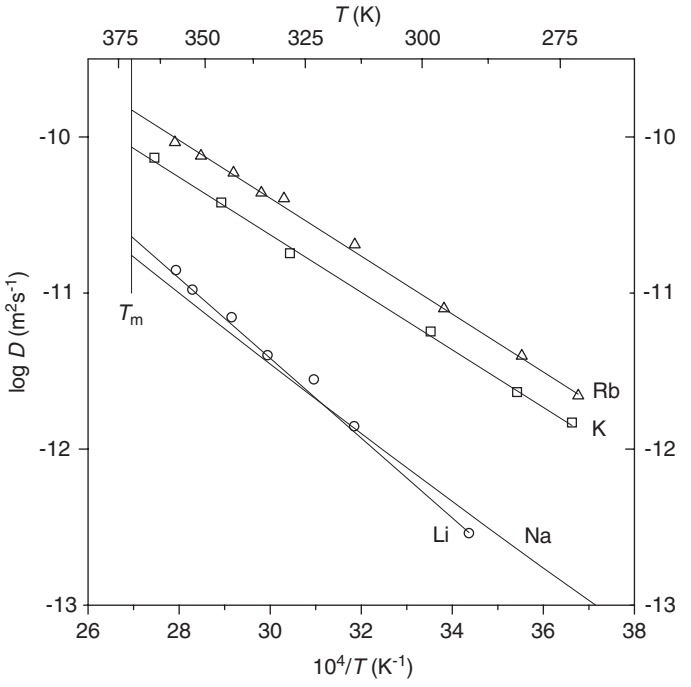

Fig. 12.05 Impurity diffusion in sodium. K in Na: □, Barr [12.09]; Li in Na: ○, Naumov [12.10]; Rb in Na: △, Barr [12.09].

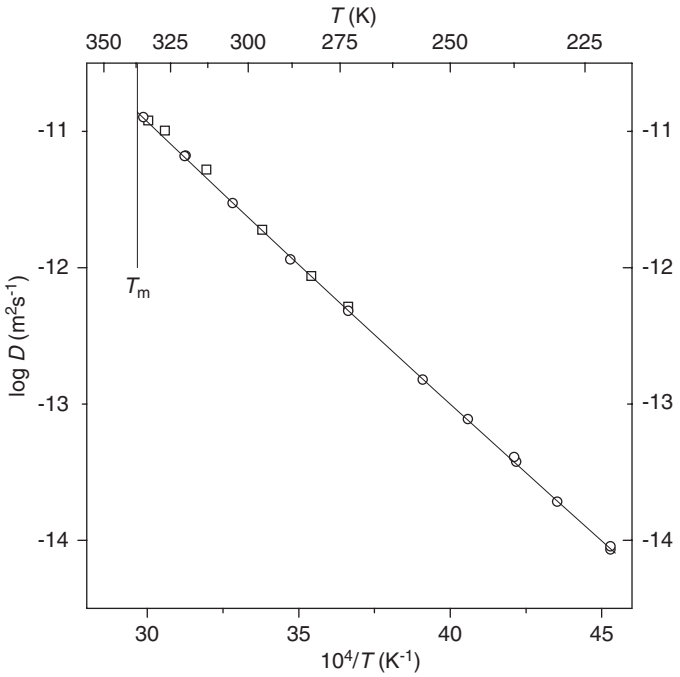

Fig. 13.01 Self-diffusion in potassium. □, Mundy [13.01]; ○, Mundy [13.02]. Two-exponential fit according to [13.02].

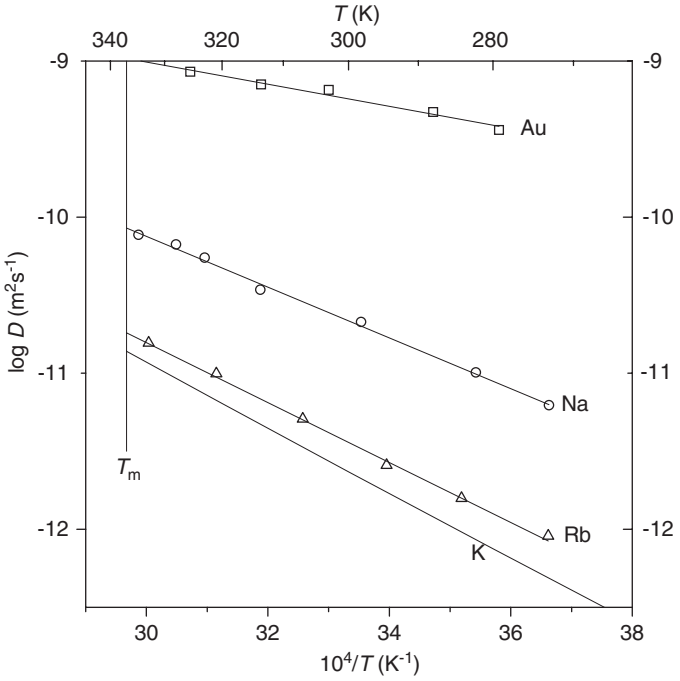

Fig. 13.02 Impurity diffusion in potassium. Au in K: □, Smith [13.03]; Na in K: ○, Barr [13.04]; Rb in K: △, Smith [13.05].

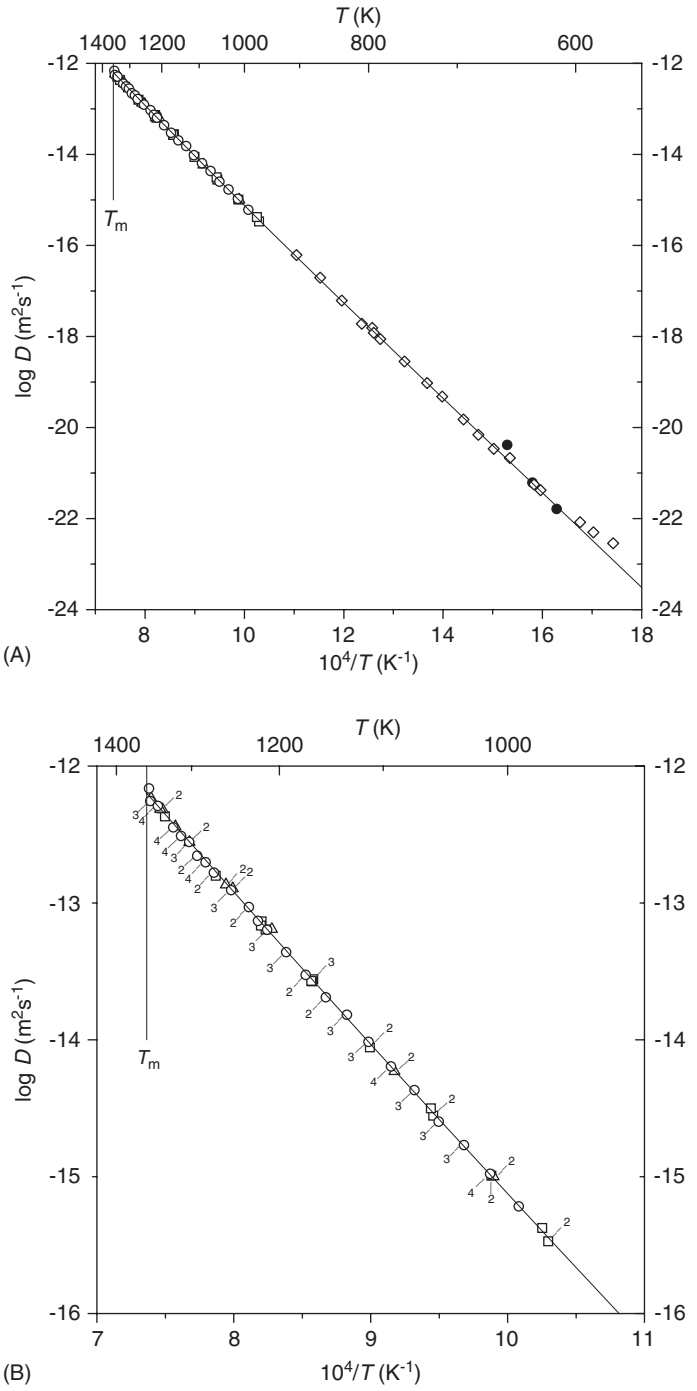

Fig. 14.01 (A) Self-diffusion in copper. □, Rothman [14.04]; ●, Lam [14.09]; ◇, Maier [14.11]; △, Bartdorff [14.12]; ○, Fujikawa [14.14]. Fitting line according to [14.12]. (B) (Detail) Self-diffusion in copper. □, Rothman [14.04]; △, Bartdorff [14.12]; ○, Fujikawa [14.14].

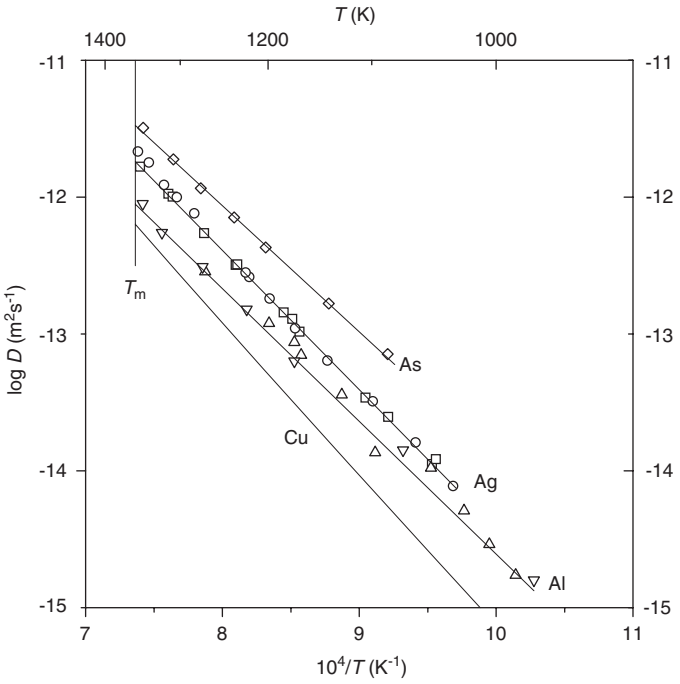

Fig. 14.02 Impurity diffusion in copper. Ag in Cu: □, Gorbachev [14.18]; ○, Krautheim [14.19]. Fitting line according to [14.18]. Al in Cu: △, Oikawa [14.20]; ▽, Fogelson [14.21]. Fitting line estimated ($D^0 = 0.11 \times 10^{-4} m^2 s^{-1}$, $Q = 1.906$ eV). As in Cu: ◇, Klotsman [14.22].

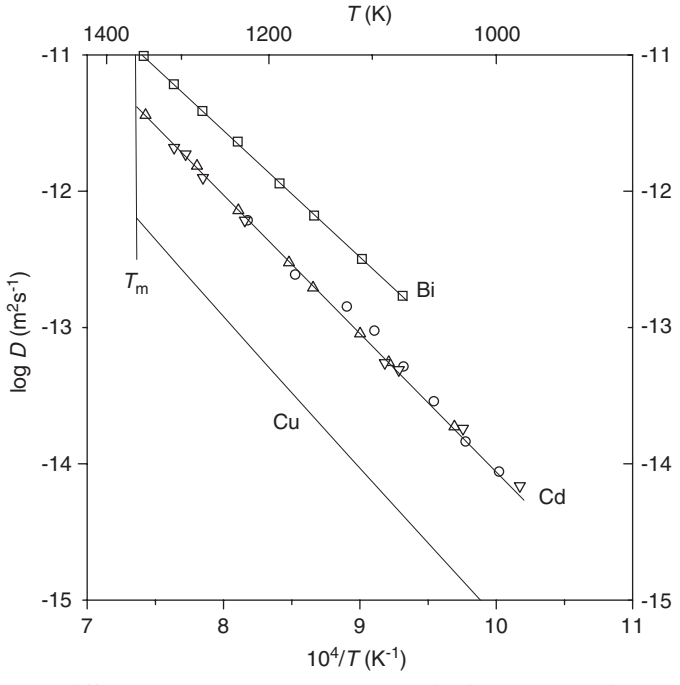

Fig. 14.03 Impurity diffusion in copper. Bi in Cu: □, Gorbachev [14.24]; Cd in Cu: ○, Hirone [14.30]; Δ, Gorbachev [14.18]; ▽, Hoshino [14.31]. Fitting line according to [14.18].

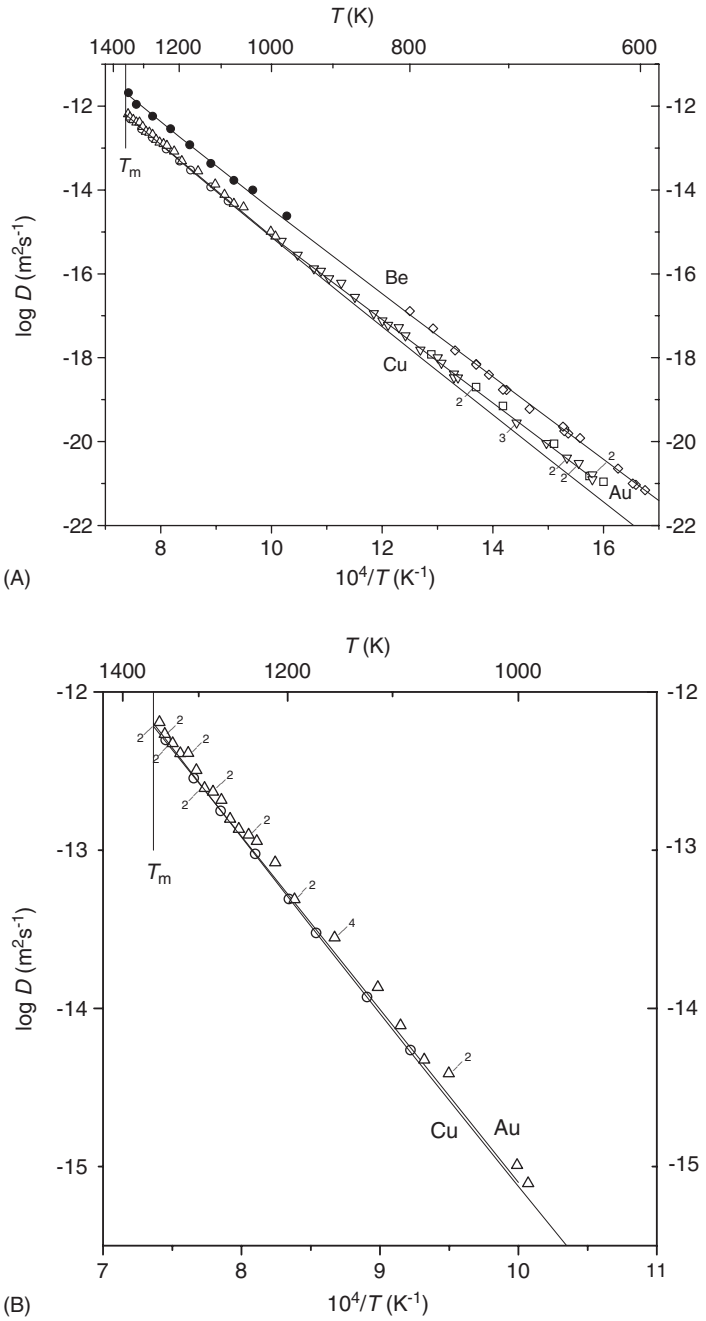

Fig. 14.04 (A) Impurity diffusion in copper. Au in Cu: □, Sippel [14.23]; ○, Gorbachev [14.24]; ∇, Fujikawa [14.27]; △, Fujikawa [14.25, 14.26]. Fitting line according to [14.24, 14.27]. Be in Cu: ●, Fogelson [14.28]; ◇, Almazouzi [14.29]. Fitting line according to [14.29]. (B) (Detail) Impurity diffusion in copper. Au in Cu: ○, Gorbachev [14.24]; △, Fujikawa [14.25, 14.26].

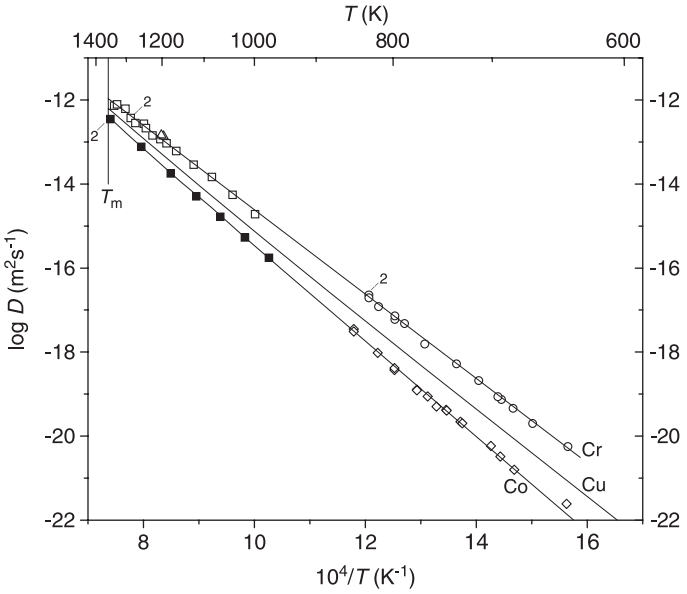

Fig. 14.05 Impurity diffusion in copper. Co in Cu: ■, Mackliet [14.32]; ◇, Döhl [14.33]. Fitting line according to Neumann [14.34]. Cr in Cu: □, Hoshino [14.35]; △, Rockosch [14.36]; ○, Almazouzi [14.37]. Fitting line according to [14.37].

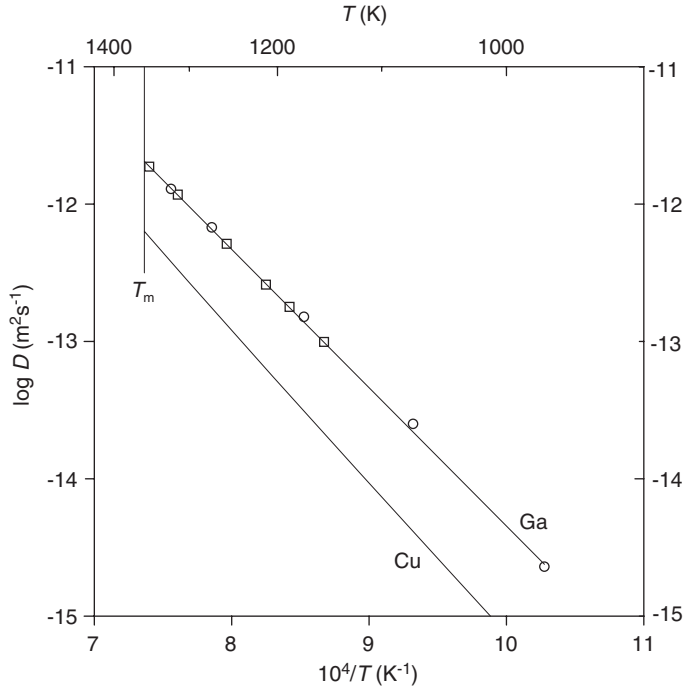

Fig. 14.06 Impurity diffusion in copper. Ga in Cu: □, Klotsman [14.43]; ○, Fogelson [14.44]. Fitting line according to [14.43].

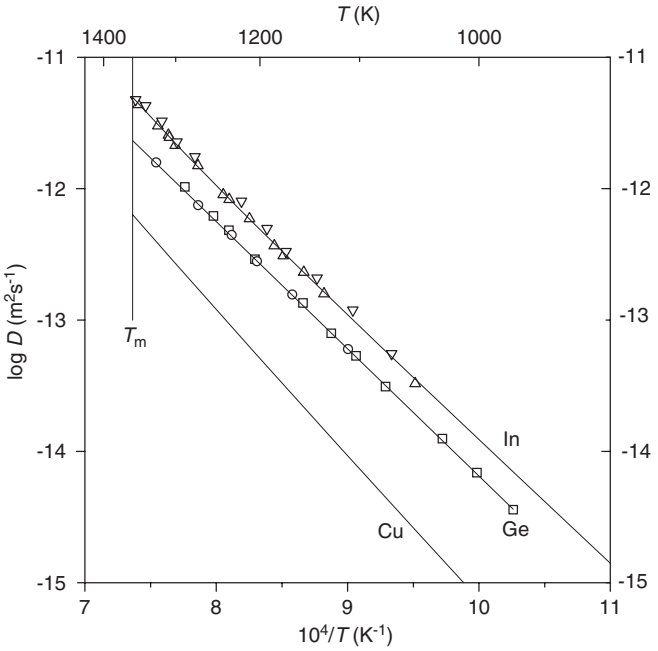

Fig. 14.07 Impurity diffusion in copper. Ge in Cu: □, Reinke [14.45]; ○, Klotsman [14.43]. Fitting line according to [14.43]. In in Cu: △, Gorbachev [14.18]; ∇, Krautheim [14.46]. Fitting line according to Neumann [14.34].

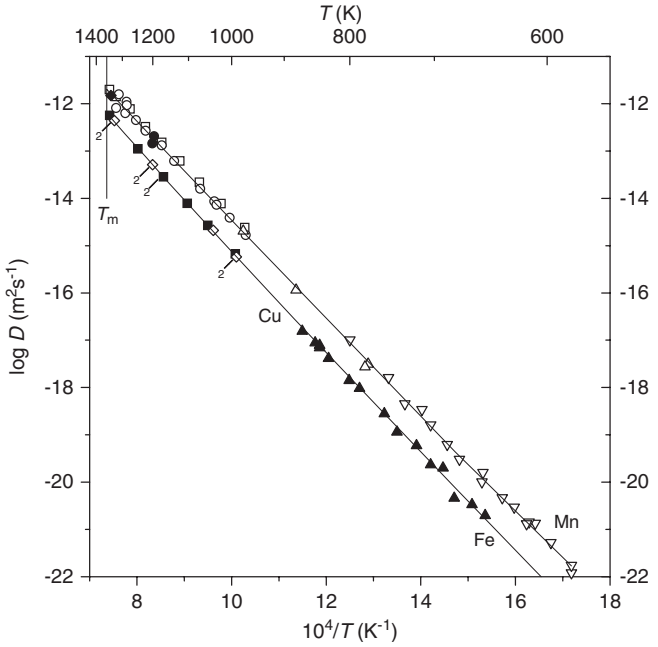

Fig. 14.08 Impurity diffusion in copper. Fe in Cu: ■, Mackliet [14.32]; ◇, Mullen [14.38]; ▲, Almazouzi [14.42]. Fitting line according to [14.42]. (The fitting lines of Fe and Cu nearly coincide.) Mn in Cu: □, Fogelson [14.49]; ○, Hoshino [14.35]; △, Maier [14.50]; ●, Rockosch [14.36]; ∇, Almazouzi [14.37]; ♦, Mackliet [14.32]. Fitting line according to [14.37].

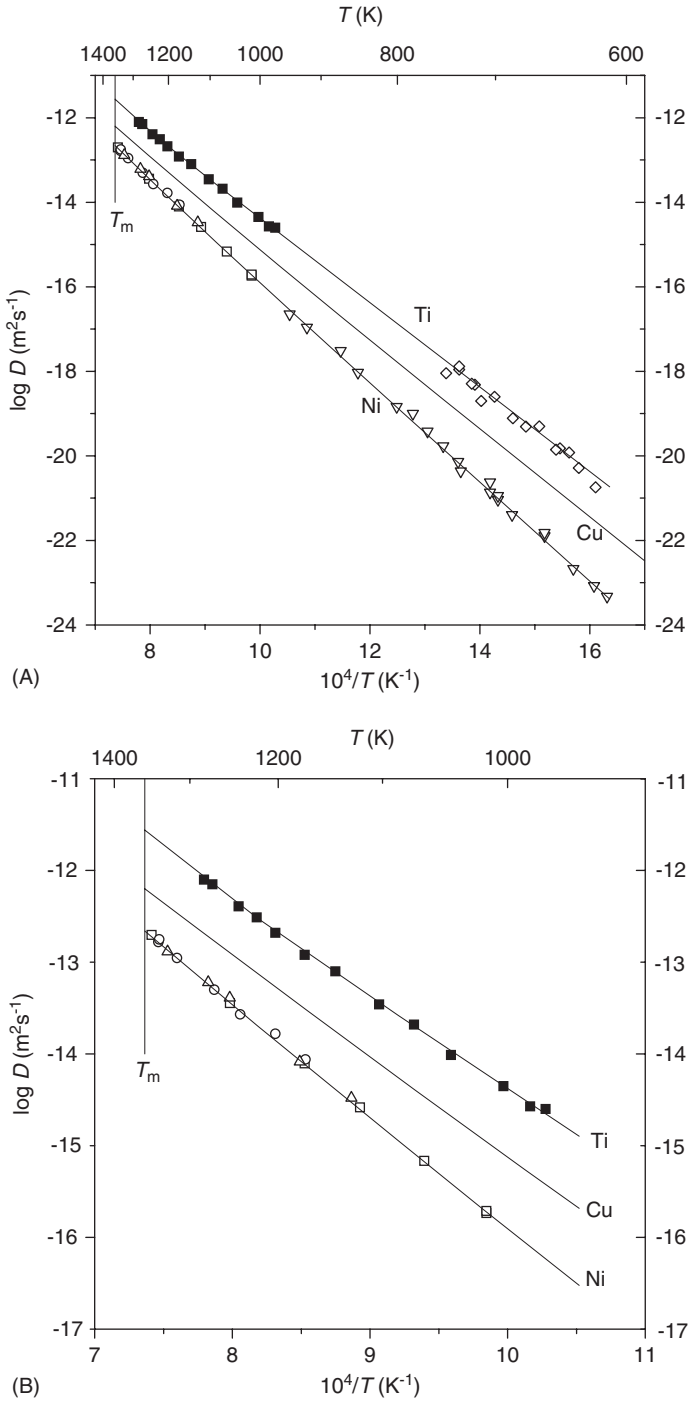

Fig. 14.09 (A) Impurity diffusion in copper. Ni in Cu: □, Mackliet [14.32]; ○, Monma [14.02]; △, Anusavice [14.08]; ▽, Almazouzi [14.42]. Fitting line according to [14.42]. Ti in Cu: ■, Iijima [14.66]; ◇, Almazouzi [14.37]. Fitting line according to [14.37]. (B) (Detail) Impurity diffusion in copper. Ni in Cu: □, Mackliet [14.32]; ○, Monma [14.02]; △, Anusavice [14.08]. Ti in Cu: ■, Iijima [14.66].

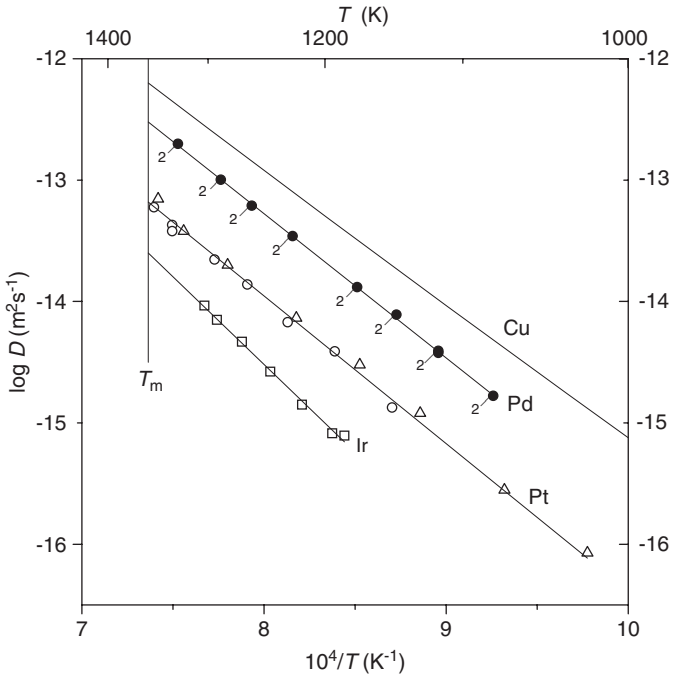

Fig. 14.10 Impurity diffusion in copper. Ir in Cu: □, Klotsman [14.48]. Pd in Cu: ●, Peterson [14.55]. Pt in Cu: △, Fogelson [14.56]; ○, Neumann [14.57]. Fitting line estimated ($D^0 = 0.61 \times 10^{-4}\,m^2\,s^{-1}$, $Q = 2.415\,eV$).

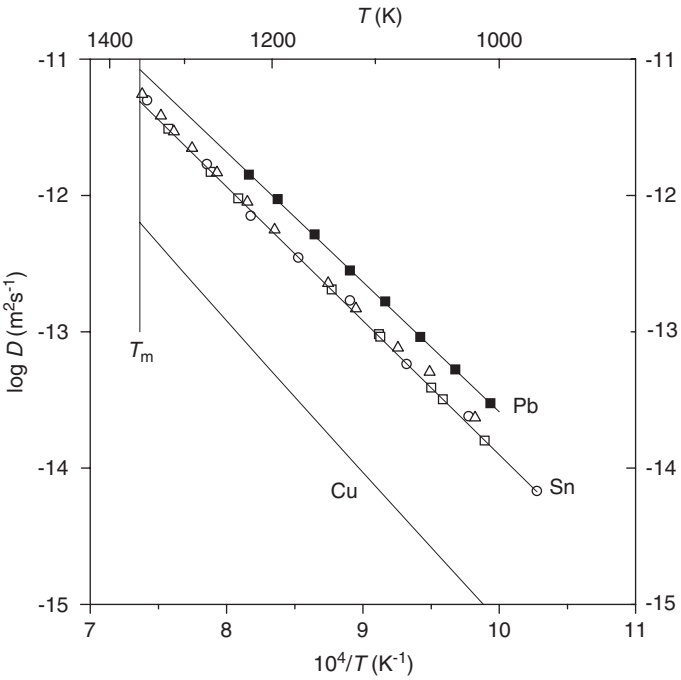

Fig. 14.11 Impurity diffusion in copper. Pb in Cu: ■, Gorbachev [14.24]. Sn in Cu: □, Gorbachev [14.62]; ○, Fogelson [14.65]; △, Krautheim [14.63]. Fitting line according to [14.62].

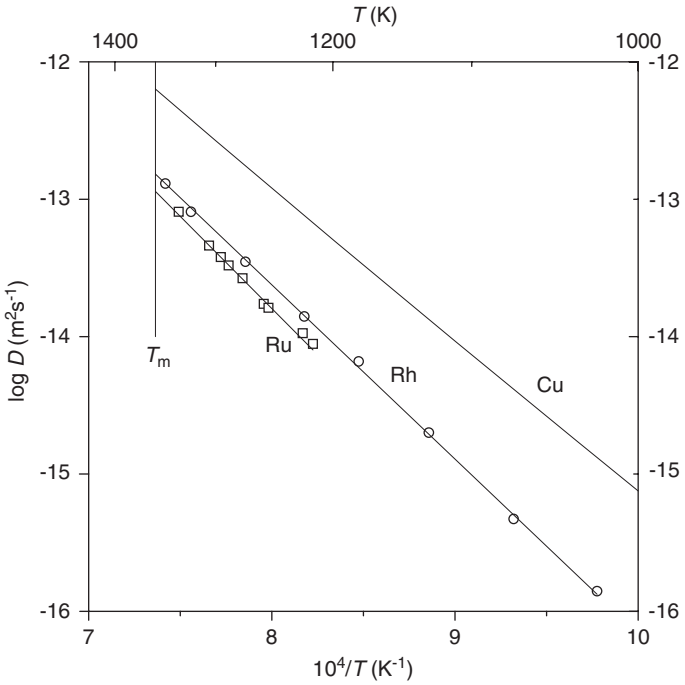

Fig. 14.12 Impurity diffusion in copper. Rh in Cu: ○, Fogelson [14.58]. Ru in Cu: □, Bernardini [14.40].

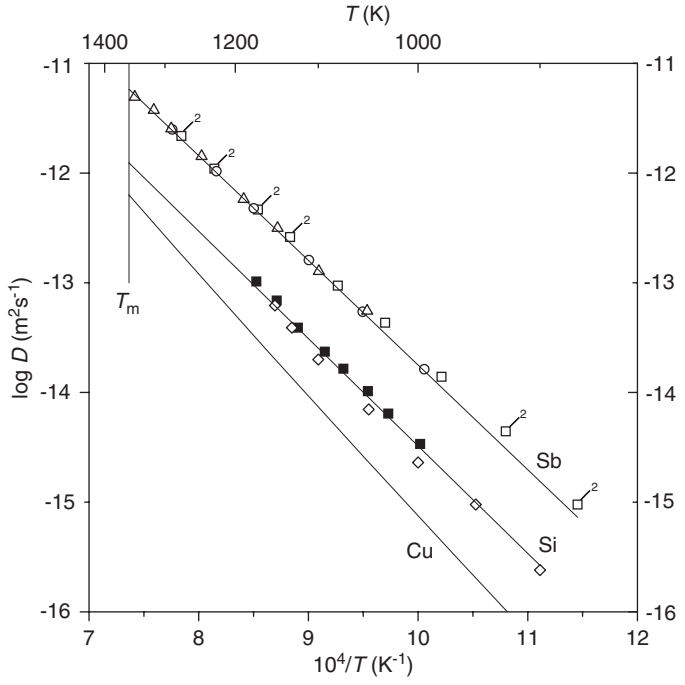

Fig. 14.13 Impurity diffusion in copper. Sb in Cu: □, Inman [14.61]; ○, Gorbachev [14.62]; △, Krautheim [14.63]. Fitting line according to [14.62]. Si in Cu: ■, Minamino [14.65]; ◇, Iijima [14.66]. Fitting line using $D^0 = 0.2 \times 10^{-4}\,\mathrm{m^2\,s^{-1}}$, $Q = 1.942\,\mathrm{eV}$.

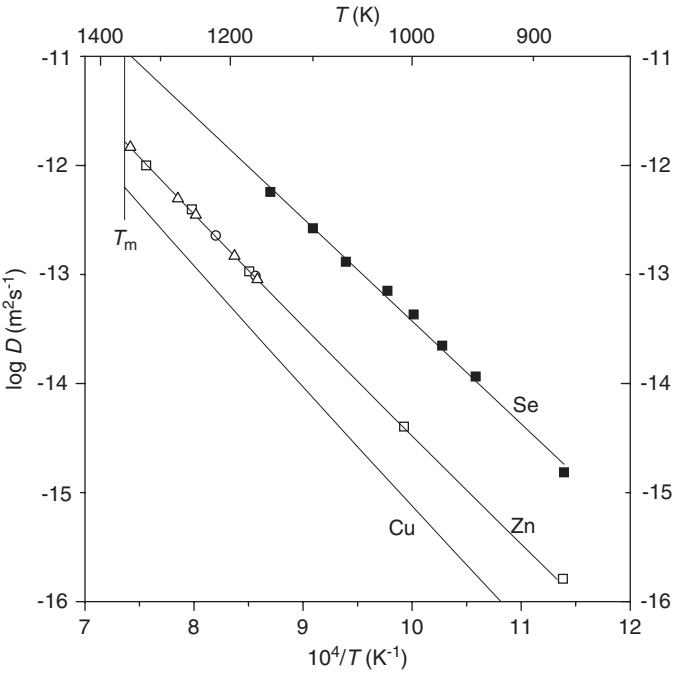

Fig. 14.14 Impurity diffusion in copper. Se in Cu: ■, Rummel [14.64]. Zn in Cu: □, Hino [14.68]; ○, Peterson [14.69]; △, Klotsman [14.70]. Approximative fitting line using $D^0 = 0.54 \times 10^{-4}\,m^2\,s^{-1}$, $Q = 2.03\,eV$.

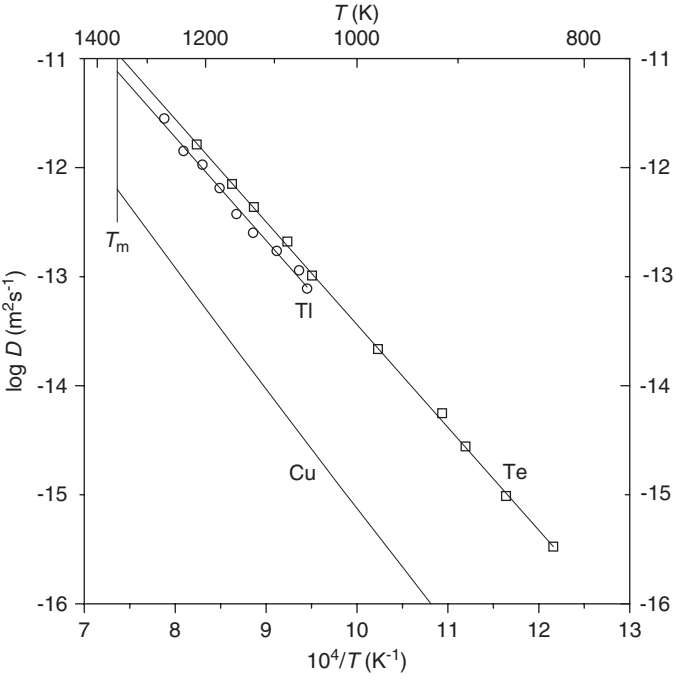

Fig. 14.15 Impurity diffusion in copper. Te in Cu: □, Rummel [14.64]. Tl in Cu: ○, Komura [14.67].

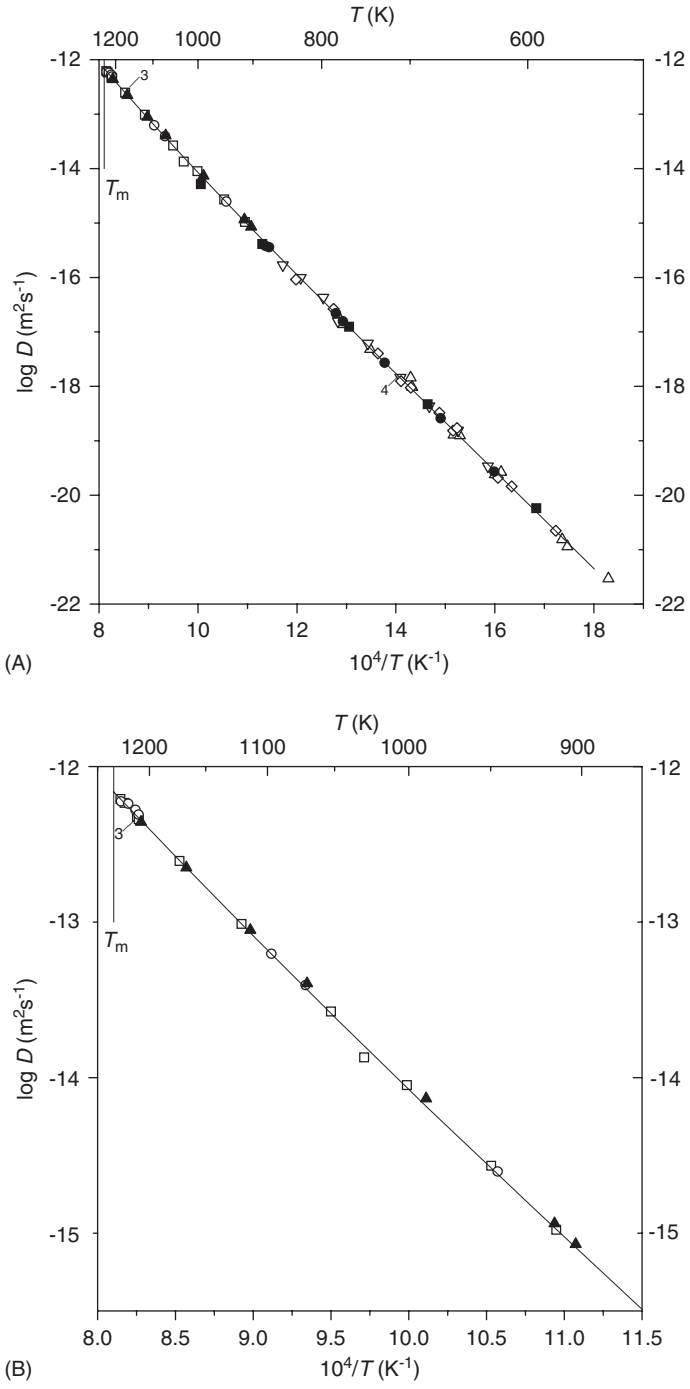

Fig. 15.01 (A) Self-diffusion in silver. ▲, Tomizuka [15.01]; □, Rothman [15.03]; ○, Reimers [15.04]; Δ, Lam [15.05]; ∇, Backus [15.06]; ◇, Bihr [15.07]; ■, Rein [15.08]; ●, Mehrer [15.09]. Fitting line according to Neumann [15.10]. (B) (Detail) Self-diffusion in silver. ▲, Tomizuka [15.01]; □, Rothman [15.03]; ○, Reimers [15.04]. Fitting line according to Neumann [15.10].

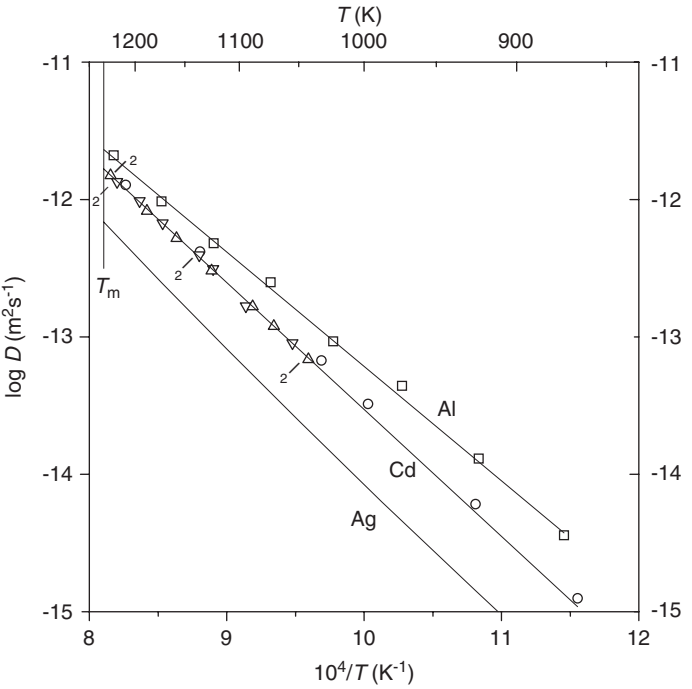

Fig. 15.02 Impurity diffusion in silver. Al in Ag: □, Fogelson [15.11]. Cd in Ag: ○, Tomizuka [15.16]; Δ, (serial sectioning) and ∇, (residual activity) Kaygorodov [15.17]. Fitting line according to [15.17].

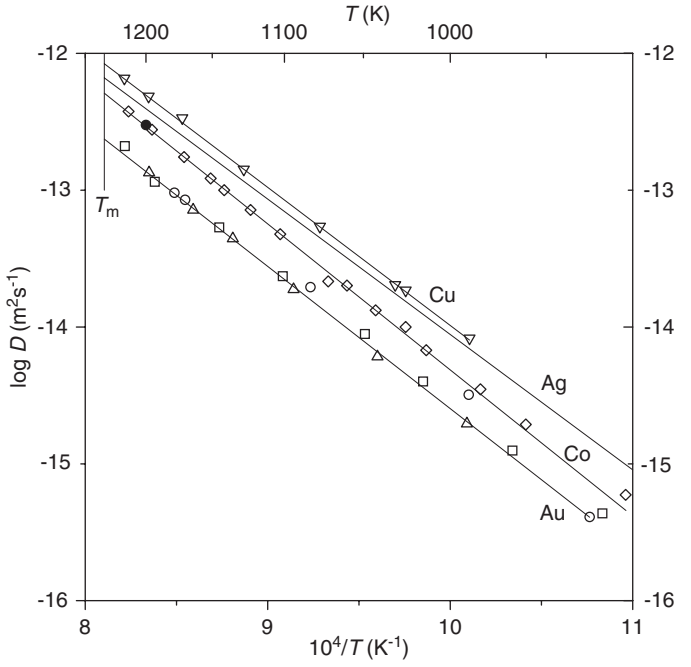

Fig. 15.03 Impurity diffusion in silver. Au in Ag: □, Jaumot [15.13]; ○, Mead [15.14]; Δ, Mallard [15.15]. Fitting line estimated ($D^0 = 0.62 \times 10^{-4}\,m^2\,s^{-1}$, $Q = 2.061\,eV$). Co in Ag: ◇, Bernardini [15.19]; ●, Lundy [15.18]. Fitting line according to [15.19]. Cu in Ag: ∇, Sawatzky [15.22].

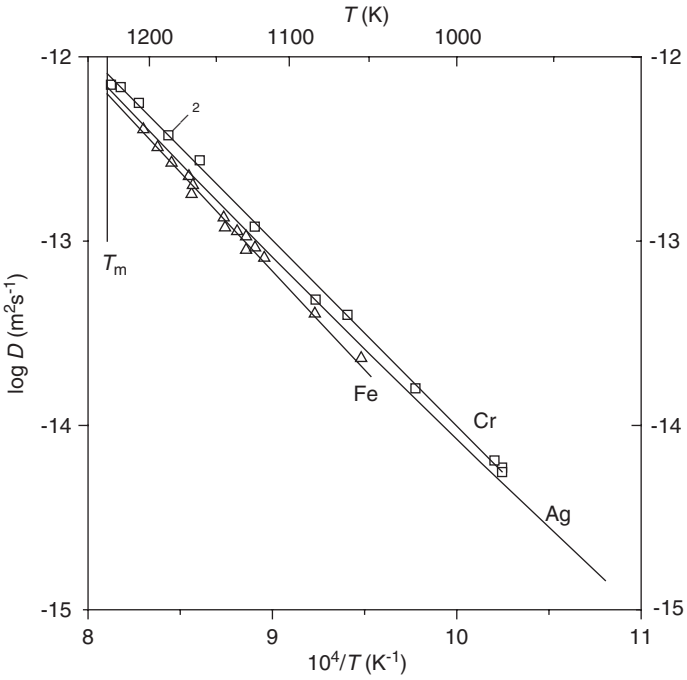

Fig. 15.04 Impurity diffusion in silver. Cr in Ag: □, Neumann [15.21]. Fe in Ag: Δ, Bernardini [15.19].

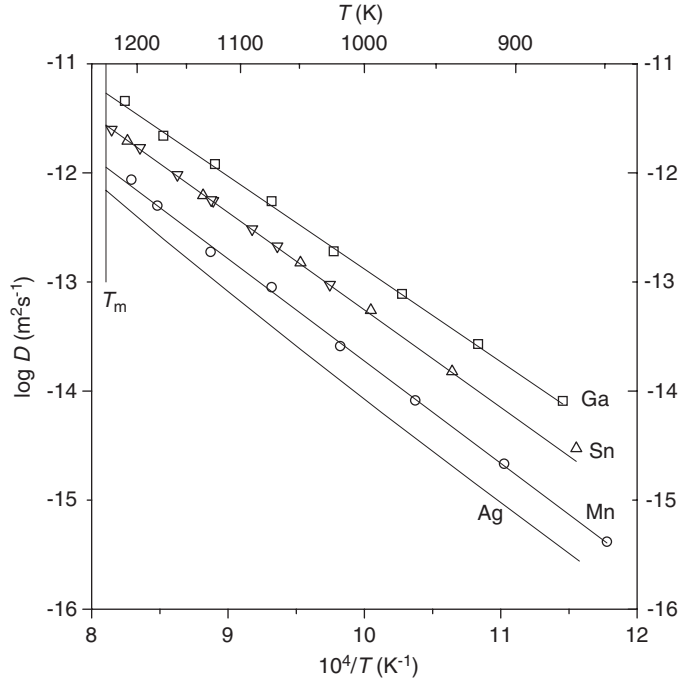

Fig. 15.05 Impurity diffusion in silver. Ga in Ag: □, Fogelson [15.26]; Mn in Ag: ○, Barclay [15.30]; Sn in Ag: △, Tomizuka [15.16]; ∇, Kaygorodov [15.45]. Fitting line according to [15.45].

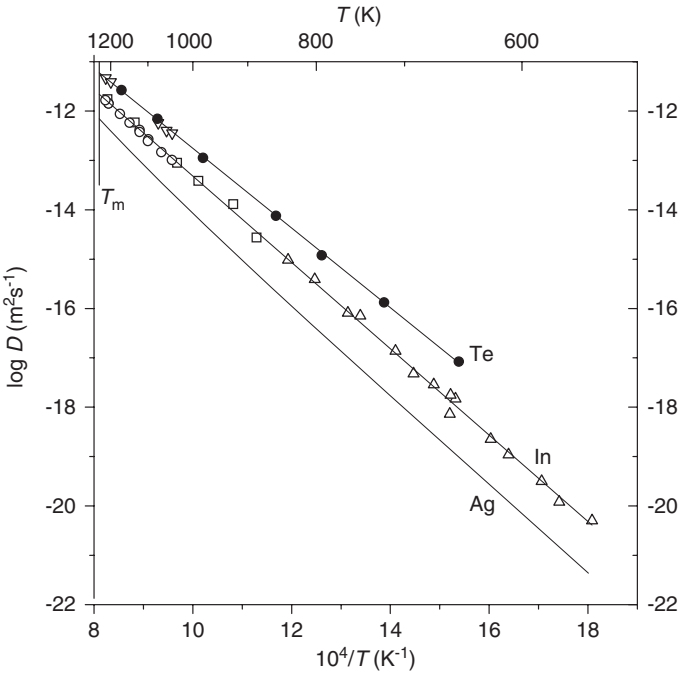

Fig. 15.06 Impurity diffusion in silver. In in Ag: □, Tomizuka [15.16]; ○, Kaygorodov [15.28]; △, Mehrer [15.29]. Fitting line: forced fit. Te in Ag: ▽, Kaygorodov [15.45]; ●, Geise [15.46]. Fitting line according to [15.46].

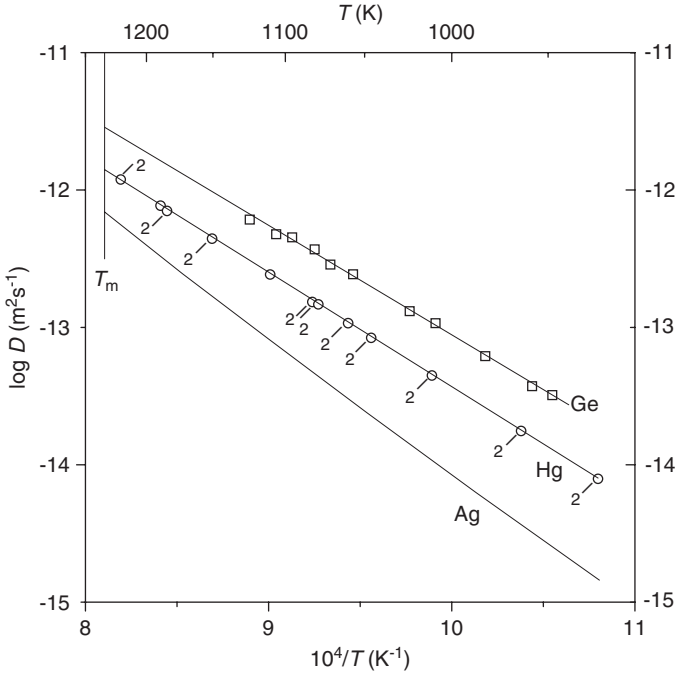

Fig. 15.07 Impurity diffusion in silver. Ge in Ag: □, Hoffmann [15.27]. Hg in Ag: ○, Sawatzky [15.22].

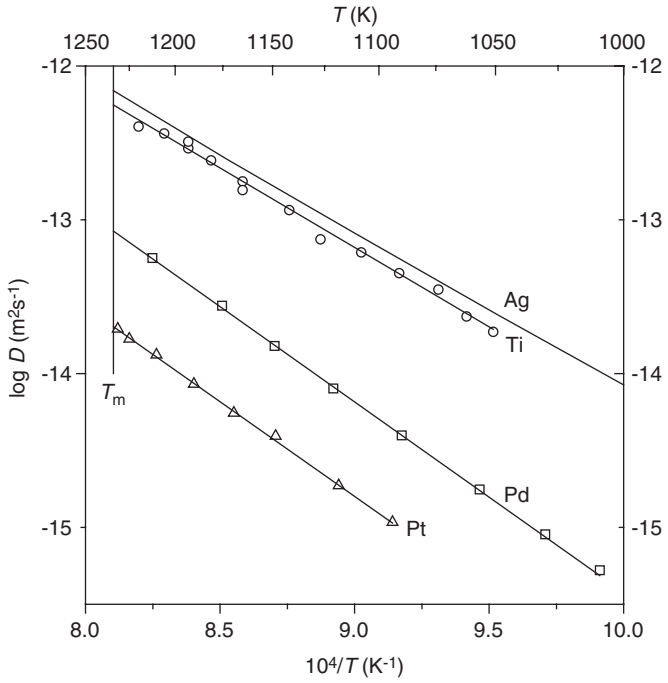

Fig. 15.08 Impurity diffusion in silver. Pd in Ag: □, Peterson [15.35]; Ti in Ag: ○, Makuta [15.20]; Pt in Ag: Δ, Neumann [15.37].

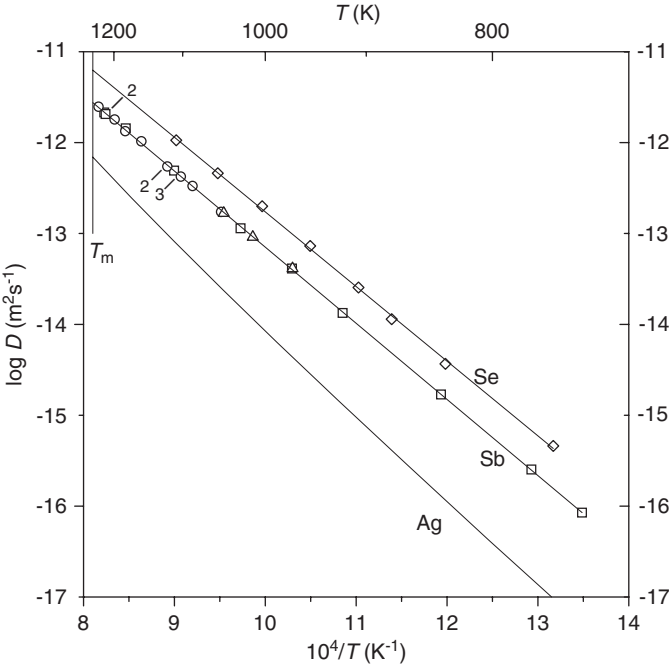

Fig. 15.09 Impurity diffusion in silver. Sb in Ag: □, Sonder [15.41]; ○, Kaygorodov [15.42]; Δ, Hagenschulte [15.43]. Fitting line according to [15.41]. Se in Ag: ◇, Rummel [15.44].

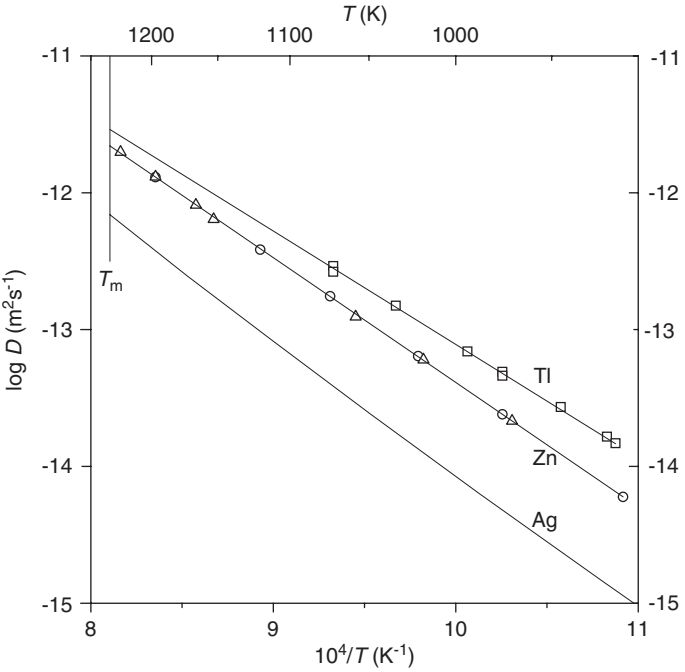

Fig. 15.10 Impurity diffusion in silver. Tl in Ag: □, Hoffmann [15.27]. Zn in Ag: ○, Sawatzky [15.47]; Δ, Rothman [15.48]. Fitting line according to [15.47, 15.48].

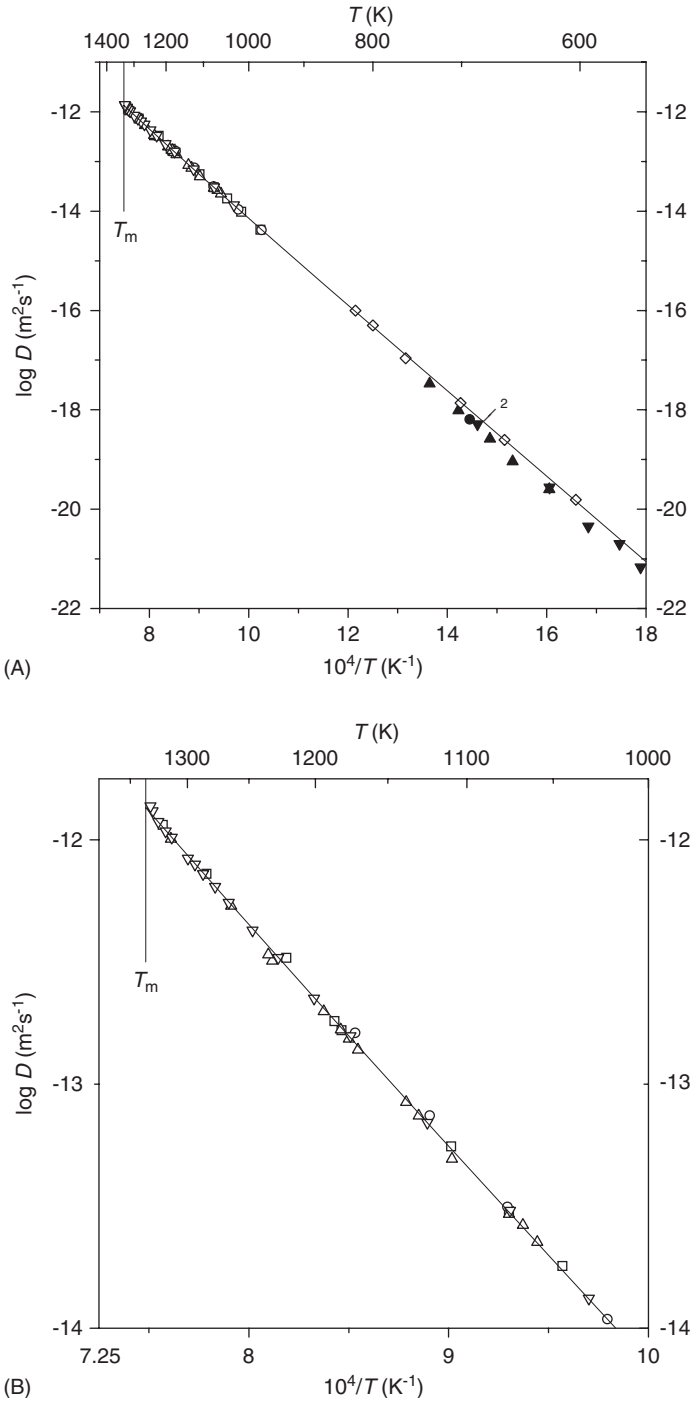

Fig. 16.01 (A) Self-diffusion in gold. □, Makin [16.01]; ○, Duhl [16.02]; ▲, Gainotti [16.04]; ▼, Rupp [16.06]; Δ, Dreyer [16.07]; ∇, Herzig [16.08]; ●, Rein [16.09]; ◇, Werner [16.10]. Fitting line: two-exponential fit according to Neumann [16.11]. (B) (Detail) Self-diffusion in gold. □, Makin [16.01]; ○, Duhl [16.02]; Δ, Dreyer [16.07]; ∇, Herzig [16.08]. Fitting line: two-exponential fit according Neumann [16.11].

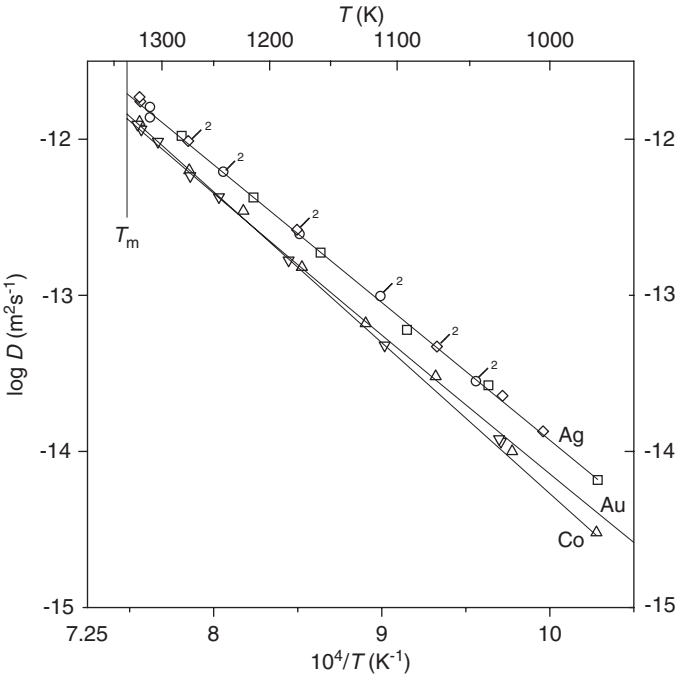

Fig. 16.02 Impurity diffusion in gold. Ag in Au: □, Mallard [16.12]; ○, Klotsmann [16.13]; ◇, Herzig [16.14]. Fitting line according to [16.13]. Co in Au: Δ, Fogelson [16.16]; ∇, Herzig [16.08]. Fitting line according to [16.08].

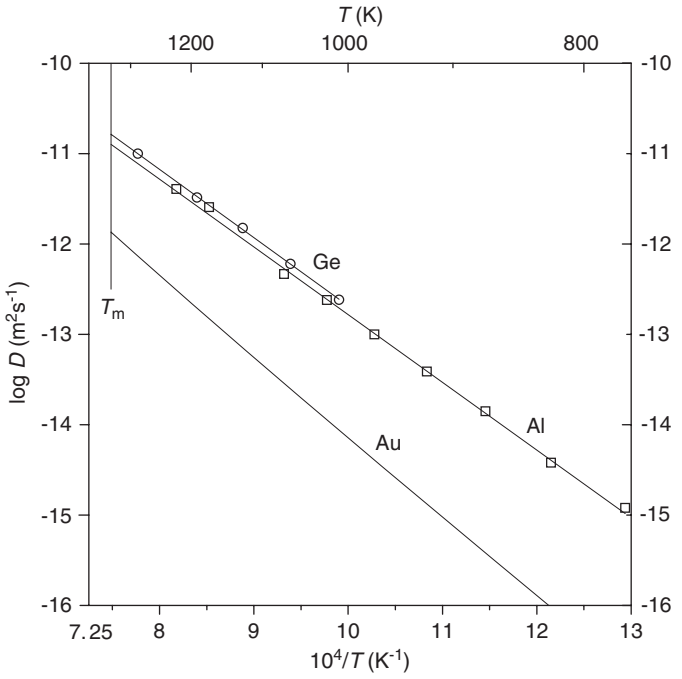

Fig. 16.03 Impurity diffusion in gold. Al in Au: □, Fogelson [16.15]. Ge in Au: ○, Cardis [16.19].

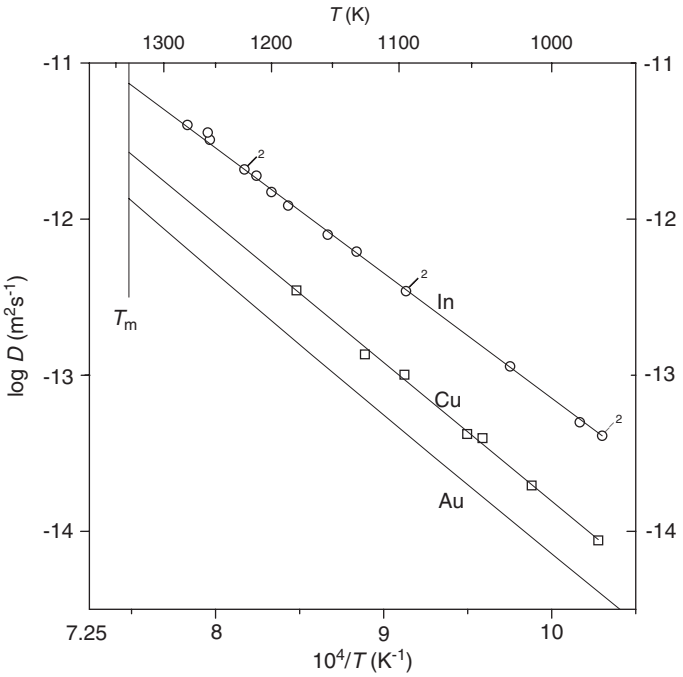

Fig. 16.04 Impurity diffusion in gold. Cu in Au: □, Vignes [16.18]. In in Au: ○, Dreyer [16.07].

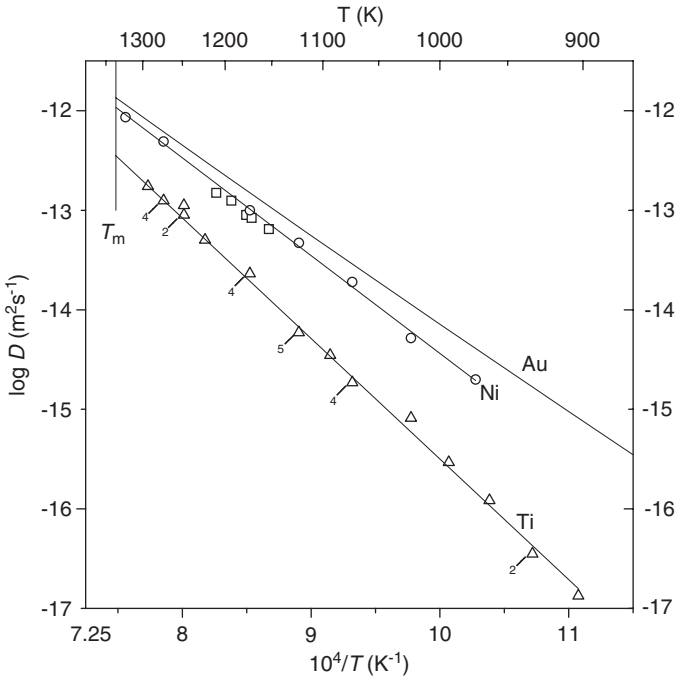

Fig. 16.05 Impurity diffusion in gold. Ni in Au: □, Reynolds [16.21]; ○, Fogelson [16.22]. Fitting line according to [16.22]. Ti in Au: Δ, Richter [16.17]. Fitting line according to present recalculation ($D^0 = 4.1 \times 10^{-4}\,m^2\,s^{-1}$, $Q = 2.403\,eV$).

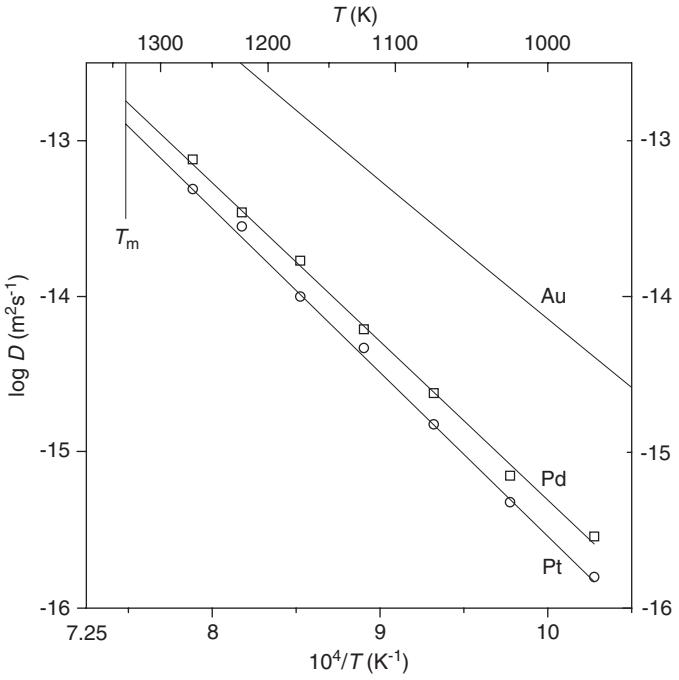

Fig. 16.06 Impurity diffusion in gold. Pd in Au: □, Fogelson [16.23]. Pt in Au: ○, Fogelson [16.23].

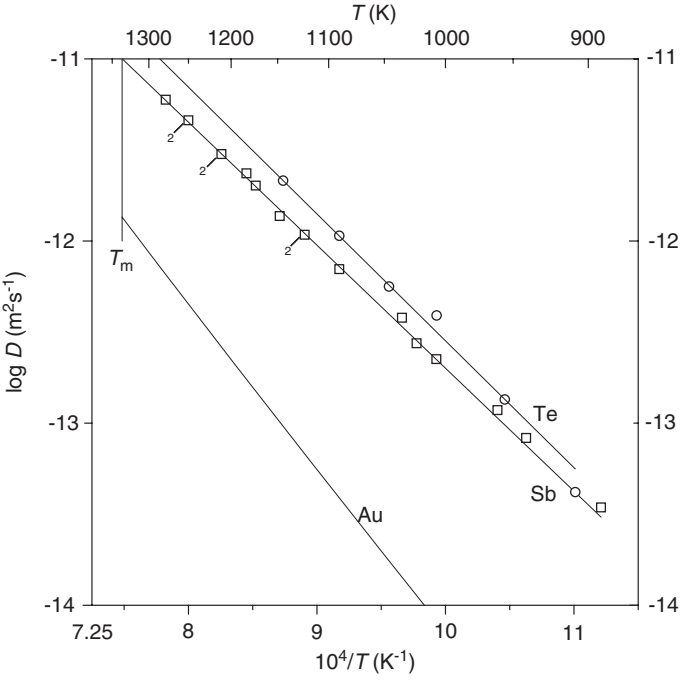

Fig. 16.07 Impurity diffusion in gold. Sb in Au: □, Herzig [16.24]; Te in Au: ○, Rummel [16.26].

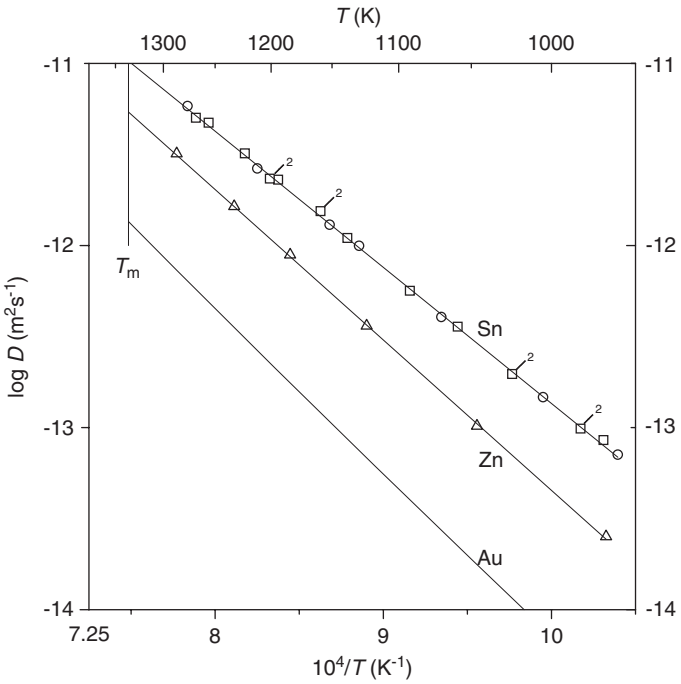

Fig. 16.08 Impurity diffusion in gold. Sn in Au: □, EPMA and ○, tracer Herzig [16.25]. Zn in Au: Δ, Cardis [16.19].

REFERENCES

References to Chapter 1.1

[11.01] D.F. Holcomb, R.E. Norberg, Phys. Rev. **98** (1955) 1074.
[11.02] A.N. Naumov, G.Ya. Ryskin, Zh. Tekh. Fiz. **29** (1959) 189; Sov. J. Techn. Phys. **4** (1959) 162 (English transl.).
[11.03] D.C. Ailion, C.P. Slichter, Phys. Rev. **137** (1965) A 235.
[11.04] A. Lodding, J.N. Mundy, A. Ott, Phys. Stat. Sol. **38** (1970) 559.
[11.05] M. Weithase, F. Noack, Phys. Stat. Sol. (b) **57** (1973) K111.
[11.06] R. Messer, F. Noack, Appl. Phys. **6** (1975) 79.
[11.07] R. Messer, in: *Magnetic Resonance and Related Phenomena*, Proc. 19th Congress Ampère, Heidelberg, Ed. H. Brunner, Heidelberg Groupement Ampère (1976), p. 269.
[11.08] P. Heitjans, A. Körblein, H. Ackermann, D. Dubbers, F. Fujara, H.J. Stöckmann, J. Phys. F: Metal Phys. **15** (1985) 41.
[11.09] M. Mali, J. Roos, M. Sonderegger, D. Brinkmann, P. Heitjans, J. Phys. F: Metal Phys. **18** (1988) 403.
[11.10] R. Messer, A. Seeger, K. Zick, Z. Metallk. **80** (1989) 299.
[11.11] O. Wieland, H.D. Carstanjen, Defect and Diffusion Forum **194–199** (2001) 35.
[11.12] A. Ott, A. Nordén-Ott, Z. Naturforsch. (23a) (1968) 473.
[11.13] J.N. Mundy, W.D. McFall, Phys. Rev. B **7** (1973) 4363.

[11.14] A. Ott, J. Appl. Phys. **42** (1971) 2999.
[11.15] A. Ott, A. Lodding, D. Lazarus, Phys. Rev. **188** (1969) 1088.
[11.16] A. Ott, Z. Naturforsch. **25a** (1970) 1477.
[11.17] J.N. Mundy, W.D. McFall, Phys. Rev. B **8** (1973) 5477.
[11.18] A. Ott, Z. Naturforsch. **23a** (1968) 2126.
[11.19] J.N. Mundy, A. Ott, L. Löwenberg, A. Lodding, Z. Naturforsch. **22a** (1967) 2113.
[11.20] J.N. Mundy, A. Ott, L. Löwenberg, A. Lodding, Phys. Stat. Sol. **35** (1969) 359.

Further Investigations

Li [11.21] R.A. Hultsch, R.G. Barnes, Phys. Rev. **125** (1962) 1832; NMR
Li [11.22] A. Ott, J.N. Mundy, L. Löwenberg, A. Lodding, Z. Naturforsch. **23a** (1968) 771.
Li [11.23] J.M. Titman, B.M. Moores, J. Phys. F: Met. Phys. **2** (1972) 592; NMR
Li [11.24] H. Ackermann, D. Dubbers, M. Grupp, P. Heitjans, R. Messer, H.J. Stöckmann, Phys. Stat. Sol. (b) **71** (1975) K91; β-NMR, precursor to Ref. [11.08].
Au [11.25] A. Ott, Z. Naturforsch. **23a** (1968) 1683; precursor to Ref. [11.14].
Cu [11.26] A. Ott, J. Appl. Phys. **40** (1969) 2395.

References to Chapter 1.2

[12.01] N.H. Nachtrieb, E. Catalano, J.A. Weil, J. Chem. Phys. **20** (1952) 1185.
[12.02] D.F. Holcomb, R.E. Norberg, Phys. Rev. **98** (1955) 1074.
[12.03] J.N. Mundy, Phys. Rev. B **3** (1971) 2431.
[12.04] G. Brünger, O. Kanert, D. Wolf, Solid State Comm. **33** (1980) 569.
[12.05] G. Neumann, V. Tölle, Phil. Mag. A **61** (1990) 563.
[12.06] M. Neumann, P. Scharwaechter, A. Seeger, W. Frank, K. Freitag, M. Konuma, G. Majer, Defect and Diffusion Forum **143–147** (1997) 85.
[12.07] L.W. Barr, F.A. Smith, in: DIMETA 82, *Diffusion in Metals and Alloys*, Eds. F.J. Kedves, D.L. Beke, Trans. Tech. Publ., Switzerland (1983), p. 325.
[12.08] L.W. Barr, J.N. Mundy, F.A. Smith, Phil. Mag. **20** (1969) 389.
[12.09] L.W. Barr, J.N. Mundy, F.A. Smith, Phil. Mag. **16** (1967) 1139.
[12.10] A.N. Naumov, Fiz. Tverd. Tela **6** (1964) 2517; Soviet Phys. Solid State **6** (1965) 1997 (English transl.).

Further Investigations

Na [12.11] R.A. Hultsch, R.G. Barnes, Phys. Rev. **125** (1962) 1832; NMR
Na [12.12] L.W. Barr, J.N. Mundy, in: *Diffusion in Body-Centered Cubic Metals*, Eds. J.A. Wheeler, F.R. Winslow, American Society for Metals, Metals Park (1965), p. 171.
Na [12.13] J.N. Mundy, L.W. Barr, F.A. Smith, Phil. Mag. **14** (1966) 785; precursor to Ref. [12.03].
Na [12.14] M. Ait-Salem, T. Springer, A. Heidemannn, B. Alefeld, Phil. Mag. A **39** (1979) 797; QNS.
Na [12.15] G. Göltz, A. Heidemann, H. Mehrer, A. Seeger, D. Wolf, Phil. Mag. A **41** (1980) 723; QNS.
Au [12.16] L.W. Barr, J.N. Mundy, F.A. Smith, Phil. Mag. **14** (1966) 1299; precursor to Ref. [12.08].
Li see Ref. [12.07].

References to Chapter 1.3

[13.01] J.N. Mundy, L.W. Barr, F.A. Smith, Phil. Mag. **15** (1967) 411.
[13.02] J.N. Mundy, T.E. Miller, R.J. Porte, Phys. Rev. B **3** (1971) 2445.
[13.03] F.A. Smith, L.W. Barr, Phil. Mag. **21** (1970) 633.
[13.04] L.W. Barr, J.N. Mundy, F.A. Smith, Phil. Mag. **16** (1967) 1139.
[13.05] F.A. Smith, L.W. Barr, Phil. Mag. **20** (1969) 205.

References to Chapter 1.4

[14.01] A. Kuper, H. Letaw, L. Slifkin, E. Sonder, C.T. Tomizuka, Phys. Rev. **96** (1954) 1224; erratum ibid. **98** (1955) 1870.
[14.02] K. Monma, H. Suto, H. Oikawa, J. Japan Inst. Metals **28** (1964) 192.
[14.03] M. Beyeler, Y. Adda, J. Physique **29** (1968) 345.
[14.04] S.J. Rothman, N.L. Peterson, Phys. Stat. Sol. **35** (1969) 305.
[14.05] U. El-Hanany, D. Zamir, Phys. Rev. **183** (1969).
[14.06] H.G. Bowden, R.W. Balluffi, Phil. Mag. **19** (1969) 1001.
[14.07] J. Kučera, B. Million, Metall. Trans. **1** (1970) 2599.
[14.08] K.J. Anusavice, R.T. DeHoff, Metall. Trans. **3** (1972) 1279.
[14.09] N.Q. Lam, S.J. Rothman, L.J. Nowicki, Phys. Stat. Sol. (a) **23** (1974) K35.
[14.10] M. Weithase, F. Noack, Z. Physik **270** (1974) 319.
[14.11] K. Maier, Phys. Stat. Sol. (a) **44** (1977) 567.
[14.12] D. Bartdorff, G. Neumann, P. Reimers, Phil. Mag. A **38** (1978) 157.
[14.13] G. Krautheim, A. Neidhardt, U. Reinhold, A. Zehe, Kristall und Technik **14** (1979) 1491.
[14.14] S. Fujikawa, K. Hirano, in: *Point Defects and Defect Interactions*, Eds. J. Takamura, M. Doyama, K. Kiritani, The University of Tokyo Press, Tokyo (1982), p. 554; private communication to the authors.
[14.15] S. Ushino, S. Fujikawa, K. Hirano, Res. Rep. Lab. Nucl. Sci., Tohoku Univ. **22** (1989) 204.
[14.16] N.H. Nachtrieb, C.T. Tomizuka, L.G. Schulz, Report AFOSR-TR-60-23, The University of Chicago (1960).
[14.17] G. Barreau, G. Brunel, G. Cizeron, C.R. Acad. Sci. Paris **270C** (1970) 516.
[14.18] V.A. Gorbachev, S.M. Klotsman, Ya.A. Rabovskiy, V.K. Talinskiy, A.N. Timofeyev, Fiz. Met. Metalloved. **34** (1972) 879; Phys. Met. Metallogr. **34** (4) (1972) 202 (English transl.).
[14.19] G. Krautheim, A. Neidhardt, U. Reinhold, Phys. Stat. Sol. (a) **49** (1978) K125.
[14.20] H. Oikawa, T. Obara, S. Karashima, Metall. Trans. **1** (1970) 2969.
[14.21] R.L. Fogelson, Ya.A. Ugay, A.V. Pokoyev, Izv. Vyssh. Uchebn. Zaved., Tsvetn. Metall. (3) (1973) 143.
[14.22] S.M. Klotsman, Ya.A. Rabovskiy, V.K. Talinskiy, A.N. Timofeyev, Fiz. Met. Metalloved. **29** (1970) 803; Phys. Met. Metallogr. **29** (4) (1970) 127 (English transl.).
[14.23] R.F. Sippel, Phys. Rev. **115** (1959) 1441.
[14.24] V.A. Gorbachev, S.M. Klotsman, Ya.A. Rabovskiy, V.K. Talinskiy, A.N. Timofeyev, Fiz. Met. Metalloved. **44** (1977) 214; Phys. Met. Metallogr. **44** (1) (1977) 191 (English transl.).
[14.25] S. Fujikawa, A. Seeger, Res. Rep. Nucl. Sci., Tohoku Univ. **20** (1987) 375.
[14.26] S. Fujikawa, M. Werner, H. Mehrer, A. Seeger, Mater. Sci. Forum **15–18** (1987) 431.
[14.27] S. Fujikawa, H. Mehrer, in: *Application of Ion Beams in Materials Science*, Hosei Univ. Press, Tokyo (1988), p. 265.
[14.28] R.L. Fogelson, Ya.A. Ugay, A.V. Pokoyev, I.A. Akimova, V.D. Kretinin, Fiz. Met. Metalloved. **35** (1973) 1307; Phys. Met. Metallogr. **35** (6) (1973) 176 (English transl.).
[14.29] A. Almazouzi, M.P. Macht, V. Naundorf, G. Neumann, Phys. Stat. Sol. (a) **133** (1992) 305.
[14.30] T. Hirone, N. Kunitomi, M. Sakamoto, H. Yamaki, J. Phys. Soc. Japan **13** (1958) 838.
[14.31] K. Hoshino, Y. Iijima, K. Hirano, in: *Point Defects and Defect Interactions*, Eds. J. Takamura, M. Doyama, K. Kiritani, The University of Tokyo Press, Tokyo (1982), p. 562.
[14.32] C.A. Mackliet, Phys. Rev. **109** (1958) 1964.
[14.33] R. Döhl, M.P. Macht, V. Naundorf, Phys. Stat. Sol. (a) **86** (1984) 603.
[14.34] G. Neumann, V. Tölle, Phil. Mag. A **57** (1988) 319.
[14.35] K. Hoshino, Y. Iijima, K. Hirano, Metall. Trans. **8A** (1977) 469.
[14.36] H.J. Rockosch, Ch. Herzig, Phys. Stat. Sol. (b) **119** (1983) 199.
[14.37] A. Almazouzi, M.P. Macht, V. Naundorf, G. Neumann, Phys. Stat. Sol. (a) **167** (1998) 15.
[14.38] J.G. Mullen, Phys. Rev. **121** (1961) 1649.
[14.39] G. Barreau, G. Brunel, G. Cizeron, C.R. Acad. Sci. Paris **272C** (1971) 618.
[14.40] J. Bernardini, J. Cabané, Acta Metall. **21** (1973) 1561.
[14.41] S.K. Sen, M.B. Dutt, A.K. Barua, Phys. Stat. Sol. (a) **45** (1978) 657.
[14.42] A. Almazouzi, M.P. Macht, V. Naundorf, G. Neumann, Phys. Rev. B **54** (1996) 857.
[14.43] S.M. Klotsman, Ya.A. Rabovskiy, V.K. Talinskiy, A.N. Timofeyev, Fiz. Met. Metalloved. **31** (1971) 429; Phys. Met. Metallogr. **31** (2) (1971) 214 (English transl.).

[14.44] R.L. Fogelson, Ya.A. Ugay, I.A. Akimova, Izv. Vyssh. Uchebn. Zaved., Tsvetn. Metall. (1) (1977) 172.
[14.45] F.D. Reinke, C.E. Dahlstrom, Phil. Mag. **22** (1970) 57.
[14.46] G. Krautheim, A. Neidhardt, U. Reinhold, Kristall und Technik **13** (1978) 1335.
[14.47] W. Gust, C. Ostertag, B. Predel, U. Roll, A. Lodding, H. Odelius, Phil. Mag. A **47** (1983) 395.
[14.48] S.M. Klotsman, Ya.A. Rabovskiy, V.K. Talinskiy, A.N. Timofeyev, Fiz. Met. Metalloved. **45** (1978) 1104; Phys. Met. Metallogr. **45** (5) (1978) 181 (English transl.).
[14.49] R.L. Fogelson, Ya.A. Ugay, A.V. Pokoyev, Izv. Vyssh. Uchebn. Zaved., Chern. Metall. (9) (1973) 136.
[14.50] K. Maier, R. Kirchheim, G. Tölg, Microchim. Acta **8**(Suppl.) (1979) 125.
[14.51] M.C. Saxena, B.D. Sharma, Trans. Indian Inst. Metals **23** (1970) 16.
[14.52] A. Ikushima, J. Phys. Soc. Japan **14** (1959) 1636.
[14.53] R.L. Fogelson, Ya.A. Ugay, A.V. Pokoyev, I.A. Akimova, Fiz. Tverd. Tela **13** (1971) 1028; Soviet Phys. Solid State **13** (1971) 856 (English transl.).
[14.54] P. Spindler, K. Nachtrieb, Phys. Stat. Sol. (a) **37** (1976) 449; see also Metall. Trans. **9A** (1978) 763.
[14.55] N.L. Peterson, Phys. Rev. **132** (1963) 2471.
[14.56] R.L. Fogelson, Ya.A. Ugay, A.V. Pokoyev, Fiz. Met. Metalloved. **33** (1972) 1102; Phys. Met. Metallogr. **33** (5) (1972) 194 (English transl.).
[14.57] G. Neumann, M. Pfundstein, P. Reimers, Phil. Mag. A **45** (1982) 499.
[14.58] R.L. Fogelson, Ya.A. Ugay, A.V. Pokoyev, Fiz. Met. Metalloved. **34** (1972) 1104; Phys. Met. Metallogr. **34** (5) (1972) 198 (English transl.).
[14.59] F. Moya, G.E. Moya-Goutier, F. Cabané-Brouty, Phys. Stat. Sol. **35** (1969) 893.
[14.60] S.J. Wang, H.J. Grabke, Z. Metallk. **61** (1970) 597.
[14.61] M.C. Inman, L.W. Barr, Acta Metall. **8** (1960) 112.
[14.62] V.A. Gorbachev, S.M. Klotsman, Ya.A. Rabovskiy, V.K. Talinskiy, A.N. Timofeyev, Fiz. Met. Metalloved. **35** (1973) 889; Phys. Met. Metallogr. **35** (4) (1973) 226 (English transl.).
[14.63] G. Krautheim, A. Neidhardt, U. Reinhold, A. Zehe, Phys. Lett. **72A** (1979) 181.
[14.64] G. Rummel, H. Mehrer, Defect and Diffusion Forum **66–69** (1989) 453; G. Rummel, Diploma work, Univ. Münster (1987).
[14.65] Y. Minamino, T. Yamane, T. Kimura, J. Mater. Sci. Lett. **7** (1988) 365.
[14.66] Y. Iijima, Y. Wakabayashi, T. Itoga, K. Hirano, Mater. Trans. Japan Inst. Metals **32** (1991) 457.
[14.67] R.L. Fogelson, Ya.A. Ugay, I.A. Akimova, Fiz. Met. Metalloved. **37** (1974) 1107; Phys. Met. Metallogr. **37** (5) (1974) 201 (English transl.).
[14.68] Y. Iijima, K. Hoshino, K. Hirano, Metall. Trans. **8A** (1977) 997.
[14.69] S. Komura, N. Kunitomi, J. Phys. Soc. Japan **18**(Suppl II) (1963) 208.
[14.70] J. Hino, C.T. Tomizuka, C.A. Wert, Acta Metall. **5** (1957) 41.
[14.71] N.L. Peterson, S.J. Rothman, Phys. Rev. **154** (1967) 558.
[14.72] S.M. Klotsman, Ya.A. Rabovskiy, V.K. Talinskiy, A.N. Timofeyev, Fiz. Met. Metalloved. **28** (1969) 1025; Phys. Met. Metallogr. **28** (6) (1969) 66 (English transl.).
[14.73] M.B. Dutt, S.K. Sen, Japan J. Appl. Phys. **18** (1979) 1025.

Further Investigations

Cu [14.74] W.L. Mercer, *Thesis*, Univ. of Leeds (1955); from D.B. Butrymowicz, J.R. Manning, M.E. Read, J. Chem. Ref. Data **3** (1974) 527.
Cu [14.75] K. Maier, C. Bassani, W. Schüle, Phys. Lett. **44A** (1973) 539; precursor to Ref. [14.11].
Al [14.76] J. Hirvonen, J. Appl. Phys. **52** (1981) 6143; Al implanted, NRA
Au [14.77] A.B. Martin, R.D. Johnson, F. Asaro, J. Appl. Phys. **25** (1954) 364.
Au [14.78] T.F. Archbold, W.H. King, Trans. AIME **233** (1965) 839.
Au [14.79] A. Chatterjee, D.J. Fabian, Acta Metall. **17** (1969) 1141.
Co [14.80] M. Sakamoto, J. Phys. Soc. Japan **13** (1958) 845.
Co [14.81] S. Badrinarayanan, H.B. Mathur, Indian J. Pure Appl. Phys. **10** (1972) 512.
Co [14.82] F.J. Bruni, J.W. Christian, Acta Metall. **21** (1973) 385; EPMA.
Co [14.83] M.P. Macht, V. Naundorf, R. Döhl, in: DIMETA 82, *Diffusion in Metals and Alloys*, Eds. F.J. Kedves, D.L. Beke, Trans. Tech. Publ., Switzerland (1983), p. 516; precursor to Ref. [14.33].

Cr [14.84] W.L. Seitz, *Thesis*, Univ. of Arizona (1963); from D.B. Butrymowicz, J.R. Manning, M.E. Read, J. Chem. Ref. Data **4** (1975) 177
Cr see Ref. [14.39].
Cr [14.85] M.C. Saxena, Trans. Indian Inst. Metals **24** (4) (1971) 56.
Fe [14.86] Y. Tomono, A. Ikushima, J. Phys. Soc. Japan **13** (1958) 762.
Fe [14.87] G. Salje, M. Feller-Kniepmeier, J. Appl. Phys. **49** (1978) 229; EPMA.
Fe [14.88] K.H. Steinmetz, G. Vogl, W. Petry, K. Schroeder, Phys. Rev. B **34** (1986) 107; QMS.
Mn [14.89] A. Ikushima, J. Phys. Soc. Japan **14** (1959) 111.
Ni [14.90] K.J. Anusavice, J.J. Pinajian, H. Oikawa, R.T. DeHoff, Trans. AIME **242** (1968) 2027; precursor to Ref. [14.08].
Ni [14.91] G. Brunel, G. Cizeron, P. Lacombe, C.R. Acad. Sci. Paris **270C** (1970) 393.
Ni [14.92] T.J. Renouf, Phil. Mag. **22** (1970) 359; autoradiography.
Ni [14.93] J.L. Seran, Acta Metall. **24** (1976) 627; ^{58}Ni, ^{64}Ni (stable isotopes), SIMS analysis.
Ni [14.94] M.B. Dutt, S.K. Sen, A.K. Barua, Phys. Stat. Sol. (a) **56** (1979) 149; resistometric method.
Ni see Ref. [14.83]; precursor to Ref. [14.42].
S [14.95] F. Moya, F. Cabané-Brouty, C.R. Acad. Sci. Paris **264C** (1967) 1543; precursor to Ref. [14.59].
S [14.96] J. Ladet, B. Augray, F. Moya, Met. Sci. **12** (1978) 195.
Sb [14.97] T.J. Renouf, Phil. Mag. **9** (1964) 781; autoradiography.
Sn [14.98] S.D. Gertsriken, A.L. Revo, Ukr. Fiz. Zh. **6** (1961) 398.
Sn [14.99] S.K. Sen, M.B. Dutt, A.K. Barua, Phys. Stat. Sol. (a) **32** (1975) 345; resistometric method.
Sn [14.100] K. Hoshino, Y. Iijima, K. Hirano, Trans. Japan Inst. Metals **21** (1980) 674; EPMA.
Zn [14.101] R.T. DeHoff, A.G. Guy, K.J. Anusavice, Trans. AIME **236** (1966) 881; precursor to Ref. [14.08].
Zn [14.102] H. Oikawa, K.J. Anusavice, R.T. DeHoff, A.G. Guy, Trans. ASM (Trans. Quart.) **61** (1968) 354; precursor to Ref. [14.08].
Zn [14.103] J. Kučera, B. Million, J. Plšková, Phys. Stat. Sol. (a) **11** (1972) 361.

References to Chapter 1.5

[15.01] C.T. Tomizuka, E. Sonder, Phys. Rev. **103** (1956) 1182.
[15.02] V.N. Kaygorodov, S.M. Klotsman, A.N. Timofeyev, I.Sh. Trakhtenberg, Fiz. Met. Metalloved. **25** (1968) 910; Phys. Met. Metallogr. **25** (5) (1972) 150 (English transl.).
[15.03] S.J. Rothman, N.L. Peterson, J.T. Robinson, Phys. Stat. Sol. **39** (1970) 635.
[15.04] P. Reimers, D. Bartdorff, Phys. Stat. Sol. (b) **50** (1972) 305.
[15.05] N.Q. Lam, S.J. Rothman, H. Mehrer, L.J. Nowicki, Phys. Stat. Sol. (b) **57** (1973) 225.
[15.06] J.G.E.M. Backus, H. Bakker, H. Mehrer, Phys. Stat. Sol. (b) **64** (1974) 151.
[15.07] J. Bihr, H. Mehrer, K. Maier, Phys. Stat. Sol. (a) **50** (1978) 171.
[15.08] G. Rein, H. Mehrer, Phil. Mag. A **45** (1982) 467.
[15.09] H. Mehrer, F. Hutter, in: *Point Defects and Defect Interactions in Metals*, Eds. J. Takamura, M. Doyama, M. Kiritani, Univ. of Tokyo Press, Tokyo (1982), p. 558.
[15.10] G. Neumann, V. Tölle, Phil. Mag. A **54** (1986) 619.
[15.11] R.L. Fogelson, Ya.A. Ugay, I.A. Akimova, Izv. Vyssh. Uchebn. Zaved., Tsvetn. Metall. (2) (1975) 142.
[15.12] Th. Hehenkamp, R. Wübbenhorst, Z. Metallk. **66** (1975) 275.
[15.13] F.E. Jaumot, A. Sawatzky, J. Appl. Phys. **27** (1956) 1186.
[15.14] H.W. Mead, C.E. Birchenall, Trans. AIME **209** (1957) 874.
[15.15] W.C. Mallard, A.B. Gardner, R.F. Bass, L.M. Slifkin, Phys. Rev. **129** (1963) 617.
[15.16] C.T. Tomizuka, L.M. Slifkin, Phys. Rev. **96** (1954) 610.
[15.17] V.N. Kaygorodov, S.M. Klotsman, A.N. Timofeyev, I.Sh. Trakhtenberg, Fiz. Met. Metalloved. **27** (1969). 1048; Phys. Met. Metallogr. **27** (6) (1969) 91 (English transl.).
[15.18] T.S. Lundy, R.A. Padgett, Trans. AIME **242** (1968) 1897.
[15.19] J. Bernardini, J. Cabané, Acta Metall. **21** (1973) 1561.
[15.20] F. Makuta, Y. Iijima, K. Hirano, Trans. Japan Inst. Metals **20** (1979) 551.
[15.21] G. Neumann, M. Pfundstein, P. Reimers, Phys. Stat. Sol. (a) **64** (1981) 225.

[15.22] A. Sawatzky, F.E. Jaumot, Trans. AIME **209** (1957) 1207.
[15.23] P. Dorner, W. Gust, M.B. Hintz, A. Lodding, H. Odelius, P. Predel, Acta Metall. **28** (1980) 291.
[15.24] J.G. Mullen, Phys. Rev. **121** (1961) 1649.
[15.25] S. Bharati, S. Badrinarayanan, A.P.B. Sinha, Phys. Stat. Sol. (a) **43** (1977) 653.
[15.26] R.L. Fogelson, Ya.A. Ugay, I.A. Akimova, Izv. Vyssh. Uchebn. Zaved., Tsvetn. Metall. (1) (1977) 172.
[15.27] R.E. Hoffmann, Acta Metall. **6** (1958) 95.
[15.28] V.N. Kaygorodov, Ya.A. Rabovskiy, V.K. Talinskiy, Fiz. Met. Metalloved. **24** (1967) 117; Phys. Met. Metallogr. **24** (1) (1967) 115 (English transl.).
[15.29] H. Mehrer, D. Weiler, Z. Metallk. **75** (1984) 203.
[15.30] R.S. Barclay, P. Niessen, Trans. ASM (Trans. Quart.) **62** (1969) 721.
[15.31] T. Hirone, Sh. Miura, T. Suzuoka, J. Phys. Soc. Japan **16** (1961) 2456.
[15.32] J. Ladet, J. Bernardini, F. Cabané-Brouty, Scr. Metall. **10** (1976) 195.
[15.33] S.K. Sen, M.B. Dutt, A.K. Barua, Phys. Stat. Sol. (a) **45** (1978) 657.
[15.34] R.E. Hoffmann, D. Turnbull, E.W. Hart, Acta Metall. **3** (1955) 417.
[15.35] N.L. Peterson, Phys. Rev. **132** (1963) 2471.
[15.36] R.L. Fogelson, Ya.A. Ugay, I.A. Akimova, Fiz. Met. Metalloved. **39** (1975) 447; Phys. Met. Metallogr. **39** (2) (1975) 212 (English transl.).
[15.37] G. Neumann, M. Pfundstein, P. Reimers, Phil. Mag. A **45** (1982) 499.
[15.38] C.B. Pierce, D. Lazarus, Phys. Rev. **114** (1959) 686.
[15.39] N. Barbouth, J. Oudar, J. Cabané, C.R. Acad. Sci. Paris **264C** (1967) 1029.
[15.40] S.J. Wang, H.J. Grabke, Z. Metallk. **61** (1970) 597.
[15.41] E. Sonder, L.M. Slifkin, C.T. Tomizuka, Phys. Rev. **93** (1954) 970.
[15.42] V.N. Kaygorodov, Ya.A. Rabovskiy, V.K. Talinskiy, Fiz. Met. Metalloved. **24** (1967) 661; Phys. Met. Metallogr. **24** (4) (1967) 78 (English transl.).
[15.43] H. Hagenschulte, Th. Heumann, J. Phys. Condens. Matter **1** (1989) 3601.
[15.44] G. Rummel, H. Mehrer, Defect and Diffusion Forum **66–69** (1989) 453; G. Rummel, Diploma work, Univ. Münster (1987).
[15.45] V.N. Kaygorodov, S.M. Klotsman, A.N. Timofeyev, I.Sh. Trakhtenberg, Fiz. Met. Metalloved. **28** (1969) 128; Phys. Met. Metallogr. **28** (1) (1969) 128 (English transl.).
[15.46] J. Geise, H. Mehrer, Ch. Herzig, G. Weyer, Mater. Sci. Forum **15–18** (1987) 443.
[15.47] A. Sawatzky, F.E. Jaumot, Phys. Rev. **100** (1955) 1627.
[15.48] S.J. Rothman, N.L. Peterson, Phys. Rev. **154** (1967) 552.

Further Investigations

Ag [15.49] R.E. Hoffmann, D. Turnbull, E.W. Hart, J. Appl. Phys. **22** (1951) 634; Erratum ibid. **22** (1951) 984.
Ag [15.50] L. Slifkin, D. Lazarus, T. Tomizuka, J. Appl. Phys. **23** (1952) 1032; precursor to Ref. [15.01].
Ag [15.51] A.A. Zhukhovitskii, V.A. Geodyakin, Dokl. Akad. Nauk. **102** (1955) 301.
Ag [15.52] N.H. Nachtrieb, J. Petit, J. Wehrenberg, J. Chem. Phys. **26** (1957) 106.
Ag [15.53] V.A. Geodakyan, A.A. Zhukhovitskii, Zh. Fiz. Khim. **31** (1957) 2295.
Ag [15.54] M.E. Yanitskaya, A.A. Zhukhovitskii, S.Z. Bokshtein, Dokl. Akad. Nauk. (112) (1957) 720.
Ag [15.55] A.V. Savitskii, Fiz. Met. Metalloved. **10** (1960) 564; Phys. Met. Metallogr. **10** (4) (1960) 71 (English transl.).
Ag [15.56] P. Reimers, Metall. **22** (1968) 577.
Ag [15.57] A. Brun, J. Bernardini, J. Cabané, Scr. Metall. **2** (1968) 515.
Ag [15.58] C.T. Lai, H.M. Morrison, Can. J. Phys. **48** (1970) 1548.
Ag see Ref. [15.19].
Cd [15.59] S. Bharati, A.P.B. Sinha, Phys. Stat. Sol. (a) **44** (1977) 391.
Co [15.60] T. Hirone, H. Yamamoto, J. Phys. Soc. Japan **16** (1961) 455.
Co [15.61] J. Bernardini, A. Combe-Brun, J. Cabané, Scr. Metall. **4** (1970) 985; precursor to Ref. [15.19].
Co [15.62] S. Badrinarayanan, H.B. Mathur, Indian J. Chem. **11** (1973) 465.
Fe [15.63] J. Bernardini, A. Combe-Brun, J. Cabané, C.R. Acad. Sci. Paris **269C** (1969) 287; Scr. Metall. **3** (1969) 591; precursor to Ref. [15.19].
Pb [15.64] S.K. Sen, M.B. Dutt, A.K. Barua, Phys. Stat. Sol. (a) **32** (1975) 345; resistometric method.

S [15.65] J. Ladet, B. Augray, F. Moya, Met. Sci. **12** (1978) 195.
Sb [15.66] L. Slifkin, D. Lazarus, T. Tomizuka, J. Appl. Phys. **23** (1952) 1405; precursor to Ref. [15.41].
Sn [15.67] P. Gas, J. Bernardini, Scr. Metall. **12** (1978) 367.
Zn [15.68] M.B. Dutt, S.K. Sen, Japan J. Appl. Phys. **18** (1979) 1025.

References to Chapter 1.6

[16.01] S.M. Makin, A.H. Rowe, A.D. Le Claire, Proc. Phys. Soc. B **70** (1957) 545.
[16.02] D. Duhl, K. Hirano, M. Cohen, Acta Metall. **11** (1963) 1.
[16.03] H.M. Gilder, D. Lazarus, J. Phys. Chem. Sol. **26** (1965) 2081.
[16.04] A. Gainotti, L. Zecchina, Nuovo Cimento **40** (1965) 295.
[16.05] M. Beyeler, Y. Adda, J. Physique **29** (1968) 345.
[16.06] W. Rupp, U. Ermert, R. Sizmann, Phys. Stat. Sol. **33** (1969) 509.
[16.07] K. Dreyer, Ch. Herzig, Th. Heumann, in: *Atomic Transport in Solids and Liquids*, Eds. A. Lodding, T. Lagerwall, Verlag der Zeitschrift für Naturforschung, Tübingen (1971), p. 237.
[16.08] Ch. Herzig, H. Eckseler, W. Bussmann, D. Cardis, J. Nucl. Mater. **69/70** (1978) 61.
[16.09] G. Rein, H. Mehrer, Phil. Mag. A **45** (1982) 467.
[16.10] M. Werner, H. Mehrer, in: DIMETA 82, *Diffusion in Metals and Alloys*, Eds. F.J. Kedves, D.L. Beke, Trans. Tech. Publ., Switzerland (1983), p. 393.
[16.11] G. Neumann, V. Tölle, Phil. Mag. A **54** (1986) 619.
[16.12] W.C. Mallard, A.B. Gardner, R.F. Bass, L.M. Slifkin, Phys. Rev. **129** (1963) 617.
[16.13] S.M. Klotsman, N.K. Arkhipova, A.N. Timofeyev, I.Sh. Trakhtenberg, Fiz. Met. Metalloved. **20** (1965) 390; Phys. Met. Metallogr. **20** (3) (1965) 70 (English transl.).
[16.14] Ch. Herzig, D. Wolter, Z. Metallk. **65** (1974) 273.
[16.15] R.L. Fogelson, N.N. Trofimova, Izv. Vyssh. Uchebn. Zaved., Tsvetn. Metall. (4) (1978) 152.
[16.16] R.L. Fogelson, N.N. Kazimirov, I.V. Soshnikova, Fiz. Met. Metalloved. **43** (1977) 1105; Phys. Met. Metallogr. **43** (5) (1977) 185 (English transl.).
[16.17] K. Richter, *Doctoral Thesis*, TU Bergakademie, Freiberg (1998); see also K. Richter, D. Bergner, A. Müller, C. Kirbach, A. Plötsch, S. Lorenz, Ch. Raub, D. Ott, Defect and Diffusion Forum **143–147** (1997) 103; 109.
[16.18] A. Vignes, J.P. Haeussler, Mém. Sci. Rev. Métall. **63** (1966) 1091; C.R. Acad. Sci. Paris **263C** (1966) 1504.
[16.19] D. Cardis, *Doctoral Thesis*, Univ. Münster (1977).
[16.20] A.J. Mortlock, A.H. Rowe, Phil. Mag. **11** (1965) 1157.
[16.21] J.E. Reynolds, B.L. Averbach, M. Cohen, Acta Metall. **5** (1957) 29.
[16.22] R.L. Fogelson, Ya.A. Ugay, I.A. Akimova, Fiz. Met. Metalloved. **41** (1976) 653; Phys. Met. Metallogr. **41** (3) (1976) 180 (English transl.).
[16.23] R.L. Fogelson, I.M. Voronina, T.I. Somova, Fiz. Met. Metalloved. **46** (1978) 190; Phys. Met. Metallogr. **46** (1) (1978) 163 (English transl.).
[16.24] Ch. Herzig, Th. Heumann, Z. Naturforsch. **27a** (1972) 613.
[16.25] Ch. Herzig, Th. Heumann, Z. Naturforsch. **27a** (1972) 1109.
[16.26] G. Rummel, H. Mehrer, Defect and Diffusion Forum **66–69** (1989) 453; G. Rummel, Diploma work, Univ. Münster (1987).

Further Investigations

Au [16.27] B. Okkerse, Phys. Rev. **103** (1956) 1246.
Au [16.28] H.W. Mead, C.E. Birchenall, Trans. AIME **209** (1957) 874.
Au [16.29] J.L. Whitton, G.V. Kidson, Can. J. Phys. **46** (1968) 2589; low temperature investigations.
Au [16.30] H.M. Morrison, V.L.S. Yuen, Can. J. Phys. **49** (1971) 2704; low temperature investigations.
Pt [16.31] A.J. Mortlock, A.H. Rowe, A.D. Le Claire, Phil. Mag. **5** (1960) 803.
Sn see Ref. [16.07]; precursor to Ref. [16.25].

CHAPTER 2

Self-Diffusion and Impurity Diffusion in Group II Metals

Contents

Tables
- 2.1. Beryllium (Be) 100
- 2.2. Magnesium (Mg) 102
- 2.3. Calcium (Ca) 104
- 2.4. Zinc (Zn) 105
- 2.5. Cadmium (Cd) 107

Figures
- Beryllium 109
- Magnesium 110
- Calcium 112
- Zinc 113
- Cadmium 116

References 118

For **strontium** (Sr), **barium** (Ba), **radium** (Ra) and **mercury** (Hg) no data are available.

Most of the group II metals have a hexagonal lattice structure. The respective c/a axis ratios deviate from the ideal value $\sqrt{8/3} \approx 1.633$ for the hexagonal closed packed (hcp) structure (see Table 2.0). The deviation of c/a from 1.633 leads to an anisotropy of the diffusivity.

Frequently, the single crystals used in the diffusion measurements deviate from the ideal crystallographic direction by an angle θ. In those cases $D_{\perp}$ and $D_{//}$ are calculated according to Eq. (02.18), using two crystals with different θ.

In Table 2.0 lattice structure, lattice constants c and a, c/a ratio and melting temperature of group II metals are listed.

Table 2.0 Lattice structure, lattice constants c and a, c/a ratio and melting temperature T_m

Metal	Be	Mg	Ca	Zn	Cd
Structure	hcp	hcp	hcp[1]	hcp	hcp
c (nm)	3.58	5.21	6.52	4.95	5.62
a (nm)	2.27	3.21	3.98	2.66	2.99
c/a	1.58	1.62	1.64	1.86	1.88
T_m (K)	1,560	922	1,116	693	594

[1] At $T > 723$ K.

Table 2.1 Diffusion in beryllium (References, see page 118)

(1)	(2a)	(2b)	(3)	(4)	(5)	(6)	(7)	(8)	(9)	(10)	(11)	(12)
X	D^0 (10^{-4} m^2 s^{-1})	Q (eV) and (kJ mole^{-1})	$D(T_m)$ (10^{-12} m^2 s^{-1})	T-range (K) ($\overline{T}/T_m$)	No. of data points	Material, purity	Experimental method	Remarks on the pp	Further remarks	Also studied	Figure	Reference
Self-diffusion												
Be	$\perp$ 0.52	1.631 (157.4)	280	836–1,342 (0.70)	16 (7 T)	sc[61]	^{7}Be, dried-on from salt solution[73]; residual activity	1 example (log dI/dx vs. x^2, slight NSE)	Marked data scatter		21.01	Dupouy (1966) [21.01]
	// 0.62	1.709 (165.0)	190	841–1,321 (0.69)	12 (7 T)							
Be	0.36	1.665 (160.8)	150	923–1,473 (0.77)	14 (7 T)	pc 4N	^{7}Be, vapour deposition of $^7BeCl_2$[73]; residual activity	5 examples[84]			–	Pavlinov (1968) [21.02]
Be	–	–		966	2[51]	sc[61]	^{7}Be[72]; residual activity	No	$D_\perp = 1.6 \times 10^{-13}$ m^2 s^{-1}, $D_{//} = 8.3 \times 10^{-14}$ m^2 s^{-1}	$\Delta V/V_0 = 1.2$; Al in Al	21.01	Beyeler (1970) [21.03]
Impurity diffusion												
Al	1.0	1.743 (168.3)	230	1,068–1,356 (0.78)	5	pc 3N	^{26}Al, dried-on from salt solution; residual activity	No[81]	Pronounced data scatter	$c_s = 0.13 \cdot \exp(-0.55\,\text{eV}/kT)$	–	Gladkov (1976) [21.04]
Ag	6.2	2.00 (193.0)	215	923–1,183	8	pc 2N75	^{110}Ag, vapour deposition; residual activity	No	Pronounced data scatter	Fe in Be	–	Naik (1966) [21.05]
	$\perp$ 1.76	1.873 (180.9)	155	929–1,170 (0.67)	6	sc					21.02	
	// 0.43	1.704 (164.5)	134	929–1,170	5							
Au	$\perp$ (9.0)$^+$	(2.327)$^+$ (224.7)		938, 1,053 (0.64)	6 (2 T)	sc, pc (10 µm) 3N5	Au, implanted; RBS	–	$^+$Present calculation; D_{pc} is 20 and 30 times larger than $D_\perp$ and $D_{//}$, respectively	Ag in Be at 1,053 K	–	Myers (1975) [21.06]
	// (41)$^+$	(2.50)$^+$ (241.4)										
Ce	(310)	(3.14) (304)	–	1,223–1,528 (0.88)	9	pc 2N7	^{141}Ce, dried-on from salt solution; residual activity	No	Considerable data scatter, abnormal increase of D at $T > 1{,}500$ K	Nb, V in Be; c_s = 16–45 ppma	–	Ananin (1976) [21.07]

Co	27	2.975 (287)	0.66	1,253–1,493 (0.88)	6	pc 2N8	^{57}Co, dried-on from solution; residual activity	No	Pronounced data scatter		–	Gladkov (1979) [21.08]
Cu	⊥ 0.35	1.990 (192.2)	13	972–1,273 (0.72)	5	sc[61]	^{64}Cu*, vapour deposition; residual activity	No	*Cu activated after sectioning		21.02	Dupouy (1965) [21.09]
	// 0.90	2.147 (207.3)	10.4		5							
Cu	– –	– –		673–1,073* 693–913	(9) 7	sc[61]	Cu, vapour deposition*; ion implantation, RBS	2 examples ($c - x$)	*Data not used because of surface oxidation [x]Fit together with the data of [21.09]		21.02	Myers (1974) [21.10]
	⊥ 0.416[x]	2.00[x] (193.2)	14[x]	(693–1,273)	(10)							
	// 0.381[x]	2.056[x] (198.5)	8.6[x]	(693–1,273)	(8)							
Fe	1.0	2.298 (221.9)	3.7	1,073–1,373 (0.78)	10 (4T)	pc	Fe, EPMA Be/Be(X% Fe) (Matano)		*$X = 0.05$, 0.1, 0.2		–	Donze (1962) [21.11]
Fe	0.53	2.246 (216.9)	2.9	973–1,349 (0.74)	8	pc 2N75	^{59}Fe, vapour deposition; residual activity	No		Ag in Be	–	Naik (1966) [21.05]
Nb	(2×10^4)	(3.73) (360)	–	1,318–1,538 (0.92)	7	pc 2N7	^{95}Nb, dried-on from salt solution; residual activity	No	Considerable data scatter, abnormal increase of D at $T >$ 1,500 K	Ce, V in Be; $c_s = 150$-390 ppma at $T =$ 1,173–1,423 K	–	Ananin (1976) [21.07]
Ni	(0.2)	(2.515) (242.8)	–	1,123–1,523 (0.85)	5[51]	pc 2N7	^{63}Ni, dried-on from salt solution; residual activity	No	Considerable data scatter, abnormal increase of D at $T >$ 1,500 K	Ni in Be(Ni)	–	Ananin (1970) [21.12]
V	(29)	(2.515 (242.8)	–	1,173–1,423 (0.83)	6	pc 2N7	^{48}V, dried-on from salt solution; residual activity	No	Considerable data scatter	Ce, Nb in Be	–	Ananin (1976) [21.07]

Table 2.2 Diffusion in magnesium (References, see page 118)

(1)	(2a)	(2b)	(3)	(4)	(5)	(6)	(7)	(8)	(9)	(10)	(11)	(12)
X	D^0 (10^{-4} m^2 s^{-1})	Q (eV) and (kJ mole^{-1})	$D(T_m)$ (10^{-12} m^2 s^{-1})	T-range (K) ($\overline{T}/T_m$)	No. of data points	Material, purity	Experimental method	Remarks on the pp	Further remarks	Also studied	Figure	Reference
Self-diffusion												
Mg	(1.0) 1.2$^+$	1.388 (134.0)	 3.1$^+$	741–900 (0.89)	5 (3T)	pc 3N	^{28}Mg, vapour deposition[73]; lathe (50 μm sections)	All	$^+$Present recalculation		–	Shewmon (1954) [22.01]
Mg	⊥ 1.5	1.409 (136.1)	3.0	741–849 (0.86)	4	sc* 3N5	^{28}Mg, vapour deposition[73]; lathe (40 μm sections)	All	*Two crystals deviating 7° and 78°, respectively, from the c-axis		–	Shewmon (1956) [22.02]
	// 1.0	1.396 (134.8)	2.3	740–908 (0.89)	6							
Mg	⊥ (1.75) 1.68$^+$	1.431 (138.2)	 2.5$^+$	775–906 (0.91)	9	sc 4N	^{28}Mg, dried-on from salt solution[73]; grinder and residual activity	2 examples	$^+$Present recalculation		22.01	Combronde (1971) [22.03]
	// (1.78) 1.64$^+$	1.440 (139.0)	 2.2$^+$	775–906 (0.91)	10							
Impurity diffusion												
Ag	0.34	1.236 (119.3)	5.9	750–894 (0.89)	7 (6T)	pc ~3N	^{110}Ag; grinder and residual activity			In, Zn in Mg	–	Lal (1967) [22.04]
Ag	⊥ (17.9) 17.0$^+$	1.535 (148.2)	 6.9$^+$	752–912 (0.90)	7	sc 4N	^{110}Ag, vapour deposition[73]; grinder and residual activity	2 examples	$^+$Present recalculation	Cd, In, Sb, Sn in Mg	22.02	Combronde (1972) [22.05]
	// (3.62) 3.47$^+$	1.379 (133.2)	 10.0$^+$		7							
Be	(8.06) 5.6$^+$	1.626 (157.0)	 0.72$^+$	773–873 (0.89)	7* (6T)	pc[61]	Be, Mg/Mg (0.2% Be) diffusion couple; spectral analysis	4 examples[81] ($c - x$)	$^+$Present recalculation *$p = 0.60$ MPa ($\Delta V/V_0 \approx 0$)	c_s = (130–250) ppma	22.03	Yerko (1966) [22.06]
Cd	⊥ 0.46	1.375 (132.7)	1.40	733–899 (0.88)	8	sc 4N	^{109}Cd, dried-on from salt solution[73]; grinder and residual activity; EPMA at 722 K	No		Ag, In, Sb, Sn in Mg	22.02	Combronde (1972) [22.05]
	// 1.29	1.457 (140.7)	1.39		6 2	pc 4N						
Ce	450	1.82 (175.8)	5.0	823–871 (0.92)	4	pc[61]	Ce, dissolution of precipitates in diffusion couple; EPMA			La in Mg	–	Lal (1966) [22.07]

Fe	4×10^{-6}	0.919 (88.8)	0.0038	673–873 (0.84)	10 (5T)	pc 3N5	^{59}Fe, vapour deposition[73]; residual activity	2 examples[81]		Ni, U in Mg, Ca, Fe, Ni, U in Ca	–	Pavlinov (1968) [22.08]
Ga	–	–		639–872 (0.82)	9	pc (1 mm)	^{67}Ga, vapour deposition; residual activity*	1 example (log $c - x$)	*Simultaneous evaluation of lattice and gb diffusion; low-temperature data extrapolated	gb diffusion	22.03	Stloukal (2003) [22.09]
	1.2	1.391 (134.3)	3.0	777–872 (0.89)	5	3N7						
In	0.052	1.231 (118.9)	0.96	745–883 (0.88)	8 (6T)	pc ~3N	^{114}In; residual activity			Ag, Zn in Mg	–	Lal (1967) [22.04]
In	⊥ (1.88) 1.79^{+}	1.474 (142.4)	1.55^{+}	776–906 (0.91)	6	sc 4N	^{114}In; vapour deposition[73]; grinder and residual activity	No	$^{+}$Present recalculation	Ag, Cd, Sb, Sn in Mg	22.04	Combronde (1972) [22.05]
	// (1.75) 1.65^{+}	1.485 (143.4)	1.25^{+}	748–906 (0.90)	7							
La	0.022	1.058 (102.2)	3.6	813–868 (0.91)	4	pc[61]	La, dissolution of precipitates in diffusion couple; EPMA			Ce in Mg	–	Lal (1966) [22.07]
Ni	(1.2×10^{-5}) $5 \times 10^{-6\ +}$	0.993 (95.9)	0.002^{+}	673–873 (0.84)	12 (6T)	pc 3N5	^{63}Ni, vapour deposition[73]; residual activity	No[81]	$^{+}$Correct value	Fe, U in Mg, Ca, Fe, Ni, U in Ca	–	Pavlinov (1968) [22.08]
Sb	⊥ (3.27) 3.0^{+}	1.431 (138.2)	4.5^{+}	781–896 (0.91)	7	sc 4N	^{124}Sb, vapour deposition[73], ^{125}Sb, dried-on from salt solution; residual activity	4 examples[81]	$^{+}$Present recalculation	Ag, Cd, In, Sn in Mg	22.04	Combronde (1972) [22.05]
	// (2.57) 2.4^{+}	1.422 (137.3)	4.0^{+}	781–884 (0.90)	8							
Sn	⊥ 1.84^{+}	1.496^{+} (144.5)	1.2^{+}	858, 902	2	sc 4N	^{113}Sn, vapour deposition[73]; residual activity	No	$^{+}$Present recalculation	Ag, Cd, In, Sb in Mg	22.03	Combronde (1972) [22.05]
	// (4.27) 3.63^{+}	1.553 (149.9)	1.18^{+}	748–902 (0.89)	4							
U	(1.6×10^{-5}) $2.5 \times 10^{-5\ +}$	1.188 (114.7)	$8 \times 10^{-4\ +}$	773–893 (0.90)	4	pc 3N5	^{235}U, vapour deposition[73]; residual activity	2 examples[81]	$^{+}$Present recalculation	Fe, Ni in Mg, Ca, Fe, Ni, U in Ca	–	Pavlinov (1968) [22.08]
Zn	(0.41) 0.385^{+}	1.240 (119.8)	6.4^{+}	740–893 (0.89)	5	pc ~3N	^{65}Zn; residual activity		$^{+}$Present approximation	Ag, In in Mg	22.05	Lal (1967) [22.04]
Zn	(1.05)	(1.303) (125.8)		648–848 (0.81)	5	pc 3N8	^{65}Zn, vapour deposition and dried-on from salt solution; grinder and residual activity	All[83]	$^{+}$Present approximation	gb diffusion	22.05	Čermák (2006) [22.10]
	1.73^{+}	1.335^{+} (128.9)	8.7^{+}									
Zn	1.0	1.303 (125.8)	7.5	(648–893) (0.84)	(10)				Present rough fit to the data of [22.09, 22.10]		22.05	

Table 2.3 Diffusion in calcium (References, see page 118)

(1)	(2a)	(2b)	(3)	(4)	(5)	(6)	(7)	(8)	(9)	(10)	(11)	(12)
X	D^0 (10^{-4} m^2 s^{-1})	Q (eV) and (kJ mole^{-1})	$D(T_m)$ (10^{-12} m^2 s^{-1})	T-range (K) ($\overline{T}/T_m$)	No. of data points	Material, purity	Experimental method	Remarks on the pp	Further remarks	Also studied	Figure	Reference
Self-diffusion and impurity diffusion												
Ca	8.3	1.670 (161.2)	24	773–1,073 (0.83)	14 (7T)	pc 3N5	^{45}Ca, vapour deposition[73]; residual activity	2 examples (extremely flat pp)		Fe, Ni, U in Ca and Mg	23.01	Pavlinov (1968) [23.01]
Fe	(3.2×10^{-5}) 3.7×10^{-5} +	1.292 (124.8)	0.0054+	823–1,073 (0.85)	12 (6T)	pc 3N5	^{59}Fe, vapour deposition[73]; residual activity	2 examples[81]	+Present recalculation	Ca, Ni, U in Ca, Fe, Ni, U in Mg	–	Pavlinov (1968) [23.01]
Ni	(1.0×10^{-5}) 4×10^{-5} +	1.253 (121.0)	0.0087+	823–1,073 (0.85)	12 (6T)	pc 3N5	^{63}Ni, vapour deposition[73]; residual activity	No[81]	+Present recalculation	Ca, Fe, U in Ca, Fe, Ni, U in Mg	–	Pavlinov (1968) [23.01]
U	(1.1×10^{-5}) 1.35×10^{-4} +	1.509 (145.7)	0.002+	773–973 (0.78)	10 (5T)	pc 3N5	^{235}U, vapour deposition[73]; residual activity	2 examples[81]	+Present recalculation	Ca, Fe, Ni in Ca, Fe, Ni, U in Mg	–	Pavlinov (1968) [23.01]

Table 2.4 Diffusion in zinc (References, see page 118)

(1)	(2a)	(2b)	(3)	(4)	(5)	(6)	(7)	(8)	(9)	(10)	(11)	(12)
X	D^0 (10^{-4} m^2 s^{-1})	Q (eV) and (kJ mole^{-1})	$D(T_m)$ (10^{-12} m^2 s^{-1})	T-range (K) ($\overline{T}/T_m$)	No. of data points	Material, purity	Experimental method	Remarks on the pp	Further remarks	Also studied	Figure	Reference
Self-diffusion and impurity diffusion												
Zn	$\perp$ 0.58	1.054 (101.7)	1.25	513–683 (0.86)	15 (14T)	sc* 5N	^{65}Zn, electroplated; lathe (50 μm sections)	2 examples	*$<10°$ deviating from c- and a-axis direction +Present fit to the experimental data		24.01	Shirn (1953) [24.01]
	// (0.13)	0.945			6							
	0.115+	(91.3)	1.53+									
Zn	–	–		625–685 (0.95)	8	sc 5N	^{65}Zn, ^{69}Zn, electroplated; lathe	4 examples		$E \approx 0.67$; Cd in Zn	24.01	Batra (1967) [24.02]
Zn	$\perp$ 0.18	0.997 (96.3)	1.00	513–691 (0.86)	8	sc 5N	^{65}Zn, ^{69}Zn, electroplated; lathe	3 examples		$E_\perp \approx 0.74$, $E_{//} \approx 0.70$	24.01	Peterson (1967) [24.03]
	// 0.13	0.950 (91.7)	1.60		8							
Ag	$\perp$ 0.45	1.197 (115.6)	0.09	544–686 (0.89)	8[51]	sc* > 5N	^{110}Ag, plated from cyanide solution; lathe	1 example	*About 20° deviating from c- and a-axis direction +Present fit to the depicted data	In in Zn	24.02	Rosolowski (1961) [24.04]
	// (0.32)	1.128			7[51]							
	0.28+	(108.9)	0.18+									
Au	$\perp$ 0.29	1.289 (124.4)	0.012	620–688 (0.94)	4	sc* 5N	^{198}Au, plated from salt solution; lathe (20 μm sections)	1 example	*Deviating from c- and a-axis direction	Cd in Zn	24.02	Ghate (1963) [24.05]
	// 0.97	// 1.289 (124.4)	0.04	588–688 (0.92)	5							
Cd	$\perp$ 0.117	0.886 (85.5)	4.2	498–689 (0.86)	6	sc* 5N	^{115}Cd, dried-on from salt solution; lathe (35 μm sections)	1 example[85]	*Deviating from c- and a-axis direction	Au in Zn	24.03	Ghate (1963) [24.05]
	// 0.114	0.891 (86.0)	3.8		6							
Cd	–	–		617, 683	4	sc 5N	^{109}Cd, ^{115}Cd, electroplated; lathe	4 examples		$E = 0.27$–0.51; Zn in Zn	24.03	Batra (1967) [24.02]

Table 2.4 (*Continued*)

(1)	(2a)	(2b)	(3)	(4)	(5)	(6)	(7)	(8)	(9)	(10)	(11)	(12)
X	D^0 (10^{-4} $m^2 s^{-1}$)	Q (eV) and (kJ $mole^{-1}$)	$D(T_m)$ (10^{-12} $m^2 s^{-1}$)	T-range (K) ($\overline{T}/T_m$)	No. of data points	Material, purity	Experimental method	Remarks on the pp	Further remarks	Also studied	Figure	Reference
Impurity diffusion												
Cr	⊥ (165)	(1.387)		573–633	5^{51}	sc	^{51}Cr,		Experimental and		–	Chandramouli
		(133.9)		(0.87)		3N8	electroplated;		calculated data			(1974) [24.06]
	// (170)	(1.303)			5^{51}		lathe		(from D^0 and Q)			
		(125.8)							differ by a factor			
									of 20–300			
Cu	⊥ 2.00	1.298	0.073	611–688	8	sc*	^{64}Cu,	1 example	*Deviating from	Ga in Zn	24.04	Batra (1966)
		(125.3)		(0.94)		5N	electroplated;		*c*- and *a*-axis			[24.07]
	// 2.22	1.281	0.11		8		lathe		direction			
		(123.6)										
Ga	⊥ 0.018	0.787	3.4	513–676	8	sc*	^{72}Ga,	1 example	*Deviating from	Cu in Zn	24.05	Batra (1966)
		(76.0)		(0.86)		5N	electroplated;		*c*- and *a*-axis			[24.07]
	// 0.016	0.798	2.5		10		lathe		direction			
		(77.0)										
Hg	⊥ 0.073	0.875	3.1	533–686	7	sc*	^{203}Hg,	2 examples[85]	*Deviating from		24.06	Batra (1967)
		(84.5)		(0.88)		5N	electroplated;		*c*- and *a*-axis			[24.08]
	// 0.056	0.854	3.4		7		lathe		direction			
		(82.5)										
In	⊥ 0.14	0.850	9.2	444–689	7^{51}	sc*	^{114}In, chemically	1 example[84]	*About 20°	Ag in Zn	24.03	Rosolowski
		(82.1)		(0.82)		>5N	plated; lathe		deviating from			(1961) [24.04]
	// 0.062	0.828	5.9		7^{51}				*c*- and *a*-axis			
		(80.0)							direction			
Ni	⊥ 0.43	1.258	0.03	564–664	8	sc	^{63}Ni,		Pronounced data		–	Mortlock
		(121.5)		(0.89)		5N	electroplated;		scatter			(1967) [24.09]
	// 8.1	1.415	0.04		8		autoradiography					
		(136.6)										
Sn	⊥ (0.13)	(0.798)		571–673	4	sc*	^{113}Sn,	No; NSE at	*Deviating from		24.05	Warford (1970)
		(77.0)		(0.90)		5N	electroplated;	lower	*c*- and *a*- axis			[24.10]
	0.185$^+$	0.812$^+$	23$^+$				lathe	temperatures	direction			
		(78.4)							$^+$Present fit to the			
	// (0.15)	0.841			4				experimental data			
	0.16$^+$	(81.4)	12$^+$									

Table 2.5 Diffusion in cadmium (References, see page 119)

(1)	(2a)	(2b)	(3)	(4)	(5)	(6)	(7)	(8)	(9)	(10)	(11)	(12)
X	D^0 (10^{-4} $m^2 s^{-1}$)	Q (eV) and (kJ $mole^{-1}$)	$D(T_m)$ (10^{-12} $m^2 s^{-1}$)	T-range (K) ($\overline{T}/T_m$)	No. of data points	Material, purity	Experimental method	Remarks on the pp	Further remarks	Also studied	Figure	Reference
Self-diffusion												
Cd	⊥ (0.10)	0.828		402–583	10	sc*	^{115}Cd,	2 examples	*<10° deviating	gb diffusion	25.01	Wajda (1955)
	0.115$^+$	(80.0)	1.1$^+$	(0.83)		2N5	electroplated;		from c- and			[25.01]
	// (0.05)	(0.789)		402–582	7		lathe (40 μm		a-axis direction			
		(76.2)		(0.83)			sections)		$^+$Present fit to the			
	0.024$^+$	0.749$^+$	1.1$^+$						experimental			
		(72.3)							data			
Cd	// 0.68	0.893	1.8	453–560	5^{51}	sc	^{115}Cd, vapour	No		Ag, Zn in Cd	–	Hirschwald
		(86.3)		(0.85)		4N	deposition;					(1967) [25.02]
							absorption					
Cd	⊥ 0.183	0.850	1.1	411–587	6^{51}	sc*	^{115}Cd,	No	*<10° deviating	Ag, Au, Hg,	25.01	Mao (1972)
		(82.0)		(0.84)		5N	electroplated;		from c- and a-axis	In, Zn in Cd		[25.03]
	// (0.118)	(0.807)			6^{51}		lathe		direction			
		(77.9)							$^+$Present fit to the			
	0.165$^+$	0.829$^+$	1.5$^+$						depicted data			
		(80.0)										
Cd	⊥ 0.43	0.911	0.8	524–592	4	sc*	^{109}Cd,	4 examples	*<10° deviating	Pressure	25.01	Buescher (1973)
		(87.9)		(0.94)		5N	electroplated;	(at high	from c- and	dependence		[25.04]
	// 0.32	0.861	1.6		4		lathe	pressure)	a-axis direction	(0–0.8 Gpa)		
		(83.2)										
Impurity diffusion												
Ag	// 2.21	1.102	0.10	457–574	4^{51}	sc	^{110}Ag, vapour	No		Cd, Zn in Cd	–	Hirschwald
		(106.4)		(0.87)		4N	deposition;					(1967) [25.02]
							absorption					
Ag	⊥ (0.68)	1.087		479–582	6^{51}	sc*	^{110}Ag,	No	*<10° deviating	Au, Cd, Hg,	25.02	Mao (1972)
	0.60$^+$	(105.0)	0.04$^+$	(0.89)		5N	electroplated;		from c- and	In, Zn in Cd		[25.03]
	// (1.40)	1.069			6^{51}		lathe		a-axis direction			
	1.25$^+$	(103.2)	0.11$^+$						$^+$Present fit to the			
									depicted data			
Au	⊥ 3.16	1.146	0.06	452–577	5^{51}	sc*	^{195}Au,	No	*<10° deviating	Ag, Cd, Hg,	25.03	Mao (1972)
		(110.7)		(0.87)		5N	electroplated;		from c- and	In, Zn in Cd		[25.03]
	// 1.40	1.105	0.06		5^{51}		lathe		a-axis direction			
		(106.6)										

Table 2.5 (*Continued*)

(1)	(2a)	(2b)	(3)	(4)	(5)	(6)	(7)	(8)	(9)	(10)	(11)	(12)
X	D^0 (10^{-4} m^2 s^{-1})	Q (eV) and (kJ mole^{-1})	$D(T_m)$ (10^{-12} m^2 s^{-1})	T-range (K) ($\overline{T}/T_m$)	No. of data points	Material, purity	Experimental method	Remarks on the pp	Further remarks	Also studied	Figure	Reference
Hg	⊥ 0.21	0.814 (78.6)	2.6	422–572 (0.84)	7[51]	sc* 5N	^{203}Hg, electroplated; lathe	No	*<10° deviating from *c*- and *a*-axis direction	Ag, Au, Cd, In, Zn in Cd	25.02	Mao (1972) [25.03]
	// 0.21	0.814 (78.6)	2.6		7[51]							
In	⊥ 0.09	0.735 (70.9)	5.2	434–571 (0.85)	5[51]	sc* 5N	^{114}In, electroplated; lathe	No	*<10° deviating from *c*- and *a*-axis direction	Ag, Au, Cd, Hg, Zn in Cd	25.03	Mao (1972) [25.03]
	// 0.10	0.757 (73.1)	3.8		5[51]							
Pb	⊥ 0.071	0.681 (65.8)	11.7	514–571 (0.91)	5	sc 5N	^{210}Pb, electroplated; lathe	1 example	*1°–18° deviating from *c*- and *a*-axis direction		25.04	Yeh (1981) [25.05]
	// 0.060	0.714 (68.9)	5.3		5							
Zn	⊥ 0.084	0.781 (75.4)	2.0	430–588 (0.86)	12[51]	sc* 5N	^{65}Zn, electroplated; lathe	2 examples	*<10° deviating from *c*- and *a*-axis direction	Ag, Au, Cd, Hg, In in Cd; E(472 K) for Zn in Cd	25.04	Mao (1972) [25.03]
	// 0.13	0.782 (75.5)	3.0		11[51]							

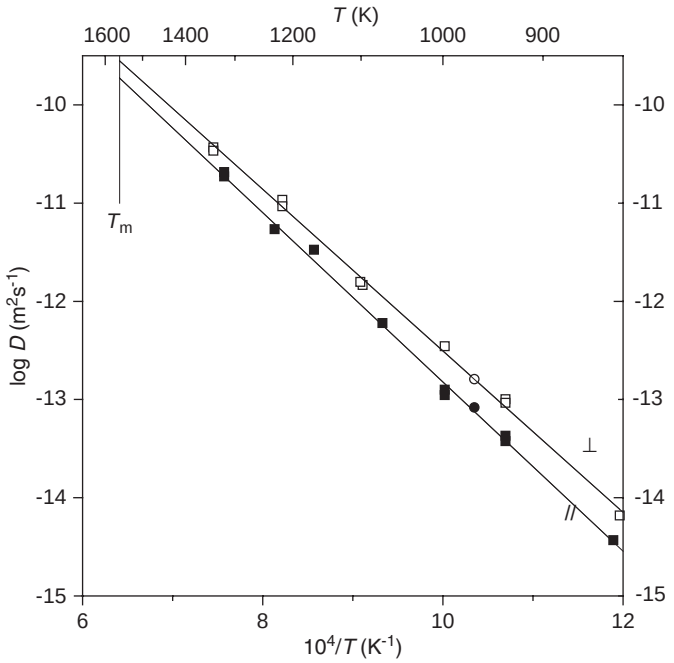

Fig. 21.01 Self-diffusion in beryllium. □ and ■, Dupouy [21.01]; ○ and ●, Beyeler [21.03]. Fitting lines according to [21.01].

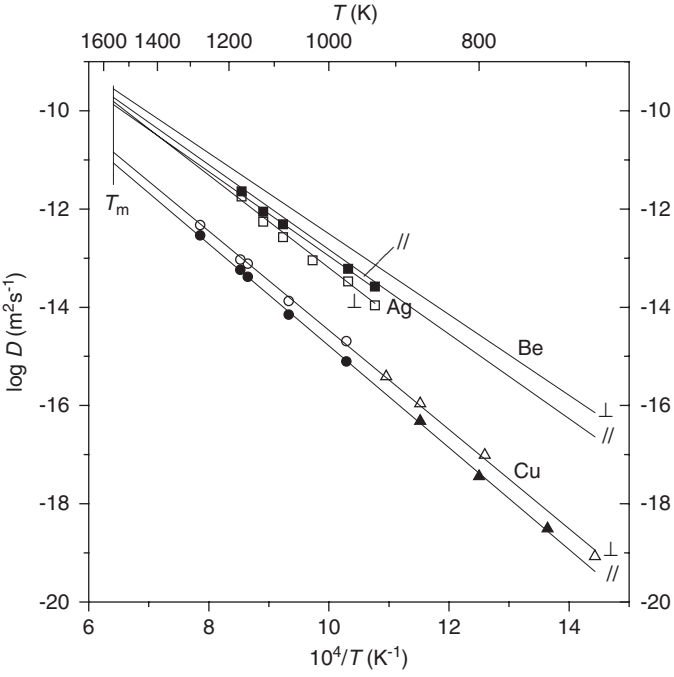

Fig. 21.02 Impurity diffusion in beryllium. Ag in Be: □ and ■, Naik [21.05]; Cu in Be: ○ and ●, Dupouy [21.09]; △ and ▲, Myers [21.10]. Fitting lines according to [21.10].

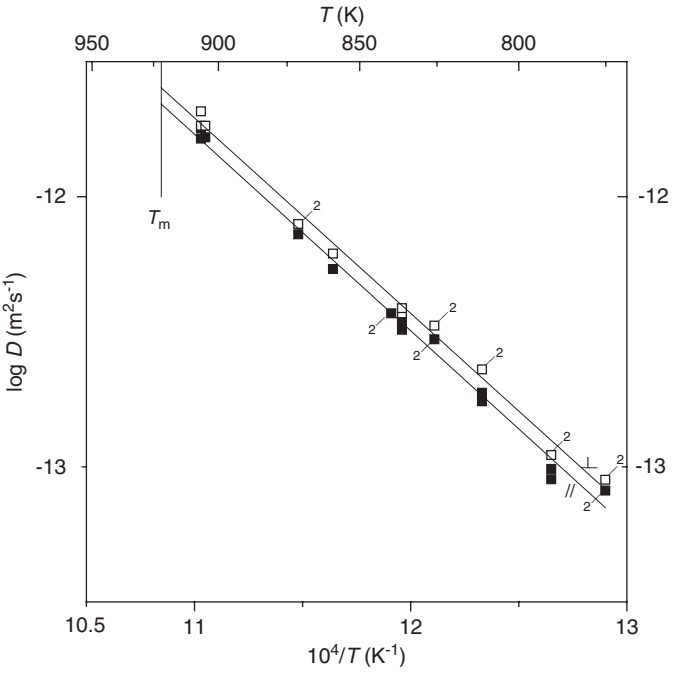

Fig. 22.01 Self-diffusion in magnesium. □ and ■, Combronde [22.03].

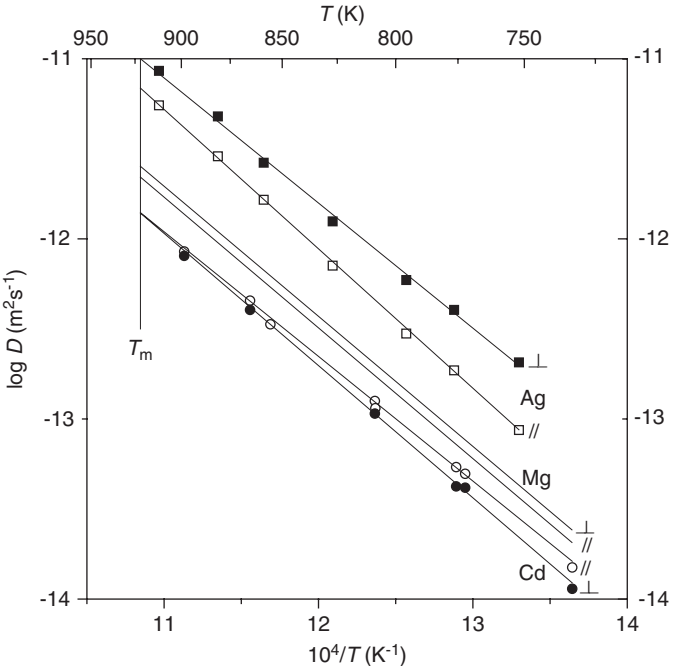

Fig. 22.02 Impurity diffusion in magnesium. Ag in Mg: □ and ■, Combronde [22.05]; Cd in Mg: ○ and ●, Combronde [22.05].

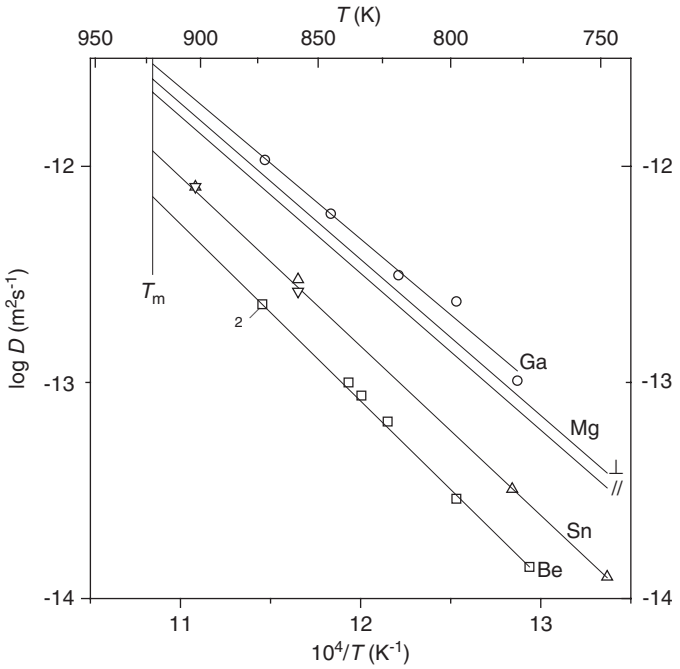

Fig. 22.03 Impurity diffusion in magnesium. Be in Mg: □, Yerko [22.06]; Ga in Mg: ○, Stloukal [22.09]; Sn in Mg: △ (//) and ▽ (⊥), Combronde [22.05]. Fitting line for $D_{//}$.

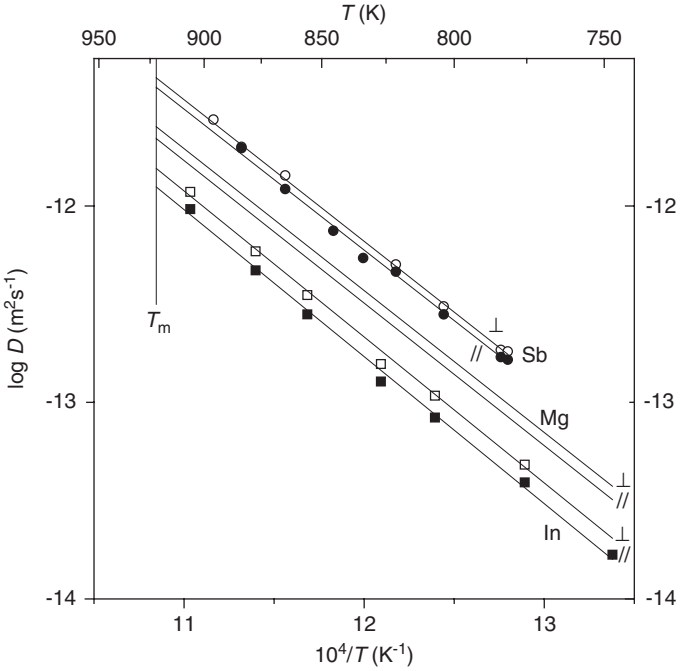

Fig. 22.04 Impurity diffusion in magnesium. In in Mg: □ and ■, Combronde [22.05]; Sb in Mg: ○ and ●, Combronde [22.03].

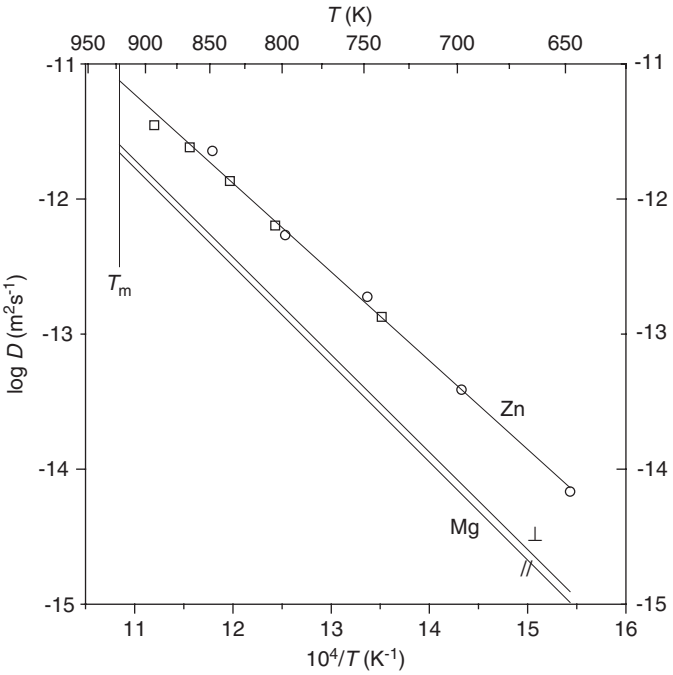

Fig. 22.05 Impurity diffusion in magnesium. Zn in Mg: □, Lal [22.09]; ○, Čermák [22.10]. Fitting line using $D^0 = 1.0 \times 10^{-4}\,m^2\,s^{-1}$ and $Q = 1.303\,eV$.

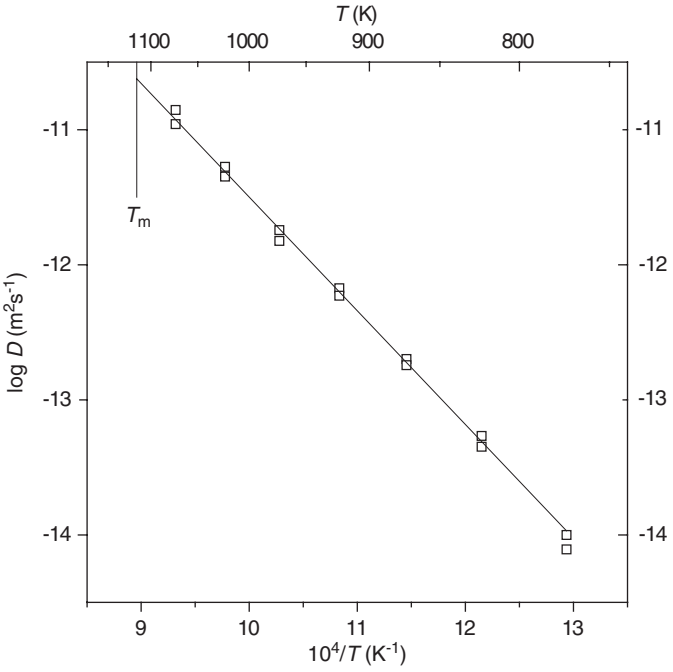

Fig. 23.01 Self-diffusion in Ca. □, Pavlinov [23.01].

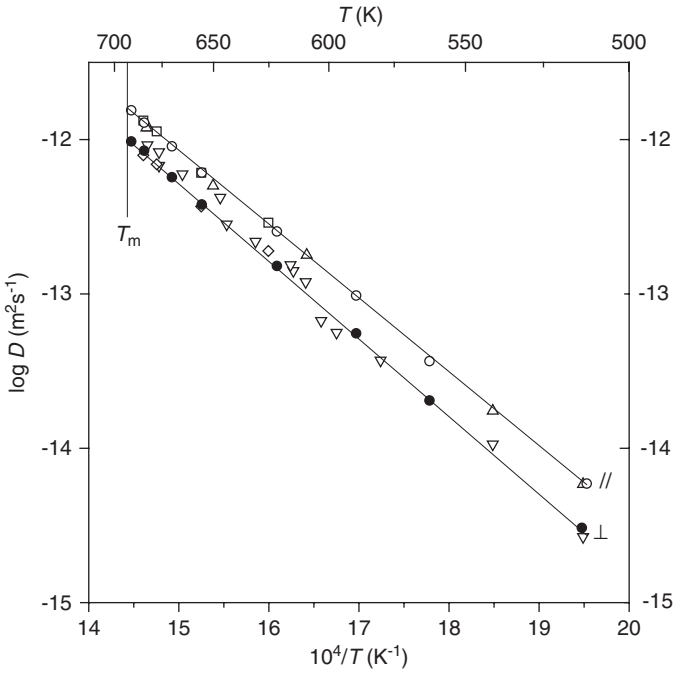

Fig. 24.01 Self-diffusion in zinc. △ and ▽, Shirn [24.01]; □ and ◇, Batra [24.02]; ○ and ●, Peterson [24.03]. Fitting line according to [24.03].

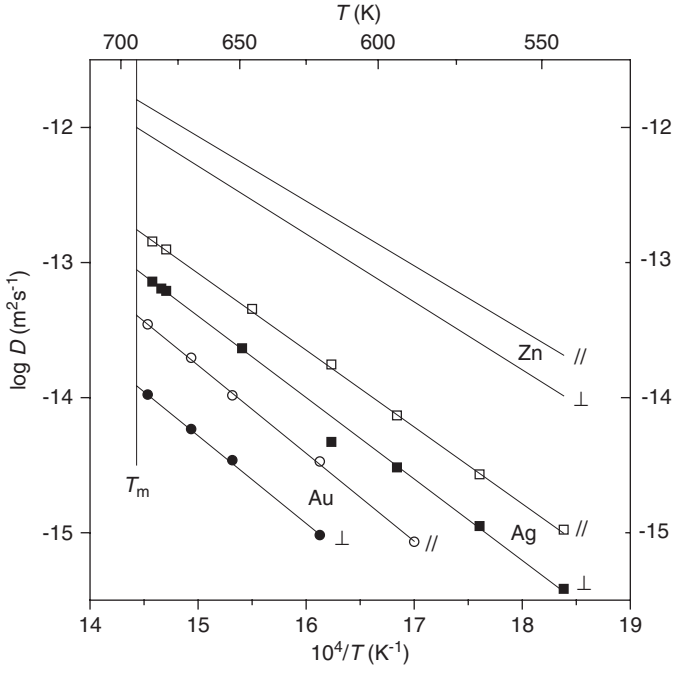

Fig. 24.02 Impurity diffusion in zinc. Ag: □ and ■, Rosolowski [24.04]; Au: ○ and ●, Ghate [24.05].

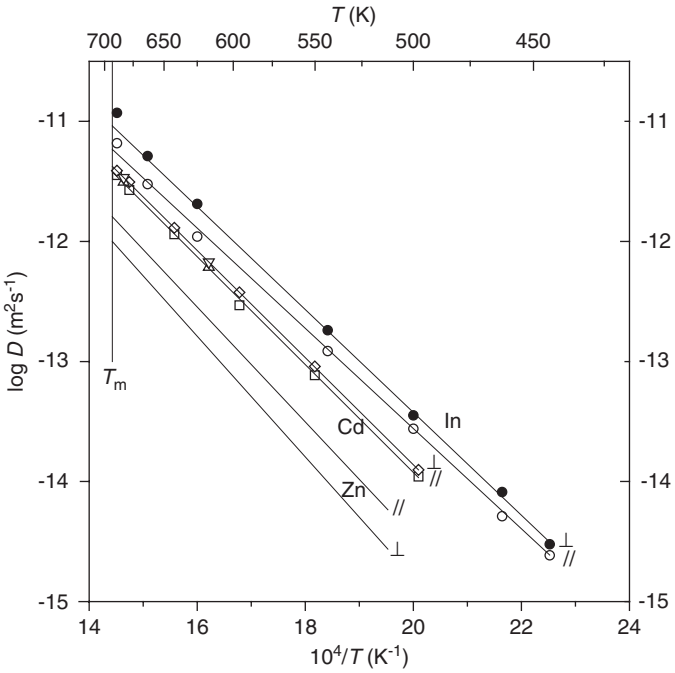

Fig. 24.03 Impurity diffusion in zinc. Cd: □ and ◇, Ghate [24.05]; △ and ▽, Batra [24.02]. Fitting lines according to [24.05]. In: ○ and ●, Rosolowski [24.04].

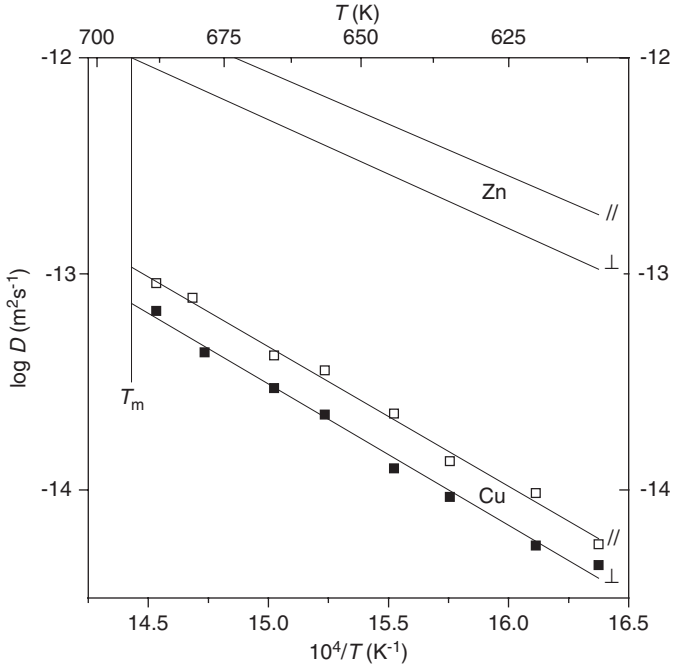

Fig. 24.04 Impurity diffusion in zinc. Cu: □ and ■, Batra [24.07].

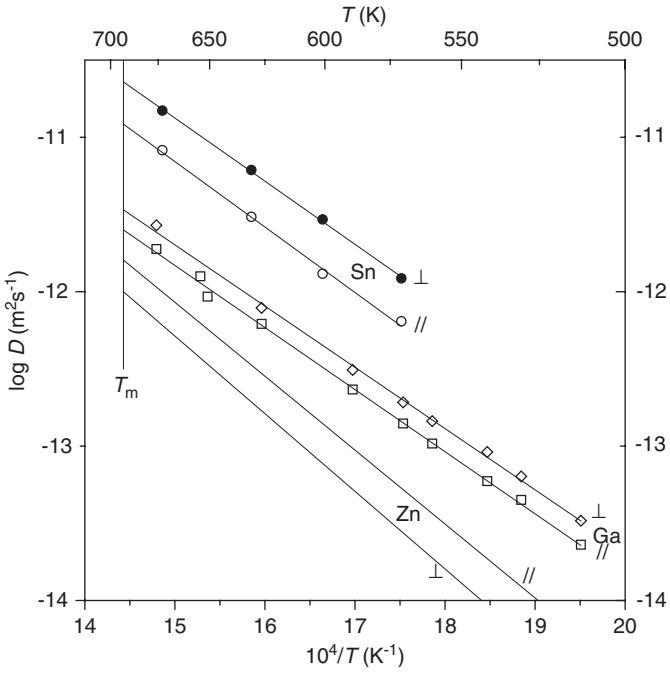

Fig. 24.05 Impurity diffusion in zinc. Ga: □ and ◇, Batra [24.07]; Sn: ○ and ●, Warford [24.10].

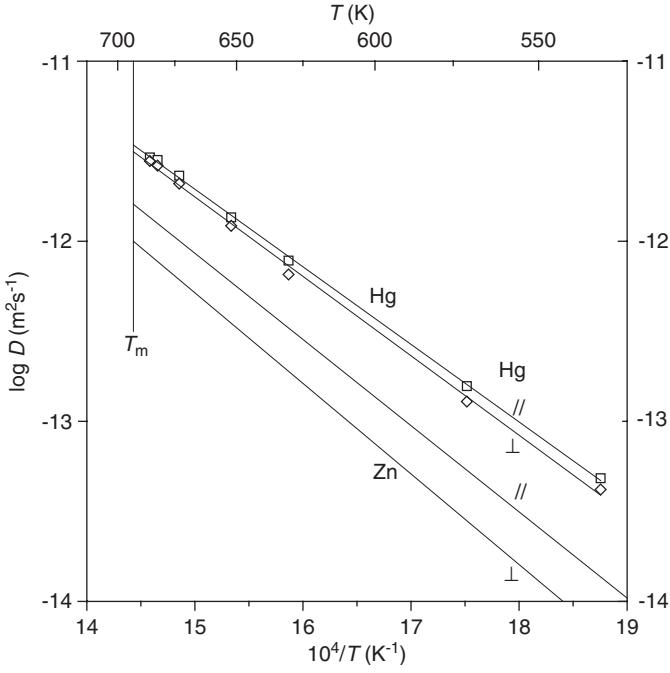

Fig. 24.06 Impurity diffusion in zinc. Hg: □ and ◇, Batra [24.08].

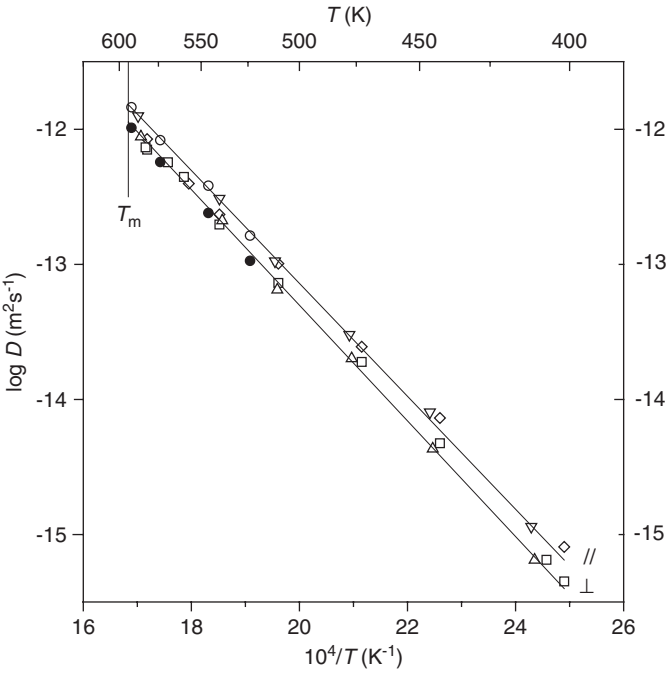

Fig. 25.01 Self-diffusion in cadmium. ◇ and □, Wajda [25.01]; ▽ and △, Mao [25.03]; ○ and ●, Buescher [25.04]. Fitting lines according to [25.03].

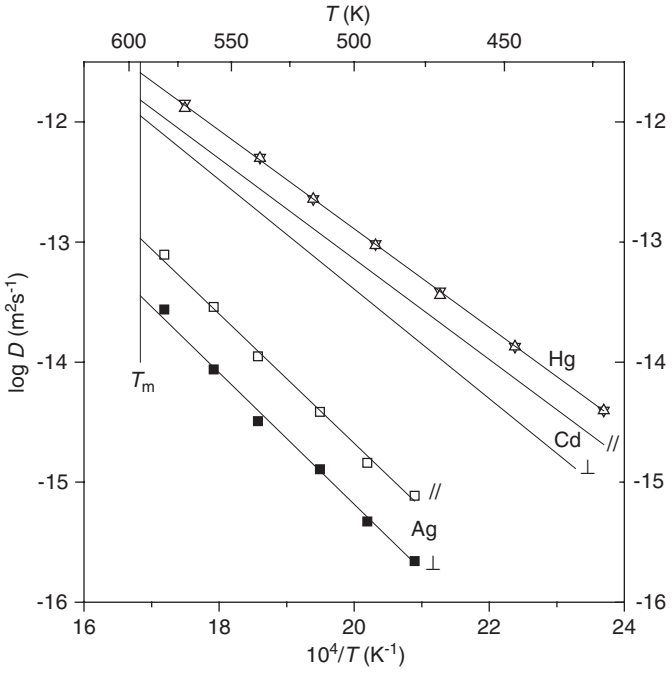

Fig. 25.02 Impurity diffusion in cadmium. Ag: □ and ■, Mao [25.03]; Hg: ▽ and △, Mao [25.03].

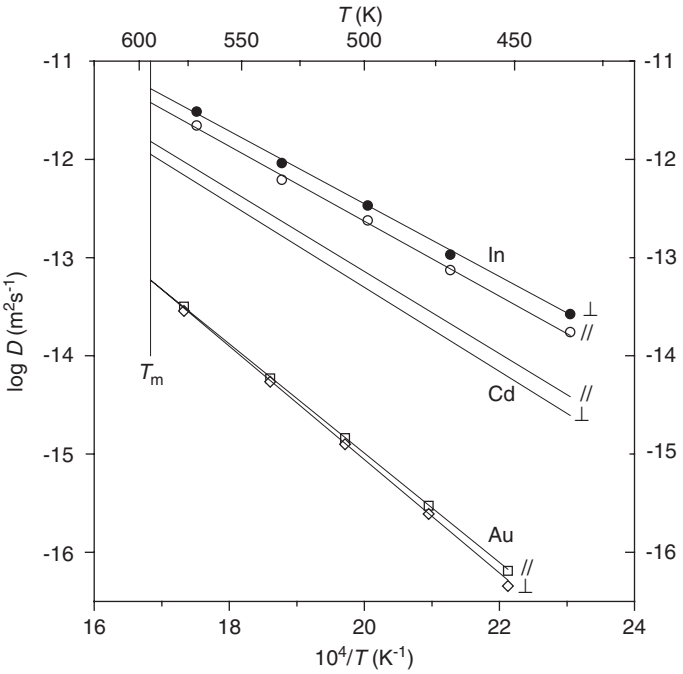

Fig. 25.03 Impurity diffusion in cadmium. Au: □ and ◇, Mao [25.03]; In: ○ and ●, Mao [25.03].

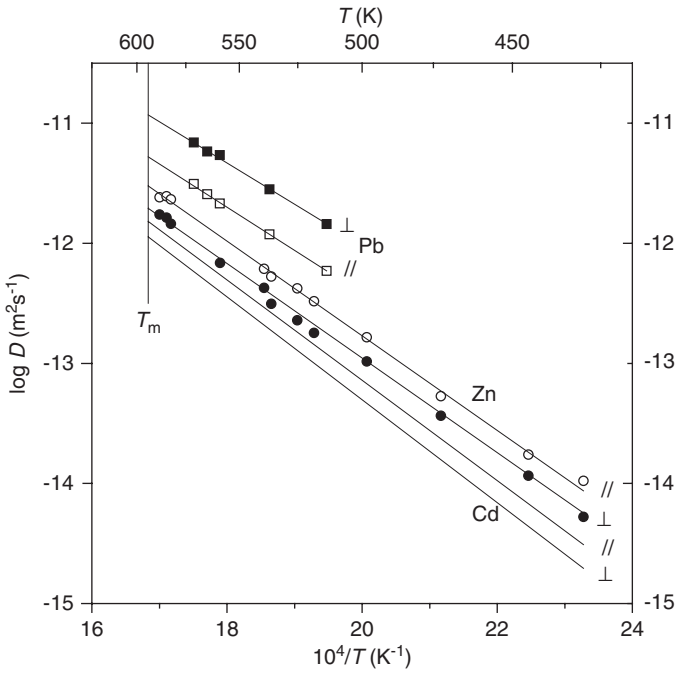

Fig. 25.04 Impurity diffusion in cadmium. Pb: □ and ■, Yeh [25.05]; Zn: ○ and ●, Mao [25.03].

REFERENCES

References to Chapter 2.1

[21.01] J.M. Dupouy, J. Mathie, Y. Adda, Mém. Sci. Rev. Métall. **63** (1966) 481.
[21.02] L.V. Pavlinov, G.V. Grigoryev, Yu.G. Sevastyanov, Fiz. Met. Metalloved. **25** (1968) 565; Phys. Met. Metallogr. **25** (3) (1968) 201 (English transl.).
[21.03] M. Beyeler, D. Lazarus, Mém. Sci. Rev. Métall. **67** (1970) 395.
[21.04] V.P. Gladkov, A.V. Svetlov, D.M. Skorov, A.N. Shabalin, Atomn. Energiya **40** (1976) 257; Sov. Atom. Energy **40** (1976) 306 (English transl.).
[21.05] M.C. Naik, J.M. Dupouy, Y. Adda, Mém. Sci. Rev. Métall. **63** (1966) 488.
[21.06] S.M. Myers, R.A. Langley, J. Appl. Phys. **46** (1975) 1034.
[21.07] V.M. Ananin, V.P. Gladkov, A.V. Svetlov, D.M. Skorov, V.I. Tenishev, Atomn. Energiya **40** (1976) 256; Sov. Atom. Energy **40** (1976) 304 (English transl.).
[21.08] V.P. Gladkov, A.V. Svetlov, D.M. Skorov, A.N. Shabalin, Fiz. Met. Metalloved. **48** (1979) 871; Phys. Met. Metallogr. **48** (4) (1979) 170 (English transl.).
[21.09] J.M. Dupouy, J. Mathie, Y. Adda, Proc. Intern. Conf. Metall. Beryllium, Grenoble (1965) p.159.
[21.10] S.M. Myers, S.T. Pricaux, T.S. Prevender, Phys. Rev. B **9** (1974) 3953.
[21.11] G. Donze, R. Le Hazif, F. Maurice, D. Dutilloy, Y. Adda, C.R. Acad. Sci. Paris **254** (1962) 2328.
[21.12] V.M. Ananin, V.P. Gladkov, V.S. Zotov, D.M. Skorov, V.I. Tenishev, Atomn. Energiya **29** (1970) 220; Sov. Atom. Energy **29** (1970) 941 (English transl.).

References to Chapter 2.2

[22.01] P.G. Shewmon, F.N. Rhines, Trans. AIME **200** (1954) 1021.
[22.02] P.G. Shewmon, Trans. AIME **206** (1956) 918.
[22.03] J. Combronde, G. Brebec, Acta Metall. **19** (1971) 1393.
[22.04] K. Lal, Rep. No. CEA-R 3136 (Saclay) (1967); see Diffusion Data **3** (1969) 144.
[22.05] J. Combronde, G. Brebec, Acta Metall. **20** (1972) 37.
[22.06] V.F. Yerko, V.F. Zelenskiy, V.S. Krasnorutskiy, Fiz. Met. Metalloved. **22** (1966) 112; Phys. Met. Metallogr. **22** (1) (1966) 112 (English transl.).
[22.07] K. Lal, V. Lévy, C. R. Acad. Sci. Paris **262C** (1966) 107.
[22.08] L.V. Pavlinov, A.M. Gladyshev, V.N. Bykov, Fiz. Met. Metalloved. **26** (1968) 823; Phys. Met. Metallogr. **26** (5) (1968) 53 (English transl.).
[22.09] I. Stloukal, J. Čermák, Scr. Mater. **49** (2003) 557; see also Defect and Diffusion Forum **237–240** (2005) 1287.
[22.10] J. Čermák, I. Stloukal, Phys. Stat. Sol. (a) **203** (2006) 2386.

References to Chapter 2.3

[23.01] L.V. Pavlinov, A.M. Gladyshev, V.N. Bykov, Fiz. Met. Metalloved. **26** (1968) 823; Phys. Met. Metallogr. **26** (5) (1968) 59 (English transl.).

References to Chapter 2.4

[24.01] G.A. Shirn, E.S. Wajda, H.B. Huntington, Acta Metall. **1** (1953) 513.
[24.02] A.P. Batra, Phys. Rev. **159** (1967) 487.
[24.03] N.L. Peterson, S.J. Rothman, Phys. Rev. **163** (1967) 645.
[24.04] J.H. Rosolowski, Phys. Rev. **124** (1961) 1828.
[24.05] P.B. Ghate, Phys. Rev. **131** (1963) 174.

[24.06] M. Chandramouli, V.S. Venkatasubramanian, Proc. Nucl. Phys. Sol. State Symp. **17C** (1974) 167.
[24.07] A.P. Batra, H.B. Huntington, Phys. Rev. **145** (1966) 542.
[24.08] A.P. Batra, H.B. Huntington, Phys. Rev. **154** (1967) 569.
[24.09] A.J. Mortlock, P.M. Ewans, Phys. Rev. **156** (1967) 814.
[24.10] J.S. Warford, H.B. Huntington, Phys. Rev. B **1** (1970) 1867.

Further Investigations

Zn [24.11] H.B. Huntington, G.A. Shirn, E.S. Wajda, Phys. Rev. **87** (1952) 211; precursor to Ref. [24.01].
Zn [24.12] T. Liu, H.G. Drickamer, J. Chem. Phys. **22** (1954) 312.
Zn [24.13] F.E. Jaumot, R.L. Smith, Trans. AIME **206** (1956) 137.
Zn [24.14] J.E. Hilliard, B.L. Averbach, M. Cohen, Acta Metall. **7** (1959) 86; polycrystalline Zn.
Zn [24.15] H.M. Gilder, B.J. Buescher, L.C. Chhabildas, in: *Atomic Transport in Solids and Liquids*, Eds. A. Lodding, T. Lagerwall, Verlag der Zeitschrift für Naturforschung, Tübingen (1971), p. 33.
Zn [24.16] L.C. Chhabildas, H.M. Gilder, Phys. Rev. B **5** (1972) 2135; pressure dependence of *D*.

References to Chapter 2.5

[25.01] E.S. Wajda, G.A. Shirn, H.B. Huntington, Acta Metall. **3** (1955) 39.
[25.02] W. Hirschwald, W. Schrödter, Z. Phys. Chem. N.F. **53** (1967) 392.
[25.03] Ch. Mao, Phys. Rev. B **5** (1972) 4693.
[25.04] B.J. Buescher, H.M. Gilder, N. Shea, Phys. Rev. B **7** (1973) 2261.
[25.05] D.C. Yeh, L.A. Acuna, H.B. Huntington, Phys. Rev. B **23** (1981) 1771.

Further Investigations

Cd [25.06] K.A. Mahmoud, R. Kamel, Radioisotopes in Scientific Research **1** (1958) 271; Acta Metall. **5** (1957) 476 (Abstract); absorption.
Cd [25.07] Y. Masuda, J. Phys. Soc. Japan **13** (1958) 597; polycrystalline Cd, NMR.
Cd [25.08] W. Chomka, Zeszyty Nauk Politech. Gdansk. Fis. (1) (1967) 39, see Diffusion Data **4** (1970) 17.
Cd [25.09] K. Apel, S. Hänsch, K. Prescher, Z. Metallk. **58** (1967) 401; polycrystalline Cd.
Ag [25.10] A.K. Iha, U.P. Sinha, Scr. Metall. **6** (1972) 495; polycrystalline Cd.
Zn see Ref. [25.02].

CHAPTER 3

Self-Diffusion and Impurity Diffusion in Group III Metals

Contents

Tables
- 3.1. Scandium (Sc) 123
- 3.2. Yttrium (Y) 124
- 3.3. Lanthanum (La) 125
- 3.4. Aluminium (Al) 126
- 3.5. Indium (In) 133
- 3.6. Thallium (Tl) 134

Figures
- Yttrium 135
- Lanthanum 135
- Aluminum 136
- Indium 143
- Thallium 144

References 145

Lanthanides (rare earth metals) and **Actinides** are treated in Chapters 9 and 10.

Diffusion investigations in aluminium are accompanied by considerable experimental problems. In air at room temperature oxide films are formed, which can become up to 100 μm thick. This leads to a tracer hold-up in the penetration profiles (near-surface effect, NSE) (see Figure 01.07). Especially, when the tracer layer is dried-on from a salt solution, a pronounced NSE is observed (see e.g. Ref. [34.12]). Careful surface preparation respectively tracer implantation prevent the formation of a marked NSE.

In the early tracer investigations applying residual activity measurements and grinder sectioning technique penetration profiles with an entire depth of 5–15 μm (i.e. within the NSE range) were used for the determination of D. The resulting diffusion coefficients are orders of magnitude smaller than the real values (see e.g. [34.55]). Typical values of D^0 and Q are 10^{-13} to $10^{-10}\,m^2\,s^{-1}$ and 0.6–0.9 eV [30.01–30.05] (for V, Cr, Fe, Co, Ni, Nb, Mo in Al).

For self-diffusion investigations an additional difficulty is that the only available radiotracer ^{26}Al has an extremely low specific activity, which needs the deposition of a thick layer. Again, the oxide hold-up results in too small D-values, an effect that increases with decreasing temperature. Only for high temperatures

(>873 K) the measured self-diffusion coefficients [34.01] are assumed to be quite accurate [34.07].

For **actinium** (Ac) no data are available.

For **gallium** (Ga) only self-diffusion was investigated close to T_m [30.06]. As in the early diffusion investigations in Al, the evaluated diffusion coefficients of ^{67}Ga in Ga are extremely small.

In Table 3.0 lattice structure, lattice constants, melting and phase transition temperatures of group III metals are listed.

Table 3.0 Lattice structure, lattice constants *a* and *c*, phase transition (T_{ij}) and melting temperature T_m

Metal	Sc		Y	La		Al	In	Tl	
Phase	α	β	α	β	γ			α	β
Structure	fcc	hcp	hcp	fcc	bcc	fcc	fct	hcp	bcc
T_{ij} (K)	1,608		1,752	1,134				507	
T_m (K)	1,812		1,803	1,193		933	430	577	
a (nm)	0.453	0.331	0.363	0.531		0.404	0.458	0.345	0.387
c (nm)		0.527	0.575				0.494	0.551	
c/*a*		1.59	1.58				1.07	1.60	

Table 3.1 Impurity diffusion in scandium (References, see page 145)

(1)	(2a)	(2b)	(3)	(4)	(5)	(6)	(7)	(8)	(9)	(10)	(11)	(12)
X	D^0 (10^{-4} m^2 s^{-1})	Q (eV) and (kJ mole^{-1})	$D(T_m)$ (10^{-12} m^2 s^{-1})	T-range (K) ($\overline{T}/T_m$)	No. of data points	Material, purity	Experimental method	Remarks on the pp	Further remarks	Also studied	Figure	Reference
Fe	1.5×10^{-3}*	0.599* (54)	–	1,241–1,790 (0.84)	9	pc 3N5	Fe; mass spectroscopy Sc/Sc(X% Fe)^x (Grube)	1 example (probability plot)	*Valid for the α-phase $^x100X = 1.2$, 2.5, 4.3	Electro-transport	–	Axtell (1986) [31.01]

Table 3.2 Self-diffusion and impurity diffusion in α-yttrium (References, see page 145)

(1)	(2a)	(2b)	(3)	(4)	(5)	(6)	(7)	(8)	(9)	(10)	(11)	(12)
X	D^0 (10^{-4} m^2 s^{-1})	Q (eV) and (kJ mole^{-1})	$D(T_m)$ (10^{-12} m^2 s^{-1})	T-range (K) ($\overline{T}/T_m$)	No. of data points	Material, purity	Experimental method	Remarks on the pp	Further remarks	Also studied	Figure	Reference
Y	⊥ 5.2	2.910 (281.9)	–	1,173–1,573 (0.76)	5	sc[61]	[91]Y, dried-on from salt solution; residual activity, abrasive paper	1 example			32.01	Gornyy (1970) [32.01]
	// 0.82	2.615 (252.5)			5							
Ag	0.0054	0.797 (77)	–	1,178–1,453* (0.73)	6	pc 2N4	[110]Ag; diffusion couple; lathe	No	*Temperature uncertainty about ±10 K	Fe in α-Y; electro-transport	32.01	Murphy (1975) [32.02]
Co	0.014	0.863 (83.3)	–	1,290–1,620 (0.81)	5	pc 2N6	Co; laser ionization mass spectroscopy, Y/Y (0.05% Co)	1 example (probability plot)	Pronounced data scatter	Fe, Ni in α-Y; electro transport	–	Okafor (1982) [32.03]
Fe	0.018	0.880 (85)	–	1,173–1,603* (0.77)	8	pc 2N4	[59]Fe; diffusion couple; lathe	No	*Temperature uncertainty about ±10 K	Ag in α-Y; electro transport	32.01	Murphy (1975) [32.02]
Fe	0.040	0.954 (92.1)	–	1,355, 1,495	2	pc 2N6	Fe; laser ionization mass spectroscopy	No		Co, Ni in α-Y; electro-transport	32.01	Okafor (1982) [32.03]
Ni	0.058	1.00 (96.5)	–	1,290–1,580 (0.80)	6	pc 2N6	Ni; laser ionization mass spectroscopy	No	Pronounced data scatter	Co, Fe in α-Y; electro-transport	–	Okafor (1982) [32.03]

Table 3.3 Self-diffusion and impurity diffusion in lanthanum (References, see page 146)

(1)	(2a)	(2b)	(3)	(4)	(5)	(6)	(7)	(8)	(9)	(10)	(11)	(12)
X	D^0 (10^{-4} m^2 s^{-1})	Q (eV) and (kJ mole^{-1})	$D(T_m)$ (10^{-12} m^2 s^{-1})	T-range (K) ($\bar{T}/T_m$)	No. of data points	Material, purity	Experimental method	Remarks on the pp	Further remarks	Also studied	Figure	Reference
La	1.5	1.956 (188.8)	–	934–1,116 (0.86) β-La	6[51]	pc (0.1–0.2 mm) 3N7	^{140}La, vapour deposition; lathe	3 examples		Au in La	33.01	Dariel (1969) [33.01]
La	0.013	1.062 (102.6)	41	1,140–1,170 (0.97) γ-La	7[51]	pc 3N7	^{140}La, vapour deposition; lathe	2 examples		La in Ce	33.01	Dariel (1973) [33.02]
La	0.11	1.297 (125.2)	37	1,151–1,183 (0.98) γ-La	8	pc 2N85	^{140}La, electroplated; lathe	1 example			33.01	Languille (1974) [33.03]
Au	0.022	0.785 (75.8)	–	888–1,071 (0.82) β-La	4[51]	pc (0.1–0.2 mm) 3N7	^{198}Au, vapour deposition; lathe	2 examples		La in La	33.02	Dariel (1969) [33.01]
Ce	(0.018) 0.02$^+$	1.084 (104.7)	52$^+$	1,139–1,170 (0.97) γ-La	9 (5T)	pc[61]	^{141}Ce, electroplated; grinder	4 examples at 1,146 K	$^+$Present approxi-mation		33.02	Fromont (1976) [33.04]

Table 3.4 Diffusion in aluminium (References, see page 146)

(1)	(2a)	(2b)	(3)	(4)	(5)	(6)	(7)	(8)	(9)	(10)	(11)	(12)
X	D^0 (10^{-4} m^2 s^{-1})	Q (eV) and (kJ mole^{-1})	$D(T_m)$ (10^{-12} m^2 s^{-1})	T-range (K) ($\overline{T}/T_m$)	No. of data points	Material, purity	Experimental method	Remarks on the pp	Further remarks	Also studied	Figure	Reference
Self-diffusion												
Al	1.71	1.474 (142.4)	1.85	729–916 (0.88)	11 (10T)	pc (~5 mm) 4N	^{26}Al, diffusion couple (150 µm foil of activated Al); lathe	1 example[84, 87] (oxide hold-up, see Figure 01.07)	See introduction page	Mn in Al	34.01	Lundy (1962) [34.01]
Al	2.20$^+$	1.496 (144.4)	1.81$^+$	673–883 (0.83)	10 (6T)	sc[61]	^{26}Al, dried-on from salt solution; grinder (abrasive paper)	No	See introduction page $^+$Present approximation	Au in Au, Cu in Cu; $\Delta V/V_0 = 1.29$	34.01	Beyeler (1968) [34.02]
Al	0.176	1.31 (126.5)		358–482 (0.45)	9	pc (100 µm foil) 6N	Al; void shrinkage (TEM)	–			–	Volin (1968) [34.03]
Al	0.137*	1.28 (123.6)	1.66	515–770 (0.69)	~50[51]	pc (~30 µm foil) 6N	Al; NMR, SLRT $T_{1\rho}$ (^{27}Al signal)	–	*Recalculated to correlated diffusion		34.01	Messer (1974) [34.04]
Al	–	–		722	1*	sc 5N	^{26}Al, diffusion couple; lathe		*$D(722\,\mathrm{K}) = 1.05 \times 10^{-14}$ m^2 s^{-1}		34.01	Hood (1985) [34.05]
Al	0.1[21] (90)[21] 9*	1.26[21] (121.7) 1.79[21] (172.8)	1.75	515–916					Reanalysis of the data of [34.04], two-exponential fit of the data of [34.01, 34.02, 34.04] *Corrected value		–	Dais (1987) [34.06]
Impurity diffusion												
Ag	0.118	1.207 (116.5)	3.6	644–928 (0.84)	9*	sc 5N	^{110}Ag, vapour deposition; microtome	1 example	*Deviating $D(928\,\mathrm{K})$ and $D(921\,\mathrm{K})$ are not shown in the figure	Au, Co, Cr, Cu, Ga, Ge, Zn in Al	34.02	Peterson (1970) [34.07]

Ag	0.13	1.214 (117.2)	3.6	615–883 (0.80)	5	sc 5N	^{110}Ag, AgCl deposition; lathe	No		Au, Cd, Cu, Fe in Al; Ag in Al (1% X) X = Ag, Cu, Zn	34.02	Alexander (1970) [34.08]
Ag	0.16	1.232 (118.9)	3.5	665–868 (0.82)	10 (9T)	sc 4N5	^{110}Ag, vapour deposition; grinder and EPMA (vapour deposition of inactive Ag)	No		Au, Cu in Al	–	Beyeler (1970) [34.09]
Au	0.131	1.205 (116.4)	4.0	642–928 (0.84)	8	sc 5N	^{198}Au, vapour deposition; microtome	1 example		Ag, Co, Cr, Cu, Ga, Ge, Zn in Al	34.03	Peterson (1970) [34.07]
Au	0.077	1.171 (113.0)	3.6	696–832 (0.82)	6 (5T)	sc 5N	^{198}Au, $AuCl_3$ deposition; lathe	No		Ag, Cd, Cu, Fe in Al	34.03	Alexander (1970) [34.08]
Au	0.27	1.253 (121.0)	4.6	723–873 (0.86)	8	sc 4N5	^{198}Au, vapour deposition; grinder and EPMA (vapour deposition of inactive Au)	No		Ag, Cu in Al	–	Beyeler (1970) [34.09]
Au	–	–		785–873	3[51]	sc 5N5	^{195}Au, implanted; microtome	3 examples at high pressure		Fe, Zn in Al; $\Delta V/V_0 \approx 1.0$	34.03	Becker (1989) [34.10]
Cd	1.04	1.288 (124.3)	11.4	714–907 (0.87)	5	sc 5N	^{115}Cd, $CdCl_2$ deposition; lathe	3 examples (slight NSE)		Ag, Au, Cu, Fe in Al	34.04	Alexander (1970) [34.08]
Co	464	1.810 (174.8)	7.7	695–927 (0.87)	10	sc 5N	^{60}Co, vapour deposition; microtome	6 examples (marked NSE at lower T, oxide hold-up)		Ag, Au, Cr, Cu, Ga, Ge, Zn in Al	34.05	Peterson (1970) [34.07]
Co	506	1.82 (175.7)	7.4	724–930 (0.89)	4	sc 5N	^{60}Co, implanted; lathe	All			34.05	Hood (1983) [34.11]
Co	193	1.744 (168.4)	7.3	603–897 (0.80)	5	sc 5N5	^{57}Co, implanted; microtome	All	Additional investigations using tracer layers dried-on from $^{57}CoCl_2$ solution, see introduction page	Cr, Fe, Mn in Al	34.05	Rummel (1995) [34.12]
Cr	(5×10^4) 1,800[+]	(2.515) (243) 2.62 (253)	1.3×10^{-3} [+]	859–923 (0.95)	3	sc 5N	^{51}Cr, vapour deposition; microtome	No	[+]Present approxi-mation	Ag, Au, Co, Cu, Ga, Ge, Zn in Al	34.06	Peterson (1970) [34.07]

Table 3.4 *(Continued)*

(1)	(2a)	(2b)	(3)	(4)	(5)	(6)	(7)	(8)	(9)	(10)	(11)	(12)
X	D^0 (10^{-4} m^2 s^{-1})	Q (eV) and (kJ mole^{-1})	$D(T_m)$ (10^{-12} m^2 s^{-1})	T-range (K) ($\overline{T}/T_m$)	No. of data points	Material, purity	Experimental method	Remarks on the pp	Further remarks	Also studied	Figure	Reference
Cr	6,430*	2.715* (262.1)	1.4×10^{-3}	833–928 (0.94)	12 (10T)	pc	Cr; EPMA Al/Al (X% Cr)	1 example (probability plot)	*$\tilde{D}$ valid for $X/2$; $X = 0.1, 0.26$	Mo, Ti, V, W in Al	34.06	Chi (1977) [34.13]
Cr	2,900	2.662 (257)	1.2×10^{-3}	873–923 (0.96)	8[51]	pc 4N3	Cr; EPMA Al/Al (0.15% Cr) (Matano, Hall)	1 example (c–x)		Hf, Mn in Al	34.06	Minamino (1987) [34.14]
Cr	10^5	2.921 (282)	1.7×10^{-3}	873–923 (0.96)	6	sc 5N5	[51]Cr, implanted; microtome	4 examples		Co, Fe, Mn in Al	34.06	Rummel (1995) [34.12]
Cu	(2.02) 1.82+	1.474 (142.4)	2.0+	714–887 (0.86)	7	pc (wire) 4N5	Cu, electroplated; resistometric method	–	+Present approximation		34.02	Ceresara (1968) [34.15]
Cu	0.647	1.399 (135.1)	1.8	706–925 (0.87)	8	sc 5N	[64]Cu, vapour deposition; microtome	1 example		Ag, Au, Co, Cr, Ga, Ge, Zn in Al	34.02	Peterson (1970) [34.07]
Cu	(1.3) 1.05+	1.431 (138.2)	2.0+	648–892 (0.83)	4	pc 4N8	[64]Cu, electroplated; residual activity	3 examples	+Present approximation	Au in Al	34.02	Fujikawa (1971) [34.16]
Cu	–	–		858, 929	2	sc 5N	[64]Cu, [67]Cu, electroplated; microtome	No		E(929 K) = 0.81, E(858 K) = 0.89; Zn in Al	34.02	Peterson (1978) [34.17]
Cu	(0.654) 0.59+	1.41 (136.1)	1.4+	594–928 (0.82)	18 (14T)	pc 5N	[67]Cu, [64]Cu, [61]Cu, electroplated; microtome and residual activity (SiC paper)	Numerous examples (partly very flat pp, NSE at low temperatures)	+Present approximation		34.02	Fujikawa (1989) [34.18]
Cu	0.9[21] 500[21]	1.440[21] (139) 2.175[21] (210)	1.6	667–930 (0.86)	26	sc 5N5	[67]Cu, [64]Cu, [61]Cu, electroplated; microtome	6 examples		Isotope effect	34.02	Ushino (1991) [34.19]

Fe				792–931	11 (9T)	sc, pc 5N, 4N	^{59}Fe, vapour deposition and implantation; lathe	6 examples	D(792 K) and D(830 K) are disregarded in the least-squares fit		34.06	Hood (1970) [34.20]
	9.1×10^5	2.68 (258.8)	0.30	850–931 (0.95)	9 (7T)							
Fe	135	1.995 (192.6)	0.22	823–909 (0.93)	8	sc 5N	^{59}Fe, $FeCl_2$ deposition; lathe	3 examples (slight NSE)	Only 8 of 20 samples show Gaussian pp	Ag, Au, Cd, Cu in Al	34.06	Alexander (1970) [34.08]
Fe	–	–		857, 896	2^{51}	sc 5N5	^{59}Fe, implanted; microtome	3 examples at high pressure		Au, Zn in Al, $\Delta V/V_0 \approx 1.5$	34.06	Becker (1989) [34.10]
Fe	7,700	2.289 (221)	0.33	723–931 (0.89)	10	sc 5N5	^{59}Fe, implanted; microtome	Numerous examples		Co, Cr, Mn in Al	34.06	Rummel (1995) [34.12]
Ga	(0.49) 0.46$^+$	1.268 (122.4)	6.5$^+$	680–925 (0.86)	9	sc 5N	^{72}Ga, vapour deposition; microtome	1 example	$^+$Present approximation	Ag, Au, Co, Cr, Cu, Ge, Zn in Al	34.07	Peterson (1970) [34.07]
Ga	(0.475) 0.51$^+$	1.274 (123)	6.7$^+$	712–853 (0.84)	6^{51}	pc 4N3	Ga; EPMA Al/Al (1.16% Ga) (Matano, Hall)	No	$^+$Present approximation to the depicted data	Ge in Al	34.07	Minamino (1989) [34.21]
Ge	0.481	1.257 (121.3)	7.8	674–926 (0.86)	9	sc 5N	^{71}Ge, vapour deposition; microtome	1 example		Ag, Au, Co, Cr, Cu, Ga, Zn in Al	34.08	Peterson (1970) [34.07]
Ge	0.276	1.222 (118)	6.9	693–873 (0.84)	7^{51}	pc 4N3	Ge; EPMA Al/Al (X% Ge) (Matano, Hall)	No	$X = 0.78$; 1.38	Ga in Al	34.08	Minamino (1989) [34.21]
Ge	0.339	1.237 (119.4)	7.1	572–916 (0.80)	12 (11T)	sc 5N5	^{71}Ge, vapour deposition and implantation	Numerous examples		$\Delta V/V_0 \approx 1.2$	34.08	Thürer (1995) [34.22]
Hg	(15.3)	(1.469) (141.8)	(18)	718–862 (0.85)	9 (8 T)	pc 5N	^{203}Hg, electroplated; residual activity	1 example (NSE, oxide hold-up)	Pronounced data scatter	Pb, Tl in Al	–	Sawayanagi (1978) [34.23]
Hf	(120) 114$^+$	2.506 (242)	$3.3 \times 10^{-4+}$	873–923 (0.96)	10^{51}	pc 4N3	Hf; EPMA Al/Al (0.1% Hf) (Matano, Hall)	1 example	$^+$Present fit to the depicted data	Cr, Mn in Al	34.09	Minamino (1987) [34.14]
In	(1.16) 1.38$^+$	1.27 (122.6)	19$^+$	715–929 (0.88)	6	sc 5N	^{114}In, implanted; microtome	All	$^+$Present approximation		34.07	Hood (1971) [34.24]
Ir	0.049	1.135 (109.6)	3.6	592–909 (0.80)	10	sc 5N5	^{192}Ir, vapour deposition; microtome	Several examples		Pd in Al	34.10	Khoukaz (2000) [34.25]

Table 3.4 *(Continued)*

(1)	(2a)	(2b)	(3)	(4)	(5)	(6)	(7)	(8)	(9)	(10)	(11)	(12)
X	D^0 (10^{-4} m^2 s^{-1})	Q (eV) and (kJ mole^{-1})	$D(T_m)$ (10^{-12} m^2 s^{-1})	T-range (K) ($\overline{T}/T_m$)	No. of data points	Material, purity	Experimental method	Remarks on the pp	Further remarks	Also studied	Figure	Reference
Li	(0.53)*	(1.315)* (127)	(4.1)*	803–923 (0.92)	6	pc 4N3	Li; resistometric method	–	*$\tilde{D}$ valid for $X \approx 0.35$ at % Li		–	Minamino (1987) [34.26]
	0.35[x]	1.305[x] (126)	3.1[x]						[x]Recalculated to $D(X=0)$			
Mg	1.0*	1.344* (129.8)	5.4	523–713 (0.66)	6	pc[61]	Mg; EPMA Al/Al (X% Mg) (Hall)	1 example (c–x)	*$\tilde{D}$ valid for $X=0$; $X=5$ to 20		–	Moreau (1971) [34.27]
Mg	1.24	1.351 (130.4)	6.2	667–928 (0.85)	6	sc 5N	[28]Mg, vapour deposition; microtome	2 examples[85]			34.11	Rothman (1974) [34.28]
Mn	(104) 130[+]	2.19 (211.4)	0.019[+]	730–921 (0.88)	13 (10T)	sc, pc 5N	[55]Mn, [56]Mn, implanted; microtome	4 examples	[+]Present approxi-mation		34.06	Hood (1971) [34.29]
Mn	37	2.102 (203)	0.016	863–923 (0.96)	9	pc 4N3	Mn; EPMA Al/Al (0.25% Mn) (Matano, Hall)	1 example (c–x)		Cr, Hf in Al	–	Minamino (1987) [34.14]
Mn	(317) 300[+]	2.247 (217)	0.022[+]	843–927 (0.95)	15 (9T)	pc 4N	[54]Mn, dried-on from salt solution; microtome	4 examples	[+]Present approxi-mation		34.06	Fujikawa (1987) [34.30]
Mn	87	2.156 (208.2)	0.019	743–929 (0.90)	10	sc 5N5	[54]Mn, implanted; microtome	All		Co, Cr, Fe in Al	34.06	Rummel (1995) [34.12]
Mo	14*	2.589* (250)	1.4×10^{-5}	898–928 (0.98)	9	pc 4N	Mo; EPMA Al/Al (X% Mo)	No	* $\tilde{D}$ valid for $X/2$; $X=0.05, 0.08$	Cr, Ti, V, W in Al	34.09	Chi (1977) [34.13, 34.31]
Na	(6.7×10^{-4})	(1.006) (97.1)		719–863 (0.57)	5	pc[61]	[24]Na, n irradiated Al foil; absorption	–			–	Sudár (1977) [34.32]
Ni	(4.4) 4.65[+]	1.51 (145.8)	3.2[+]	742–924 (0.89)	15 (10T)	pc 4N5	Ni, dried-on from salt solution; resistometric method	–	[+]Present approxi-mation	Co, Zn in Al	34.11	Erdélyi (1978) [34.33]
Pb	(50)	(1.508) (145.6)	(36)	777–876 (0.89)	7	pc 5N	[210]Pb, electroplated; residual activity	1 example (NSE, oxide hold-up)	Pronounced data scatter	Hg, Tl in Al	–	Sawayanagi (1978) [34.23]

Pd	(14)	(1.786)	(0.32)	650–929	8	sc	^{103}Pd, implanted; microtome and IBS	Several examples	$^{+}$Present approximation	Ir in Al	34.10	Khoukaz (2000) [34.25]
		(172.4)		(0.85)		5N5						
	(170)	1.974		749–929	6							
	193^{+}	(190.6)	0.42^{+}	(0.90)								
Ru	410	2.065	0.28	719–873	4	pc	^{103}Ru, electroplated and dried-on from salt solution; Ru, sputter deposition; HIRBS	All[84]		Ru in Ru	–	Dyment (2005) [34.34]
		(199.4)		(0.85)		(3 mm)						
				632, 673	2	6N						
Sb	(0.09)	(1.261)		721–893	12	pc	^{124}Sb, vapour deposition[73]; residual activity	3 examples[84]	$^{+}$Present fit to the experimental data	Ag in Al	–	Badrinarayanan (1968) [34.35]
		(121.7)		(0.86)	(6T)	specpure						
	0.05^{+}	1.205^{+}	1.5^{+}									
		(116.3)										
Sc	4.31	1.792	0.090	813–928	15[51]	sc	^{44}Sc, dried-on from salt solution; microtome	2 examples	Erfc-solution, incorrect ln c–x^2 evaluation		–	Fujikawa (1997) [34.36]
		(173)		(0.93)	(12T)	5N5						
Si	0.35*	1.284*	4.1	623–903	15	pc	Si; EPMA Al/Al (0.5% Si)	3 examples (c–x)	* $\tilde{D}$ valid for X/2		–	Bergner (1973) [34.37]
		(123.9)		(0.82)	(10T)	4N						
Si	2.02	1.409	4.9	753–893	11	pc	Si; EPMA Al/Al (X% Si) (Matano, Darken)	–	$X = 0.58, 0.87, 1.15$		–	Fujikawa (1978) [34.38]
		(136)		(0.88)		5N						
Sn	0.84	1.228	19	649–905	8	sc	^{113}Sn, implanted; microtome	Several examples		$\Delta V/V_0 = 0.87$ at $T = 787$ K	34.08	Erdélyi (1991) [34.39]
		(118.6)		(0.83)		5N8						
Sn	–	–		624–796	6	sc	^{113}Sn, implanted; microtome	3 examples (erfc and ln c–x^2 evaluation)	*D(erfc) fit together with the data of [34.39]	gb-diffusion	34.08	Erdélyi (1991) [34.40]
	0.454*	1.186*	18	(0.76)		5N2						
		(114.5)										
Ti	1,120	2.693	3.2×10^{-4}	843–928	11	pc	Ti; EPMA Al/Al (0.1% Ti)	1 example (probability plot)		Cr, Mo, V, W in Al	34.06	Chi (1977) [34.13, 34.41]
		(260.0)		(0.95)		4N						
Tl	(116)	(1.582)	(33)	737–876	7	pc	^{204}Tl, electroplated; residual activity	1 example (NSE, oxide hold-up)	Pronounced data scatter	Hg, Pb in Al	–	Sawayanagi (1978) [34.23]
		(152.7)		(0.86)		5N						
U	(0.1)	(1.214)	(2.7)	798–898	6	pc[61]	^{235}U, vapour deposition of UO_2; nuclear fission technique	1 example (only deeper penetration)			–	Blechet (1968) [34.42]
		(117.2)		(0.91)	(5T)							
V	(1.6×10^4)*	3.135*		843–928	14	pc	V; EPMA Al/Al (X% V)	No	*$\tilde{D}$ valid for X/2 $^{+}$Present approximation; $X = 0.14, 0.19$	Cr, Mo, Ti, W in Al	34.06	Chi (1977) [34.13, 34.41]
	1.45×10^5 $^{+}$	(302.7)	$1.7 \times 10^{-4+}$	(0.95)	(12T)	4N						

Table 3.4 *(Continued)*

(1)	(2a)	(2b)	(3)	(4)	(5)	(6)	(7)	(8)	(9)	(10)	(11)	(12)
X	D^0 (10^{-4} m^2 s^{-1})	Q (eV) and (kJ mole^{-1})	$D(T_m)$ (10^{-12} m^2 s^{-1})	T-range (K) ($\overline{T}/T_m$)	No. of data points	Material, purity	Experimental method	Remarks on the pp	Further remarks	Also studied	Figure	Reference
W	(2.2×10^5) (325) (10.6)	(3.366) (0.98) (2.579) (249)	(1.4×10^{-5}) 1.2×10^{-5}	903–928 911–928	6 (5T) 4	pc 4N	W; EPMA Al/Al (0.027% W)	No	Abnormal data scatter	Cr, Mo, Ti, V in Al	–	Chi (1977) [34.13, 34.31]
Zn	0.259	1.252 (120.8)	4.5	630–926 (0.83)	16	sc 5N	^{65}Zn, vapour deposition; microtome	1 example		Ag, Au, Co, Cr, Cu, Ga, Ge in Al	34.04	Peterson (1970) [34.07]
Zn	0.30	1.258 (121.4)	4.8	699–920 (0.87)	15[51] (10T)	pc (1.5 mm) 4N	^{65}Zn, electroplated; grinder and residual activity	No			34.04	Gödény (1972) [34.43]
Zn	0.177	1.223 (118.1)	4.4	438–918 (0.73)	30 (19T)	pc 5N	^{65}Zn, electroplated[73]; residual activity	Numerous examples	Marked data scatter	Zn in Al(Zn,Mg)	–	Fujikawa (1976) [34.44]
Zn	0.27	1.247 (120.4)	4.9	614–890 (0.81)	8	pc 4N	^{65}Zn, electroplated; grinder	No		Zn in Al(X), X = Zn, Mg	34.04	Beke (1977) [34.45]
Zn	(0.325) 0.28$^+$	(1.221) (117.9) 1.252$^+$ (120.8)	(8.2) 4.8$^+$	688–928 (0.87)	11	sc 5N	^{65}Zn, ^{69}Zn, electroplated; microtome	1 example	$^+$Present approxi-mation	$E = 0.37$ to 0.61 for $T = 688$ to 928 K; Cu in Al	34.04	Peterson (1978) [34.17]
Zn	0.406	1.285 (124.0)	4.7	757–881 (0.88)	6	pc 4N6	Zn; EPMA Al/Al (3.5% Zn), (Matano, Hall)	1 example (c–x)			–	Minamino (1982) [34.46]
Zn	0.16 0.245*	1.212 (117.0) 1.239* (119.6)	4.5 4.9*	714–893 (0.86)	7	pc (1 mm) 4N	^{65}Zn, electroplated; microtome	1 example	*Fit together with the data of [34.42, 34.44]	Zn in Al(X), X = Cu, Zn, Si	34.04	Beke (1983) [34.47]
Zn	– (1.43)$^+$	– (1.367)$^+$ (132.0)	(5.9)$^+$	793–913 (0.91)	3	sc 5N5	^{65}Zn, electroplated; microtome	No	$^+$Present approxi-mation	Au, Fe in Al; $\Delta V/V_0 \approx 1$	–	Becker (1989) [34.10]
Zr	728	2.507 (242.0)	2.1×10^{-3}	804–913 (0.92)	8 (7T)	pc 5N	^{95}Zr, $ZrCl_4$ deposition; residual activity	Several examples	Pronounced data scatter	Zr in Al(Fe), Al(Si)	–	Marumo (1973) [34.48]

Table 3.5 Self-diffusion and impurity diffusion in indium (References, see page 148)

(1)	(2a)	(2b)	(3)	(4)	(5)	(6)	(7)	(8)	(9)	(10)	(11)	(12)
X	D^0 (10^{-4} m^2 s^{-1})	Q (eV) and (kJ mole^{-1})	$D(T_m)$ (10^{-12} m^2 s^{-1})	T-range (K) ($\overline{T}/T_m$)	No. of data points	Material, purity	Experimental method	Remarks on the pp	Further remarks	Also studied	Figure	Reference
In	– 1.02	– 0.776 (74.9)	 0.08	(323–429) 323–428	(10) 4	pc 4N75	^{114}In, electroplated; microtome	1 example (close to T_m, abrupt slope change)	Abnormal enhanced diffusivity at $T>428$ K	Tl in In	–	Eckert (1952) [35.01]
In	⊥ 3.7 // 2.7	0.813 (78.5) 0.813 (78.5)	0.11 0.08	312–417 (0.85) 312–417 (0.85)	10^{51} 8^{51}	sc 3N7, 4N5	^{114}In, electroplated; microtome	2 examples (all pp exhibit short-circuit contributions at deeper penetration)			35.01	Dickey (1959) [35.02]
Ag	⊥ (0.52) 0.49$^+$ // 0.11	0.555 (53.6) 0.499 (48.2)	 15.2$^+$ 15.7	296–415 (0.83) 304–418 (0.84)	8^{51} 6^{51}	sc 4N	^{110}Ag, dried-on from salt solution; microtome	No	$^+$Present fit to the depicted data	Au in In	35.02	Anthony (1966) [35.03]
Au	0.009	0.291 (28.1)	350	297–415 (0.83)	9^{51} (8T)	sc* 4N	^{198}Au, dried-on from salt solution; microtome	No	*Randomly oriented	Ag in In	35.02	Anthony (1966) [35.03]
Co	(1.2×10^{-5})	(0.26) (25.1)	(1.1)	363–425 (0.92)	20^{51} (14 T)	sc* 4N7	^{60}Co, electroplated; microtome	Several examples[81,84]	*Diffusion in <111> direction; extreme data scatter; authors guess diffusion along dislocations	c_s is in ppb range	–	Albrecht (1974) [35.04]
Tl	– 0.049	– 0.672 (64.9)	 0.065	(322–429) 322–412 (0.85)	(9) 5	pc 3N	^{204}Tl, electroplated; microtome	No	Abnormal enhanced diffusivity at $T>423$ K	In in In	35.02	Eckert (1952) [35.01]

Table 3.6 Self-diffusion and impurity diffusion in thallium (References, see page 148)

(1) X	(2a) D^0 (10^{-4} m^2 s^{-1})	(2b) Q (eV) and (kJ mole^{-1})	(3) $D(T_m)$ (10^{-12} m^2 s^{-1})	(4) T-range (K) ($\overline{T}/T_m$)	(5) No. of data points	(6) Material, purity	(7) Experimental method	(8) Remarks on the pp	(9) Further remarks	(10) Also studied	(11) Figure	(12) Reference
Tl	$\perp$ (0.4) 0.44$^+$ // (0.4) 0.48$^+$	0.980 (94.6) 0.993 (95.9)	–	423–502 (0.80) 423–496 (0.80) (α-Tl)	10^{51} (5T) 4^{51} (3T)	sc 3N	^{204}Tl, electroplated; lathe	No	$^+$Present fit to the depicted data		36.01	Shirn (1955) [36.01]
	(0.7) 0.83$^+$	0.867 (83.7)	2.2$^+$	514–549 (0.92) (β-Tl)	6^{51} (3T)							
Tl	0.42	0.831 (80.2)	2.3	513–573 (0.94) (β-Tl)	17	sc 5N	^{204}Tl, electroplated; lathe	All			36.01	Chiron (1985) [36.02]
Ag	$\perp$ 0.038	0.512 (49.4)	–	360, 473 (0.72)	2^{51}	sc 6N	^{110}Ag, dried-on from salt solution; microtome	No	$^+$Present fit to the depicted data	Au in Tl	36.02	Anthony (1968) [36.03]
	// 0.027	0.486 (46.9)	–	(α-Tl)	2^{51}							
	(0.042) 0.040$^+$	0.516 (49.8)	124$^+$	510–572 (0.94) (β-Tl)	7^{51}	pc (5 mm) 6N						
Au	$\perp$ (5.3×10^{-4}) 4.8×10^{-4} $^+$	0.226 (21.8)	–	388–490 (0.76)	5^{51}	sc 6N	^{198}Au, dried-on from salt solution; microtome	2 examples	$^+$Present fit to the depicted data	Ag in Tl	36.02	Anthony (1968) [36.03]
	// (2.0×10^{-5}) 1.9×10^{-5} $^+$	0.121 (11.7)	–	(α-Tl)	4^{51}							
	(5.2×10^{-4}) 4.8×10^{-4} $^+$	0.260 (25.1)	260$^+$	515–568 (0.94) (β-Tl)	6^{51}	pc (5 mm) 6N						

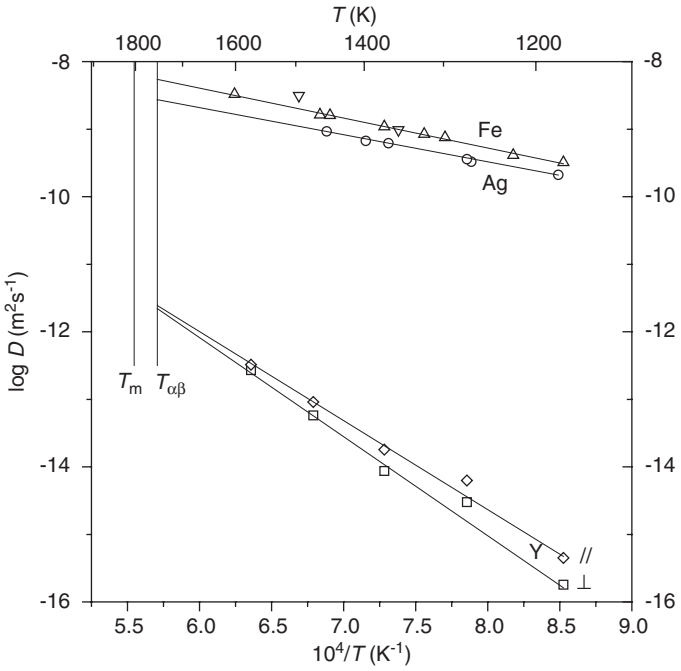

Fig. 32.01 Self-diffusion and impurity diffusion in yttrium. Self-diffusion: □ and ◇, Gornyy [32.01]. Ag in α-Y: ○, Murphy [32.02]; Fe in α-Y: △, Murphy [32.02]; ▽, Okafor [32.03].

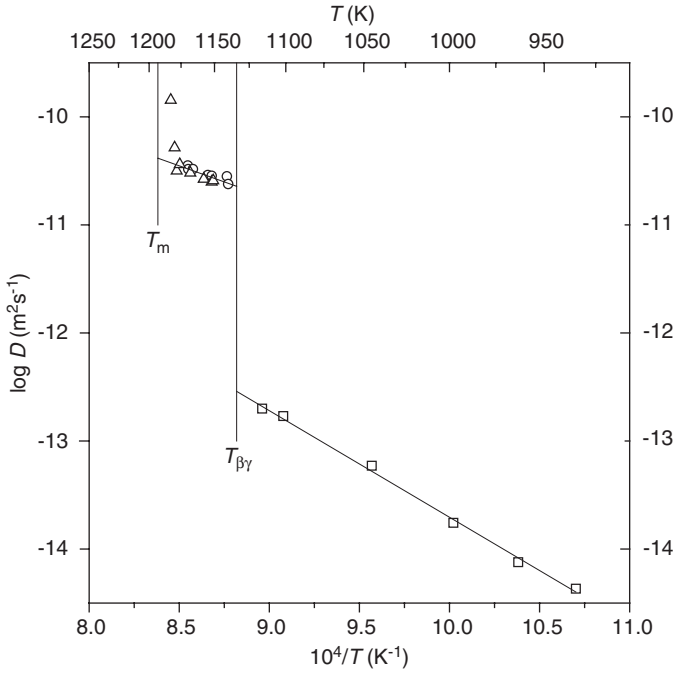

Fig. 33.01 Self-diffusion in lanthanum. Self-diffusion in β-La: □, Dariel [33.01]; in γ-La: ○, Dariel [33.02]; △, Languille [33.03]. Fitting line using the average $D^0 = 0.04 \times 10^{-4}\,\mathrm{m^2\,s^{-1}}$ and $Q = 1.18\,\mathrm{eV}$.

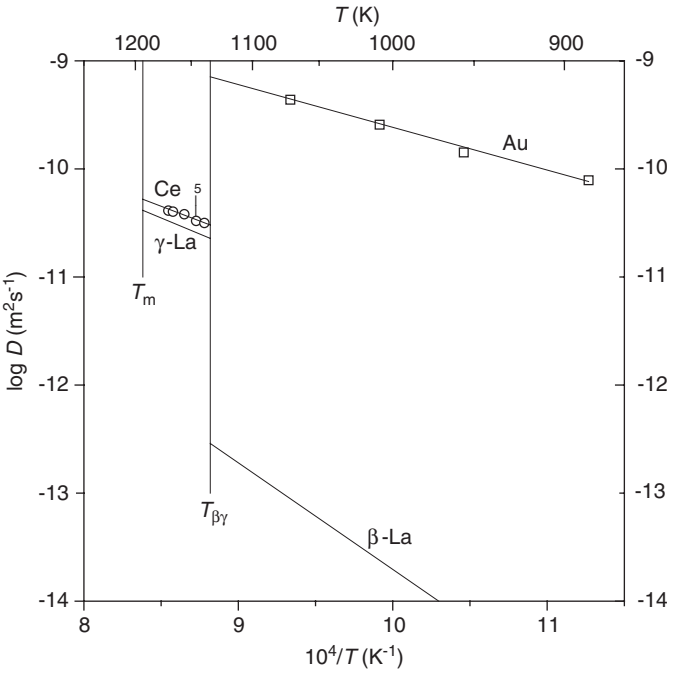

Fig. 33.02 Impurity diffusion in lanthanum. Au in β-La: □, Dariel [33.01]; Ce in γ-La: ○, Fromont [33.04].

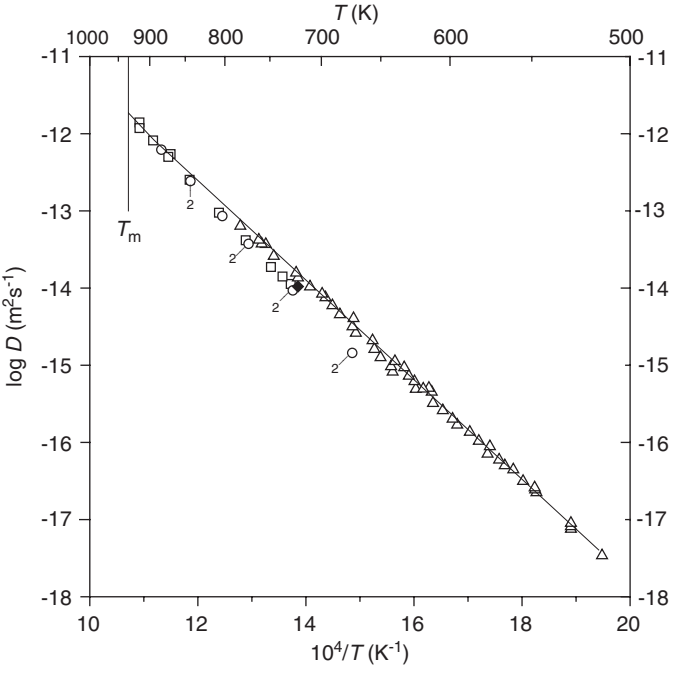

Fig. 34.01 Self-diffusion in aluminium. □, Lundy [34.01]; ○, Beyeler [34.02]; △, Messer [34.04]; ♦, Hood [34.05]. The fitting line consists of two linear branches, from T_m to 933 K according to [34.01] and below 933 K according to [34.04].

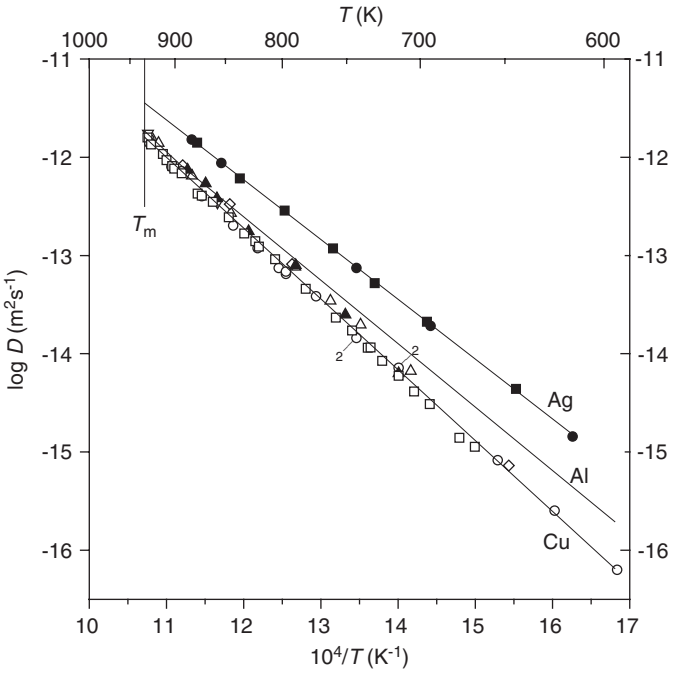

Fig. 34.02 Impurity diffusion in aluminuim. Ag in Al: ■, Peterson [34.07]; ●, Alexander [34.08]. Fitting line according to [34.07]. Cu in Al: ▲, Ceresara [34.15]; △, Peterson [34.07]; ▽, Peterson [34.17]; ◇, Fujikawa [34.16]; ○, Fujikawa [34.18]; □, Ushino [34.19]. Approximative fitting line using $D^0 = 0.85 \times 10^{-4}\,m^2\,s^{-1}$ and $Q = 1.43\,eV$.

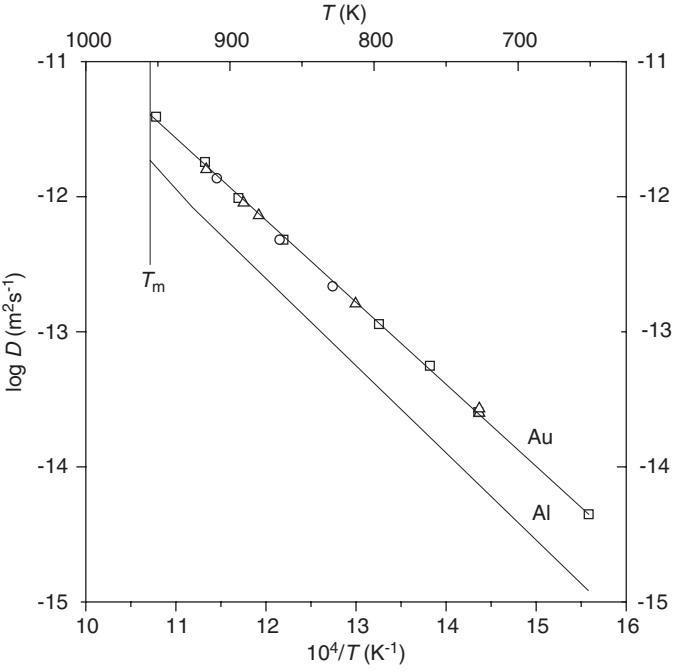

Fig. 34.03 Impurity diffusion in aluminium. Au in Al: □, Peterson [34.07]; △, Alexander [34.08]; ○, Becker [34.10]. Approximative fitting line using $D^0 = 0.1 \times 10^{-4}\,m^2\,s^{-1}$ and $Q = 1.188\,eV$.

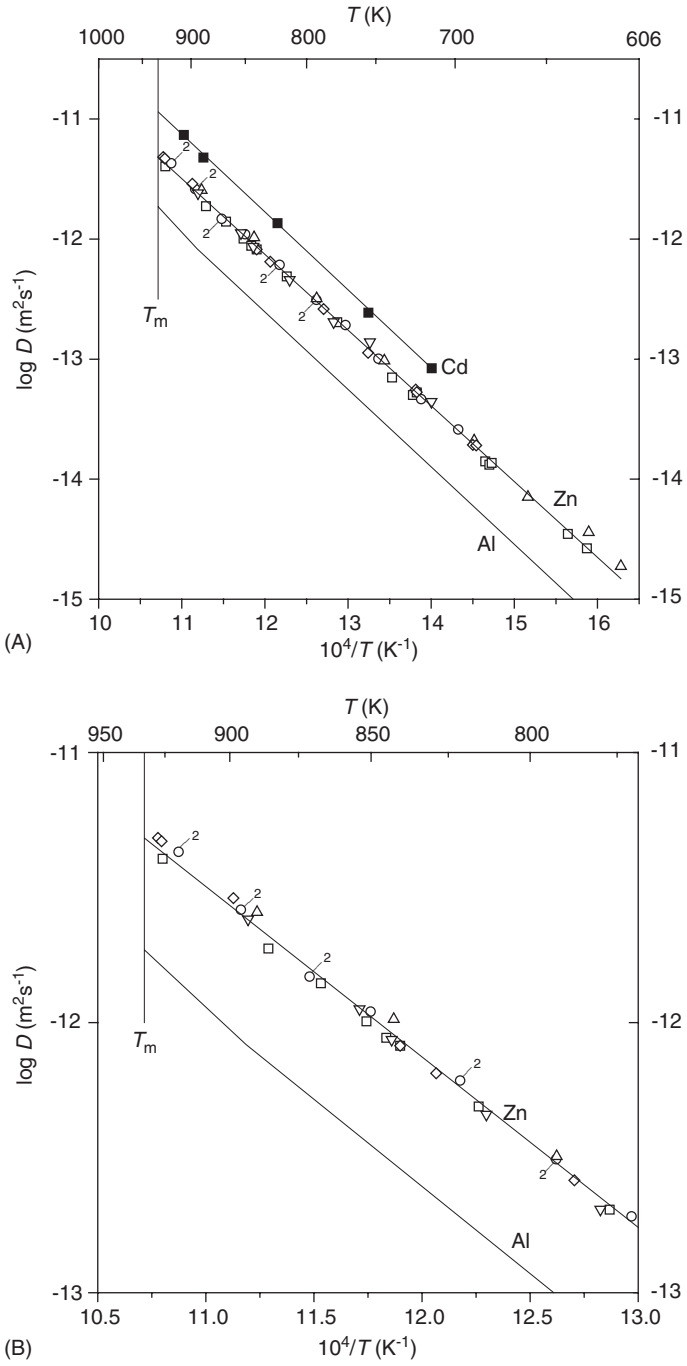

Fig. 34.04 (A) Impurity diffusion in aluminium. Cd in Al: ■, Alexander [34.08]; Zn in Al: □, Peterson [34.07]; ○, Gödény [34.43]; △, Beke [34.45]; ◇, Peterson [34.17]; ▽, Beke [34.47]. Fitting line according to [34.47]. (B) (Detail). Impurity diffusion in Al. Zn in Al: □, Peterson [34.07]; ○, Gödény [34.43]; △, Beke [34.45]; ◇, Peterson [34.17]; ▽, Beke [34.47]. Fitting line according to [34.47].

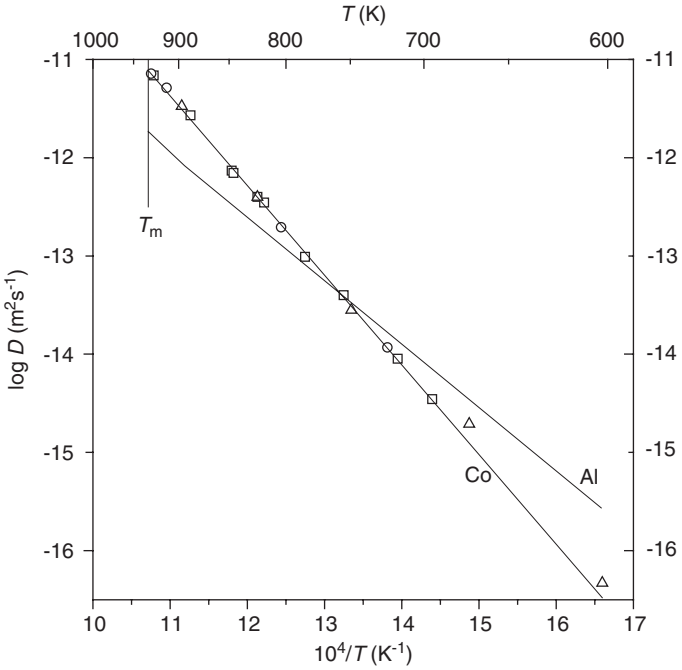

Fig. 34.05 Impurity diffusion in aluminium. Co in Al: □, Peterson [34.07]; ○, Hood [34.11]; △, Rummel [34.12]. Fitting line according to [34.07].

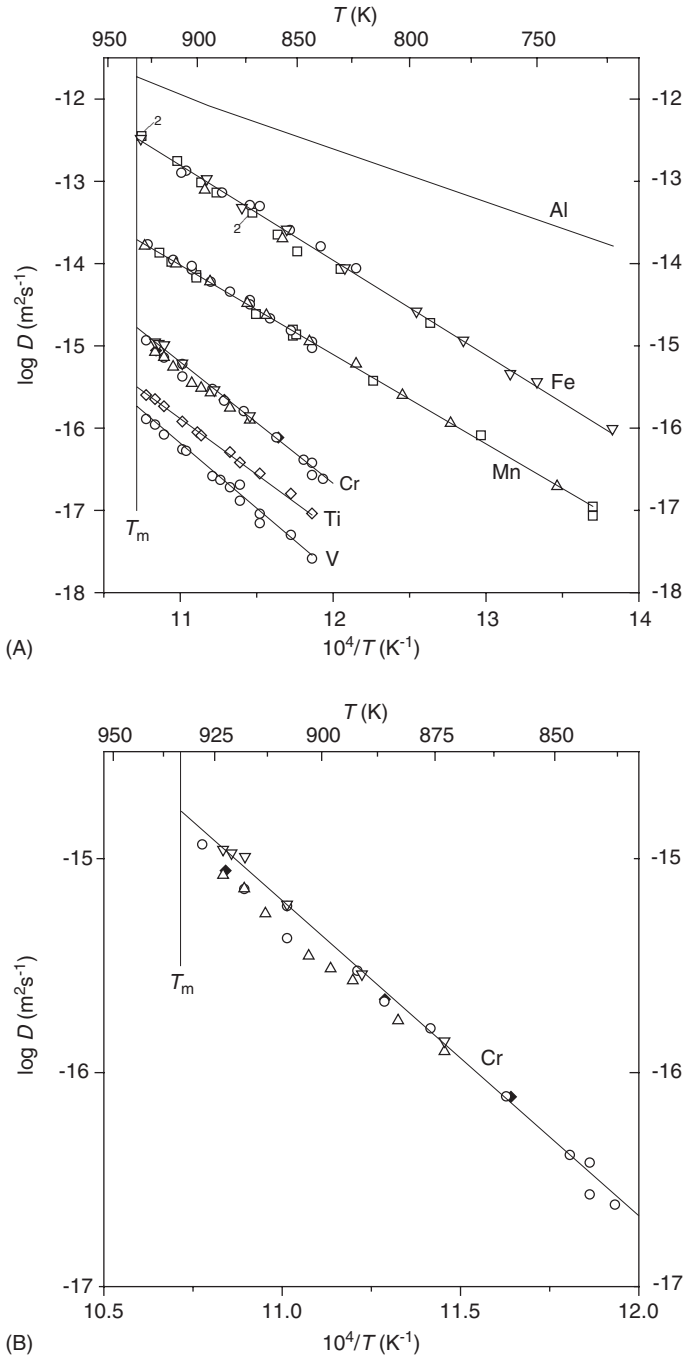

Fig. 34.06 (A) Impurity diffusion in aluminium. Cr in Al: ◆, Peterson [34.07]; ○, Chi [34.13]; △, Minamino [34.14]; ▽, Rummel [34.12]. Fitting line according to [34.12]. Fe in Al: □, Hood [34.20]; ○, Alexander [34.08]; △, Becker [34.10]; ▽, Rummel [34.12]. Fitting line according to [34.12]. Mn in Al: □, Hood [34.29]; ○, Fujikawa [34.30]; △, Rummel [34.12]. Fitting line according to [34.12]. Ti in Al: ◇, Chi [34.13]; V in Al: ○, Chi [34.13]. (B) (Detail). Impurity diffusion in aluminium. Cr in Al: ◆, Peterson [34.07]; ○, Chi [34.13]; △, Minamino [34.14]; ▽, Rummel [34.12]. Fitting line according to [34.12].

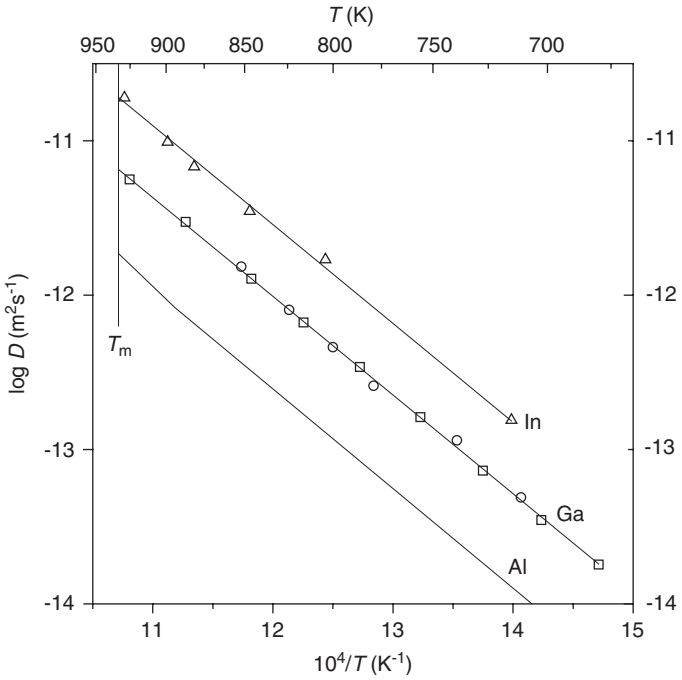

Fig. 34.07 Impurity diffusion in aluminium. Ga in Al: □, Peterson [34.07]; ○, Minamino [34.21]. Fitting line according to [34.07]. In in Al: △, Hood [34.24].

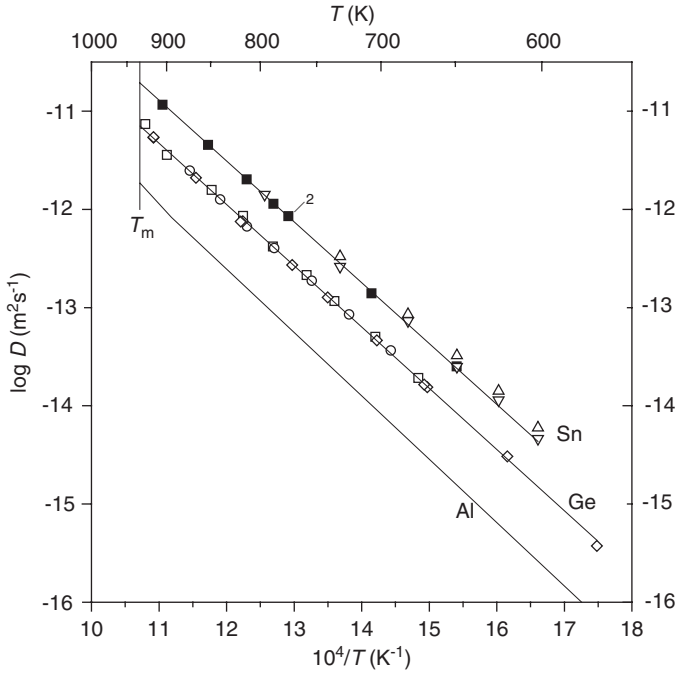

Fig. 34.08 Impurity diffusion in aluminium. Ge in Al: □, Peterson [34.07]; ○, Minamino [34.21]; ◇, Thürer [34.22]. Fitting line according to [34.22]. Sn in Al: ■, Erdélyi [34.39]; △, Erdélyi [34.40] (erfc); ▽, Erdélyi [34.40] (Gauss). Fitting line according to [34.39].

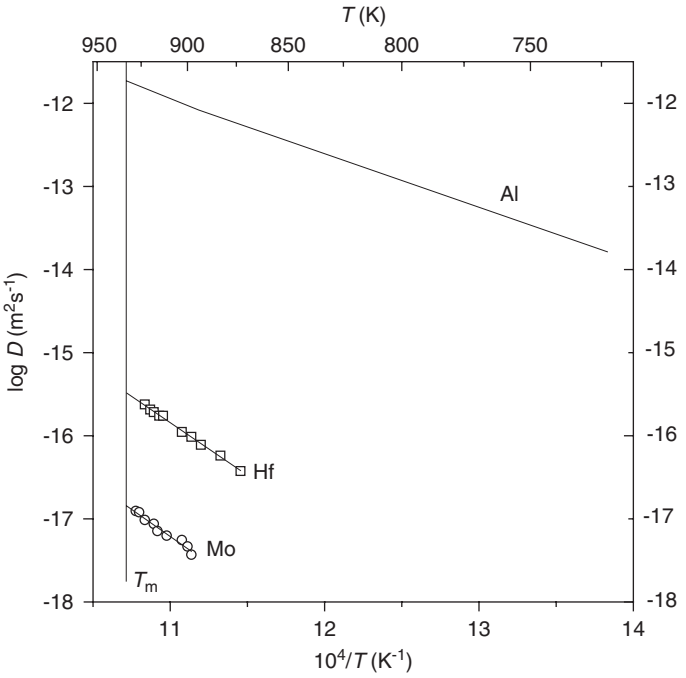

Fig. 34.09 Impurity diffusion in aluminium. Hf in Al: □, Minamino [34.14]. Mo in Al: ○, Chi [34.13, 34.31].

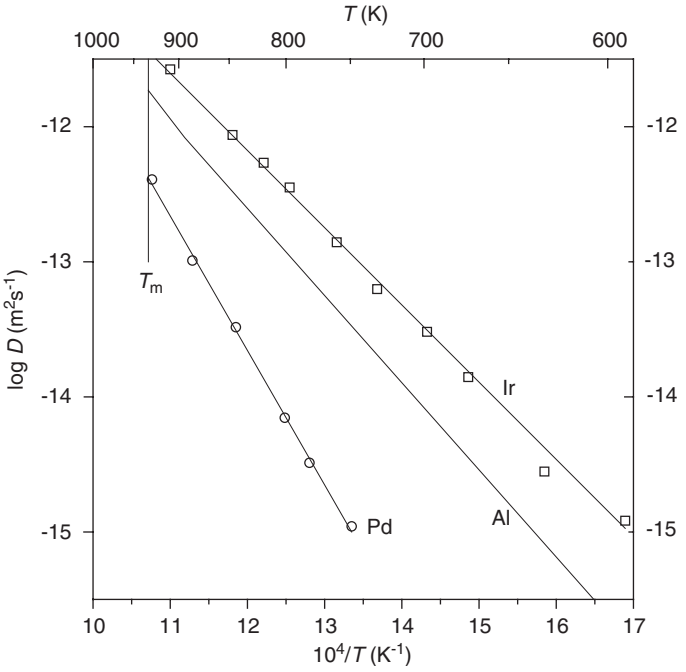

Fig. 34.10 Impurity diffusion in aluminium. Ir in Al: □, Khoukaz [34.25]; Pd in Al: ○, Khoukaz [34.25].

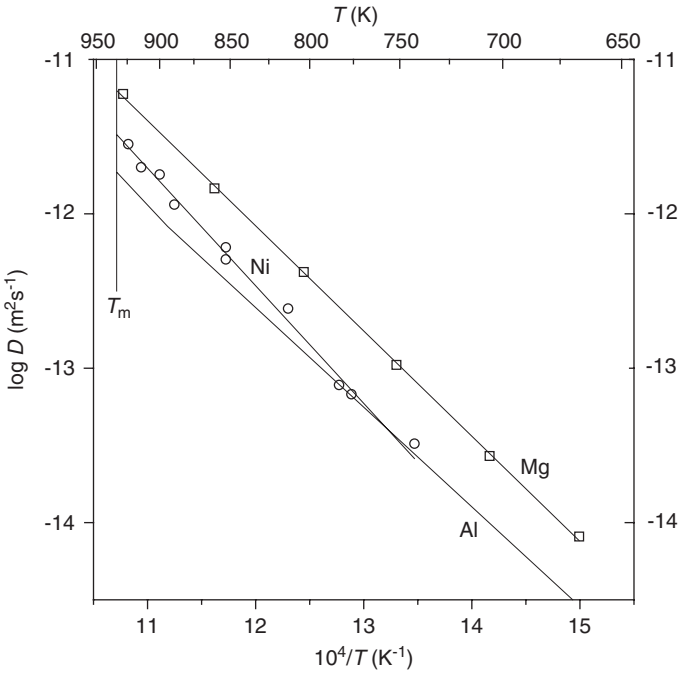

Fig. 34.11 Impurity diffusion in aluminium. Mg in Al: □, Rothman [34.28]; Ni in Al: ○, Erdélyi [34.33].

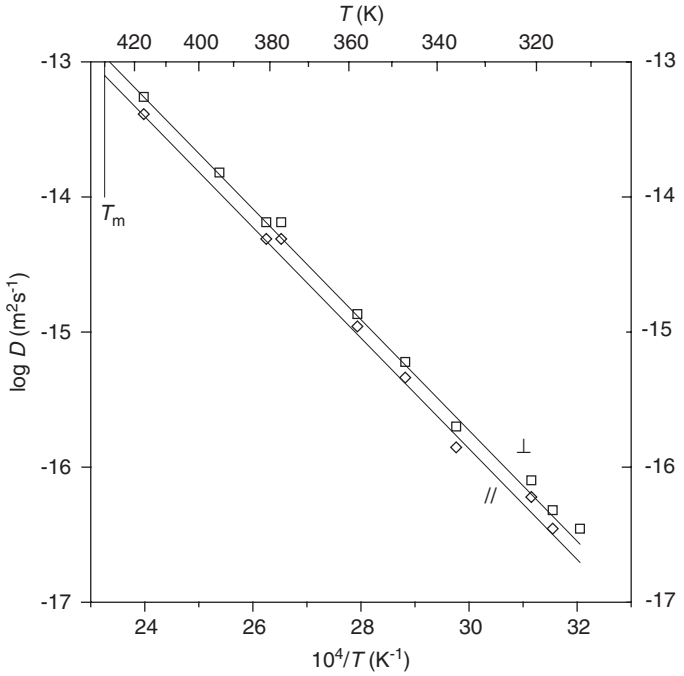

Fig. 35.01 Self-diffusion in indium. □ and ◇, Dickey [35.02].

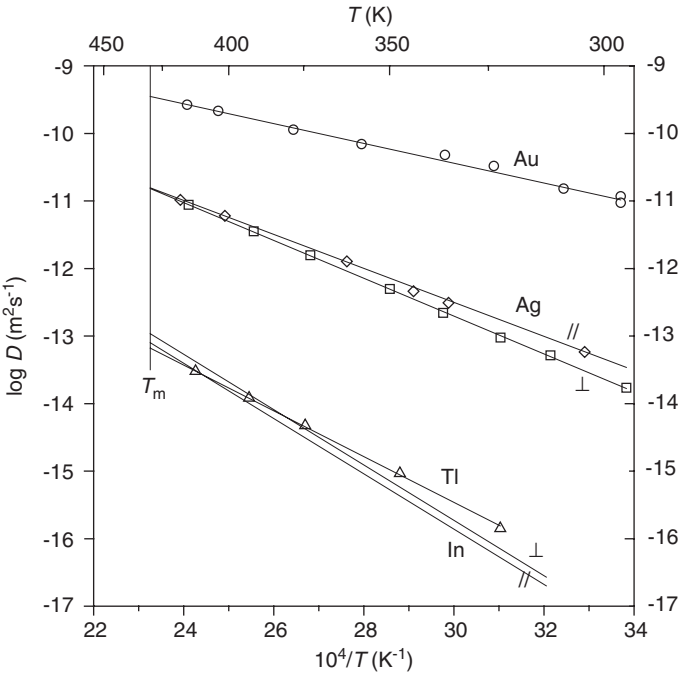

Fig. 35.02 Impurity diffusion in indium. Ag in In: □ and ◇, Anthony [35.03]; Au in In: ○, Anthony [35.03]; Tl in In: △, Eckert [35.01].

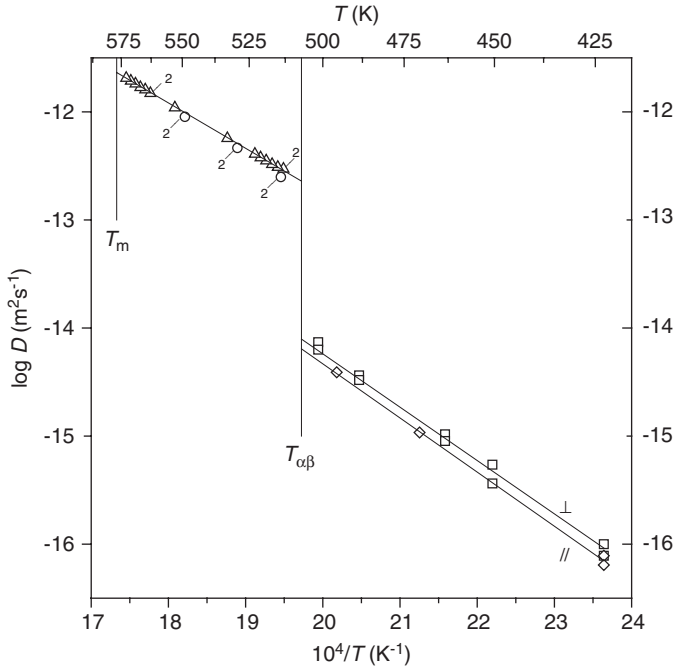

Fig. 36.01 Self-diffusion in thallium. In α-Tl: □ and ◇, Shirn [36.01]; in β-Tl: ○, Shirn [36.01]; △, Chiron [36.02]. Fitting line according to [36.02].

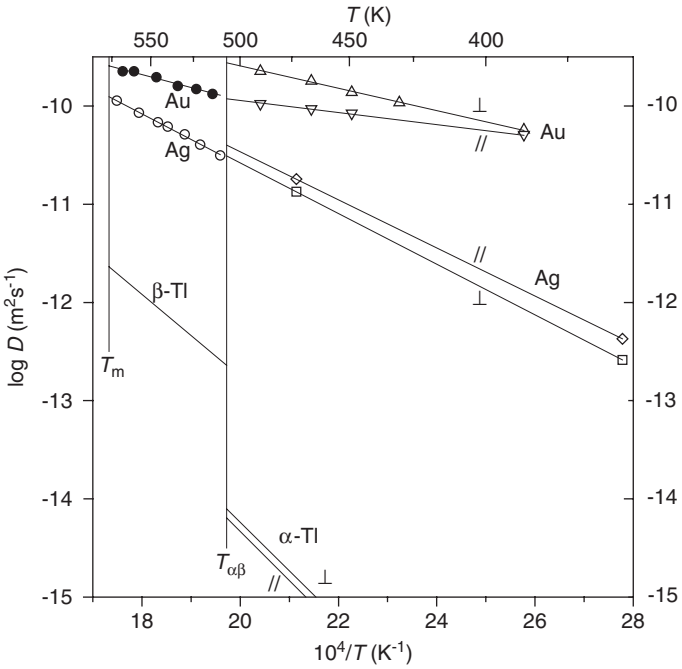

Fig. 36.02 Impurity diffusion in thallium. Ag in α-Tl: □ and ◇; Ag in β-Tl: ○, Anthony [36.03]; Au in α-Tl: △ and ▽; Au in β-Tl: ●, Anthony [36.03]

REFERENCES

References to Chapter 3.0

[30.01] K. Hirano, R.P. Agarwala, M. Cohen, Acta Metall. **10** (1962) 857.
[30.02] R.P. Agarwala, S.P. Murarka, M.S. Anand, Acta Metall. **12** (1964) 871.
[30.03] G.P. Tiwari, B.D. Sharma, Trans. Indian Inst. Met. **20** (1967) 83.
[30.04] A.R. Paul, R.P. Agarwala, J. Appl. Phys. **38** (1967) 3790.
[30.05] S.P. Murarka, M.S. Anand, R.P. Agarwala, Acta Metall. **16** (1968) 69.
[30.06] A.C. Carter, C.G. Wilson, Brit. J. Appl. Phys. (J. Phys. D) **1** (1968) 515.

References to Chapter 3.1

[31.01] S.C. Axtell, I.C.I. Okafor, R.J. Conzemius, O.N. Carlson, J. Less-Common Metals **115** (1986) 269.

References to Chapter 3.2

[32.01] D.S. Gornyy, R.M. Altovskiy, Fiz. Met. Metalloved. **30** (1970) 85; Phys. Met. Metallogr. **30** (1) (1970) 87 (English transl.).
[32.02] J.E. Murphy, G.H. Adams, W.N. Cathey, Metall. Trans. **6A** (1975) 343.
[32.03] I.C.I. Okafor, O.N. Carlson, J. Less-Common Metals **84** (1982) 65.

References to Chapter 3.3

[33.01] M.P. Dariel, G. Erez, G.M.J. Schmidt, Phil. Mag. **19** (1969) 1053.
[33.02] M.P. Dariel, Phil. Mag. **28** (1973) 915.
[33.03] A. Languille, D. Calais, B. Coqblin, J. Phys. Chem. Sol. **35** (1974) 1461.
[33.04] M. Fromont, J. Physique Lett. **37** (1976) L117.

References to Chapter 3.4

[34.01] T.S. Lundy, J.F. Murdock, J. Appl. Phys. **33** (1962) 1671.
[34.02] M. Beyeler, Y. Adda, J. Physique **29** (1968) 345.
[34.03] T.E. Volin, R.W. Balluffi, Phys. Stat. Sol. **25** (1968) 163.
[34.04] R. Messer, S. Dais, D. Wolf, in: Proc. 18th Ampère Congress, Eds. P.S. Allen, E.R. Andrews, C.A. Bates, Nottingham (1974), p. 327.
[34.05] G.M. Hood, in: *Solute-Defect Interaction-Theory and Experiment*, Eds. S. Saimoto, G.R. Purdy, Pergamon Press, Oxford (1985), p. 83.
[34.06] S. Dais, R. Messer, A. Seeger, Mater. Sci. Forum **15–18** (1987) 419.
[34.07] N.L. Peterson, S.J. Rothman, Phys. Rev. B **1** (1970) 3264.
[34.08] W.B. Alexander, L.M. Slifkin, Phys. Rev. B **1** (1970) 3274.
[34.09] M. Beyeler, F. Maurice, R. Seguin, Mém. Sci. Rev. Métall. **67** (1970) 295.
[34.10] Ch. Becker, G. Erdélyi, G.M. Hood, H. Mehrer, Defect and Diffusion Forum **66–69** (1989) 409.
[34.11] G.M. Hood, R.J. Schultz, J. Armstrong, Phil. Mag. A **47** (1983) 775.
[34.12] G. Rummel, Th. Zumkley, M. Eggersmann, K. Freitag, H. Mehrer, Z. Metallk. **86** (1995) 122.
[34.13] N. van Chi, *Doctoral Thesis*, Bergakademie Freiberg (1977); Neue Hütte **23** (1978) 147.
[34.14] Y. Minamino, T. Yamane, Sh. Nakagawa, H. Araki, K. Hirao, J. Japan Inst. Light Metals **37** (1987) 72.
[34.15] S. Ceresara, Phys. Stat. Sol. **27** (1968) 517.
[34.16] S. Fujikawa, K. Hirano, Trans. Japan Inst. Metals **12** (1971) 435; J. Japan Inst. Light Metals **20** (1970) 267.
[34.17] N.L. Peterson, S.J. Rothman, Phys. Rev. B **17** (1978) 4666.
[34.18] S. Fujikawa, K. Hirano, Defect and Diffusion Forum **66–69** (1989) 447.
[34.19] S. Ushino, S. Fujikawa, K. Hirano, J. Japan Inst. Light Metals **41** (1991) 433.
[34.20] G.M. Hood, Phil. Mag. **21** (1970) 305.
[34.21] Y. Minamino, T. Yasuda, H. Araki, T. Yamane, Defect and Diffusion Forum **66–69** (1989) 1251.
[34.22] A. Thürer, G. Rummel, Th. Zumkley, K. Freitag, H. Mehrer, Phys. Stat. Sol. (a) **149** (1995) 535.
[34.23] F. Sawayanagi, R.R. Hasiguti, J. Japan Inst. Metals **42** (1978) 1155.
[34.24] G.M. Hood, R.J. Schultz, Phys. Rev. B **4** (1971) 2339.
[34.25] Ch. Khoukaz, H. Mehrer, Z. Metallk. **91** (2000) 888.
[34.26] Y. Minamino, T. Yamane, H. Araki, Metall. Trans. **18A** (1987) 1536.
[34.27] G. Moreau, J.A. Cornet, D. Calais, J. Nucl. Mater. **38** (1971) 197.
[34.28] S.J. Rothman, N.L. Peterson, L.J. Nowicki, L.C. Robinson, Phys. Stat. Sol. (b) **63** (1974) K29.
[34.29] G.M. Hood, R.J. Schultz, Phil. Mag. **23** (1971) 1479.
[34.30] S. Fujikawa, K. Hirano, Mater. Sci. Forum **13/14** (1987) 539.
[34.31] N. van Chi, D. Bergner, in: DIMETA 82, *Diffusion in Metals and Alloys*, Eds. F.J. Kedves, D.L.Beke, Trans. Tech. Publ., Switzerland (1983), p. 334.
[34.32] S. Sudár, J. Csikai, M. Buszkó, Z. Metallk. **68** (1977) 740.
[34.33] G. Erdélyi, D.L. Beke, F.J. Kedves, I. Gödény, Phil. Mag. B **38** (1978) 445.
[34.34] F. Dyment, S. Balart, C. Lugo, R.A. Perez, N. Di Lalla, M.J. Iribarren, Defect and Diffusion Forum **237–240** (2005) 402.
[34.35] S. Badrinarayanan, H.B. Mathur, Int. J. Appl. Radiat. Isot. **19** (1968) 353.
[34.36] S. Fujikawa, Defect and Diffusion Forum **143–147** (1997) 115.
[34.37] D. Bergner, E. Cyrener, Neue Hütte **18** (1973) 356.
[34.38] S. Fujikawa, K. Hirano, Y. Fukushima, Metall. Trans. **9A** (1978) 1811.

[34.39] G. Erdélyi, K. Freitag, H. Mehrer, Phil. Mag. A **63** (1991) 1167.
[34.40] G. Erdélyi, K. Freitag, G. Rummel, H. Mehrer, Appl. Phys. A **53** (1991) 297.
[34.41] D. Bergner, N. van Chi, Wiss. Zeitschrift der Pädagogischen Hochschule N.K. Krupskaja, Halle, **15** (3) (1977) 15.
[34.42] J.J. Blechet, A. van Craeynest, D. Calais, J. Nucl. Mater. **27** (1968) 112.
[34.43] I. Gödény, D.L. Beke, F.J. Kedves, Phys. Stat. Sol. (a) **13** (1972) K155.
[34.44] S. Fujikawa, K. Hirano, Trans. Japan Inst. Metals **17** (1976) 809.
[34.45] D.L. Beke, I. Gödény, F.J. Kedves, G. Groma, Acta Metall. **25** (1977) 539.
[34.46] Y. Minamino, T. Yamane, M. Koizumi, M. Shimada, N. Ogawa, Z. Metallk. **73** (1982) 124.
[34.47] D.L. Beke, I. Gödény, F.J. Kedves, Phil. Mag. A **47** (1983) 281.
[34.48] T. Marumo, S. Fujikawa, K. Hirano, J. Japan Inst. Light Metals **23** (1973) 17.

Further Investigations

Al [34.49] J.J. Spokas, C.P. Slichter, Phys. Rev. **113** (1959) 1462; NMR.
Al [34.50] T.G. Stoebe, R.D. Gulliver, T.O. Ogurtani, R.A. Huggins, Acta Metall. **13** (1965) 701; NMR.
Al [34.51] F.Y. Fradin, *Doctoral Thesis*, Univ. Illinois (1967); F.Y. Fradin, T.J. Rowland, Appl. Phys. Lett. **11** (1967) 207; NMR.
Al [34.52] R.D. Engardt, R.G. Barnes, Phys. Rev. B **3** (1971) 2391; NMR.
Al [34.53] Ch.Y. Sun, *Doctoral Thesis*, Univ. of Illinois (1971); NMR; see also A. Seeger, D. Wolf, H. Mehrer, Phys. Stat. Sol. (b) **48** (1971) 481.
Ag [34.54] Th. Heumann, S. Dittrich, Z. Elektrochemie **61** (1957) 1138; Interdiffusion, potentiometric titration.
Ag [34.55] M.S. Anand, R.P. Agarwala, Trans. AIME **239** (1967) 1848.
Ag [34.56] Th. Heumann, H. Böhmer, J. Phys. Chem. Sol. **29** (1968) 237; Kryukov absorption method; D^0 corrected to $0.24 \times 10^{-4}\,m^2\,s^{-1}$.
Ag see Ref. [34.35].
Ag [34.57] D. Bartdorff, P. Reimers, Phys. Stat. Sol. (a) **28** (1975) 433; isotope effect.
Au see Ref. [34.16].
Au [34.58] D. Acker, M. Beyeler, G. Brebec, M. Bendazzoli, J. Gilbert, J. Nucl. Mater. **50** (1974) 281; low temperature measurements.
Co [34.59] M.S. Anand, R.P. Agarwala, Phil. Mag. **26** (1972) 297.
Co [34.60] R.V. Patil, G.P. Tiwari, Trans. Indian Inst. Metals **27** (1974) 215.
Co see Ref. [34.33]; resistometric method.
Cr [34.61] W.G. Fricke, in: *Aluminum*, Vol. **1**, Ed. K.R. van Horn, ASM Metals Park (1967); see also Scr. Metall. **6** (1972) 1139; EPMA.
Cu [34.62] J.B. Murphy, Acta Metall. **9** (1961) 563; Interdiffusion, spectrophotometric analysis.
Cu [34.63] M.S. Anand, S.P. Murarka, R.P. Agarwala, J. Appl. Phys. **36** (1965) 3860.
Cu see Ref. [34.08].
Cu see Ref. [34.09].
Cu see Ref. [34.58]; low temperature measurements.
Fe [34.64] S. Mantl, W. Petry, K. Schroeder, G. Vogl, Phys. Rev. B **27** (1983) 5313; QMS.
Fe [34.65] D.L. Beke, I. Gödény, I.A. Szabo, G. Erdélyi, F.J. Kedves, Phil. Mag. A **55** (1987) 425.
In [34.66] M.S. Anand, R.P. Agarwala, Phys. Stat. Sol. (a) **1** (1970) K41.
Li [34.67] C.J. Wen, W. Weppner, B.A. Boukamp, R.A. Huggins, Metall. Trans. **11B** (1980) 131; Interdiffusion, electrochemical technique.
Li [34.68] C. Moreau, A. Allouche, E.J. Knystautas, J. Appl. Phys. **58** (1985) 4582; Interdiffusion, low temperature measurements.
Mg [34.69] S. Fujikawa, K. Hirano, Mater. Sci. Eng. **27** (1977) 25.
Mn see Ref. [34.61]; EPMA.
Mn [34.70] D. Bergner, E. Cyrener, Neue Hütte **18** (1973) 9.
Mn [34.71] D.L. Beke, I. Gödény, I. Móricz, F.J. Kedves, Phil. Mag. Lett. **60** (1989) 219.
Sn see Ref. [34.66].

Zn [34.72] J.E. Hilliard, B.L. Averbach, M. Cohen, Acta Metall. **7** (1959) 86.
Zn [34.73] S. Ceresara, T. Federighi, F. Pieragostini, Phys. Stat. Sol. **16** (1966) 439; resistometric method.
Zn see Ref. [34.69].
Zn see Ref. [34.33]; resistometric method.
Zn [34.74] Y. Minamino, T. Yamane, K. Tokuda, Z. Metallk. **71** (1980) 90.
Zn [34.75] S. Varadarajan, R.A. Fournelle, Acta Metall. Mater. **40** (1992) 1847; low temperature measurements, X-ray analysis, TEM.

References to Chapter 3.5

[35.01] R.E. Eckert, H.G. Drickamer, J. Chem. Phys. **20** (1952) 13.
[35.02] J.E. Dickey, Acta Metall. **7** (1959) 350.
[35.03] T.R. Anthony, D. Turnbull, Phys. Rev. **151** (1966) 495.
[35.04] W.W. Albrecht, G. Frohberg, H. Wever, Z. Metallk. **65** (1974) 279.

References to Chapter 3.6

[36.01] G. Shirn, Acta Metall. **3** (1955) 87.
[36.02] R. Chiron, G. Faivre, Phil. Mag. A **51** (1985) 865; Rev. Phys. Appl. **20** (1985) 553.
[36.03] T.R. Anthony, B.F. Dyson, D. Turnbull, J. Appl. Phys. **39** (1968) 1391.

CHAPTER 4

Self-Diffusion and Impurity Diffusion in Group IV Metals

Contents

Tables
- 4.1. Titanium (Ti) 151
- 4.2. Zirconium (Zr) 162
- 4.3. Hafnium (Hf) 172
- 4.4. Tin (Sn) 173
- 4.5. Lead (Pb) 176

Figures
- Titanium 181
- Zirconium 191
- Hafnium 197
- Tin 200
- Lead 203

References 206

Silicon (Si) and **germanium** (Ge) are not topic of the present data collection. Self-diffusion and impurity diffusion data in the semi-conductors Si and Ge are collected in Refs. [40.01–40.03].

Anomalous diffusion behaviour is observed in α-Ti and especially in α-Zr. Interstitially dissolved 3d group metals, particularly iron, enhance self-diffusion and impurity diffusion in α-Ti and α-Zr, caused by highly mobile Fe-interstitial/vacancy pairs [40.04]. Whereas in α-Ti the enhancement results in a linear Arrhenius plot with low diffusion energy, in α-Zr ln$D$ vs. $1/T$ is divided into three regions (see Fig. 40.01). Region I, at high temperatures, represents intrinsic diffusion with normal values of D^0 and Q. In region II, at intermediate temperatures, Fe-enhanced extrinsic self-diffusion exceeds that intrinsic diffusion, where the enhancement is directly proportional to the Fe content of the sample. In region III the solubility limit of Fe is exceeded, which leads to Fe precipitation and a reduced influence of Fe on the diffusivity [40.04].

Lead was the first solid metal on which self-diffusion was studied. In 1896 Roberts-Austen had investigated the extremely fast diffusion of Au [40.05]. Later on Seith and co-workers had investigated impurity diffusion in lead using optical spectrum analysis [40.06–40.12] and self-diffusion with the aid of radio isotopes [40.13].

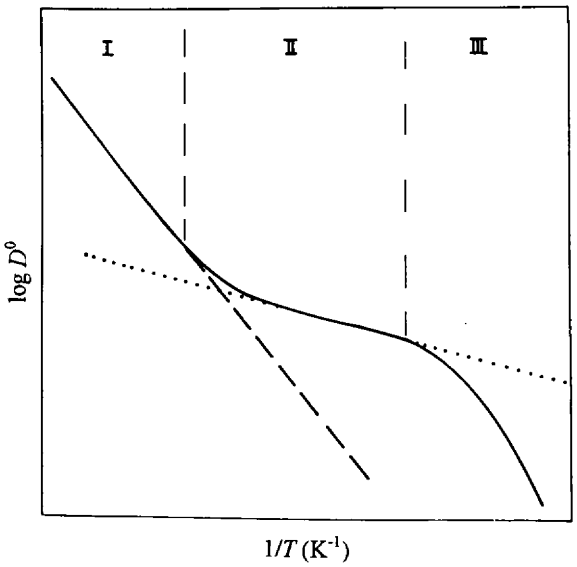

Fig. 40.01 Schematic illustration of self-diffusion in α-Zr. The influence of Fe impurities (according to Ref. [40.04]). See text for details.

In Table 4.0 lattice structure, lattice constants, melting and phase transition temperatures of the group IV metals are listed.

Table 4.0 Lattice structure, lattice constants *a* and *c*, phase transition temperature T_{ij} and melting temperature T_m

Metal	Ti		Zr		Hf		Sn	Pb
phase	α	β	α	β	α	β	β	
Structure	hcp	bcc	hcp	bcc	hcp	bcc	bct	fcc
T_{ij} (K)	1,155		1,136		2,013		434	
T_m (K)	1,940		2,125		2,500		505	601
a (nm)	0.295	0.331	0.323	0.362	0.320	0.360	0.583	0.495
c (nm)	0.469		0.515		0.506		0.318	

Table 4.1 Diffusion in titanium (References, see page 206)

(1)	(2a)	(2b)	(3)	(4)	(5)	(6)	(7)	(8)	(9)	(10)	(11)	(12)
X	D^0 (10^{-4} m^2 s^{-1})	Q (eV) and (kJ mole^{-1})	D (T_m) (10^{-12} m^2 s^{-1})	T-range (K) ($\overline{T}/T_m$)	No. of data points	Material, purity	Experimental method	Remarks on the pp	Further remarks	Also studied	Figure	Reference
Self-diffusion												
Ti	3.58×10^{-4} [21]	1.353[21] (130.6)	30	1,172–1,813 (0.77)	14	pc 3N	^{44}Ti, dried-on from salt solution; lathe	3 examples (50 μm sections)		V in β-Ti	41.01	Murdock (1964) [41.01]
	1.09[21]	2.602[21] (251.2)		β-Ti								
Ti	3.5[22]	3.4[22] (328.3)	31	1,176–1,893 (0.79) β-Ti	10	pc ~3N8	^{44}Ti, dried-on from salt solution; lathe	All	Ω-fit with Ω = 4.1		41.01	Köhler (1987) [41.02]
Ti	1.27×10^{-4} [21]	1.24[21] (119.7)	32	(1,172–1,893) β-Ti	(24)				Two-exponential fit to the data of [41.01,41.02]		–	Neumann (1990) [41.03]
	0.45[21]	2.41[21] (232.7)										
Ti	⊥ (1.7×10^{-4})*	(2.00)* (192.8)	–	858–1,127 (0.51) α-Ti	6 (5T)	sc ~3N*	^{44}Ti, vapour deposition; microtome and IBS	No	*~30 ppma Fe and Ni impurities, see introduction page	Co in α-Ti	–	Herzig (1991) [41.04]
Ti	⊥ 13.5	3.138 (303)	–	873–1,133 (0.52)	7	sc ultra-	^{44}Ti, vapour deposition; IBS	All (total depth: 0.5–4 μm)	*~0.025 ppma Fe and Ni impurities, see introduction page	Al in α-Ti	41.13	Köppers (1997) [41.05]
	// –	–	–	923, 1,023 α-Ti	2	pure*						
Impurity diffusion												
Ag	(0.003[x])	1.865[x]		1,213–1,863 (0.79) β-Ti	11[51] (9T)	pc 3N5	^{110}Ag[72]; lathe	No (linear pp)	[x]Almost linear ln $D - 1/T$ plot [+]Present fit to the depicted data	Sc in β-Ti	–	Askill (1971) [41.06]
	0.0026[+]	(180.0)	37[+]									
Ag	10.8[22]	3.656[22] (353)	31	1,173–1,773 (0.76) β-Ti	13	pc 3N5	Ag; EPMA Ti/Ti(2.76% Ag) (Matano)	No	Ω-fit with Ω = 4.52	Cu in β-Ti	41.02	Lee (1990) [41.07]
Ag	(0.065)	(2.486) (240)	–	1,030–1,120 (0.55) α-Ti	5[51]	pc* (1–2 mm) 2N7	Ag; EPMA Ti/Ti(3.19% Ag) (Matano)	No	*Fe content not specified, see introduction page [+]Present fit to the depicted data	Au, Cu in α-Ti	–	Taguchi (1995) [41.08]
	0.25[+]	2.620[+] (253)										

Table 4.1 *(Continued)*

(1)	(2a)	(2b)	(3)	(4)	(5)	(6)	(7)	(8)	(9)	(10)	(11)	(12)
X	D^0 (10^{-4} m^2 s^{-1})	Q (eV) and (kJ mole^{-1})	D (T_m) (10^{-12} m^2 s^{-1})	T-range (K) ($\overline{T}/T_m$)	No. of data points	Material, purity	Experimental method	Remarks on the pp	Further remarks	Also studied	Figure	Reference
Ag	1.0	2.890 (279)	–	823–1,073 (0.49) α-Ti	6	pc 3N*, 4N^{x}	Ag, implanted; RBS	All	Fe content *<150 ^{x}3.8 ppma; D (uncertainty 20–25%) is independent of the impurity content	Al in α-Ti	41.14	Araujo (2000) [41.09]
Al	1.2×10^{-3} *	1.554* (150)	(11)*	1,223–1,573 (0.72) β-Ti	8	pc 2N9	Al; EPMA Ti/Ti(2.1% Al) (Boltzmann–Matano, Hall)	1 example (probability plot)	*Forced fit		41.03	Araki (1994) [41.10]
Al	–	–		1,193–1,873 (0.79) β-Ti	6[51]	pc[61]	Al; SIMS				41.03	Köppers (2000) [41.11]
Al	0.114[23]	2.207[23] (213.1)	21	1,193–1,873 β-Ti	14				Present α-fit with $\alpha = 6.7$ and $T_0 = T_m$ to the data of [41.10, 41.11]		41.03	
Al	⊥ (66)^{x}	(3.407)^{x} (329)	–	935–1,140 (0.53)	11 (8T)	sc, pc ultrapure*	Al, vapour deposition; SIMS	Several examples (total depth: 0.5–5 μm)	*Fe, Ni content 0.025 ppma $^{x}D_{pc} \approx D_{\perp}$ $^{+}$Present approximation	Ti in α-Ti	41.14	Köppers (1997) [41.05]
	⊥ 80^{+}	3.433^{+} (331.5)	–	α-Ti 1,036, 1,073	2							
	// –	–	–									
Al	140	3.376 (326)	–	948–1,073 (0.52) α-Ti	6	pc 3N, 4N	Al, implanted; NRA (^{27}Al(p,γ)^{28}Si)	All (total depth: ≤ 0.2 μm)	Uncertainty of D: 20–25%	Ag in α-Ti	–	Araujo (2000) [41.09]
Au	9.32[22]	3.604[22] (348)	27	1,173–1,823 (0.77) β-Ti	14	pc (2 mm) 3N5	Au; EPMA Ti/Ti(1.26% Au) (Matano)	No	Ω-fit with $\Omega = 4.2$		41.02	Lee (1993) [41.12]

Au	(0.19) $(0.24)^{+}$	(2.693) (260)	–	823–973 (0.46) α-Ti	5	pc 3N*	Au, implanted; RBS	3 examples[81]	*Fe, Ni content ~150 ppma, see introduction page +Present approximation	c_s is 0.2–0.35 at %	–	dos Santos (1994) [41.13]
Au	(2.5×10^{-4}) $(2.0 \times 10^{-4})^{+}$	(1.947) (188)	–	980–1,120 (0.54) α-Ti	5[51]	pc (1–2 mm) 2N7*	Au; EPMA Ti/Ti(0.61% Au) (Matano)	No	*Fe content not specified +Present fit to the depicted data	Ag, Cu in α-Ti	–	Taguchi (1995) [41.08]
Be	0.8	1.743 (168.3)		1,188–1,573 (0.71) β-Ti	10[51] (5T)	pc 2N62	^{7}Be; residual activity	No		Be in β-Zr	–	Pavlinov (1969) [41.14]
Be	(1.4×10^{4}) $(2{,}400)^{+}$	(2.693) (260) $(2.514)^{+}$ (242.8)	–	993–1,133 (0.55) α-Ti	4	pc 2N5*	^{7}Be, dried-on from salt solution; residual activity	3 examples	*Fe content 0.25% +Present approximation		–	Shabalin (1979) [41.15]
Co	0.0121	1.327 (128.1)		1,191–1,497 (0.69) β-Ti	11[51]	pc (5–10 mm) 2N7	^{60}Co, electroplated; autoradiography	No		Fe, Mn, Nb, Ni in β-Ti	–	Peart (1962) [41.16]
Co	(0.012^{21}) 0.0105^{+} (2.0^{21}) 2.8^{+}	1.327^{21} (128.1) 2.277^{21} (219.8)	710^{+}	1,188–1,899 (0.80) (β-Ti)	25[51] (20T)	pc 2N7	^{60}Co, electroplated; lathe	1 example (~80 μm sections)	Approximative two-exponential fit; + Present rough fit to the depicted data	Cr, Fe, Mn, Mo, Nb, Ni in β-Ti	41.04	Gibbs (1963) [41.17]
Co	–	–		1,223 β-Ti	1	pc ~3N	Co; EPMA Ti/Ti(2.25% Co) (Boltzmann–Matano, Hall)	No	$D(1{,}223\,\mathrm{K}) = 3.64 \times 10^{-12}\,\mathrm{m^2\,s^{-1}}$	$\Delta V/V_0 = 0.22$	41.04	Araki (1997) [41.18]
Co	⊥ 0.032	1.315 (126.1)	–	871–1,135 (0.52)	6	sc 3N6*	^{60}Co, electroplated[73]; lathe	2 examples	*Fe content ~7.5 ppma		41.15	Nakajima (1983) [41.19]
	// 0.019	1.182 (114.1)	–	α-Ti	6							
Co	0.03^{x}	1.315^{x} (127)	–	619–823 (0.37) α-Ti	5	pc 3N*	^{60}Co, vapour deposition; microtome	All (partly erfc-solution)	*Fe, Co, Ni content < 200 ppma, see introduction page $^{x}D_{pc} \approx D_{\perp}$		41.15	Pérez (1995) [41.20]
Cr	0.01	1.636 (158.0)	56	1,199–1,466 (0.69) β-Ti	8	pc ~2N7	^{51}Cr, vapour deposition; autoradiography	1 example		Ti in Ti(Cr)	–	Mortlock (1959) [41.21]

Table 4.1 *(Continued)*

(1)	(2a)	(2b)	(3)	(4)	(5)	(6)	(7)	(8)	(9)	(10)	(11)	(12)
X	D^0 (10^{-4} m^2 s^{-1})	Q (eV) and (kJ mole^{-1})	D (T_m) (10^{-12} m^2 s^{-1})	T-range (K) ($\overline{T}/T_m$)	No. of data points	Material, purity	Experimental method	Remarks on the pp	Further remarks	Also studied	Figure	Reference
Cr	0.005[21] 4.9[21]	1.531[21] (147.8) 2.645[21] (255.4)	(115)	1,284–1,895 (0.82) β-Ti	20[51] (10T)	pc 2N7	[51]Cr, vapour deposition[73]; auto-radiography	No	Approximative two-exponential fit together with the data of [41.21]	Co, Fe, Mn, Mo, Nb, Ni in β-Ti	–	Gibbs (1963) [41.17]
Cr	0.084[22]	2.154[22] (208)	68	1,173–1,823 (0.77) β-Ti	14	pc ~3N5	Cr; EPMA Ti/Ti(4.62% Cr) (Matano, Darken)	No	Ω-fit with $\Omega = 1.16$	Pd in β-Ti	41.04	Lee (1991) [41.22]
Cr	0.0038[x] 0.0212[x]	1.522[x] (147) 1.730[x] (167)	68	1,173–1,573 (0.71) β-Ti	7	pc ~3N	Cr; EPMA Ti/Ti(4.81% Cr) (Boltzmann–Matano, Hall)	1 example ($c - x$)	[x]Two linear branches below and above 1,370 K	$\Delta V/V_0 =$ 0.4–0.45	41.04	Araki (2006) [41.23]
Cr	$\perp$ 0.020 // 0.022	1.755 (169.4) 1.714 (165.5)	–	875–1,123 (0.51) α-Ti	6 6	sc ~3N8*	[51]Cr, dried-on from salt solution; lathe	All	*Fe, Ni content <60 ppma	Cr in α-Ti(X) X = Al, Sn	41.15	Nakajima (1990) [41.24]
Cu	0.0021[21] 11.3[21]	1.266[21] (122.3) 2.611[21] (252.1)	(290)	1,233–1,733 (0.76) β-Ti	11	pc ~2N8	Cu; EPMA				41.02	Caloni (1969) [41.25]
Cu	0.57[22]	2.496[22] (241)	190	1,173–1,773 (0.76) β-Ti	13	pc ~3N5	Cu; EPMA Ti/Ti(2.28% Cu) (Matano, Darken)	No	Ω-fit with $\Omega = 2.3$	Ag in β-Ti	41.02	Lee (1990) [41.07]
Cu	(0.38) 0.34[+]	2.029 (195)	–	1,030–1,100 (0.55) α-Ti	4[51]	pc (1–2 mm) 2N7*	Cu; EPMA Ti/Ti(0.91% Cu) (Matano)	No	*Fe content not specified, see introduction page [+]Present fit to the depicted data	Ag, Au in α-Ti	–	Taguchi (1995) [41.08]
Fe	0.0078 0.0085	1.370 (132.3) 1.388 (134.0)	– –	1,183–1,468 (0.68) 1,177–1,557 (0.70) β-Ti	8* 11[x]	pc (5–10 mm) 2N7, 3N	[55]Fe*, [59]Fe[x], electro-plated; auto-radiography	1 example		Co, Mn, Nb, Ni in β-Ti; Fe in Ti(Fe) Fe in Ti(Nb)	41.05	Peart (1962) [41.16]

Fe	0.0078[21] 2.7[21]	1.370[21] (132.3) 2.385[21] (230.3)	390	1,242–1,918 (0.81) 1,256–1,490 (0.71) β-Ti	18[51]* (10T) 6[51 x]	pc 2N7	^{59}Fe*, ^{55}Fe^{x}, electro-plated[73]; lathe and auto-radiography	No	Approximative two-exponential fit together with the ^{55}Fe data of [41.16]	Co, Cr, Mn, Mo, Nb, Ni in β-Ti; $E<0.1$	41.05	Gibbs (1963) [41.17]
Fe	$\perp$ 0.064 // 0.0047	1.493 (144.2) 1.163 (112.3)	– –	877–1,137 (0.52) α-Ti	6 6	sc 3N5*	^{59}Fe, electro-plated; lathe	No (2 examples in Ref. [41.36])	*Fe content <10 ppma		41.16	Nakajima (1983) [41.26]
Ga	(6.35[22]) 6.7^{+}	3.480[22] (336)	33^{+}	1,223–1,823 (0.79) β-Ti	13	pc 3N5	Ga; EPMA Ti/Ti(1.71% Ga) (Matano, Darken)	No	Ω-fit with $\Omega = 4.0$ $^{+}$Present approximation	In in β-Ti	41.03	Lee (1993) [41.27]
Ga	$\perp$ 21^{x}	3.06^{x} (295.5)	–	873–1,143 (0.52) α-Ti	9[51]	pc ultra-pure*	Ga; SIMS analysis	5 examples (at lower T non-linear in ln $c - x^2$)	$^{x}D_{pc} \approx D_{\perp}$ *Fe, Ni content ~ 0.03 ppma	Ti, Al, In in α-Ti	41.16	Köppers (1997) [41.28], [41.29]
Ga	(25) 34^{+}	3.190 (308)	–	873–1,123 (0.51) α-Ti	6	pc $\sim$4N*	Ga, implanted; RBS	3 examples	*Fe, Ni content $\sim$ 150 ppma, see introduction page $^{+}$Present approximation		–	Behar (2003) [41.30]
Ge	0.792[22]	2.921[22] (282)	43	1,173–1,823 (0.77) β-Ti	14	pc $\sim$3N5	Ge; EPMA Ti/Ti(2% Ge) (Matano, Darken)	No	Ω-fit with $\Omega = 3.05$	Si, Sn in β-Ti	41.06	Iijima (1993) [41.31]
Hf	– 0.0069^{+} – 1.2×10^{-4}+	1.761* (170) 1.191* (115)	18^{+}	1,623–1,873 (0.90) 1,273–1,573 (0.73) β-Ti	5 6	pc 2N7	Hf; EPMA Ti/Ti(X % Hf) (Den Broeder)	No	$X = 50$–100 *Two linear branches $^{+}$Present approximation		–	Le Gall (1987) [41.32]
Hf	(1.5)	(2.9) (280)	–	(823–1,023) 823–973 (0.46) α-Ti	(6) 5	pc $\sim$3N6*	Hf, vapour deposition; RBS		*Fe content <40 ppma, see introduction page		–	Behar (1991) [41.33]
Hf	(0.04)	(2.631) (254)	–	902–1,145 (0.53) α-Ti	6	pc 3N*	Hf, vapour deposition; RBS, HIRBS	All[85]	*Fe content $\sim$100 ppma, see introduction page		–	Pérez (1993) [41.34]

Table 4.1 *(Continued)*

(1)	(2a)	(2b)	(3)	(4)	(5)	(6)	(7)	(8)	(9)	(10)	(11)	(12)
X	D^0 (10^{-4} m^2 s^{-1})	Q (eV) and (kJ mole^{-1})	D (T_m) (10^{-12} m^2 s^{-1})	T-range (K) ($\overline{T}/T_m$)	No. of data points	Material, purity	Experimental method	Remarks on the pp	Further remarks	Also studied	Figure	Reference
In	(1.39[22]) 1.32$^+$	3.263[22] (315)	20$^+$	1,173–1,823 (0.77) β-Ti	14	pc 3N5	In; EPMA Ti/Ti(1.71% In) (Matano, Darken)	No	Ω-fit with $\Omega = 3.83$ $^+$Present approximation	Ga in β-Ti	41.07	Lee (1993) [41.27]
In	$\perp$ 31^x	3.41^x (329.2)	–	990–1,142 (0.55) α-Ti	6[51]	pc ultra-pure*	In; SIMS analysis	No	$^xD_{pc} \approx D_\perp$ *Fe, Ni content $\sim$0.03 ppma	Ti, Al, Ga in α-Ti	41.18	Köppers (1997) [41.28]
In	(0.02)	(2.692) (260)	–	823–1,073 (0.49) α-Ti	6	pc 3N*	In, implanted; RBS	All	*Fe content $\sim$100 ppma, see introduction page		–	Pérez (1997) [41.35]
Mn	0.0061	1.461 (141.1)		1,213–1,492 (0.70) β-Ti	9[51] (8T)	pc (5–10 mm) 2N7	^{54}Mn, electro-plated; auto-radiography	No		Co, Fe, Nb, Ni in β-Ti	–	Peart (1962) [41.16]
Mn	(0.0061[21]) 0.0054$^+$ (4.3[21]) 3.8$^+$	1.461[21] (141.1) 2.515[21] (242.8)	200$^+$	1,213–1,897 (0.80) β-Ti	26[51] (17T)	pc 2N7	^{54}Mn, electro-plated; lathe	1 example ($\sim$80 µm sections)	Approximative two-exponential fit $^+$Present rough fit to the depicted data	Co, Cr, Fe, Mo, Nb, Ni in β-Ti	41.05	Gibbs (1963) [41.17]
Mn	$\perp$ 0.6	1.960 (189.2)	–	878–1,135 (0.52)	6	sc, pc 3N5	^{54}Mn, dried-on from salt solution; lathe	All	Fe, Ni content $\sim$60 ppma	Mn in α-Ti(O)	41.16	Nakamura (1988) [41.36]
	// 0.049	1.662 (160.5)		α-Ti	6							
Mo	(0.008[21]) 0.007$^+$ (20[21]) 15$^+$	1.865[21] (180.0) 3.166[21] (305.7)	19$^+$	1,179–1,899 (0.79) β-Ti	24[51] (17T)	pc 2N7	^{99}Mo, electro-plated; lathe	1 example ($\sim$80 µm sections)	Approximative two-exponential fit $^+$Present rough fit to the depicted data	Co, Cr, Fe, Mn, Nb, Ni in β-Ti	41.08	Gibbs (1963) [41.17]
Nb	0.005	1.704 (164.5)		1,270–1,532 (0.72) β-Ti	6[51]	pc (5–10 mm) 2N7	^{95}Nb, electro-plated; auto-radiography	No		Co, Fe, Mn, Ni in β-Ti; Nb in Ti(Nb), Nb in Ti(Fe)	41.08	Peart (1962) [41.16]

Nb	(0.005[21])	1.704[21] (164.5)		1,311–1,890 (0.83) β-Ti	15[51] (8T)	pc 2N7	[95]Nb, electroplated; autoradiography	No	Approximative two-exponential fit together with the data of [41.16] [+]Present rough fit to the depicted data	Co, Cr, Fe, Mn, Mo, Ni in β-Ti; Nb in Ti(Nb)	41.08	Gibbs (1963) [41.17]
	(20[21])	3.166[21] (305.7)										
	0.003[21+]	1.684[21 +] (159.1)	21[+]									
	10[21+]	3.166[21 +] (305.7)										
Ni	0.0092	1.284 (123.9)		1,209–1,511 (0.70) β-Ti	10[51]	pc (5–10 mm) 2N7	[63]Ni, electroplated; autoradiography	No		Co, Fe, Mn, Nb in β-Ti	41.05	Peart (1962) [41.16]
Ni	(0.0092[21])	1.284[21] (123.9)	790[+]	1,220–1,911 (0.81) β-Ti	16[51] (11T)	pc 2N7	[63]Ni, electroplated; autoradiography	No	Approximative two-exponential fit together with the data of [41.16] [+]Present rough fit to the depicted data	Co, Cr, Fe, Mn, Mo, Nb in β-Ti	41.05	Gibbs (1963) [41.17]
	0.008[+]											
	(2.0[21])	2.277[21] (219.8)										
	3.5[+]											
Ni	–	–		912–1,141 (0.53) α-Ti	5	pc "high-pure"*	[63]Ni, electroplated; lathe (50 µm sections)	All (partly marked NSE)	*Fe content not specified [+]Present approximation	Co, Fe, Ni in α-Zr	–	Hood (1972) [41.37]
	0.061[+]	1.445[+] (139.5)	–									
Ni	⊥ 0.054	1.469 (141.8)	–	876–1,103 (0.51) α-Ti	5[51]	sc ~3N*	[63]Ni, electroplated; lathe	No	*Fe, Ni content ~100 ppma, see introduction page	Ni in α-Ti(O)	41.19	Nakajima (1985) [41.38]
	// 0.056	1.421 (137.2)	–		5[51]							
P	0.00362[21]	1.045[21] (100.9)	910	1,218–1,873 (0.80) β-Ti	15 (10T)	pc 2N7	[32]P, electroplated; lathe	No	Approximative two-exponential fit	Sc, Sn in β-Ti	41.10	Askill (1965) [41.39]
	5[21]	2.450[21] (236.6)										
P				(872–1,123)*	(14)	sc 3N6[x]	[32]P, dried-on from salt solution; lathe	4 examples	*Marked downward curvature of ln D – 1/T below 973 K [x]Fe content <7.5 ppma	P in Ti(O)	41.19	Nakajima (1986) [41.40]
	⊥ 0.155	1.431 (138.2)	–	973–1,123 (0.54) α-Ti	4							
	// 4.7	1.785 (172.3)	–		4							
Pb	$(8 \times 10^{-4})^{+}$	$(2.351)^{+}$ (227)	–	823–973 (0.46) α-Ti	5 (4T)	pc 3N*	Pb, implanted; RBS	2 examples	*Fe, Ni content <150 ppma, see introduction page [+]Present approximation		41.18	Mirassou (1996) [41.41]

Table 4.1 *(Continued)*

(1)	(2a)	(2b)	(3)	(4)	(5)	(6)	(7)	(8)	(9)	(10)	(11)	(12)
X	D^0 (10^{-4} m^2 s^{-1})	Q (eV) and (kJ $mole^{-1}$)	D (T_m) (10^{-12} m^2 s^{-1})	T-range (K) ($\overline{T}/T_m$)	No. of data points	Material, purity	Experimental method	Remarks on the pp	Further remarks	Also studied	Figure	Reference
Pb	0.056	2.693 (260)	–	913–1,123 (0.52) α-Ti	7	pc 3N*	Pb, vapour deposition; HIRBS	1 example	*Fe content ~100 ppma, see introduction page	Ag in α-Ti	41.18	Mirassou (1997) [41.42]
Pd	5.70[22]	3.21[22] (310)	62	1,173–1,823 (0.77) β-Ti	14	pc ~3N5	Pd; EPMA Ti/Ti(1.84% Pd) (Boltzmann–Matano, Hall)	No	Ω-fit with Ω = 3.18	Cr in β-Ti	41.09	Lee (1991) [41.22]
Pd	(20) 29^+	2.734 (264)	–	723–1,073 (0.45) α-Ti	8	pc 4N*	Pd, implanted; RBS	All	*Fe, Ni content <3 ppma +Present recalculation		41.17	Behar (2000) [41.43]
Pu	(1×10^{-6}) $(1.5 \times 10^{-6})^+$	(0.663) (64.1)		1,178–1,400 (0.68) β-Ti	5[51]	pc[61]	Pu, diffusion couple; α-auto-radiography	No	+Present fit to the depicted data	Pu in Ti(Pu)	–	Languille (1971) [41.44]
Sc	0.0021[x]	1.418[x] (136.9)	43	1,192–1,563 (0.71) β-Ti	8	pc 2N7	^{46}Sc, vapour deposition; lathe	No	[x]Forced fit	P, Sn in β-Ti	41.10	Askill (1965) [41.39]
Sc	(0.004[x]) 0.0019[+]	1.405[x] (135.7)	42^+	1,213–1,843 (0.79) β-Ti	12[51] (11T)	pc 3N5	^{46}Sc[72]; Lathe	No	[x]Forced fit +Present fit to the depicted data	Ag in β-Ti	41.10	Askill (1971) [41.06]
Si	0.422[22]	2.682[22] (259)	56	1,173–1,823 (0.77) β-Ti	14	pc ~3N5	Si; EPMA Ti/Ti(1.02% Si) (Matano, Darken)	No	Ω-fit with Ω = 2.52	Ge, Sn in β-Ti	41.06	Iijima (1993) [41.31]
Si	(4.4×10^{-7})	(1.09) (105.2)	–	923–1,073 (0.51) α-Ti	4	pc 3N*	Si, implanted; NRA ($^{30}Si(p,\gamma)^{31}P$)	No	*Fe content not specified		–	Räisänen (1986) [41.45]
Sn	$(3.8 \times 10^{-4}$ [21]) 3.6×10^{-4} [+] (9.5[21]) 13^+	1.370[21] (132.3) 3.001[21] (289.7)	30^+	1,226–1,868 (0.80) β-Ti	17 (10T)	pc 2N7	^{113}Sn, electro-plated; lathe	No	Approximative two-exponential fit +Present rough approximation	P, Sc in β-Ti	–	Askill (1965) [41.39]

Sn	– 0.007^{+}	– 1.714^{+} (165.5)	25^{+}	1,245–1,798 (0.78) β-Ti	5	pc 3N7	^{113}Sn, ^{121}Sn, electro-plated; lathe	No	Pronounced data scatter $^{+}$Present rough approximation	$E = 0.18$–0.37	–	Jackson (1977) [41.46]
Sn	0.69^{22}	3.117^{22} (301)	18	1,173–1,823 (0.77) β-Ti	14	pc ~3N5	Sn; EPMA Ti/Ti(1.65% Sn) (Matano, Darken)	No	Ω-fit with $\Omega = 3.50$	Ge, Si in β-Ti	41.06	Iijima (1993) [41.31]
Sn	2.69^{22}	3.407^{22} (329)	21	1,173–1,773 (0.76) β-Ti	8	pc ~3N	Sn; EPMA Ti/Ti(4.9% Sn) (Matano, Hall)	1 example (probability plot)	Ω-fit with $\Omega = 4.0$	$\Delta V/V_0 =$ 0.28–.41	41.06	Araki (1993) [41.47]
Sn	(40) 36^{+} –	3.5 (338) –	–	873–1,098 (0.51) 923–1,073 α-Ti	7* 3^{x}	pc 3N* ^{x}	Sn, implanted; RBS	Several examples	Fe, Ni content *<150 ppma ^{x}500 ppma, see introduction page $^{+}$Present approximation		41.20	Pérez (1997) [41.48]
Ta	$(3 \times 10^{-4}$ $^{21})$ $2.8 \times 10^{-4+}$ (13^{21}) 11^{+}	1.453^{21} (140.3) 3.209^{21} (309.8)	9.7^{+}	1,187–1,869 (0.79) β-Ti	15	pc 2N7	^{182}Ta^{72}; lathe	No	Approximative two-exponential fit $^{+}$Present rough approximation		41.11	Askill (1966) [41.49]
Ta	0.15^{22}*	2.973^{22}* (287)	7.5	1,273–1,873 (0.81)	12	pc ~3N5	Ta; EPMA Ti/Ta diffusion couple (Den Broeder, Hall)	No	* $\tilde{D}$ extrapolated to $x = 0$; D(Hall) $\approx 0.9\tilde{D}(0)$; Ω-fit with $\Omega = 3.28$		41.11	Ansel (1998) [41.50]
Ta	(10) 11^{+} $(0.25)^{x}$	3.294 (318) $(2.986)^{x}$ (275.7)	–	911–1,123 (0.52) 911, 1,043 α-Ti	7 2	pc 4N* $3N^{x}$	Ta, vapour deposition; RBS, HIRBS	All	*Fe, Ni content <3 ppma; ^{x}Fe, Ni content <150 ppma $^{+}$Present approximation		41.20	Pérez (2003) [41.51]
U	(5.1×10^{-4}) (4.9×10^{-4})*	(1.271) (122.7) –		1,188–1,473 (0.69) 1,188–1,373 β-Ti	11 (6T) 9 (5T)	pc 2N7	^{235}U, vapour deposition[73]; residual activity and absorption	No	*According to [41.65]		–	Pavlinov (1966) [41.52]

Table 4.1 *(Continued)*

(1)	(2a)	(2b)	(3)	(4)	(5)	(6)	(7)	(8)	(9)	(10)	(11)	(12)
X	D^0 (10^{-4} m^2 s^{-1})	Q (eV) and (kJ mole^{-1})	D (T_m) (10^{-12} m^2 s^{-1})	T-range (K) ($\overline{T}/T_m$)	No. of data points	Material, purity	Experimental method	Remarks on the pp	Further remarks	Also studied	Figure	Reference
U	(0.002)	(1.43) (138.1)		1,188–1,298 (0.64) β-Ti	4	pc ~2N3	U(natural), vapour deposition; fission fragment radiography	1 example		U in γ-Fe	–	de Keroulas (1967) [41.53]
U	(1.6×10^{-5} [21]) (0.02 [21]) (4.1×10^{-7}) (2.3×10^{-7})$^+$	(0.924 [21]) (89.2) (1.995 [21]) (192.6) (1.186) (114.1)	(19) –	1,182–1,775 (0.76) β-Ti 1,022–1,123 (0.55) α-Ti	7[51] 3[51]		Experimental details not reported		$^+$Present fit to the depicted data		–	Fedorov (1978) [41.54]
V	3.1×10^{-4} [21] 1.37[21]	1.396[21] (134.8) 2.481[21] (239.5)	56	1,175–1,816 (0.77) β-Ti	13	pc 3N	^{48}V, dried-on from salt solution; lathe	3 examples (50 µm sections)		Ti in β-Ti	41.09	Murdock (1964) [41.01]
V	8×10^{-6} [21] 0.21[21] 33[22]	1.05[21] (101.4) 2.16[21] (208.6) 3.66[22] (353.4)	53 56	(1,175–1,816) β-Ti	(13)				Two-exponential and Ω-fit to the data of [41.01] with $\Omega = 4.0$		41.09	Neumann (1991) [41.55]

W	180[22]	4.464[22] (431)	13	1,173–1,773 (0.76) β-Ti	13[51]	pc 3N	W; EPMA Ti/W diffusion couple (Matano, Darken)	No	Ω-fit with $\Omega = 5.64$	$\Delta V/V_0 =$ 0.30 ± 0.02 for 1,323–1,573 K $\Delta V/V_0 = 0.385$ for 1,623, 1,673 K	41.12	Minamino (1993) [41.56]
Zr	1.59[22]	3.273[22] (316)	37	1,173–1,773 (0.76) β-Ti	9[51]	pc 2N5	Zr; EPMA Ti/Ti(3.06% Zr) (Boltzmann–Matano, Hall)	No	Ω-fit with $\Omega = 4.34$	$\Delta V/V_0 =$ 0.22–0.35	41.07	Araki (1996) [41.57]
Zr	43 –	3.149 (304) –	–	873–1,133 (0.52) 823–1,012 α-Ti	9 (8T) 6[x]	pc 3N*	Zr, vapour deposition; HIRBS, RBS[x]	All	*Fe, Ni content < 150 ppma [x]Pronounced data scatter		41.17	Pérez (1994) [41.58]
Zr	– –	– –	– –	922–1,123 931–1,127 (0.53) α-Ti	4* 3[x]	pc[61]	Zr, vapour deposition; HIRBS	No	Fe content *200 ppma [x]500 ppma		41.17	Pérez (1996) [41.59]

Table 4.2 Diffusion in zirconium (References, see page 209)

(1)	(2a)	(2b)	(3)	(4)	(5)	(6)	(7)	(8)	(9)	(10)	(11)	(12)
X	D^0 (10^{-4} $m^2 s^{-1}$)	Q (eV) and (kJ mole^{-1})	$D(T_m)$ (10^{-12} $m^2 s^{-1}$)	T-range (K) ($\overline{T}/T_m$)	No. of data points	Material, purity	Experimental method	Remarks on the pp	Further remarks	Also studied	Figure	Reference
Self-diffusion												
Zr	2.4×10^{-4}	1.305 (126.0)		1,441–1,776 (0.76) β-Zr	11 (7T)	pc 3N	^{95}Zr, vapour deposition; lathe	1 example			42.01	Kidson (1961) [42.01]
Zr	– 0.85[21]* 1.34[21]*	– 1.201[21]* (116.0) 2.827[21]* (273.0)	29*	1,174–-2,020 (0.75) β-Zr	18	pc 3N4	^{95}Zr, dried-on from oxalate solution; lathe	3 examples	Erroneous thermal expansion correction *Two-exponential fit according to Kidson [42.03]	Nb in β-Zr	42.01	Federer (1963) [42.02]
Zr	–	–		1,215–2,088 (0.78) β-Zr	8 (4T)	pc (>5 mm)	^{95}Zr, ^{89}Zr; mechanical sectioning			$E \approx 0$	42.01	Graham (1970) [42.04]
Zr	1.0×10^{-6} [21] 0.01[21]	0.74[21] (71.4) 1.91[21] (184.4)	31	1,189–2,000 (0.75) β-Zr	18 (15T)	pc (1–3 mm) 3N8	^{95}Zr, ^{88}Zr, dried-on from oxalate solution; lathe	5 examples		E = 0.29–0.41 (1,189–2,000 K)	42.01	Herzig (1979) [42.05]
Zr	3.1×10^{-5}	1.090 (105.3)		1,173–1,473 (0.62) β-Zr	7*	pc ~3N	^{95}Zr, dried-on from oxalate solution; serial sectioning	1 example	*The tabulated data were calculated from D^0 and Q	Mn in β-Zr; Zr, Mn in Zr(Mn)	–	Pruthi (1979) [42.06]
Zr	2.8×10^{-6} [21] 0.0173[21] 1.2[22]	0.84[21] (81.1) 2.01[21] (194.1) 3.53[22] (304.8)	32 34	(1,174–2,020) β-Zr	(31)				Two-exponential and Ω-fit ($\Omega = 4.2$) of the data of [42.03, 42.05]		42.01	Neumann (1990) [42.07]
Zr	1.74×10^{-5}	1.031 (99.5)		1,200–1,518 (0.64) β-Zr	19 (10T)	pc[61]	^{95}Zr, vapour deposition; grinder	No		Zr in Zr(Ag)	–	Patil (1992) [42.08]

Zr	–	–	–	1,124 α-Zr	2	sc 3N3	^{97}Zr, vapour deposition; microtome	2 examples		Several impurities in α-Zr at about 1,110 K	42.08	Hood (1974) [42.09]
Zr	–	–	–	779–1,128 (0.45) α-Zr	10	sc* 4N^{x}	^{95}Zr, electroplated; IBS	All	*Tilted 36° to the *c*-axis ^{x}Fe content 2 ppma		42.08	Horvath (1984) [42.10]
Zr	⊥ –	–	–	871–1,074 (0.46)	4 (2T)	sc nominally pure^{x}	^{95}Zr, vapour deposition; IBS	All[84,85]	*Tilted 14° to the *c*-axis ^{x}Fe content 90–230 ppma		42.08	Lübbehusen (1991) [42.11]
	≈ // –	–	–	α-Zr	5*							
Zr	⊥, //–	–	–	1,107	4	sc	^{95}Zr, vapour deposition; microtome and IBS	4 examples	^{x}Fe content 47, 57, <1 ppma		42.08	Hood (1995) [42.12]
	⊥, //–	–	–	868–1,107 (0.46)	6	nominally pure^{x}						
	⊥, //–	–	–	1,110 α-Zr	2							
Zr	⊥ – // 0.9	– 3.17 (306.1)	– –	937–1,099 (0.48) α-Zr	3 3	sc[61] *	^{95}Zr, vapour deposition; IBS	no	^{x} Fe content <1 ppma	Hf in α-Zr; Zr in α-Zr(Nb), Hf, Zr in α-Zr(Ti)	42.08	Hood (1997) [42.13]
Impurity diffusion												
Ag	(5.7×10^{-4}) $6.1 \times 10^{-4+}$	1.418 (136.9)		1,221–1,457 (0.63) β-Zr	6[51]	pc 4N	^{110}Ag, dried-on from salt solution; serial sectioning (lapping)	2 examples	$^{+}$Present fit to the depicted data	Ag in α-Zr	42.02	Tendler (1974) [42.14]
Ag	4.2×10^{-4} [21] 190.5[21]	1.37[21] (132.3) 3.36[21] (324.4)	225	1,199–1,988 (0.75) β-Zr	12	pc 3N8	^{110}Ag, ^{105}Ag, dried-on from salt solution; lathe	6 examples (partly[85])		$E = 0.4 \pm 0.04$; Zr in β-Zr at 1,913 K: $D = 1.2 \times 10^{-11}$ m^2 s^{-1}	42.02	Manke (1982) [42.15]
Ag	3.9×10^{-4} [21] 109[21] 980[22]	1.36[21] (131.3) 3.27[21] (315.7) 4.78[22] (461.5)	215 165	(1,199–1,988) β-Zr	(12)				Two-exponential and Ω-fit (Ω = 5.9) of the data of [42.15]		42.02	Neumann (1991) [42.16]
Ag	2.5×10^{-4}	1.326 (128)		1,200–1,290 (0.59) β-Zr	4[51]	pc 2N6	Ag; EPMA Zr/Zr (1.27% Ag) (Sauer, Freise)	No		Ag in α-Zr Cu in β-Zr	–	Iijima (1995) [42.17]
Ag	–	–	–	1,094 α-Zr	1^{x}	sc* 3N3	^{110}Ag; lathe		*Orientation not specified $^{x}D = 4.0 \times 10^{-16}$ m^2 s^{-1}	Au, Zn in α-Zr	42.09	Hood (1971) [42.18]

Table 4.2 *(Continued)*

(1)	(2a)	(2b)	(3)	(4)	(5)	(6)	(7)	(8)	(9)	(10)	(11)	(12)
X	D^0 (10^{-4} $m^2 s^{-1}$)	Q (eV) and (kJ mole^{-1})	$D(T_m)$ (10^{-12} $m^2 s^{-1}$)	T-range (K) ($\overline{T}/T_m$)	No. of data points	Material, purity	Experimental method	Remarks on the pp	Further remarks	Also studied	Figure	Reference
Ag	5.1×10^{-3}	1.938 (187.2)	–	1,037–1,120 (0.51) α-Zr	6[51]	pc 4N*	^{110}Ag, electroplated; serial sectioning (lapping)	3 examples[83]	*Fe content 900 ppma (see [42.20])	Ag in β-Zr	42.09	Tendler (1974) [42.14]
Ag	$\perp$ 5.9×10^{-4}	1.8 (173.8)	–	1,063–1,118 (0.51)	4	sc 4N6*	^{110}Ag, electroplated; grinder	All	*Fe content 20 ppma $^{x}D(\theta)$ recalculated to $D^{//}$ according to Eq. (02.18)		42.09	Tobar (1989) [42.19]
	// 0.067	2.2 (212.4)	–	α-Zr	4[x]							
Ag	2.20	2.537 (245)	–	938–1,117 (0.48)	5	sc[x] 3N3[1]	^{110}Ag, electroplated; microtome and grinder	All[83]	[x]Tilted 22° from the c-axis; Fe content [1]107, [2]192, [3]20 ppma		42.09	Vieregge (1989) [42.20]
	0.068	2.175 (210)	–	895–1,110 (0.47) α-Zr	7	pc 4N3[2] 3N6[3]						
Ag	0.017	2.113 (204)	–	1,028–1,104 (0.50) α-Zr	4[51]	pc 2N6	Ag, EPMA Zr/Zr (0.34% Ag) (Sauer, Freise)	No		Ag, Cu in β-Zr	–	Iijima (1995) [42.17]
Al	0.056	2.280 (220.1)		1,203–1,323 (0.59) β-Zr	5	pc 3N	Al; EPMA Zr/Zr (10% Al) (Hall)	No			42.03	Laik (2002) [42.21]
Al	–	–	–	1,108 α-Zr	1[x]	sc* 3N3	^{26}Al, dried-on from salt solution; microtome	Slight NSE	*Orientation not specified $^{x}D = 3.4 \times 10^{-17}$ $m^2 s^{-1}$	Several impurities in α-Zr at about 1,100 K	–	Hood (1974) [42.09]
Al	(17)	(2.9) (280)	–	873–1,073 (0.46) α-Zr	5	pc 2N8*	Al, implanted; NRA (^{27}Al (p,γ) ^{28}Si)	1 example ($c - x$)	*Fe content not specified; For comparison with [42.09]: D(1,108 K) = 1.1×10^{-16} $m^2 s^{-1}$	Al in α-Hf	–	Räisänen (1985) [42.22]
Au	–	–	–	1,143 α-Zr	1[x]	sc* 3N3	^{198}Au; lathe		*Orientation not specified $^{x}D = 1.3 \times 10^{-15}$ $m^2 s^{-1}$	Ag, Au in α-Zr	–	Hood (1971) [42.18]
Be	0.0833	1.349 (130.2)		1,188–1,573 (0.65) β-Zr	8[51] (5T)	pc 2N7	^{7}Be; residual activity	No		Be in β-Ti	–	Pavlinov (1969) [42.23]

Be	–	–		1,318, 1,421 β-Zr	2	pc (>2 mm)	^{7}Be, electroplated; serial sectioning (lapping)	All (erfc-solutions for α-Zr)			–	Tendler (1976) [42.24]
	0.33	1.383 (133.6)	–	1,013–1,120 (0.50) α-Zr	4	4N						
Ce	0.032[21]	1.8[21] (173.8)	270	1,153–1,873 (0.71)	11	pc (3–4 mm)	^{141}Ce; residual activity			Mo in β-Zr	42.04	Paul (1968) [42.25]
	42.2[21]	3.22[21] (310.9)		β-Zr		"high purity"						
Co	(3.26×10^{-3}) 3.45×10^{-3} [+]	0.946 (91.4)	2,000	1,193–1,977 (0.75) β-Zr	16 (14T)	pc 4N	^{60}Co, vapour deposition; lathe	Several examples (total penetration 2,500 µm, gb contributions at lower T)	[+]Present fit to the tabulated data		42.05	Kidson (1969) [42.26]
Co	3.3×10^{-3}	0.95 (91.7)	1,850	1,193–1,741 (0.69) β-Zr	7[51]	pc 3N8	^{60}Co, ^{57}Co[72]; lathe	No		$E = 0.23 \pm 0.05$; Fe in β-Zr; Co in β-Zr(Nb)	42.05	Herzig (1987) [42.27]
Co	4.7×10^{-3}	1.00 (96.6)	2,000	1,600–1,950 (0.84) β-Zr	4	pc "high purity"	^{60}Co, dried-on from salt solution; lathe	No		Cr, Fe in β-Zr; electro-transport	42.05	Zee (1989)[42.28]
Co	–	–	–	1,049–1,103 (0.51)	5 (3T)	pc[61]	^{58}Co, implanted; microtome	All[85] (partly erfc-solutions)	Tilted $^{1}42°$, $^{2}14°$, $^{3}87°$ from the c-axis, $D(\theta)$ recalculated to $D_{\perp}$ and $D_{//}$		–	Kidson (1981) [42.29]
	$\perp$ 37 [▽]	1.51 [▽] (145.8)		873–1,023	4	sc[61, 1]						
	$\perp$ 1,200 [Δ]	1.9 [Δ] (183.4)		860–990	4	sc[2, *] ~3N			Fe content [*] ~500 ppma			
	// 4×10^{4}	1.98 (191.2)		825–1,044 (0.44) α-Zr	6	sc[3, x] ~2N7			[x] ~1,250 ppma; see introduction page; D^{0} and Q valid for [▽] > 923 K, [Δ] < 873 K			
Cr	4.17×10^{-3}	1.388 (134.0)		1,173–1,673 (0.67) β-Zr	12[51] (6T)	pc 2N7	^{51}Cr; residual activity	No		Fe, Mo, W in β-Zr, Mo, W, Zr in β-Ti	–	Pavlinov (1967) [42.30]

Table 4.2 *(Continued)*

(1)	(2a)	(2b)	(3)	(4)	(5)	(6)	(7)	(8)	(9)	(10)	(11)	(12)
X	D^0 ($10^{-4}\,m^2\,s^{-1}$)	Q (eV) and (kJ mole^{-1})	$D(T_m)$ ($10^{-12}\,m^2\,s^{-1}$)	T-range (K) ($\overline{T}/T_m$)	No. of data points	Material, purity	Experimental method	Remarks on the pp	Further remarks	Also studied	Figure	Reference
Cr	7×10^{-3}	1.474 (142.4)		1,187–1,513 (0.64) β-Zr	11 (10T)	pc[61] (0.6 – 2 mm)	^{51}Cr, dried-on from salt solution and electroplated; serial sectioning (lapping)	4 examples (partly erfc-solution)			42.05	Nicolai (1979) [42.31]
Cr	4.53×10^{-3}	1.427 (137.8)		1,201–1,479 (0.63) β-Zr	6 (4T)	pc 3N5	^{51}Cr, dried-on from salt solution; grinder (SiC papers)	No		Zr, Fe in β-Zr; Zr in Zr(X), X = Cr, Fe	42.05	Patil (1981) [42.32]
Cr	3.1	2.27 (219.2)	1,300	1,630–1,910 (0.83) β-Zr	5	pc "high purity"	^{51}Cr, dried-on from salt solution; lathe	No		Co, Fe in β-Zr; electro-transport	42.05	Zee (1989) [42.28]
Cr	(4.9×10^{-3})	(1.305) (126.0)	–	896–1,105 (0.47)	11[51] (9T)	pc (0.2–2 mm)	^{51}Cr, electroplated; residual activity	2 examples	$^{+}$Present fit to the depicted data		–	Tendler (1972) [42.33]
	0.012^{+}	1.40^{+} (135)		α-Zr		5N, 2N5						
Cr	$\perp$ 0.2	1.688 (163)	–	1,023–1,121 (0.50)	4	sc* $\sim$4N^{x}	^{51}Cr, electroplated; serial sectioning (lapping)	Several examples (partly erfc-solutions)	*Single crystals of different orientation, $D(\theta)$ recalculated to $D_\perp$ and $D_{//}$ according to Eq. (02.18) ^{x}Fe content 20 ppma, see introduction page		42.10	Balart (1983) [42.34]
	// 0.2	1.585 (153)		α-Zr	5 (4T)							
Cr	–	–		799–1,057	6	sc[61 x]	^{51}Cr, dried-on from salt solution; microtome	1 example[84]	^{x}Fe content <3 ppma		42.10	Hood (1993) [42.35]
	$\perp$ 0.1	1.62 (156.4)	–	886–1,057 (0.46)	5							
	–	–		724–1,057	8							
	// 0.024	1.39 (134.2)	–	886–1,057 α-Zr	5							
Cu	0.1	1.605 (155)		1,173–1,290 (0.58) β-Zr	5[51]	pc 2N6	Cu, EPMA Zr/Zr(1.57% Cu) (Sauer, Freise)	No		Ag in α-Zr and β-Zr	42.05	Iijima (1995) [42.17]

Cu	⊥ 0.25	1.60 (154.5)	–	933–1,132 (0.49)	6	sc 3N6[x]	[64]Cu, implanted; lathe	Several examples	*Tilted 10° from the *c*-axis [x]Fe content 55 ppma		42.11	Hood (1975) [42.36]
	// 0.40	1.54 (148.7)	–	888–1,132 (0.48)	8							
	0.42*	1.62* (156.4)	–	887–1,117 α-Zr	5							
Fe	5.3×10^{-3}	1.08 (104.3)	1,450	1,172–1,886 (0.72) β-Zr	12	pc 3N7	[59]Fe, dried-on from salt solution; lathe	Several examples		Fe, Zr in β-Zr(Fe)	42.05	Trampenau (1990) [42.37]
Fe	–	–	–	973, 1,071 α-Zr	2[x]	pc (2–3 mm) 3N3	[59]Fe, vapour deposition; lathe	All	[x]$D(973\,\mathrm{K}) = 3.7 \times 10^{-12}$ [x]$D(1{,}071\,\mathrm{K}) = 3.5 \times 10^{-11}\,\mathrm{m^2\,s^{-1}}$	Co, Ni in α-Zr, Ni in α-Ti	42.12	Hood (1972) [42.38]
Fe	–	–	–	1,113 α-Zr	1[x]	sc* 3N3	[59]Fe, vapour deposition; lathe	pp with slight NSE	*Orientation not specified [x]$D = 7 \times 10^{-11}\,\mathrm{m^2\,s^{-1}}$	Several impurities in α-Zr at about 1,100 K	42.12	Hood (1974) [42.09]
Fe	–	–	–	891, 1,096 α-Zr	3[51] (2T)	pc (> 2 mm) 4N	[59]Fe, electroplated; residual activity	No		Cr, Zn in β-Zr, Co, Cr, Zn in α-Zr	42.12	Tendler (1975) [42.39]
Fe	–	–		871–1,131	4	sc 3N8[x]	[59]Fe, implanted and dried-on from salt solution; lathe	4 examples[83]	Downward curvature of ln $D - 1/T$ at higher temperature [x]Fe content 88 ppma [+]Present approximation	Fe in α-Zr(Fe)	42.12	Nakajima (1988) [42.40]
	⊥ (57)	(1.68) (162.2)		871–1,032 (0.47)	3							
	60[+]	1.69[+] (163.2)	–									
	–	–		765–1,133	9							
	// (1,700)	(1.81) (174.8)		765–980	5							
	300[+]	1.69[+] (163.2)	–	765–1,032 (0.45) α-Zr	6							
Hf	–	–		1,192–1,973 (0.74) β-Zr	12 (11T)	pc 3N8	[181]Hf; experimental details not reported	No		$E \approx 0.45$	42.06	Herzig (1987) [42.41]
Hf	2.8×10^{-5} [21]	1.11[21] (107.2)	27	(1,192–1,973) β-Zr	(11) (10T)				Two-exponential and Ω-fit ($\Omega = 3.5$) of the data of [42.41]		42.06	Neumann (1991) [42.16]
	0.30[21]	2.60[21] (251.0)										
	0.23[22]	3.18[22] (307.0)	22									

Table 4.2 *(Continued)*

(1)	(2a)	(2b)	(3)	(4)	(5)	(6)	(7)	(8)	(9)	(10)	(11)	(12)
X	D^0 ($10^{-4}\,m^2\,s^{-1}$)	Q (eV) and (kJ mole^{-1})	$D(T_m)$ ($10^{-12}\,m^2\,s^{-1}$)	T-range (K) ($\overline{T}/T_m$)	No. of data points	Material, purity	Experimental method	Remarks on the pp	Further remarks	Also studied	Figure	Reference
Hf	0.26	3.1 (299.3)	–	873–1,111 (0.47) α-Zr	12 (5T)	pc (1–2 mm) ~4N*	Hf, sputter deposition; SIMS analysis	2 examples ($c - x$)	*Fe content <1 ppma; pronounced data scatter	Hf in sc α-Zr (Fe content ~50 ppma)	–	Hood (1992) [42.42]
Mn	5.6×10^{-3}	1.431 (138.2)		1,220–1,420 (0.62) β-Zr	5[51]	pc (> 2 mm) 2N5	[54]Mn, deposition in metallic form or as $MnCl_2$; residual activity	2 examples		Mn in α-Zr	42.06	Tendler (1973) [42.43]
Mn	5.38×10^{-3}	1.457 (140.7)		1,173–1,473 (0.62) β-Zr	7*	pc 3N	[54]Mn, dried-on from salt solution; serial sectioning	1 example	*The tabulated data were calculated from D^0 and Q	Zr in β-Zr; Zr, Mn in Zr(Mn)	–	Pruthi (1979) [42.06]
Mn	2.4×10^{-3}	1.310 (126.4)	–	898–1,111 (0.47) α-Zr	5[51]	pc (> 2 mm) 5N, 2N5	[54]Mn, electroplated; residual activity	1 example		Mn in β-Zr	42.11	Tendler (1973) [42.43]
Mn	–	–	–	1,105 α-Zr	1[x]	sc* 3N3	[54]Mn, electroplated; lathe	1 example	*Orientation not specified [x]$D = 2.8 \times 10^{-13}\,m^2\,s^{-1}$	Several impurities in α-Zr at about 1,100 K	42.11	Hood (1974) [42.09]
Mo	(1.99×10^{-4}) [21] $2.15 \times 10^{-4+}$ (2.63)[21] 2.50[+]	1.53[21] (147.7) 2.97[21] (286.8)	27.5[+]	1,173–1,873 (0.72) β-Zr	10	pc (3–4 mm) "high purity"	[99]Mo; residual activity		[+]Present approximation	Ce in β-Zr	42.07	Paul (1968) [42.25]
Nb	-*	-*		1,155–2,031 (0.75) β-Zr	15	pc 3N4	[95]Nb, dried-on from oxalate solution; lathe	3 examples	*Unusual evaluation of the curved Arrhenius plot; erroneous thermal expansion correction	Zr in β-Zr	42.07	Federer (1963) [42.02]
Nb	–	–		1,510–1,995 (0.82) β-Zr	8[51]	pc[61]	[95]Zr; experimental details not reported	No		Hf in β-Hf	42.07	Herzig (1982) [42.44]
Nb	2.7×10^{-5} [21] 0.26[21] 12[22]	1.21[21] (116.8) 2.47[21] (238.5) 3.94[22] (380.4)	40 40	(1,155–2,031) (β-Zr)	(15)				Two-exponential and Ω-fit (Ω = 4.3) of the data of [42.03]		42.07	Neumann (1991) [42.16]

Nb	1.88*	2.69* (259.7)	–	1,002–1,097 (0.49) α-Zr	17 (7T)	sc[61] [x]	[93]Nb, [94]Nb, dried-on from salt solution; microtome and IBS	No	*Common fit for $D_{\perp}$ and $D_{//}$ [x]Fe content < 0.1 ppma		42.09	Hood (1997) [42.45]
Ni	–	–	–	971–1,103 (0.49) α-Zr	4	sc* (2–3 mm) 3N3	[63]Ni, vapour deposition; lathe	All[84]	*Unspecified orientation	Co, Fe in α-Zr; Ni in α-Ti	42.13	Hood (1972) [42.38]
Ni	–	–	–	1,123 α-Zr	2*	sc[61]	[63]Ni, dried-on from salt solution; lathe	All	*$D_{\perp} = 1.6 \times 10^{-10}$ *$D_{//} = 6.0 \times 10^{-10}\ m^2\ s^{-1}$	Ni in α-Zr(Nb)	42.13	Hood (1987) [42.46]
P	0.33	1.444 (139.4)		1,223–1,473 (0.63) β-Zr	10 (6T)	pc 3N4	[32]P; residual activity	No		P in V	–	Vandyshev (1970) [42.47]
Pb	–	–	–	872–1,098 (0.46) α-Zr	6 (4T)	sc ~3N8*	Pb, sputter deposition; RBS	No	*Fe content 30 and 60 ppma; non-linear in ln $D - 1/T$; $D(T)$ is about one order of magnitude smaller than in Ref. [42.49]	Hf, Ta in α-Zr	–	Hood (1991) [42.48]
Pb	–	–	–	823–1,123 (0.46)	7	pc ~3N7*	Pb, vapour deposition; HIRBS	All	*Fe content ~80 ppma		–	Pérez (1999) [42.49]
	(1.9×10^{-3})	(2.330) (225)		953–1,123								
	(53)	(3.304) (319)		823–893 α-Zr								
Rb	– (8.8×10^{-4})	– (1.592) (153.7)		1,040–1,302 1,159–1,302 (0.58) β-Zr	14 (9T) 5 (4T)	pc[61]	Rb; out-diffusion from Rb doped Zr filaments, mass spectroscopy	No	Pronounced data scatter	U in W	–	Schwegler (1968) [42.50]
Ru	–	–		1,194 β-Zr	1	pc[61] * sc[61]	[103]Ru, electroplated and vapour deposition; grinder	All (partly erfc-solutions)	*Fe content 20 ppma; $D(1{,}194\ K) = 1.3 \times 10^{-13}$, $D(1{,}093\ K) = 1.2 \times 10^{-11}\ m^2\ s^{-1}$		–	Balart (1989) [42.51]
	–	–	–	1,092–1,100 α-Zr	4 (3T)							
S	27.6	1.683 (162.5)		1,155–1,250 (0.57) β-Zr	8 (4T)	pc 3N3	[35]S, dried-on from benzene solution, forming a constant source of ZrS_2[73]; serial sectioning	No[81]	[a, b]Different pre-annealing procedures		–	Vandyshev (1967) [42.52]
	(8.9[a])	(1.917[a]) (185.7)	–	870–1,080 (0.46)	10 (5T)							
	(3.1[b])	(1.782[b]) (172.1)	–	α-Zr								

Table 4.2 *(Continued)*

(1)	(2a)	(2b)	(3)	(4)	(5)	(6)	(7)	(8)	(9)	(10)	(11)	(12)
X	D^0 ($10^{-4}\,m^2s^{-1}$)	Q (eV) and (kJ mole^{-1})	$D(T_m)$ ($10^{-12}\,m^2s^{-1}$)	T-range (K) ($\overline{T}/T_m$)	No. of data points	Material, purity	Experimental method	Remarks on the pp	Further remarks	Also studied	Figure	Reference
Sb	–	–	–	1,120 α-Zr	2^x (1T)	sc* 3N3	^{122}Sb, ion implantation; microtome	1 example (pronounced dislocation tail)	*Orientation not specified $^xD = (2\pm0.6)\times10^{-17}\,m^2s^{-1}$	Several impurities in α-Zr at about 1,100 K	–	Hood (1974) [42.09]
Sn	(5.0×10^{-3}) 0.011^+	(1.691) (163.3) 1.77^+ (171)		1,193–1,523 (0.64) β-Zr	6^{51}	pc 2N, 3N	^{113}Sn; residual activity	No	$^+$Present fit to the depicted data	Zr in β-Zr, Zr, Sn in β-Zr(Sn)	–	Fedorov (1959) [42.53]
Sn	– $8.5\times10^{-3\,+}$	– 1.755^+ (169.5)		1,279–1,723 (0.71) β-Zr	8 (4T)	pc 3N7	^{113}Sn, dried-on from salt solution[73]; microtome	All	$^+$Present approximation	Fe in β-Zr at $T = 1{,}223$ K	42.03	Chelluri (1981) [42.54]
Sn	(2×10^{-8})*	(0.954)* (92.1)	–	923–1,093 (0.47) α-Zr	4	pc[61]	^{113}Sn; residual activity	No	*Abnormally small values of D^0 and Q	Sn, Zr in α-Zr(Sn)	–	Fedorov (1959) [42.55]
Ta	5.5×10^{-5}	1.171 (113.0)		1,173–1,473 (0.62) β-Zr		pc 2N6	^{182}Ta; residual activity			Zr in α-Zr and β-Zr	–	Borisov (1958) [42.56]
	100	3.036 (293.1)	–	973–1,073 (0.48) α-Zr								
Ta	–	–	–	872–1,096 (0.46) α-Zr	4 (3T)	sc* ~3N8	Ta, sputter deposition; RBS	No	*Fe content 30 and 60 ppma; non-linear in $\ln D - 1/T$	Hf, Pb in α-Zr	–	Hood (1991) [42.48]
Ti	–	–	–	1,116 α-Zr	1^x	sc* 3N3	^{44}Ti, dried-on from salt solution; microtome	1 example	*Orientation not specified $^xD = 9.4\times10^{-17}\,m^2s^{-1}$	Several impurities in α-Zr at about 1,100 K	42.10	Hood (1974) [42.09]
Ti	⊥– //– 17	– – 2.93 (282.9)	–	773–1,124 (0.45) 773–1,124 1,037–1,124 (0.51) α-Zr	$10^{*\,0}$ 14^0 7	sc^{61x}	^{44}Ti, dried-on from salt solution; microtome and Ti sputter deposition; SIMS	4 examples	*Pronounced data scatter ^{0}Pronounced NSE at lower T ^{x}Fe content 30–60 ppma		42.10	Hood (1994) [42.57]
U	8.15×10^{-5}	1.154 (111.4)		1,223–1,573 (0.66) β-Zr	10 (5T)	pc 2N6	^{235}U; Kryukov absorption	No			–	Pavlinov (1970) [42.58]

U	$(5.3 \times 10^{-6}$ [21])	(0.854)[21] (82.5)		1,223–1,773 (0.70) β-Zr	6	pc[61]	^{235}U; vapour deposition; serial sectioning	No	$D(T)$ calculated by use of $D^0_{1,2}$ and $Q_{1,2}$ does not fit to D_{exp}	U in Mo, Nb, V, Ta, W	–	Fedorov (1971) [42.59]
	(0.36[21])	(2.515)[21] (242.8)										
V	–	–		1,143–1,673 (0.66)	7	pc ($\sim$1 mm)	^{48}V, dried-on from $VOCl_3$ solution; residual activity	2 examples	$^{+}$Present approximation; the results of [42.60] and [42.61] differ by a factor 5–25	V in α-Zr, V in V, Nb	–	Agarwala (1968) [42.60]
	(0.32)	(2.480) (239.5)		1,473–1,673 (0.74)	3	$\sim$3N						
	0.075^{+}	2.267^{+} (218.9)										
	(7.6×10^{-3}) 8.0×10^{-3} $^{+}$	1.986 (191.8)		1,143–1,473 (0.62) β-Zr	5							
V	8.9×10^{-5}	1.207 (116.6)		1,166–1,480 (0.62) β-Zr	7*	pc $\sim$3N	^{48}V, dried-on from salt solution; serial sectioning	1 example	*The tabulated data were calculated from D^0 and Q; the results of [42.60] and [42.61] differ by a factor 5–25	V, Zr in Zr (0.5–2% V)	–	Pruthi (1982) [42.61]
V	(1.12×10^{-8})	(0.993) (95.9)	–	873–1,123 (0.47) α-Zr	6	pc* ($\sim$1 mm) $\sim$3N	^{48}V, dried-on from $VOCl_3$ solution; residual activity	1 example	*Fe content $\sim$1,000 ppma	V in β-Zr, V in V, Nb	–	Agarwala (1968) [42.60]
W	0.41	2.420 (233.6)		1,173–1,523 (0.63) β-Zr	19[51] (8T)	pc 2N7	^{185}W; absorption			Cr, Fe, Mo in β-Zr, Mo, W, Zr in β-Ti	–	Pavlinov (1967) [42.30]
Y	8×10^{-5}	1.032 (99.7)		1,373–1,608 (0.70) β-Zr	4	pc[61]	^{90}Y, vapour deposition; residual activity	No	*$D = 3.5 \times 10^{-17}$ m^2 s^{-1}		–	Fedorov (1966) [42.62]
	–	–		1,073 α-Zr	1*							
Zn	0.082	1.904 (183.8)		1,273–1,453 (0.64) β-Zr	6[51]	pc ($>$ 2 mm) 3N2, 4N	^{65}Zn, vapour deposition; residual activity	No (pp linear in ln $c - x^2$ up to 400 μm)		Cr, Fe in β-Zr, Co, Cr, Fe, Zn in α-Zr	–	Tendler (1975) [42.39]
Zn	–	–	–	1,099 α-Zr	1[x]	sc* 3N3	^{65}Zn; lathe		*Orientation not specified [x]$D = 2.8 \times 10^{-15}$ m^2 s^{-1}	Ag, Au in α-Zr	–	Hood (1971) [42.18]
Zn	1.65	2.320 (224.0)	–	1,002–1,114 (0.50) α-Zr	12[51] (9T)	pc ($>$ 2 mm) 3N2, 4N	^{65}Zn, vapour deposition; residual activity	No (partly NSE)	Pronounced data scatter	Cr, Fe, Zn in β-Zr, Co, Cr, Fe in α-Zr	–	Tendler (1975) [42.39]

Table 4.3 Diffusion in hafnium

(References, see page 211)

(1) X	(2a) D^0 (10^{-4} m^2 s^{-1})	(2b) Q (eV) and (kJ mole^{-1})	(3) $D(T_m)$ (10^{-12} m^2 s^{-1})	(4) T-range (K) ($\overline{T}/T_m$)	(5) No. of data points	(6) Material, purity	(7) Experimental method	(8) Remarks on the pp	(9) Further remarks	(10) Also studied	(11) Figure	(12) Reference
Self-diffusion												
Hf	1.2×10^{-3}	1.678 (162.0)	50	2,068–2,268 (0.87) β-Hf	6 (5T)	pc (4.0 at % Zr)	^{181}Hf, vapour deposition; lathe	No (linear in ln $c - x^2$)			43.01	Winslow (1965) [43.01]
Hf	1.1×10^{-3}	1.65 (159.3)	52	2,013–2,351 (0.87) β-Hf	7[51] (6T)	pc (5.5 at % Zr)	^{181}Hf; serial sectioning	No		$E = 0.36-0.28$; Nb in β-Zr; Nb in β-Zr(Nb)	43.01	Herzig (1982) [43.02]
Hf	$\perp$, // –	–		1,437–1,883	27	sc (4.0 at % Zr)	^{181}Hf, vapour deposition; lathe	3 examples (dislocation tails at lower T)	Pronounced data scatter		43.02	Davis (1972) [43.03]
	$\perp$ 0.28	3.606 (348.3)	–	1,473–1,883 (0.67)	10 (9T)							
	// 0.86	3.833 (370.1)	–	α-Hf	10 (9T)							
Hf	0.054	3.345 (323)	–	1,173–1,633 (0.56) α-Hf	6[51]	pc ~3N	Experimental details not reported	No		Al in α-Hf	43.02	Herzig (2002) [43.04]
Impurity diffusion												
Al	–	–	–	1,073–1,870 (0.59) α-Hf	6[51]	pc ~3N	Al; SIMS analysis	No	[+]Present approximation	Hf in α-Hf	43.03	Herzig (2002) [43.04]
	1.0[+]	3.42[+] (330)										
Al	(3) ~5[+]	3.490 (337)	–	973–1,298 (0.45) α-Hf	8	pc ~2N*	Al, implanted; NRA (^{27}Al (p,γ) ^{28}Si)	Several examples	[+]Present approximation *Fe content ~600 ppma		–	Bernardi (2005) [43.05]
Co	5.3×10^{-3}	0.99 (95.5)	–	1,106–1,798 (0.58) α-Hf	6	pc (5.1 at % Zr)	^{60}Co, electroplated; serial sectioning	1 example		Cr in α-Hf and β-Hf	43.04	Dyment (1976) [43.06]
Cr	0.14*	2.216* (214.0)	–	2,073–2,173 (0.85) β-Hf	3	pc (5.1 at % Zr)	^{51}Cr, electroplated; serial sectioning	3 examples	*Common fit for α- and β-phase; pronounced data scatter	Co in α-Hf	–	Dyment (1976) [43.06]
				1,183–1,983 (0.63) α-Hf	11							
Ti	0.27*	3.335* (322)	– –	1,075–1,858 (0.59) α-Hf	$\perp$ 15 // 6	sc[x] ~3N	^{44}Ti, dried-on from salt solution; microtome; Ti, vapour deposition; SIMS analysis	Numerous examples	*Common fit for $D_\perp$ and $D_{//}$ [x]Fe content < 80 ppma		43.05	Köppers (1993) [43.07]

Table 4.4 Diffusion in tin

(References, see page 211)

(1) X	(2a) D^0 (10^{-4} m^2 s^{-1})	(2b) Q (eV) and (kJ mole^{-1})	(3) $D(T_m)$ (10^{-12} m^2 s^{-1})	(4) T-range (K) ($\overline{T}/T_m$)	(5) No. of data points	(6) Material, purity	(7) Experimental method	(8) Remarks on the pp	(9) Further remarks	(10) Also studied	(11) Figure	(12) Reference
Self-diffusion												
Sn	⊥ 1.4	1.010 (97.6)	0.011	451–495 (0.94)	8	sc 4N8	^{113}Sn, electroplated[73]; microtome	2 examples			44.01	Meakin (1960) [44.01]
	// 8.2	1.110 (107.2)	6.8×10^{-3}		8							
Sn	⊥ 10.7	1.089 (105.1)	0.015	434–499 (0.92)	6	sc 5N	^{113}Sn, vapour deposition[73]; microtome	1 example		$\Delta V/V_0 =$ 0.33	44.01	Coston (1964) [44.02]
	// 7.7	1.110 (107.2)	6.4×10^{-3}		5							
Sn	⊥ 21.0	1.123 (108.5)	0.013	455–499 (0.94)	5[51]	sc 5N	^{113}Sn, electroplated[73]; lathe	No		Cd, Sb, Zn in Sn	44.01	Huang (1974) [44.03]
	// 12.8	1.127 (108.9)	7.1×10^{-3}		5[51]							
Impurity diffusion												
Ag	⊥ 0.18	0.798 (77.0)	0.19	414–495	8[51]	sc[61]	^{110}Ag, chemical deposition from nitrate solution; microtome	No		Au in Sn	44.02	Dyson (1966) [44.04]
	// 7.1×10^{-3}	0.533 (51.5)	3.4	405–499 (0.90)	8[51]							
Au	⊥ 0.16	0.768 (74.1)	0.35	420–500 (0.91)	7[51]	sc[61]	^{198}Au, chemical deposition from chloride solution; microtome	No		Ag in Sn	44.02	Dyson (1966) [44.04]
	//(5.8×10^{-3})	0.477 (46.1)	10	407–483 (0.88)	7[51]							
Cd	⊥ 120	1.197 (115.6)	0.014	458–500 (0.95)	7[51]	sc 5N	^{109}Cd, electroplated[73]; lathe	No		Sn, Sb, Zn in Sn	44.03	Huang (1974) [44.03]
	// 220	1.223 (118.1)	0.013		7[51]							
Co	⊥ – (150$^+$)	– (1.088$^+$) (105)	(0.21)	399–502 (0.89)	6[51]	sc 4N5	^{60}Co, electroplated; residual activity	2 examples[84]	$^+$Present rough fit to the depicted data; abnormally low D values for 3d impurities, see Ni in Sn for comparison	Fe in Sn	–	Brik (1982) [44.05]
	// – (13$^+$)	– (1.067$^+$) (103)	(0.03)		6[51]							

Table 4.4 *(Continued)*

(1) X	(2a) D^0 (10^{-4} m^2 s^{-1})	(2b) Q (eV) and (kJ mole^{-1})	(3) $D(T_m)$ (10^{-12} m^2 s^{-1})	(4) T-range (K) ($\overline{T}/T_m$)	(5) No. of data points	(6) Material, purity	(7) Experimental method	(8) Remarks on the pp	(9) Further remarks	(10) Also studied	(11) Figure	(12) Reference
Cu	$\perp (2.4 \times 10^{-3})$	(0.343) (33.1)	(90)	408–495 (0.89)	4[51]	sc[61]	Cu[71]; microtome	No[84]	Pronounced data scatter		–	Dyson (1967) [44.06]
	$//(\sim 1 \times 10^{-3})^x$	$(\sim 0.173)^x$ (16.7)	(2×10^3)		1*				[x]Estimated [*]$D_{//}$ (298 K) $\approx 2 \times 10^{-10}$ m^2 s^{-1}			
Fe	(4.8×10^{-4})	(0.47) (45.4)	(0.25)	387–462 (0.84)	4[51]	pc 5N5	[57]Co, electroplated; Mößbauer spectroscopy [57]Fe signal				–	Shimotomai (1978) [44.07]
Fe	$\perp$ – (42^+)	– (1.10^+) (106)	(0.05)	399–502 (0.89)	5[51]	sc 4N5	[55]Fe, [59]Fe, electroplated; residual activity	No	[+]Present rough fit to the depicted data; see Co in Sn	Co in Sn	–	Brik (1982) [44.05]
	// – (2.7^+)	– (1.046^+) (101)	(0.01)		5[51]							
Hg	$\perp$ *30.1	1.162 (112.2)	7.5×10^{-3}	448–499	10	sc 6N	[203]Hg, chemical deposition from nitrate solution; microtome	1 example	*D measured in [110] direction		44.04	Warburton (1972) [44.08]
	// 7.5	1.097 (105.9)	8.4×10^{-3}	448–497 (0.94)	9							
In	$\perp$ 34.1	1.119 (108.0)	0.023	454–494 (0.94)	10 (5T)	sc* 4N8	[114]In, electroplated[73]; lathe	3 examples	Erroneous thermal expansion correction		44.05	Sawatzky (1958) [44.09]
	// (12.2) 13.2$^+$	1.110 (107.2)	0.011^+		9 (5T)				[*]Deviating 5° and 10° from the c-axis, $D_\perp$ and $D_{//}$ calculated according to Eq. (02.18) [+]Present approximation			

Ni	$\perp$ 0.0187	0.561 (54.2)	4.7	393–474 (0.86)	5^{51}	sc 5N	^{63}Ni, electroplated; lathe	No			44.06	Yeh (1984) [44.10]
	// 0.0199	0.187 (18.1)	(3×10^{-4})	298–373 (0.66)	5^{51}							
Sb	$\perp$ 76.6	1.275 (123.1)	1.4×10^{-3}	466–498 (0.95)	7 (6T)	sc* 5N	^{124}Sb, electroplated[73]; lathe	4 examples	*Crystals of different orientation, $D_{\perp}$ and $D_{//}$ calculated according to Eq. (02.18)		44.05	Huang (1971) [44.11], [44.03]
	// 79.1	1.262 (121.8)	2.0×10^{-3}		7 (6T)							
Tl	(1.2×10^{-3})	(0.637) (61.5)	(0.05)	410–489 (0.85)	10 (7T)	pc 5N	^{204}Tl, electroplated; lathe and auto-radiography (3T)	No	gb-diffusion enhanced	gb-diffusion	–	Bartha (1969) [44.12]
Zn	$\perp$ 8.4	0.924 (89.2)	0.50	409–499	6	sc 5N	^{65}Zn, electroplated[73]; lathe	2 examples	$^{+}$Present approximation	Sn, Cd, Sb in Sn	44.07	Huang (1974) [44.03]
	// (0.011) 0.0115^{+}	0.520 (50.2)	7.3^{+}	409–496 (0.90)	4							

Table 4.5 Diffusion in lead

(References, see page 212)

(1) X	(2a) D^0 (10^{-4} m^2 s^{-1})	(2b) Q (eV) and (kJ mole^{-1})	(3) $D(T_m)$ (10^{-12} m^2 s^{-1})	(4) T-range (K) ($\overline{T}/T_m$)	(5) No. of data points	(6) Material, purity	(7) Experimental method	(8) Remarks on the pp	(9) Further remarks	(10) Also studied	(11) Figure	(12) Reference
Self-diffusion												
Pb	0.281	1.050 (101.3)	0.044	447–595 (0.87)	7	sc 5N	^{210}Pb, vapour deposition; microtome	1 example			45.01	Nachtrieb (1955) [45.01]
Pb	1.372	1.130 (109.1)	0.046	480–596 (0.90)	5	pc 4N	^{210}Pb, vapour deposition; microtome	No		Bi, Tl in Pb; Pb, Bi, Tl in Pb(Tl)	45.01	Resing (1961) [45.02]
Pb	0.463	1.075 (103.8)	0.044	477–571 (0.87)	6[51]	pc 6N	^{210}Pb, electroplated; electrochemical sectioning	No		$\Delta V/V_0$ = 0.57–0.63 (p = 0–4.0 GPa)	45.01	Hudson (1961) [45.03]
Pb	0.887	1.107 (106.9)	0.046	470–574 (0.87)	9[51] (8T)	sc 6N	^{210}Pb, electroplated; microtome	No		Cd in Pb; Pb in Pb(Cd)	45.01	Miller (1969) [45.04]
Pb	0.88	1.106 (106.8)	0.047	487–568 (0.88)	5	sc 6N	^{210}Pb, electroplated; lathe	No (linear in $\ln c - x^2$)		Hg in Pb; Pb, Hg in Pb(Hg)	45.01	Warburton (1973) [45.05]
Impurity diffusion												
Ag	– 0.048*	– 0.63* (60.8)	 25*	473–578 (0.87)	5[51]	sc 5N	^{110}Ag, vapour deposition; microtome	No (linear in $\ln c - x^2$)	Marked data scatter *Fit for p = 0 according to Decker [45.32]	$\Delta V/V_0 = 0.35$ (p = 0–3.9 GPa) according to Ref. [45.32]	–	Curtin (1965) [45.06]
Ag	0.046	0.626 (60.5)	26	398–594 (0.83)	8[51]	sc[61]	^{110}Ag, electroplated; microtome	No (linear in $\ln c - x^2$)		Cu in Pb	45.02	Dyson (1966) [45.07]
Ag	–	–		553–575 (0.94)	8 (4T)	pc 5N5	^{111}Ag, ^{105}Ag, chemical deposition; microtome	All (slight NSE)		$E \approx 1$	45.02	Herzig (1971) [45.08]
Ag	–	–		423–576 (0.83)	4	sc 6N	^{110}Ag, ^{105}Ag, electroplated; microtome	2 examples		E = 0.31–0.19	45.02	Miller (1973) [45.09]
Ag	0.0442	0.630 (60.8)	23	437–572 (0.84)	5	sc 4N8	^{110}Ag, chemical deposition; microtome	1 example		$\Delta V/V_0 = 0.37$ (p = 0–0.9 GPa)	–	Ascoli (1974) [45.10]
Ag	–	–		423–477 (0.75)	3	sc 6N	^{110}Ag, electroplated; lathe	No		Ag in Pb(Ag); c_s = 75–300 ppma	45.02	Cohen (1975) [45.11]

Ag	0.046	0.63 (60.8)	24	423–573 (0.83)	7 (4T)	pc (0.2 mm) 5N	^{110}Ag, chemical deposition; microtome	1 example		Ni in Pb; Ag, Ni in Pb(Sn)	45.02	Hu (1982) [45.12]
Ag	0.046	0.624 (60.3)	27	423–513 (0.78)	3[51]	pc (0.5 mm) 5N	^{110}Ag[72], microtome	No		Ag, Au, Cu in Pb(In)	45.02	Shi (1987) [45.13]
Ag	0.048^{+}	0.628^{+} (60.6)	26^{+}	398–594 (0.83)	(33)				$^{+}$Present fit to the data of [45.07–45.09], [45.11–45.13]		45.02	
Au	2.8×10^{-3}	0.386 (37.3)	160	463–569 (0.86)	8	pc[61] (1–9 mm)	^{198}Au (neutron irradiation of Au after the diffusion run), vapour deposition*; microtome (250 μm sections)	1 example	*$\sim$0.2 μm layer; see column (9) in Ref. [45.19]		–	Ascoli (1956) [45.14]
Au	4.1×10^{-3}	0.405 (39.1)	160	367–598 (0.80)	23 (15T)	sc 5N	^{195}Au, electroplated; microtome	1 example	*$<$0.2 μm layers; see column (9) in Ref. [45.19]		–	Ascoli (1961) [45.15]
Au	2.5×10^{-3}	0.379 (36.6)	170	357–526 (0.73)	4[51]	sc 5N	^{198}Au (neutron irradiation of Au after the diffusion run), electroplated*; microtome (50 μm sections)		*$\sim$0.2 μm layers; see column (9) in Ref. [45.19]	p-dependence of D (p = 0–1.0 GPa)	–	Ascoli (1966) [45.16]
Au	8.7×10^{-3}	0.434 (41.9)	200	461–592 (0.88)	14[51]	sc 5N	^{198}Au, ^{199}Au, vapour deposition; microtome	3 examples	See column (9) in Ref. [45.19]		–	Kidson (1966) [45.17]
Au	5.6×10^{-3}*	0.411* (39.7)	200*	(443–640)	0 (at $p = 0$)	sc 6N	^{198}Au (neutron irradiation of Au after the diffusion run), electroplated; ($\sim$10 nm layers); microtome	No	*$D(p)$ recalculated to $D(p = 0)$	$\Delta V/V_0 \approx 0.30$ (p = 2.1 – 4.6 GPa)	–	Weyland (1971) [45.18]
	5.8×10^{-3} x	0.417x (40.3)	185x						xReanalysis using a new pressure calibration [45.32]			
Au	3.62×10^{-3}	0.388 (37.4)	230	410–511 (0.77)	10	sc 6N	^{195}Au, electroplated; lathe	1 example	Au additions to Pb drastically de-enhance the diffusivity of Au (and Pb). In the earlier papers probably too thick Au layers lead to reduced diffusivities.	Au in Pb(Au)	45.02	Warburton (1975) [45.19]

Table 4.5 *(Continued)*

(1) X	(2a) D^0 (10^{-4} m^2 s^{-1})	(2b) Q (eV) and (kJ mole^{-1})	(3) $D(T_m)$ (10^{-12} m^2 s^{-1})	(4) T-range (K) ($\overline{T}/T_m$)	(5) No. of data points	(6) Material, purity	(7) Experimental method	(8) Remarks on the pp	(9) Further remarks	(10) Also studied	(11) Figure	(12) Reference
Au	5.2×10^{-3}	0.400 (38.6)	230	334–563 (0.75)	14 (13T)	pc 6N	^{195}Au (carrier free), chemical deposition; microtome	3 examples (erfc-solution at low T)		Au in Pb(Ag) and Pb(Pd)	45.02	Decker (1979) [45.20]
Bi	12.0$^+$	1.191$^+$ (115.0)	0.12$^+$	564, 596	2	pc 4N	^{210}Bi, vapour deposition*; microtome	No	$^+$Present calculation *Daughter of ^{210}Pb	Pb, Tl in Pb and Pb(Tl)	45.03	Resing (1961) [45.02]
Cd	0.409	0.920 (88.9)	0.78	423–594 (0.85)	9[51]	sc 6N	^{115}Cd, electroplated; microtome	2 examples (dislocation tail at low T)		Pb in Pb and Pb(Cd)	45.04	Miller (1969) [45.04]
Cd	0.92	0.961 (92.8)	0.79	523–570 (0.91)	8[51]	sc 6N	^{109}Cd, electroplated; microtome	1 example		$\Delta V/V_0 \approx 0.32$ ($p = 0$–4.0 GPa); Hg in Pb	–	Vanfleet (1977) [45.21]
Co	9×10^{-3}	0.481 (46.4)	84	372–552 (0.77)	6[51]	pc (3–4 mm) 6N	^{60}Co (neutron irradiation of Co after the diffusion run), implanted; microtome (30 μm sections)	1 example[84]			–	Kusunoki (1978) [45.22]
Cr	8.7×10^{-3}	0.577 (55.7)	130	502–591 (0.91)	[52]	sc 4N5	^{51}Cr, electroplated; lathe	No (linear in $\ln c - x^2$)		Cs in Pb	–	Chandramouli (1974) [45.23]
Cs	2.03	1.080 (104.3)	0.18	504–590 (0.91)	[52]	sc 4N5	^{137}Cs, implanted; lathe	No (linear in $\ln c - x^2$)		Cr in Pb	–	Chandramouli (1974) [45.23]
Cu	7.9×10^{-3}	0.348 (33.6)	950	497–591 (0.91)	8[51]	sc[61]	^{64}Cu, chemical deposition; microtome	2 examples (partly oxide hold-up)		Ag in Pb	45.02	Dyson (1966) [45.07]
Cu	(8×10^{-4})	(0.243) (23.4)		491–600 (0.91)	[52]	sc 6N	^{64}Cu, chemical deposition; microtome (20 μm sections)	1 example[84]	*Fit for $p = 0$ according to Decker [45.32]	Pressure dependence of D ($p = 0$–5.6 GPa)	–	Candland (1972) [45.24]
	8.6×10^{-3}*	0.354* (34.2)	920*									
Cu	–	–		592, 595	2	sc 6N	^{64}Cu, ^{67}Cu, chemical deposition; microtome	2 examples		$E = 0.23$; c_s(594 K) ≈ 13 ppma	45.02	Mundy (1974) [45.25]
Cu	–	0.343 (33.1)		508–575 (0.90)	4[51] *				*Pre-annealed samples used in Ref. [45.24] ($p = 0$)		45.02	Decker (1975) [45.26]

Cu	5.5×10^{-3}	0.331 (32.0)	910	(497–595)	(14)				Present fit to the data of [45.07, 45.25, 45.26]		45.02	
Hg	1.05	0.984 (95.0)	0.58	466–573 (0.86)	6	sc 6N	^{203}Hg, electroplated; lathe	No (dislocation tails at deep penetrations)		Pb in Pb; Hg, Pb in Pb(Hg)	45.03	Warburton (1973) [45.05]
Hg	1.50*	1.002* (96.7)	0.59	526–582 (0.92)	4[51]	sc 6N	^{203}Hg, electroplated; microtome	No	*Fit together with the data of [45.05]	$\Delta V/V_0 \approx 0.52$ ($p = 0$–3.8 GPa); Cd in Pb	45.03	Vanfleet (1977) [45.21]
In	(33) (17$^+$)	(1.162) (112.2) (1.136$^+$) (109.7)	 (0.50$^+$)	437–493 (0.77)	10 (4T)	sc 5N	In, 5 µm film deposited on the crystal; microtome, EPMA	1 example	$^+$Present approximation; the results of [45.27] and [45.28] at 516 K differ by a factor of 10		–	Kučera (1969) [45.27]
In	–	–		516	1*	pc 5N	^{114}In, electroplated; microtome	No	*$D = 1.3 \times 10^{-15}$ m^2 s^{-1}; see Ref. [45.27]	Pb in Pb(In)	–	Cheriet (1987) [45.28]
Ir	(2.1×10^{-3}) ($3.3 \times 10^{-3+}$)	(0.462) (44.6) (0.487$^+$) (47.0)	 (27$^+$)	419–574 (0.83) 514–574 (0.91)	8 (7T) 7 (6T)	sc 5N	^{192}Ir, dried-on from salt solution; microtome	Numerous examples[81]	Pronounced data scatter $^+$Present approximation		–	Zeiger (1982) [45.29]
Na	(6.3)	(1.127) (118.5)	(0.032)	522–586 (0.92)	10[51] (7T)	sc 6N	^{22}Na, pressure welding of ^{22}Na–Pb alloys with pure lead; microtome	1 example[81]	Pronounced data scatter		–	Owens (1972) [45.30]
Ni	9.4×10^{-3}	0.461 (44.5)	130	483–596 (0.90)	11[51]	sc 6N	^{63}Ni, electroplated; microtome	1 example		$\Delta V/V_0 \approx 0.13$ ($p = 0$–5.0 GPa)	45.05	Candland (1973) [45.31]
Ni	0.019*	0.495* (47.8)	135		(33)*				*Fit for $p = 0$ to the data of Ref. [45.31]		–	Decker (1975) [45.32]
Ni	0.011	0.47 (45.4)	125	485–554 (0.86)	5[51]	pc (0.2 mm) 5N	^{63}Ni, electroplated; microtome	1 example		Ag in Pb; Ag, Ni in Pb(Sn)	45.05	Hu (1982)[45.12]
Ni	–	–		433–556 (0.82)	5[51]	pc 5N	^{63}Ni, electroplated; microtome	No			45.05	Mei (1987) [45.33]
Pd	3.4×10^{-3}	0.367 (35.4)	280	482–585 (0.89)	10[51]	sc 6N	^{109}Pd, chemical deposition; microtome	1 example		$\Delta V/V_0 \approx 0.04$ ($p = 0$–4 GPa)	45.05	Decker (1975) [45.32]

Table 4.5 *(Continued)*

(1) X	(2a) D^0 ($10^{-4}\,m^2\,s^{-1}$)	(2b) Q (eV) and (kJ mole^{-1})	(3) $D(T_m)$ ($10^{-12}\,m^2\,s^{-1}$)	(4) T-range (K) ($\overline{T}/T_m$)	(5) No. of data points	(6) Material, purity	(7) Experimental method	(8) Remarks on the pp	(9) Further remarks	(10) Also studied	(11) Figure	(12) Reference
Pt	0.011	0.438 (42.3)	230	490–593 (0.90)	13[51] (11T)	sc 6N	Pt, chemical deposition; microtome	2 examples (partly erfc-solutions)	Pt content of each slice was determined by observing the variation of the melting curve	$c_s \approx 100$–400 ppma	45.06	Vanfleet (1980) [45.34]
Sb	(0.29) 38[+]	(0.963) (93.0) 1.20[+] (115.9)	0.33[+]	461–588 (0.87) 521–588 (0.92)	9 7	sc 6N	[124]Sb, dried-on from salt solution; microtome	2 examples	[+]Present fit to the upper temperature range		45.04	Nishikawa (1972) [45.35]
Sn	0.41	1.03 (99.4)	0.094	517–599 (0.93)	13[51] (12T)	sc 6N	[113]Sn, electroplated; microtome	No		$\Delta V/V_0 \approx 0.52$ ($p = 0$–2.9 GPa)	45.04	Decker (1977) [45.36]
Tl	(0.511) 0.53[+]	1.055 (101.9)	0.075[+]	480–595 (0.89)	6	pc 4N	[204]Tl, vapour deposition; microtome	No	[+]Present approximation	Pb, Bi in Pb; Pb, Bi, Tl in Pb(Tl)	45.03	Resing (1961) [45.02]
Zn	0.016	0.490 (47.3)	125	455–572 (0.85)	7[51]	sc 6N	[65]Zn, electroplated; microtome	2 examples[81,85]		$\Delta V/V_0 \approx 0.21$ ($p = 0$–4.7 GPa)	45.06	Ross (1974) [45.37], [45.38]

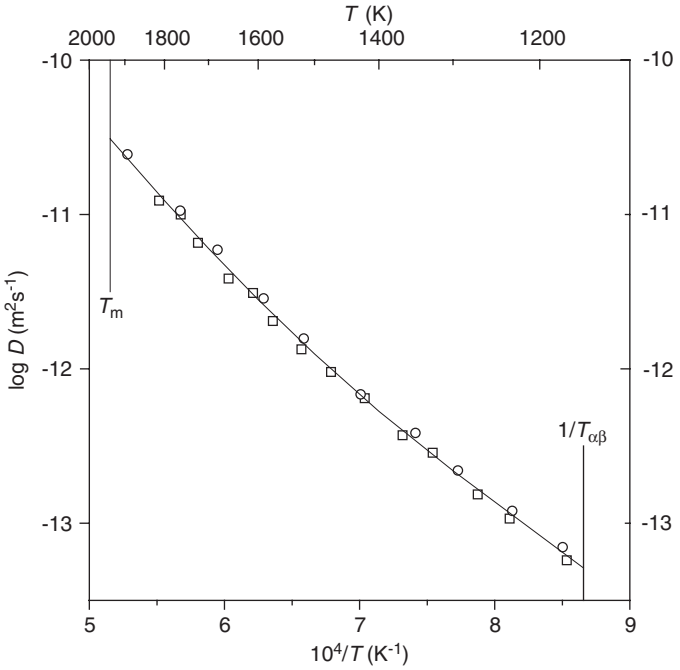

Fig. 41.01 Self-diffusion in β-titanium. □, Murdock [41.01]; ○, Köhler [41.02]. Fitting line: Ω-fit according to [41.02].

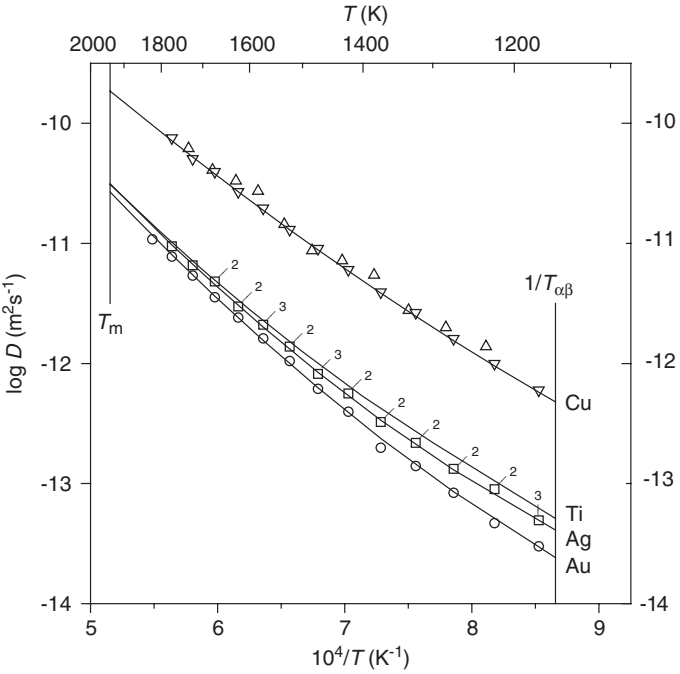

Fig. 41.02 Impurity diffusion in β-titanium. Ag in Ti: □, Lee [41.07]; Au in Ti: ○, Lee [41.12]; Cu in Ti: Δ, Caloni [41.25]; ∇, Lee [41.07]. Fitting line: Ω-fit according to [41.07].

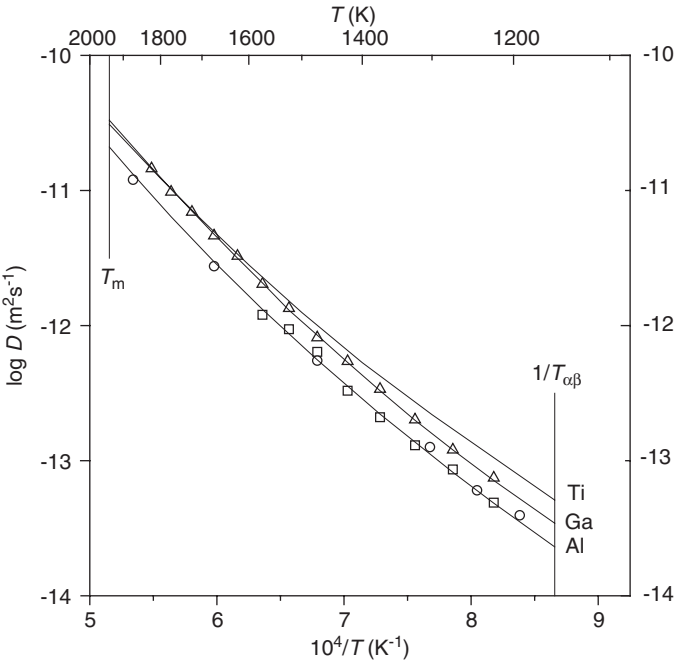

Fig. 41.03 Impurity diffusion in β-titanium. Al in Ti: □, Araki [41.10]; ○, Köppers [41.11]. Fitting line: α-fit with $D^0 = 0.114 \times 10^{-4}\,m^2\,s^{-1}$, $Q = 2.207\,eV$, $T_0 = T_m$ and $\alpha = 6.7$. Ga in Ti: Δ, Lee [41.27].

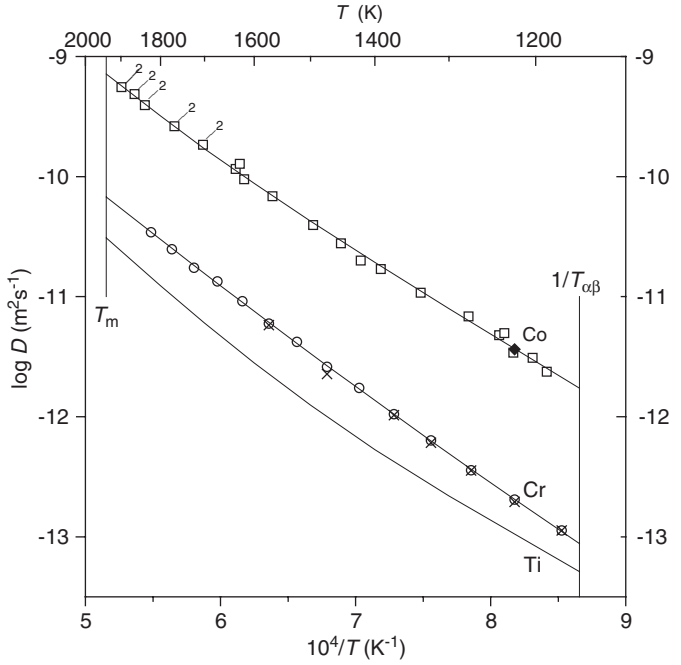

Fig. 41.04 Impurity diffusion in β-titanium. Co in Ti: □, Gibbs [41.17]; ♦, Araki [41.18]; Cr in Ti: ○, Lee [41.22]; x, Araki [41.23]. Fitting line: Ω-fit according to [41.22].

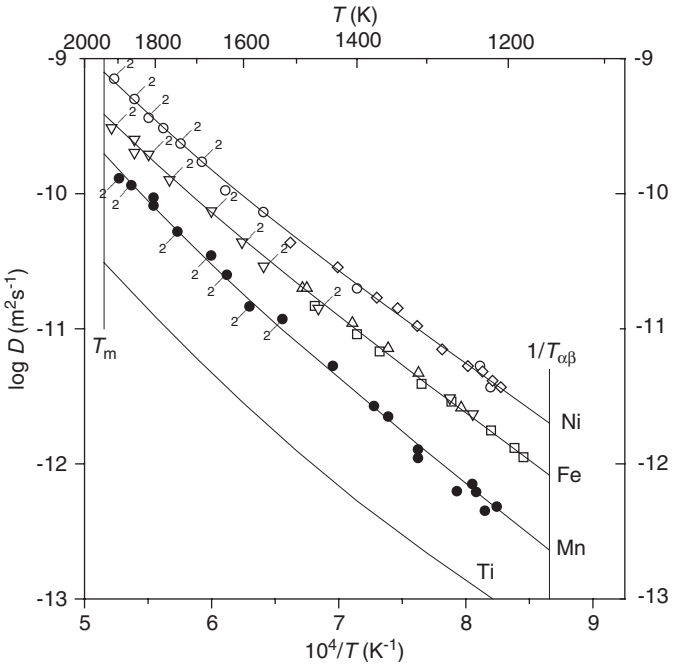

Fig. 41.05 Impurity diffusion in β-titanium. Fe in Ti: ^{55}Fe: □, Peart [41.16]; Δ, Gibbs [41.17]; ^{59}Fe: ∇, Gibbs [41.17]. Fitting line according to [41.17]. Mn in Ti: ●, Gibbs [41.17]; Ni in Ti: ◇, Peart [41.16]; ○, Gibbs [41.17]. Fitting line: present approximation.

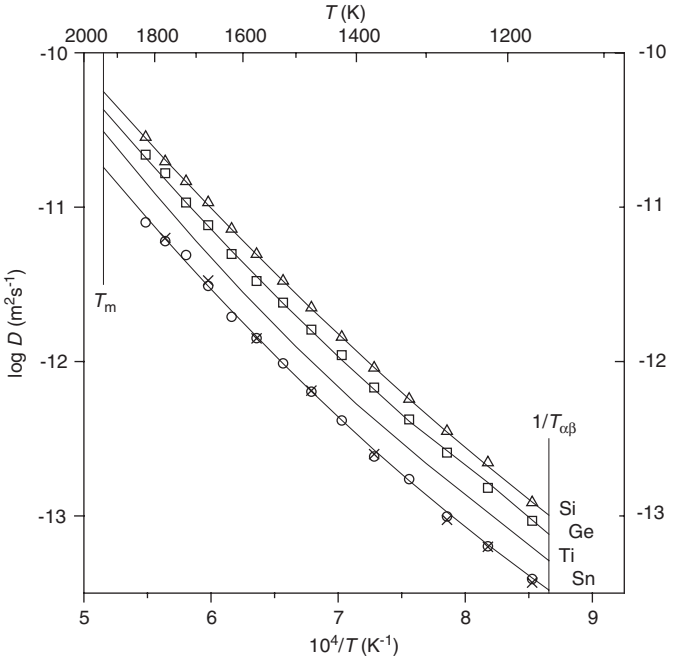

Fig. 41.06 Impurity diffusion in β-titanium. Ge in Ti: □, Iijima [41.31]; Si in Ti: Δ, Iijima [41.31]; Sn in Ti: ○, Iijima [41.31]; x, Araki [41.47]. Fitting line according to [41.31].

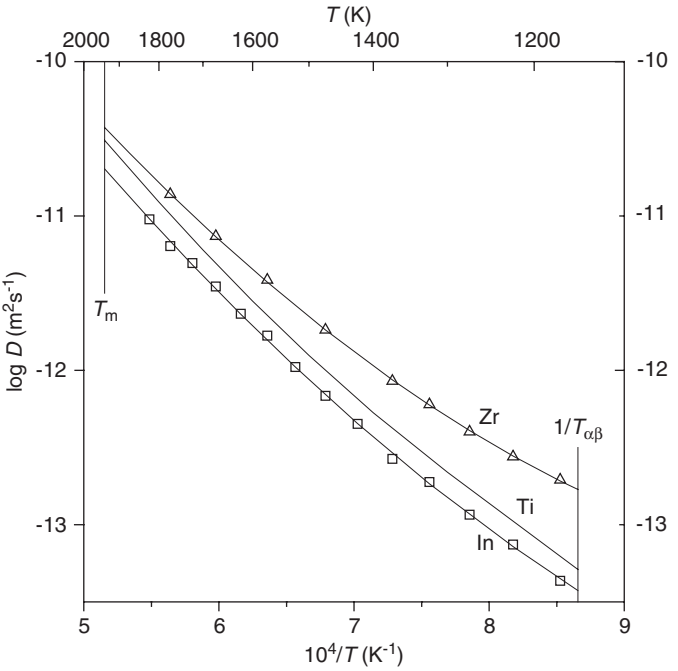

Fig. 41.07 Impurity diffusion in β-titanium. In in Ti: □, Lee [41.27]; Zr in Ti: Δ, Araki [41.57].

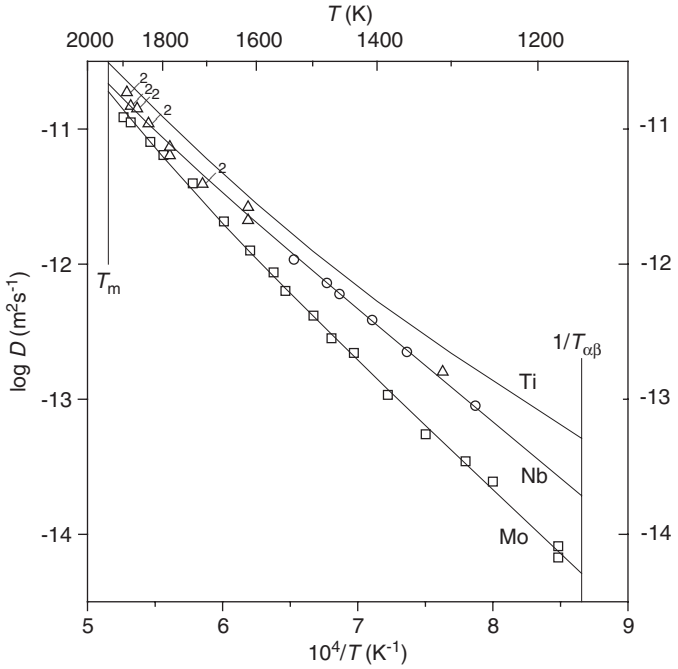

Fig. 41.08 Impurity diffusion in β-titanium. Mo in Ti: □, Gibbs [41.17]; Nb in Ti: ○, Peart [41.16]; Δ, Gibbs [41.17]. Fitting line: present fit.

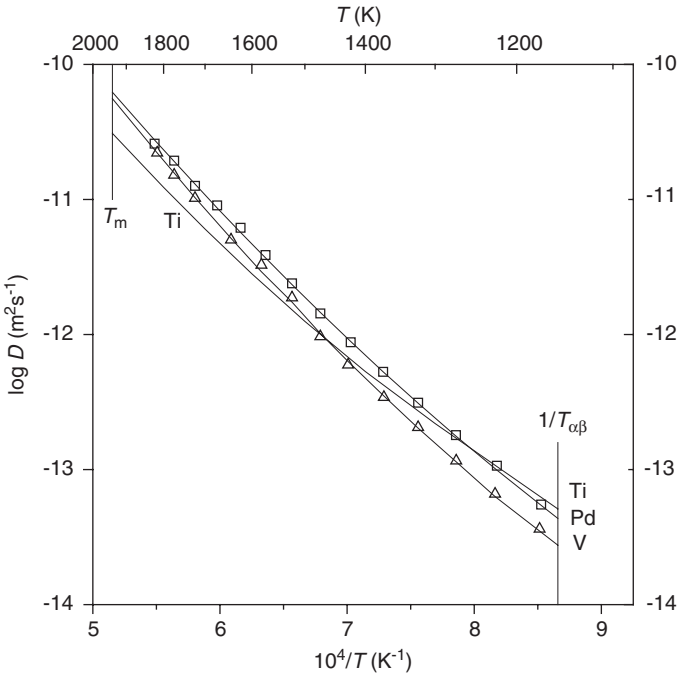

Fig. 41.09 Impurity diffusion in β-titanium. Pd in Ti: □, Lee [41.22]; V in Ti: ○, Murdock [41.01]. Fitting line: Ω-fit according to Neumann [41.55].

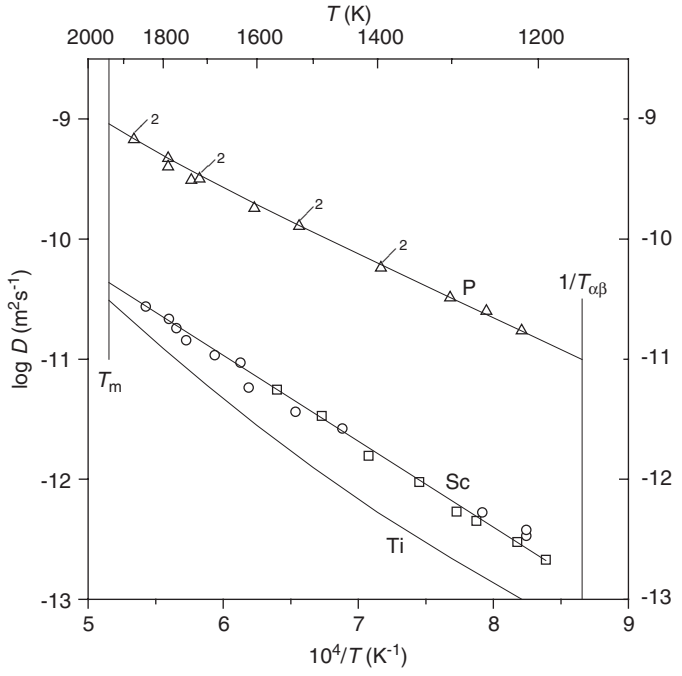

Fig. 41.10 Impurity diffusion in β-titanium. P in Ti: Δ, Askill [41.39]; Sc in Ti: □, Askill [41.39]; ○, Askill [41.06]. Fitting line according to [41.39].

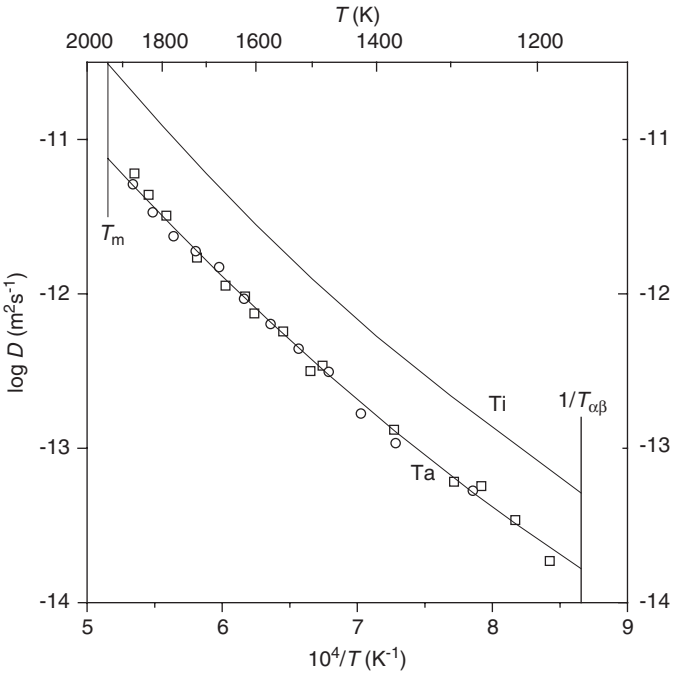

Fig. 41.11 Impurity diffusion in β-titanium. Ta in Ti: □, Askill [41.49]; ○, Ansel [41.50]. Fitting line: Ω-fit according to [41.50].

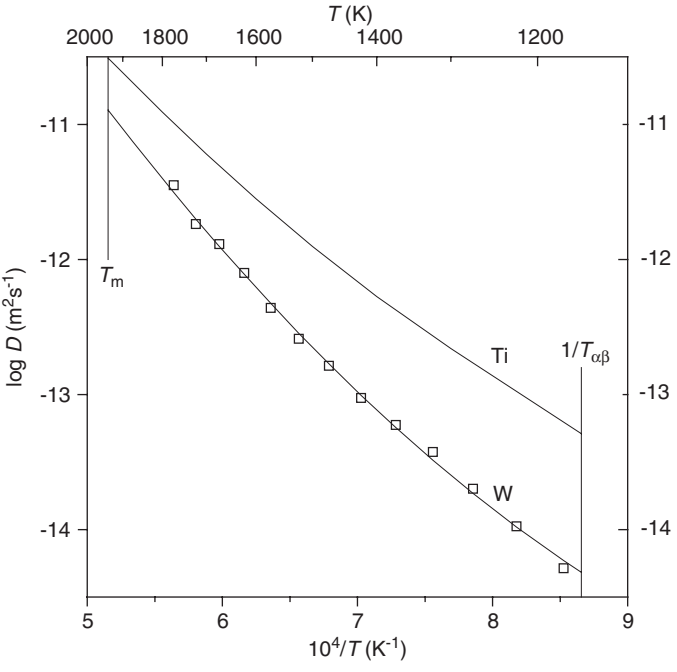

Fig. 41.12 Impurity diffusion in β-titanium. W in Ti: □, Minamino [41.56].

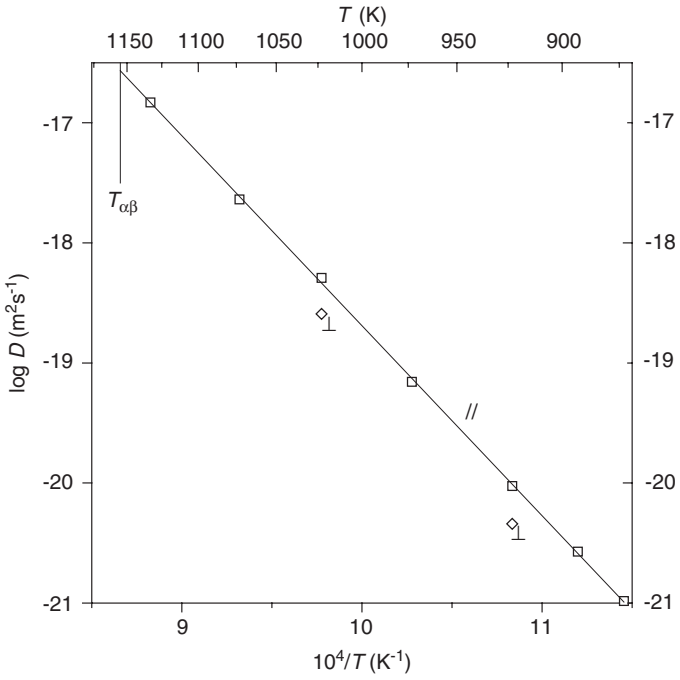

Fig. 41.13 Self-diffusion in α-titanium. □ and ◇, Köppers [41.05].

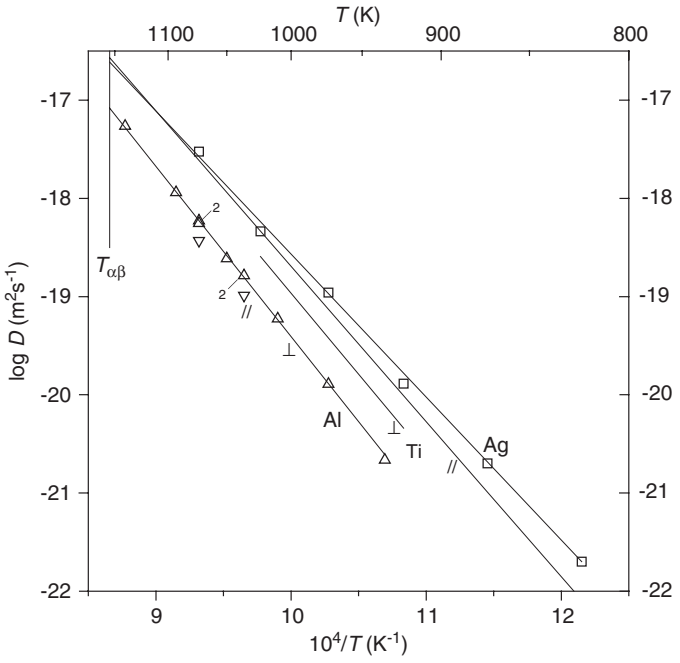

Fig. 41.14 Impurity diffusion in α-titanium. Ag in Ti: □, Araujo [41.09]; Al in Ti: Δ and ∇, Köppers [41.05].

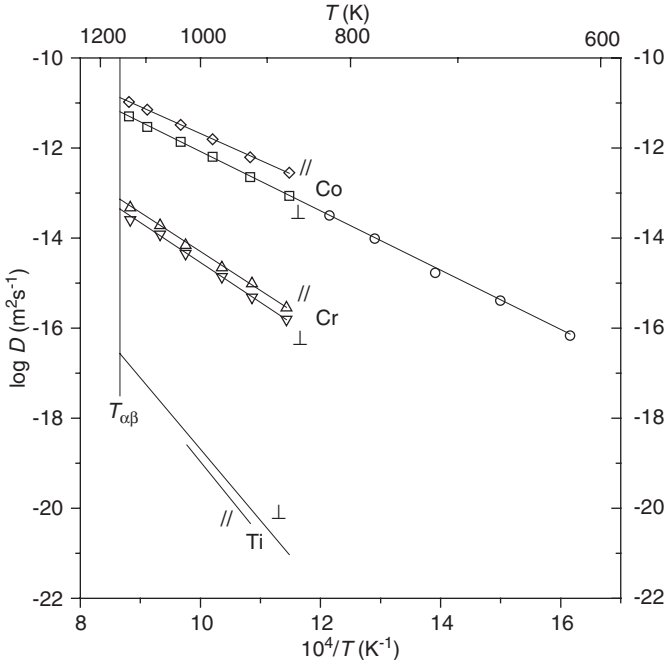

Fig. 41.15 Impurity diffusion in α-titanium. Co in Ti: □ and ◇, Nakajima [41.19]; ○, Perez [41.20]. Fitting line according to [41.19]. Cr in Ti: Δ and ∇, Nakajima [41.24].

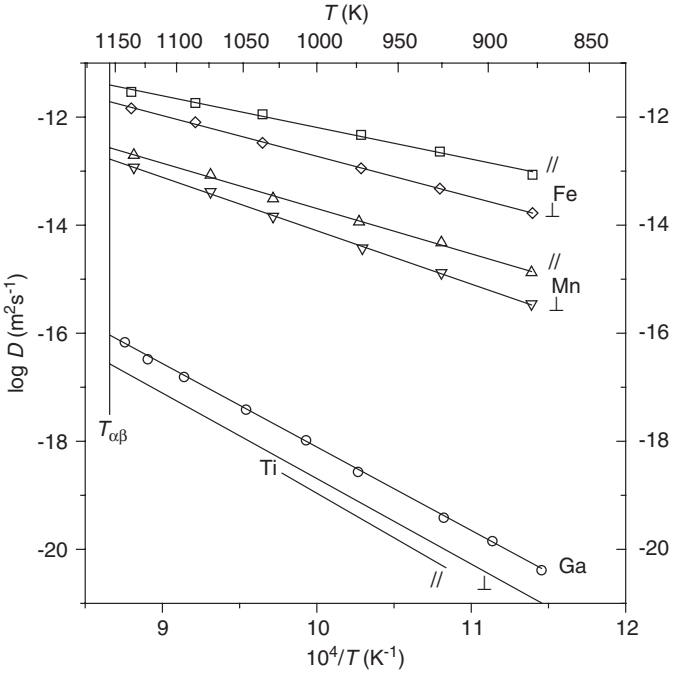

Fig. 41.16 Impurity diffusion in α-titanium. Fe in Ti: □ and ◇, Nakajima [41.26]; Mn in Ti: Δ and ∇, Nakamura [41.36]; Ga in Ti: ○, Köppers [41.28], [41.29].

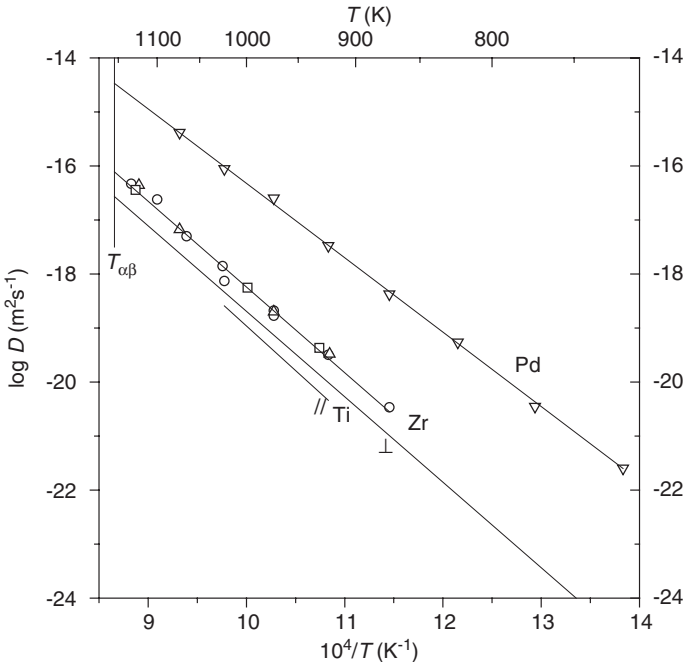

Fig. 41.17 Impurity diffusion in α-titanium. Pd in Ti: ∇, Behar [41.43]; Zr in Ti: ○, Perez [41.58]; □, Δ, Perez [41.59]. Fitting line according to [41.58].

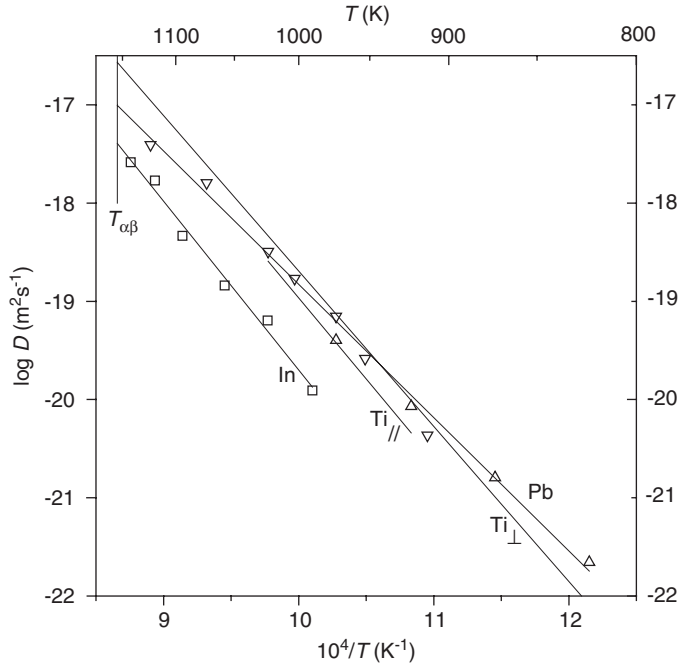

Fig. 41.18 Impurity diffusion in α-titanium. In in Ti: □, Köppers [41.28]; Pb in Ti: Δ, Mirassou [41.41]; ∇, Mirassou [41.42]. Fitting line according to [41.42].

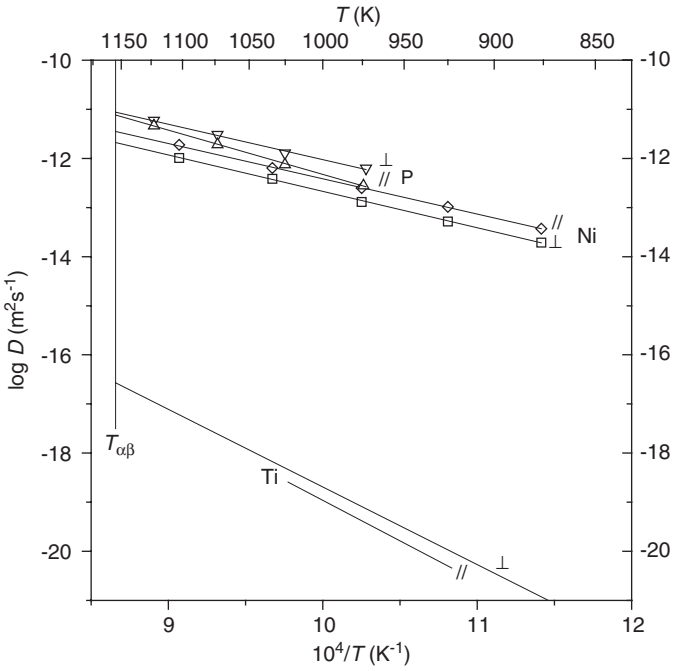

Fig. 41.19 Impurity diffusion in α-titanium. Ni in Ti: □ and ◇, Nakajima [41.38]; P in Ti: Δ and ∇, Nakajima [41.40].

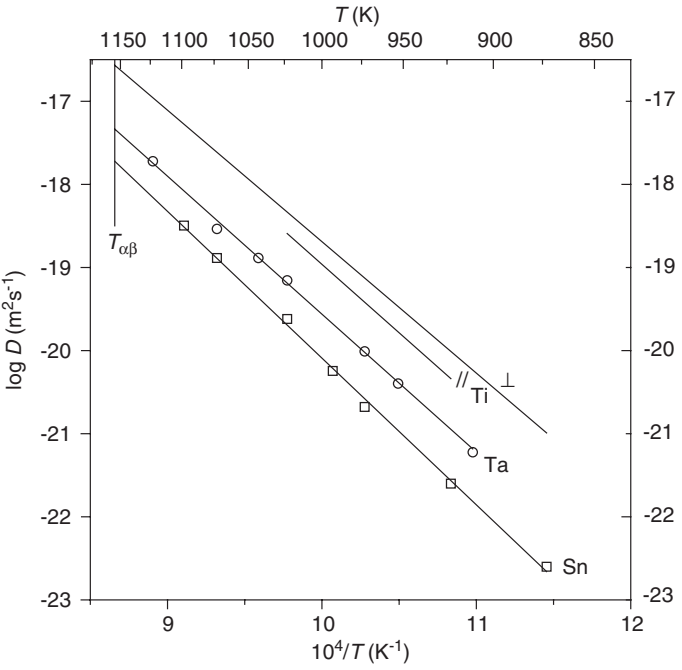

Fig. 41.20 Impurity diffusion in α-titanium. Sn in Ti: □, Perez [41.48]; Ta in Ti: ○, Perez [41.51].

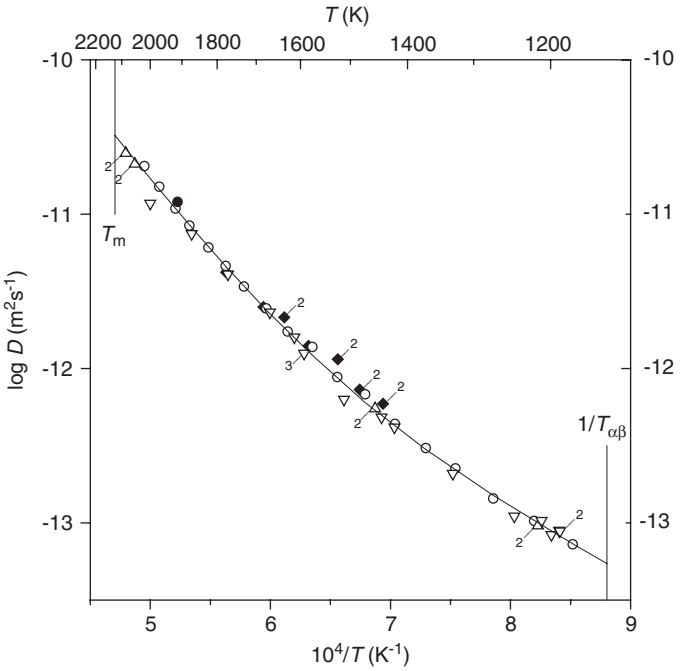

Fig. 42.01 Self-diffusion in β-zirconium. ♦, Kidson [42.01]; ○, Federer [42.02]; Δ, Graham [42.04]; ∇, Herzig [42.05]; ●, Manke [42.15]. Fitting line: two-exponential fit according to Neumann [42.07].

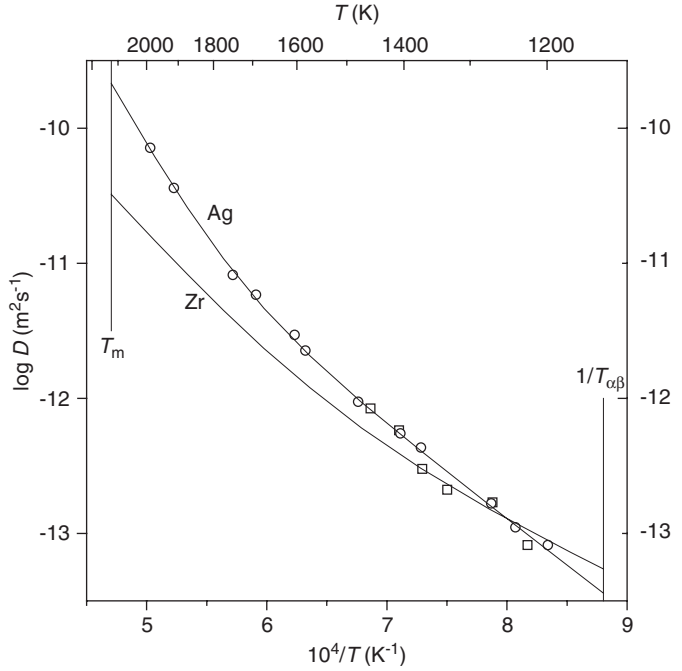

Fig. 42.02 Impurity diffusion in β-zirconium. Ag in Zr: □, Tendler [42.14]; ○, Manke [42.15]. Fitting line: two-exponential fit according to Neumann [42.16].

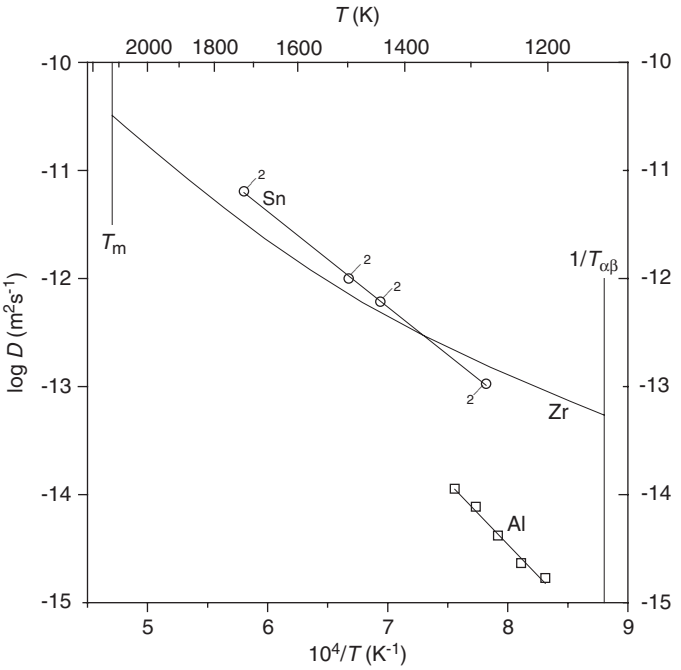

Fig. 42.03 Impurity diffusion in β-zirconium. Al in Zr: □, Laik [42.21]; Sn in Zr: ○ Chelluri [42.54].

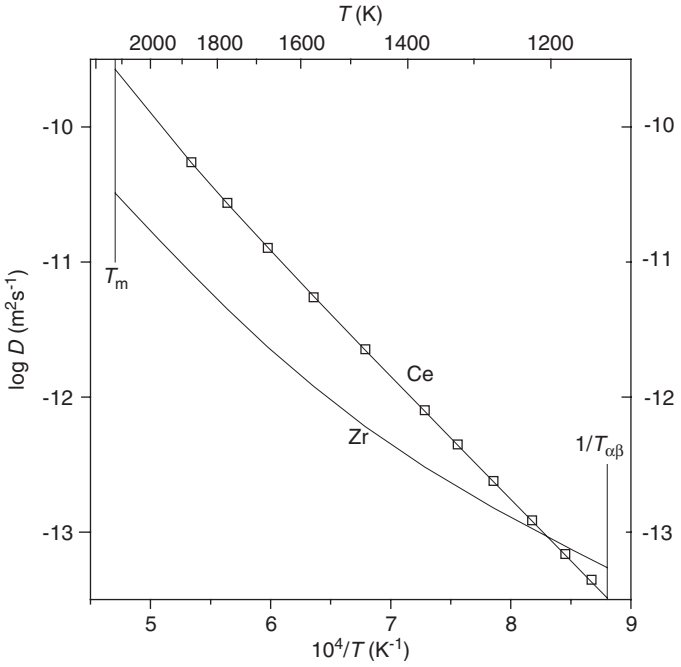

Fig. 42.04 Impurity diffusion in β-zirconium. Ce in Zr: □, Paul [42.25].

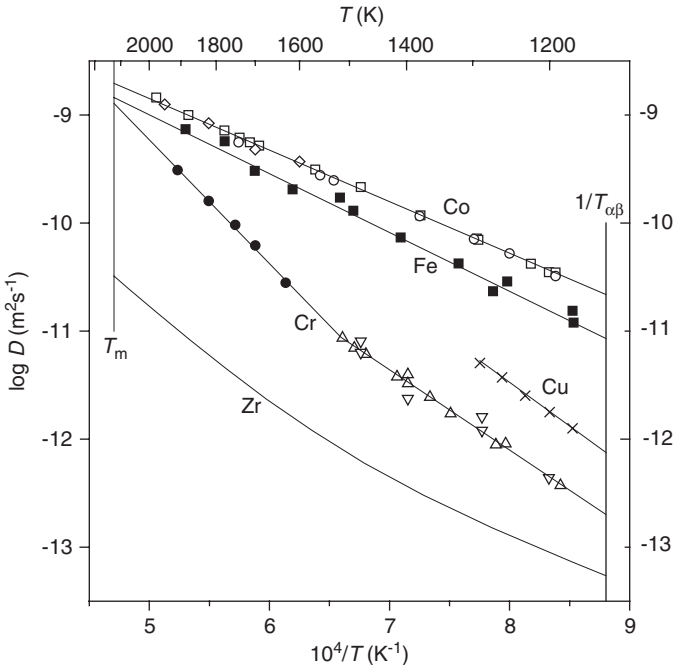

Fig. 42.05 Impurity diffusion in β-zirconium. Co in Zr: □, Kidson [42.26]; ○, Herzig [42.27]; ◇, Zee [42.28]. Fitting line according to [42.26]. Cr in Zr: Δ, Nicolai [42.31]; ∇, Patil [42.32]; ●, Zee [42.28]. Fitting line: two linear branches above and below 1,516 K according to [42.28] and [42.31]. Cu in Zr: x, Iijima [42.17]; Fe in Zr: ■, Trampenau [42.37].

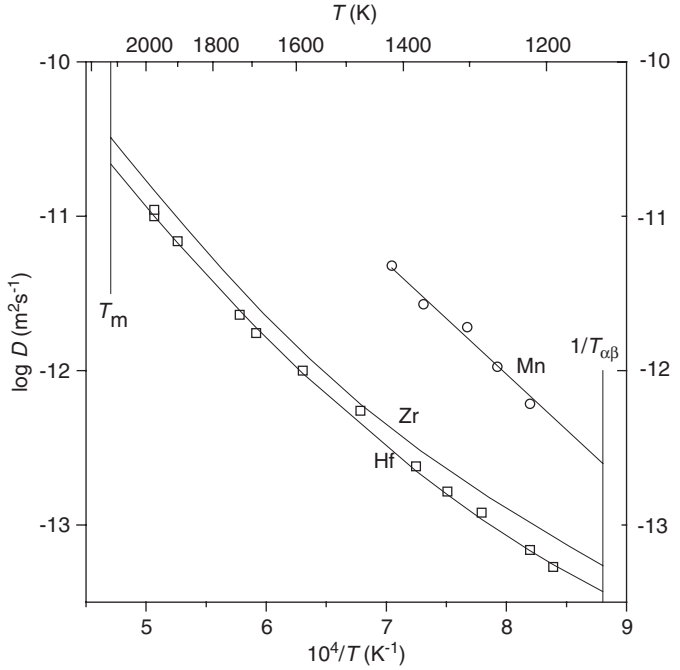

Fig. 42.06 Impurity diffusion in β-zirconium. Hf in Zr: □, Herzig [42.41]. Fitting line: Ω-fit according to Neumann [42.16]. Mn in Zr: ○, Tendler [42.43].

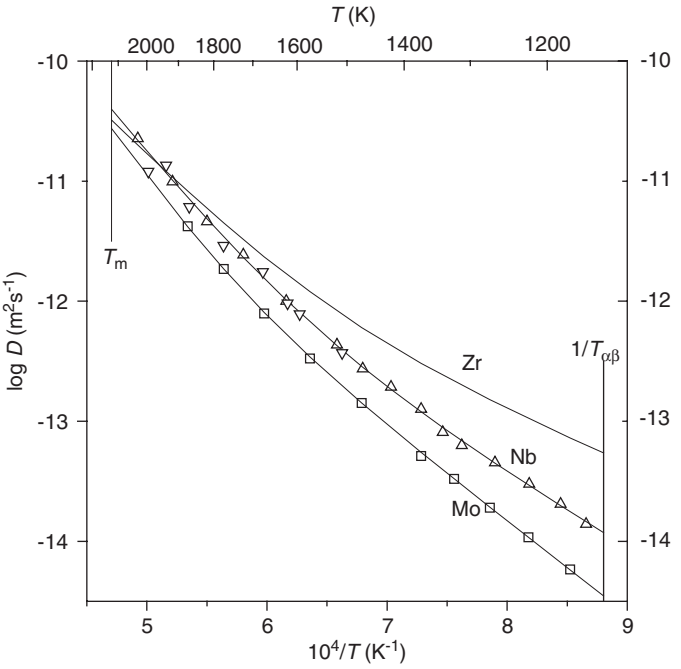

Fig. 42.07 Impurity diffusion in β-zirconium. Mo in Zr: □, Paul [42.25]; Nb in Zr: Δ, Federer [42.02]; ∇, Herzig [42.44]. Fitting line: two-exponential fit according to Neumann [42.16].

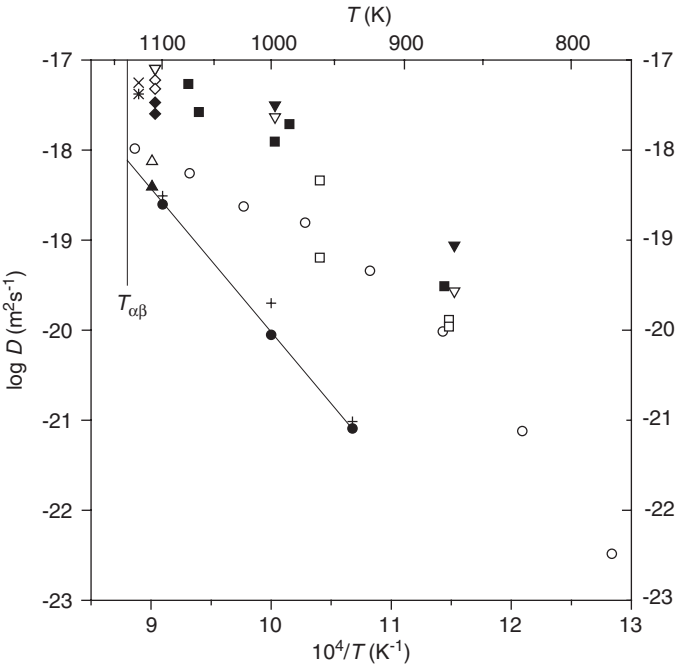

Fig. 42.08 Self-diffusion in α-zirconium in dependence of the Fe content. ○, Horvath [42.10], 2 ppma Fe. $D_{//}$ and $D_{\perp}$: □ and ■, Lübbehusen [42.11] (100–200 ppma Fe); x and $*$, Hood [42.09] (Fe content not specified); ♦ and ◇, ▼ and ∇, Hood [42.12] (47 and 57 ppma Fe, respectively); ▲ and Δ, Hood [42.12] ($<$ 1 ppma); ● and +, Hood [42.13] ($<$ 1 ppma). Fitting line for $D_{//}$ according to [42.13]. (See introduction page.)

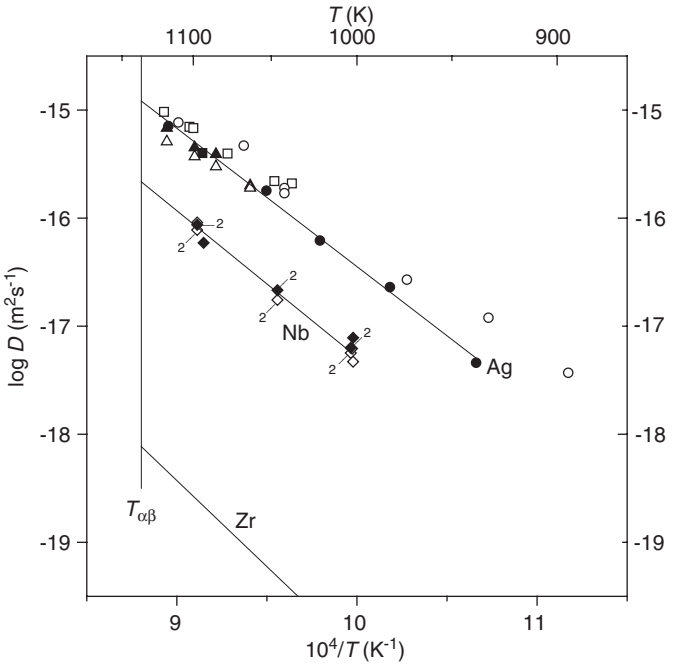

Fig. 42.09 Impurity diffusion in α-zirconium. Ag in Zr single crystals: ■, Hood [42.18] (280 ppma Fe); ●, Vieregge [42.20] (107 ppma Fe); ▲ and Δ, Tobar [42.19] (20 ppma Fe) (// and ⊥ to the *c*-axis); Ag in Zr polycrystals: □, Tendler [42.14] (900 ppma Fe); ○, Vieregge [42.20] (20 and 192 ppma Fe). Fitting line for single crystals according to [42.20]; Nb in Zr: ◇ and ◆, Hood [42.45].

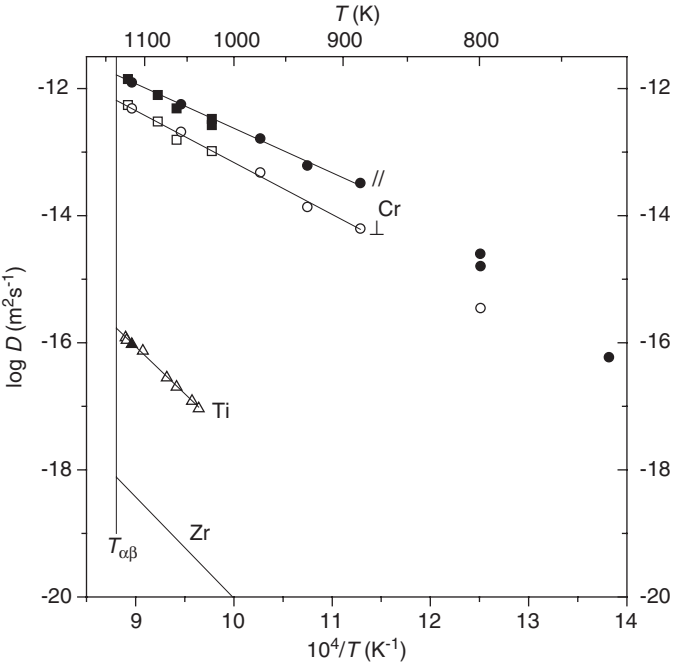

Fig. 42.10 Impurity diffusion in α-zirconium. Cr in Zr: □ and ■, Balart [42.34]; ○ and ●, Hood [42.35]. Fitting line according to [42.35]. Ti in Zr: Δ, Hood [42.57]; ▲, Hood [42.09].

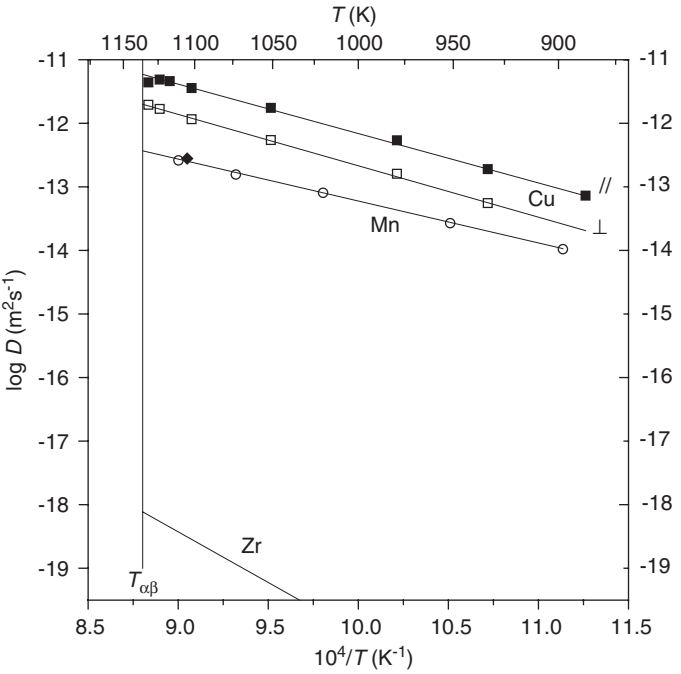

Fig. 42.11 Impurity diffusion in α–zirconium. Cu in Zr: □ and ■, Hood [42.36]; Mn in Zr: ○, Tendler [42.43]; ♦, Hood [42.09]. Fitting line according to [42.43].

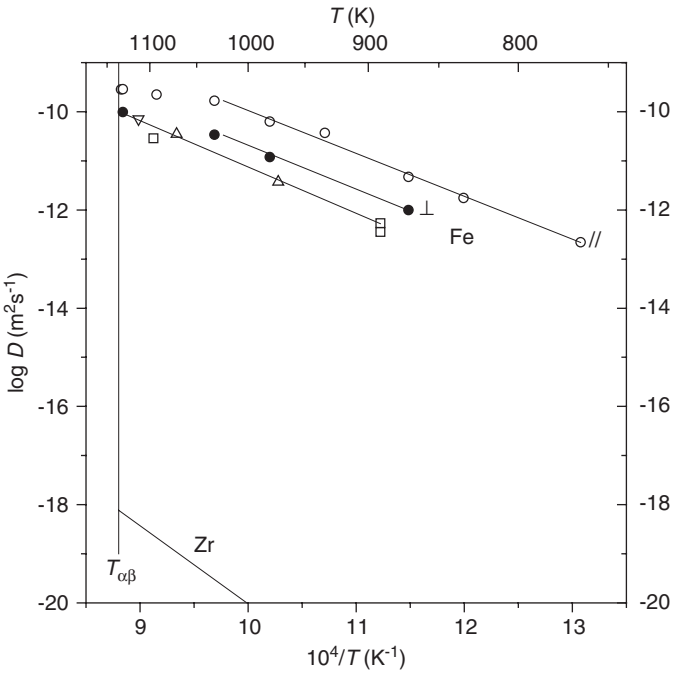

Fig. 42.12 Impurity diffusion in α-zirconium. Fe in Zr: Δ, Hood [42.38] (pc); ∇, Hood [42.09] (sc); □, Tendler [42.39] (pc); ● and ○, Nakajima [42.40]. Tentative fitting line using $D^0 = 0.02\,m^2\,s^{-1}$, $Q = 1.87\,eV$ (pc).

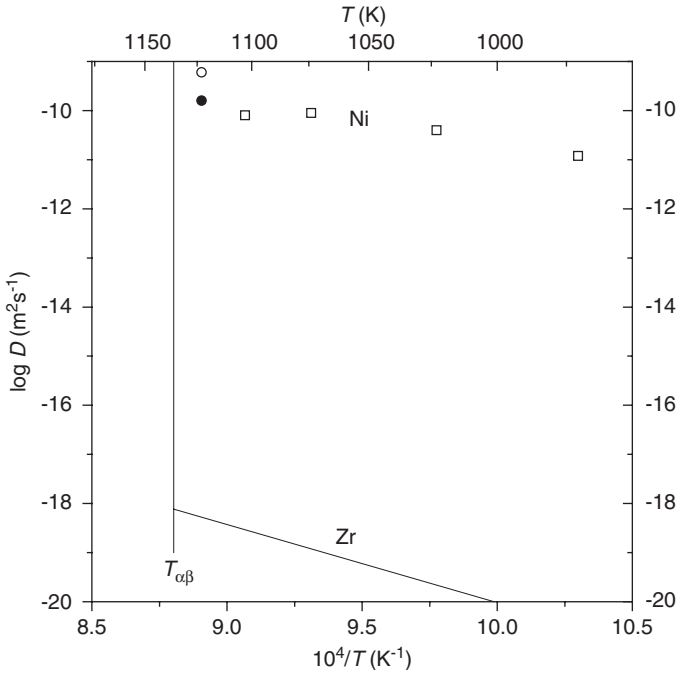

Fig. 42.13 Impurity diffusion in α–zirconium. Ni in Zr: □, Hood [42.38]; ○ and ●, Hood [42.46].

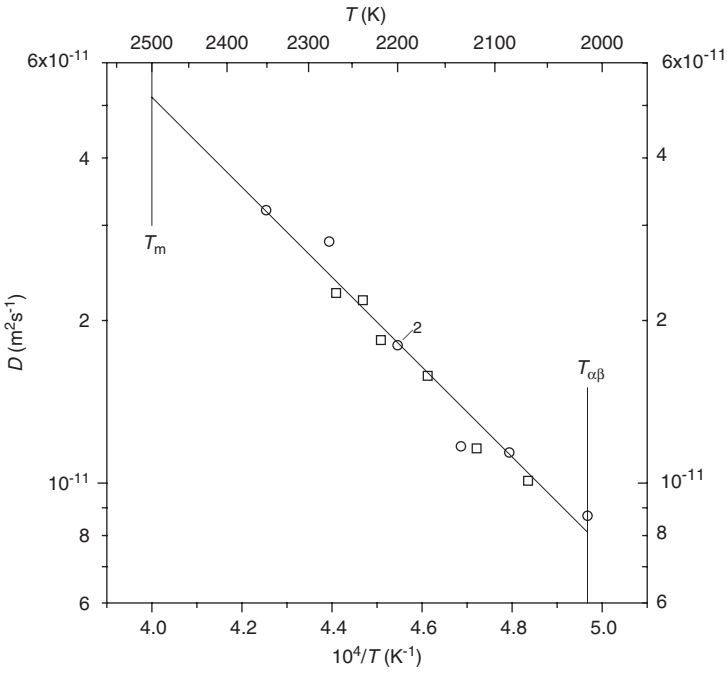

Fig. 43.01 Self-diffusion in β-hafnium. □, Winslow [43.01]; ○, Herzig [43.02]. Fitting line according to [43.02].

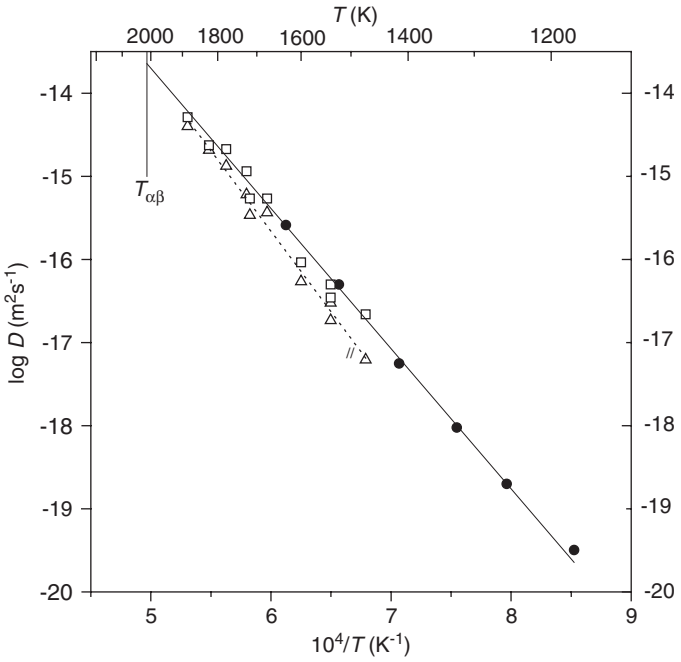

Fig. 43.02 Self-diffusion in α–hafnium. ●, Herzig [43.04]; Δ (parallel) and □ (perpendicular), Davis [43.03]. Fitting lines: solid line for D_{pc} according to [43.04] and dotted line for $D_{//}$ according to [43.03].

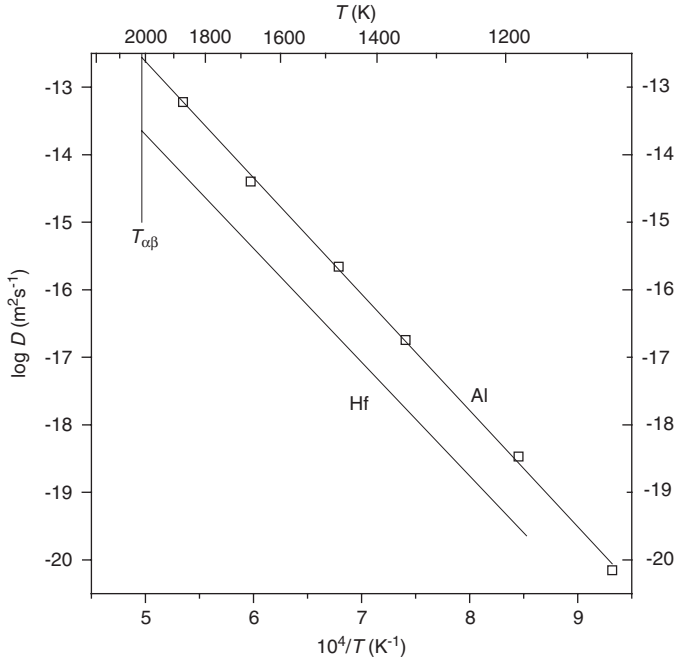

Fig. 43.03 Impurity diffusion in α-hafnium. Al in α-Hf: □, Herzig [43.04].

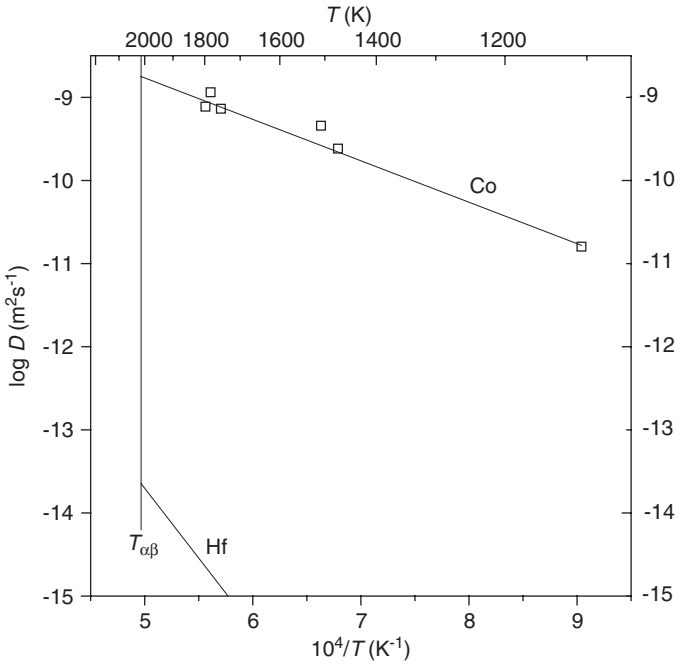

Fig. 43.04 Impurity diffusion in α-hafnium. Co in α-Hf: □, Dyment [43.06].

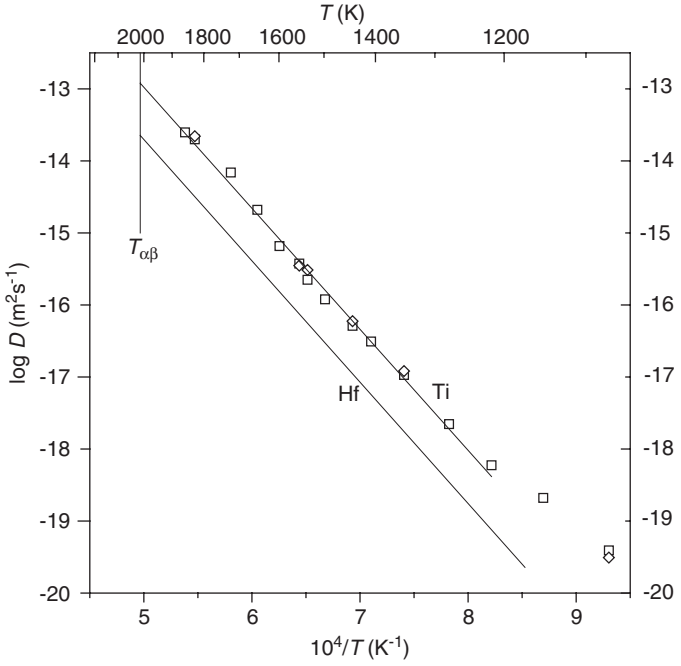

Fig. 43.05 Impurity diffusion in α-hafnium. Ti in α-Hf: □ (perpendicular) and ◇ (parallel), Köppers [43.07].

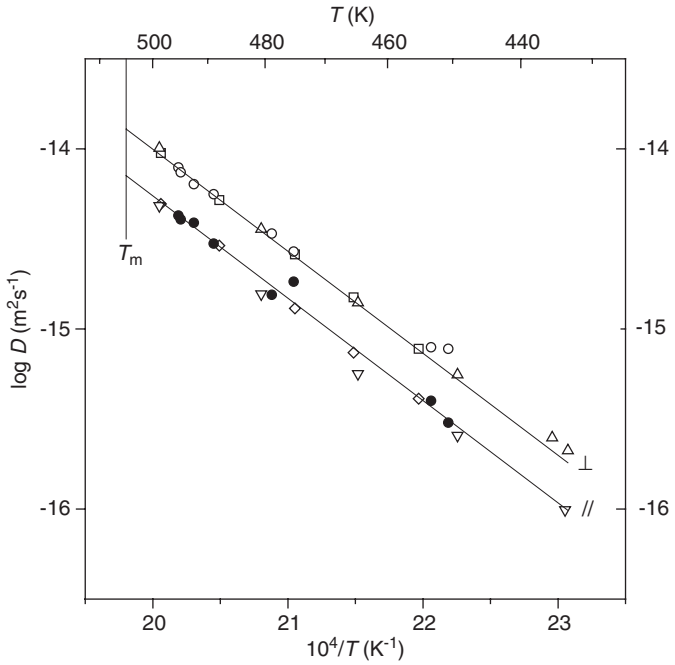

Fig. 44.01 Self-diffusion in tin. ○ and ●, Meakin [44.01]; Δ and ∇, Coston [44.02]; □ and ◇ Huang [44.03]. Fitting lines according to [44.03].

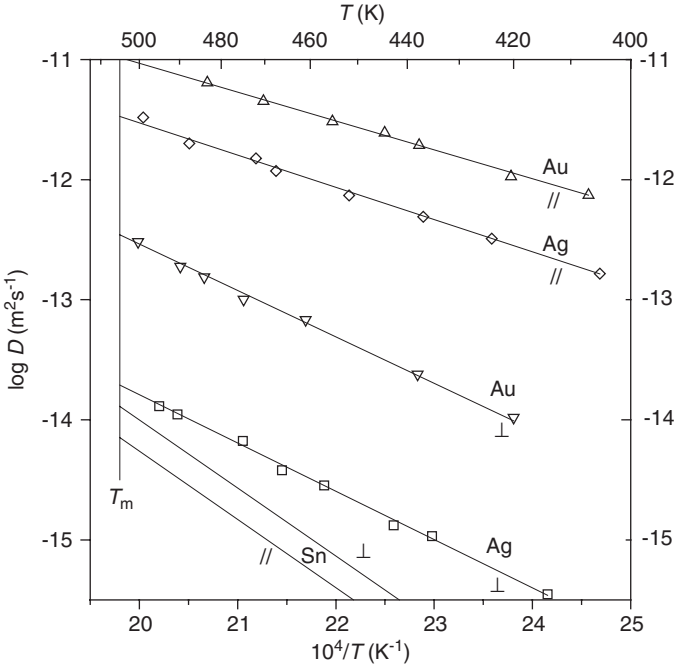

Fig. 44.02 Impurity diffusion in tin. Ag in Sn: □ and ◇, Dyson [44.04]; Au in Sn: Δ and ∇, Dyson [44.04].

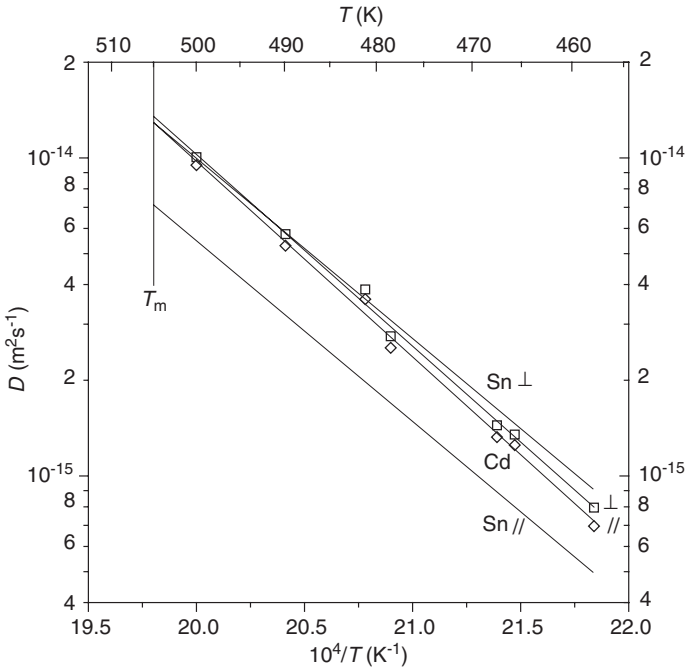

Fig. 44.03 Impurity diffusion in tin. Cd in Sn: □ and ◇, Huang [44.03].

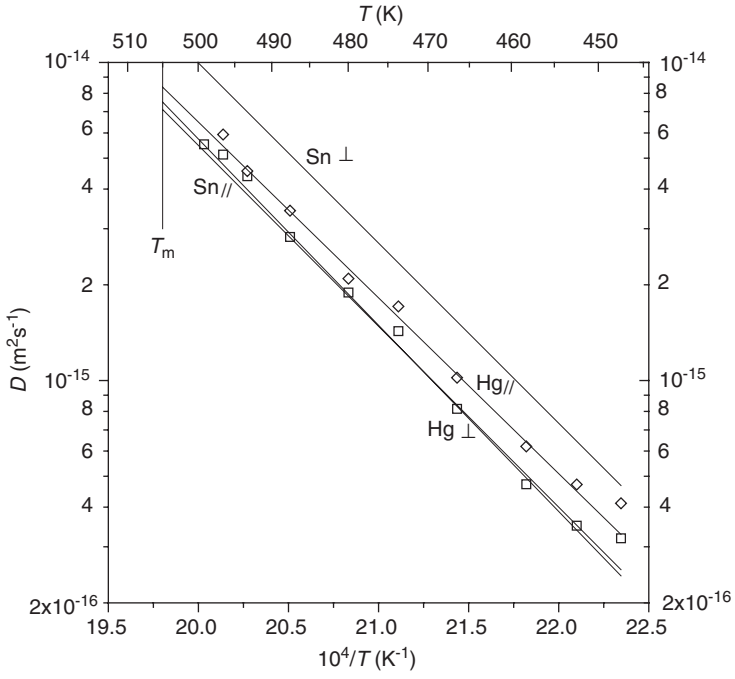

Fig. 44.04 Impurity diffusion in tin. Hg in Sn: □ and ◇, Warburton [44.08].

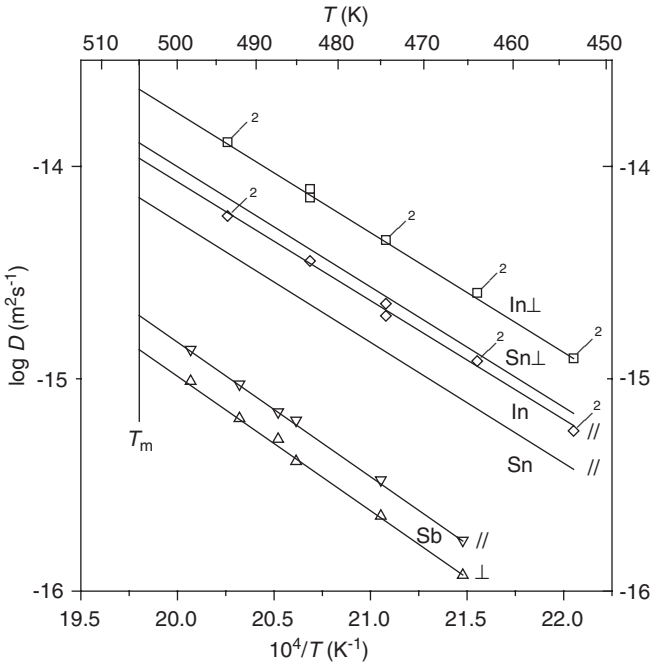

Fig. 44.05 Impurity diffusion in tin. In in Sn: □ and ◇, Sawatzky [44.09]; Sb in Sn: Δ and ∇, Huang [44.11, 44.03].

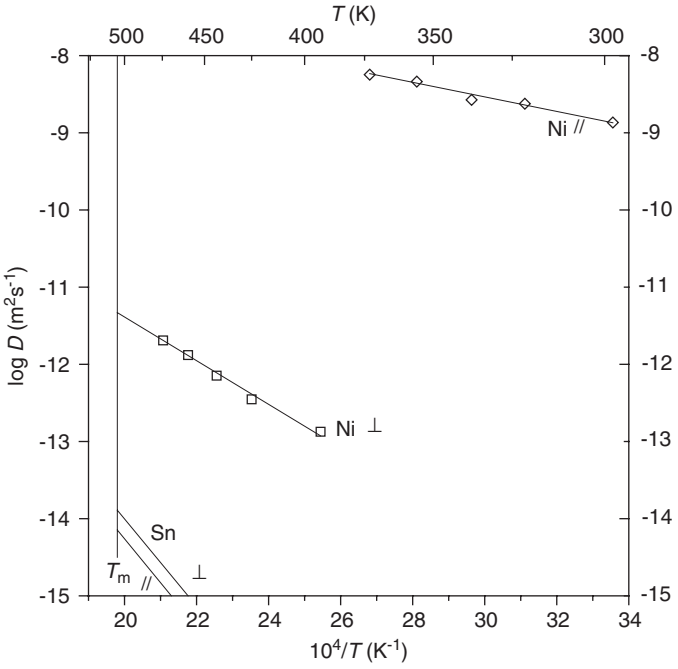

Fig. 44.06 Impurity diffusion in tin. Ni in Sn: □ and ◇, Yeh [44.10].

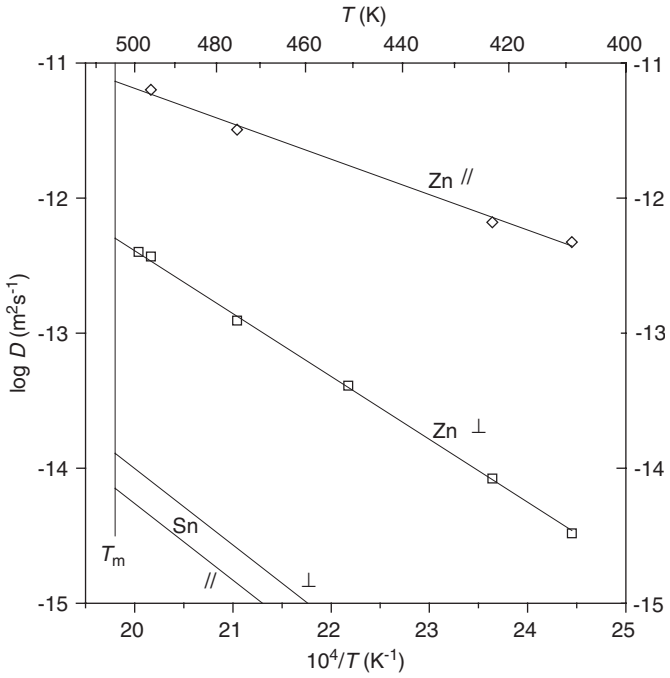

Fig. 44.07 Impurity diffusion in tin. Zn in Sn: □ and ◇, Huang [44.03].

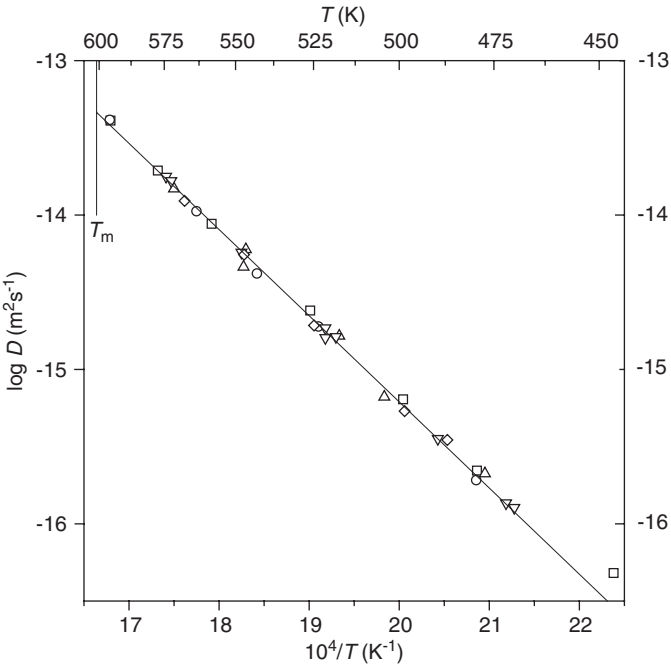

Fig. 45.01 Self-diffusion in lead. □, Nachtrieb [45.01]; ○, Resing [45.02]; Δ, Hudson [45.03]; ∇, Miller [45.04]; ◇, Warburton [45.05]. Fitting line according to [45.04].

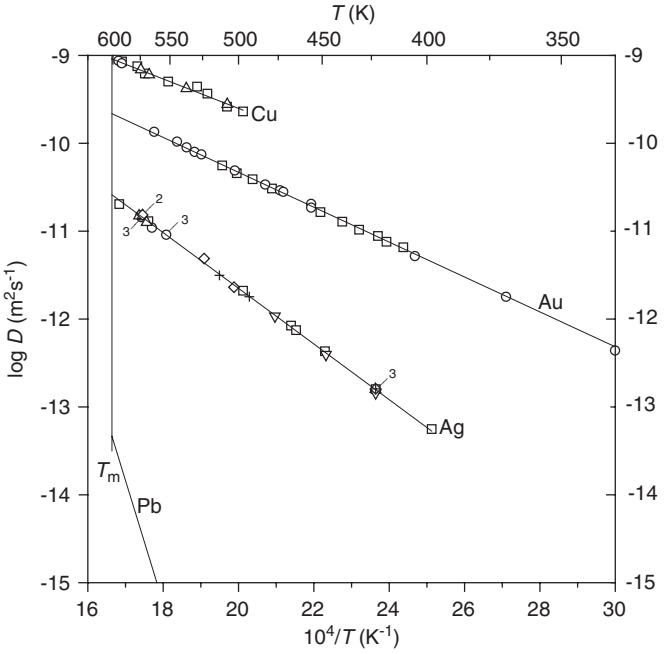

Fig. 45.02 Impurity diffusion in lead. Ag in Pb: □, Dyson [45.07]; ○, Herzig [45.08]; Δ, Miller [45.09]; ∇, Cohen [45.11]; ◇, Hu [45.12]; +, Shi [45.13]. Fitting line using $D^0 = 4.8 \times 10^{-6}\,m^2\,s^{-1}$, $Q = 0.628\,eV$. Au in Pb: □, Warburton [45.19]; ○, Decker [45.20]. Fitting line using $D^0 = 4.4 \times 10^{-7}\,m^2\,s^{-1}$, $Q = 0.394\,eV$; Cu in Pb: □, Dyson [45.07]; ○, Mundy [45.25]; Δ, Decker [45.26]. Fitting line: present approximation using $D^0 = 5.5 \times 10^{-7}\,m^2\,s^{-1}$, $Q = 0.331\,eV$.

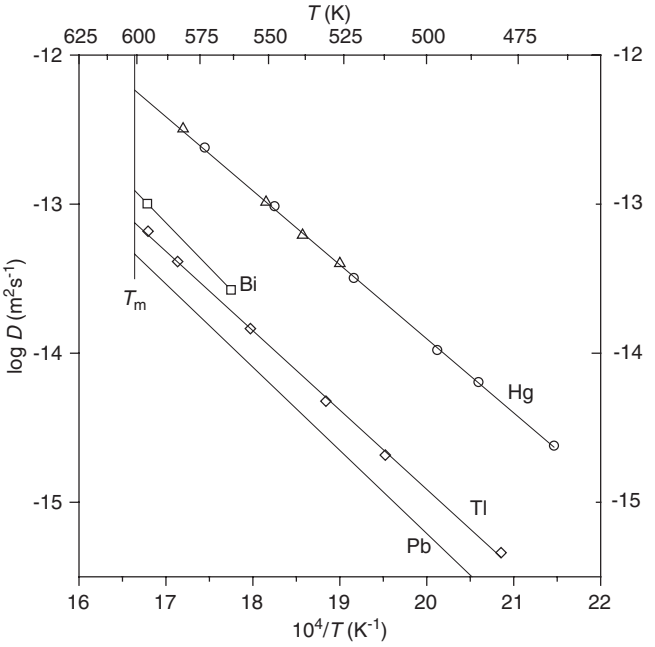

Fig. 45.03 Impurity diffusion in lead. Bi in Pb: □, Resing [45.02]; Hg in Pb: ○, Warburton [45.05]; Δ, Vanfleet [45.21]. Fitting line according to [45.05]. Tl in Pb: ◇, Resing [45.02].

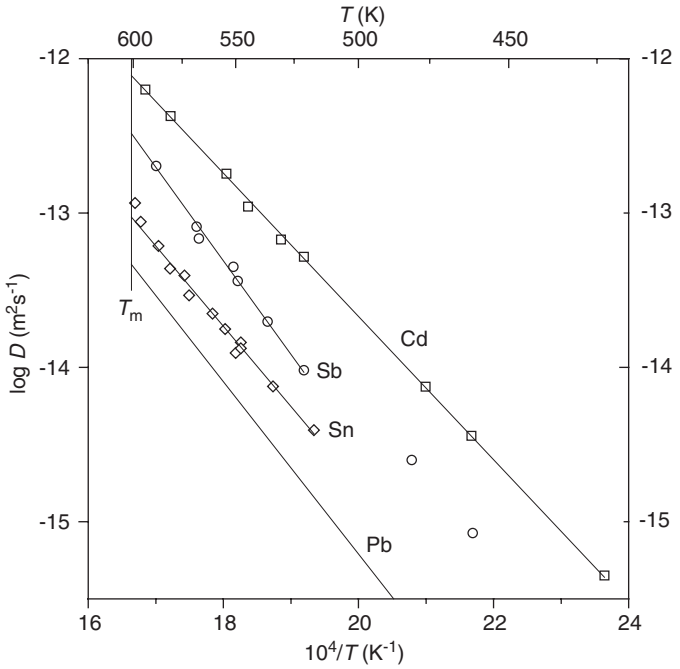

Fig. 45.04 Impurity diffusion in lead. Cd in Pb: □, Miller [45.04]; Sb in Pb: ○, Nishikawa [45.35]; Sn in Pb: ◇, Decker [45.36].

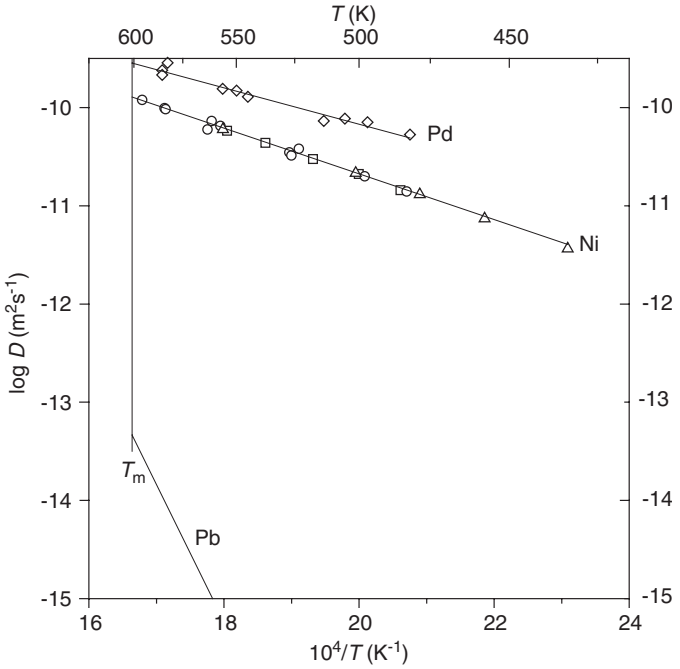

Fig. 45.05 Impurity diffusion in lead. Ni in Pb: □, Hu [45.12]; ○, Candland [45.31]; Δ, Mei [45.33]. Fitting line according to [45.31]. Pd in Pb: ◇, Decker [45.32].

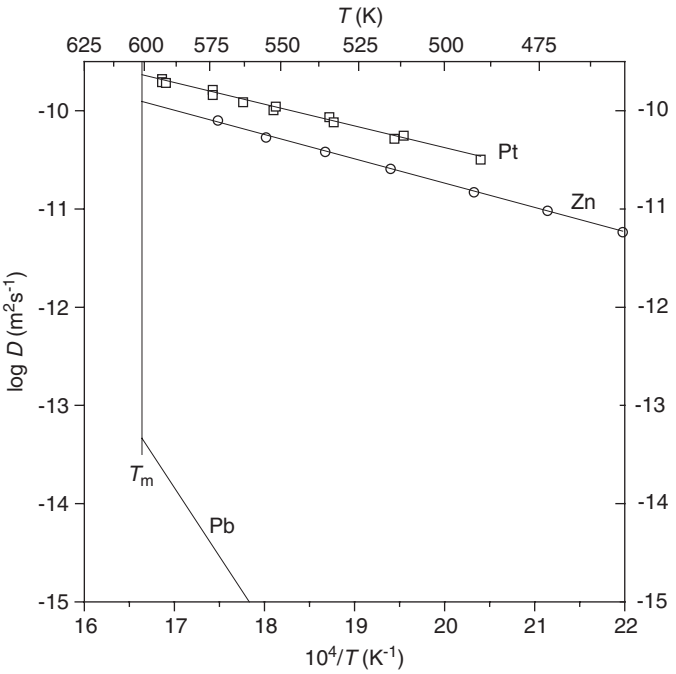

Fig. 45.06 Impurity diffusion in lead. Pt in Pb: □, Vanfleet [45.34]; Zn in Pb: ○, Ross [45.37].

REFERENCES

References to Chapter 4.0

[40.01] M. Schulz, in: *Landolt-Börnstein*, New Series III **22b**, Eds. O. Madelung, M. Schulz, Springer, Berlin (1989), Chapter 4.2, p. 207.
[40.02] N.A. Stolwijk, in: *Landolt-Börnstein*, New Series III **22b**, Eds. O. Madelung, M. Schulz, Springer, Berlin (1989), Chapter 4.3, p. 439.
[40.03] B.L. Sharma, Defect and Diffusion Forum **70/71** (1990).
[40.04] A.D. King, G.M. Hood, R.A. Holt, J. Nucl. Mater. **185** (1991) 174.
[40.05] W.C. Roberts-Austen, Proc. Roy. Soc. London **59** (1896) 281; ibid. 67 (1900) 101.
[40.06] G.v. Hevesy, W. Seith, Z. Elektrochemie **37** (1931) 528.
[40.07] W. Seith, J.G. Laird, Z. Metallk. **24** (1932) 193.
[40.08] W. Seith, A. Keil, Z. Phys. Chem. B **22** (1933) 350.
[40.09] W. Seith, E. Hofer, H. Etzold, Z. Elektrochem. **40** (1934) 322.
[40.10] W. Seith, H. Etzold, Z. Elektrochem. **40** (1934) 829.
[40.11] W. Seith, H. Etzold, Z. Elektrochem. **41** (1935) 122.
[40.12] W. Seith, Z. Elektrochem. **41** (1935) 872.
[40.13] G.v. Hevesy, W. Seith, A. Keil, Z. Phys. **79** (1932) 197.

References to Chapter 4.1

[41.01] J.F. Murdock, T.S. Lundy, E.E. Stansbury, Acta Metall. **12** (1964) 1033.
[41.02] U. Köhler, Ch. Herzig, Phys. Stat. Sol. (b) **144** (1987) 243.

[41.03] G. Neumann, V. Tölle, Phil. Mag. A **61** (1990) 563.
[41.04] Ch. Herzig, R. Willecke, K. Vieregge, Phil. Mag. A **63** (1991) 949.
[41.05] M. Köppers, Ch. Herzig, M. Friesel, Y. Mishin, Acta Mater. **45** (1997) 4181; see also Ref. [41.28].
[41.06] J. Askill, Phys. Stat. Sol. (b) **43** (1971) K1.
[41.07] S.Y. Lee, Y. Iijima, O. Taguchi, K. Hirano, J. Jpn. Inst. Met. **54** (1990) 502.
[41.08] O. Taguchi, Y. Iijima, Phil. Mag. A **72** (1995) 1649.
[41.09] L.L. Araújo, M. Behar, Appl. Phys. A **71** (2000) 169.
[41.10] H. Araki, T. Yamane, Y. Minamino, S. Saji, Y. Hana, S.B. Jung, Metall. Mater. Trans. A **25** (1994) 874.
[41.11] M. Köppers, M. Friesel, Ch. Herzig, to be published; see Y. Mishin, Ch. Herzig, Acta Mater. **48** (2000) 589.
[41.12] S.Y. Lee, Y. Iijima, K. Hirano, Defect and Diffusion Forum **95–98** (1993) 623.
[41.13] J.H.R. dos Santos, P.F.P. Fichtner, M. Behar, R.A. Pérez, F. Dyment, Appl. Phys. A **58** (1994) 453.
[41.14] L.V. Pavlinov, G.V. Grigoryev, G.O. Gromyko, Izv. Akad. Nauk SSSR, Met. (3) (1969) 207.
[41.15] A.N. Shabalin, V.P. Gladkov, P.L. Gruzin, A.V. Svetlov, Fiz. Met. Metalloved. **48** (1979) 663; Phys. Met. Metallogr. **48** (3) (1979) 182 (English transl.).
[41.16] R.F. Peart, D.H. Tomlin, Acta Metall. **10** (1962) 123.
[41.17] G.B. Gibbs, D. Graham, D.H. Tomlin, Phil. Mag. **8** (1963) 1269; the recalculated diffusion parameters in Ref. [41.39] do not improve the agreement between experimental and calculated diffusion coefficients.
[41.18] H. Araki, Y. Minamino, T. Yamane, Y. Shirai, Y. Miyamoto, Defect and Diffusion Forum **143–147** (1997) 125.
[41.19] H. Nakajima, M. Koiwa, Y. Minonishi, S. Ono, Trans. Jpn. Inst. Met. **24** (1983) 655.
[41.20] R.A. Pérez, F. Dyment, Phil. Mag. A **71** (1995) 965.
[41.21] A.J. Mortlock, D.H. Tomlin, Phil. Mag. **4** (1959) 628.
[41.22] S.Y. Lee, Y. Iijima, K. Hirano, Mater. Trans. Jpn. Inst. Met. **32** (1991) 451.
[41.23] H. Araki, T. Yamane, T. Nakatuka, Y. Minamino, Z. Metallk. **97** (2006) 22.
[41.24] H. Nakajima, K. Ogasawara, S. Yamaguchi, Mater. Trans. Jpn. Inst. Met. **31** (1990) 249.
[41.25] O. Caloni, A. Ferrari, P.M. Strocchi, Electrochim. Metal. **4** (1969) 45; from Diff. Data 4 (1970) 65.
[41.26] H. Nakajima, M. Koiwa, S. Ono, Scr. Metall. **17** (1983) 1431.
[41.27] S.Y. Lee, Y. Iijima, K. Hirano, Phys. Stat. Sol. (a) **136** (1993) 311.
[41.28] M. Köppers, D. Derdau, M. Friesel, Ch. Herzig, Defect and Diffusion Forum **143–147** (1997) 43.
[41.29] Ch. Herzig, M. Friesel, D. Derdau, S.V. Divinski, Intermetallics **7** (1999) 1141.
[41.30] M. Behar, J.H.R. dos Santos, F. Bernardi, F. Dyment, Defect and Diffusion Forum **213–215** (2003) 1.
[41.31] Y. Iijima, S.Y. Lee, K. Hirano, Phil. Mag. A **68** (1993) 901.
[41.32] G. Le Gall, D. Ansel, J. Debuigne, Acta Metall. **35** (1987) 2297.
[41.33] M. Behar, F. Dyment, R.A. Pérez, J.H.R. dos Santos, R.L. Maltez, E.J. Savino, Phil. Mag. A **63** (1991) 967.
[41.34] R.A. Pérez, F. Dyment, G. García Bermúdez, H. Somacal, D. Abriola, J. Nucl. Mater. **207** (1993) 221; see also Ref. [41.42].
[41.35] R.A. Pérez, M.R.F. Soares, M. Behar, F. Dyment, J. Nucl. Mater. **249** (1997) 52.
[41.36] Y. Nakamura, H. Nakajima, S. Ishioka, M. Koiwa, Acta Metall. **36** (1988) 2787.
[41.37] G.M. Hood, R.J. Schultz, Phil. Mag. **26** (1972) 329.
[41.38] H. Nakajima, M. Koiwa, Titanium, Sci. Technol. (1985) 1759; see also H. Nakajima, S. Maekawa, Y. Aoki, M. Koiwa, Trans. Jpn. Inst. Met. **26** (1985) 1.
[41.39] J. Askill, G.B. Gibbs, Phys. Stat. Sol. **11** (1965) 557.
[41.40] H. Nakajima, J. Nakazawa, Y. Minonishi, M. Koiwa, Phil. Mag. A **53** (1986) 427.
[41.41] M.L. Mirassou, R.A. Pérez, F. Dymont, J.H.R. dos Santos, M. Behar, Scr. Mater. **34** (1996) 1537.
[41.42] M.L. Mirassou, R.A. Pérez, F. Dyment, Defect and Diffusion Forum **143–147** (1997) 67.
[41.43] M. Behar, M.R.F. Soares, F. Dyment, R.A. Pérez, S. Balart, Phil. Mag. A **80** (2000) 1319.
[41.44] A. Languille, Mém. Sci. Rev. Métall. **63** (1971) 435.
[41.45] J. Räisänen, J. Keinonen, Appl. Phys. Lett. **49** (1986) 773.

[41.46] M.S. Jackson, D. Lazarus, Phys. Rev. B **15** (1977) 4644.
[41.47] H. Araki, T. Yamane, Y. Minamino, S. Saji, Y. Fujiishi, Y. Miyamoto, Mater. Trans. Jpn. Inst. Met. **34** (1993) 763.
[41.48] R.A. Pérez, M. Behar, F. Dyment, Phil. Mag. A **75** (1997) 993.
[41.49] J. Askill, Phys. Stat. Sol. **16** (1966) K63.
[41.50] D. Ansel, I. Thibon, M. Boliveau, J. Debuigne, Acta Mater. **46** (1998) 423.
[41.51] R.A. Pérez, F. Dyment, G. García Bermúdez, D. Abriola, M. Behar, Appl. Phys. A **76** (2003) 247.
[41.52] L.V. Pavlinov, A.I. Nakaneshnikov, Met. Metalloved. Chist. Met. (5) (1966) 124.
[41.53] F. de Keroulas, J. Mory, Y. Quéré, J. Nucl. Mater. **22** (1967) 276.
[41.54] G.B. Fedorov, E.A. Smirnov, Diffuziya v Reaktornykh Materialakh. Moscow, Atomizdat Publ. (1978), Diffusion in Reactor Materials, Trans. Tech. Publ., Switzerland (1984) (English transl.).
[41.55] G. Neumann, V. Tölle, Z. Metallk. **82** (1991) 741.
[41.56] Y. Minamino, H. Araki, T. Yamane, S. Ogino, S. Saji, Y. Miyamoto, Defect and Diffusion Forum **95–98** (1993) 685; see also H. Araki, Y. Minamino, T. Yamane, S. Saji, S. Ogino, Y. Miyamoto, J. Jpn. Inst. Met. **57** (1993) 501.
[41.57] H. Araki, Y. Minamino, T. Yamane, T. Nakatsuka, Y. Miyamoto, Metall. Mater. Trans. **27A** (1996) 1807.
[41.58] R.A. Pérez, F. Dyment, Hj. Matzke, G. Linker, H. Dhers, J. Nucl. Mater. **217** (1994) 48; see also Ref. [41.42].
[41.59] R.A. Pérez, M.L. Aguirre, F. Dyment, J. Nucl. Mater. **229** (1996) 15.

Further Investigations

β-titanium

Ti [41.60] N.E. Walsoë de Reca, C.M. Libanati, Acta Metall. **16** (1968) 1297.
Ti [41.61] A.E. Ponteau, D. Lazarus, Phys. Rev. B **19** (1979) 4027.
Fe [41.62] K. Ouchi, Y. Iijima, K. Hirano, Titanium, Sci. Technol. (1980) 559; EPMA.
Fe [41.63] L.G. Korneluk, L.M. Mirsky, B.S. Bokshtein, Titanium, Sci. Technol. (1973) 905.
Mo [41.64] L.V. Pavlinov, Fiz. Met. Metalloved. **24** (1967) 272; Phys. Met. Metallogr. 24 (2) (1967) 70 (English transl.).
Nb see Ref. [41.61].
U [41.65] L.V. Pavlinov, A.I. Nakonechnikov, V.N. Bykov, Atomn. Energiya **19** (1965) 521; Sov. Atom. Energy 19 (1965) 1495 (English transl.); precursor to Ref. [41.52].
W see Ref. [41.64].
Zr see Ref. [41.64].

α-titanium

Ti [41.66] C.M. Libanati, F. Dyment, Acta Metall. **11** (1963) 1263.
Ti [41.67] F. Dyment, Titanium, Science and Technology (1980) 519.
Al [41.68] A.V. Pokoyev, V.M. Mironov, L.K. Kudryavtseva, Izv. Vyssh. Uchebn. Zaved., Tsvetn. Metall. **19**(2), (1976) 130; Sov. Non-ferrous Met. Res. **4** (2) (1976) 81 (English transl.); X-ray diffraction method.
Al [41.69] J. Räisänen, A. Anttila, J. Keinonen, J. Appl. Phys. **57** (1985) 613; NRA.
Al see Ref. [41.62].
Co [41.70] E. Santos, F. Dyment, Phil. Mag. **31** (1975) 809.
Co [41.71] H. Nakajima, Sh. Ishioka, M. Koiwa, Phil. Mag. A **52** (1985) 743; isotope effect measurement.
Co see Ref. [41.04].
Fe see Ref. [41.63].
Fe [41.72] H. Nakajima, M. Ohno, S. Yamaguchi, M. Koiwa, Scr. Metall. **22** (1988) 1455; influence of oxygen on the diffusion.
Hf [41.73] R.A. Pérez, F. Dyment, G. García Bermúdez, H. Somacal, J. Nucl. Mater. **186** (1992) 206; precursor to Ref. [41.34].
Mn see Ref. [41.70].
Zr see Ref. [41.73]; precursor to Ref. [41.58].

References to Chapter 4.2

[42.01] G.V. Kidson, J. McGurn, Can. J. Phys. **39** (1961) 1146.
[42.02] J.I. Federer, T.S. Lundy, Trans. AIME **227** (1963) 592.
[42.03] G.V. Kidson, Can. J. Phys. **41** (1963) 1563.
[42.04] D. Graham, E.R. Hanes, NASA TN D **5905** (1970); unpublished; see Ref. [42.05].
[42.05] Ch. Herzig, H. Eckseler, Z. Metallk. **70** (1979) 215.
[42.06] D.D. Pruthi, M.S. Anand, R.P. Agarwala, Phil. Mag. A **39** (1979) 173; see also Ref. [42.61].
[42.07] G. Neumann, V. Tölle, Phil. Mag. A **61** (1990) 563.
[42.08] R.V. Patil, J. Nucl. Mater. **187** (1992) 197.
[42.09] G.M. Hood, R.J. Schultz, Acta Metall. **22** (1974) 459.
[42.10] J. Horvath, F. Dyment, H. Mehrer, J. Nucl. Mater. **126** (1984) 206.
[42.11] M. Lübbehusen, K. Vieregge, G.M. Hood, H. Mehrer, Ch. Herzig, J. Nucl. Mater. **182** (1991) 164.
[42.12] G.M. Hood, H. Zou, D. Gupta, R.J. Schultz, J. Nucl. Mater. **223** (1995) 122.
[42.13] G.M. Hood, H. Zou, R.J. Schultz, N. Matsuura, J.A. Roy, J.A. Jackman, Defect and Diffusion Forum **143–147** (1997) 49.
[42.14] R. Tendler, C.F. Varotto, J. Nucl. Mater. **54** (1974) 212.
[42.15] L. Manke, Ch. Herzig, Acta Metall. **30** (1982) 2092.
[42.16] G. Neumann, V. Tölle, Z. Metallk. **82** (1991) 741.
[42.17] Y. Iijima, O. Taguchi, J. Mater. Sci. Lett. **14** (1995) 486.
[42.18] G.M. Hood, in: *Diffusion Processes*, Eds. J.N. Sherwood, A.V. Chadwick, W.M. Muir, F.L. Swinton, Gordon and Breach, London (1971), p. 361.
[42.19] G. Tobar, S. Balart, Defect and Diffusion Forum **66–69** (1989) 381.
[42.20] K. Vieregge, Ch. Herzig, J. Nucl. Mater. **165** (1989) 65.
[42.21] A. Laik, K. Bhanumurthy, G.B. Kale, J. Nucl. Mater. **305** (2002) 124.
[42.22] J. Räisänen, J. Keinonen, Appl. Phys. A **36** (1985) 175.
[42.23] L.V. Pavlinov, G.V. Grigoryev, G.O. Gromyko, Izv. Akad. Nauk SSSR, Met. (3) (1969) 207.
[42.24] R. Tendler, J. Abriata, C.F. Varotto, J. Nucl. Mater. **59** (1976) 215.
[42.25] A.R. Paul, M.S. Anand, M.C. Naik, R.P. Agarwala, Intern. Conf. Vacancies and Interstitials in Metals, Jülich, Vol. 1 (1968) 105.
[42.26] G.V. Kidson, G.J. Young, Phil. Mag. **26** (1969) 1047.
[42.27] Ch. Herzig, J. Neuhaus, K. Vieregge, L. Manke, Mat. Sci. Forum **15–18** (1987) 481.
[42.28] R.H. Zee, J. Phys.: Condens. Matter **1** (1989) 5631.
[42.29] G.V. Kidson, Phil. Mag. A **44** (1981) 341.
[42.30] L.V. Pavlinov, Fiz. Met. Metalloved. **24** (1967) 272; Phys. Met. Metallogr. 24 (2) (1967) 70 (English transl.).
[42.31] L.I. Nicolai, R.H. de Tendler, J. Nucl. Mater. **87** (1979) 401.
[42.32] R.V. Patil, G.P. Tiwari, B.D. Sharma, Phil. Mag. A **44** (1981) 717.
[42.33] R. Tendler, C.F. Varotto, J. Nucl. Mater. **44** (1972) 99.
[42.34] S.N. Balart, N. Varela, R.H. de Tendler, J. Nucl. Mater. **119** (1983) 59.
[42.35] G.M. Hood, R.J. Schultz, J. Nucl. Mater. **200** (1993) 141.
[42.36] G.M. Hood, R.J. Schultz, Phys. Rev. B **11** (1975) 3780.
[42.37] J. Trampenau, Ch. Herzig, J. Phys.: Condens. Matter **2** (1990) 9345.
[42.38] G.M. Hood, R.J. Schultz, Phil. Mag. **26** (1972) 329.
[42.39] R. Tendler, E. Santos, J. Abriata, C.F. Varotto, in: *Thermodynamics of Nuclear Materials 1974*, Vol. **2**, Intern. Atomic Energy Agency, Vienna (1975), p. 71.
[42.40] H. Nakajima, G.M. Hood, R.J. Schultz, Phil. Mag. B **58** (1988) 319.
[42.41] Ch. Herzig, U. Köhler, Mater. Sci. Forum **15–18** (1987) 301.
[42.42] G.M. Hood, H. Zou, R.J. Schultz, J.A. Roy, J.A. Jackman, J. Nucl. Mater. **189** (1992) 226.
[42.43] R. Tendler, C.F. Varotto, J. Nucl. Mater. **46** (1973) 107.
[42.44] Ch. Herzig, L. Manke, W. Bussmann, in: *Point Defects and Defect Interactions in Metals*, Eds. J.I. Takamura, M. Doyama, M. Kiritani, Univ. Tokyo Press, Tokyo (1982), p. 578.
[42.45] G.M. Hood, H. Zou, R.J. Schultz, N. Matsuura, Defect and Diffusion Forum **143–147** (1997) 55.

[42.46] G.M. Hood, R.J. Schultz, Mater. Sci. Forum **15–18** (1987) 475.
[42.47] B.A. Vandyshev, A.S. Panov, Izv. Akad. Nauk. SSSR, Met. (1) (1970) 231.
[42.48] G.M. Hood, T. Laursen, J.A. Jackman, R. Belec, R.J. Schultz, J.L. Whitton, Phil. Mag. A **63** (1991) 937.
[42.49] R.A. Pérez, F. Dyment, Appl. Phys. A **68** (1999) 667.
[42.50] E.Ch. Schwegler, F.A. White, Intern. J. Mass Spectrom. Ion Phys. (1) (1968) 191.
[42.51] S. Balart, R. Tendler, A. Amalric, F. Carbone, F. Gaioli, J. Nucl. Mater. **168** (1989) 346.
[42.52] B.A. Vandyshev, A.S. Panov, P.L. Gruzin, Fiz. Met. Metalloved. **23** (1967) 908; Phys. Met. Metallogr. **23** (5) (1967) 133 (English transl.).
[42.53] G.B. Fedorov, V.D. Gulyakin, Met. Metalloved. Chist. Met. (1) (1959) 170.
[42.54] B. Chelluri, D. Lazarus, C.A. Wert, Phys. Rev. B **23** (1981) 4849.
[42.55] G.B. Fedorov, F.I. Zhomov, Met. Metalloved. Chist. Met. (1) (1959) 162.
[42.56] E.V. Borisov, Yu.G. Godin, P.L. Gruzin, A.I. Eustyukin, V.S. Emelyanov, Met. Met., Izdatel Akad. Nauk. SSSR, Moscow (1958), NP-TR-448 (1960) 196 (English transl.).
[42.57] G.M. Hood, H. Zou, R.J. Schultz, E.H. Bromley, J.A. Jackman, J. Nucl. Mater. **217** (1994) 229.
[42.58] L.V. Pavlinov, Fiz. Met. Metalloved. **30** (1970) 367; Phys. Met. Metallogr. **30** (2) (1970) 149 (English transl.).
[42.59] G.B. Fedorov, E.A. Smirnov, F.I. Zhomov, V.N. Gusev, S.A. Paraev, Met. Metalloved. Chist. Met. (9) (1971) 30; see also Atomn. Energiya 31 (1971) 516, Sov. Atom. Energy **31** (1971) 1280 (English transl.).
[42.60] R.P. Agarwala, S.P. Murarka, M.S. Anand, Acta Metall. **16** (1968) 61.
[42.61] D.D. Pruthi, R.P. Agarwala, Phil. Mag. A **46** (1982) 841.
[42.62] G.B. Fedorov, F.I. Zhomov, E.A. Smirnov, Met. Metalloved. Chist. Met. (5) (1966) 22.

Further Investigations

β-zirconium

Zr [42.63] P.L. Gruzin, V.S. Emelyanov, G.G. Ryabova, G.B. Fedorov, Proc. 2nd U.N. Intern. Conf. Peaceful Uses of Atomic Energy, Geneva 1958, **19** (1958) 187.
Zr see Ref. [42.56].
Zr see Ref. [42.53].
Zr [42.64] V.S. Lyachenko, V.N. Bykov, L.V. Pavlinov, Fiz. Met. Metalloved. **8** (1959) 362; Phys. Met. Metallogr. **8** (3) (1959) 40 (English transl.)
Zr [42.65] D. Volokoff, S. May, Y. Adda, C.R. Acad. Sci. Paris **251** (1960) 2341.
Zr see Ref. [42.32].
Cr [42.66] R.P. Agarwala, S.P. Murarka, M.S. Anand, Trans. AIME **233** (1965) 986.
Cr see Ref. [42.39].
Fe [42.67] A.M. Blinkin, V.V. Vorobiov, Ukr. Fiz. Zh. **9**(1), (1964) 91.
Fe see Ref. [42.30].
Fe see Ref. [42.54].
Fe see Ref. [42.27]; precursor to Ref. [42.37].
Fe see Ref. [42.28].
Hf [42.68] D. Ansel, A.M. Margottet, M. Boliveau, J. Debuigne, Scr. Metall. **34** (1996) 749; EPMA.
Mo see Ref. [42.30].
Mo [42.69] G.B. Fedorov, E.A. Smirnov, V.N. Gusev, F.I. Zhomov, V.L. Gorbenko, Met. Metalloved. Chist. Met. (10) (1973) 62.
Nb [42.70] G.B. Fedorov, E.A. Smirnov, S.M. Novikov, Met. Metalloved. Chist. Met. (8) (1969) 41.
Nb [42.71] G.P. Tiwari, B.D. Sharma, V.S. Raghunathan, R.V. Patil, J. Nucl. Mater. **46** (1973) 35.
U [42.72] L.V. Pavlinov, A.I. Nakonechnikov, V.N. Bykov, Atomn. Energiya **19** (1965) 521; Soviet Atom. Energy **19** (1965) 1495 (English transl.).
U [42.73] G.B. Fedorov, E.A. Smirnov, F.I. Zhomov, Met. Metalloved. Chist. Met. (7) (1968) 116.

α-zirconium
Zr see Ref. [42.64].
Zr see Ref. [42.56].
Zr see Ref. [42.65].
Zr see Ref. [42.53].
Zr [42.74] P. Flubacher, Eidgenössisches Institut für Reaktorforschung, EIR-Report No. 49 (1963)
Zr [42.75] F. Dyment, C.M. Libanati, J. Mater. Sci. **3** (1968) 349.
Co see Ref. [42.38].
Co see Ref. [42.09].
Co see Ref. [42.39].
Cr see Ref. [42.66].
Cu see Ref. [42.18].
Fe see Ref. [42.67].
Hf [42.76] F. Dyment, M. Behar, H. Dhers, P.L. Grande, E. Savino, F.C. Zawislak, Appl. Phys. A **51** (1990) 29; RBS.
Hf see Ref. [42.48].
Hf [42.77] G.M. Hood, H. Zou, J.A. Roy, R.J. Schultz, N. Matsuura, J.A. Jackman, J. Nucl. Mater. **228** (1996) 43; SIMS.
Nb see Ref. [42.75].
Pb [42.78] C.R.S. da Silva, F. Zawislak, Mat. Res. Symp. Proc. **316** (1994) 173.

References to Chapter 4.3

[43.01] F.R. Winslow, T.S. Lundy, Trans. AIME **233** (1965) 1790.
[43.02] Ch. Herzig, L. Manke, W. Bussmann, in: *Point Defects and Defect Interactions in Metals*, Eds. J.I. Takamura, M. Doyama, M. Kiritani, Univ. Tokyo Press, Tokyo (1982), p. 578.
[43.03] B.E. Davis, W.D. McMullen, Acta Metall. **20** (1972) 593.
[43.04] Ch. Herzig, Y. Mishin, S.V. Divinski, Metall. Mater. Trans. A **33A** (2002) 765.
[43.05] F. Bernardi, M. Behar, J.H.R. dos Santos, F. Dyment, Appl. Phys. A **80** (2005) 69.
[43.06] F. Dyment, J. Nucl. Mater. **61** (1976) 271.
[43.07] M. Köppers, Ch. Herzig, U. Södervall, A. Lodding, Defect and Diffusion Forum **95–98** (1993) 783.

Further Investigations

Hf [43.08] N.E. Walsöe de Reca, C.M. Libanati, Acta Metall. **16** (1968) 1297.
Hf [43.09] F. Dyment, C.M. Libanati, J. Mater. Sci. **3** (1968) 349.
Al [43.10] J. Räisänen, J. Keinonen, Appl. Phys. A **36** (1985) 175; NRA.

References to Chapter 4.4

[44.01] J.D. Meakin, E. Klokholm, Trans. AIME **218** (1960) 463.
[44.02] C. Coston, N.H. Nachtrieb, J. Phys. Chem. **68** (1964) 2219.
[44.03] F.H. Huang, H.B. Huntington, Phys. Rev. B **9** (1974) 1479.
[44.04] B.F. Dyson, J. Appl. Phys. **37** (1966) 2375.
[44.05] V.B. Brik, Phys. Met. Metalloved. **53** (1982) 600; Phys. Met. Metallogr. **53** (3) (1982) 176 (English transl.).
[44.06] B.F. Dyson, T.R. Anthony, D. Turnbull, J. Appl. Phys. **38** (1967) 3408.
[44.07] M. Shimotomai, R.R. Hasiguti, S. Umeyama, Phys. Rev. B **18** (1978) 2097.
[44.08] W.K. Warburton, Phys. Rev. B **6** (1972) 2161.
[44.09] A. Sawatzky, J. Appl. Phys. **29** (1958) 1303.
[44.10] D.C. Yeh, H.B. Huntington, Phys. Rev. Lett. **53** (1984) 1469.
[44.11] F.H. Huang, H.B. Huntington, Scr. Metall. **5** (1971) 705.
[44.12] L. Bartha, T. Szalay, Intern. J. Appl. Rad. Isotopes **20** (1969) 825.

Further Investigations

Sn [44.13] W. Lange, A. Hässner, I. Berthold, Phys. Stat. Sol. **1** (1961) 50.
Sn [44.14] D. Bergner, W. Lange, Phys. Stat. Sol. **18** (1966) 67.
Zn see Ref. [44.14].

References to Chapter 4.5

[45.01] N.H. Nachtrieb, G.S. Handler, J. Chem. Phys. **23** (1955) 1569.
[45.02] H.A. Resing, N.H. Nachtrieb, J. Phys. Chem. Sol. **21** (1961) 40.
[45.03] J.B. Hudson, R.E. Hoffman, Trans. AIME **221** (1961) 761.
[45.04] J.W. Miller, Phys. Rev. **181** (1969) 1095.
[45.05] W.K. Warburton, Phys. Rev. B **7** (1973) 1330.
[45.06] H.R. Curtin, D.L. Decker, H.B. Vanfleet, Phys. Rev. **139** (1965) A1552.
[45.07] B.F. Dyson, T.R. Anthony, D. Turnbull, J. Appl. Phys. **37** (1966) 2370.
[45.08] Ch. Herzig, Th. Heumann, D. Wolter, Z. Naturforsch. **26a** (1971) 1477.
[45.09] J.W. Miller, J.N. Mundy, L.C. Robinson, R.E. Loess, Phys. Rev. B **8** (1973) 2411.
[45.10] A. Ascoli, L. Filoni, G. Poletti, S.L. Rossi, Phys. Rev. B **10** (1974) 5003.
[45.11] B.M. Cohen, W.K. Warburton, Phys. Rev. B **12** (1975) 5682.
[45.12] C.K. Hu, H.B. Huntington, Phys. Rev. B **26** (1982) 2782.
[45.13] J. Shi, S. Mei, H.B. Huntington, J. Appl. Phys. **62** (1987) 451.
[45.14] A. Ascoli, E. Germagnoli, L. Mongini, Nuovo Cimento **4** (1956) 123.
[45.15] A. Ascoli, J. Inst. Met. **89** (1961) 218.
[45.16] A. Ascoli, B. Bollani, G. Guarini, D. Kustudic, Phys. Rev. **141** (1966) 732.
[45.17] G.V. Kidson, Phil. Mag. **13** (1966) 247.
[45.18] J.A. Weyland, D.L. Decker, H.B. Vanfleet, Phys. Rev. B **4** (1971) 4225.
[45.19] W.K. Warburton, Phys. Rev. B **11** (1975) 4945.
[45.20] D.L. Decker, J.G. Melville, H.B. Vanfleet, Phys. Rev. B **20** (1979) 3036.
[45.21] H.B. Vanfleet, J.D. Jorgensen, J.D. Schmutz, D.L. Decker, Phys. Rev. B **15** (1977) 5545.
[45.22] K. Kusunoki, S. Nishikawa, Scr. Metall. **12** (1978) 615.
[45.23] M. Chandramouli, N.K. Mishra, V.S. Venkatasubramanian, Proc. Nucl. Phys. Sol. State Phys. Symp. **17C** (1974) 91; Defect Diffusion Data **13** (1976) 83.
[45.24] C.T. Candland, D.L. Decker, H.B. Vanfleet, Phys. Rev. B **5** (1972) 2085.
[45.25] J.N. Mundy, J.W. Miller, S.J. Rothman, Phys. Rev. B **10** (1974) 2275.
[45.26] D.L. Decker, Phys. Rev. B **11** (1975) 1770.
[45.27] J. Kučera, K. Stránský, Can. Metall. Quart. **8** (1969) 91.
[45.28] L. Cheriet, H.B. Huntington, Acta Metall. **35** (1987) 1649.
[45.29] H. Ziegler, Diploma Work, Univ. Münster (1982), unpublished.
[45.30] C.W. Owens, D. Turnbull, J. Appl. Phys. **43** (1972) 3933.
[45.31] C.T. Candland, H.B. Vanfleet, Phys. Rev. B **7** (1973) 575.
[45.32] D.L. Decker, C.T. Candland, H.B. Vanfleet, Phys. Rev. B **11** (1975) 4885.
[45.33] S. Mei, J. Shi, H.B. Huntington, J. Appl. Phys. **62** (1987) 444.
[45.34] H.B. Vanfleet, Phys. Rev. B **21** (1980) 4337.
[45.35] S. Nishikawa, K. Tsumuraya, Phil. Mag. **26** (1972) 941.
[45.36] D.L. Decker, J.D. Weiss, H.B. Vanfleet, Phys. Rev. B **16** (1977) 2392.
[45.37] R.A. Ross, H.B. Vanfleet, D.L. Decker, Phys. Rev. B **9** (1974) 4026.
[45.38] D.L. Decker, R.A. Ross, W.E. Evenson, H.B. Vanfleet, Phys. Rev. B **15** (1977) 507.

Further Investigations

Pb [45.39] B. Okkerse, Acta Metall. **2** (1954) 551.
Au [45.40] W.K. Warburton, Scr. Metall. **7** (1973) 105; precursor to Ref. [45.19].
Au [45.41] C.K. Hu, H.B. Huntington, J. Appl. Phys. **58** (1985) 2564; Diffusion in Pb(Sn).
Au see Ref. [45.13].
Cu see Ref. [45.13].
Ni [45.42] H. Amenzou-Badrour, G. Moya, J. Bernardini, Acta Metall. **36** (1988) 767.
Sn [45.43] S. Mei, H.B. Huntington, C.K. Hu, M.J. McBride, Scr. Metall. **21** (1987) 153.
Sn [45.44] S.K. Sen, A. Ghorai, Phil. Mag. A **59** (1989) 707; resistometric method.

CHAPTER 5

Self-Diffusion and Impurity Diffusion in Group V Metals

Contents

Tables
5.1. Vanadium (V) 217
5.2. Niobium (Nb) 220
5.3. Tantalum (Ta) 224
5.4. Antimony (Sb) 226
Figures
Vanadium 227
Niobium 230
Tantalum 234
Antimony 235
References 236

Phosphorus (P) and **arsenic** (As) are not topic of this data collection.

In **vanadium** oxygen impurities enhance the diffusivity at lower temperatures (see Refs. [51.01, 51.04]). This effect is not observed in **niobium** (see Refs. [52.01, 52.03]).

Diffusion coefficients derived from out-diffusion investigations of spallation products in **niobium** (Sr, Y, Zn, Zr) [50.01] and in **tantalum** (rare earth metals, As, Ba, Cs, Hf, Rb, Sr and Y) [50.02] are not taken into consideration in this data collection (see Chapter 0.1).

Legoux and Merini have studied the diffusion of actinides in **tantalum** (summarized in Ref. [50.03]). The α-emitting actinides were generated by ion bombardment of heavy elements and implanted into a Ta foil. The results of the investigations between about 1,000 and 1,700 K ($\bar{T}/T_m \approx 0.4$) exhibit an extreme data scatter. Because of the very low diffusion energies, probably not representative for lattice diffusion, the reported diffusion parameters are not considered in Table 5.3.

Diffusion of the almost insoluble alkaline metals was investigated in single as well as polycrystals of **vanadium** (Cs [50.04]), **niobium** (Na, K [50.05], Cs [50.04]) and **tantalum** (Cs [50.04]) at temperatures lower than 0.7 T_m. The results refer to dominating grain-boundary and dislocation diffusion. Note that Cs could not be detected in single crystals of V, Nb and Ta [50.04]. The results of the alkaline diffusion are not considered in Tables 5.1–5.3.

In **bismuth** (Bi) only self-diffusion of ^{210}Bi in single crystals was investigated [50.06]. Anomalous penetration plots, however, do not permit the determination of credible diffusion coefficients.

In Table 5.0 lattice structure, lattice constant and melting temperature of group V metals are listed.

Table 5.0 Lattice structure, lattice constants a and c and melting temperature T_m

Metal	V	Nb	Ta	Sb
Structure	bcc	bcc	bcc	Trigonal
T_m (K)	2,175	2,740	3,288	904
a (nm)	0.302	0.330	0.331	0.431
c (nm)				1.125

Table 5.1 Diffusion in vanadium (References, see page 236)

(1)	(2a)	(2b)	(3)	(4)	(5)	(6)	(7)	(8)	(9)	(10)	(11)	(12)
X	D^0 (10^{-4} m^2 s^{-1})	Q (eV) and (kJ mole^{-1})	$D(T_m)$ (10^{-12} m^2 s^{-1})	T-range (K) ($\bar{T}/T_m$)	No. of data points	Material, purity	Experimental method	Remarks on the pp	Further remarks	Also studied	Figure	Reference
Self-diffusion												
V	58	3.968 (383.1)	3.7	1,771–2,161 (0.90)	8	sc 2N7*	^{48}V, electroplated; lathe	4 examples	*Oxygen content 880 ppm, see introduction page		51.01	Lundy (1965) [51.01]
	(0.011)	(2.645) (255.4)		1,275–1,674 (0.67)	7 (5T)							
V	214	4.082 (394.2)	7.4	1,629–2,106 (0.85)	12 (10T)	sc 4N*	^{48}V, electroplated and vapour deposition[73]; lathe and chemical etching	Numerous examples	*Oxygen content 5 ppm, see introduction page	Fe in V	51.01	Peart (1965) [51.02]
	0.36	3.194 (308.4)		1,153–1,590 (0.63)	21 (13T)	pc 3N*						
	500[21]	4.272[21] (412.4)	7.0	1,153–2,106					[x]Corrected value			
	0.065[21x]	3.014[21] (291.0)										
V	173	4.239 (409.3)	2.6	1,915–2,115 (0.93)	6	sc >3N*	^{48}V, dried-on from salt solution; lathe, grinder and anodizing and stripping	Numerous examples, short circuit tails at low T and deeper penetrations	*Oxygen content not specified		51.01	Pelleg (1974) [51.03]
	0.288	3.206 (309.6)		997–1,865 (0.66)	34 (26T)							
V	79.9	3.99 (385.2)	4.5	1,695–2,166 (0.89)	23 (12T)	sc ~2N7*	^{48}V, dried-on from salt solution[73]; lathe	Several examples	*Oxygen content 940 ppm, see introduction page		51.01	Macht (1979) [51.04]
	0.0208	2.82 (272.3)		1,446–1,641 (0.71)	12 (6T)							
V	–	–		1,323–2,147	18	sc	^{48}V[72]; residual activity	Numerous examples	*Oxygen content 170 ppm, see introduction page	V in V(Fe) and V(Ta)	51.01	Ablitzer (1983) [51.05]
	26.8	3.857 (372.4)	3.1	1,806–2,147 (0.91)	9	3N7* pc						
	1.79	3.438 (331.9)		1,521–1,757 (0.75)	6							
V	0.10*	3.09 (298.3)		1,335–1,845 (0.73)	15[51]	pc 3N5 2N8	^{51}V; NMR SLRT $T_{1\rho}$		*$D^0 = f_{1V} D^0_{NMR}$ (see Chapter 0.2)		–	Günther (1983) [51.06]
V	118	4.032 (389.3)	5.3	1,578–1,888 (0.80)	7	pc 3N5*	^{48}V, dried-on from salt solution; serial sectioning	1 example	*Oxygen content not specified	Zr in V; V, Zr in V(Zr)	51.01	Pruthi (1984) [51.07]

Table 5.1 *(Continued)*

(1)	(2a)	(2b)	(3)	(4)	(5)	(6)	(7)	(8)	(9)	(10)	(11)	(12)
X	D^0 (10^{-4} m^2 s^{-1})	Q (eV) and (kJ mole^{-1})	$D(T_m)$ (10^{-12} m^2 s^{-1})	T-range (K) ($\bar{T}/T_m$)	No. of data points	Material, purity	Experimental method	Remarks on the pp	Further remarks	Also studied	Figure	Reference
V	2,420	3.21 (310.0)	4.2	(997–2,166)	(133)				Two-exponential fit to the data of [51.01–51.05]		51.01	Neumann (1990) [51.08]
	0.31	4.70 (453.8)										
V	0.359	3.201 (309.1)		1,220–1,694 (0.67)	6	pc >3N*	^{48}V, dried-on from salt solution; grinder	1 example	*Oxygen content not specified	V in V(Co)	51.01	Segel (1997) [51.09]
Impurity diffusion												
Al	0.084	2.778 (268.2)		1,273–1,773 (0.70)	7	pc[61]	Al, vapour deposition; X-ray diffraction method	–			51.02	Maslov (1985) [51.10]
Co	1.12	3.055 (295.0)	9.3	1,298–2,126 (0.79)	23	sc >3N	^{60}Co, dried-on from salt solution; grinder and lathe	Numerous examples			51.03	Pelleg (1975) [51.11]
Co	(0.7)	(2.391) (283)		1,337–1,521 (0.66)	4	pc 3N8	^{60}Co, dried-on from salt solution; grinder	2 examples	+Present approximation	Co in V(Co)	–	Pelleg (1995) [51.12]
	0.66+	3.020+ (291.6)										
Cr	100	3.913 (377.8)		1,424–1,873 (0.76)	12	pc 3N8*	^{51}Cr, dried-on from salt solution; grinder	Several examples	*Oxygen content 725 ppm; pronounced data scatter		–	Pelleg (1995) [51.13]
Fe	0.60	3.057 (295.2)		1,115–1,444 (0.59)	8 (4T)	sc 4N	^{59}Fe, dried-on from salt solution[73]; chemical etching	1 example		V in V	–	Peart (1965) [51.02]
Fe	274	3.997 (385.9)	15	1,618–2,090 (0.85)	9 (8T)	sc[61]	^{59}Fe, ^{55}Fe, dried-on from salt solution; lathe and chemical etching	Numerous examples		$E = 0.70–0.30$	51.03	Coleman (1968) [51.14]
	0.37	3.079 (279.3)		1,253–1,570 (0.65)	7 (5T)							
	2,280[21]	4.402[21] (425.0)	17	1,253–2,090								
	0.0936[21]	2.932[21] (283.0)										

Fe	–	–		1,211–2,088	44 (34T)	sc pc	[59]Fe, electroplated and dried-on from salt solution; lathe, grinder (residual activity) and anodizing; Fe, vapour deposition; EPMA	Numerous examples			51.03	Ablitzer (1981) [51.15]
	31.7	3.694 (356.6)	8.7	1,839–2,088 (0.90)	8	3N						
	2.48	3.301 (318.7)		1,484–1,788 (0.75)	23 (18T)							
Fe	2,030[21]	4.45[21] (429.7)	12.6	(1,253–2,090)	(49)				Two-exponential fit to the data of [51.14, 51.15]		51.03	Neumann (1991) [51.16]
	0.38[21]	3.08[21] (297.4)										
Mo	0.185	3.176 (306.7)		1,340–1,868 (0.74)	10	pc[61]	[99]Mo, dried-on from salt solution; grinder	All			51.02	Pelleg (1991) [51.17]
Nb	–	–		1,673–2,023 (0.85)	6	pc ~2N7	Nb, EPMA, thin film of V in a Nb/V/Nb sandwich sample (Hall)	No	[+]Present rough approximation	X in Nb(X) X = Mo, Ti, V, W, Zr (EPMA)	–	Roux (1970) [51.18]
	68[+]	3.90[+] (376.6)	6.2[+]									
Ni	0.18	2.758 (266.2)		1,175–1,948 (0.72)	24 (20T)	sc pc 3N	[63]Ni, dried-on from salt solution; residual activity	Numerous examples (very flat pp)	Pronounced data scatter		–	Pelleg (1986) [51.19]
P	0.0245	2.160 (208.5)		1,473–1,723 (0.73)	10 (5T)	pc 2N8	[32]P; residual activity	No	Marked gb contributions cannot be excluded	P in β-Zr	–	Vandyshev (1970) [51.20]
S	0.031	1.474 (142.4)		1,320–1,520 (0.65)	8 (5T)	pc 2N8	[35]S; residual activity	No	Marked gb contributions cannot be excluded	S in Ta	–	Vandyshev (1969) [51.21]
Ta	0.244	3.121 (301.4)	14	1,371–2,076 (0.79)	18	sc pc 3N	[182]Ta, dried-on from salt solution; grinder	Numerous examples[84] (very flat pp)	Pronounced data scatter		–	Pelleg (1977) [51.22]
Ti	–	–		1,373–2,076	15	pc	[44]Ti, dried-on from salt solution; lathe	No	[x]Fit according to Ref. [51.24] *Oxygen content 112 ppm, see introduction page	Ti, V in V(Ti)	51.04	Murdock (1968) [51.23]
	34.1[x]	3.769[x] (363.9)	6.3	1,623–2,076 (0.85)	10	3N8*						
	(0.1[x])	(2.952[x]) (285.0)		1,373–1,573	5							
U	2.0×10^{-4} [x]	2.663 (257.1)		1,373–1,773 (0.72)	5[51]	pc[61]	[235]U, experimental details not reported	No	[x]Corrected value	U in β-Zr, Nb, Ta, W	–	Fedorov (1971) [51.25]
Zr	81	3.824 (369.2)		1,578–1,883 (0.80)	7	pc 3N5*	[95]Zr dried-on from salt solution; serial sectioning	1 example	*Oxygen content not specified	V in V; V, Zr in V(Zr)	51.04	Pruthi (1984) [51.07]

Table 5.2 Diffusion in niobium (References, see page 237)

(1)	(2a)	(2b)	(3)	(4)	(5)	(6)	(7)	(8)	(9)	(10)	(11)	(12)
X	D^0 (10^{-4} $m^2 s^{-1}$)	Q (eV) and (kJ mole)	$D(T_m)$ (10^{-12} $m^2 s^{-1}$)	T-range (K) ($\bar{T}/T_m$)	No. of data points	Material, purity	Experimental method	Remarks on the pp	Further remarks	Also studied	Figure	Reference
Self-diffusion												
Nb	1.1	4.163 (402.0)		1,151–2,668 (0.70)	32 (31T)	sc pc 2N75	^{95}Nb, dried-on from oxalate solution; lathe, grinder, anodizing and stripping	Several examples	Erroneous thermal expansion correction; no influence of oxygen on the diffusivity observed	Ta in Nb	52.01	Lundy (1965) [52.01]
Nb	0.61	4.115 (397.3)		1,421–2,509 (0.72)	11	sc 3N pc[61]	^{95}Nb, electroplated and dried-on from salt solution; residual activity, grinder, anodizing and stripping	3 examples		Co, Cu, Fe, Ni in Nb	52.01	Ablitzer (1977) [52.02]
Nb	3.7[21] 0.008[21]	4.54[21] (438.3) 3.62[21] (349.5)	1.8[21]	1,354–2,695 (0.74)	36 (19T)	sc 3N8	^{95}Nb, dried-on from oxalate solution; grinder, anodizing and stripping	5 examples	No influence of oxygen on the diffusivity observed		52.01	Einziger (1978) [52.03]
Nb	– 4.6[21]* 0.015[21] *	– 4.59[21] * (443.2) 3.67[21]* (354.3)	1.9[21]*	1,929–2,673 (0.84)	14	sc[61]	^{95}Nb, ^{92}Nb, dried-on from salt solution; lathe	Several examples	*Two-exponential fit to the data of [52.03]	Isotope effect, E-values ranging from 0.35 to 0.48, maximum at ~2,200 K	52.01	Bussmann (1981) [52.04]
Nb	(1.1)*	(4.163)* (402.0)		2,300–2,510 (0.88)	5	pc 4N	^{95}Nb, dried-on from salt solution; serial sectioning	1 example (in [52.10])	For experimental details, see Ref. [52.10] *The temperatures of the measured D values are fitted to $D(T)$ acc. to [52.01]	Co, Cr, Fe, Ta in Nb; electro-transport	–	Serruys (1983) [52.05], [52.06]
Nb	65[21] 0.115[21]	5.21[21] (503.0) 3.88[21] (374.6)	2.5[21]	(1,151–2,695)	(88)		Two-exponential fit to the data of [52.01–52.04]				52.01	Neumann (1990) [52.07]

Impurity diffusion

Al	(0.11*) 0.055^{+}	3.476 (335.7)	1,623–1,823 (0.63)	5	pc 4N	Al; EPMA Nb/Nb (4.5% Al) (Boltzmann–Matano)	2 examples (c–x)	*Average (corrected value) $^{+}$Present extrapolation to $c = 0$		–	Ruiz-Aparicio (1993) [52.08]
Co	0.0418	2.664 (257.2)	1,347–2,173 (0.64)	19 (18T)	sc[61]	^{60}Co; vapor deposition; grinder	Several examples	Marked data scatter		52.02	Pelleg (1976) [52.09]
Co	(0.11) 0.115^{+}	2.845 (274.7)	1,580–1,920 (0.64)	6	pc[61]	Co, vapour deposition; EPMA Nb/Co*/Nb	2 examples (see Figure 01.02)	$^{+}$Present approximation *Thin film	Nb, Cu, Fe, Ni in Nb	52.02	Ablitzer (1977) [52.02]
Co	(0.11)*	(2.845)* (274.7)	1,582–2,163 (0.68)	6	pc 4N	^{60}Co, dried-on from salt solution; serial sectioning	No	*The temperatures of the measured D-values are fitted to $D(T)$ acc. to [52.02]	Nb, Cr, Fe in Nb; electro-transport	–	Serruys (1982) [52.10, 52.06]
Co	–	–	1,422–1,561 (0.54)	4	sc pc $>$4N	^{60}Co, vapour deposition; chemical sectioning	2 examples			52.02	Wenwer (1989) [52.11]
Cr	0.30	3.621 (349.6)	1,226–1,708 (0.54)	20 (12T)	sc $\sim$3N8	^{51}Cr, vapour deposition; anodizing and stripping	6 examples (total penetration depth $<1.5\,\mu$m; pronounced NSE at lower T)	Marked data scatter		–	Pelleg (1969) [52.12]
Cr	0.13	3.495 (337.5)	1,220–1,766 (0.54)	24 (17T)	pc $\sim$3N7	^{51}Cr, vapour deposition; anodizing and stripping	6 examples (total penetration depth $<2\,\mu$m; partly very flat pp)	Pronounced data scatter		–	Pelleg (1969) [52.13]
Cu	– (11.2)$^{+}$	$\sim$3.12 (301) (3.80)$^{+}$ (367)	1,829, 1,909 (0.68)	2	pc[61]	Co; EPMA Nb/Co*/Nb	No	$^{+}$Present calculation *Thin film	Nb, Co, Fe, Ni in Nb	–	Ablitzer (1977) [52.02]
Fe	0.14	3.049 (294.3)	1,664–2,168 (0.70)	9	pc[61]	^{59}Fe, electroplated and dried-on from salt solution; grinder and lathe	No		Nb, Co, Cu, Ni in Nb	52.02	Ablitzer (1977) [52.02]

Table 5.2 *(Continued)*

(1)	(2a)	(2b)	(3)	(4)	(5)	(6)	(7)	(8)	(9)	(10)	(11)	(12)
X	D^0 (10^{-4} m^2 s^{-1})	Q (eV) and (kJ mole)	$D(T_m)$ (10^{-12} m^2 s^{-1})	T-range (K) ($\bar{T}/T_m$)	No. of data points	Material, purity	Experimental method	Remarks on the pp	Further remarks	Also studied	Figure	Reference
Fe	(0.14)*	(3.049)* (294.3)		1,865–2,379 (0.77)	5	pc 4N	^{59}Fe, dried-on from salt solution; serial sectioning	No	*The temperatures of the measured D-values are fitted to $D(T)$ acc. to [52.02]	Nb, Co, Cr, Ni in Nb; electro-transport	–	Serruys (1982) [52.10], [52.06]
Mo	(92) (510.8)	(5.291)		1,998–2,455 (0.81)	7	pc ~2N7	Mo; EPMA thin film of Mo in Nb/Mo/Nb sandwich sample (Hall)	1 example	+Present approximation	Ti, V, W, Zr in Nb, Nb in V	52.03	Roux (1970) [52.14]
	200+	5.437+ (525.0)	2.0+									
Ni	0.077	2.736 (264.2)		1,434–1,533 (0.54)	10*	pc[61]	^{63}Ni, electroplated and dried-on from salt solution; residual activity	No	*Two strongly deviating data points	Nb, Co, Cu, Fe in Nb	52.04	Ablitzer (1977) [52.02]
P	(0.051) 0.057+	2.233 (215.6)		1,573–2,073 (0.67)	15 (6T)	sc 3N	^{32}P, surface reaction with H_3PO_4; residual activity	1 example	+Present approximation	P in Mo	52.04	Vandyshev (1968) [52.15]
Pd	2.4+	4.143+ (400)		1,965–2,341 (0.79)	6	pc[61]	Pd, vapour deposition (6 μm film); EPMA Nb/Pd/Nb	1 example	+Present approximation	Ru in Nb	52.05	Sathyaraj (1979) [52.16]
Ru	29+	4.764+ (460)		2,026–2,342 (0.80)	7	pc[61]	^{103}Ru, dried-on from salt solution; grinder and residual activity	2 examples	+Present approximation	Pd in Nb	52.06	Sathyaraj (1979) [52.16]
S	2,600	3.170 (306.1)		1,370–1,770 (0.57)	10[51] (7T)	sc pc ~2N5	^{35}S, dried-on from salt solution; serial sectioning	No			–	Vandyshev (1968) [52.17]
Sn	0.14	3.422 (330.4)	7.1	2,123–2,663 (0.88)	8 (5T)	pc (2–4 mm) 2N85	^{113}Sn, dried-on from salt solution[73]; lathe	No			52.06	Askill (1965) [52.18]
Ta	– 1.0	– 4.306 (415.8)		(1,376–2,346) 1,526–2,346 (0.71)	(11) 8	sc pc 2N75	^{182}Ta, dried-on from oxalate solution; grinder and anodizing and stripping	2 examples	Erroneous thermal expansion correction; pronounced data scatter	Nb in Nb	52.05	Lundy (1965) [52.01]

Ti	0.099	3.770 (364.0)		1,267–1,765 (0.55)	32 (17T)	sc ∼3N8	^{44}Ti, dried-on from salt solution; anodizing and stripping	5 examples[84] (total penetration depth $<1.5\,\mu$m)			–	Pelleg (1970) [52.19]
Ti	(0.4) 0.225^{+}	(3.838) (370.5) 3.739^{+} (361)	 3.0^{+}	1,898–2,348 (0.77)	11	pc ∼2N7	Ti; EPMA Nb/Nb (X% Ti)* (Hall)	1 example	$^{+}$Present approximation *X = 15–26	Mo, V, W, Zr in Nb, Nb in V	52.03	Roux (1970) [52.14]
U	(0.089)	(3.330) (321.6)		1,773–2,273 (0.74)	10^{51} (5T)	pc 2N55	^{235}U, vapour deposition; residual activity	No		U in β-Ti, β-Zr, Nb, Mo	–	Pavlinov (1965) [52.20]
U	(5×10^{-6})	(3.326) (321.1)		1,973–2,273 (0.77)	4^{51}	pc[61]	^{235}U, vapour deposition; serial sectioning	No		U in β-Zr, V, Nb, Ta, Mo, W	–	Fedorov (1971) [52.21]
V	0.47	4.293 (414.5)	3.1	1,898–2,348 (0.77)	8	pc ∼2N7	V; EPMA Nb/Nb (X% V)* (Hall)	No	*X = 4.7–20	Mo, Ti, W, Zr in Nb, Nb in V	52.07	Roux (1970) [52.14]
W	(7×10^{4}) $5\times10^{4+}$	(6.765) (653.2) 6.667^{+} (643.7)	 2.7^{+}	2,175–2,443 (0.84)	6	pc ∼2N7	W; EPMA Nb/Nb (X% W)* (Hall)	No	$^{+}$Present approximation *X = 16–18	Mo, Ti, V, Zr in Nb, Nb in V	–	Roux (1970) [52.14]
Y	1.5×10^{-3}	2.411 (232.8)		1,473–1,873 (0.61)	10 (5T)	sc 2N8	^{91}Y, dried-on from salt solution[73]; residual activity	No		Y in Ta, Mo, W	–	Gornyy (1971) [52.22]
Zr	0.47	3.773 (364.3)	5.4	1,855–2,357 (0.77)	7	pc ∼2N7	Zr; EPMA Nb/Nb (X% Zr)* (Hall)	No	*X = 13–21	Mo, Ti, V, W in Nb, Nb in V	52.07	Roux (1970) [52.14]
Zr	0.85	3.93 (379.5)	5.0	1,773–2,523 (0.79)	12 (8T)	sc 3N8	^{95}Zr, dried-on from oxalate solution*; grinder and anodizing and stripping	1 example	*Co-diffusion of ^{95}Nb and ^{95}Zr		52.07	Einziger (1978) [52.23]
Zr	0.28	3.70 (357.2)	4.3	1,855–2,523 (0.80)	(15)				Present rough fit to the data of [52.14, 52.23]		52.07	

Table 5.3 Diffusion in tantalum (References, see page 238)

(1)	(2a)	(2b)	(3)	(4)	(5)	(6)	(7)	(8)	(9)	(10)	(11)	(12)
X	D^0 (10^{-4} m^2 s^{-1})	Q (eV) and (kJ mole^{-1})	$D(T_m)$ (10^{-12} m^2 s^{-1})	T-range (K) ($\check{T}/T_m$)	No. of data points	Material, purity	Experimental method	Remarks on the pp	Further remarks	Also studied	Figure	Reference
Self-diffusion												
Ta	(0.124*) 0.09$^+$	4.280 (413.3)		1,523–2,578 (0.62)	14	sc pc 2N7	^{182}Ta, dried-on from oxalate solution^x and vapour deposition^x at $T<1{,}773$ K; grinder (3 samples) and anodizing and stripping (11 samples)	1 example	Erroneous thermal expansion correction *Calculated from $D_{Nb}/D_{Ta} \approx 1.85$ $^+$Present rough fit, disregarding the grinder results ^{x}Simultaneous diffusion of ^{182}Ta and ^{95}Nb	Nb in Ta	53.01	Pawel (1965) [53.01]
Ta	0.21 1.3×10^{-3} [21] ^{x} 1.0[21] ^{x}	4.39 (423.9) 3.80[21] ^{x} (366.9) 4.74[21] ^{x} (457.7)	5.6[21]	1,261–2,993 (0.65)	17	sc ~3N5	^{182}Ta, vapour deposition; grinder and IBS	Several examples	^{x}Two-exponential fit together with the data of [53.01]		53.01	Weiler (1983) [53.02]
Ta	1.89×10^{-3} [21] 1.16[21]	3.84[21] (370.8) 4.78[21] (461.5)	5.7[21]		(31)				Two-exponential fit to the data of [53.01, 53.02]		53.01	Neumann (1990) [53.03]
Impurity diffusion												
Al	(1.5)	(3.172) (306.2)		1,780–2,000 (0.57)	10[51]	pc[61]	Al; out-diffusion method; atomic absorption	–	Pronounced data scatter		–	Nikolaev (1978) [53.04]
Co	(0.93)$^+$	3.728$^+$ (360)		2,128, 2,330^x	2[51]	pc[61]	Co; EPMA, Ta/Co*/Ta	No	$^x D(2{,}128\,\text{K}) = 8.0 \times 10^{-13}$, $D(2{,}330\,\text{K}) = 1.4 \times 10^{-13}$ m^2 s^{-1} $^+$Present calculation *Thin film	Fe, Ni in Ta	53.02	Ablitzer (1976) [53.05]

Fe	0.059	3.417 (329.9)		2,050–2,330 (0.67)	4[51]	pc[61]	Fe; EPMA Ta/Fe*/Ta	No	*Thin film	Co, Ni in Ta	53.02	Ablitzer (1976) [53.05]
Mo	1.8×10^{-3}	3.513 (339.1)		2,023–2,503 (0.69)	3	pc[61]	^{99}Mo; residual activity		Probably dominated by gb diffusion	Co, Cr, Ta, W in Mo, Mo in Ni	–	Borisov (1968) [53.06]
Mo	0.28	4.553 (439.6)		2,198–2,449 (0.70)	4[51]	pc ~2N7	Mo; EPMA Ta/Mo (Hall)	No		Nb, Ta, V, W in Mo	53.03	Roux (1972) [53.07]
Nb	(0.23)	(4.280) (413.3)		1,194–2,757 (0.60)	25	sc pc	^{95}Nb, dried-on from salt solution[x] and vapour deposition[x]; lathe, grinder, anodizing and stripping	3 examples	Erroneous thermal expansion correction [x]Simultaneous diffusion of ^{95}Nb and ^{182}Ta	Ta in Ta	53.03	Pawel (1965) [53.01]
	0.32	4.384 (423.3)		2,376–2,757	8	2N7						
	0.068	4.133 (399.0)		1,194–2,278	17							
Nb	13.6[21]	5.30[21] (511.7)	12[21]	(1,194–2,757)	(25)				Two-exponential fit to the data of [53.01]		53.03	Neumann (1991) [53.08]
	0.0205[21]	3.96[21] (382.4)										
Ni	0.19[+]	3.335[+] (322)		2,050, 2,330	2[51]	pc[61]	Ni; EPMA Ta/Ni*/Ta	No	[x]$D(2{,}050\ \mathrm{K}) = 1.2 \times 10^{-13}$, $D(2{,}330\ \mathrm{K}) = 1.15 \times 10^{-12}\ \mathrm{m^2\ s^{-1}}$ [+]Present calculation *Thin film		53.02	Ablitzer (1976) [53.05]
S	100	3.036 (293.1)		1,970–2,110 (0.62)	4	pc 2N	^{35}S; residual activity	No	Marked gb contributions cannot be excluded	S in V	–	Fedorov (1969) [53.09]
U	(7.6 10^{-5}) 1.5 10^{-4} [+]	3.660 (353.4)		1,865–2,400 (0.65)	5[51]	pc[61]	^{235}U, vapour deposition; residual activity	No	[+]Corrected value	U in Mo, Nb, V, W, β-Zr	–	Fedorov (1971) [53.10]
Y	0.12	3.131 (302.3)		1,473–1,773 (0.49)	8 (4T)	sc 2N8	^{91}Y, dried-on from salt solution[73]; residual activity	1 example		Y in Mo, Nb, W	–	Gornyy (1971) [53.11]

Table 5.4 Self-diffusion and impurity diffusion in antimony (References, see page 238)

(1)	(2a)	(2b)	(3)	(4)	(5)	(6)	(7)	(8)	(9)	(10)	(11)	(12)
X	D^0 (10^{-4} m^2 s^{-1})	Q (eV) and (kJ mole^{-1})	$D(T_m)$ (10^{-12} m^2 s^{-1})	T-range (K) ($\hat{T}/T_m$)	No. of data points	Material, purity	Experimental method	Remarks on the pp	Further remarks	Also studied	Figure	Reference
Sb	$\perp$ 16.6	1.925 (185.9)	0.030	763–863 (0.90)	9[51] (8T)	sc 4N8	^{124}Sb, electroplated; grinder	2 examples (pronounced dislocation tail)	Extreme data scatter of $D_\perp$		–	Huntigton (1964) [54.01]
	// 22.2	2.042 (197.2)	0.009	775–889 (0.92)	6[51]							
Sb	–	–		657–856	36* (9T)	pc 3N	^{124}Sb, electroplated; residual activity	Several examples (gb contributions at deeper penetrations)	*Marked gb contributions at lower T		–	Hässner (1965) [54.02]
	1.05	1.713 (165.4)	0.029	746–856 (0.89)	22 (6T)							
Sb	$\perp$ (0.10)	1.552 (149.9)		773–903 (0.93)	15[51] (8T)	sc 6N	^{124}Sb; chemical etching	No	$^+$Present approximation		54.01	Cordes (1966) [54.03]
	0.11$^+$		0.024$^+$									
	// 56	2.082 (201.0)	0.014		13[51] (8T)							
Sb	0.26	1.605 (154.9)	0.029	708–863 (0.87)	5	pc 3N	^{124}Sb; serial sectioning	1 example		Ag, Sn in Sb; electro-transport	–	Kuzmenko (1973) [54.04]
Ag	(67)	1.240 (119.7)		603–879 (0.82)	6	pc 3N	^{110}Ag; serial sectioning	1 example	$^+$Present approximation	Sb, Sn in Sb; electro-transport	54.02	Kuzmenko (1973) [54.04]
	81$^+$		1,000$^+$									
Sn	0.03$^+$	1.336$^+$ (129)		723–763 (0.82)	3	pc 3N	^{113}Sn, ^{123}Sn; serial sectioning	No	$^+$Present approximation	Sb, Ag in Sb; electro-transport	54.02	Kuzmenko (1973) [54.04]

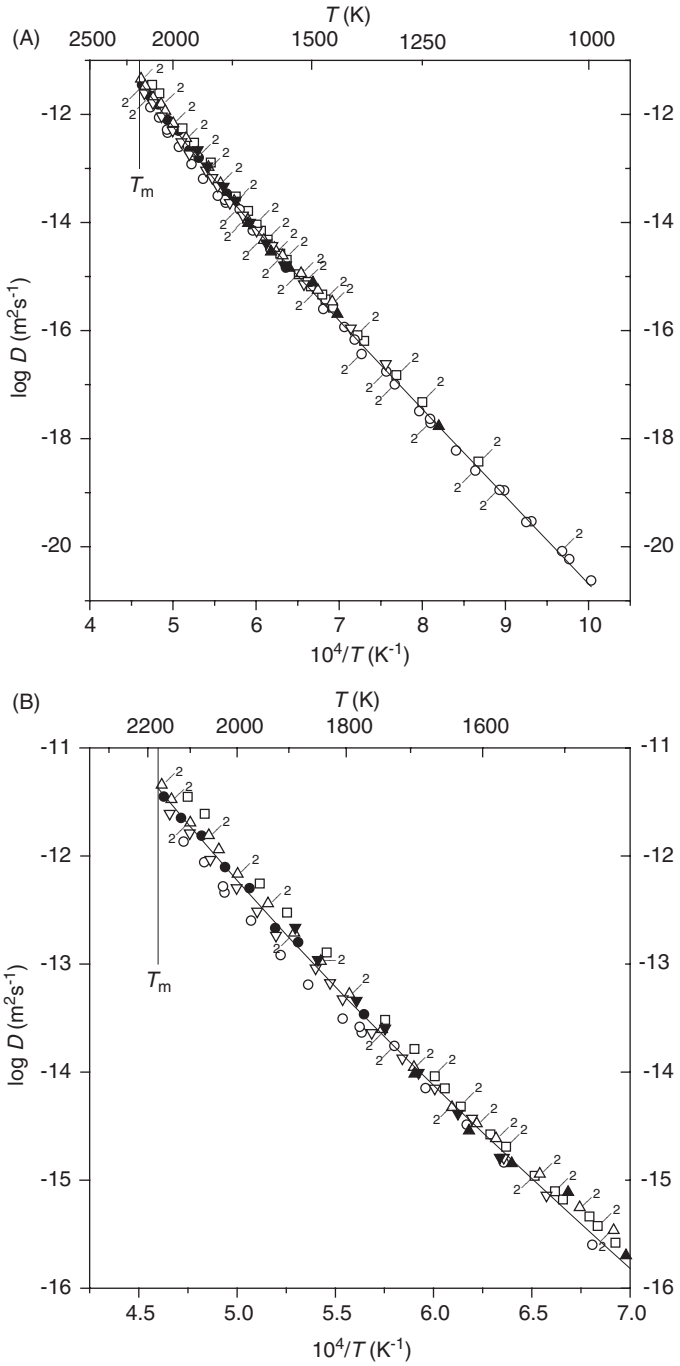

Fig. 51.01 (A) Self-diffusion in vanadium. ●, Lundy [51.01]; □, Peart [51.02]; ○, Pelleg [51.03]; △, Macht [51.04]; ▽, Ablitzer [51.05]; ▼, Pruthi [51.07]; ▲, Segel [51.09]. Fitting line: two-exponential fit according to Neumann [51.08]. (B) (Detail) Self-diffusion in vanadium. ●, Lundy [51.01]; □, Peart [51.02]; ○, Pelleg [51.03]; △, Macht [51.04]; ▽, Ablitzer [51.05]; ▼, Pruthi [51.07]; ▲, Segel [51.09]. Fitting line: two-exponential fit according to Neumann [51.08].

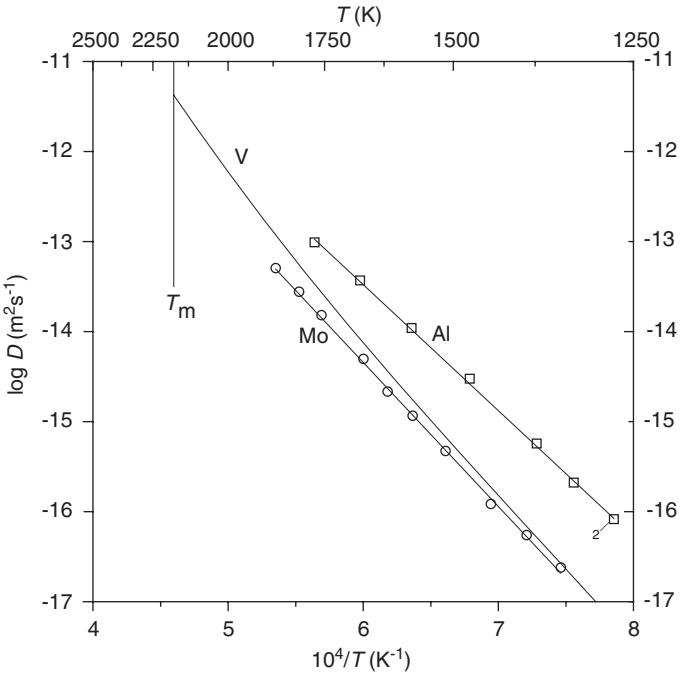

Fig. 51.02 Impurity diffusion in vanadium. Al in V: □, Maslov [51.10]; Mo in V: ○, Pelleg [51.17].

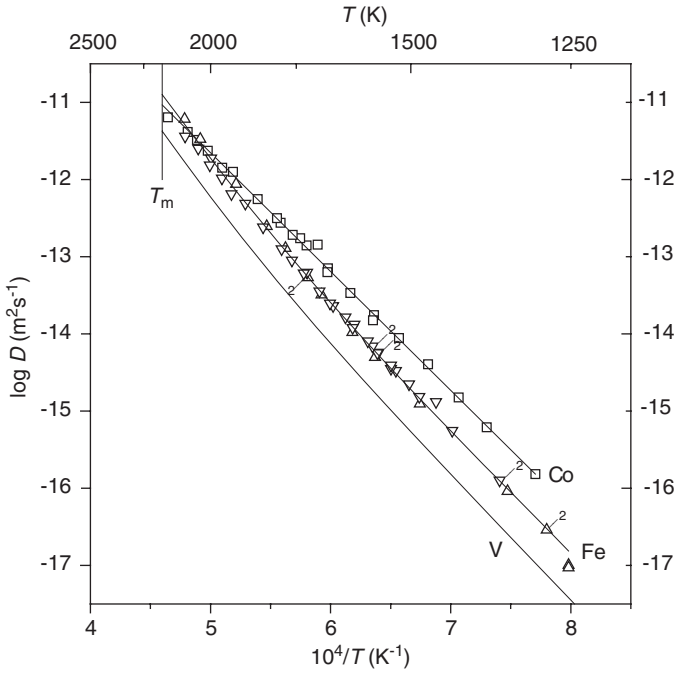

Fig. 51.03 Impurity diffusion in vanadium. Co in V: □, Pelleg [51.11]; Fe in V: △, Coleman [51.14]; ▽, Ablitzer [51.15]. Fitting line: two-exponential fit according to Neumann [51.16].

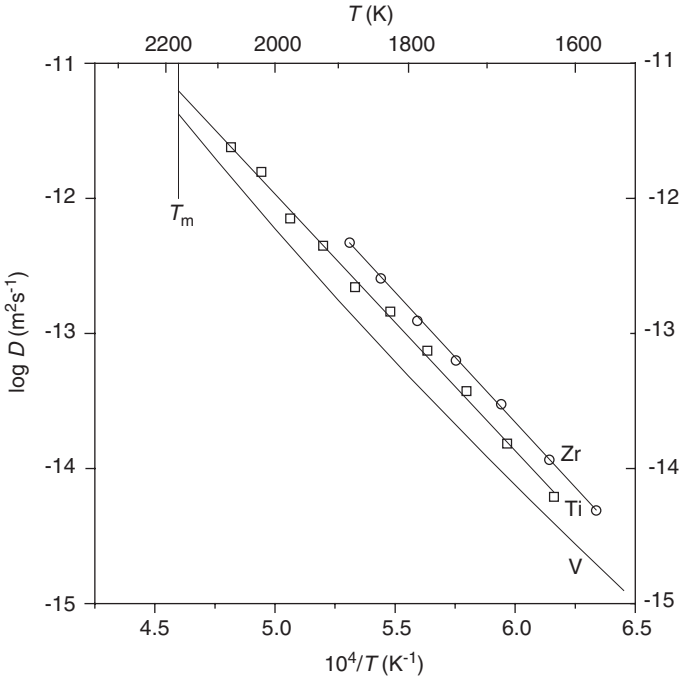

Fig. 51.04 Impurity diffusion in vanadium. Ti in V: □, Murdock [51.23]; Zr in V: ○, Pruthi [51.07].

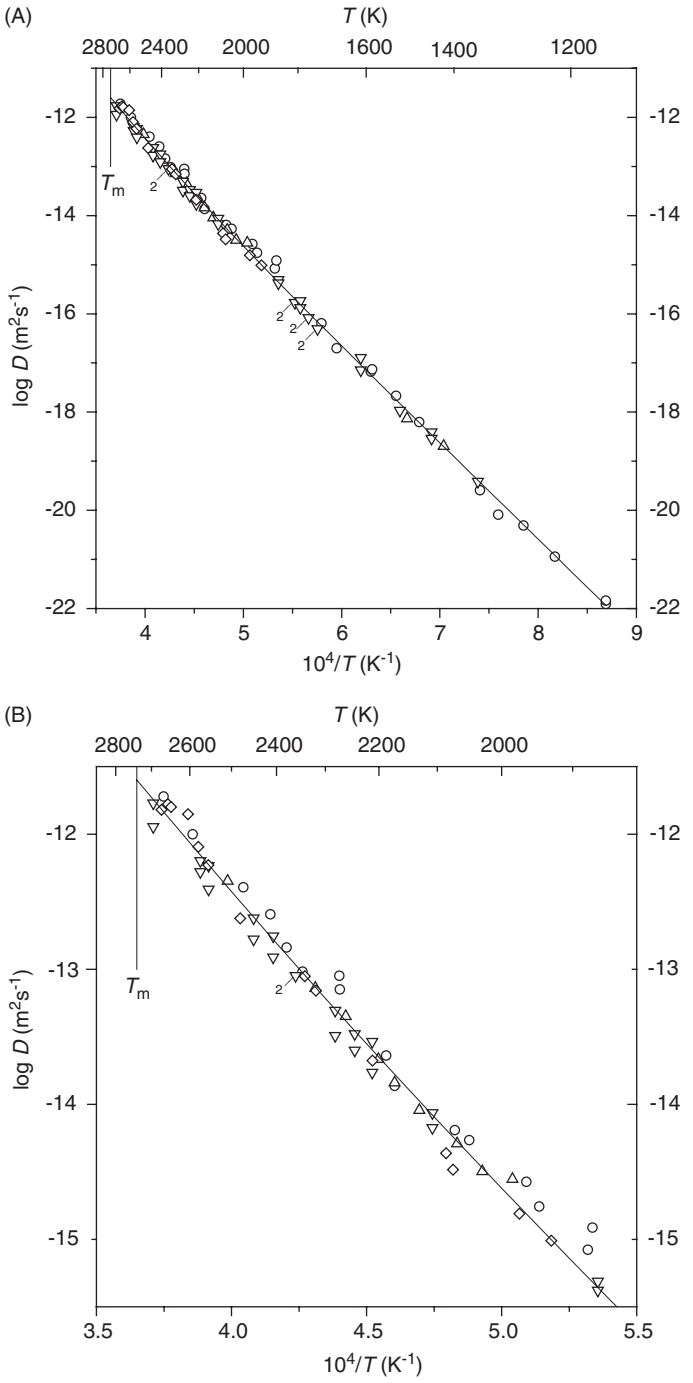

Fig. 52.01 (A) Self-diffusion in niobium. ○, Lundy [52.01] (disregarding four markedly deviating data points); △, Ablitzer [52.02]; ▽, Einziger [52.03]; ◇, Bussmann [52.04]. Fitting line: two-exponential fit according to Neumann [52.07]. (B) (Detail) Self-diffusion in niobium; ○, Lundy [52.01] (disregarding four markedly deviating data points); △, Ablitzer [52.02]; ▽, Einziger [52.03]; ◇, Bussmann [52.04]. Fitting line: two-exponential fit according to Neumann [52.07].

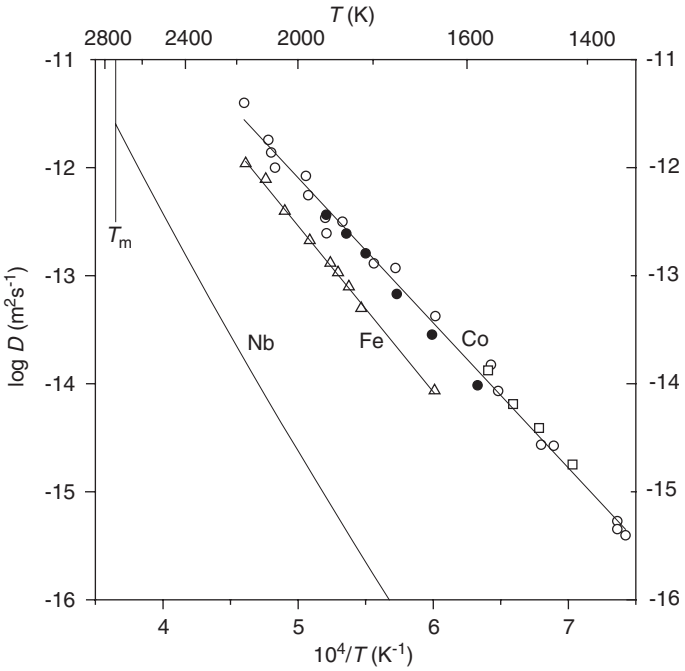

Fig. 52.02 Impurity diffusion in niobium. Co in Nb: ○, Pelleg [52.09]; ●, Ablitzer [52.02]; □, Wenwer [52.11]. Fitting line according to [52.09]. Fe in Nb: △, Ablitzer [52.02].

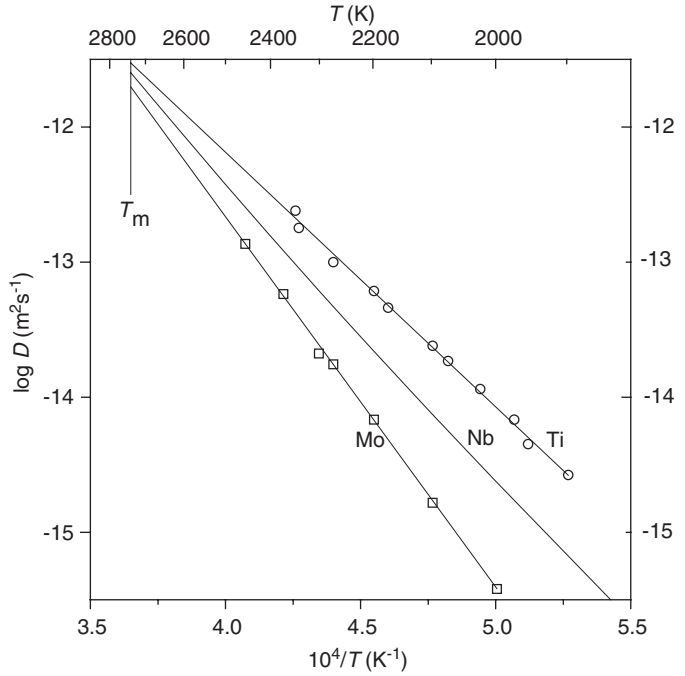

Fig. 52.03 Impurity diffusion in niobium. Mo in Nb: □, Roux [52.14]; Ti in Nb: ○, Roux [52.14].

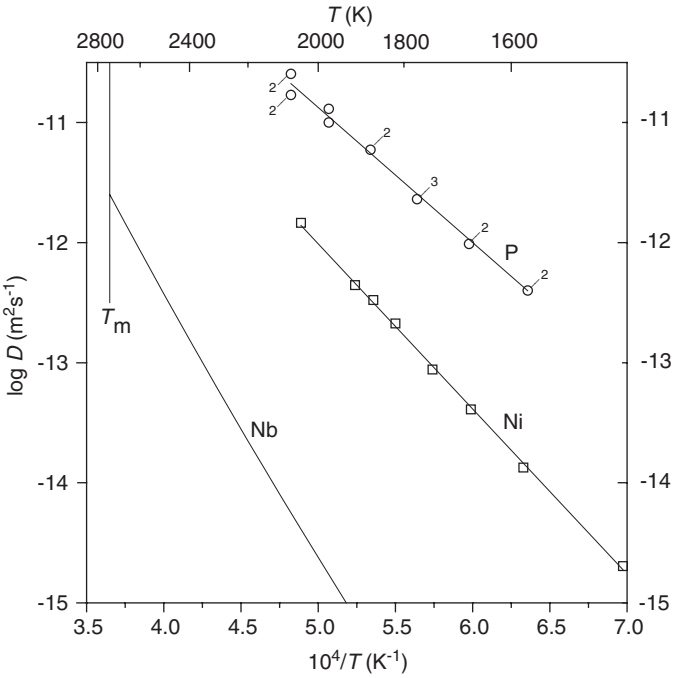

Fig. 52.04 Impurity diffusion in niobium. Ni in Nb: □, Ablitzer [52.02]; P in Nb: ○, Vandyshev [52.15].

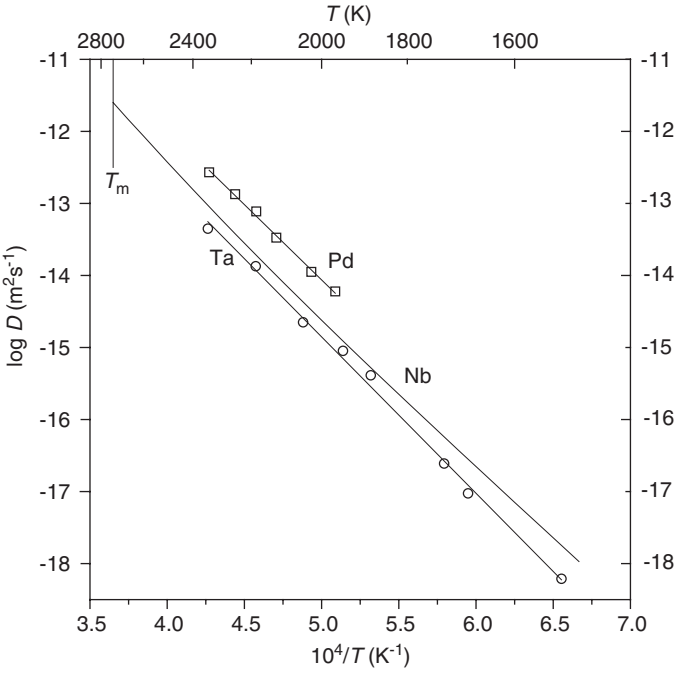

Fig. 52.05 Impurity diffusion in niobium. Pd in Nb: □, Sathyaraj [52.16]; Ta in Nb: ○, Lundy [52.01] (disregarding three markedly deviating data points).

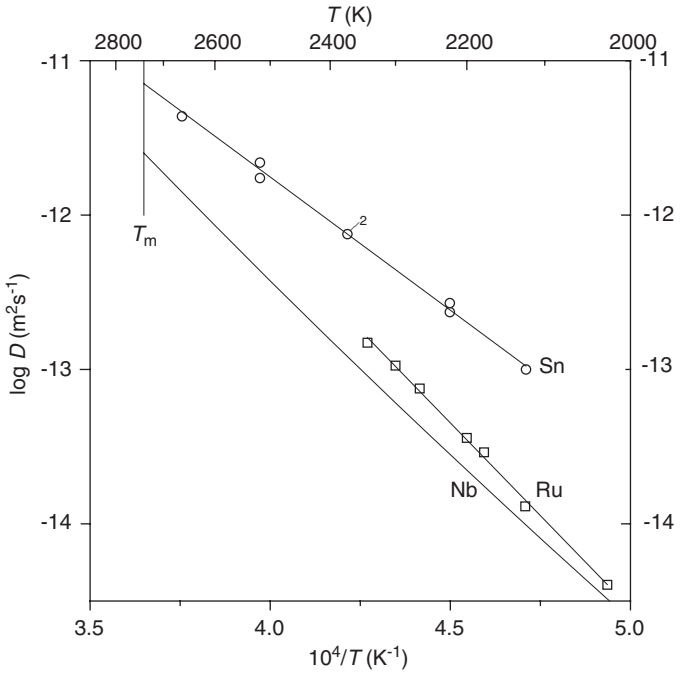

Fig. 52.06 Impurity diffusion in niobium. Ru in Nb: □, Sathyaraj [52.16]; Sn in Nb: ○, Askill [52.18].

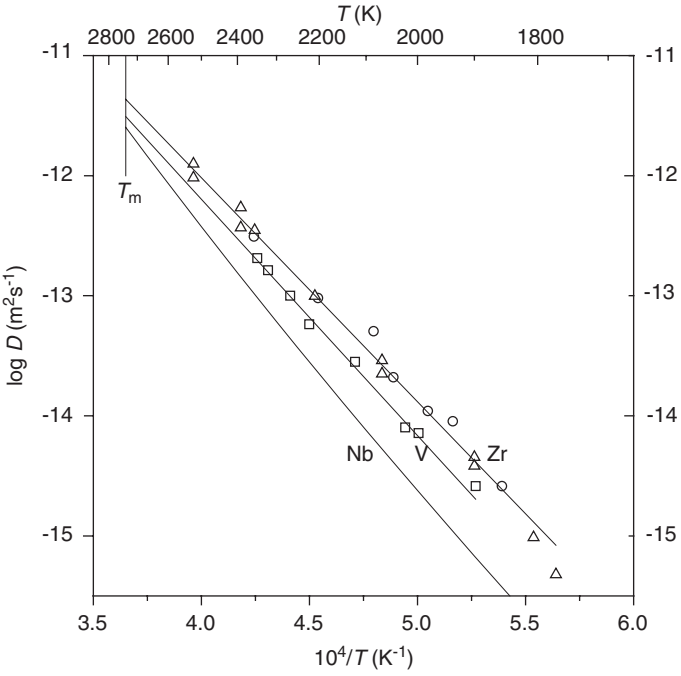

Fig. 52.07 Impurity diffusion in niobium. V in Nb: □, Roux [52.14]; Zr in Nb: ○, Roux [52.14]; Δ, Einziger [52.23]. Fitting line using $D^0 = 0.28 \times 10^{-4} m^2 s^{-1}$, $Q = 3.70$ eV.

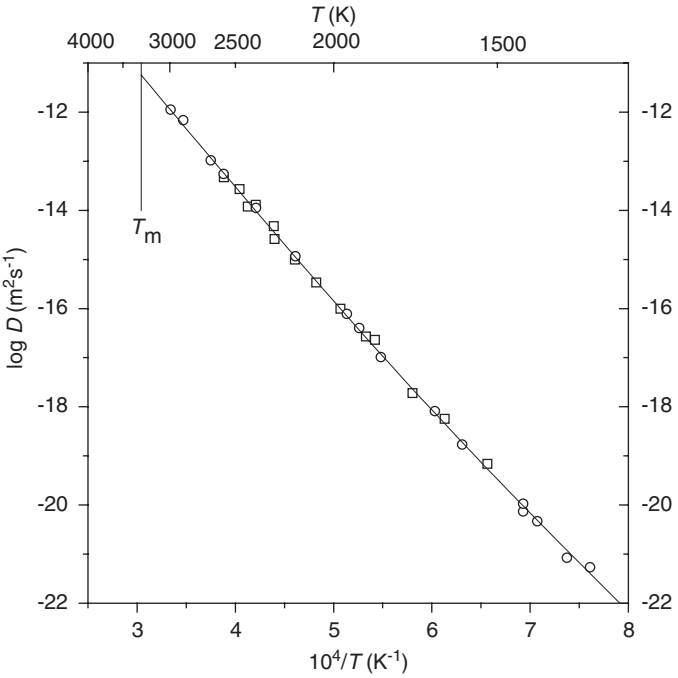

Fig. 53.01 Self-diffusion in tantalum. □, Pawel [53.01]; ○, Weiler [53.02]. Fitting line: two-exponential fit according to Neumann [53.03].

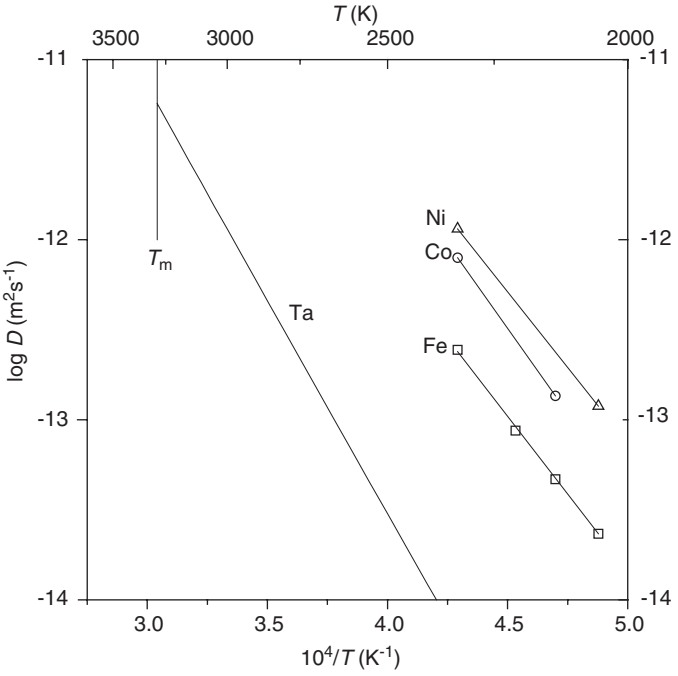

Fig. 53.02 Impurity diffusion in tantalum. Co in Ta: ○, Ablitzer [53.05]; Fe in Ta: □, Ablitzer [53.05]; Ni in Ta: △, Ablitzer [53.05].

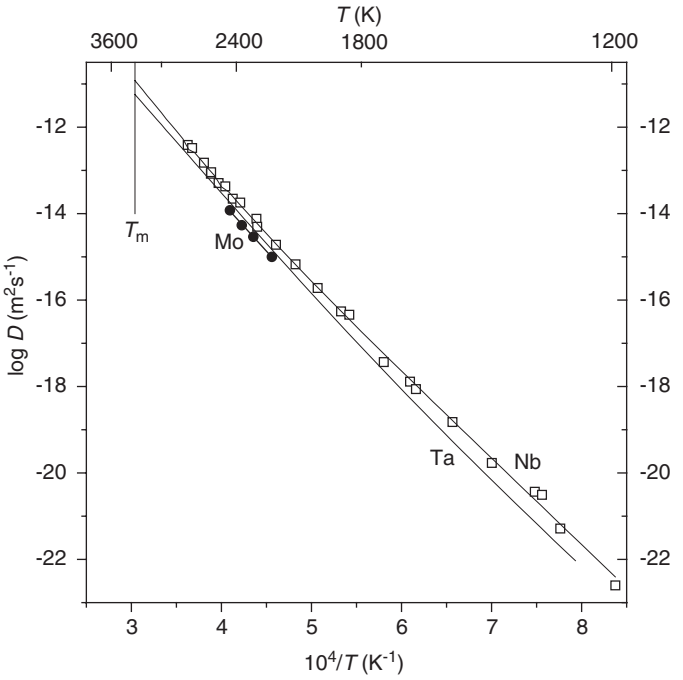

Fig. 53.03 Impurity diffusion in tantalum. Mo in Ta: ●, Roux [53.07]; Nb in Ta: □, Pawel [53.01]. Fitting line: two-exponential fit according to Neumann [53.08].

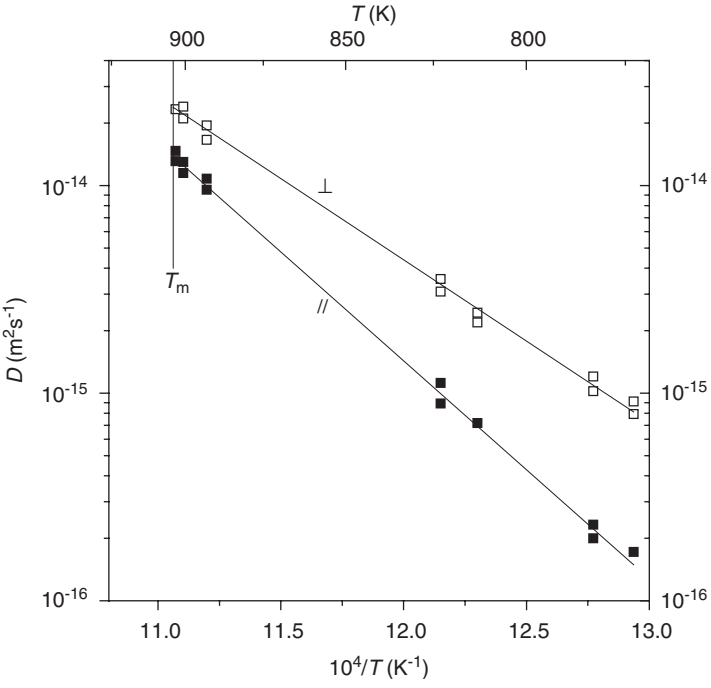

Fig. 54.01 Self-diffusion in antimony. □ and ■, Cordes [54.03].

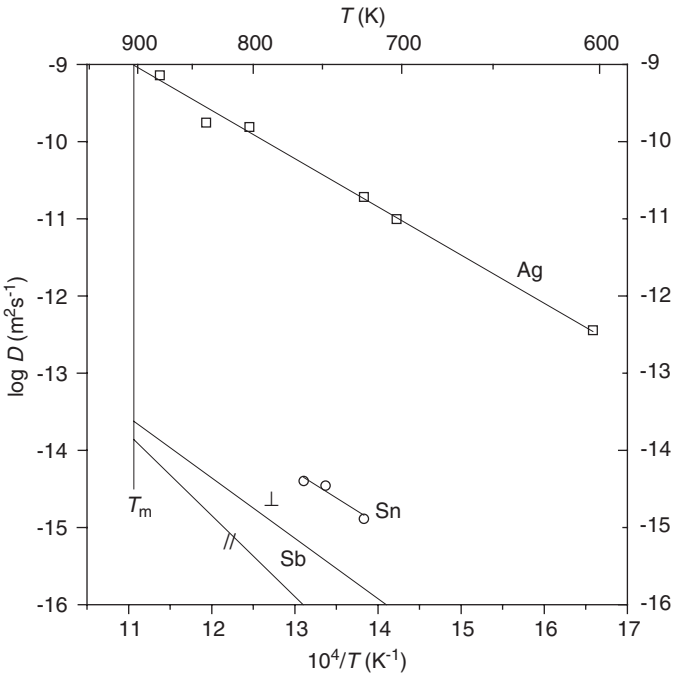

Fig. 54.02 Impurity diffusion in antimony. Ag in Sb: □, Kuzmenko [54.04]; Sn in Sb: ○, Kuzmenko [54.04].

REFERENCES

References to Chapter 5.0

[50.01] G.J. Beyer, A.F. Novgorodov, Radiochem. Radioanal. Lett. **27** (1976) 341.
[50.02] G.J. Beyer, W.D. Fromm, A.F. Novgorodov, Nucl. Instrum. Methods **146** (1977) 419.
[50.03] Y. Legoux, J. Merini, J. Less-Common Met. **166** (1990) 141.
[50.04] K.N. Gedgovd, A.I. Krasovskiy, S.M. Novikov, Fiz. Met. Metalloved. **50** (1980) 437; Phys. Met. Metallogr. **50** (2) (1980) 185 (English transl.).
[50.05] M.G. Karpman, G.V. Shcherbedinski, G.N. Dubinin, G.P. Benediktova, Metalloved. Termichesk. Obrab. Met. (3) (1967) 46.
[50.06] W.P. Ellis, N.H. Nachtrieb, J. Appl. Phys. **40** (1969) 472.

References to Chapter 5.1

[51.01] T.S. Lundy, C.J. McHargue, Trans. AIME **233** (1965) 243.
[51.02] R.F. Peart, J. Phys. Chem. Sol. **26** (1965) 1853.
[51.03] J. Pelleg, Phil. Mag. **29** (1974) 383.
[51.04] M.P. Macht, G. Frohberg, H. Wever, Z. Metallk. **70** (1979) 209.
[51.05] D. Ablitzer, J.P. Haeussler, K.V. Sathyaraj, Phil. Mag. A **47** (1983) 515.
[51.06] B. Günther, O. Kanert, Acta Metall. **31** (1983) 909.
[51.07] D.D. Pruthi, R.P. Agarwala, Phil. Mag. A **49** (1984) 263.
[51.08] G. Neumann, V. Tölle, Phil. Mag. A **61** (1990) 563.

[51.09] V. Segel, J. Pelleg, Phil. Mag. A **76** (1997) 1203.
[51.10] I.A. Maslov, V.M. Mironov, A.V. Pokoyev, Fiz. Met. Metalloved. **60** (1985) 193; Phys. Met. Metallogr. **60** (1) (1985) 180 (English transl.).
[51.11] J. Pelleg, Phil. Mag. **32** (1975) 593.
[51.12] J. Pelleg, Phil. Mag. A **72** (1995) 1547.
[51.13] J. Pelleg, Phil. Mag. A **71** (1995) 431.
[51.14] M.G. Coleman, C.A. Wert, R.F. Peart, Phys. Rev. **175** (1968) 788.
[51.15] D. Ablitzer, J.P. Haeussler, K.V. Sathyaraj, A. Vignes, Phil. Mag. A **44** (1981) 589.
[51.16] G. Neumann, V. Tölle, Z. Metallk. **82** (1991) 741.
[51.17] J. Pelleg, Y. Zaklos, Phil. Mag. A **63** (1991) 439.
[51.18] F. Roux, A. Vignes, Rev. Phys. Appl. **5** (1970) 393.
[51.19] J. Pelleg, Phil. Mag. A **54** (1986) L21.
[51.20] B.A. Vandyshev, A.S. Panov, Izv. Akad. Nauk SSSR, Met. (2) (1970) 231.
[51.21] B.A. Vandyshev, A.S. Panov, Izv. Akad. Nauk SSSR, Met. (1) (1969) 244.
[51.22] J. Pelleg, M. Herman, Phil. Mag. **35** (1977) 349.
[51.23] J.F. Murdock, C.J. McHargue, Acta Metall. **16** (1968) 493.
[51.24] J. Pelleg, Rev. High-Temp. Mater. **4** (1978) 5.
[51.25] G.B. Fedorov, E.A. Smirnov, F.I. Zhomov, V.N. Gusev, S.A. Paraev, Atomn. Energiya **31** (1971) 516; Sov. Atom. Energy **31** (1971) 1280 (English transl.).

Further Investigations

V [51.26] R.P. Agarwala, S.P. Murarka, M.S. Anand, Acta Metall. **16** (1968) 61.
V [51.27] J.F. Tiers, Y. Chabre, J. Phys. F: Metal Phys. **11** (1981) 1943; NMR
Cr [51.28] J. Pelleg, Phys. Stat. Sol. (a) **147** (1995) 361; Influence of oxygen on the diffusivity.
Cr [51.29] R.A. Wolfe, H.W. Paxton, Trans. AIME **230** (1964) 1426.

References to Chapter 5.2

[52.01] T.S. Lundy, F.R. Winslow, R.E. Pawel, C.J. McHargue, Trans. AIME **233** (1965) 1533.
[52.02] D. Ablitzer, Phil. Mag. **35** (1977) 1239.
[52.03] R.E. Einziger, J.N. Mundy, H.A. Hoff, Phys. Rev. B **17** (1978) 440.
[52.04] W. Bussmann, Ch. Herzig, H.A. Hoff, J.N. Mundy, Phys. Rev. B **23** (1981) 6216.
[52.05] Y. Serruys, Scr. Metall. **16** (1982) 365.
[52.06] Y. Serruys, G. Brebec, in: DIMETA 82, *Diffusion in Metals and Alloys*, Eds. F.J. Kedves, D.L. Beke, Trans. Tech. Publ., Aedermannsdorf, Switzerland (1983), p. 351.
[52.07] G. Neumann, V. Tölle, Phil. Mag. A **61** (1990) 563.
[52.08] J.G.L. Ruiz-Aparicio, F. Ebrahimi, J. Alloys Compds. **202** (1993) 117.
[52.09] J. Pelleg, Phil. Mag. **33** (1976) 165.
[52.10] Y. Serruys, G. Brebec, Phil. Mag. A **45** (1982) 563.
[52.11] F. Wenwer, N.A. Stolwijk, H. Mehrer, Z. Metallk. **80** (1989) 205.
[52.12] J. Pelleg, Phil. Mag. **19** (1969) 25.
[52.13] J. Pelleg, J. Less-Common Met. **17** (1969) 319.
[52.14] F. Roux, A. Vignes, Rev. Phys. Appl. **5** (1970) 393; see also F. Roux, *Thesis*, Univ. Nancy (1972).
[52.15] B.A. Vandyshev, A.S. Panov, Fiz. Met. Metalloved. **26** (1968) 517; Phys. Met. Metallogr. **26** (3) (1968) 138 (English transl.).
[52.16] K.V. Sathyaraj, D. Ablitzer, C. Demangeat, Phil. Mag. A **40** (1979) 541.
[52.17] B.A. Vandyshev, A.S. Panov, Izv. Akad. Nauk SSSR, Met. (1) (1968) 206.
[52.18] J. Askill, Phys. Stat. Sol. **9** (1965) K167.
[52.19] J. Pelleg, Phil. Mag. **21** (1970) 735.
[52.20] L.V. Pavlinov, A.I. Nakonechnikov, V.N. Bykov, Atomn. Energiya **19** (1965) 521; Sov. Atom. Energy **19** (1965) 1495 (English transl.).
[52.21] G.B. Fedorov, E.A. Smirnov, F.I. Zhomov, V.N. Gusev, S.A. Paraev, Atomn. Energiya **31** (1971) 516; Sov. Atom. Energy **31** (1971) 1280 (English transl.).

[52.22] D.S. Gornyy, R.M. Altovskiy, Fiz. Met. Metalloved. **31** (1971) 781; Phys. Met. Metallogr. **31** (4) (1971) 108 (English transl.).
[52.23] R.E. Einziger, J.N. Mundy, Phys. Rev. B **17** (1978) 449.

Further Investigations

Nb [52.24] R. Resnick, L.S. Castleman, Trans. AIME **218** (1960) 307.
Nb [52.25] R.F. Peart, D. Graham, D.H. Tomlin, Acta Metall. **10** (1962) 519.
Nb [52.26] V.D. Lyubimov, P.V. Geld, G.P. Shveykin, Izv. Akad. Nauk SSSR Metall. Gorn. Delo (5) (1964). 137; Izv. Akad. Nauk SSSR Met. (2) (1967) 84.
Nb [52.27] G.B. Fedorov, F.I. Zhomov, E.A. Smirnov, Met. Metalloved. Chist. Met. (8) (1969) 145.
Al [52.28] G.I. Nikolaev, N.V. Bodrov, Zh. Fiz. Khim. **52** (1978) 1430; Russian J. Phys. Chem. **52** (1978) 821 (English transl.); out-diffusion method.
Co see Ref. [52.25].
Cr see Ref. [52.10].
Fe see Ref. [52.25].
Mo [52.29] G.B. Fedorov, E.A. Smirnov, V.N. Gusev, F.I. Zhomov, V.L. Gorbenko, Met. Metalloved. Chist. Met. (10) (1973) 62.
Ni [52.30] R.P. Agarwala, K. Hirano, Trans. Japan Inst. Met. **13** (1972) 425.
Ta see Ref. [52.05].
V [52.31] R.P. Agarwala, S.P. Murarka, M.S. Anand, Acta Metall. **16** (1968) 61.
W see Ref. [52.27].

References to Chapter 5.3

[53.01] R.E. Pawel, T.S. Lundy, J. Phys. Chem. Sol. **26** (1965) 937.
[53.02] D. Weiler, K. Maier, H. Mehrer, in: DIMETA 82, *Diffusion in Metals and Alloys*, Eds. F.J. Kedves, D.L. Beke, Trans. Tech. Publ., Aedermannsdorf, Switzerland (1983), p. 342.
[53.03] G. Neumann, V. Tölle, Phil. Mag. A **61** (1990) 563.
[53.04] G.I. Nikolaev, N.V. Bodrov, Zh. Fiz. Khim. **52** (1978) 1430; Russian J. Phys. Chem. **52** (1978) 821 (English transl.).
[53.05] D. Ablitzer, M. Gantois, La Diffusion dans les Milieux Condensés, Théorie et Applications, Centre Etudes Nucléaires Saclay **1** (1976) 299.
[53.06] E.V. Borisov, P.L. Gruzin, S.V. Zemskii, Zash. Pokryt. Met. (2) (1968) 104; see also Diffus. Data **3** (1969) 289.
[53.07] F. Roux, *Thesis*, Univ. Nancy (1972).
[53.08] G. Neumann, V. Tölle, Z. Metallk. **82** (1991) 741.
[53.09] B.A. Vandyshev, A.S. Panov, Izv. Akad. Nauk SSSR, Met. (1) (1969) 244.
[53.10] G.B. Fedorov, E.A. Smirnov, F.I. Zhomov, V.N. Gusev, S.A. Paraev, Atomn. Energiya **31** (1971) 516; Sov. Atom. Energy **31** (1971) 1280 (English transl.).
[53.11] D.S. Gornyy, R.M. Altovskiy, Fiz. Met. Metalloved. **31** (1971) 781; Phys. Met. Metallogr. **31** (4) (1971) 108 (English transl.).

References to Chapter 5.4

[54.01] H.B. Huntington, P.B. Ghate, J.H. Rosolowski, J. Appl. Phys. **35** (1964) 3027.
[54.02] A. Hässner, R. Hässner, Phys. Stat. Sol. **11** (1965) 575.
[54.03] H. Cordes, K. Kim, J. Appl. Phys. **37** (1966) 2181.
[54.04] P.P. Kuzmenko, G.P. Grinevich, Metallofizika **47** (1973) 98.

CHAPTER 6

Self-Diffusion and Impurity Diffusion in Group VI Metals

Contents

Tables
6.1. Chromium (Cr) 240
6.2. Molybdenum (Mo) 241
6.3. Tungsten (W) 244
Figures
Chromium 247
Molybdenum 248
Tungsten 250
References 254

The first investigations of **chromium** self-diffusion were performed on polycrystalline samples at lower temperatures [60.01–60.09]. The results strongly refer to the dominance of grain-boundary diffusion with diffusion energies smaller than 3.3 eV.

Diffusion coefficients derived from out-diffusion of spallation products in **molybdenum** (Rb, Se, Sr, Y, Zn, Zr) [60.10] and **tungsten** (rare earth metals, Ba, Ce, Y) [60.11] are not taken into consideration in this data collection (see Chapter 0.1).

Diffusion of the almost insoluble alkaline metals was investigated in single as well as polycrystals of **molybdenum** (Li [60.12, 60.13], Na, K [60.14], Cs [60.15, 60.16]) and **tungsten** (Li [60.13], Na, K [60.17], Cs [60.16]) at temperatures lower than 0.7 T_m. In general, extremely low diffusion energies were observed which refer to dominating grain-boundary and dislocation diffusion. Note that Cs could not be detected in single crystals of molybdenum and tungsten. The results of alkaline metal diffusion are not listed in Tables 6.2 and 6.3.

Sulphur (S), **selenium** (Se) and **tellurium** (Te) are not topic of the present data collection.

In Table 6.0 lattice structure, lattice constant and melting temperature of the group VI metals are listed.

Table 6.0 Lattice structure, lattice constant a and melting temperature T_m

Metal	Cr	Mo	W
Structure	bcc	bcc	bcc
T_m (K)	2,130	2,893	3,673
a (nm)	0.302	0.315	0.316

Table 6.1 Self-diffusion and impurity diffusion in chromium (References, see page 255)

(1)	(2a)	(2b)	(3)	(4)	(5)	(6)	(7)	(8)	(9)	(10)	(11)	(12)
X	D^0 (10^{-4} m^2 s^{-1})	Q (eV) and (kJ mole^{-1})	$D(T_m)$ (10^{-12} m^2 s^{-1})	T-range (K) ($\overline{T}/T_m$)	No. of data points	Material, purity	Experimental method	Remarks on the pp	Further remarks	Also studied	Figure	Reference
Cr	970	4.510 (435.4)	2.1	1,369–2,093 (0.81)	31 (24T)	sc 4N5	^{51}Cr, ^{48}Cr, dried-on from salt solution and vapour deposition; grinder	3 examples		V in Cr; $E = 0.52-0.31$ (1,714–2,093 K)	61.01	Mundy (1976) [61.01]
Cr	(46) 40^+ 1,280*	4.20 (405.5) 4.58* (442.2)	1.9*	1,073–1,446 (0.59)	7 (38)	sc 4N	^{51}Cr, vapour deposition; IBS	2 examples (dislocation tails)	$^+$Present approximation *Fit together with the data of [61.01]		61.01	Mundy (1981) [61.02]
Fe	–	–		1,260–1,700	7^{51} (6T)	pc[61]	^{55}Fe, vapour deposition; residual activity	No	Strongly enhanced diffusivities below 1,523 K	Cr in V; Fe, Cr in Fe(Cr)	–	Wolfe (1964) [61.03]
	0.47	3.439 (332.0)		1,523–1,700 (0.76)	4^{51}							
Mo	($2.7\,10^{-3}$)	(2.515) (242.8)		1,373–1,693 (0.72)	5	pc[61]	^{99}Mo; residual activity		Probably dominated by gb diffusion	Mo in Ni	–	Gruzin (1963) [61.04]
V	86^+	4.09^+ (394.9)	$(1.8)^+$	1,595–2,041 (0.85)	6 (4T)	sc 4N5	^{48}V, dried-on from salt solution; grinder	No	$^+$Present approximation	Cr in Cr	61.02	Mundy (1976) [61.01]

Table 6.2 Diffusion in molybdenum (References, see page 255)

(1)	(2a)	(2b)	(3)	(4)	(5)	(6)	(7)	(8)	(9)	(10)	(11)	(12)
X	D^0 (10^{-4} m^2 s^{-1})	Q (eV) and (kJ mole^{-1})	$D(T_m)$ (10^{-12} m^2 s^{-1})	T-range (K) ($\overline{T}/T_m$)	No. of data points	Material, purity	Experimental method	Remarks on the pp	Further remarks	Also studied	Figure	Reference
Self-diffusion												
Mo	(4) 5.7[+]	4.987 (481.5)		2,073–2,448 (0.78)	5[51]	pc 2N3 (0.7% W)	[99]Mo, electroplated; residual activity	No	[+]Present fit to the depicted data	W in Mo	62.01	Borisov (1959) [62.01]
Mo	2.77	4.814 (464.8)		1,973–2,193 (0.72)	3[51]	pc (1–2 mm) ~3N	[99]Mo, electroplated; serial sectioning	No			62.01	Bronfin (1960) [62.02]
Mo	8* 139[21] 0.13[21]	5.056* (488.2) 5.69[21] (549.4) 4.53[21] (437.4)	1.8[21]	1,360–2,773 (0.71)	12 (11T)	sc 4N	[99]Mo, vapour and sputter deposition; IBS and grinder	All	*Forced fit	Ta in Mo at 2,373 K	62.01	Maier (1973) [62.03]
Impurity diffusion												
Co	3.0	4.337 (418.7)	8.3	2,213–2,603 (0.83)	6[51]	pc (1–2 mm) 3N7	[60]Co, electroplated; autoradiography*	1 example	*Annealed in argon atmosphere	Nb, Co, Fe in Nb	–	Peart (1962) [62.04]
Co	18	4.627 (446.8)	15	2,123–2,603 (0.82)	15 (9T)	pc 3N7 sc 4N	[60]Co, electroplated[73]; serial sectioning*	No	*Annealed in vacuum, strong influence of argon atmosphere observed	Nb in Mo	62.02	Askill (1965) [62.05] [62.06]
Cr	1.88	3.517 (339.6)		1,273–1,423 (0.47)	4	sc ~2N7	[51]Cr; residual activity	No	Marked gb contributions cannot be excluded		–	Mulyakayev (1971) [62.07]
Fe	0.15	3.586 (346.3)		1,273–1,623 (0.50)	16 (8T)	pc 3N6	[59]Fe; residual activity	3 examples			62.02	Nohara (1973) [62.08]
Nb	1,000	6.028 (582.0)		2,073–2,436 (0.78)	3[51]	pc	Nb; EPMA Mo/Mo (50% Nb)				62.03	Winklelman (1963) [62.09]

Table 6.2 *(Continued)*

(1)	(2a)	(2b)	(3)	(4)	(5)	(6)	(7)	(8)	(9)	(10)	(11)	(12)
X	D^0 (10^{-4} m^2 s^{-1})	Q (eV) and (kJ mole^{-1})	$D(T_m)$ (10^{-12} m^2 s^{-1})	T-range (K) ($\overline{T}/T_m$)	No. of data points	Material, purity	Experimental method	Remarks on the pp	Further remarks	Also studied	Figure	Reference
Nb	(2.9) 4.5$^+$	(5.898) (569.4) 4.974$^+$ (480.2)		2,098–2,455 (0.79)	5	pc 3N	Nb; EPMA Mo/Nb (Hall)	No	$^+$Present fit to the tabulated data	Ta, V, W in Mo, Mo in Ta, Mo, Ti, V, W, Zr in Nb	62.03	Roux (1972) [62.10]
Nb	0.017	3.929 (379.3)		1,973–2,273 (0.73)	4	pc[61]	^{95}Nb; residual activity	No		Mo, Zr in Mo	62.03	Fedorov (1973) [62.11]
P	(0.19) 0.245$^+$	3.491 (337.1)		2,273–2,493 (0.82)	10 (5T)	sc 3N7	^{32}P, surface reaction with $H_3PO_4^{73}$; residual activity	1 example	$^+$Present approximation	P in Nb	62.04	Vandyshev (1968) [62.12]
Re	0.097	4.107 (396.5)		1,973–2,373 (0.75)	6	pc[61]	^{186}Re, electroplated; serial sectioning	No			62.05	Bronfin (1964) [62.13]
S	(320) 3,800$^+$	(4.380) (422.9) 5.43$^+$ (524.3)		2,493–2,743 (0.90)	10 (5T)	sc 3N7	^{35}S, dried-on[73]; grinder	No (erfc-solutions)	$^+$Present fit to the tabulated data		62.04	Vandyshev (1968) [62.14]
Ta	1.9	4.900 (473.1)		2,098–2,449 (0.79)	5	pc 3N	Ta; EPMA Mo/Ta (Hall)	No		Nb, V, W in Mo, Mo in Ta, Mo, Ti, V, W, Zr in Nb	62.03	Roux (1972) [62.10]

Ta	–	–	2,373	1[x]	sc 4N	^{182}Ta*; grinder	1 example	*Simultaneous diffusion of ^{182}Ta and ^{99}Mo [x]$D = 1.09 \times 10^{-14}\ m^2\ s^{-1}$	Mo in Mo	62.03	Maier (1979) [62.03]
U	(7.6×10^{-3}) (3.313) (319.9)		1,773–2,273 (0.70)	10^{51} (5T)	pc 3N8	^{235}U, vapour deposition; residual activity	No		U in β-Ti, β-Zr, Nb	–	Pavlinov (1965) [62.15]
U	(1.3×10^{-6}) (3.278) (316.5)		2,073–2,373 (0.77)	5^{51}	pc[61]	^{235}U, vapour deposition; serial sectioning	No		U in β-Zr, V, Nb, Ta, W	–	Fedorov (1971) [62.16]
V	2.9 4.900 (473.1)		1,998–2,449 (0.77)	7 (6T)	pc 3N	V; EPMA Mo/V and Mo/Mo (X% V) (Hall)	No	$X = 15$–22	Nb, Ta, W in Mo, Mo in Ta, Mo, Ti, V, W, Zr in Nb	62.05	Roux (1972) [62.10]
W	(140) 150[+] 5.898 (569.4)		2,093–2,453 (0.79)	16 (12T)	pc 3N	W; EPMA Mo/W and Mo/Mo (X% W) (Hall)	No	[+]Present approximation; $X = 21$–64	Nb, Ta, V in Mo, Mo in Ta, Mo, Ti, V, W, Zr in Nb	62.05	Roux (1972) [62.10]
W	3.6 5.343 (515.8)		2,173–2,541 (0.81)	4	sc[61]	W, sputter deposition (1 μm film); EPMA	No		Mo in W	–	Erley (1974) [62.17]
Y	1.8×10^{-4} 2.225 (214.8)		1,473–1,873 (0.58)	5	sc 2N8	^{91}Y, dried-on from salt solution[73]; residual activity	No	Pronounced data scatter	Y in Nb, Ta, W	–	Gornyy (1971) [62.18]
Zr	(1.9×10^{-3}) 2.1×10^{-3} [+] 3.794 (366.4)		2,073–2,373 (0.77)	4	pc[61]	^{95}Zr; residual activity	No	[+]Present approximation	Mo, Nb in Mo	–	Fedorov (1973) [62.11]

Table 6.3 Diffusion in tungsten (References, see page 256)

(1)	(2a)	(2b)	(3)	(4)	(5)	(6)	(7)	(8)	(9)	(10)	(11)	(12)
X	D^0 (10^{-4} m^2 s^{-1})	Q (eV) and (kJ mole^{-1})	$D(T_m)$ (10^{-12} m^2 s^{-1})	T-range (K) ($\overline{T}/T_m$)	No. of data points	Material, purity	Experimental method	Remarks on the pp	Further remarks	Also studied	Figure	Reference
Self-diffusion												
W	1.88	6.084 (587.4)		2,073–2,676 (0.65)	7	sc[61]	^{188}W, vapour deposition; anodizing and stripping	No (dislocation tails at deeper penetrations; see Ta in W)	Erroneous thermal expansion corrections	Nb, Ta in W	63.01	Pawel (1969) [63.01]
W	15.3	6.487 (626.4)		2,042–2,819 (0.66)	20 (8T)	sc ~5N	^{187}W, sputter deposition; anodizing and stripping	Several examples			63.01	Arkhipova (1977) [63.02]
W	46[21] 0.04[21]	6.9[21] (666.2) 5.45[21] (526.2)	1.7[21]	1,705–3,409 (0.70)	51 (49T)	sc 5N	^{187}W, ^{185}W, vapour deposition of irradiated WCl_6; grinder and anodizing and stripping	4 examples[83]	Marked data scatter, temperature uncertainties up to ±40 K		63.01	Mundy (1978) [63.03]
W	200[21] 0.13[21]	7.33[21] (707.7) 5.62[21] (542.6)	2.0[21]	(1,705–3,409)	(52)				Two-exponential fit to the data of [63.01, 63.03]		63.01	Neumann (1990) [63.04]
Impurity diffusion												
Co	0.16 0.71$^+$	5.147 (497.0) 5.410$^+$ (522.4)		1,684–2,265 (0.54) (1,773–2,265)	7 6	sc ~5N	^{57}Co, electroplated; anodizing and stripping	All	$^+$Present approximation		63.02	Klotsman (1992) [63.05]
Cr	0.89	5.669 (547.4)		2,084–2,658 (0.65)	12 (11T)	sc[61]	Cr, sputter deposition*; SIMS	All ($(\ln c_0/c)^{½}$ vs. x)	*Simultaneous diffusion of Cr and Mo	Mo in W	63.02	Klotsman (1989) [63.06]
Fe	–	–		2,300	1*	sc ~5N	Fe; SIMS	1 example	*$D = 7.2 \times 10^{-17}$ m^2 s^{-1}; simultaneous diffusion of Fe, Mn, Ni	Mn, Ni in W at 2,300 K	63.03	Klotsman (1995) [63.07]

Hf	2.19* 3.63+	5.777* (557.8) 5.884+ (568.1)	2,017–2,571 (0.62)	8 (5T)	sc ~5N	Hf, vapour deposition[x]; SIMS	All (partly erfc-solutions)	*Disregarding three deviating data points +Present least-squares fit to all data points [x]Simultaneous diffusion of Hf and Mo	Mo in W	63.04	Klotsman (1996) [63.08]
Ir	0.32	5.243 (506.2)	2,007–2,960 (0.68)	11	sc[61]	^{192}Ir, vapour deposition; grinder and anodizing and stripping	Several examples		Os, Ta in W	63.05	Arkhipova (1984) [63.09]
Mn	–	–	2,300	1*	sc ~5N	Mn; SIMS	1 example	*$D = 5.9 \times 10^{-17}$ m^2 s^{-1}; simultaneous diffusion of Fe, Mn, Ni	Fe, Ni in W at 2,300 K	63.03	Klotsman (1995) [63.07]
Mo	1.45	5.875 (567.3)	2,084–2,529 (0.63)	9 (8T)	sc[61]	Mo, sputter deposition[x]; SIMS	All ($(\ln c_0/c)^{½}$ vs. x)	[x]Simultaneous diffusion of Mo and Cr	Cr in W	63.06	Klotsman (1989) [63.06]
Mo	1.4	5.864 (566.2)	2,017–2,483 (0.61)	18 (12T)	sc ~5N	Mo, vapour deposition[x]; SIMS	All (partly erfc-solutions)	[x]Simultaneous diffusion of Mo and Hf	Hf in W	63.06	Klotsman (1996) [63.08]
Nb	3.01	5.967 (576.1)	1,578–2,640 (0.57)	14	sc[61]	^{95}Nb, vapour deposition; anodizing and stripping	1 example	Erroneous thermal expansion correction	W, Ta in W	63.07	Pawel (1969) [63.01]
Ni	–	–	2,300	1*	sc ~5N	Ni; SIMS	1 example	*$D = 1.03 \times 10^{-16}$ m^2 s^{-1}; simultaneous diffusion of Fe, Mn, Ni	Fe, Mn in W at 2,300 K	63.03	Klotsman (1995) [63.07]
Os	0.64	5.577 (538.5)	2,105–2,928 (0.69)	12	sc[61]	^{186}Os, vapour deposition; grinder and anodizing and stripping	Several examples		Ir, Ta in W	63.05	Arkhipova (1984) [63.09]
P	26.8	5.282 (510.0)	2,153–2,453 (0.63)	12 (4T)	sc 4N	^{32}P; serial sectioning	No	Pronounced data scatter		–	Iovkov (1978) [63.10]
Re	4.0	6.184 (597.1)	2,113–2,906 (0.68)	13	sc ~4N	^{186}Re, sputter deposition; grinder and anodizing and stripping	Several examples			63.04	Arkhipova (1982) [63.11]

Table 6.3 *(Continued)*

(1)	(2a)	(2b)	(3)	(4)	(5)	(6)	(7)	(8)	(9)	(10)	(11)	(12)
X	D^0 (10^{-4} m^2 s^{-1})	Q (eV) and (kJ mole^{-1})	$D(T_m)$ (10^{-12} m^2 s^{-1})	T-range (K) ($\overline{T}/T_m$)	No. of data points	Material, purity	Experimental method	Remarks on the pp	Further remarks	Also studied	Figure	Reference
S	2.17×10^{-5}	3.027 (292.3)		2,153–2,453 (0.63)	11 (4T)		^{35}S, dried-on; serial sectioning	No	Pronounced data scatter		–	Iovkov (1972) [63.12]
Sc	2.96*	5.802* (560.2)		1,978–2,467 (0.61)	6	sc ~5N	Sc; SIMS	Several examples	*Disregarding D(2,294 K)	Ti, V in W	63.08	Klotsman (1996) [63.13]
Ta	3.05	6.067 (585.8)		1,578–2,648 (0.58)	12	sc[61] pc	^{182}Ta, vapour deposition; grinder and anodizing and stripping	4 examples (gb and dislocation tails at deeper penetrations)	Erroneous thermal expansion correction	W, Nb in W	63.08	Pawel (1969) [63.01]
Ta	6.2	6.232 (601.7)		2,102–2,906 (0.68)	8	sc[61]	^{182}Ta, vapour deposition; grinder and anodizing and stripping	All		Ir, Os in W	63.08	Arkhipova (1984) [63.09]
Ta	–	–		2,115, 2,309	2	sc[61]	Ta; SIMS	2 examples		Cr in W	63.08	Klotsman (1987) [63.14]
Ti	–	–		2,085	2* (1T)	sc ~5N	Ti; SIMS	2 examples	*D(2,085 K) = 1.18×10^{-18} m^2 s^{-1}	Sc, V in W	63.03	Klotsman (1996) [63.13]
U	0.018	4.033 (389.4)		2,030–3,000 (0.68)	13 (12T)	pc 4N	Mainly ^{235}U; out-diffusion from U-doped W filaments; mass spectrometry	No		Rb in β-Zr	–	Schwegler (1968) [63.15]
U	2×10^{-3}	4.488 (433.4)		1,973–2,473 (0.61)	5	pc[61]	^{235}U, vapour deposition; serial sectioning	No		U in Mo, Nb, Ta, V, β-Zr	–	Fedorov (1971) [63.16]
V	–	–		2,085, 2,293	2*	sc ~5N	V; SIMS	2 examples	*D(2,085 K) = 1.03×10^{-18}, D(2,293 K) = 1.99×10^{-17} m^2 s^{-1}	Sc, Ti in W	63.03	Klotsman (1996) [63.13]
Y	6.7×10^{-3}	2.953 (285.1)		1,473–1,873 (0.46)	10 (5T)	sc 2N8	^{91}Y, dried-on from salt solution[73]; residual activity	No		Y in Mo, Nb, Ta	–	Gornyy (1971) [63.17]

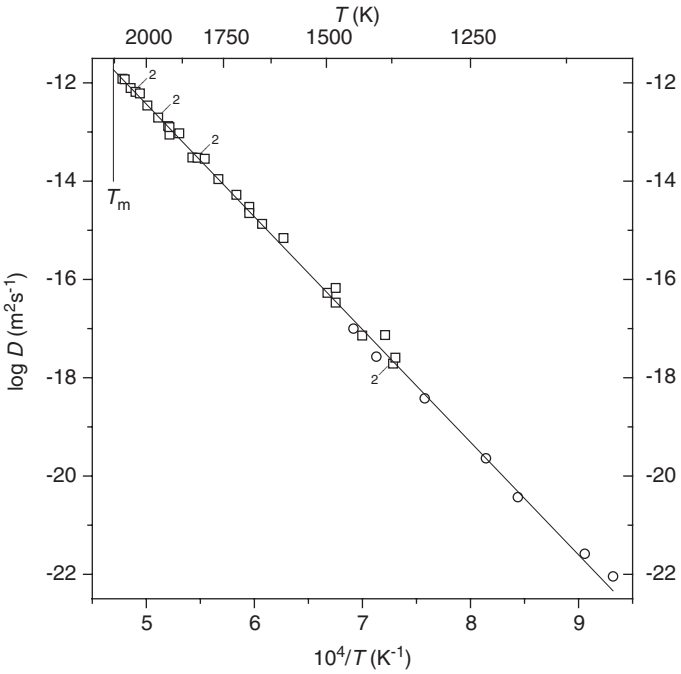

Fig. 61.01 Self-diffusion in chromium. □, Mundy [61.01]; ○, Mundy [61.02]. Fitting line using $D^0 = 0.11\,m^2\,s^{-1}$, $Q = 4.55\,eV$.

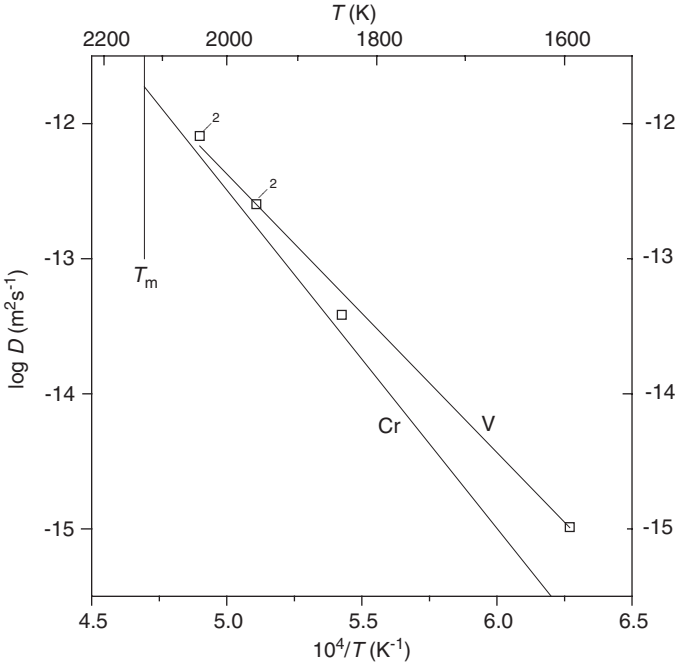

Fig. 61.02 Impurity diffusion in chromium. V in Cr: □, Mundy [61.01]. Fitting line using $D^0 = 86 \times 10^{-4}\,m^2\,s^{-1}$, $Q = 4.09\,eV$.

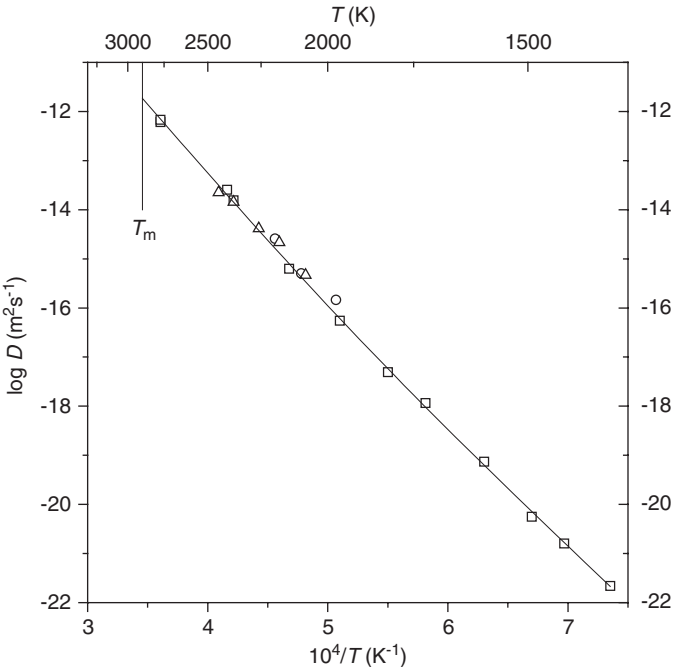

Fig. 62.01 Self-diffusion in molybdenum. △, Borisov [62.01]; ○, Bronfin [62.02]; □, Maier [62.03]. Fitting line according to [62.03].

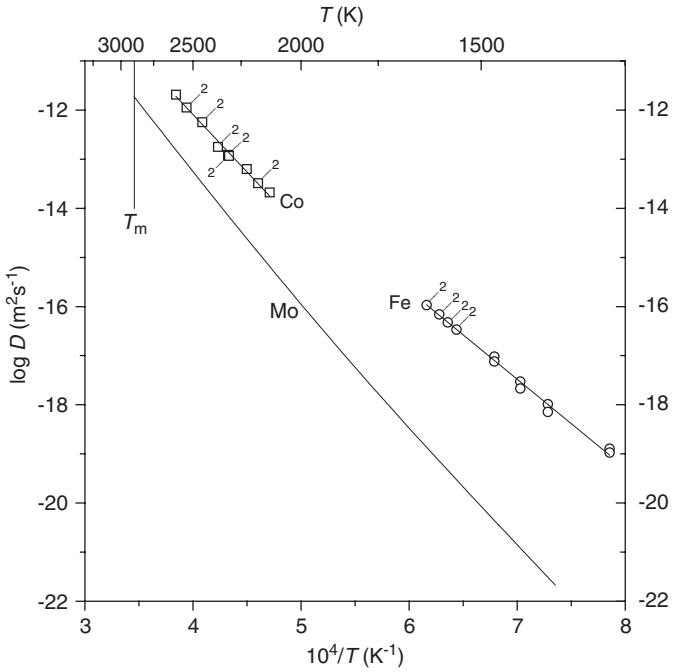

Fig. 62.02 Impurity diffusion in molybdenum. Co in Mo: □, Askill [62.05]; [62.06]. Fe in Mo: ○, Nohara [62.08].

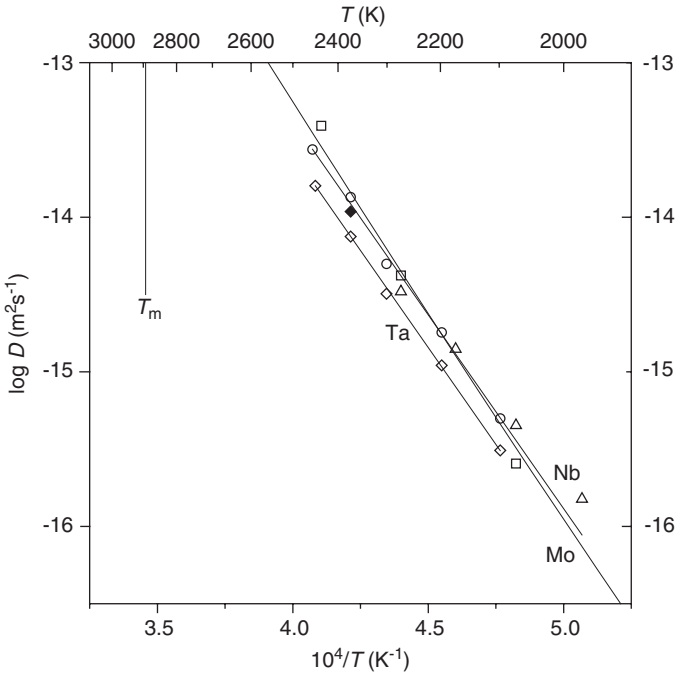

Fig. 62.03 Impurity diffusion in molybdenum. Nb in Mo: □, Winklelman [62.09]; ○, Roux [62.10]; △, Fedorov [62.11]. Fitting line according to [62.10]. Ta in Mo: ◇, Roux [62.10]; ◆, Maier [62.03]. Fitting line according to [62.10].

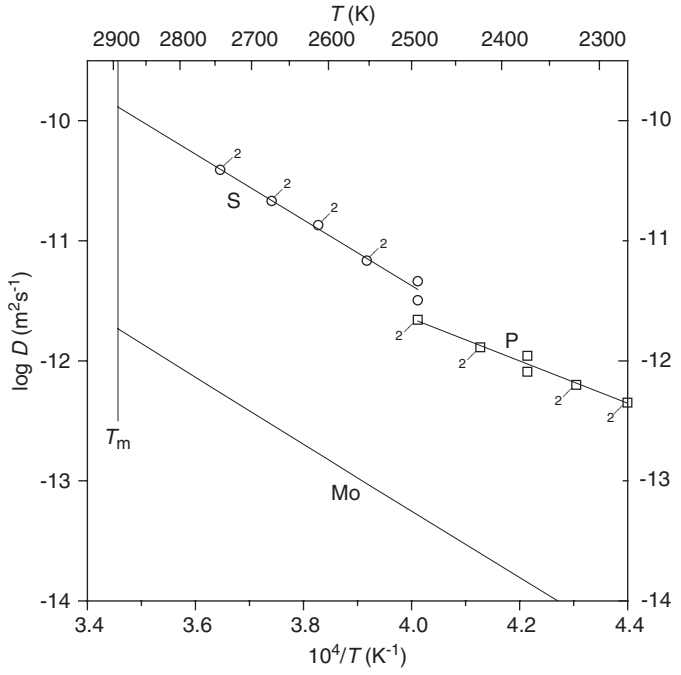

Fig. 62.04 Impurity diffusion in molybdenum. P in Mo: □, Vandyshev [62.12]. S in Mo: ○, Vandyshev [62.14].

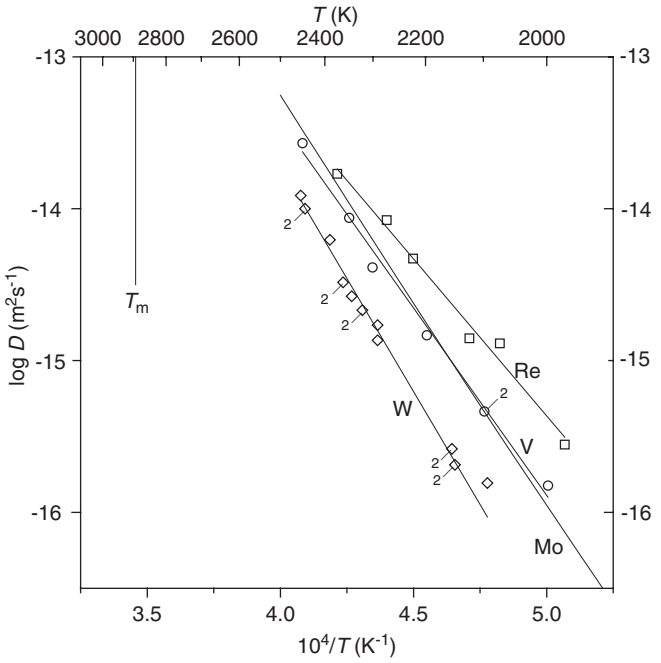

Fig. 62.05 Impurity diffusion in molybdenum. Re in Mo: □, Bronfin [62.13]. V in Mo: ○, Roux [62.10]. W in Mo: ◇, Roux [62.10]

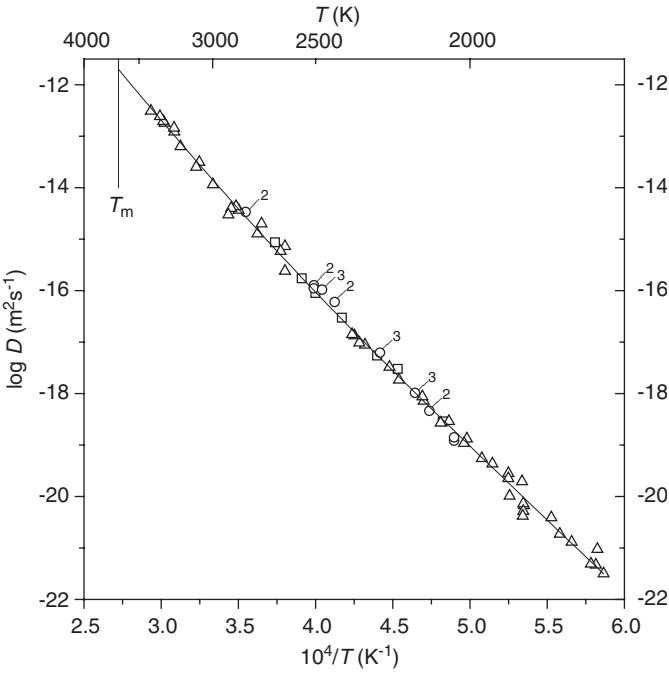

Fig. 63.01 Self-diffusion in tungsten. □, Pawel [63.01]; ○, Arkhipova [63.02]; △, Mundy [63.03]. Fitting line: two-exponential fit according to Neumann [63.04].

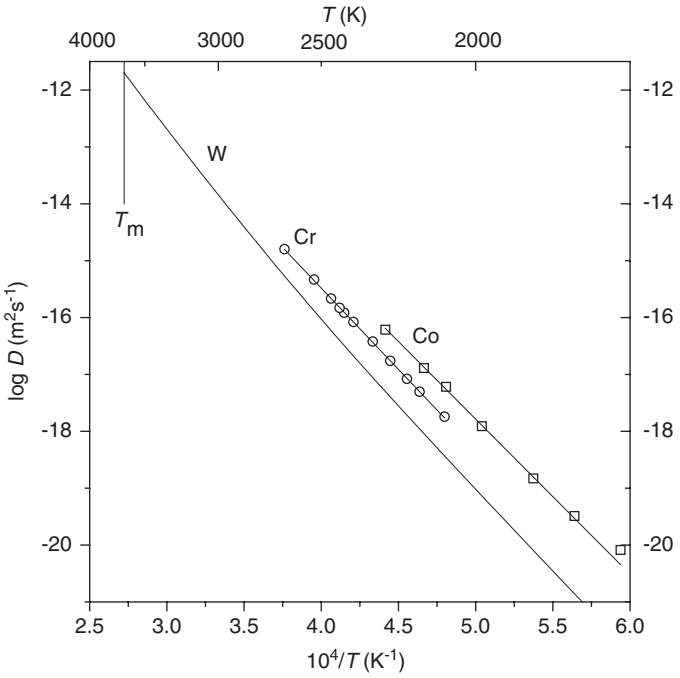

Fig. 63.02 Impurity diffusion in tungsten. Co in W: □, Klotsman [63.05]. Fitting line using $D^0 = 0.71 \times 10^{-4}\,m^2\,s^{-1}$, $Q = 5.41\,eV$; Cr in W: ○, Klotsman [63.06].

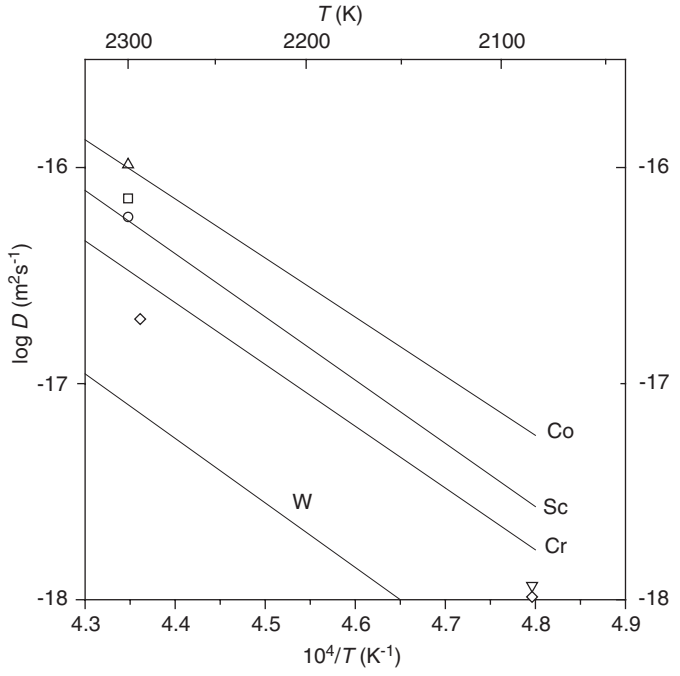

Fig. 63.03 Impurity diffusion in tungsten. Fe in W: □, Klotsman [63.07]; Mn in W: ○, Klotsman [63.07]; Ni in W: △, Klotsman [63.07]; Ti in W: ∇, Klotsman [63.13]; V in W: ◇, Klotsman [63.13].

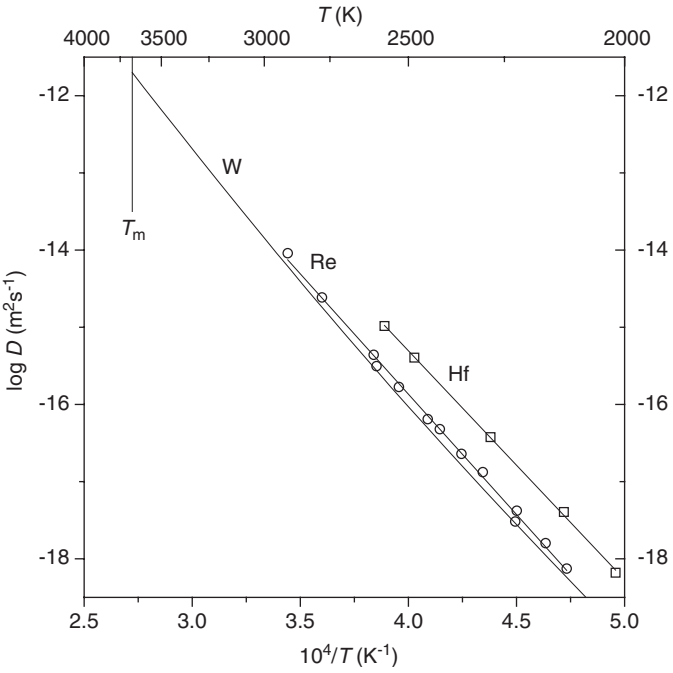

Fig. 63.04 Impurity diffusion in tungsten. Hf in W: □, Klotsman [63.08]. Fitting line using $D^0 = 3.63 \times 10^{-4}\,m^2\,s^{-1}$, $Q = 5.88\,eV$. Re in W: ○, Arkhipova [63.11].

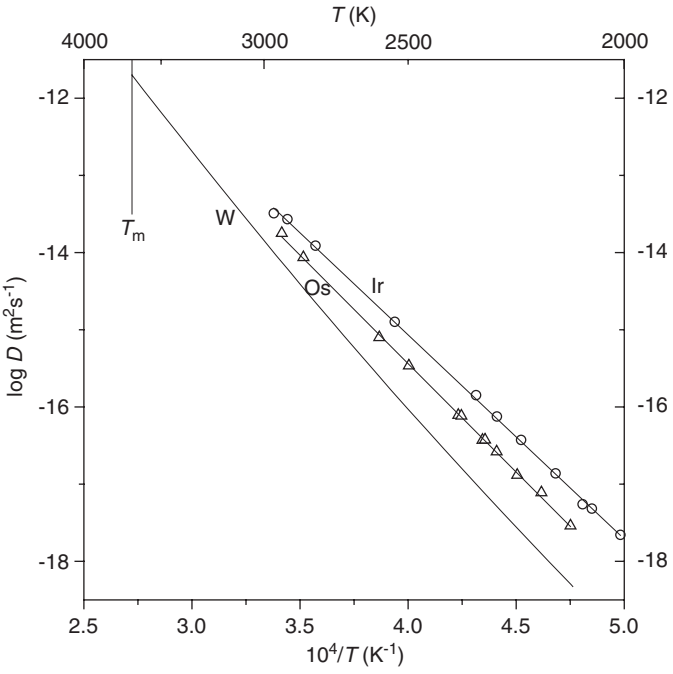

Fig. 63.05 Impurity diffusion in tungsten. Ir in W: ○, Arkhipova [63.09]; Os in W: △, Arkhipova [63.09].

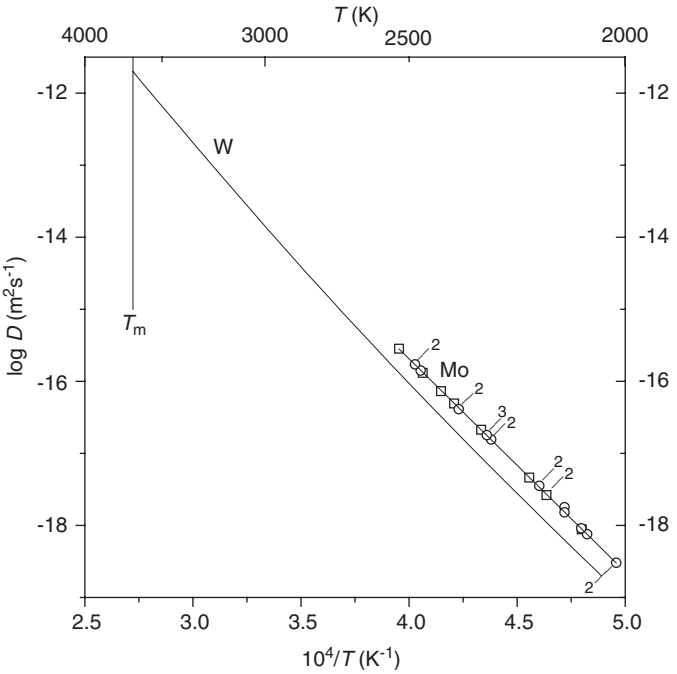

Fig. 63.06 Impurity diffusion in tungsten. Mo in W: □, Klotsman [63.06]; ○, Klotsman [63.08]. Fitting line according to [63.06].

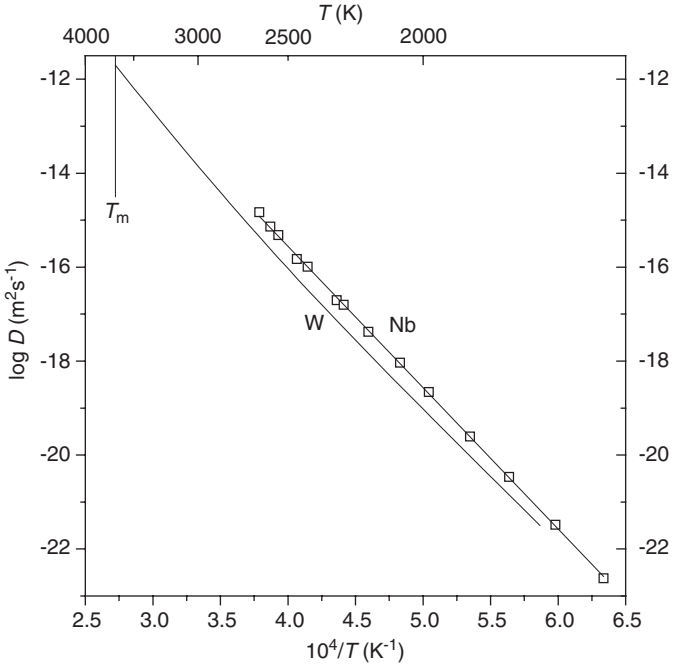

Fig. 63.07 Impurity diffusion in tungsten. Nb in W: □, Pawel [63.01].

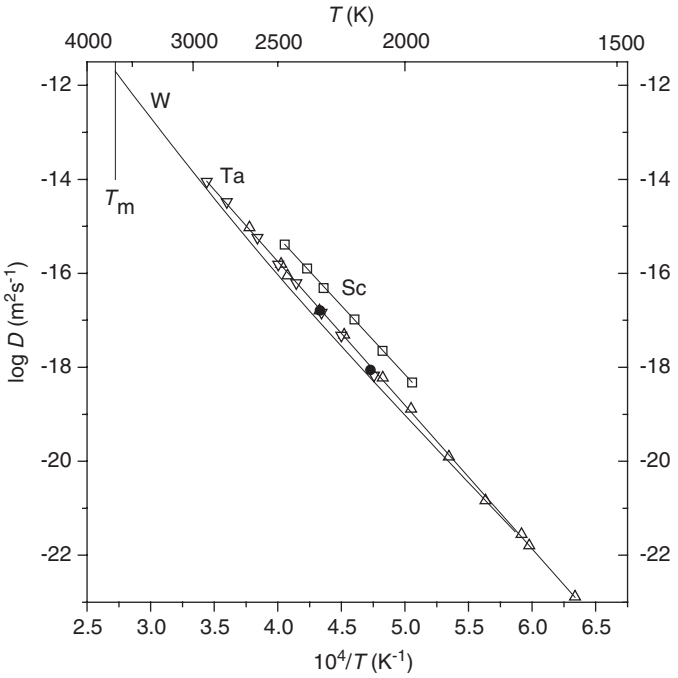

Fig. 63.08 Impurity diffusion in tungsten. Sc in W: □, Klotsman [63.13]; Ta in W: △, Pawel [63.01]; ∇, Arkhipova [63.09]; ●, Klotsman [63.14]. Fitting line according to [63.01].

REFERENCES

References to Chapter 6.0

[60.01] S.Z. Bokshtein, S.T. Kishkin, L.M. Moroz, Zavod. Lab. **23** (1957) 316.
[60.02] P.L. Gruzin, L.V. Pavlinov, A.D. Tyutyunnik, Izv. Akad. Nauk SSSR, Ser. Fiz. (5) (1959) 155.
[60.03] H.W. Paxton, E.G. Gondolf, Archiv. Eisenhüttenwesen **30** (1959) 55.
[60.04] N.A. Bogdanov, Izv. Akad. Nauk SSSR, Otd. Tekh. Nauk, Metall. Topl. (3) (1960) 99; Russian Metall. Fuels (3) (1960) 95 (English transl.).
[60.05] L.I. Ivanov, M.P. Matveeva, V.A. Morozov, D.A. Prokoshkin, Izv. Akad. Nauk SSSR, Otd. Metall. Topl. (2) (1962) 104; Russian Metall. Fuels (2) (1962) 63 (English transl.).
[60.06] W.C. Hagel, Trans. AIME **224** (1962) 430.
[60.07] J. Askill, D.H. Tomlin, Phil. Mag. **11** (1965) 467.
[60.08] G.B. Fedorov, F.I. Zhomov, E.A. Smirnov, Met. Metalloved. Chist. Met. (7) (1968) 128.
[60.09] J. Askill, Phys. Stat. Sol. (a) **8** (1971) 587.
[60.10] G.J. Beyer, ZfK-317 (Zentralinstitut für Kernforschung, Dresden) (1976).
[60.11] G.J. Beyer, ZfK-310 (Zentralinstitut für Kernforschung, Dresden) (1976).
[60.12] C.H. Wu, J. Chem. Phys. **62** (1975) 4589.
[60.13] L.N. Larikov, V.I. Isaichev, E.A. Maksimenko, B.M. Belkov, Dokl. Akad. Nauk SSSR **237** (1977) 315; Sov. Phys. Dokl. **22** (1977) 677 (English transl.).
[60.14] M.G. Karpman, G.V. Shcherbedinski, G.N. Dubinin, G.P. Benediktova, Metalloved. Termichesk. Obrab. Met. (3) (1967) 46.

[60.15] A.A. Korolev, L.V. Pavlinov, Fiz. Met. Metalloved. **29** (1970) 1326; Phys. Met. Metallogr. **29** (6) (1970) 226 (English transl.).
[60.16] K.N. Gedgovd, A.I. Krasovskiy, S.M. Novikov, Fiz. Met. Metalloved. **50** (1980) 437; Phys. Met. Metallogr. **50** (2) (1980) 185 (English transl.).
[60.17] M. Riedel, O. Kaposi, R. Karacsonyi, Ann. Univ. Budapest, Rolando Eötvös Nominatae, Sect. Chim. **12** (1971) 207; from Diffus. Data **6** (1972) 400.

References to Chapter 6.1

[61.01] J.N. Mundy, C.W. Tse, W.D. McFall, Phys. Rev. B **13** (1976) 2349.
[61.02] J.N. Mundy, H.A. Hoff, J. Pelleg, S.J. Rothman, L.J. Nowicki, F.A. Schmidt, Phys. Rev. B **24** (1981) 658.
[61.03] R.A. Wolfe, H.W. Paxton, Trans. AIME **230** (1964) 1426.
[61.04] P.L. Gruzin, S.V. Zemskii, I.B. Rodina, Met. Metalloved. Chist. Met. (4) (1963) 243.

References to Chapter 6.2

[62.01] E.V. Borisov, P.L. Gruzin, L.V. Pavlinov, G.B. Fedorov, Met. Metalloved. Chist. Met. (1) (1959) 213.
[62.02] M.B. Bronfin, S.Z. Bokshtein, A.A. Zhukhovitkii, Zavod. Lab. **26** (1960) 828; Ind. Lab. **26** (1960) 886 (English transl.).
[62.03] K. Maier, H. Mehrer, G. Rein, Z. Metallk. **70** (1979) 271.
[62.04] R.F. Peart, D. Graham, D.H. Tomlin, Acta Metall. **10** (1962) 519.
[62.05] J. Askill, in: *Diffusion in Body-Centred Cubic Metals*, Eds. J.A. Wheeler, F.R. Winslow, American Society for Metals, Metals Park (1965), p. 247.
[62.06] J. Askill, Phys. Stat. Sol. **9** (1965) K113.
[62.07] L.M. Mulyakayev, G.V. Shcherbedinskii, G.N. Dubinin, Metalloved. Termichesk, Obrab. Met. (8) (1971) 45.
[62.08] K. Nohara, K. Hirano, J. Japan Inst. Metals **37** (1973) 731.
[62.09] A.H. Winklelman, *Thesis*, Air Force Inst. Technol. (1963); from C.S. Hartley, J.E. Steedly, L.D. Parsons, in Ref. [62.05], p. 51.
[62.10] F. Roux, *Thesis*, Univ. Nancy (1972).
[62.11] G.B. Fedorov, E.A. Smirnov, V.N. Gusov, F.I. Zhomov, V.L.Gorbenko, Met. Metalloved. Chist. Met. (10) (1973) 62.
[62.12] B.A. Vandyshev, A.S. Panov, Fiz. Met. Metalloved. **26** (1968) 517; Phys. Met. Metallogr. **26** (3) (1968) 138 (English transl.).
[62.13] M.B. Bronfin, in: *Diffusion Processes, Structure and Properties of Metals*, Ed. S.Z. Bokshtein, Moscow (1964) (English transl. by Consultants Bureau Enterprises, New York (1965), p.24).
[62.14] B.A. Vandyshev, A.S. Panov, Fiz. Met. Metalloved. **25** (1968) 321; Phys. Met. Metallogr. **25** (2) (1968) 130 (English transl.).
[62.15] L.V. Pavlinov, A.I. Nakonechnikov, V.N. Bykov, Atomn. Energiya **19** (1965) 521; Sov. Atom. Energy **19** (1965) 1495 (English transl.).
[62.16] G.B. Fedorov, E.A. Smirnov, F.I. Zhomov, V.N. Gusev, S.A. Paraev, Atomn. Energiya **31** (1971) 516; Sov. Atom. Energy **31** (1971) 1280 (English transl.).
[62.17] W. Erley, H. Wagner, Phys. Stat. Sol. (a) **25** (1974) 463.
[62.18] D.S. Gornyy, R.M. Altovskiy, Fiz. Met. Metalloved. **31** (1971) 781; Phys. Met. Metallogr. **31** (4) (1971) 108 (English transl.).

Further Investigations

Mo [62.19] W. Danneberg, E. Krautz, Z. Naturforsch. **16a** (1961) 854.
Mo [62.20] L.V. Pavlinov, V.N. Bykov, Fiz. Met. Metalloved. **18** (1964) 459.
Mo [62.21] J. Askill, D.H. Tomlin, Phil. Mag. **8** (1963) 997.

Mo see Ref. [62.05].
Fe [62.22] B. Lesage, A.M. Huntz, J. Less-Common Metals **38** (1974) 149.
Nb see Ref. [62.05].
S see Ref. [62.22].
W [62.23] F. Roux, D. Ablitzer, A. Vignes, in: Proc. Thermionic Conversion Specialists Conf., Miami (1970), p. 109; precursor to Ref. [62.10].
W see Ref. [62.02].
W [62.24] S.Z. Bokshtein, M.B. Bronfin, S.T. Kishkin, in Ref. [62.13], p. 16.
W [62.25] J. Askill, Phys. Stat. Sol. **23** (1967) K21.

References to Chapter 6.3

[63.01] R.E. Pawel, T.S. Lundy, Acta Metall. **17** (1969) 979.
[63.02] N.K. Arkhipova, S.M. Klotsman, Ya.A. Rabovskiy, A.N. Timofeyev, Fiz. Met. Metalloved. **43** (1977) 779, **46** (1978) 796; Phys. Met. Metallogr. **43** (4) (1977) 88, **46** (4) (1978) 102 (English transl.).
[63.03] J.N. Mundy, S.J. Rothman, N.Q. Lam, H.A. Hoff, L.J. Nowicki, Phys. Rev. B **18** (1978) 6566.
[63.04] G. Neumann, V. Tölle, Phil. Mag. A **61** (1990) 563.
[63.05] S.M. Klotsman, S.V. Osetrov, A.N. Timofeyev, Phys. Rev. B **46** (1992) 2831.
[63.06] S.M. Klotsman, V.M. Koloskov, S.V. Osetrov, I.P. Polikarpova, G.N. Tatarinova, A.N. Timofeyev, Fiz. Met. Metalloved. **67** (1989) 767; Phys. Met. Metallogr. **67** (4) (1989) 136 (English transl.); see also Defect and Diffusion Forum **66–69** (1989) 439.
[63.07] S.M. Klotsman, S.A. Matveyev, S.V. Osetrov, A.N. Timofeyev, Fiz. Met. Metalloved. **79** (3) (1995) 126; Phys. Met. Metallogr. **79** (1995) 322 (English transl.).
[63.08] S.M. Klotsman, S.V. Osetrov, A.N. Timofeyev, Fiz. Met. Metalloved. **81** (6) (1996) 125; Phys. Met. Metallogr. **81** (1996) 668 (English transl.).
[63.09] N.K. Arkhipova, S.M. Klotsman, I.P. Polikarpova, G.N. Tatarinova, A.N. Timofeyev, L.M. Veretennikov, Phys. Rev. B **30** (1984) 1788.
[63.10] V.P. Iovkov, A.S. Panov, A.V. Ryabenko, Izv. Akad. Nauk SSSR, Metal (1) (1978) 78.
[63.11] N.K. Arkhipova, I.M. Veretennikov, S.M. Klotsman, G.N. Tatarinova, A.N. Timofeyev, Fiz. Met. Metalloved. **53** (1982) 104; Phys. Met. Metallogr. **53** (1) (1982) 92 (English transl.).
[63.12] V.P. Iovkov, A.S. Panov, A.V. Ryabenko, Fiz. Met. Metalloved. **34** (1972) 1322; Phys. Met. Metallogr. **34** (6) (1972) 203 (English transl.).
[63.13] S.M. Klotsman, S.V. Osetrov, A.N. Timofeyev, Fiz. Met. Metalloved. **81** (5) (1996) 97; Phys. Met. Metallogr. **81** (1996) 527 (English transl.).
[63.14] S.M. Klotsman, S.V. Osetrov, I.P. Polikarpova, G.N. Tatarinova, A.N. Timofeyev, O.P. Shepatkovskiy, Fiz. Met. Metalloved. **64** (1987) 148; Phys. Met. Metallogr. **64** (1) (1987) 133 (English transl.).
[63.15] E.C. Schwegler, F.A. White, J. Mass Spectrom. Ion Phys. **1** (1968) 191.
[63.16] G.B. Fedorov, E.A. Smirnov, F.I. Zhomov, V.N. Gusev, S.A. Paraev, Atomn. Energiya **31** (1971) 516; Sov. Atom. Energy **31** (1971) 1280 (English transl.).
[63.17] D.S. Gornyy, R.M. Altovskiy, Fiz. Met. Metalloved. **31** (1971) 781; Phys. Met. Metallogr. **31** (4) (1971) 108 (English transl.).

Further Investigations

W [63.18] W. Danneberg, E. Krautz, Metallurgy **15** (1961) 977.
W [63.19] R.L. Andelin, J.D. Knight, M. Kahn, Trans. AIME **233** (1965) 19.
W [63.20] L.N. Larikov, L.F. Chernaya, T.K. Yatsenko, in: *Svoystva i primeneniye zharoprochnykh splasov* (Properties and use of heat-resistant alloys), Moscow, Nauka (1966) p. 28; see Refs. [63.01, 63.02].
W [63.21] A.A. Korolev, L.V. Pavlinov, M.I. Gavrilyuk, Fiz. Met. Metalloved. **33** (1972) 295; Phys. Met. Metallogr. **33** (2) (1972) 70 (English transl.).

Cr [63.22] S.M. Klotsman, G.N. Tatarinova, A.N. Timofeyev, Mater. Sci. Forum **15–18** (1987) 457; precursor to Ref. [63.06]
Mo [63.23] L.N. Larikov, V.M. Tyshkevich, L.F. Chernaya, Ukr. Fiz. Zh. **12** (1967) 986.
Mo [63.24] W. Erley, H. Wagner, Phys. Stat. Sol. (a) **25** (1974) 463; EPMA.
Re see Ref. [63.19].
Re see Ref. [63.23].

CHAPTER 7

Diffusion in Group VII Metals

MANGANESE, RHENIUM

Preliminary results were published for self-diffusion of ^{54}Mn in polycrystalline γ- (fcc) and δ- (bcc) **manganese** [70.01]. The results suggest that grain-boundary diffusion dominates.

For **technetium** (Tc) no data are available.

Self-diffusion in **rhenium** (Re) was investigated by means of field electron microscopy (FEM) [70.02]. The kinetics of the reconstruction of the needle shape was associated with a volume diffusion process with an activation energy of 5.3 eV above 1,520 K.

REFERENCES TO CHAPTER 7

[70.01] J. Askill, Phys. Stat. Sol. **33** (1969) K105.

[70.02] Kh. Noiman, E. Kloze, I.L. Sokolskaya, Fiz. Tverd. Tela **6** (1964) 1744; Sov. Phys. Solid State **6** (1964) 1369 (English transl.).

CHAPTER 8

Self-Diffusion and Impurity Diffusion in Group VIII Metals

Contents

Tables
8.1. Iron (Fe) 261
8.2. Cobalt (Co) 274
8.3. Iridium (Ir) 277
8.4. Nickel (Ni) 278
8.5. Palladium (Pd) 286
8.6. Platinum (Pt) 287
Figures
Iron 289
Cobalt 299
Iridium 301
Nickel 302
Palladium 308
Platinum 309
References 310

Iron shows a diffusion anomaly around the Curie temperature T_C. In the present data collection, this anomaly is exclusively described by the model of Ruch et al. [02.14] (Eq. (02.19), see Chapter 0.2). Other interpretations (e.g. [80.01, 81.13, 81.56, 81.99]) are not taken into consideration for the evaluation of the diffusion parameters.

In **cobalt** this type of diffusion anomaly was also observed in some cases [82.03, 82.12, 82.13]. Reliable self-diffusion measurements [82.02], however, suggest that the anomaly is almost negligible.

In **iron**, furthermore, an experimental anomaly is observed: the marked discrepancy (20–30%) between diffusion coefficients measured by means of macrosectioning and sputter sectioning techniques for Fe and Nb in α_P-iron. Although difficult to verify, short-circuit contributions could be responsible for this discrepancy [81.16].

In **ruthenium** (Ru) self-diffusion of ^{103}Ru in polycrystalline ruthenium was investigated in the temperature range from 1,267 to 1,373 K ($\bar{T}/T_m \approx 0.5$) [80.02]. The penetration plots refer to marked grain-boundary contributions.

In **rhodium** (Rh) the activation energy for self-diffusion ($Q \approx 3.95\,\text{eV}$) was deduced from high-temperature creep investigations [80.03].

For **osmium** (Os) no data are available.

In Table 8.0 lattice structure, lattice constant, phase transition temperatures and melting temperature of the group VIII metals are listed.

Table 8.0 Lattice structure, lattice constant a, phase transition temperatures T_{ij}, Curie temperature T_C and melting temperature T_m.

	Fe			Co	Ir	Ni	Pd	Pt
Phase	α	γ	δ					
Structure	bcc	fcc	bcc	fcc	fcc	fcc	fcc	fcc
T_C (K)	1,043			1,393				
T_{ij} (K)	1,183	1,663						
T_m (K)	1,812			1,768	2,716	1,728	1,825	2,042
a (nm)	0.287	0.359		0.355	0.384	0.352	0.389	0.392

Table 8.1 Diffusion in iron (References, see page 310)

(1)	(2a)	(2b)	(3)	(4)	(5)	(6)	(7)	(8)	(9)	(10)	(11)	(12)
X	D^0 ($10^{-4}\,m^2\,s^{-1}$)	Q (eV) and ($kJ\,mole^{-1}$)	D (T_m) ($10^{-12}\,m^2\,s^{-1}$)	T-range (K) ($\tilde{T}/T_m$)	No. of data points	Material, purity	Experimental method	Remarks on the pp	Further remarks	Also studied	Figure	Reference
Self-diffusion												
Fe	–	–		1,709 δ-Fe	1	pc 3N7	^{55}Fe, electroplated; absorption	1 example	D(1,709 K)= $8.4 \times 10^{-12}\,m^2\,s^{-1}$	Fe in γ-Fe and α-Fe	81.01	Buffington (1961) [81.01]
Fe	1.9	2.472 (238.7)	25	1,687–1,781 (0.96) δ-Fe	5	pc[61]	^{59}Fe, vapour deposition; lathe and residual activity	All (probability plot)		Co in δ-Fe	–	Borg (1963) [81.02]
Fe	6.8	2.676 (258.9)	24	1,680–1,788 (0.96) δ-Fe	5 (4T)	pc 4N8	^{55}Fe, electroplated; autoradiography	1 example		Fe in γ-Fe and α-Fe	81.01	Graham (1963) [81.03]
Fe	2.01	2.493 (240.8)	23	1,701–1,765 (0.96) δ-Fe	5 (3T)	pc 3N5	^{59}Fe, electroplated; lathe and residual activity	No		Fe in α-Fe, Co in α-Fe and δ-Fe	81.01	James (1966) [81.04]
Fe	–	–		1,683–1,733 (0.94) δ-Fe	8 (4T)	pc >3N5	^{59}Fe, ^{52}Fe, electroplated; lathe	4 examples		Fe in γ-Fe and α-Fe; $E \approx 0.33$	81.01	Walter (1969) [81.05]
Fe	–	–		1,725 δ-Fe	1	pc (3–4 mm) 5N	^{59}Fe, ^{55}Fe, electroplated; lathe and microtome	1 example	D(1,725 K)= $8.32 \times 10^{-12}\,m^2\,s^{-1}$	Fe in γ-Fe and α-Fe; E=0.71	–	Graham (1969) [81.06]
Fe	0.18	2.797 (270.1)	–	1,337–1,666 (0.83) γ-Fe	12 (6T)	pc 3N7	^{55}Fe, electroplated; absorption	No		Fe in δ-Fe and α-Fe	81.01	Buffington (1961) [81.01]
Fe	(4.08) 3.7$^+$	3.222 (311.1)	–	1,223–1,473 (0.74) γ-Fe	4	pc (0.12–0.3 mm) 3N8	^{55}Fe[72]; absorption	No	$^+$Present approximation	Fe in Fe(X), X=Bi, Pb, Sb, Sn	81.01	Ivantsov (1966) [81.07]
Fe	(0.49) 0.46$^+$	2.943 (284.1)	–	1,444–1,634 (0.85) γ-Fe	15	pc (2–5 mm) 3N8	^{59}Fe, ^{55}Fe, electroplated; lathe	Several examples	$^+$Present approximation	$E \approx 0.57$	81.01	Heumann (1968) [81.08]
Fe	–	–	–	1,641 γ-Fe	2 (1T)	pc >3N5	^{59}Fe, ^{52}Fe, electroplated; lathe	1 example	D(1,641 K)= $4.5 \times 10^{-14}\,m^2\,s^{-1}$	Fe in δ-Fe and α-Fe; E=0.53	81.01	Walter (1969) [81.05]

Table 8.1 *(Continued)*

(1)	(2a)	(2b)	(3)	(4)	(5)	(6)	(7)	(8)	(9)	(10)	(11)	(12)
X	D^0 ($10^{-4}\,m^2\,s^{-1}$)	Q (eV) and ($kJ\,mole^{-1}$)	D (T_m) ($10^{-12}\,m^2\,s^{-1}$)	T-range (K) ($\bar{T}/T_m$)	No. of data points	Material, purity	Experimental method	Remarks on the pp	Further remarks	Also studied	Figure	Reference
Fe	–	–	–	1,394, 1,611 γ-Fe	2	pc (3–4 mm) 5N	^{59}Fe, ^{55}Fe, electroplated; lathe and microtome	No	D(1,611 K)= 3.47×10^{-14}, D(1,394 K)= $1.33 \times 10^{-15}\,m^2\,s^{-1}$	Fe in δ-Fe and α-Fe; E (1,611 K) = 0.79	–	Graham (1969) [81.06]
Fe	(0.41) 0.48$^+$	2.910 (280.9)	–	1,373–1,523 (0.84) γ-Fe	4	pc 3N6	^{59}Fe, electroplated; residual activity	No	$^+$Present approximation	Pd in γ-Fe, Fe, Pd in Pd; Fe, Pd in Fe(Pd)	–	Fillon (1977) [81.09]
Fe	– 118	– 2.916 (281.5)	–	1,049–1,169 1,069–1,169 α_p-Fe	6 4	pc[61] (3 mm)	^{55}Fe, vapour deposition; residual activity	2 examples			81.01	Borg (1960) [81.10]
	–	–	–	980–1,038 α_f-Fe	5 (4T)						81.01	
Fe	(900) 800$^+$	3.130 (302.2)	–	1,073-1,163 α_p-Fe	3	pc 3N8	^{55}Fe; absorption		$^+$Present approximation	Fe in Fe(X), X=Sn, Sb, $c(X) \leq$ 0.03%	–	Amonenko (1964) [81.11]
	–	–	–	1,023 α_f-Fe	1						–	
Fe	5.4	2.615 (252.5)	–	1,082–1,162 (0.62) α_p-Fe	6	pc 3N2	^{55}Fe, vapour deposition; Kryukov method	No			81.01	Angers (1968) [81.12]
Fe	–	–	–	1,168, 1,169 α_p-Fe	4 (2T)	pc > 3N5	^{59}Fe, ^{52}Fe, electroplated; grinder	2 examples		Fe in δ-Fe and γ-Fe; $E \approx$ 0.44	81.01	Walter (1969) [81.05]
Fe	–	–	–	1,142 α_p-Fe	2 (1T)	pc (3–4 mm)	^{59}Fe, ^{55}Fe, electroplated; lathe and microtome	2 examples	D(1,142 K)= 1.26×10^{-15}, D(1,043 K)= 7.35×10^{-17}, D(993 K)= $2.12 \times 10^{-17}\,m^2\,s^{-1}$	Fe in δ-Fe and γ-Fe; E=0.40–0.69	–	Graham (1969) [81.06]
	–	–	–	993, 1,043 α_f-Fe	4 (2T)	5N					–	

Fe	1.02[24]	2.53[24] (244.3)	–	784–1,017 (0.50) α_f-Fe	14 (7T)	pc 5N, sc 3N8	^{59}Fe, vapour deposition; IBS	Several examples	Fit according to Eq. (02.19) with α=0.16		81.01	Hettich (1977) [81.13]
Fe	121	2.917 (281.6)	–	1,067–1,169 (0.62) α_p-Fe	8 (6T)	pc (0.3 mm) 3N7	^{59}Fe, electroplated; microtome	3 examples		V in γ-Fe and α-Fe	81.01	Geise (1987) [81.14]
Fe	2.76[24]	2.596[24] (250.6)	–	1,052–1,148 α_p-Fe	7	pc 3N7	^{59}Fe, ^{55}Fe, electroplated; IBS	Several examples	Fit according to Eq. (02.19) with α=0.156	E=0.46–0.60	81.01	Iijima (1988) [81.15]
				766–1,042 α_f-Fe	14						81.01	
Fe	0.66[24]	2.47[24] (238.5)	–	1,054–1,163 α_p-Fe	8	sc 3N8	^{59}Fe, vapour deposition; microtome and IBS	Several examples	Fit according to Eq. (02.19) with α=0.40		81.01	Lübbehusen (1990) [81.16]
				755–1,032 α_f-Fe	14						81.01	
Impurity diffusion												
Ag	1,950*	2.992* (288.9)	–	1,081–1,161 α_p-Fe	4	pc[61]	^{110}Ag, vapour deposition; serial sectioning	2 examples (partly erfc-solution)	*Valid for the whole T-range		–	Bondy (1971) [81.17]
	–	–	–	1,021 α_f-Fe	1						–	
Ag	38	2.684 (259.2)	–	1,053–1,173 α_p-Fe	13 (7T)	pc 3N7	^{110}Ag, electroplated; residual activity	4 examples[84]	Erroneous thermal expansion correction	Ag in Ni	–	Eguchi (1973) [81.18]
	230	2.879 (278.0)	–	973–1,033 α_f-Fe	7 (4T)						–	
Al	1.8*	2.369* (228.2)	–	1,003–1,673	12	pc[61]	Al; X-ray diffraction method	–	*Valid for α-+ γ-phase; +Present approximation		–	Akimova (1983) [81.19]
			–	1,223–1,673 γ-Fe	6							
	33+	2.652+ (256.1)	–	1,048–1,183 α_p-Fe	5						81.02	
Al	0.22	2.662 (257)	–	1,230–1,473 (0.75) γ-Fe	13[51] (10T)	pc 3N	Al; EPMA, Fe (1.5% Al)/Fe/Fe (1.5% Al), (den Broeder, Hall)		Fit according to Eq. (02.19) with α=0.16		81.02	Bergner (1993) [81.20]
	5.35[24]	2.499[24] (241.3)	–	1,064–1,183 α_p-Fe	7[51]						81.02	
			–	940–1,043 α_f-Fe	4[51]							

Table 8.1 *(Continued)*

(1)	(2a)	(2b)	(3)	(4)	(5)	(6)	(7)	(8)	(9)	(10)	(11)	(12)
X	D^0 (10^{-4} m^2 s^{-1})	Q (eV) and Q (kJ mole^{-1})	D (T_m) (10^{-12} m^2 s^{-1})	T-range (K) ($\bar{T}/T_m$)	No. of data points	Material, purity	Experimental method	Remarks on the pp	Further remarks	Also studied	Figure	Reference
As	0.58	2.554 (246.6)	–	1,323–1,523 (0.79) γ-Fe	5	pc[61] (~2 mm)	As; EPMA, Fe/Fe (0.6% As) (Matano)	All (probability plot)			81.02	Božić (1976) [81.21]
As	0.019[24]	1.947[24] (188)	–	673–923 (0.44) α_f-Fe	7[51]	pc (0.5 mm) 4N	As, implanted; RBS and HIRBS	All (marked scatter)	Fit to Eq. (02.19) with α=0.2$^+$ ($^+$ present approxi-mation)		81.02	Pérez [81.22]
Au	0.81	3.004 (290)	–	1,263–1,653 (0.80) γ-Fe	7[51]	pc (2–3 mm) 4N5	Au; EPMA, Fe/Fe (X% Au) (Sauer, Freise)		X=1; 2.2	p-dependence of D	81.03	Yamazaki (2004) [81.23]
Au	31	2.706 (261.3)	–	1,055–1,174 α_p-Fe	6	pc (2 mm)	^{195}Au, electroplated; residual activity	No	$^+$Present fit of α_f-Fe data to Eq. (02.19) with α=0.12	Co, Ni in α-Fe	81.03	Borg (1963) [81.24]
	–	–	–	972–1,034 α_f-Fe	4$^+$	5N					81.03	
Be	(0.1)	(2.498) (241.2)	–	1,373–1,623 (0.83)	10 (5T)	pc 3N	^{7}Be, dried-on from salt solution[73]; residual activity	No	$^+$Present least squares fit	Be in Ni	81.03	Grigoryev (1968) [81.25]
	0.332$^+$	2.650$^+$ (255.8)		γ-Fe							81.03	
Co	5.5	2.654 (256.2)	23	1,669–1,775 (0.95) δ-Fe	5	pc[61]	^{60}Co, vapour deposition; lathe and residual activity	All (probability plot)		Fe in δ-Fe	81.04	Borg (1963) [81.02]
Co	6.38	2.663 (257.1)	25	1,702–1,794 (0.96) δ-Fe	9 (5T)	pc 3N5	^{60}Co, electroplated; lathe and residual activity	1 example	Some tabulated data had to be corrected	Fe in δ-Fe and α-Fe, Co in α-Fe	81.04	James (1966) [81.04]
Co	(1.25) 1.35$^+$	3.161 (305.2)	–	1,478–1,535 (0.83) γ-Fe	9	pc 3N8	^{60}Co, electroplated; lathe	All	$^+$Present approximation	gb-diffusion	81.04	Suzuoka (1961) [81.26]
Co	(1.0) 1.18$^+$	3.127 (301.9)	–	1,409–1,658 (0.85) γ-Fe	16 (14T)	pc 5N	Co; diffusion couple and thin film; EPMA (Hall)	2 examples	$^+$Present approximation	Ni in Fe; Fe, Ni in Co; Co, Fe in Ni	81.04	Badia (1969) [81.27]
Co	118	2.962 (286.0)	–	1,045–1,178 α_p-Fe	13	pc (2 mm)	^{60}Co, vapour deposition; residual activity	No		Au, Ni in α-Fe	81.04	Borg (1963) [81.24]
	–	–	–	963–1,034 α_f-Fe	5	5N					81.04	

Co	9.5	2.702 (260.9)	–	1,105-1,161 α_p-Fe	3[51]	pc (3 mm) ~3N	[60]Co, electroplated; lathe	1 example (gb contribution eliminated)			–	Sato (1964) [81.28]
Co	6.38	2.663 (257.1)	–	1,081–1,157 α_p-Fe	4 (3T)	pc 3N5	[60]Co, electroplated; lathe and residual activity	No		Co in δ-Fe, Fe in α-Fe and δ-Fe	– –	James (1966) [81.04]
	(7.19)	(2.697) (260.4)	–	956–1,041 α_f-Fe	3							
Co	0.99	2.50 (241.4)	–	1,059–1,164 α_p-Fe	6	sc 4N7	[57]Co, [58]Co, vapour deposition; IBS	4 examples	Data tabulated in Ref. [81.30]		81.04	Mehrer (1983) [81.29]
	–	–	–	786–1,034 α_f-Fe	17 (16T)						81.04	
Co	2.76	2.60* (251)	–	1,053–1,173 α_p-Fe	6	pc >3N5	[60]Co, [57]Co, electroplated; radio-frequency sputtering	Several examples	*Assuming D_p(Co)=D_p(Fe) and α=0.23 in Eq. (02.19)	E= 0.65–0.52	81.04	Iijima (1993) [81.31]
	–	(3.20)* (309)	–	859–1,043 α_f-Fe	11						81.04	
Cr	10.8	3.023 (291.8)	–	1,233–1,669 (0.80) γ-Fe	10[51]	pc 3N8	[51]Cr, dried-on from salt solution; residual activity	1 example		Cr in α-Fe, Hf, V in α-Fe and γ-Fe	–	Bowen (1970) [81.32]
Cr	2.53	2.493 (240.8)	–	1,058–1,148 α_p-Fe	10[51]	pc (0.6 mm) 3N5	[51]Cr, dried-on from salt solution; residual activity	No	Pronounced data scatter		–	Huntz (1967) [81.33]
Cr	8.52	2.598 (250.8)	–	1,070–1,150 α_p-Fe	4[51]	pc 3N8	[51]Cr, dried-on from salt solution; residual activity	No		Cr in γ-Fe, Hf, V in γ-Fe and α-Fe (2% V)	–	Bowen (1970) [81.32]
Cr	2.2	2.483 (239.7)	–	1,043–1,183 α_p-Fe	15[51]	pc (0.4 mm) ~3N	Cr; EPMA, Fe/Fe (1–27% Cr) (Boltzmann–Matano, Grube)	No		Cr in γ-Fe; Mo, W in γ-Fe and α-Fe	–	Alberry (1974) [81.34]
Cr	37.3[24]	2.769[24] (267.4)	–	1,049–1,174 α_p-Fe	15	pc >3N5	[51]Cr, electroplated; radio-frequency sputtering	Several examples	Fit to Eq. (02.19) with α=0.133		81.05	Lee (1990) [81.35]
				885–1,037 α_f-Fe	15 (14T)						81.05	
Cu	1.8	3.057 (295.2)	–	1,202–1,293 (0.69) γ-Fe	3[51]	pc ~3N	Cu; EPMA			Cu in α-Fe	81.06	Speich (1966) [81.36]
Cu	3.8[+]	3.21[+] (309.9)	–	1,558–1,641 (0.88) γ-Fe	6 (3T)	pc[61]	[64]Cu, vapour deposition; grinder	3 examples	[+]Present approximation	Cu in α_p-Fe	81.06	Rothman (1968) [81.37]

Table 8.1 *(Continued)*

(1)	(2a)	(2b)	(3)	(4)	(5)	(6)	(7)	(8)	(9)	(10)	(11)	(12)
X	D^0 (10^{-4} m^2 s^{-1})	Q (eV) and (kJ mole^{-1})	D (T_m) (10^{-12} m^2 s^{-1})	T-range (K) ($\tilde{T}/T_m$)	No. of data points	Material, purity	Experimental method	Remarks on the pp	Further remarks	Also studied	Figure	Reference
Cu	1.9	3.062 (295.6)	–	1,203–1,283 (0.69) γ-Fe	3[51]	pc[61]	Cu; EPMA Cu/Fe couples (Matano)	No			81.06	Tsuji (1974)[81.38]
Cu	0.19	2.823 (272.6)	–	1,198–1,323 (0.70) γ-Fe	4	pc 4N8	Cu, vapour deposition (4 μm film); EPMA	No		Cu in α_p-Fe	81.06	Salje (1977) [81.39]
Cu	4.16	3.159 (305.0)	–	1,378–1,483 (0.79) γ-Fe	5	pc 3N7	^{64}Cu, chemical deposition; residual activity	All[83]		gb-diffusion	–	Majima (1977) [81.40]
Cu	8.6	2.589 (250.0)	–	1,050–1,135 α_p-Fe	4[51]	pc ~3N	Cu; EPMA			Cu in γ-Fe	81.06	Speich (1966) [81.36]
	–	–	–	973–1,023 α_f-Fe	3[51]						81.06	
Cu	3.35$^+$	2.524$^+$ (243.7)	–	1,128–1,175 α_p-Fe	3	pc[61]	^{64}Cu, vapour deposition; grinder	No	$^+$Present approximation	Cu in γ-Fe	81.06	Rothman (1968) [81.37]
Cu	5.9*	2.559* (247.1)	–	1,069–1,143 α_p-Fe	5[51]	pc ~3N	^{64}Cu, electroplated; residual activity	No	*Valid for the whole T-range (α_p-plus α_f-phase)		81.06	Lazarev (1970) [81.41]
				981–1,028 α_f-Fe	3[51]						–	
Cu	(300)*	(2.940)* (283.9)	–	1,045–1,173 α_p-Fe	17 (11T)	sc 4N8	Cu, vapour deposition (4 μm film); EPMA	1 example ($c-x$)	*Fit to Eq. (02.19) using α=0.073;	Cu in γ-Fe	81.06	Salje (1977) [81.39]
	54$^+$	2.778$^+$ (268.2)		963–1,024 α_f-Fe	9 (5T)				$^+$ present fit to Eq. (02.19) using α=0.09		81.06	
Hf	(9×10^4)	(4.900) (473.1)	–	1,438–1,593 (0.84) γ-Fe	3[51]	pc ~3N6	^{181}Hf, electroplated; residual activity	No		Fe, Nb in γ-Fe	–	Sparke (1965) [81.42]
Hf	(3,600)	(4.219) (407.4)	–	1,371–1,628 (0.83) γ-Fe	5[51]	pc 3N8	^{181}Hf, dried-on from salt solution; residual activity	No		Cr, V in γ-Fe and α-Fe (2% V)	–	Bowen (1970) [81.32]

Mn	0.76*	2.326* (224.6)	26	1,719–1,767 (0.96) δ-Fe	3	pc[61]	Mn; EPMA Fe/Fe (2% Mn) (D independent of c(Mn))	1 example (probability plot)	*Fit together with the α_p-phase	Mn in α_p-Fe	81.07	Kirkaldy (1973) [81.43]
Mn	(0.16)	(2.710) (261.7)	–	1,201–1,581 (0.77) γ-Fe	13^{51} (9T)	pc 3N7	^{54}Mn, electroplated; residual activity	No	+Present fit to the depicted data; erroneous thermal expansion correction	Mn in Fe(Mn)	81.07	Nohara (1971) [81.44]
	0.019+	2.494+ (240.8)										
	(0.35)	(2.277) (219.8)	–	1,060–1,177 α_p-Fe	8^{51} (4T)						81.07	
	0.075+	2.105+ (203.2)										
	(1.49)	2.420 (233.6)	–	981–1,029 α_f-Fe	8^{51} (4T)						81.07	
	2.0+											
Mn	0.76*	2.326* (224.6)	–	1,067–1,174 α_p-Fe	5^{51} (4T)	pc[61]	Mn; EPMA Fe/Fe (2% Mn) (D independent of c(Mn))	No	*Fit together with the δ-phase	Mn in δ-Fe	81.07	Kirkaldy (1973) [81.43]
Mn	8.5	2.576 (248.7)	–	1,048-1,169 α_p-Fe	7	sc 3N8	^{54}Mn, vapour deposition; microtome				81.07	Lübbehusen (1984) [81.45]
Mo	25.1	3.352 (323.7)	–	1,217–1,573 (0.77) γ-Fe	9^{51} (8T)	pc 3N7	^{99}Mo; residual activity	No	The D-values for α-Fe are about a factor of two smaller than those of Ref. [81.47]	Mo, Fe in Fe(Mo)	81.08	Nohara (1976) [81.46]
	30.6	2.827 (273.0)	–	1,047–1,171 α_p-Fe	6^{51} (5T)						–	
	45.9	2.949 (284.7)	–	983–1,033 α_f-Fe	8^{51} (6T)						–	
Mo	148^{24}	2.927^{24} (282.6)	–	1,050–1,163 α_p-Fe	10 (8T)	pc (3–5 mm)	^{99}Mo, electroplated; radio-frequency sputtering and IBS	Several examples	Fit to Eq. (02.19) with α=0.074		81.08	Nitta (2002) [81.47]
			–	833-1,041 α_f-Fe	12	4N5					81.08	
Nb	(530)	(3.569) (344.6)	–	1,435–1,607 (0.81) γ-Fe	5^{51}	pc ~3N6	^{95}Nb, electroplated; residual activity	no	+Present fit to the depicted data	Fe, Hf in γ-Fe	81.09	Sparke (1965) [81.42]
	6.5+	2.983+ (288.0)										
Nb	(0.75)	2.734 (264)	–	1,221–1,474 (0.74) γ-Fe	6*	pc 4N	^{95}Nb, ^{94}Nb, electroplated; serial sectioning	1 example (gb-tail)	+Present approximation *Marked gb contributions at lower T	Nb in Fe(Mn) and Fe(Si)	81.09	Kurokawa (1983) [81.48]
	0.69+											

Table 8.1 *(Continued)*

(1)	(2a)	(2b)	(3)	(4)	(5)	(6)	(7)	(8)	(9)	(10)	(11)	(12)
X	D^0 (10^{-4} m^2 s^{-1})	Q (eV) and (kJ mole^{-1})	D (T_m) (10^{-12} m^2 s^{-1})	T-range (K) ($\bar{T}/T_m$)	No. of data points	Material, purity	Experimental method	Remarks on the pp	Further remarks	Also studied	Figure	Reference
Nb	0.83	2.760 (266.5)	–	1,210–1,604 (0.78) γ-Fe	5	pc 3N7	^{95}Nb, dried-on from oxalate solution; microtome	4 examples		gb-diffusion	81.09	Geise (1985) [81.49]
	50.2	2.610 (252)	–	1,059–1,162 α_p-Fe	5						81.09	
	–	–	–	993, 1,025 α_f-Fe	2						81.09	
Nb	*	*	–	833–1,000 α_f-Fe	5	sc 4N	^{95}Nb, dried-on from salt solution; microtome and grinder	4 examples[84]	*Fitting parameters acc. to the model of [81.13, 81.55] are presented	gb-diffusion	81.09	Herzig (2002) [81.50]
	50.2[24 +]	2.610[24 +] (252)							[+]Present approximation using D_p^0 and Q_p from [81.49] and α=0.1			
Nb	1,400[24]	3.104[24] (299.7)	–	1,053–1,163 α_p-Fe	10 (8T)	pc 4N5	^{95}Nb, electroplated; radio-frequency and magnetron sputtering and IBS	Several examples (total penetration plot in the α_f-phase $<0.5\,\mu$m)	Fit to Eq. (02.19) with α=0.061		81.09	Oono (2003) [81.51]
			–	823–1,033 α_f-Fe	10						81.09	
Ni	9.7	2.719 (262.5)	26	1,746–1,767 (0.97) δ-Fe	3[51]	pc 3N6	Ni; EPMA Fe/Fe (2% Ni) (Grube)				81.10	Moharil (1974) [81.52]
Ni	6.92	3.365 (324.9)	–	1,425–1,673 (0.85) γ-Fe	5[51]	pc 3N1	^{63}Ni, electroplated; absorption	No		Ni in Co and Ni; Ni in Fe(Ni)	81.10	MacEwan (1959) [81.53]

Ni	3.0	3.252 (314.0)	–	1,413–1,633 (0.84) γ-Fe	13 (10T)	pc 5N	Ni, diffusion couple and thin film; EPMA (Hall)	2 examples		Co in Fe; Fe, Ni in Co; Co, Fe in Ni	81.10	Badia (1969) [81.27]
Ni	1.3	2.428 (234.5)	–	1,053–1,173 α_p-Fe	12 (5T)	sc pc	^{63}Ni, electroplated; residual activity and absorption	3 examples		Ni in γ-Fe	81.10	Hirano (1961) [81.54]
	1.4	2.546 (245.8)	–	873–1,023 α_f-Fe	8 (4T)	3N7					81.10	
Ni	9.9	2.684 (259.2)	–	1,155–1,173 α_p-Fe	6	pc (2 mm)	^{63}Ni, vapour deposition; grinder	No		Au, Cu in α-Fe	81.10	Borg (1963) [81.24]
	–	–	–	973–1,023 α_f-Fe	4	5N					81.10	
Ni	–	–	–	1,048–1,160 α_p-Fe	4	pc 5N	^{63}Ni, vapour deposition; microtome	All			81.10	Čermák (1989) [81.55]
	–	–	–	788–1,014 α_f-Fe	9 (6T)						81.10	
Ni	2.3[24]	2.50[24] (241.4)	26	1,746–1,767 δ-Fe and 788–1,173 α-Fe	(46)				Present fit for α-Fe and δ-Fe to the data of [81.53, 81.55, 81.25, 81.56] according to Eq. (02.19) with α=0.12		81.10	
P	2.3$^+$	2.33$^+$ (225.0)	–	1,679, 1,723 δ-Fe	3[51] (2T)	pc 3N7	^{32}P, diffusion couple; residual activity	1 example (probability plot)	$^+$Present fit for the depicted data		81.11	Seibel (1963) [81.56, 81.57]
	(28.3)	3.027		1,553–1,623	6[51]						81.11	
	38$^+$	(292.3)		(0.88) γ-Fe								
P	287	2.807 (271)	–	1,056–1,153 α_p-Fe	4[51] (3T)	pc[61] (0.5 mm)	^{32}P, dried-on from salt solution; residual activity	No	$^+$Present approximative fit to the depicted data according to Eq. (02.19) with α=0.14	gb-diffusion; P in Fe(P)	81.11	Matsuyama (1983) [81.58]
	1.38×10^5	343.9 (332)	–	932–1,019 α_f-Fe	3[51]						81.11	
	100^{24+}	2.71^{24+} (261.7)	–									

Table 8.1 *(Continued)*

(1)	(2a)	(2b)	(3)	(4)	(5)	(6)	(7)	(8)	(9)	(10)	(11)	(12)
X	D^0 (10^{-4} m^2 s^{-1})	Q (eV) and (kJ mole^{-1})	D (T_m) (10^{-12} m^2 s^{-1})	T-range (K) ($\bar{T}/T_m$)	No. of data points	Material, purity	Experimental method	Remarks on the pp	Further remarks	Also studied	Figure	Reference
Pd	(0.41) 0.48$^+$	2.910 (281.0)	–	1,373–1,523 (0.80) γ-Fe	4	pc 3N7	^{103}Pd, electroplated; grinder	No	$^+$Present approximation	Fe in Fe, Fe, Pd in Pd; Fe, Pd in Fe(Pd)	81.12	Fillon (1977) [81.09]
Pt	(2.7) 1.2$^+$	(3.066) (296.0) 2.95$^+$ (284.8)	–	1,183–1,533 (0.75) γ-Fe	9	pc 4N	^{193}Pt, electroplated; residual activity	No	$^+$Present approxi-mation, disrega-rding D(1,183 K)	Pt in Pt, Co, Ni	81.12	Million (1973) [81.59]
S	(1.35)*	(2.10)* (202.7)	(195)	1,673–1,730 (0.94) δ-Fe	4[51]	pc 3N7	^{35}S, diffusion couple; residual activity	1 example (probability plot)	*Fit for α- plus δ-Fe together with the data of Ref. [81.95]		81.11	Seibel (1962) [81.60, 81.57]
	2.42	2.316 (223.6)	–	1,524–1,626 (0.87) γ-Fe	7[51] (6T)						81.11	
S	0.5	2.168 (209.4)	–	1,214–1,306 (0.70) γ-Fe	12[51] (4T)	pc[61]	H_2/H_2S gas mixture; resistivity change	–		S in α-Fe, Ag, Cu, Ni	81.11	Wang (1970) [81.61]
S	1.7	2.298 (221.9)	–	1,240–1,525 (0.76) γ-Fe	5[51]	pc (0.1 mm) ~3N5	^{35}S, deposition of FeS (<1 μm); residual activity	1 example[82,84]		gb-diffusion	81.11	Hoshino (1971) [81.62]
S	(2.7) 0.4$^+$	(2.125) (205.2) 1.96$^+$ (189.3)	–	1,050–1,150 α_p-Fe	12[51] (5T)	pc[61]	H_2/H_2S gas mixture; resistivity change	–	$^+$Present fit to the depicted data	S in γ-Fe, Ag, Cu, Ni	81.11	Wang (1970) [81.61]
S	34.6*	2.398* (231.5)	– –	1,073–1,173 α_p-Fe 973–1,033 α_f-Fe	3[51] 3[51]	pc >4N	^{35}S, gas mixture; residual activity	No	*Valid for the whole α-Fe range		– –	Gruzin (1972) [81.63]
S	2×10^7 1.56*	3.6 (347.6) 2.1* (202.8)	–	928–1,003 α_f-Fe	[52]	sc[61]	S; surface segregation kinetics studied with Auger electron spectroscopy	–	*Fit to Eq. (02.19) with α=0.3		–	Arabczyk (1986) [81.64]

S	1.0	2.044 (197.4)	205	1,673–1,730 δ-Fe and 1,050–1,150 α_p-Fe	(16) (9T)				Present fit for α-Fe plus δ-Fe to the data of [81.60, 81.61]		81.11	
Sb	440	2.796 (270)	–	1,058–1,150 α_p-Fe	8[51]	sc[61] pc[61]	[124]Sb, electroplated; residual activity	1 example		Sb in Fe (0.5% Mo)	81.05	Bruggeman (1975) [81.65]
	–	–	–	991–1,036 α_f-Fe	4[51]	(0.5–1 mm)					81.05	
Sb	– 260[+]	2.732 (263.8)	–	1,073–1,173 α_p-Fe	3[51]	pc (0.5–1 mm)	Sb; EPMA Fe/Fe (1–4% Sb) (Boltzmann–Matano)	No	[+]Present approximation for c(Sb)=0		81.05	Nishida (1977) [81.66]
	–	–	–	973, 1,023 α_f-Fe	2[51]	~3N8					81.05	
Sb	80	2.796 (270)	–	773–873 α_f-Fe	3	pc[61] (0.1 mm)	Sb, implanted; NRA	1 example			81.05	Myers (1978) [81.67]
Sb	(70.9)*	(2.646)* (255.5)	–	1,046–1,176 α_p-Fe	22	sc[61]	Sb, vapour–solid diffusion couple; EPMA (Matano)		*Valid for $T > 1{,}080$ K; [+]Present approximation for the whole α_p-range		81.05	Schröder (1988) [81.68]
	220[+]	2.76[+] (266.5)										
	–	–		971–1,041 α_f-Fe	9						81.05	
Sb	0.13[24]	2.092[24] (202)	–	1,053–1,073 α_p-Fe	3	pc (0.5 mm)	Sb, vapour deposition and implantation; RBS, HIRBS	Several examples (total pp <1 μm)	Fit to Eq. (02.19) with α=0.2		81.05	Pérez (2005) [81.69]
			–	695–1,023 α_f-Fe	12	4N					81.05	
Se	0.045	2.206 (213)	–	1,326–1,643 (0.82) γ-Fe	11	pc 4N	[75]Se; out-diffusion kinetics from dilute Fe(Se) alloys; residual activity	No	Pronounced data scatter		–	Foucault-Villard (1980) [81.70]
	–	–	–	1,102–1,175 α-Fe	8 (7T)						–	
Si	0.07	2.517 (243.0)	–	1,273–1,463 (0.75) γ-Fe	6 (4T)	pc 3N5	Si; EPMA Fe (2% Si)/Fe/Fe (7% Si) (Matano, Grube)	2 examples (c–x)			81.13	Bergner (1989) [81.71]
	(1.7)	(2.754) (229.1)	–	1,133, 1,173 α_p-Fe	2						–	
Sn	0.845	2.711 (261.7)	–	1,196–1,653 (0.79) γ-Fe	22 (19T)	pc (6 mm) ~3N5	[113]Sn, dried-on from salt solution; grinder	Several examples			81.13	Kimura (1986) [81.72]

Table 8.1 *(Continued)*

(1)	(2a)	(2b)	(3)	(4)	(5)	(6)	(7)	(8)	(9)	(10)	(11)	(12)
X	D^0 (10^{-4} m^2 s^{-1})	Q (eV) and (kJ mole^{-1})	D (T_m) (10^{-12} m^2 s^{-1})	T-range (K) ($\bar{T}/T_m$)	No. of data points	Material, purity	Experimental method	Remarks on the pp	Further remarks	Also studied	Figure	Reference
Sn	– 2.4	– 2.298 (221.9)	–	1,053–1,183 1,073–1,183 α_p-Fe	8[51] 4[51]	pc[61]	^{113}Sn, electroplated; residual activity	No			81.13	Treheux (1972) [81.73]
	5.4	2.407 (232.4)	–	973–1,033 α_f-Fe	5[51]						81.13	
Sn	800	2.98 (287.7)	–	773–923 α_f-Fe	4[51]	pc[61] (>0.1 mm)	Sn, implanted; RBS	3 examples			–	Myers (1984) [81.74]
Sn	6.1×10^4	3.277 (316.4)	–	896–1,023 α_f-Fe	5[51]	pc (3 mm)	^{113}Sn[72]; residual activity;	No			81.13	Hennesen (1984) [81.75]
	2.6×10^4	3.252 (314.0)	–	720–887	11[51]	~3N6 sc Fe(2% Sn)	segregation kinetics, Auger electron spectroscopy				–	
Sn	– 0.075[24] +	1.968[24] (190)	–	1,048–1,163 α_p-Fe	3	pc (0.5 mm) 4N	^{113}Sn, dried-on from salt solution; grinder;	All	Fit to Eq. (02.19) with α=0.232; +Present approximation		81.13	Torres (2000) [81.76]
			–	673–1,023 α_f-Fe	12		Sn, implanted and vapour deposition; HIRBS, RBS				81.13	
Ta	67.2	3.304 (319)	–	1,420–1,620 (0.84) γ-Fe	15[51]	pc ~3N	Ta; EPMA Fe/Fe (X% Ta) (Grube)	No	Pronounced data scatter; X=0.17, 0.05	Nb in γ-Fe	–	Shaikh (1990) [81.77]
	2.75×10^4	3.356 (324)	–	1,099–1,167 α_p-Fe	4[51]						–	
Ti	2,100[24]	3.037[24] (293.2)	–	1,053–1,174 α_p-Fe	6	sc 5N	^{44}Ti, dried-on from salt solution; microtome	All	Fit to Eq. (02.19) with α=0.079		81.14	Klugkist (1995) [81.78]
			–	948–1,042 α_f-Fe	6						81.14	
U	(7×10^{-5})	(1.38) (133.2)	–	1,223–1,348 (0.71) γ-Fe	4	pc 2N7	U (natural), vapour deposition; fission fragment radiography	No		U in β-Ti	–	de Keroulas (1967) [81.79]
V	(0.28) 0.82+	2.736 (264.2)	–	1,376–1,627 (0.83) γ-Fe	6[51]	pc 3N7	^{48}V, dried-on from salt solution; residual activity	No		Cr, Hf in γ-Fe; Cr in α-Fe; Hf, V in α-Fe (2% V)	–	Bowen (1970) [81.32]

V	0.62	2.833 (273.5)	–	1,210–1,607 (0.78) γ-Fe	5	pc (0.3 mm) 3N7	^{48}V, electroplated; microtome	Several examples		Fe in α-Fe	81.15	Geise (1987) [81.14]
	124	2.838 (274)	–	1,058-1,172 α_p-Fe	5						81.15	
W	(0.13)*	(2.770)* (267.4)	–	1,380–1,640 (0.83) γ-Fe	13[51]	pc (0.4 mm) ~3N	W; EPMA Fe/Fe (1–10% W) (Boltzmann–Matano, Grube)	No	*The D-values obtained in [81.80] and [81.34] differ by a factor of ~3	W in α-Fe, Cr, Mo in γ-Fe and α-Fe	–	Alberry (1974) [81.34]
W	(0.509)*	(2.817)* (272)	–	1,258–1,578 (0.78) γ-Fe	11 (6T)	pc ~3N7	^{185}W, electroplated; residual activity	No	*The D-values obtained in [81.34] and [81.80] differ by a factor of ~3	W in Co, Ni	–	Růžičková (1981) [81.80]
W	0.29	2.389 (230.7)	–	1,048–1,148 α_p-Fe	5	pc ~2N5	^{185}W, electroplated; residual activity	1 example (gb contribution eliminated)		Mo, V in α-Fe; Mo, V, W in α-Fe(Cr)	81.14	Kučera (1969) [81.81]
W	1.1	2.474 (238.9)	–	1,090-1,166 α_p-Fe	4[51]	pc ~3N7	W; EPMA Fe/Fe (1–10% W) (Boltzmann–Matano, Grube)	No		W in γ-Fe, Cr, Mo in γ-Fe and α-Fe	81.14	Alberry (1974) [81.34]
W	150[24]	2.972[24] (287)	–	1,053–1,173 α_p-Fe	11 (10T)	pc (3–4 mm)	^{181}W, electroplated; magnetron, radio-frequency and ion-beam sputtering (IBS)	Several examples	Fit to Eq. (02.19) with α=0.086		81.14	Takemoto (2007) [81.82]
			–	833–1,035 α_f-Fe	12 (11T)	4N			+Present approximation α=0.078		81.14	
Zn	0.22+	2.69+ (259.7)	–	1,273–1,425 (0.74) γ-Fe	5	pc (2 mm) 4N	Zn; EPMA Fe/Fe (3% Zn) (Boltzmann–Matano)	No	+Present extrapolation to c_{Zn}=0		81.06	Budurov (1973) [81.83]
Zn	60[24]	2.720[24] (262.6)	–	1,043–1,169 α_p-Fe	7	sc 4N8	Zn (vapour); EPMA	No	Fit of $D(c_{Zn}=0)$ to Eq. (02.19) with α=0.118 (best fit with α=0.11)		81.06	Richter (1981) [81.84]
			–	848–1,039 α_f-Fe	10						81.06	

Table 8.2 Diffusion in cobalt (References, see page 312)

(1)	(2a)	(2b)	(3)	(4)	(5)	(6)	(7)	(8)	(9)	(10)	(11)	(12)
X	D^0 (10^{-4} m^2 s^{-1})	Q (eV) and (kJ mole^{-1})	$D(T_m)$ (10^{-12} m^2 s^{-1})	T-range (K) ($\bar{T}/T_m$)	No. of data points	Material, purity	Experimental method	Remarks on the pp	Further remarks	Also studied	Figure	Reference
Self-diffusion												
Co	0.37	2.905 (280.5)	0.19	1,323–1,523 (0.80)	3	pc 2N7	^{60}Co, vapour deposition; absorption	–			82.01	Nix (1951) [82.01]
Co	0.55[x]	2.99[x] (288.7)	0.16	896–1,745 (0.75)	26 (24T)	pc 4N	^{60}Co, ^{57}Co, electroplated; lathe and sputter sectioning	Several examples, gb tails at lower T^{83}	[x]Forced fit to the curved Arrhenius plot	$E \approx 0.67$ (1,451–1,745 K)	82.01	Bussmann (1979) [82.02]
Co	0.146[21]	2.796[21x] (270)	0.47	923–1,743 (0.75)	44 (38T)	sc >5N	^{60}Co, ^{57}Co, electroplated; lathe and sputter sectioning	Several examples	[x]Two-exponential fit combined with Eq. (02.19)	E=0.70–0.75 (1,419–1,027 K)	82.01	Lee (1993) [82.03]
	40,400[21x]	4.599[21x] (444)										
Co	0.235	2.915 (281.5)	0.21	(896–1,745)	(25)				Two-exponential fit to the data of Ref. [82.02]; two-exponential fit to the data of Ref. [82.03]		82.01	Neumann (2001) [82.04]
	68.5	3.82 (368.8)										
	0.36	2.97 (286.8)	0.39	(923–1,743)	(44)							
	234	3.84 (370.8)										

Impurity diffusion												
Cr	(0.084)[x]	(2.628)[x] (253.7)		1,273–1,573 (0.80)	5	pc 2N7	Cr; EPMA, Co/Co (15.2% Cr) (Grube)	No	[x]$\tilde{D}$ valid for 7.6 at % Cr	Mo, V, W in Co; Cr, Mo, V, W in Ni	–	Davin (1963) [82.05]
Fe	0.21	2.719 (262.5)	0.37	1,377–1,576 (0.84)	3	pc 3N	^{55}Fe, electroplated; serial sectioning	No		Co in Co	82.02	Mead (1955) [82.06]
Fe	(0.11)	(2.624)) (253.3)		1,409-1,629 (0.86)	9 (6T)	pc 5N	Fe; EPMA, Co/Fe (Hall)	No	[x]D^0 and Q from [82.06], fit to the experimental data	Ni in Co; Co, Ni in Fe; Co, Fe in Ni	82.02	Badia (1969) [82.07]
	0.21[x]	2.719[x] (262.5)	0.37									
Mn	(0.011)	(2.255) (217.7)		1,424–1,519 (0.83) $> T_C$	8 (5T)	pc (4–5 mm) 3N5	^{54}Mn, electroplated; lathe	2 examples[82]	[+]Present approximation for the entire T-range (within the error limits no influence of the phase transition on D recognizable; see introduction page)	Mn in Co(Mn)	–	Iijima (1977) [82.08]
	(0.0315)	(2.407) (232.4)		1,133–1,378 (0.71) $< T_C$	11 (6T)							
	0.093[+]	2.524[+] (243.7)	0.60	1,133–1,519 (0.75)								
Mo	(0.231)[x]	(2.723)[x] (262.9)		1,273–1,573 (0.80)	5	pc 2N7	Mo; EPMA, Co/Co (9.6% Mo) (Grube)	No	[x]$\tilde{D}$ valid for 4.8 at % Mo	Cr, V, W in Co; Cr, Mo, V, W in Ni	–	Davin (1963) [82.05]
Ni	(1.25)	3.127		1,425–1,673	5[51]	pc	^{63}Ni, electroplated;	–	[+]Present fit to the	Ni in Ni, Fe	–	MacEwan
	2.63[+]	(301.9)	0.32[+]	(0.88)		2N5	absorption		depicted data			(1959) [82.09]
Ni	(0.4)	2.923	0.20	1,409–1,629	11	pc	Ni; EPMA, vapour	–	[+]Present	Fe in Co; Co,	82.02	Badia (1969)
	0.43[+]	(282.2)		(0.85)		5N	deposition (50–100 nm) and Co/Ni (Hall)		approximation	Ni in Fe; Co, Fe in Ni		[82.07]
Pt	0.65	2.892 (279.3)		1,354–1,481 (0.80)	6 (3T)	pc 4N	^{193}Pt, electroplated; residual activity	No		Pt in Fe, Ni	–	Million (1973) [82.10]
S	(1.3)	(2.342) (226.1)		1,423–1,523 (0.83)	3	pc 4N	^{35}S; residual activity	No	[+]Present approximation	gb-diffusion	–	Pavlyuchenko (1964) [82.11]
	0.69[+]	2.248[+] (217.0)	27[+]									

Table 8.2 *(Continued)*

(1)	(2a)	(2b)	(3)	(4)	(5)	(6)	(7)	(8)	(9)	(10)	(11)	(12)
X	D^0 (10^{-4} m^2 s^{-1})	Q (eV) and (kJ mole^{-1})	$D(T_m)$ (10^{-12} m^2 s^{-1})	T-range (K) ($\bar{T}/T_m$)	No. of data points	Material, purity	Experimental method	Remarks on the pp	Further remarks	Also studied	Figure	Reference
V	(0.021)[x] (0.016[+])	(2.298)[x] (221.9)		1,273–1,573 (0.80)	5	pc 2N7	V; EPMA, Co/Co (14.8% V) (Grube)	No	[x]$\tilde{D}$valid for 7.4 at % V [+]Present approximation	Cr, Mo, W in Co; Cr, Mo, V, W in Ni	–	Davin (1963) [82.05]
V	–	–		1,273–1,563 (0.80)	14 (7T)	pc 3N8	^{48}V, dried-on from salt solution; residual activity	No	Marked magnetic diffusion anomaly observed (see introduction page)		82.03	Kučera (1986) [82.12]
W	0.351*	2.922* (282.2)		1,258–1,578 (0.80)	12 (6T)	pc 3N7	^{185}W; electroplated; residual activity	No	*Valid for $T > T_C$, marked magnetic diffusion anomaly observed (see introduction page)	W in γ-Fe and Ni	82.03	Růžičková (1981) [82.13]
Zn	(0.32[+])	(2.66[+]) (257)		1,248–1,471 (0.77)	4	pc[61]	Zn; EPMA, Co/Co (2–17% Zn) (Boltzmann-Matano)	No	[+]Present rough extrapolation to 0% Zn		–	Budurov (1973) [82.14]
Zn	(0.08) (0.54[+]) (0.12) (0.145[+])	(2.637) (254.6) (2.89[+]) (279) (2.762) (266.7) (2.80[+]) (270.5)		1,413–1,513 (0.83) $>T_C$ 1,173–1,388 (0.72) $<T_C$	4 5	sc[61]	^{65}Zn, electroplated; residual activity	No	[+]Present approximation; for the magnetic diffusion anomaly, see introduction page	Fe in Co; Fe in Co(Fe)	–	Bristoti (1974) [82.15]

Table 8.3 Self-diffusion and impurity diffusion in iridium (References, see page 313)

(1)	(2a)	(2b)	(3)	(4)	(5)	(6)	(7)	(8)	(9)	(10)	(11)	(12)
X	D^0 (10^{-4} m^2 s^{-1})	Q (eV) and (kJ mole^{-1})	$D(T_m)$ (10^{-12} m^2 s^{-1})	T-range (K) ($\dagger/T_m$)	No. of data points	Material, purity	Experimental method	Remarks on the pp	Further remarks	Also studied	Figure	Reference
Ir	0.36	4.545 (438.8)	0.13	2,092–2,664 (0.88)	7 (6T)	sc 3N	^{192}Ir, sputter deposition; grinder	All*	*D corrected for vapourization loss		83.01	Arkhipova (1986) [83.01]
Au	0.49	4.383 (432.2)		1,373–1,898 (0.60)	13 (9T)	sc 4N	Au, in-diffusion from the gas phase*; SIMS	4 examples (deviations from linearity in ln c–x^2)	*Investigated in UHV		83.02	Ermakov (2001) [83.02]
Co	0.11	4.065 (392.5)		1,544–1,783 (0.61)	5	sc 4N	Co, in-diffusion from the gasphase*; SIMS	All	*Investigated in UHV, simultaneous diffusion with Fe and Rh	Fe, Rh in Ir	83.02	Ermakov (2004) [83.03]
Fe	–	–		1,473–2,073 (0.65)	7	sc 4N	Fe, in-diffusion from the gasphase*; SIMS	3 examples	*Investigated in UHV, simultaneous diffusion with Co and Rh; pronounced data scatter	Co, Rh in Ir	–	Ermakov (2004) [83.03]
Rh	–	–		1,473–2,073 (0.65)	6	sc 4N	Rh, in-diffusion from the gasphase*; SIMS	3 examples	*Investigated in UHV, simultaneous diffusion with Co and Fe; pronounced data scatter	Co, Fe in Ir	–	Ermakov (2004) [83.03]

Table 8.4 Diffusion in nickel (References, see page 313)

(1)	(2a)	(2b)	(3)	(4)	(5)	(6)	(7)	(8)	(9)	(10)	(11)	(12)
X	D^0 (10^{-4} m^2 s^{-1})	Q (eV) and (kJ mole^{-1})	$D(T_m)$ (10^{-12} m^2 s^{-1})	T-range (K) ($\bar{T}/T_m$)	No. of data points	Material, purity	Experimental method	Remarks on the pp	Further remarks	Also studied	Figure	Reference
Self-diffusion												
Ni	1.27	2.897 (279.7)	0.45	1,151–1,521 (0.77)	15	pc (∼1 mm) ∼3N	^{63}Ni, electroplated; absorption and residual activity	2 examples			–	Hoffman (1956) [84.01]
Ni	0.40	2.767 (267.1)	0.34	1,373–1,448 (0.82)	5	pc ∼4N	^{63}Ni, vapour deposition; grinder	No		Ni in Au; Ni in Ni(Au) (EPMA)	–	Reynolds (1957) [84.02]
Ni	–	–		1,303–1,673	13[51] (8T)	pc 3N2	^{63}Ni, electroplated; grinder and residual activity	3 examples	gb-contribution below 1,425 K		–	MacEwan (1959) [84.03]
	3.36	3.027 (292.3)	0.50	1,425–1,673 (0.90)	11[51] (6T)							
Ni	5.12	3.079 (297.3)	0.53	1,425–1,673 (0.90)	5[51]	pc 3N2	^{63}Ni, electroplated; absorption	No		Ni in Co and γ-Fe	–	MacEwan (1959) [84.04]
Ni	1.7	2.953 (285.1)		973–1,373 (0.68)	9	pc 3N8	^{63}Ni, electroplated; residual activity	No		Co in Ni, Co, Ni in Co; Co, Ni in Co(Ni)	–	Hirano (1961) [84.05, 84.06]
Ni	–	–		1,202–1,576	16 (8T)	pc 3N8	^{63}Ni, electroplated; serial sectioning (chemical polishing)	2 examples			–	Shinyaev (1963) [84.07]
	2.59	3.014 (291.0)	0.42	1,358–1,576 (0.85)	10 (5T)							
Ni	1.9	2.949 (284.7)	0.47	1,315–1,677 (0.87)	13	pc (1–4 mm) >3N5	^{63}Ni; lathe	1 example (slight NSE)		Cr in Ni; Ni, Cr in Ni(Cr)	–	Monma (1964) [84.08]
Ni	1.77	2.955 (285.3)	0.42	1,253–1,670 (0.85)	20	sc 5N	^{63}Ni, electroplated; grinder and residual activity	2 examples			84.01	Bakker (1968) [84.09]
Ni	1.33	2.91 (281.0)		815–1,195 (0.58)	10	sc 4N7	^{63}Ni, sputter deposition; IBS	All			84.01	Maier (1976) [84.10]
Ni	1.82	2.954 (285.2)	0.44	1,326–1,673 (0.87)	4	sc 3N8	^{63}Ni, electroplated; lathe	All		Co, W in Ni	84.01	Vladimirov (1978) [84.11]
Ni	0.85[21]	2.87[21] (277.1)	0.47	(879–1,670)	(28)				Two-exponential fit to the data of [84.09, 84.10]		84.01	Neumann (1986) [84.12]
	1,350[21]	4.15[21] (400.7)										

Impurity diffusion												
Ag	8.25	2.923 (282.2)		1,183–1,303 (0.72)	3[51]	sc 4N	[110]Ag, electroplated; residual activity	1 example[84]		gb-diffusion	–	Treheux (1976) [84.13]
	(22.4)	(2.923) (282.2)		1,110–1,323 (0.70)	9[51]	pc 2N3						
Ag	8.94	2.894 (279.4)	3.2	1,297–1,693 (0.87)	13	sc 3N8	[110]Ag, [105]Ag, electroplated; lathe and residual activity	All (partly corrected for vapourization loss of tracers)		gb-diffusion	84.02	Vladimirov (1978) [84.14]
Al	1.87*	2.775* (268.0)	1.5	1,372–1,553 (0.85)	6	pc (0.5–10 mm) 2N8	Al, pressure-welded diffusion couples, Ni/Ni (0.7% Al); lathe, spectrophotometry (Grube)	No	*$\tilde{D}$, valid for 0–0.7 at % Al	Mn, Ti, W in Ni	84.03	Swalin (1956) [84.15]
Al	1.0	2.693 (260)		914–1,212 (0.62)	7 (5T)	sc 4N	Al, vapour deposition; SIMS	1 example			84.03	Gust (1981) [84.16]
As	1.39	2.608 (251.9)	3.4	1,239–1,634 (0.83)	10 (9T)	sc 3N8	[73]As, vapour deposition; lathe	All			84.04	Vladimirov (1979) [84.17]
Au	(2.0)	(2.819) (272.2)		1,068–1,378 (0.71)	3[51]	pc (4 mm) 3N8	[198]Au, vapour deposition; autoradiography	1 example	+Present fit to the depicted data; marked gb contributions cannot be excluded	Au in Ni(Au)	–	Kurtz (1955) [84.18]
	(90)+	(3.00)+ (289.7)										
Au	(0.02)*	(2.385)* (230.3)		1,026–1,325 (0.68)	5[51]*	sc 5N, pc	[198]Au, electroplated; lathe	1 example	*Valid for sc samples +Present fit to the depicted data	gb-diffusion	–	Chatterjee (1968) [84.19]
	(0.021)*+	(2.27)*+ (219.2)										
Be	(0.019)	(2.004) (193.4)	(2.7)	1,293–1,673 (0.86)	10 (5T)	pc 3N	[7]Be, dried-on from salt solution; residual activity	3 examples	+Present approximation disregarding the lowest T	Be in γ-Fe	–	Grigoryev (1968) [84.20]
	(0.118)+	(2.263)+ (218.5)	(3.0)+	1,473–1,673 (0.91)	8 (4T)							
Ce	(0.66)	(2.637) (254.6)		973–1,370 (0.68)	10 (9T)	pc (4 mm) 4N	[141]Ce, vapour deposition; residual activity	2 examples (gb tails)		Nd in Ni; gb-diffusion	–	Paul (1971) [84.21]
Co	0.75	2.806 (270.9)		1,021–1,465 (0.72)	9	pc 3N8	[60]Co, electroplated; residual activity	No		Ni in Ni, Co, Ni in Co; Co, Ni in Co(Ni)	–	Hirano (1962) [84.06]

Table 8.4 *(Continued)*

(1)	(2a)	(2b)	(3)	(4)	(5)	(6)	(7)	(8)	(9)	(10)	(11)	(12)
X	D^0 (10^{-4} m^2 s^{-1})	Q (eV) and (kJ mole^{-1})	$D(T_m)$ (10^{-12} m^2 s^{-1})	T-range (K) ($\check{T}/T_m$)	No. of data points	Material, purity	Experimental method	Remarks on the pp	Further remarks	Also studied	Figure	Reference
Co	– 0.98$^+$	(2.875) (277.6) 2.837$^+$ (274.0)		1,368, 1,466	2	pc ∼2N8	^{60}Co, electroplated; lathe	2 examples	$^+$Present calculation		84.05	McCoy (1963) [84.22]
Co	1.11	2.814 (271.7)	0.68	1,430–1,644 (0.89)	10[51] (5T)	pc 2N8	^{60}Co, electroplated[73]; residual activity	No		Ni in Ni, Co, Ni in Co; Co, Ni in Ni(Co)	–	Hässner (1965) [84.23]
Co	0.59	2.793 (269.6)	0.42	1,409–1,643 (0.88)	9	pc 5N	Co, diffusion couple Ni/Co; EPMA (Hall)	No		Fe in Ni; Fe, Ni in Co; Co, Ni in Fe	–	Badia (1969) [84.24]
Co	0.55	2.749 (265.5)		855–1,255 (0.61)	6[51]	pc 4N	^{57}Co, electroplated; absorption and residual activity	No		Co in Ni(Co)	–	Million (1972) [84.25]
Co	2.77	2.953 (285.1)	0.67	1,335–1,696 (0.88)	13 (10T)	sc 3N8	^{57}Co, electroplated; lathe	All		Ni, W in Ni	84.05	Vladimirov (1978) [84.11]
Co	1.8	2.921 (282)	0.54	1,323–1,648 (0.86)	10[51]	pc 3N7	Co; EPMA, Ni/Ni (4.85% Co) (Boltzmann–Matano, Hall)	No		Cr, Ti in Ni	84.05	Jung (1992) [84.26]
Co	2.26	2.937 (283.6)	0.61	(1,323–1,696) (0.87)	(25)				Present fit to the data of [84.11, 84.22, 84.26]		84.05	
Cr	1.1	2.823 (272.6)	0.64	1,373–1,541 (0.84)	9	pc (1–4 mm) >3N5	^{51}Cr; lathe	1 example (slight NSE, 40 μm sections)		Ni in Ni; Ni, Cr in Ni(Cr)	–	Monma (1964) [84.08]
Cr	8.52	3.025 (292.1)		1,223–1,423 (0.77)	5	pc 3N	^{51}Cr, electroplated; residual activity	No		Cr in γ-Fe; Ni, Cr in Ni(Cr), Cr, Fe in Fe(Cr)	–	Růžičková (1981) [84.27]

Cr	5.2	2.993 (289)	0.96	1,323–1,648 (0.86)	10^{51}	pc 3N7	Cr; EPMA, Ni/Ni (5.06% Cr) (Boltzmann–Matano, Hall)	No		Co, Ti in Ni	84.06	Jung (1992) [84.26]
Cu	0.57	2.676 (258.3)	0.90	1,327–1,632 (0.86)	5	pc (1–4 mm) >3N5	^{64}Cu; lathe	1 example (40 μm sections)		Cu in Cu; Ni, Cu in Ni(Cu)	–	Monma (1964) [84.28]
Cu	(0.724) 0.66^{+}	2.645 (255.4)		1,123–1,323 (0.71)	5	pc (~3 mm) 3N5	^{64}Cu, electroplated; residual activity	1 example	$^{+}$Present approximation	Cu in Al	84.02	Anand (1965) [84.29]
Cu	0.27	2.646 (255.5)		1,048–1,323 (0.69)	6	sc 5N	Cu, vapour deposition (1–2 μm film); EPMA	1 example			–	Helfmeier (1970) [84.30]
Cu	0.61	2.641 (255)	1.2	1,080–1,613 (0.78)	16 (13T)	pc (1–3 mm) 3N5	Cu; serial sectioning, atomic absorption analysis	3 examples			84.02	Taguchi (1984) [84.31]
Fe	(0.22) 0.92^{+}	(2.619) (252.9) 2.773^{+} (267.7)	 0.75^{+}	1,409–1,629 (0.88)	9 (6T)	pc 5N	Fe, diffusion couple Ni/Fe; EPMA (Hall)	No	$^{+}$Present approximation	Co in Ni; Fe, Ni in Co; Ni, Co in Fe	84.04	Badia (1969) [84.24]
Fe	1.0	2.79 (269.4)	0.73	1,478–1,669 (0.91)	9	sc 5N	^{59}Fe, electroplated; grinder (lapping)	1 example		Fe in Ni(Fe)	84.04	Bakker (1971) [84.32]
Ge	(2.1) 2.9^{+}	(2.74) (264) 2.776^{+} (268)	 2.3^{+}	940–1,676 (0.76)	12 (11T)	sc 4N 4N6	^{68}Ge, implanted; grinder and IBS	4 examples	$^{+}$Present approximation		84.07	Mantl (1983) [84.33]
Ge	2.6	2.776 (268)	2.1	1,373–1,598 (0.86)	10^{51}	pc 3N7	Ge; EPMA, Ni/Ni (5.19% Ge) (Matano, Hall)	No		In, W in Ni	84.07	Takahashi (1996) [84.34]
Hf	(2.65)* 2.76^{+}	2.645* (255.4)		1,023–1,423 (0.71)	6	pc 4N	Hf; EPMA, Ni/Ni (0.3% Hf)/ Ni (4.5% Hf)	1 example (probability plot)	$^{+}$Present approximation *$\tilde{D}$ valid for 0.15 at % Hf		84.08	Bergner (1972) [84.35]
In	6.78	2.801 (270.4)	4.6	1,274–1,659 (0.85)	9 (8T)	sc 3N8	^{114}In, sputter deposition; lathe	All			84.03	Vladimirov (1978) [84.36]
In	1.1	2.589 (250)		777–1,513 (0.66)	16 (12T)	sc 4N	In, vapour deposition; SIMS	1 example[85]	Marked data scatter		84.03	Gust (1981) [84.37]
In	1.26[21] 1.9×10^{4} [21]	2.60[21] (251.0) 4.12[21] (397.8)	5.1	(789–1,659)	(22)				Two-exponential fit to the data of [84.36, 84.37]		84.03	Neumann (1988) [84.38]

Table 8.4 *(Continued)*

(1)	(2a)	(2b)	(3)	(4)	(5)	(6)	(7)	(8)	(9)	(10)	(11)	(12)
X	D^0 (10^{-4} m^2 s^{-1})	Q (eV) and (kJ mole^{-1})	$D(T_m)$ (10^{-12} m^2 s^{-1})	T-range (K) ($\tilde{T}/T_m$)	No. of data points	Material, purity	Experimental method	Remarks on the pp	Further remarks	Also studied	Figure	Reference
In	1.9	2.641 (255)	3.7	1,323–1,548 (0.83)	10[51]	pc 3N7	In; EPMA, Ni/Ni (0.9% In) (Matano, Hall)	1 example (probability plot)		Ge, W in Ni	84.03	Takahashi (1996) [84.34]
Ir	1.11*	3.217* (310.6)	0.046	1,173–1,573 (0.79)	5	pc (>0.5 mm) 3N8	Ir; EPMA, Ni/Ni (3.28% Ir) (Boltzmann–Matano, Sauer–Freise)	No	*$\tilde{D}$, average for 0–3.28 at % Ir	Pd, Pt, Rh, Ru in Ni	84.05	Karunaratse (2003) [84.39]
Mg	6.32*	2.765* (267)		1,145–1,400 (0.74)	7	pc 3N	Mg; EPMA, Ni/Ni (0.08% Mg)	2 examples (probability plot)	*$\tilde{D}$ valid for 0.04 at % Mg		–	Bergner (1981) [84.40]
Mn	7.5*	2.910* (280.9)	2.4	1,376–1,566 (0.85)	6	pc (0.5–10 mm) ~2N8	Mn, pressure welded diffusion couples, Ni/Ni (1.7–4.0% Mn); lathe, spectrophotometry (Grube)	No	*$\tilde{D}$, valid for 0–4 at % Mn	Al, Ti, W in Ni	84.09	Swalin (1956) [84.15]
Mo	1.3	2.931 (283)	0.37	1,323–1,623 (0.85)	7[51]	pc 3N7	Mo; EPMA, Ni/Ni (2.97% Mo) (Matano, Hall)	No		Pt in Ni; Mo, Pt in Ni_3Al	84.06	Minamino (1997) [84.41]
Mo	1.15*	2.913* (281.3)	0.36	1,173–1,573 (0.79)	5	pc 3N8	Mo; EPMA, Ni/Ni (6.5% Mo) (Boltzmann–Matano, den Broeder)	No	*$\tilde{D}$, average for 0–6.5 at % Mo	Nb in Ni	84.06	Karunaratse (2005) [84.42]
Nb	1.3	2.710 (261.7)	1.6	1,116–1,527 (0.76)	6[51]	pc 4N	Nb; EPMA, diffusion couple*	No	*Nb concentration not reported	Hf, Ta, Ti, W, Zr in Ni	84.10	Bergner (1977) [84.43]
Nb	0.88*	2.662* (257)	1.5	1,173–1,500 (0.77)	5	pc 3N8	Nb; EPMA, Ni/Ni (3% Nb) (Boltzmann–Matano, den Broeder)	No	*$\tilde{D}$, average for 0–3 at % Nb	Mo in Ni	84.10	Karunaratse (2005) [84.42]

Nd	(0.44)	(2.594) (250.5)		973–1,373 (0.68)	10 (9T)	pc (4 mm) 4N	^{147}Nd, vapour deposition; residual activity	2 examples (gb tails)		Ce in Ni; gb-diffusion	–	Paul (1971) [84.21]
Pd	0.69*	2.752* (265.7)	0.65	1,173–1,573 (0.79)	5	pc (>0.5 mm) 3N8	Pd; EPMA, Ni/Ni (5.78% Pd) (Boltzmann–Matano, Sauer–Freise)	No	*$\tilde{D}$, average for 0–5.78 at % Pd	Ir, Pt, Rh, Ru in Ni	84.11	Karunaratse (2003) [84.39]
Pt	0.35	2.900 (280)	0.12	1,323–1,623 (0.85)	7[51]	pc 3N7	Pt; EPMA, Ni/Ni (3.01% Pt) (Matano, Hall)	No		Mo in Ni; Mo, Pt in Ni_3Al	84.05	Minamino (1997) [84.41]
Pt	0.92*	3.016* (291.2)	0.15	1,173–1,573 (0.79)	5	pc (>0.5 mm) 3N8	Pt; EPMA, Ni/Ni (3.24% Pt) (Boltzmann–Matano, Sauer–Freise)	No	*$\tilde{D}$, average for 0–3.24 at % Pt	Ir, Pd, Rh, Ru in Ni	84.05	Karunaratse (2003) [84.39]
Pu	(0.17) (0.21^{+})	(2.233) (215.6)		1,298–1,398 (0.78)	5	pc ~3N	Pu[71], diffusion couple; autoradiography	4 examples (c–x), erfc-solution	$^{+}$Present approximation; marked gb contributions cannot be excluded	c_s=40–80 ppma (1,300–1,400 K)	–	Blechet (1968) [84.44]
Re	8.2×10^{-3}*	2.641* (255)	0.016	1,173–1,573 (0.79)	5[51]	pc (>0.5 mm) 3N8	Re; EPMA, Ni/Ni (3% Re) (Boltzmann–Matano, Sauer–Freise)	No	*$\tilde{D}$, average for 0–3 at % Re	Ta, W in Ni	–	Karunaratse (2000) [84.45]
Rh	0.87*	2.959* (285.7)	0.20	1,173–1,573 (0.79)	5	pc (>0.5 mm) 3N8	Rh; EPMA, Ni/Ni (5.96% Rh) (Boltzmann–Matano, Sauer–Freise)	No	*$\tilde{D}$, average for 0–6 at % Rh	Ir, Pd, Pt, Ru in Ni	84.11	Karunaratse (2003) [84.39]
Ru	2.48*	3.142 (303.4)	0.16	1,173–1,573 (0.79)	5	pc (>0.5 mm)	Ru; EPMA, Ni/Ni (X% Ru) (Boltzmann–Matano, Sauer–Freise)	No	X=2.97; 6.06, *$\tilde{D}$, average for 0–2.97 at % Ru	Ir, Pd, Pt, Rh in Ni	84.11	Karunaratse (2003) [84.39]
	(0.62)^{x}	(2.991)^{x} (288.8)			5	3N8			^{x}Resp. for 0–6.06 at % Ru		–	
S	1.40	2.268 (219.0)		1,078–1,495 (0.74)	19 (18T)	sc 3N8	^{35}S, vapour deposition; lathe	All			84.12	Vladimirov (1975) [84.46]
S	–	–		1,153–1,331 (0.72)	7 (6T)	sc[61]	^{35}S, sulphurization of Ni foils; absorption	–		c_s(1,173 K)=350 ppma	84.12	Arbuzov (1980) [84.47]

Table 8.4 *(Continued)*

(1)	(2a)	(2b)	(3)	(4)	(5)	(6)	(7)	(8)	(9)	(10)	(11)	(12)
X	D^0 (10^{-4} m^2 s^{-1})	Q (eV) and (kJ mole^{-1})	$D(T_m)$ (10^{-12} m^2 s^{-1})	T-range (K) ($\bar{T}/T_m$)	No. of data points	Material, purity	Experimental method	Remarks on the pp	Further remarks	Also studied	Figure	Reference
Sb	3.85	2.735 (264.0)	4.1	1,203–1,674 (0.83)	12	sc 3N8	^{125}Sb, electroplated; lathe	All			84.09	Vladimirov (1976) [84.48]
Si	1.5*	2.676* (258.3)	2.3	1,387–1,572 (0.86)	5[51]	pc (0.5–10 mm) ~2N8	Si, pressure welded diffusion couples, Ni/Ni (<1% Si); lathe, spectrophotometry (Grube)	No	*$\tilde{D}$, valid for 0–1 at % Si	Mg, Mo in Ni	–	Swalin (1957) [84.49]
Sn	4.56	2.767 (267.2)	3.9	1,242–1,642 (0.83)	11 (10T)	sc 3N8	^{113}Sn, electroplated; lathe	1 example			84.07	Vladimirov (1979) [84.50]
Ta	0.4	2.667 (257.5)	0.66	1,117–1,532 (0.77)	6[51]	pc 4N	Ta; EPMA, diffusion couple*	No	*Ta concentration not reported	Hf, Nb, Ti, W, Zr in Ni	84.10	Bergner (1977) [84.43]
Ta	0.219*	2.600* (251)	0.57	1,173–1,573 (0.79)	5[51]	pc (> 0.5 mm) 3N8	Ta; EPMA, Ni/Ni (3% Ta) (Boltzmann–Matano, Sauer–Freise)	No	*$\tilde{D}$, average for 0–3 at % Ta	Re, W in Ni	84.10	Karunaratse (2000) [84.45]
Te	–	–		(958–1,553)	(7)	sc	^{123}Te, vapour	3 examples		gb-diffusion	84.12	Neuhaus
	2.6	2.631 (254)	5.5	1,135–1,553 (0.78)	5	4N	deposition; microtome					(1989) [84.51]
Ti	0.86*	2.663* (257.1)	1.5	1,377–1,555 (0.85)	6	pc (0.5–10 mm) ~2N8	Ti, pressure welded diffusion couples, Ni/Ni (0.9% Ti); lathe, spectrophotometry (Grube)	1 example (probability plot)	*$\tilde{D}$, valid for 0–0.9 at % Ti	Al, Mn, W in Ni	84.08	Swalin (1956) [84.15]
Ti	(1.4)	(2.732) (263.8)		1,025–1,424 (0.70)	7[51]	pc 4N	Ti; EPMA, diffusion couple*	No	+Present fit to the depicted data; *Ti concentration not reported; [x]See also Ref. [84.35]	Hf, Nb, Ta, W, Zr in Ni	84.08	Bergner (1977) [84.43][x]
	7.3+	2.911+ (281.0)										

Ti	4.1	2.848 (275)	2.0	1,323–1,648 (0.86)	10^{51}	pc 3N7	Ti; EPMA, Ni/Ni (3.41% Ti) (Boltzmann–Matano, Hall)	No		Co, Cr in Ti	84.08	Jung (1992) [84.26]
U	1.0	2.446 (236.2)		1,248–1,348 (0.75)	10 (5T)	pc 4N8	U^{71}, vapour deposition[73]; fissiography	1 example			–	Zanghi (1971) [84.52]
V	0.87	2.884 (278.4)		1,073–1,573 (0.77)	7	pc 4N	^{48}V, dried-on from salt solution; residual activity	1 example		V in Al	–	Murarka (1968) [84.53]
W	(2.0) 1.8^{+}	3.101 (299.4)	0.16^{+}	1,373–1,568 (0.85)	5	pc (1–4 mm) > 3N5	^{185}W; lathe	1 example (40 μm sections)	$^{+}$Present approximation	Ni, W in Ni(W)	–	Monma (1964) [84.54]
W	2.87	3.192 (308.2)	0.14	1,346–1,668 (0.87)	11 (9T)	sc 3N8	^{181}W, electroplated; lathe	All		Ni, Co in Ni	84.06	Vladimirov (1978) [84.11]
W	2.1	3.138 (303)	0.15	1,423–1,623 (0.88)	9^{51}	pc 3N7	W; EPMA, Ni/Ni (1.94% W) (Matano, Hall)	No		Ge, In in Ni	84.06	Takahashi (1996) [84.34]
Zn	(2.8)* 2.56^{+}	2.859* (276)		1,123–1,323 (0.71)	6^{51}	pc 3N5	Zn; EPMA, Ni/Ni (X% Zn)^{x} (Boltzmann–Matano)	No	*Extrapolated to $X=0$ $^{x}X=45$; 40 $^{+}$Present fit to the depicted data		–	Yamamoto (1979) [84.55]
Zr	6.1	2.754 (265.9)		Not reported	[52]	pc 4N	$^{95}Zr^{72}$; microtome	No		Hf, Nb, Ta, Ti, W in Ni	–	Bergner (1977) [84.43]

Table 8.5 Self-diffusion and impurity diffusion in palladium (References, see page 315)

(1)	(2a)	(2b)	(3)	(4)	(5)	(6)	(7)	(8)	(9)	(10)	(11)	(12)
X	D^0 (10^{-4} m^{2}s^{-1})	Q (eV) and (kJ mole^{-1})	$D(T_m)$ (10^{-12} m^2 s^{-1})	T-range (K) ($\bar{T}/T_m$)	No. of data points	Material, purity	Experimental method	Remarks on the pp	Further remarks	Also studied	Figure	Reference
Pd	0.205	2.758 (266.3)	0.49	1,330–1,776 (0.85)	20 (10T)	sc 5N	^{103}Pd, ^{112}Pd, electroplated[73]; lathe	Numerous examples		$E \approx 0.81$ (1,726, 1,776 K)	85.01	Peterson (1964) [85.01]
Pd	(0.04) 0.045$^+$	2.585 (249.6)		1,373–1,523 (0.79)	4	pc 3N5	^{103}Pd, electroplated; grinder	No	$^+$Present approximation	Fe in Pd; Fe, Pd in Fe; Fe, Pd in Pd(Fe)	–	Fillon (1977) [85.02]
Fe	(0.18) 0.206$^+$	2.693 (260.0)		1,373–1,523 (0.79)	4	pc 3N5	^{59}Fe, electroplated; grinder	No	$^+$Present approximation	Pd in Pd; Fe, Pd in Fe; Fe, Pd in Pd(Fe)	85.01	Fillon (1977) [85.02]

Table 8.6 Diffusion in platinum (References, see page 316)

(1)	(2a)	(2b)	(3)	(4)	(5)	(6)	(7)	(8)	(9)	(10)	(11)	(12)
X	D^0 (10^{-4} m^2 s^{-1})	Q (eV) and (kJ mole^{-1})	$D(T_m)$ (10^{-12} m^2 s^{-1})	T-range (K) ($\tilde{T}/T_m$)	No. of data points	Material, purity	Experimental method	Remarks on the pp	Further remarks	Also studied	Figure	Reference
Self-diffusion												
Pt	(0.33) 0.37[+]	2.958 (285.6)	1.8	1,598–1,873 (0.85)	5	pc 4N	^{193}Pt, ^{195}Pt, ^{197}Pt, (neutron irradiated pure Pt); serial sectioning		[+]Present approximation		86.01	Kidson (1957) [86.01]
Pt	0.22	2.89 (279.0)	1.6	1,523–1,998 (0.86)	10	pc (>1 mm) 5N	^{195}Pt, electroplated; absorption				86.01	Cattaneo (1962) [86.02]
Pt	0.05 0.06[21] (0.6–6)[21]	2.67 (257.8) 2.690[21] (259.7) (3.78–4.02)[21] (365–388)		850–1,265 (0.52)	9	sc 4N	^{197}Pt, sputter deposition[x]; IBS	All	[x]Simultaneous diffusion of Pt and Au; two-exponential fit to the data of [86.01–86.03]	Au in Pt	86.01	Rein (1978) [86.03]
Pt	0.034[21] 88.6[21]	2.64[21] (254.9) 4.05[21] (391.0)	1.9	(850–1,998)	(24)				Two-exponential fit to the data of [86.01–86.03]		86.01	Neumann (1986) [86.04]

Table 8.6 *(Continued)*

(1)	(2a)	(2b)	(3)	(4)	(5)	(6)	(7)	(8)	(9)	(10)	(11)	(12)
X	D^0 (10^{-4} m^2 s^{-1})	Q (eV) and (kJ mole^{-1})	$D(T_m)$ (10^{-12} m^2 s^{-1})	T-range (K) ($\dot{T}/T_m$)	No. of data points	Material, purity	Experimental method	Remarks on the pp	Further remarks	Also studied	Figure	Reference
Impurity diffusion												
Ag	0.13*	2.673* (258.1)	3.3	1,473–1,873 (0.82)	3	pc (1.5 mm) 4N	Ag; EPMA, Pt/Pt (4.3% Ag)	1 example (probability plot)	*$\tilde{D}$ valid for 2.15 at % Ag	Al, Fe in Pt	–	Bergner (1978) [86.05]
Al	$1.3 \cdot 10^{-3}$*	2.005* (193.6)		1,373–1,873 (0.79)	4	pc (1.5 mm) 4N	Al; EPMA, Pt/Pt (7% Al)	1 example (probability plot)	*$\tilde{D}$ valid for 3.5 at % Al	Ag, Fe in Pt	–	Bergner (1978) [86.05]
Au	(0.13) 0.15$^+$	2.61 (252.0)		850–1,265 (0.52)	9	sc 4N	^{199}Au, sputter deposition^x; IBS		^{x}Simultaneous diffusion of Au and Pt; $^+$Present approximation disregarding D(1,080 K)	Pt in Pt	86.02	Rein (1978) [86.03]
Co	–	–		1,023–1,323	26 (7T)	pc (~0.5 mm)	^{57}Co, electroplated; absorption		Considerable gb contributions		–	Kučera (1968) [86.06]
	(19.6)	(3.218) (310.7)		1,173–1,323 (0.61)	12 (4T)	3N 4N						
Fe	0.025*	2.521* (243.4)		1,373–1,673 (0.75)	4	pc (1.5 mm) 4N	Fe; EPMA, Pt/Pt (6.8% Fe)	1 example (probability plot)	* $\tilde{D}$ valid for 3.4 at % Fe	Ag, Al in Pt	–	Bergner (1978) [86.05]

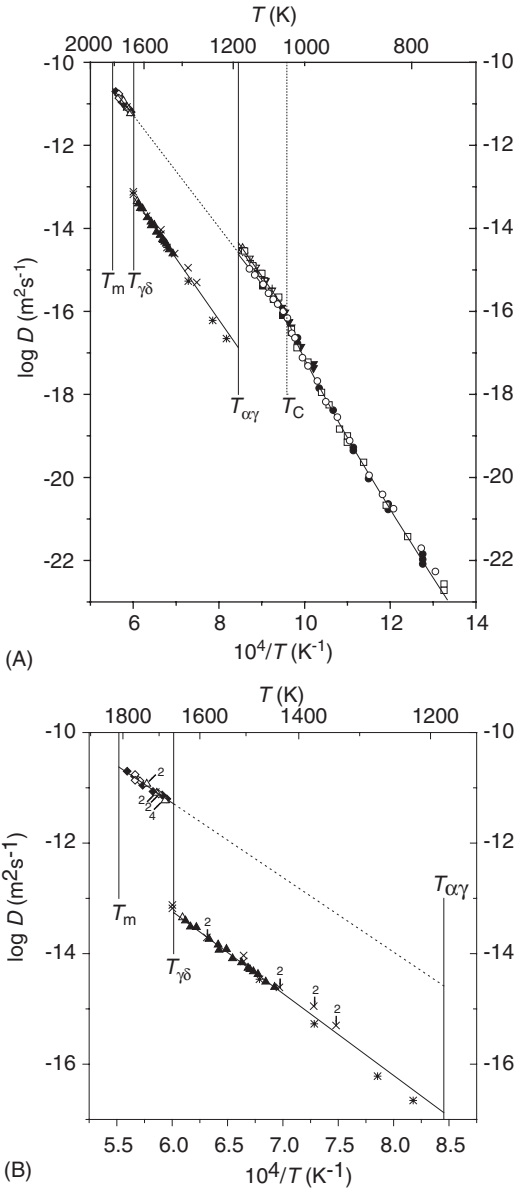

Fig. 81.01 (A) Self-diffusion in iron. ×, Buffington [81.01]; ◆, Graham [81.03]; ◇, James [81.04]; Δ, Walter [81.05]; ▲, Heumann [81.08]; ▼, Borg [81.10]; +, Angers [81.12]; ●, Hettich [81.13]; ∇, Geise [81.14]; ○, Iijima [81.15]; □ and ■, Lübbehusen [81.16]; ∗, Ivantsov [81.07]. For fitting lines, see detail figures. (B) (Detail). Self-diffusion in δ- and γ-iron. ×, Buffington [81.01]; ◆, Graham [81.03]; ◇, James [81.04]; Δ, Walter [81.05]; ▲, Heumann [81.08]; ∗, Ivantsov [81.07]. Fitting line for δ-iron using $D^0=6.6\times10^{-4}\,m^2\,s^{-1}$, Q=2.676 eV. Fitting line for γ-iron according to [81.08]. (C) (Detail). Self-diffusion in α_p-iron. Discrepancy between macrosectioning and sputtering data. Macrosectioning: Δ, Walter [81.05]; ▼, Borg [81.10]; ∇, Geise [81.14]; □, Lübbehusen [81.16]; sputtering: ■, Lübbehusen [81.16]; ○, Iijima [81.15]. Fitting line for macrosectioning data according to [81.14], for sputtering data according to [81.15]. (D) Detail. Self-diffusion in α-iron. Δ, Walter [81.05]; ▼, Borg [81.10]; +, Angers [81.12]; ●, Hettich [81.13]; ∇, Geise [81.14]; ○, Iijima [81.15]; □ and ■, Lübbehusen [81.16]. Fitting line for α_f- plus α_p-iron according to [81.15], for macrosectioning data in α_p-iron according to [81.14].

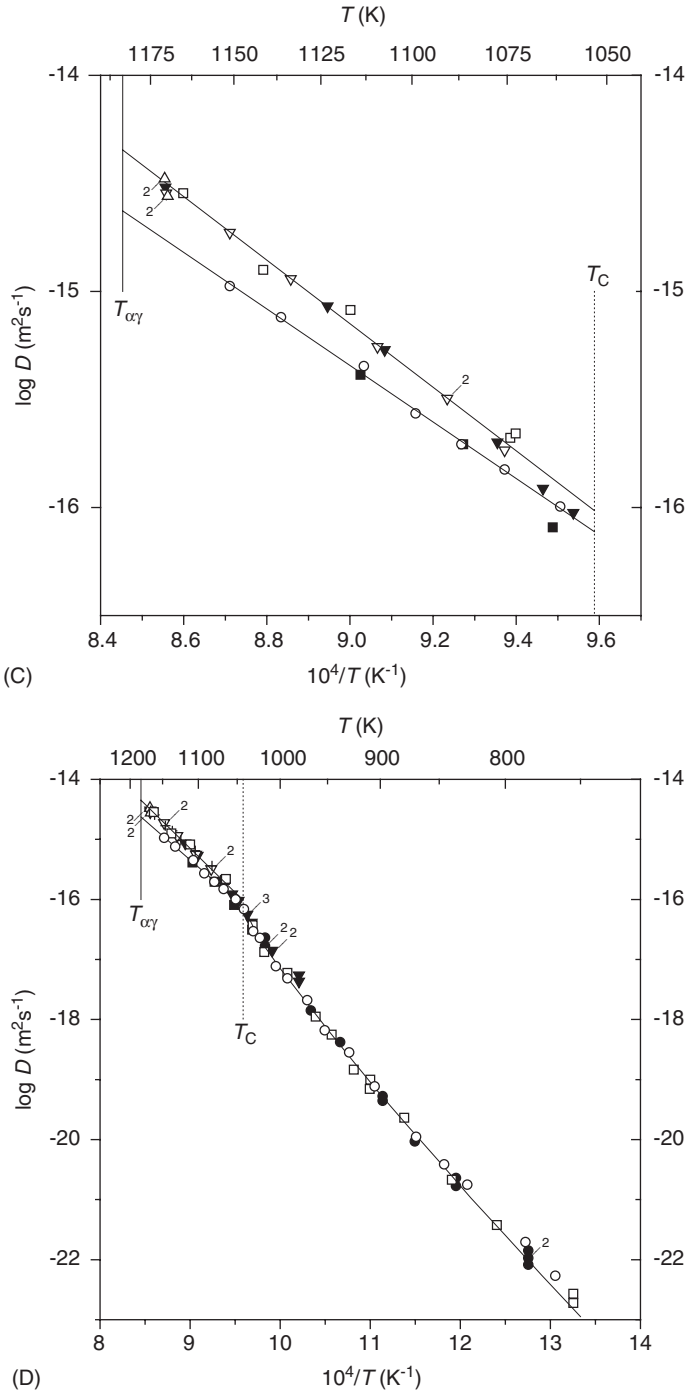

Fig. 81.01 (*Continued*)

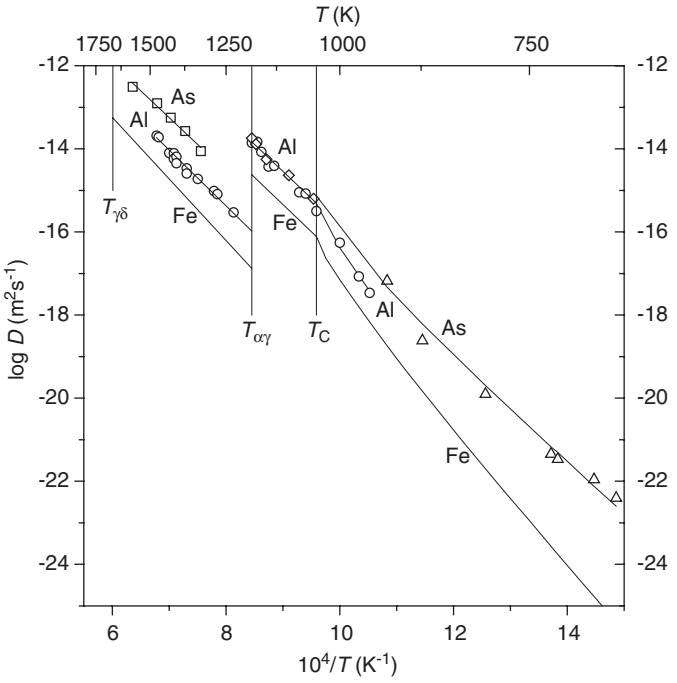

Fig. 81.02 Impurity diffusion in iron. Al in γ- and α-Fe: $\diamond$, Akimova [81.19]; $\bigcirc$, Bergner [81.20]. Fitting line for γ-iron according to [81.20]. Tentative fitting line for α-Fe using $D_p^0 = 14 \times 10^{-4}\,\mathrm{m^2\,s^{-1}}$, $Q_p = 2.58\,\mathrm{eV}$, $\alpha = 0.16$. As in γ- and α-Fe: $\square$, Božić [81.21]; Δ, Pérez [81.22].

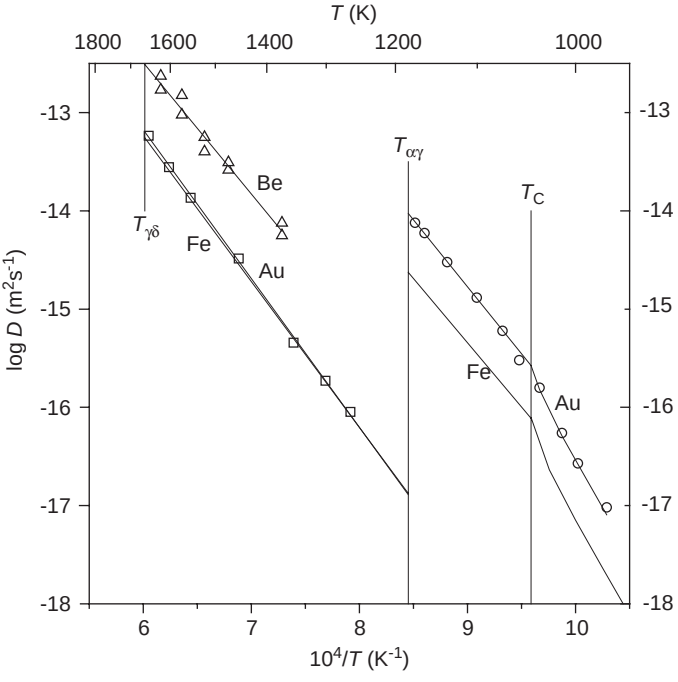

Fig. 81.03 Impurity diffusion in iron. Au in γ-Fe: $\square$, Yamazaki [81.23]; Au in α-Fe: $\bigcirc$, Borg [81.24]; Be in γ-Fe: Δ, Grigoryev [81.25].

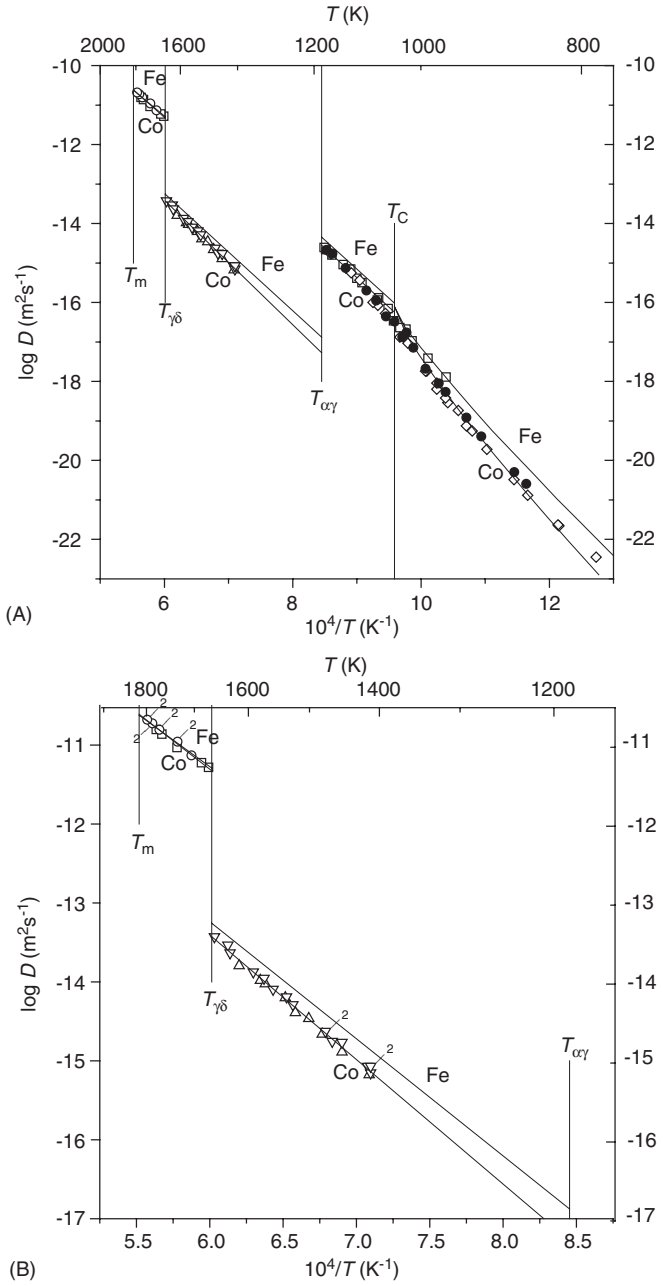

Fig. 81.04 (A) Impurity diffusion in iron. Co in δ-Fe: □, Borg [81.02]; ○, James [81.04]. Fitting line using D^0=23.4 × 10^{-4} m^2 s^{-1}, Q=2.869 eV; Co in γ-Fe: Δ, Suzuoka [81.26]; ∇, Badia [81.27]. Fitting line using D^0=1.12 × 10^{-4} m^2 s^{-1}, Q=3.127 eV. Co in α-Fe: □, Borg [81.24]; ◇, Mehrer [81.29]; ●, Iijima [81.31]. Fitting line: for α_p-Fe according to [81.24], for α_f-Fe according to [81.31]. (B) (Detail) Impurity diffusion in δ and γ-iron; Co in δ-Fe: □, Borg [81.02]; ○, James [81.04]. Fitting line using D^0=23.4 × 10^{-4} m^2 s^{-1}, Q=2.869 eV. Co in γ-Fe: Δ, Suzuoka [81.26]; ∇, Badia [81.27]. Fitting line using D^0=1.12 × 10^{-4} m^2 s^{-1}, Q=3.127 eV. The fitting lines of Co and Fe in δ-Fe nearly coincide. (C) (Detail) Impurity diffusion in α-iron. Co in α-Fe: □, Borg [81.24]; ◇, Mehrer [81.29]; ●, Iijima [81.31]. Fitting line: for α_p-Fe according to [81.24], for α_f-Fe according to [81.31].

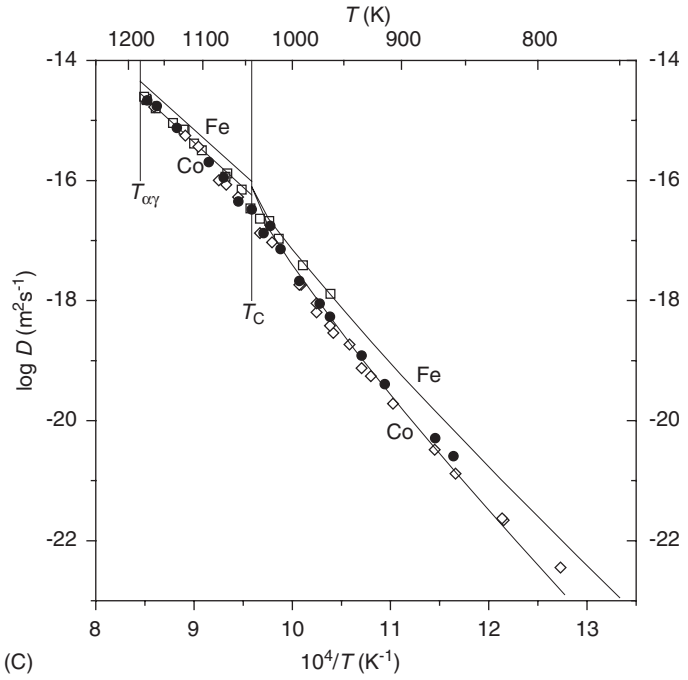

Fig. 81.04 (*Continued*)

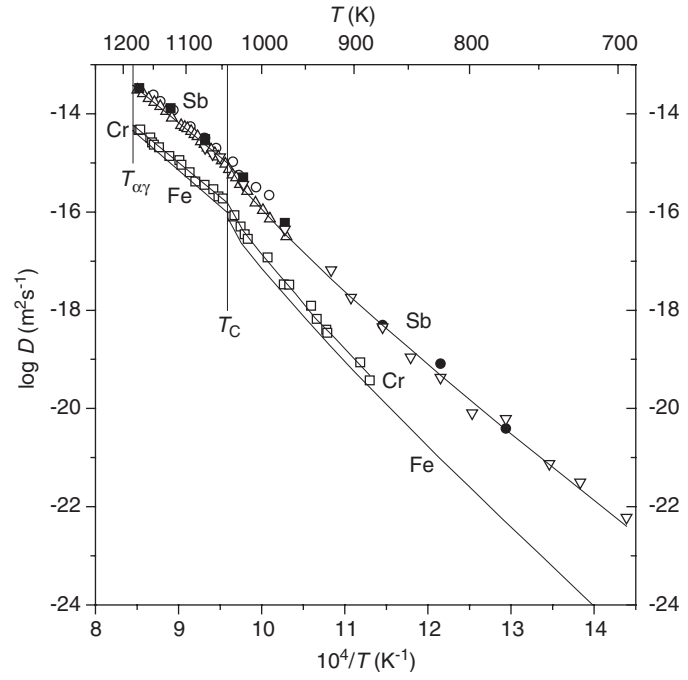

Fig. 81.05 Impurity diffusion in α-iron. Cr in α-Fe: □, Lee [81.35]; fitting line for α_p-Fe according to [81.35]; for α_f-Fe according to Eq. (02.19); Sb in α-Fe: ○, Bruggeman [81.65]; ■, Nishida [81.66]; ●, Myers [81.67]; Δ, Schröder [81.68]; ∇, Pérez [81.69]. Fitting line for α_p-Fe using D^0=220 × 10^{-4} m^2 s^{-1}, Q=2.76 eV, for α_f-Fe according to [81.69].

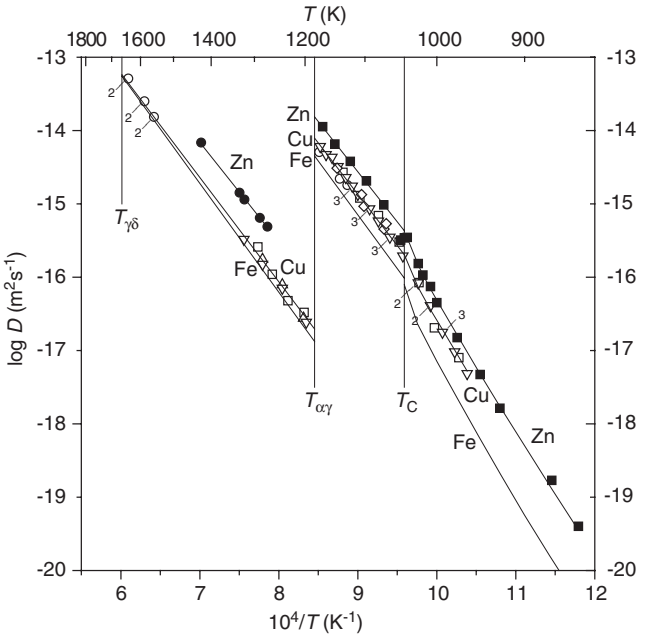

Fig. 81.06 Impurity diffusion in iron. Cu in γ-Fe: □, Speich [81.36]; ○, Rothman [81.37]; Δ, Tsuji [81.38]; ∇, Salje [81.39]. Fitting line using $D^0 = 0.21 \times 10^{-4}\,m^2\,s^{-1}$, $Q = 2.823$ eV. Cu in α-Fe: □, Speich [81.36]; ○, Rothman [81.37]; ◇, Lazarev [81.41]; ∇, Salje [81.39]. Fitting line using $D_p^0 = 54 \times 10^{-4}\,m^2\,s^{-1}$, $Q = 2.778$ eV, $\alpha = 0.09$; Zn in γ-Fe: ●, Budurov [81.83]; Zn in α-Fe: ■, Richter [81.84]; fitting line according to [81.84] with $\alpha = 0.11$.

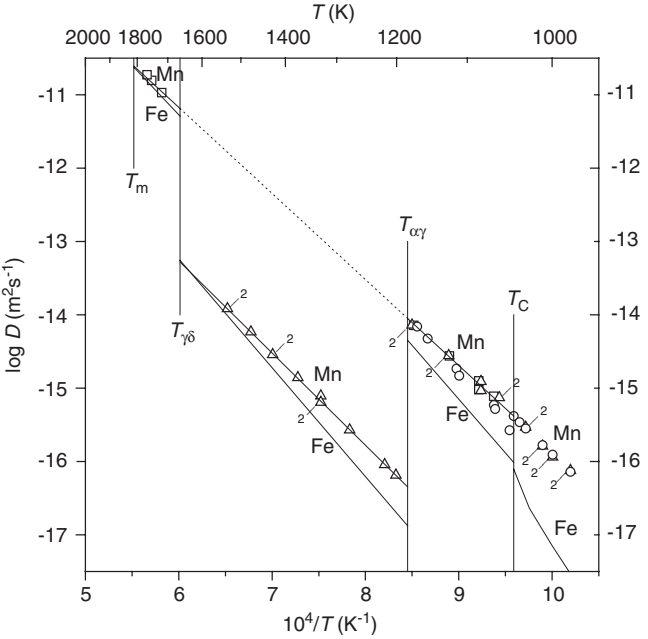

Fig. 81.07 Impurity diffusion in iron. Mn in δ-Fe: □, Kirkaldy [81.43]; Mn in γ-Fe: Δ, Nohara [81.44]; Mn in α-Fe: □, Kirkaldy [81.43]; ○, Lübbehusen [81.45]. Fitting line using $D^0 = 0.73 \times 10^{-4}\,m^2\,s^{-1}$, $Q = 2.326$ eV, $\alpha = 0.013$.

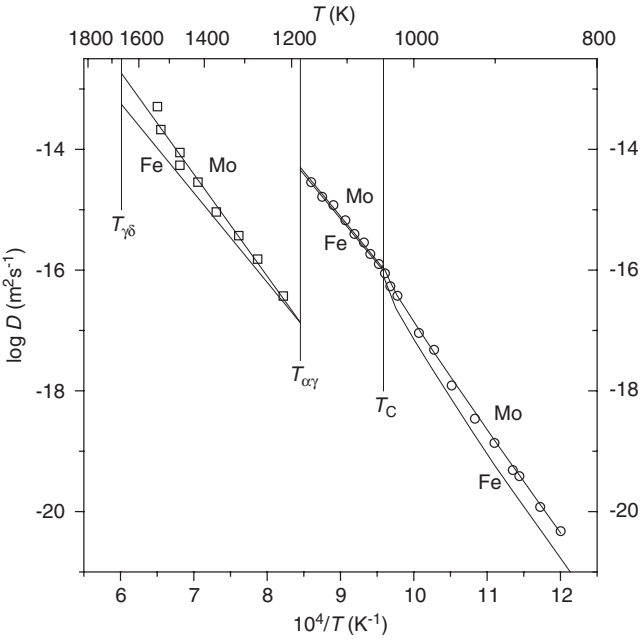

Fig. 81.08 Impurity diffusion in iron. Mo in γ-Fe: □, Nohara [81.46]; Mo in α-Fe: ○, Nitta [81.47].

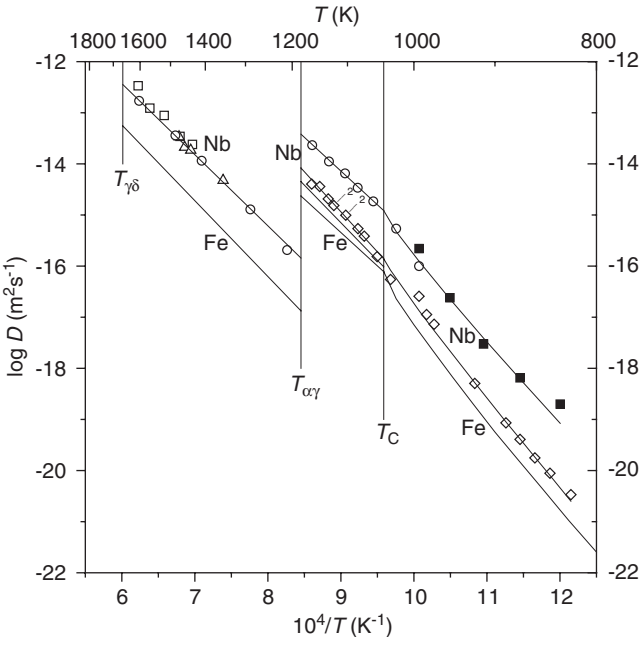

Fig. 81.09 Impurity diffusion in iron. Nb in γ-Fe: □, Sparke [81.42]; Δ, Kurokawa [81.48]; ○, Geise [81.49]. Fitting line according to [81.49]. Nb in α-Fe: (microsectioning) ◇, Oono [81.51]. Fitting line according to Eq. (02.19) with α=0.061 [81.51]; (macrosectioning) ■, Herzig [81.50]. Fitting line according to [81.50] with α=0.1. For Fe in α_p-Fe the fitting lines for macrosectioning and sputter data are shown.

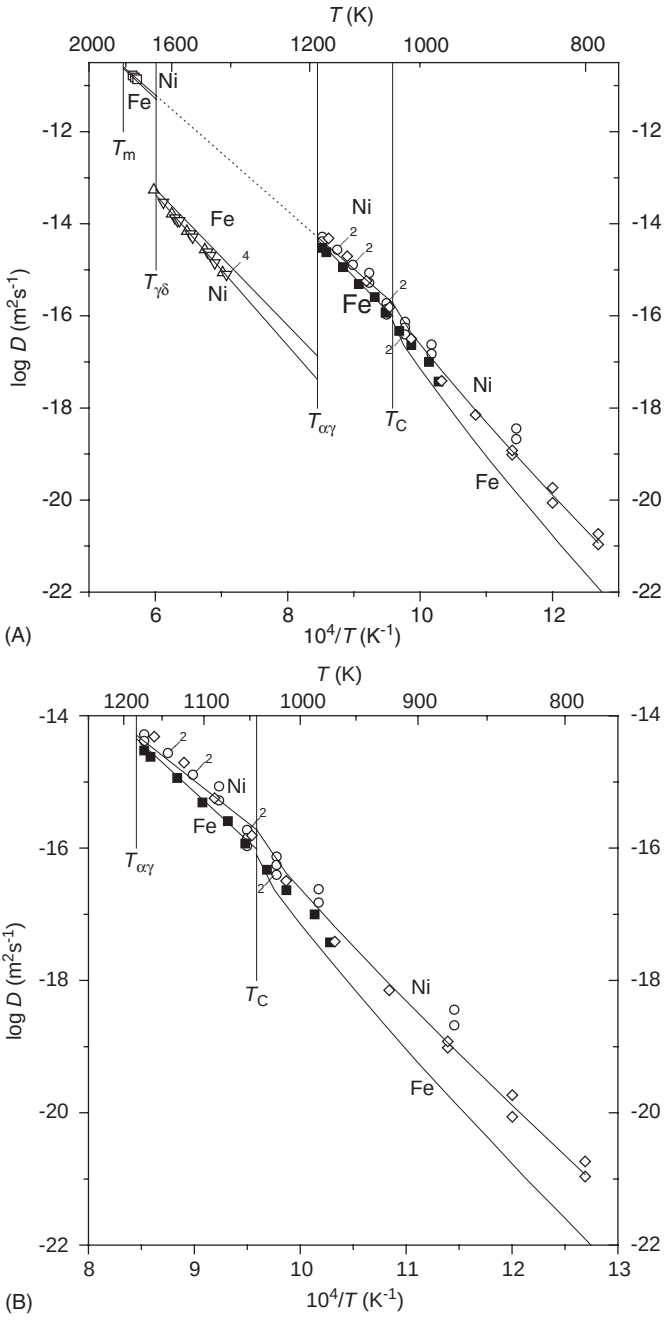

Fig. 81.10 (A) Impurity diffusion in iron. Ni in δ-Fe: □, Moharil [81.52]; Ni in γ-Fe: Δ, McEwan [81.53]; ∇, Badia [81.27]. Fitting line according to [81.27]; Ni in α-Fe: ○, Hirano [81.54]; ■, Borg [81.24]; ◇, Čermák [81.55]. Fitting line: fit to α-Fe and δ-Fe to according to Eq. (02.19) using $D^0=2.3\times10^{-4}\,m^2\,s^{-1}$, Q=2.5 eV and α=0.12. (B) (Detail) Impurity diffusion in α-iron. Ni in α-Fe: ○, Hirano [81.54]; ■, Borg [81.24]; ◇, Čermák [81.55]. Fitting line: fit to α-Fe and δ-Fe according to Eq. (02.19) using $D^0=2.3\times10^{-4}\,m^2\,s^{-1}$, Q=2.5 eV and α=0.12.

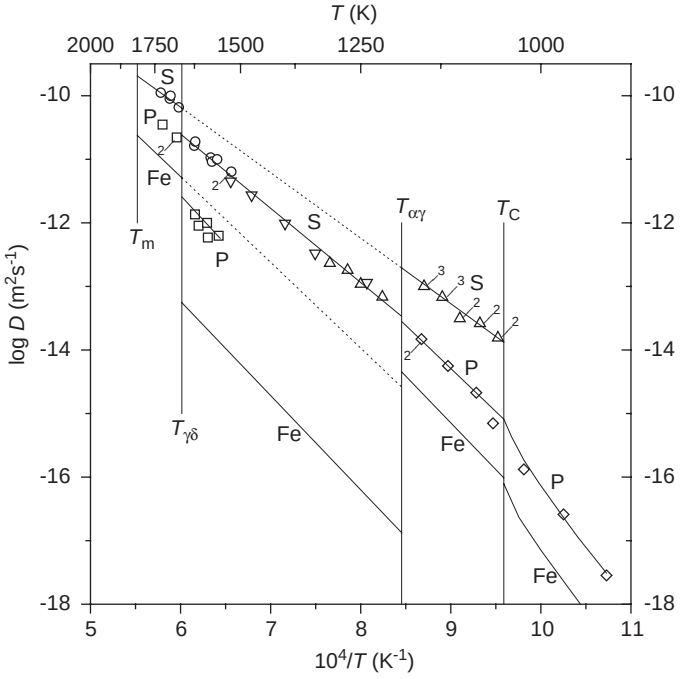

Fig. 81.11 Impurity diffusion in iron. P in δ- and γ-Fe: □, Seibel [81.56, 81.57]; P in α-Fe: ◇, Matsuyama [81.58]; S in δ- and γ-Fe: ○, Seibel [81.60, 81.58]; S in γ-Fe: Δ, Wang [81.61]; ∇, Hoshino [81.62]. Fitting line using D^0=2.5 × 10^{-4} m^2 s^{-1}, Q=2.31 eV. S in α-Fe: Wang [81.61]. Fitting line to α-Fe and δ-Fe: fit using D^0=1.0 × 10^{-4} m^2 s^{-1}, Q=2.044 eV.

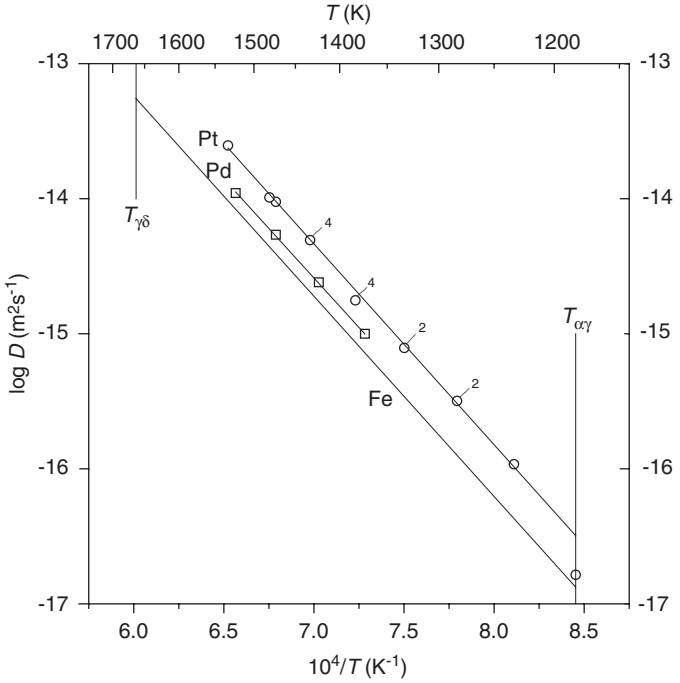

Fig. 81.12 Impurity diffusion in iron. Pd in γ-Fe: □, Fillon [81.09]; Pt in γ-Fe: ○, Million [81.59].

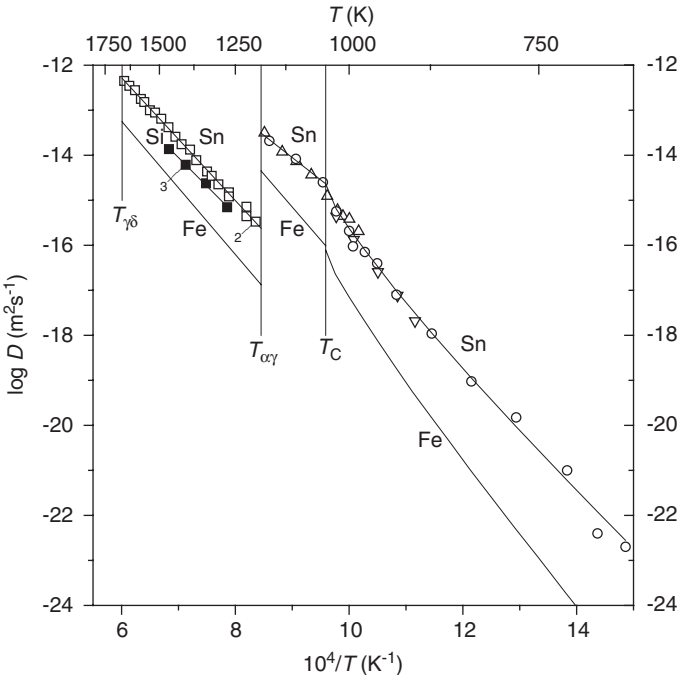

Fig. 81.13 Impurity diffusion in iron. Si in γ-Fe: ■, Bergner [81.71]; Sn in γ-Fe: □, Kimura [81.72]; Sn in α-Fe: Δ, Treheux [81.73]; ∇, Hennesen [81.75]; ○, Torres [81.76]. Fitting line for α-Fe according to [81.76].

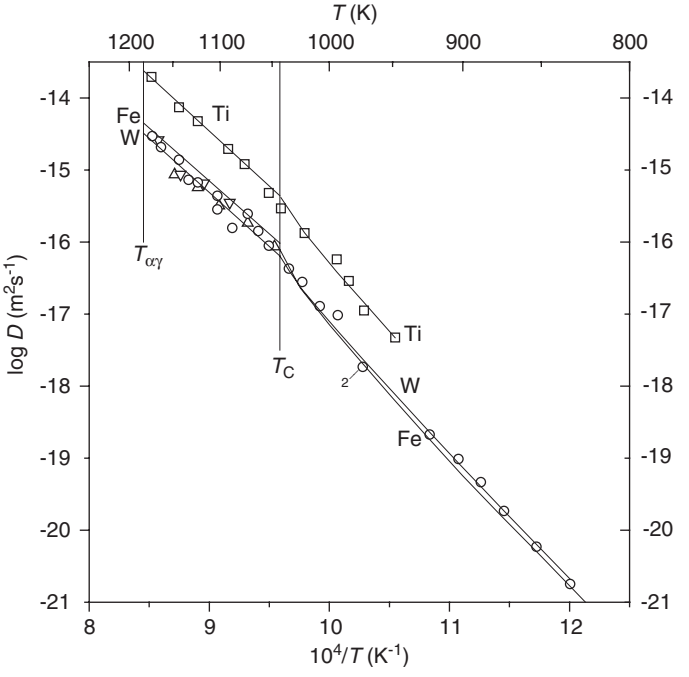

Fig. 81.14 Impurity diffusion in iron. Ti in α-Fe: □, Klugkist [81.78]. W in α-Fe: Δ, Kučera [81.81]; ∇, Alberry [81.34]; ○, Takemoto [81.82]. Fitting line according to [81.83] with α=0.078.

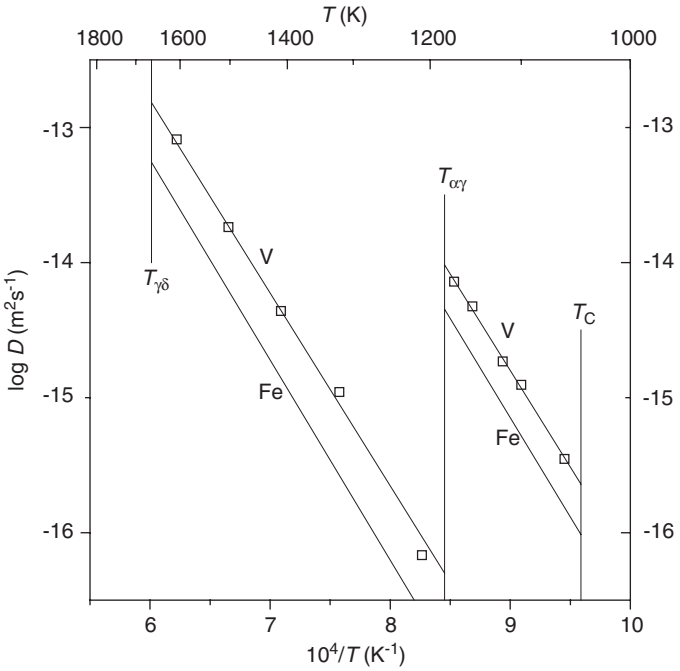

Fig. 81.15 Impurity diffusion in iron. V in γ- and α-Fe: □, Geise [81.14].

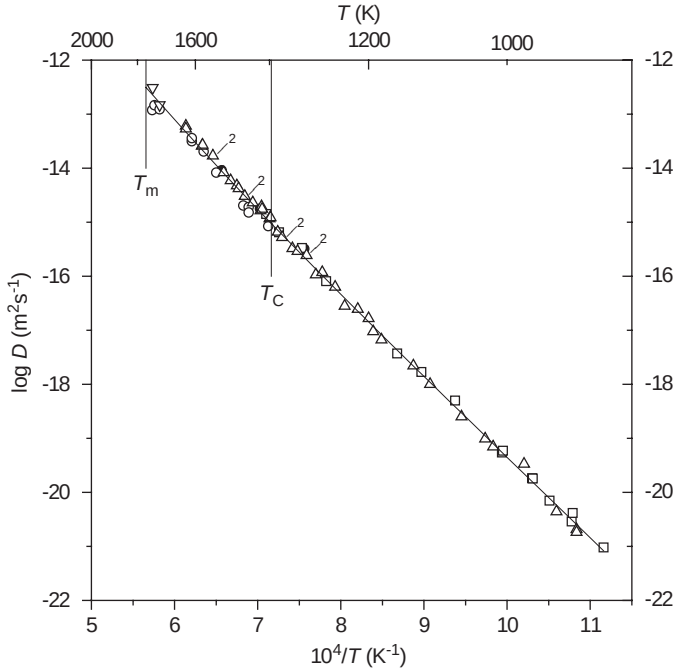

Fig. 82.01 Self-diffusion in cobalt. ●, Nix [82.01]; ○, (lathe sectioning) and □, (sputter sectioning) Bussmann [82.02]; ∇, (lathe sectioning) and Δ, (sputter sectioning) Lee [82.03]. Fitting line: two-exponential fit according to Neumann [82.04], using the average parameter set $D_1^0 = 0.3 \times 10^{-4}\,m^2\,s^{-1}$, $Q_1 = 2.943$ eV, $D_2^0 = 150 \times 10^{-4}\,m^2\,s^{-1}$, $Q_2 = 3.82$ eV, $D(T_m) = 3.1 \times 10^{-13}\,m^2\,s^{-1}$.

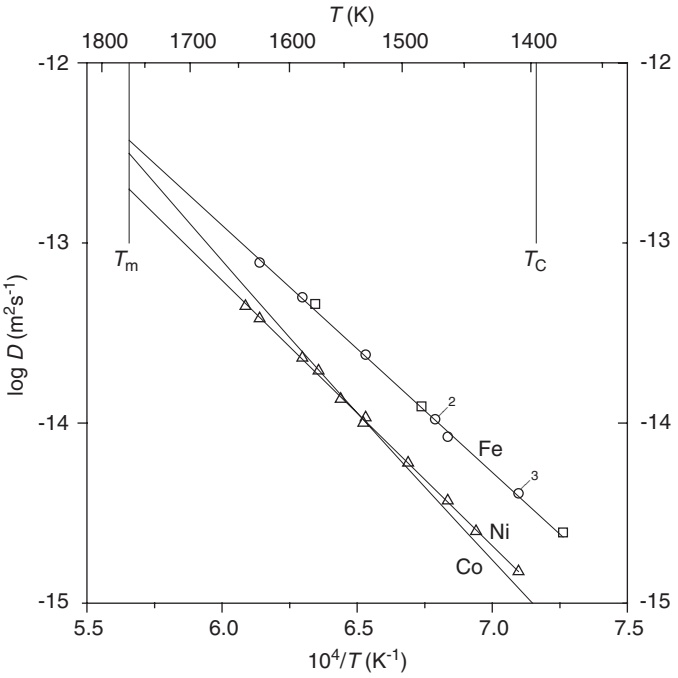

Fig. 82.02 Impurity diffusion in cobalt. Fe in Co: □, Mead [82.06]; ○, Badia [82.07]. Fitting line according to [82.06]; Ni in Co: Δ, Badia [82.07].

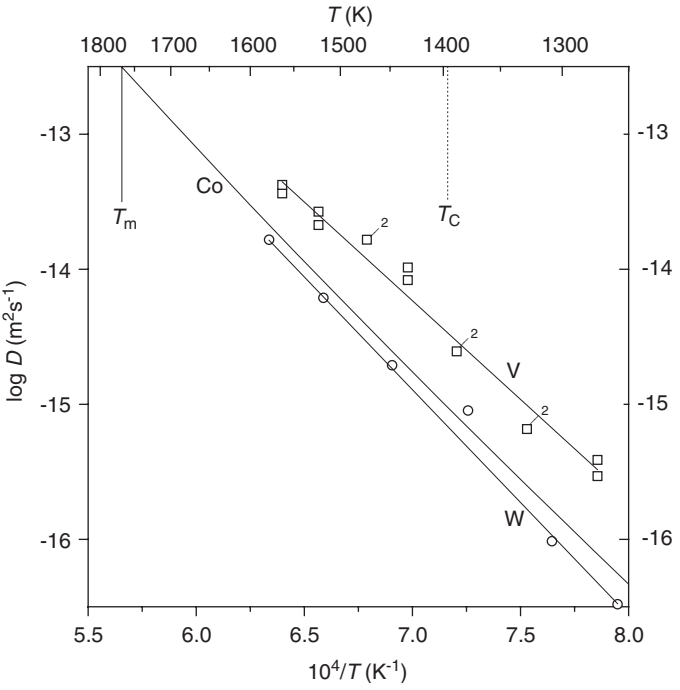

Fig. 82.03 Impurity diffusion in cobalt. V in Co: □, Kučera [82.12]. Fitting line: eye-fit using D^0=1.0 × 10^{-4} m^2 s^{-1}, Q=2.90 eV. W in Co: ○, Růžičková [82.13]. Fitting line: eye-fit using D^0=6.6 × 10^{-4} m^2 s^{-1}, Q=3.32 eV.

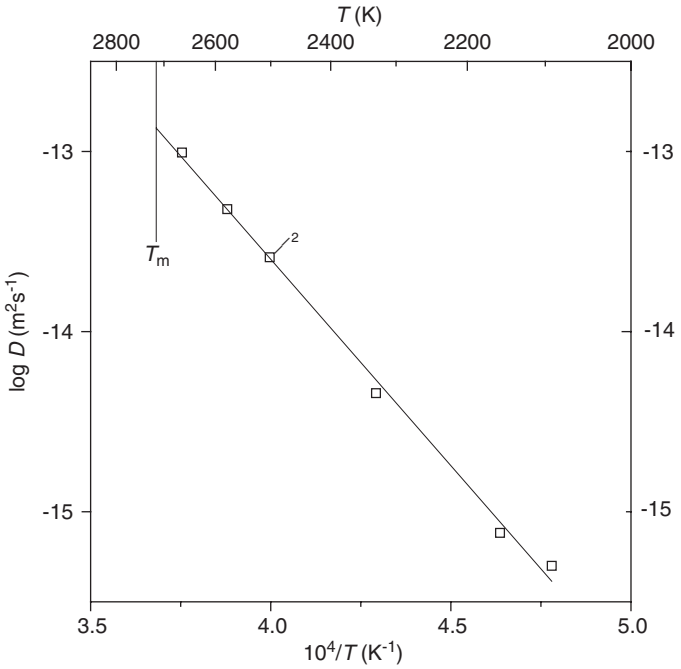

Fig. 83.01 Self-diffusion in iridium. □, Arkhipova [83.01].

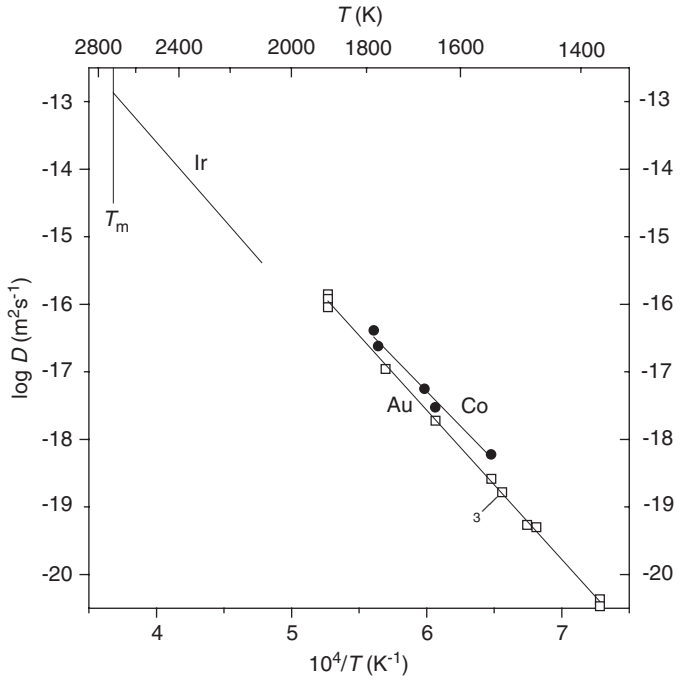

Fig. 83.02 Impurity diffusion in iridium. Au in Ir: □, Ermakov [83.02]; Co in Ir: ○, Ermakov [83.03].

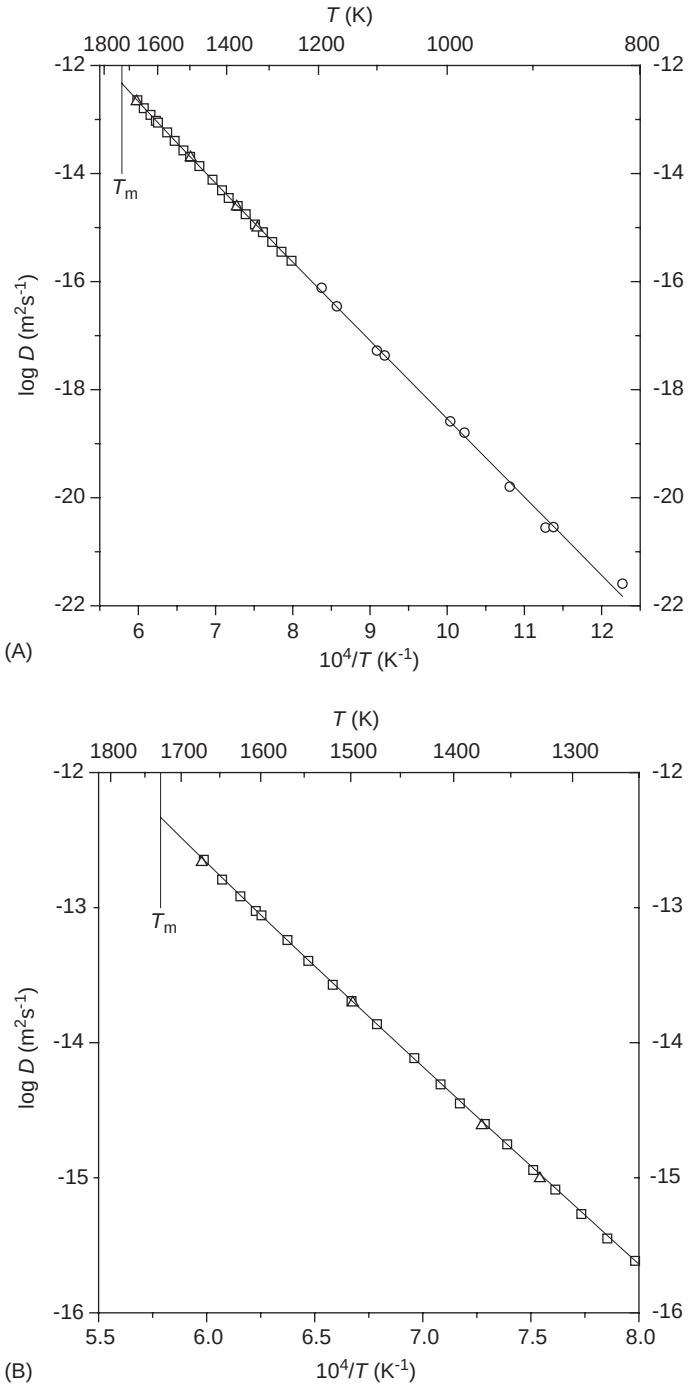

Fig. 84.01 (A) Self-diffusion in nickel. □, Bakker [84.09]; ○, Maier [84.10]; Δ, Vladimirov [84.11]. Fitting line: two-exponential fit according to Neumann [84.12]. (B) Detail. Self-diffusion in nickel; □, Bakker [84.09]; Δ, Vladimirov [84.11]. Fitting line: two-exponential fit according to Neumann [84.12].

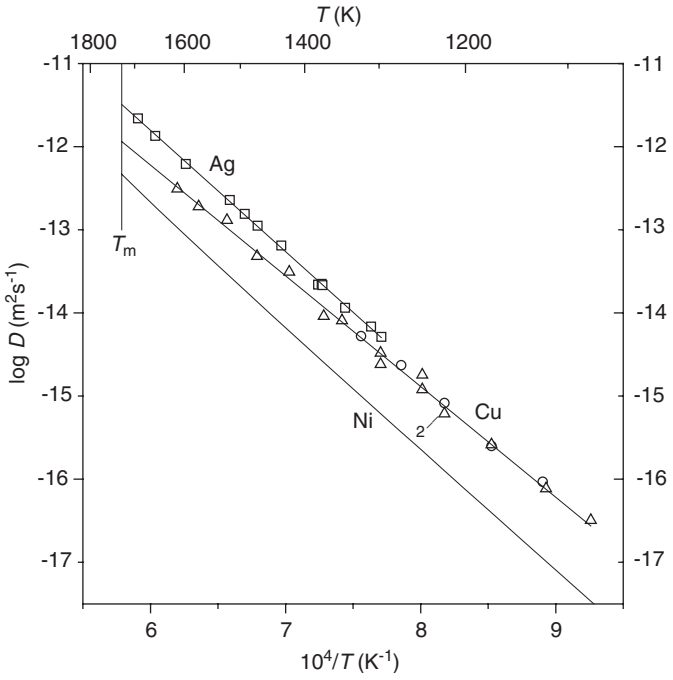

Fig. 84.02 Impurity diffusion in nickel. Ag in Ni: □, Vladimirov [84.14]; Cu in Ni: ○, Anand [84.29]; Δ, Taguchi [84.31]. Fitting line according to [84.31].

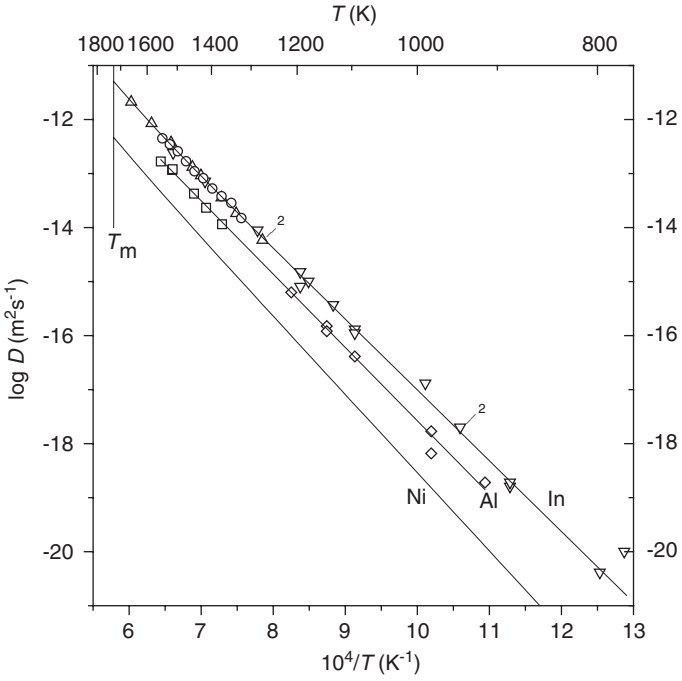

Fig. 84.03 Impurity diffusion in nickel. Al in Ni: □, Swalin [84.15]; ◇, Gust [84.16]; fitting line according to [84.16]; In in Ni: Δ, Vladimirov [84.36]; ∇, Gust [84.37]; ○, Takahashi [84.34]. Fitting line: two-exponential fit according to Neumann [84.38].

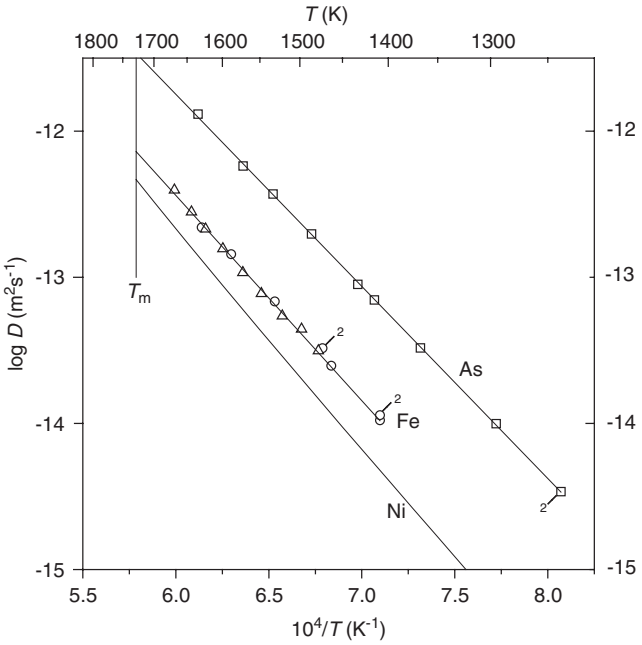

Fig. 84.04 Impurity diffusion in nickel. As in Ni: □, Vladimirov [84.17]; Fe in Ni: ○, Badia [84.24]; Δ, Bakker [84.32]. Fitting line according to [84.32].

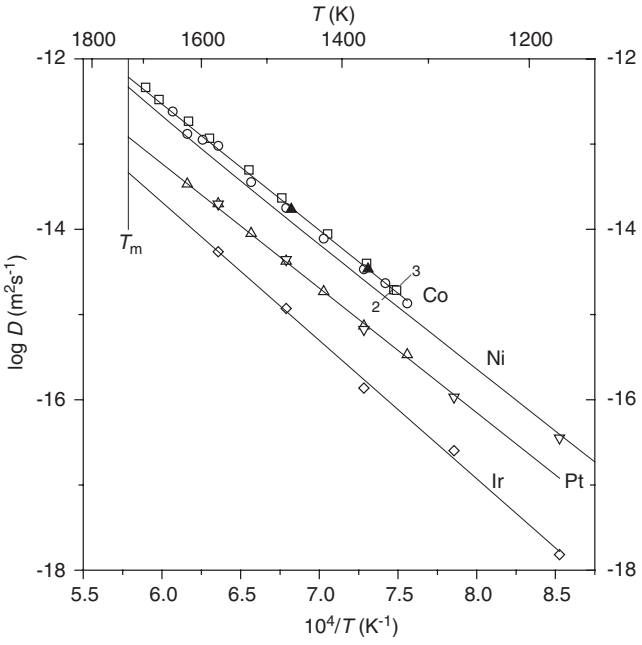

Fig. 84.05 Impurity diffusion in nickel. Co in Ni: □, Vladimirov [84.11]; ○, Jung [84.26]; ▲, McCoy [84.22]. Fitting line using $D^0 = 2.26 \times 10^{-5}\,m^2\,s^{-1}$, $Q = 2.937$ eV. Ir in Ni: ◇, Karunaratse [84.39]; Pt in Ni: Δ, Minamino [84.41]; ∇, Karunaratse [84.39]. Fitting line according to [84.41].

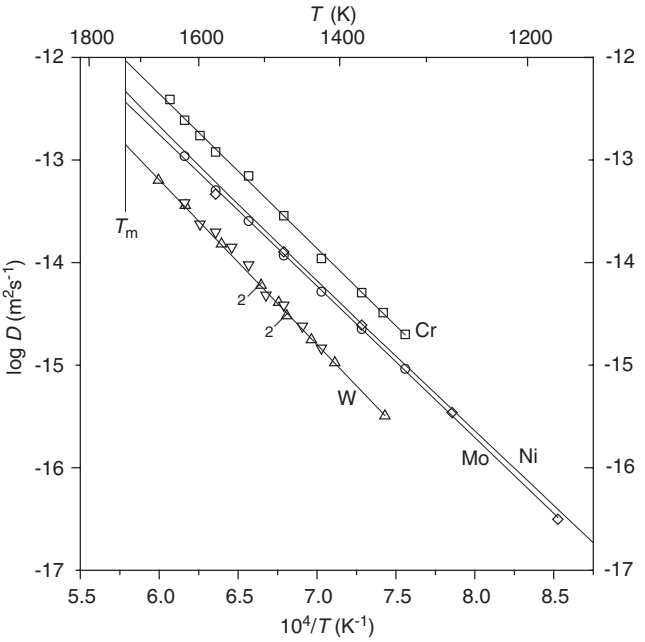

Fig. 84.06 Impurity diffusion in nickel. Cr in Ni: □, Jung [84.26]; Mo in Ni: ○, Minamino [84.41]; ◇, Karunaratse [84.42]. Fitting line according to [84.41]. W in Ni: Δ, Vladimirov [84.11]; ∇, Takahashi [84.34]. Fitting line according to [84.11].

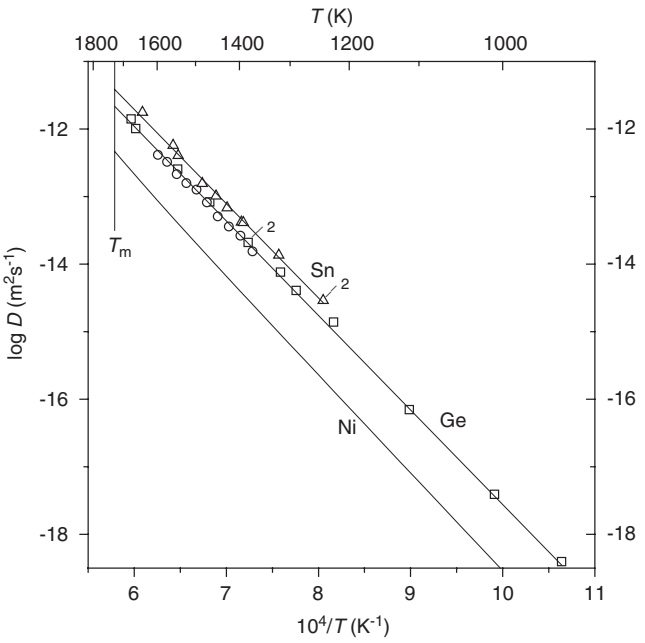

Fig. 84.07 Impurity diffusion in nickel. Ge in Ni: □, Mantl [84.33]; ○, Takahashi [84.34]. Fitting line using $D^0=2.7\times10^{-4}\,m^2\,s^{-1}$, $Q=2.68$ eV. Sn in Ni: Δ, Vladimirov [84.50].

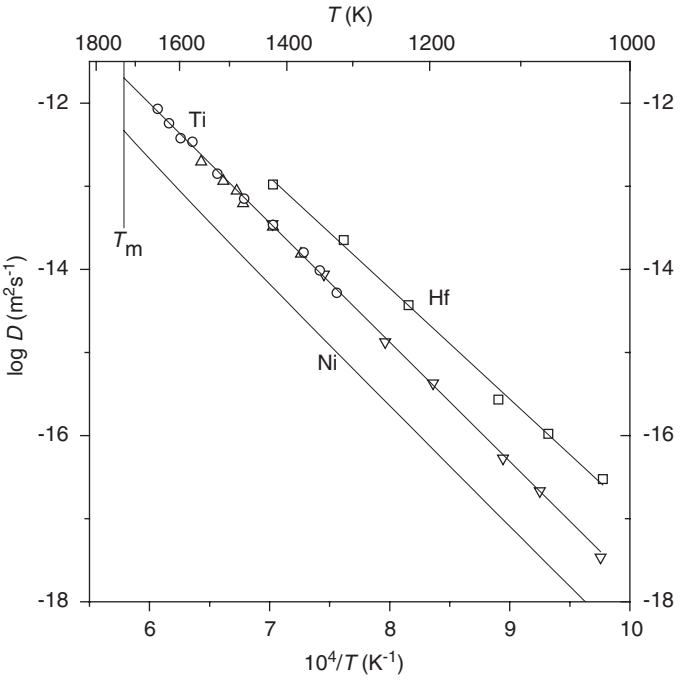

Fig. 84.08 Impurity diffusion in nickel. Hf in Ni: □, Bergner [84.35]; Ti in Ni: Δ, Swalin [84.15]; ∇, Bergner [84.43]; ○, Jung [84.26]. Fitting line according to [84.26].

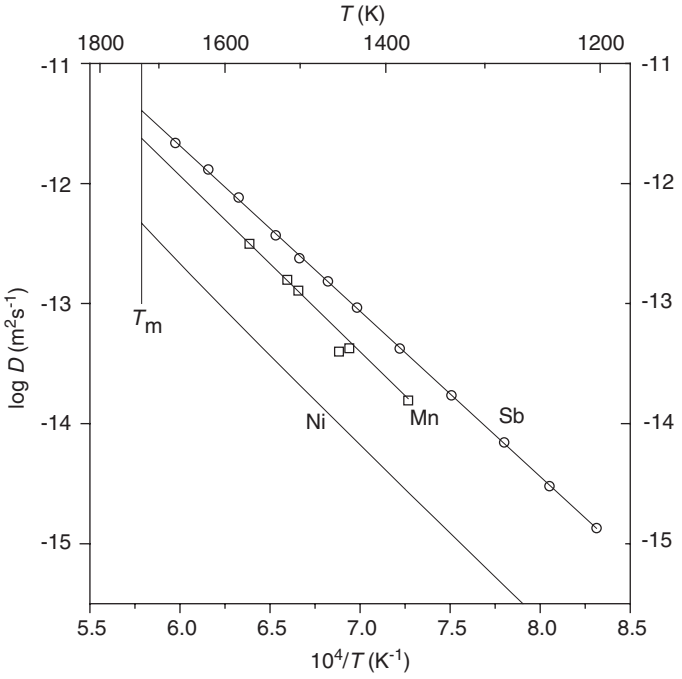

Fig. 84.09 Impurity diffusion in nickel. Mn in Ni: □, Swalin [84.15]; Sb in Ni: ○, Vladimirov [84.48].

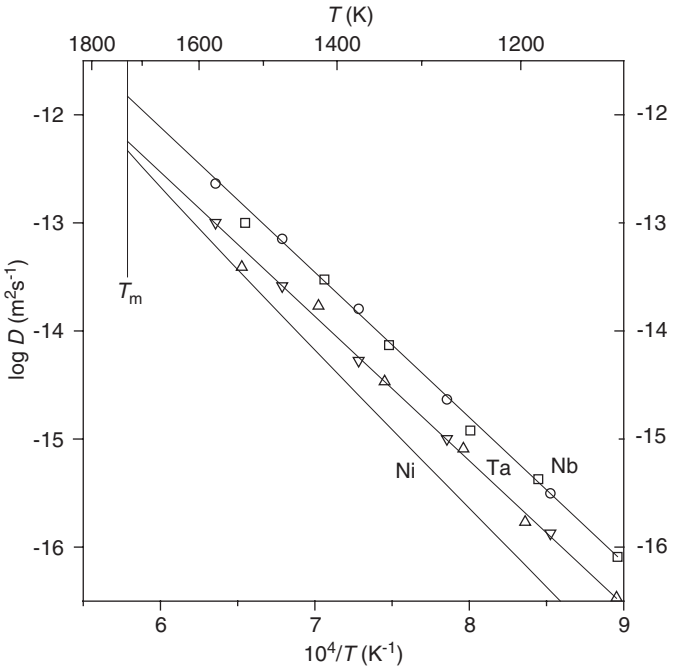

Fig. 84.10 Impurity diffusion in nickel. Nb in Ni: □, Bergner [84.43]; ○, Karunaratse [84.42]. Fitting line according to [84.42]; Ta in Ni: Δ, Bergner [84.43]; ∇, Karunaratse [84.45]. Fitting line using $D^0 = 0.3 \times 10^{-4} \times m^2 \times s^{-1}$, $Q = 2.64$ eV.

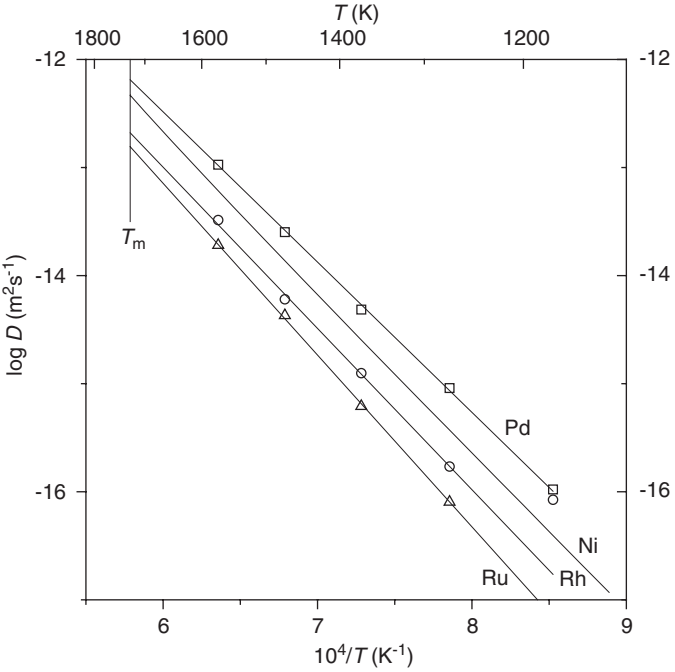

Fig. 84.11 Impurity diffusion in nickel. Pd in Ni: □, Karunaratse [84.39]; Rh in Ni: ○, Karunaratse [84.39]; Ru in Ni: Δ, Karunaratse [84.39].

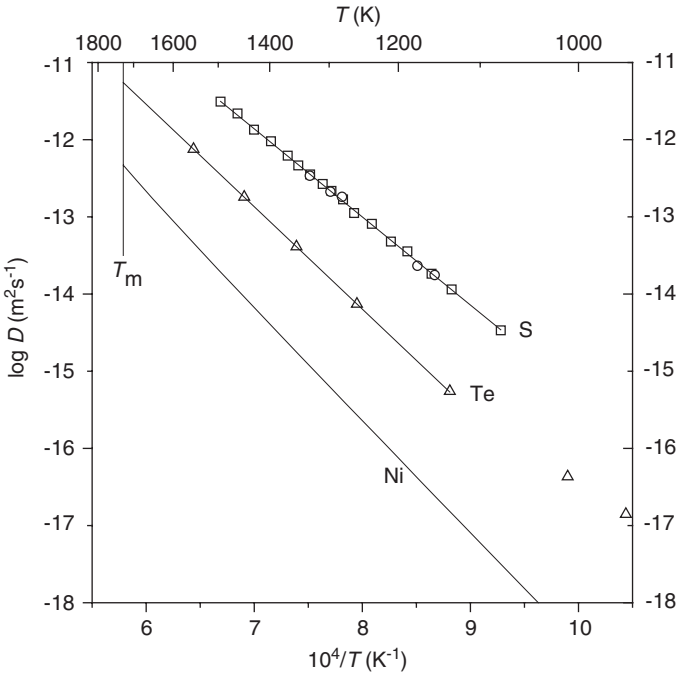

Fig. 84.12 Impurity diffusion in nickel. S in Ni: □, Vladimirov [84.46]; ○, Arbuzov [84.47]. Fitting line according to [84.46]. Te in Ni: Δ, Neuhaus [84.51].

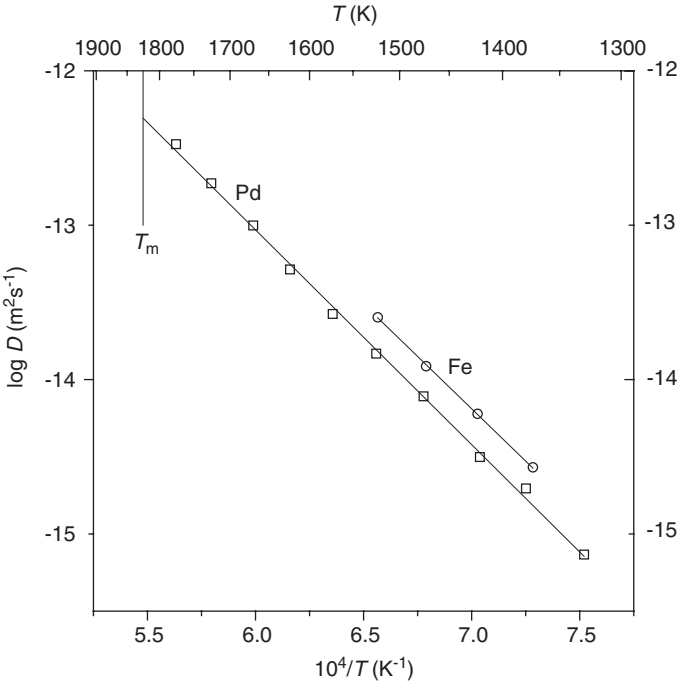

Fig. 85.01 Self-diffusion and impurity diffusion in palladium. Pd in Pd: □, Peterson [85.01]; Fe in Pd: ○, Fillon [85.02].

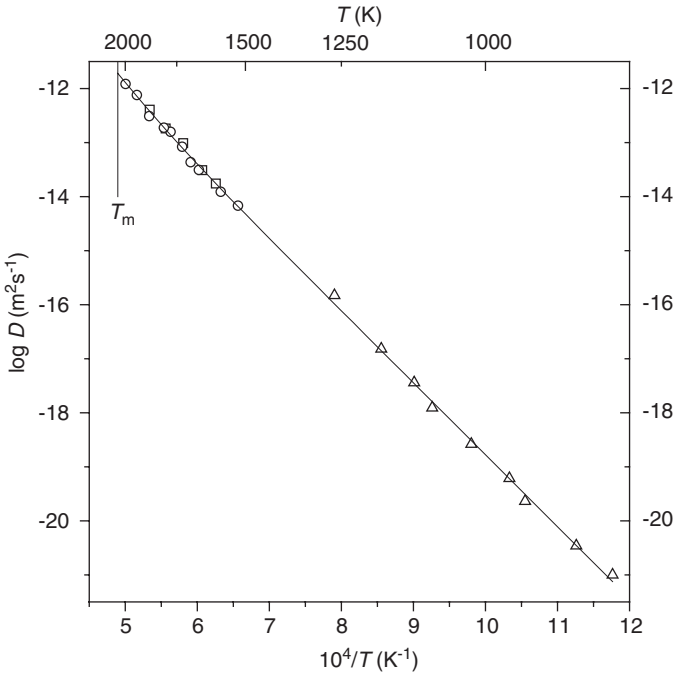

Fig. 86.01 Self-diffusion in platinum. □, Kidson [86.01]; ○, Cattaneo [86.02]; Δ, Rein [86.03]. Fitting line: two-exponential fit according to Neumann [86.04].

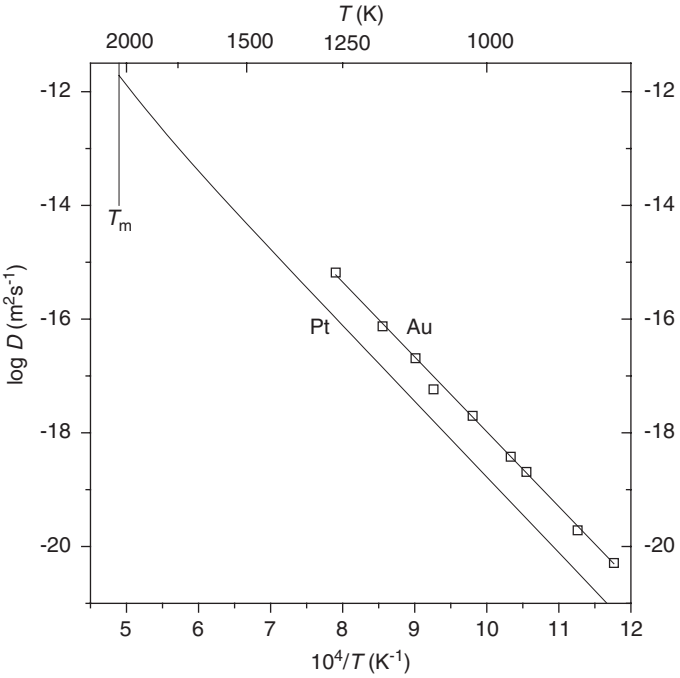

Fig. 86.02 Impurity diffusion in platinum. Au in Pt: □, Rein [86.03].

REFERENCES

References to Chapter 8.0

[80.01] J. Kučera, Czech. J. Phys. B **29** (1979) 797.
[80.02] F. Dyment, S. Balart, C. Lugo, R.A. Pérez, N. Di Lalla, M.J. Iribarren, Defect and Diffusion Forum **237–240** (2005) 402.
[80.03] V.I. Shalayev, I.B. Trachenko, V.A. Pavlov, N.I. Timofeyev, A.V. Guchshina, Fiz. Met. Metalloved. **29** (1970) 1061; Phys. Met. Metallogr. **29** (5) (1970) 170 (English transl.).

References to Chapter 8.1

[81.01] F.S. Buffington, K. Hirano, M. Cohen, Acta Metall. **9** (1961) 434.
[81.02] R.J. Borg, D.Y.F. Lai, O.H. Krikorian, Acta Metall. **11** (1963) 867.
[81.03] D. Graham, D.H. Tomlin, Phil. Mag. **8** (1963) 1581.
[81.04] D.W. James, G.M. Leak, Phil. Mag. **14** (1966) 701.
[81.05] C.M. Walter, N.L. Peterson, Phys. Rev. **178** (1969) 922.
[81.06] D. Graham, J. Appl. Phys. **40** (1969) 2386.
[81.07] I.G. Ivantsov, A.M. Blinkin, Fiz. Met. Metalloved. **22** (1966) 876; Phys. Met. Metallogr. **22** (6) (1966) 68 (English transl.).
[81.08] Th. Heumann, R. Imm, J. Phys. Chem. Sol. **29** (1968) 1613.
[81.09] J. Fillon, D. Calais, J. Phys. Chem. Sol. **38** (1977) 81.
[81.10] R.J. Borg, C.E. Birchenall, Trans. AIME **218** (1960) 980.
[81.11] V.M. Amonenko, A.M. Blinkin, I.G. Ivantsov, Fiz. Met. Metalloved. **17** (1964) 56; Phys. Met. Metallogr. **17** (1) (1964) 54 (English transl.).
[81.12] R. Angers, F. Claisse, Can. Metall. Quart. **7** (2), (1968) 73.
[81.13] G. Hettich, H. Mehrer, K. Maier, Scr. Metall. **11** (1977) 795.
[81.14] J. Geise, Ch. Herzig, Z. Metallk. **78** (1987) 291.
[81.15] Y. Iijima, K. Kimura, K. Hirano, Acta Metall **36** (1988) 2811.
[81.16] M. Lübbehusen, H. Mehrer, Acta Metall. Mater. **38** (1990) 283.
[81.17] A. Bondy, V. Lévy, C.R. Acad. Sci. Paris **272C** (1971) 19.
[81.18] T. Eguchi, Y. Iijima, K. Hirano, Crystal Latt. Defects **4** (1973) 265.
[81.19] I.A. Akimova, V.M. Mironov, A.V. Pokoyev, Fiz. Met. Metalloved. **56** (1983) 1225; Phys. Met. Metallogr. **56** (6) (1983) 175 (English transl.).
[81.20] D. Bergner, Y. Khaddour, Defect and Diffusion Forum **95–98** (1993) 709.
[81.21] B.I. Božić, R.J. Lučić, J. Mater. Sci. **11** (1976) 887.
[81.22] R.A. Pérez, D.N. Torres, F. Dyment, M. Weissman, Defect and Diffusion Forum **237–240** (2005) 462.
[81.23] Y. Yamazaki, Y. Iijima, M. Okada, Acta Mater. **52** (2004) 1247; Defect and Diffusion Forum **233–234** (2004) 115
[81.24] R.J. Borg, D.Y.F. Lai, Acta Metall. **11** (1963) 861.
[81.25] G.V. Grigoryev, L.V. Pavlinov, Fiz. Met. Metalloved. **25** (1968) 836; Phys. Met. Metallogr. **25** (5) (1968) 79 (English transl.).
[81.26] T. Suzuoka, Trans. Jpn. Inst. Metals **2** (1961) 176.
[81.27] M. Badia, A. Vignes, Acta Metall. **17** (1969) 177.
[81.28] K. Sato, Trans. Jpn. Inst. Metals **5** (1964) 91.
[81.29] H. Mehrer, D. Höpfel, G. Hettich, in: DIMETA 82, *Diffusion in Metals and Alloys*, Eds. F.J. Kedves, D.L. Beke, Trans. Tech. Publ., Switzerland (1983), p. 360.
[81.30] J. Kučera, L. Kozak, H. Mehrer, Phys. Stat. Sol. (a) **81** (1984) 497.
[81.31] Y. Iijima, K. Kimura, C.G. Lee, K. Hirano, Mater. Trans. Jpn. Inst. Metals **34** (1993) 20.
[81.32] A.W. Bowen, G.M. Leak, Metall. Trans. **1** (1970) 1695.
[81.33] A.M. Huntz, M. Aucouturier, P. Lacombe, C.R. Acad. Sci. Paris **265C** (1967) 554.

[81.34] P.J. Alberry, C.W. Haworth, Met. Sci. **8** (1974) 407.
[81.35] C.G. Lee, Y. Iijima, T. Hiratani, K. Hirano, Mater. Trans. Jpn. Inst. Metals **31** (1990) 255.
[81.36] G.R. Speich, J.A. Gula, R.M. Fisher, in: *The Electron Microprobe*, Eds. T.D. McKinley, K.F. Heinrich, D.B. Wittry, Wiley, New York (1966), p. 525.
[81.37] S.J. Rothman, N.L. Peterson, C.M. Walter, L.J. Nowicki, J. Appl. Phys. **39** (1968) 5041.
[81.38] S. Tsuji, K. Yamanaka, J. Jpn. Inst. Metals **38** (1974) 415.
[81.39] G. Salje, M. Feller-Kniepmeier, J. Appl. Phys. **48** (1977) 1833.
[81.40] K. Majima, H. Mitani, J. Jpn. Inst. Metals **41** (1977) 1207; Trans. Jpn. Inst. Metals **19** (1978) 663.
[81.41] V.A. Lazarev, V.M. Golikov, Fiz. Met. Metalloved. **29** (1970) 598; Phys. Met. Metallogr. **29** (3) (1970) 154 (English transl.).
[81.42] B. Sparke, D.W. James, G.M. Leak, J. Iron Steel Inst. **203** (1965) 152.
[81.43] J.S. Kirkaldy, P.N. Smith, R.C. Sharma, Metall. Trans. **4** (1973) 624.
[81.44] K. Nohara, K. Hirano, Trans. Iron Steel Inst. Jpn. (Suppl.) **11** (1971) 1267.
[81.45] M. Lübbehusen, Diploma work, Univ. Münster (1984), unpublished; from Ref. [81.78].
[81.46] K. Nohara, K. Hirano, J. Jpn. Inst. Metals **40** (1976) 1053.
[81.47] H. Nitta, Y. Yamamoto, R. Kanno, K. Takasawa, T. Iida, Y. Yamazaki, S. Ogu, Y. Iijima, Acta Mater. **50** (2002) 4117.
[81.48] S. Kurokawa, J.E. Ruzzante, A.M. Hey, F. Dyment, Met. Sci. **17** (1983) 433.
[81.49] J. Geise, Ch. Herzig, Z. Metallk. **76** (1985) 622.
[81.50] Ch. Herzig, J. Geise, S.V. Divinski, Z. Metallk. **93** (2002) 1180.
[81.51] N. Oono, H. Nitta, Y. Iijima, Mater. Trans. Jpn. Inst. Metals **44** (2003) 2078.
[81.52] D.B. Moharil, I. Jin, G.R. Purdy, Metall. Trans. **5** (1974) 59.
[81.53] J.R. MacEwan, J.U. MacEwan, L. Yaffe, Can. J. Chem. **37** (1959) 1629.
[81.54] K. Hirano, M. Cohen, B.L. Averbach, Acta Metall. **9** (1961) 440.
[81.55] J. Čermák, M. Lübbehusen, H. Mehrer, Z. Metallk. **80** (1989) 213.
[81.56] G. Seibel, C.R. Acad. Sci. Paris **256** (1963) 4661.
[81.57] G. Seibel, Mém. Sci. Rev. Métall. **61** (1964) 413.
[81.58] T. Matsuyama, H. Hosokawa, H. Suto, Trans. Jpn. Inst. Metals **24** (1983) 594.
[81.59] B. Million, J. Kučera, Kovové Mater. **11** (1973) 300.
[81.60] G. Seibel, C.R. Acad. Sci. Paris **255** (1962) 3182.
[81.61] S.J. Wang, H.J. Grabke, Z. Metallk. **61** (1970) 597.
[81.62] A. Hoshino, T. Araki, Trans. Natl. Res. Inst. Metals **13** (1971) 99.
[81.63] P.L. Gruzin, V.V. Mural, A.P. Fokin, Fiz. Met. Metalloved. **34** (1972) 1326; Phys. Met. Metallogr. **34** (6) (1972) 209 (English transl.).
[81.64] W. Arabczyk, M. Militzer, H.J. Müssig, J. Wieting, Scr. Metall. **20** (1986) 1549.
[81.65] G.A. Bruggeman, J.A. Roberts, Metall. Trans. **6A** (1975) 755.
[81.66] K. Nishida, H. Murohashi, T. Yamamoto, J. Jpn. Inst. Metals **41** (1977) 1101.
[81.67] S.M. Myers, H.J. Rack, J. Appl. Phys. **49** (1978) 3246.
[81.68] A. Schröder, M. Feller-Kniepmeier, Phys. Stat. Sol. (a) **110** (1988) 107.
[81.69] R.A. Pérez, D.N. Torres, F. Dyment, Appl. Phys. A **81** (2005) 787.
[81.70] M. Foucault-Villard, P. Benaben, J. Le Coze, C.R. Acad. Sci. Paris **291C** (1980) 169.
[81.71] D. Bergner, Y. Khaddour, S. Lörx, Defect and Diffusion Forum **66–69** (1989) 1407.
[81.72] K. Kimura, Y. Iijima, K. Hirano, Trans. Jpn. Inst. Metals **27** (1986) 1.
[81.73] D. Treheux, D. Marchive, J. Delagrange, P. Guiraldenq, C. R. Acad. Sci. Paris **274C** (1972) 1260.
[81.74] S.M. Myers, in: *Nontraditional Methods in Diffusion*, Eds. G.E. Murch, H.K. Birnbaum, J.R. Cost, Metall. Soc. AIME, Warrendale (1984), p. 137.
[81.75] K. Hennesen, H. Keller, H. Viefhaus, Scr. Metall. **18** (1984) 1319.
[81.76] D.N. Torres, R.A. Pérez, F. Dyment, Acta Mater. **48** (2000) 2925.
[81.77] O.A. Shaikh, Mater. Sci. Technol. **6** (1990) 1177.
[81.78] P. Klugkist, Ch. Herzig, Phys. Stat. Sol. (a) **148** (1995) 413.
[81.79] F. de Keroulas, J. Mory, Y. Quéré, J. Nucl. Mater. **22** (1967) 276.
[81.80] J. Růžičková, B. Million, J. Kučera, Kovové Mater. **19** (1981) 3.

[81.81] J. Kučera, B. Million, K. Ciha, Kovové Mater. **7** (1969) 97.
[81.82] S. Takemoto, H. Nitta, Y. Iijima, Y. Yamazaki, Phil. Mag. **87** (2007) 1619.
[81.83] S. Budurov, P. Kovatchev, Z. Kamenova, Z. Metallk. **64** (1973) 652.
[81.84] I. Richter, M. Feller-Kniepmeier, Phys. Stat. Sol. (a) **68** (1981) 289.

Further Investigations

γ-iron

Fe [81.85] P.L. Gruzin, Izv. Akad. Nauk SSSR, Otd. Tekhn. Nauk (3) (1953) 383.
Fe [81.86] A.A. Zhukhovitskii, V.A. Geodakyan, Zh. Fiz. Khim. **29** (1955) 1334.
Fe see Ref. [81.03].
Fe see Ref. [81.42].
Fe [81.87] A. Heiming, K.H. Steinmetz, G. Vogl, Y. Yoshida, J. Phys. F: Metal Phys. **18** (1988) 1491; QMS.
Al [81.88] J. Hirvonen, J. Räisänen, J. Appl. Phys. **53** (1982) 3314; NRA.
Al [81.89] O. Taguchi, M. Hagiwara, Y. Yamazaki, Y. Iijima, Defect and Diffusion Forum **194–199** (2001) 91; absorptiometry.
Co [81.90] K. Hirano, M. Cohen, Trans. Jpn. Inst. Metals **13** (1972) 96.
Cr see Ref. [81.34].
Cr [81.91] A.M. Huntz, P. Guiraldenq, M. Aucouturier, P. Lacombe, Mém. Sci. Rev. Mét. **66** (1969) 85.
Cu see Ref. [81.89].
Mo see Ref. [81.34].
Nb see Ref. [81.77].
Ni see Ref. [81.54].
Ni [81.92] J.I. Goldstein, R.E. Hanneman, R.E. Ogilvie, Trans. AIME **233** (1965) 812.
Ni [81.93] Y. Hanatate, K. Majima, H. Mitani, J. Jpn. Inst. Metals **41** (1977) 1211; Trans. Jpn. Inst. Metals **19** (1978) 669.
P [81.94] P.L. Gruzin, V.V. Minal, Fiz. Met. Metalloved. **16** (1963) 551; Phys. Met. Metallogr. **16** (4) (1963) 50 (English transl.).
S [81.95] N.G. Ainslie, A.U. Seyboldt, J. Iron Steel Inst. **194** (1960) 341.
S [81.96] V.V. Mural, A.P. Fokin, Metalloved. Termichesk. Obrab. Met. (6) (1978) 67.

α-iron

Fe see Ref. [81.01].
Fe see Ref. [81.03].
Fe see Ref. [81.04].
Fe see Ref. [81.06].
Fe [81.97] J. Kučera, B. Million, J. Růičkov, V. Foldyna, A. Jakobová, Acta Metall. **22** (1974) 135.
Co [81.98] K. Hirano, Y. Iijima, Defect and Diffusion Forum **66–69** (1989) 1039; precursor to Ref. [81.31].
Cr see Ref. [81.98]; precursor to Ref. [81.35].
Cr [81.99] R. Braun, M. Feller-Kniepmeier, Phys. Stat. Sol. (a) **90** (1985) 553; EPMA.
Cu [81.100] C.G. Lee, J.H. Lee, B.S. Lee, Y.I. Lee, T. Shimozaki, T. Okina, Defect and Diffusion Forum **237–240** (2005) 266; Laser induced break-down spectroscopy.
Mn [81.101] V. Irmer, M. Feller-Kniepmeier, J. Phys. Chem. Sol. **33** (1972) 2141.
Mo see Ref. [81.34].
P see Ref. [81.94].
P [81.102] P.L. Gruzin, V.V. Mural, A.P. Fokin, Fiz. Met. Metalloved. **17** (1964) 384.
Sb [81.103] R.A. Pérez, D.N. Torres, M. Weissman, F. Dyment, Defect and Diffusion Forum **194–199** (2001) 97; precursor to [81.69].
V see Ref. [81.81].

References to Chapter 8.2

[82.01] F.C. Nix, F.E. Jaumot, Phys. Rev. **82** (1951) 72.
[82.02] W. Bussmann, Ch. Herzig, W. Rempp, K. Maier, H. Mehrer, Phys. Stat. Sol. (a) **56** (1979) 87.

[82.03] C.G. Lee, Y. Iijima, K. Hirano, Defect and Diffusion Forum **95–98** (1993) 723.
[82.04] G. Neumann, V. Tölle, C. Tuijn, Physica B **304** (2001) 298.
[82.05] A. Davin, V. Leroy, D. Coutsouradis, L. Habraken, Kobalt **19** (1963) 51; Mém. Sci. Rev. Métall. **60** (1963) 275.
[82.06] H.W. Mead, C.E. Birchenall, Trans. AIME **203** (1955) 994.
[82.07] M. Badia, A. Vignes, Acta Metall. **17** (1969) 177; see also Ref. [82.21].
[82.08] Y. Iijima, K. Hirano, O. Taguchi, Phil. Mag. **35** (1977) 229.
[82.09] J.R. MacEwan, J.U. MacEwan, L. Yaffe, Can. J. Chem. **37** (1959) 1629.
[82.10] B. Million, J. Kučera, Kovové Mater. **4** (1973) 300.
[82.11] M.M. Pavlyuchenko, I.F. Kononyuk, Dokl. Akad. Nauk Belorussk. SSR **8** (1964) 157.
[82.12] J. Kučera, B. Million, J. Růžičková, Phys. Stat. Sol. (a) **96** (1986) 177.
[82.13] J. Růžičková, B. Million, J. Kučera, Kovové Mater. **19** (1981) 3.
[82.14] St. Budurov, P. Kovatchev, Z. Kamenova, Z. Metallk. **64** (1973) 377.
[82.15] A. Bristoti, A.R. Wazzan, Rev. Brasil. Fis. **4** (1974) 1.

Further Investigations

Co [82.16] R.C. Ruder, C.E. Birchenall, Trans. AIME **191** (1951) 142; absorption.
Co [82.17] P.L. Gruzin, Dokl. Akad. Nauk **86** (1952) 289.
Co see Ref. [82.06]
Co [82.18] S.D. Gertsriken, T.K. Yatsenko, L.F. Slastnikov, Voprosy Fiz. Met. Metalloved. **9** (1959) 154.
Co [82.19] K. Hirano, R.P. Agarwala, B.L. Averbach, M. Cohen, J. Appl. Phys. **33** (1962) 3049.
Co [82.20] A. Hässner, W. Lange, Phys. Stat. Sol. **8** (1965) 77.
Co [82.21] B. Million, J. Kučera, Acta Metall. **17** (1969) 339.
Co [82.22] M. Badia, *Thesis*, Univ. Nancy (1969).
Fe [82.23] M. Aucouturier, M.P.R. de Castro, P. Lacombe, Acta Metall. **13** (1965) 125; see also Kobalt **28** (1965) 1.
Fe see Ref. [82.14].
Ni see Ref [82.18].
Ni see Ref. [82.19].
Ni [82.24] B. Million, J. Kučera, Czech. J. Phys. B **21** (1971) 161.
W see [82.05].

References to Chapter 8.3

[83.01] N.K. Arkhipova, S.M. Klotsman, I.P. Polikarpova, A.N. Timofeyev, O.P. Shepatkovskiy, Fiz. Met. Metalloved. **62** (1986) 1181; Phys. Met. Metallogr. **62** (6) (1986) 127 (English transl.).
[83.02] A.V. Ermakov, S.M. Klotsman, S.A. Matveyev, G.N. Tatarinova, A.N. Timofeyev, V.K. Rudenko, N.I. Timofeyev, Fiz. Met. Metalloved. **92** (2), (2001) 87; Phys. Met. Metallogr. **92** (2001) 185 (English transl.).
[83.03] A.V. Ermakov, S.M. Klotsman, S.A. Matveyev, G.N. Tatarinova, A.N. Timofeyev, G.F. Kuzmenko, V.K. Rudenko, N.I. Timofeyev, Fiz. Met. Metalloved. **97** (5), (2004) 82; Phys. Met. Metallogr. **97** (2004) 507 (English transl.).

References to Chapter 8.4

[84.01] R.E. Hoffman, F.W. Pikus, R.A. Ward, Trans. AIME **206** (1956) 483.
[84.02] J.E. Reynolds, B.L. Averbach, M. Cohen, Acta Metall. **5** (1957) 29.
[84.03] J.R. MacEwan, J.U. MacEwan, L. Yaffe, Can. J. Chem. **37** (1959) 1623.
[84.04] J.R. MacEwan, J.U. MacEwan, L. Yaffe, Can. J. Chem. **37** (1959) 1629.
[84.05] K. Hirano, M. Cohen, B.L. Averbach, Trans. ASM **53** (1961) 910.
[84.06] K. Hirano, R.P. Agarwala, B.L. Averbach, M. Cohen, J. Appl. Phys. **33** (1962) 3049.
[84.07] A.Ya. Shinyayev, Fiz. Met. Metalloved. **15** (1963) 100.
[84.08] K. Monma, H. Suto, H. Oikawa, J. Jpn. Inst. Metals **28** (1964) 188.

[84.09] H. Bakker, Phys. Stat. Sol. **28** (1968) 569.
[84.10] K. Maier, H. Mehrer, E. Lessmann, W. Schüle, Phys. Stat. Sol. (b) **78** (1976) 689.
[84.11] A.B. Vladimirov, V.N. Kaygorodov, S.M. Klotsman, I.Sh. Trakhtenberg, Fiz. Met. Metalloved. **46** (1978) 1232; Phys. Met. Metallogr. **46** (6) (1978) 94 (English transl.).
[84.12] G. Neumann, V. Tölle, Phil. Mag. A **54** (1986) 619.
[84.13] D. Treheux, A. Heurtel, P. Guiraldenq, Acta Metall. **24** (1976) 503.
[84.14] A.B. Vladimirov, V.N. Kaygorodov, S.M. Klotsman, I.Sh. Trakhtenberg, Fiz. Met. Metalloved. **45** (1978) 1015; Phys. Met. Metallogr. **45** (5) (1978) 100 (English transl.).
[84.15] R.A. Swalin, A. Martin, Trans. AIME **206** (1956) 567.
[84.16] W. Gust, M.B. Hintz, A. Lodding, H. Odelius, B. Predel, Phys. Stat. Sol. (a) **64** (1981) 187.
[84.17] A.B. Vladimirov, S.M. Klotsman, I.Sh. Trakhtenberg, Fiz. Met. Metalloved. **48** (1979) 1113; Phys. Met. Metallogr. **48** (5) (1979) 193 (English transl.).
[84.18] A.D. Kurtz, B.L. Averbach, M. Cohen, Acta Metall. **3** (1955) 442.
[84.19] A. Chatterjee, D.J. Fabian, J. Inst. Metals **96** (1968) 186.
[84.20] G.V. Grigoryev, L.V. Pavlinov, Fiz. Met. Metalloved. **25** (1968) 836; Phys. Met. Metallogr. **25** (5) (1968) 79 (English transl.).
[84.21] A.R. Paul, R.P. Agarwala, Metall. Trans. **2** (1971) 2691.
[84.22] H.E. McCoy, J.F. Murdock, Trans. Quart. **56** (1963) 11.
[84.23] A. Hässner, W. Lange, Phys. Stat. Sol. **8** (1965) 77.
[84.24] M. Badia, A. Vignes, Acta Metall. **17** (1969) 177.
[84.25] B. Million, Z. Metallk. **63** (1972) 484.
[84.26] S.B. Jung, T. Yamane, Y. Minamino, K. Hirao, H. Araki, S. Saji, J. Mater. Sci. Lett. **11** (1992) 1333.
[84.27] J. Růžičková, B. Million, Mater. Sci. Eng. **50** (1981) 59.
[84.28] K. Monma, H. Suto, H. Oikawa, J. Jpn. Inst. Metals **28** (1964) 192.
[84.29] M.S. Anand, S.P. Murarka, R.P. Agarwala, J. Appl. Phys. **36** (1965) 3860.
[84.30] H. Helfmeier, M. Feller-Kniepmeier, J. Appl. Phys. **41** (1970) 3202.
[84.31] O. Taguchi, Y. Iijima, K. Hirano, J. Jpn. Inst. Metals **48** (1984) 20.
[84.32] H. Bakker, J. Backus, F. Waals, Phys. Stat. Sol. (b) **45** (1971) 633.
[84.33] S. Mantl, S.J. Rothman, L.J. Nowicki, J.L. Lerner, J. Phys. F: Metal Phys. **13** (1983) 1441.
[84.34] T. Takahashi, Y. Minamino, T. Asada, S.B. Jung, T. Yamane, J. High-Temp. Soc. **22** (1996) 121.
[84.35] D. Bergner, Kristall und Technik **7** (1972) 651.
[84.36] A.B. Vladimirov, V.N. Kaygorodov, S.M. Klotsman, I.Sh. Trakhtenberg, Fiz. Met. Metalloved. **45** (1978) 1301; Phys. Met. Metallogr. **45** (6) (1978) 160 (English transl.).
[84.37] W. Gust, M.B. Hintz, A. Lodding, H. Odelius, B. Predel, Acta Metall. **30** (1982) 75.
[84.38] G. Neumann, V. Tölle, Phil. Mag. A **57** (1988) 621.
[84.39] M.S.A. Karunaratse, R.C. Reed, Acta Mater. **51** (2003) 2905.
[84.40] D. Bergner, A. Meier, Microchim. Acta Suppl. **9** (1981) 99.
[84.41] Y. Minamino, H. Yoshida, S.B. Jung, K. Hirao, T. Yamane, Defect and Diffusion Forum **143–147** (1997) 257.
[84.42] M.S.A. Karunaratse, R.C. Reed, Defect and Diffusion Forum **237–240** (2005) 420.
[84.43] D. Bergner, *Habilitation Thesis*, Bergakademie Freiberg, Germany (1977).
[84.44] J.J. Blechet, A. van Craeynest, D. Calais, J. Nucl. Mater. **28** (1968) 177.
[84.45] M.S.A. Karunaratse, P. Carter, R.C. Reed, Mater. Sci. Eng. A **281** (2000) 229.
[84.46] A.B. Vladimirov, V.N. Kaygorodov, S.M. Klotsman, I.Sh. Trakhtenberg, Fiz. Met. Metalloved. **39** (1975) 319; Phys. Met. Metallogr. **39** (2) (1975) 82 (English transl.).
[84.47] V.L. Arbuzov, A.B. Vladimirov, S.Ye. Danilov, S.M. Klotsman, I. Sh. Trakhtenberg, Fiz. Met. Metalloved. **49** (1980) 356; Phys. Met. Metallogr. **49** (2) (1980) 113 (English transl.).
[84.48] A.B. Vladimirov, V.N. Kaygorodov, S.M. Klotsman, I.Sh. Trakhtenberg, Fiz. Met. Metalloved. **41** (1976) 429; Phys. Met. Metallogr. **41** (2) (1976) 181 (English transl.).
[84.49] R.A. Swalin, A. Martin, R. Olson, Trans. AIME **209** (1957) 936.
[84.50] A.B. Vladimirov, V.N. Kaygorodov, S.M. Klotsman, I.Sh. Trakhtenberg, Fiz. Met. Metalloved. **48** (1979) 352, Phys. Met. Metallogr. **48** (2) (1979) 107 (English transl.).
[84.51] P. Neuhaus, Ch. Herzig, Z. Metallk. **80** (1989) 220.

[84.52] J.P. Zanghi, A. van Craeynest, D. Calais, J. Nucl. Mater. **39** (1971) 133; Mém. Sci. Rev. Métall. **69** (1972) 73.
[84.53] S.P. Murarka, M.S. Anand, R.P. Agarwala, Acta Metall. **16** (1968) 69.
[84.54] K. Monma, H. Suto, H. Oikawa, J. Jpn. Inst. Metals **28** (1964) 197.
[84.55] T. Yamamoto, T. Takashima, K. Nishida, J. Jpn. Inst. Metals **43** (1979) 1196.

Further Investigations

Ni [84.56] A. Messner, R. Benson, J.E. Dorn, Trans. ASM **53** (1961) 227; absorption
Ni [84.57] G.B. Fedorov, V.M. Raetskii, E.A. Smirnov, Met. Metalloved. Chist. Met., Sb. Nauchn. Rabot (3) (1961) 203.
Ni [84.58] A.R. Wazzan, J.E. Dorn, J. Appl. Phys. **36** (1965) 222; absorption
Ni see Ref. [84.23].
Ni [84.59] I.G. Ivantsov, Fiz. Met. Metalloved. **22** (1966) 725; Phys. Met. Metallogr. **22** (5) (1966) 77 (English transl.); absorption.
Ni [84.60] V.M. Amonenko, I.G. Ivantsov, A.M. Blinkin, Fiz. Met. Metalloved. **27** (1969) 466; Phys. Met. Metallogr. **27** (3) (1969) 83 (English transl.); absorption.
Ni [84.61] B. Million, J. Kučera, Czech. J. Phys. B **21** (1971) 161.
Ni [84.62] M.B. Bronfin, G.S. Bulatov, I.A. Drugova, Fiz. Met. Metalloved. **40** (1975) 363; Phys. Met. Metallogr. **40** (2) (1975) 115 (English transl.); absorption
Ni [84.63] M. Feller-Kniepmeier, H. Helfmeier, Z. Metallk. **67** (1976) 533; absorption.
Ni [84.64] B. Million, J. Růžičková, J. Velišek, J. Vřeštal, Mater. Sci. Eng. **50** (1981) 43.
Ag [84.65] D. Treheux, A. Heurtel, P. Guiraldenq, C. R. Acad. Sci. Paris **280C** (1975) 1191; precursor to Ref. [84.13].
Co see Ref. [84.57].
Co [84.66] M. Badia, A. Vignes, C. R. Acad. Sci. Paris **264C** (1967) 858; precursor to Ref. [84.24].
Cr [84.67] A. Davin, V. Leroy, D. Coutsouradis, L. Habraken, Kobalt **19** (1963) 51; Mém. Sci. Rev. Métall. **60** (1963) 275.
Fe [84.68] M. Badia, A. Vignes, C. R. Acad. Sci. Paris **264C** (1967) 1528; precursor to Ref. [84.24].
Fe see Ref. [84.64].
Mg see Ref. [84.49].
Mo see Ref. [84.49].
Mo see Ref. [84.67].
Mo [84.69] Yu.E. Ugaste, V.N. Pimenov, Fiz. Met. Metalloved. **33** (1972) 1034; Phys. Met. Metallogr. **33** (5) (1972) 125 (English transl.); EPMA.
Mo [84.70] C.P. Heijwegen, G.D. Rieck, Acta Metall. **22** (1974) 1269; EPMA.
Nb [84.71] R.V. Patil, G.B. Kale, J. Nucl. Mater. **230** (1996) 57; EPMA.
Pt [84.72] B. Million, J. Kučera, Kovové Mater. **4** (1973) 300.
S [84.73] S.J. Wang, H.J. Grabke, Z. Metallk. **61** (1970) 597; Resistivity measurement
Sn [84.74] D. Marchive, D. Duc, M. Treheux, P. Guiraldenq, C. R. Acad. Sci. Paris **280C** (1975) 25.
V see Ref. [84.67].
W see Ref. [84.15].
W [84.75] H.W. Allison, G.E. Moore, J. Appl. Phys. **29** (1959) 842.
W see Ref. [84.67].
W [84.76] D. Bergner, Microchim. Acta Suppl. **3** (1968) 19; see also Ref. [84.43]; EPMA
W [84.77] J. Růžičková, B. Million, J. Kučera, Met. Mater. **19** (1981) 3; see also Ref. [84.64]
W see Ref. [84.45].

References to Chapter 8.5

[85.01] N.L. Peterson, Phys. Rev. **136A** (1964) A568.
[85.02] J. Fillon, D. Calais, J. Phys. Chem. Sol. **38** (1977) 81.

References to Chapter 8.6

[86.01] G.V. Kidson, R. Ross, in: Proc. Intern. Conf. in Science and Research, Paris, **1** (1957) p. 185.
[86.02] F. Cattaneo, E. Germagnoli, F. Grasso, Phil. Mag. **7** (1962) 1373.
[86.03] G. Rein, H. Mehrer, K. Maier, Phys. Stat. Sol. (a) **45** (1978) 253.
[86.04] G. Neumann, V. Tölle, Phil. Mag. A **54** (1986) 619.
[86.05] D. Bergner, K. Schwarz, Neue Hütte **23** (1978) 210.
[86.06] J. Kučera, T. Zemčik, Can. Metall. Quart. **7** (2), (1968) 83.

CHAPTER 9

Self-Diffusion and Impurity Diffusion in Rare Earth Metals

Contents

Tables
- 9.1. Cerium (Ce) 319
- 9.2. Praseodymium (Pr) 321
- 9.3. Neodymium (Nd) 324
- Europium (Eu) 324
- Gadolinium (Gd) 324
- Erbium (Er) 325
- Ytterbium (Yb) 325

Figures
- Cerium 326
- Praseodymium 327
- Neodymium 329
- Europium 330
- Gadolinium 330
- Erbium 331
- Ytterbium 331

References 332

For **promethium** (Pm), **samarium** (Sm), **terbium** (Tb), **dysprosium** (Dy), **holmium** (Ho), **thulium** (Tm) and **lutetium**(Lu) no data are available. Only self-diffusion was studied in **europium** (Eu), **gadolinium** (Gd) and **ytterbium** (Yb).

In Table 9.0 lattice structure, lattice constants, melting temperature and phase transition of the rare earths are listed.

Table 9.0 Lattice structure, lattice constants a and c, phase transition (T_{ij}) and melting temperature T_m

Metal	Ce		Pr		Nd		Eu	Gd	Er	Yb	
Phase	δ	γ	β	α	β	α		β		γ	α
Structure	bcc	fcc	bcc	dhcp[1]	bcc	dhcp[1]	bcc	bcc	hcp	bcc	hcp
T_{ij} (K)	992		1,068		1,145			1,538		993	
T_m (K)	1,071		1,205		1,289		1,099	1,585	1,795	1,097	
a (nm)	0.419	0.516	0.420	0.363	0.418	0.362	0.461	0.410	0.346	0.547	0.387
c (nm)				1.195		1.192			0.576		0.645
c/a				3.29		3.28			1.67		1.67

[1] In the double-hcp structure the stacking of the close-packed planes is ABACABAC…, compared to the simple hcp structure with an ABAB… stacking.

Table 9.1 Diffusion in cerium (References, see page 332)

(1)	(2a)	(2b)	(3)	(4)	(5)	(6)	(7)	(8)	(9)	(10)	(11)	(12)
X	D^0 (10^{-4} m^2 s^{-1})	Q (eV) and (kJ/mole)	$D(T_m)$ (10^{-12} m^2 s^{-1})	T-range (K) ($\overline{T}/T_m$)	No. of data points	Material, purity	Experimental method	Remarks on the pp	Further remarks	Also studied	Figure	Reference
Self-diffusion												
Ce	0.012	0.932 (90.0)	49	992–1,044 (0.95) δ-Ce	9	pc 3N	^{141}Ce, vapour deposition; lathe	3 examples			91.01	Dariel (1971) [91.01]
	0.55	1.587 (153.2)	–	801–965 (0.82) γ-Ce	10 (8T)							
Ce	7×10^{-3}	0.878 (84.7)	52	1,018–1,064 (0.97) δ-Ce	5	pc 3N	^{141}Ce, vapour deposition; lathe and residual activity	2 examples			91.01	Languille (1973) [91.02]
Ce	–	–		1,003, 1,028 δ-Ce	2	pc 3N	^{141}Ce, electroplated; lathe	3 examples at high p		$\Delta V/V_0 < 0$	91.01	Languille (1974) [91.03]
Ce	–	–		930 γ-Ce	1*	pc 3N	^{141}Ce, electroplated; lathe	No	*D(930 K) = 1.09×10^{-13} m^2 s^{-1}	$\Delta V/V_0 < 0$	–	Marbach (1976) [91.04]
Impurity diffusion												
Ag	0.12	0.963 (93.0)	360	996–1,049 (0.95) δ-Ce	6	pc ~3N	^{110}Ag, vapour deposition; lathe	1 example		Au in Ce	91.02	Dariel (1972) [91.05]
	0.025	0.915 (88.3)	–	853–968 (0.85) γ-Ce	7							
Ag	1.4	1.214 (117.2)	–	873–973 (0.86) γ-Ce	4	pc 2N8	^{110}Ag, precipitated as hydroxide; absorption and lathe	No		Co, Fe in γ-Ce; electrotransport	–	Cathey (1973) [91.06]
Au	0.095	0.889 (85.8)	620	999–1,047 (0.96) δ-Ce	6	pc 3N	^{198}Au, vapour deposition and electroplated; lathe	3 examples (NSE at lower T after vapour deposition)		Ag in Ce	91.02	Dariel (1972) [91.05]
	4.4×10^{-3}	0.646 (62.4)	–	824–973 (0.84) γ-Ce	7							

Table 9.1 *(Continued)*

(1)	(2a)	(2b)	(3)	(4)	(5)	(6)	(7)	(8)	(9)	(10)	(11)	(12)
X	D^0 (10^{-4} m^2 s^{-1})	Q (eV) and (kJ/mole)	$D(T_m)$ (10^{-12} m^2 s^{-1})	T-range (K) ($\overline{T}/T_m$)	No. of data points	Material, purity	Experimental method	Remarks on the pp	Further remarks	Also studied	Figure	Reference
Co	0.01	0.477 (46.1)	–	823–923 (0.82) γ-Ce	3	pc 2N8	^{60}Co, precipitated as hydroxide; absorption and lathe			Ag, Fe in γ-Ce; electrotransport	–	Cathey (1973) [91.06]
Co	1.2×10^{-3}	0.347 (33.5)	2,800	(1,003–1,071) (0.97) δ-Ce	[52]	pc[61]	^{60}Co, electroplated; lathe	No (erfc-solutions)		Gd in δ-Ce	–	Marbach (1976) [91.07]
	1.6×10^{-3}	0.369 (35.6)	–	(800–1,000) (0.84) γ-Ce	[52]							
Fe	3.3×10^{-4}	0.20 (19.2)	–	700–923 (0.76) γ-Ce	4	pc 2N8	^{59}Fe, precipitated as hydroxide; absorption and lathe			Ag, Co in γ-Ce; electrotransport	–	Cathey (1973) [91.06]
Fe	2.0×10^{-3}	0.334 (32.2)	5,400	1,004–1,048 (0.96) δ-Ce	6[51]	pc 3N	^{59}Fe, vapour deposition*; lathe	2 examples	*Simultaneous diffusion of Fe and Mn	Mn in Ce, Pr, Nd; Fe in Pr, Nd	91.02	Dariel (1975) [91.08]
	0.017	0.516 (49.8)	–	876–993 (0.87) γ-Ce	10[51]							
Gd	0.012	1.041 (100.5)	15	(1,003–1,071) (0.97) δ-Ce	[52]	pc[61]	^{159}Gd, electroplated; lathe	No		Co in Ce	–	Marbach (1976) [91.07]
La	0.038	1.062 (102.6)	38	999–1,045 (0.95) δ-Ce	6[51]	pc 3N5	^{140}La, vapour deposition; lathe	2 examples		La in La	91.02	Dariel (1973) [91.09]
Mn	–	–		1,041 δ-Ce	1[51x]	pc 3N	^{54}Mn, vapour deposition*; lathe	No	*Simultaneous diffusion of Fe and Mn; $^{x}D(1{,}041\ \mathrm{K}) = 3.10 \times 10^{-10}$ m^2 s^{-1}	Fe in Ce, Pr, Nd; Mn in Pr, Nd	91.02	Dariel (1975) [91.08]
	$4.5 \times 10^{-4+}$	0.532$^+$ (51.3)	–	887–975 (0.87) γ-Ce	3[51]							

Table 9.2 Diffusion in praseodymium (References, see page 332)

(1)	(2a)	(2b)	(3)	(4)	(5)	(6)	(7)	(8)	(9)	(10)	(11)	(12)
X	D^0 (10^{-4} m^2 s^{-1})	Q (eV) and (kJ/mole)	$D(T_m)$ (10^{-12} m^2 s^{-1})	T-range (K) ($\overline{T}/T_m$)	No. of data points	Material, purity	Experimental method	Remarks on the pp	Further remarks	Also studied	Figure	Reference
Self-diffusion												
Pr	0.087	1.275 (123.1)	40	1,073–1,198 (0.94) β-Pr	6^{51}	pc 3N6	^{142}Pr, vapour deposition; lathe	2 examples	*Data depicted in Ref. [92.02]: $D(1{,}064\,K) = 1.7 \times 10^{-13}$, $D(1{,}041\,K) = 1.2 \times 10^{-13}$ m^2 s^{-1}	Ho, In, La in Pr	92.01	Dariel (1969) [92.01]
	–	–		1,041, 1,064* α-Pr	2^{51}							
Impurity diffusion												
Ag	0.032	0.932 (90.0)	400	1,082–1,194 (0.95) β-Pr	6^{51}	pc 3N3	^{110}Ag, vapour deposition; lathe	Several examples		Au, Co in Pr	92.02	Dariel (1969) [92.02]
	0.14	1.102 (106.4)	–	885–1,039 (0.80) α-Pr	6^{51}							
Au	0.033	0.872 (84.2)	750	1,075–1,187 (0.94) β-Pr	5^{51}	pc 3N3	^{198}Au, vapour deposition; lathe	No		Ag, Co in Pr	92.02	Dariel (1969) [92.02]
	0.043	0.854 (82.5)	–	873–1,014 (0.78) α-Pr	4^{51}							
Au	–	–	–	1,013, 1,053 α-Pr	4*	sc[61]	^{198}Au, vapour deposition; lathe	All (erfc-solution)	*$D_\perp(1{,}053\,K) = 4.0 \times 10^{-10}$, $D_{//}(1{,}053\,K) = 4.6 \times 10^{-10}$, $D_\perp(1{,}013\,K) = 3.7 \times 10^{-10}$, $D_{//}(1{,}013\,K) = 4.4 \times 10^{-10}$ m^2 s^{-1}		92.02	Dariel (1981) [92.03]
Co	–	–		1,151, 1,192 β-Pr	2^{51}*	pc 3N3	^{60}Co, vapour deposition; lathe	No	*$D(1{,}036\,K) = 5.0 \times 10^{-9}$, $D(1{,}151\,K) = 4.8 \times 10^{-9}$ m^2 s^{-1}	Ag, Au in Pr	92.03	Dariel (1969) [92.02]
	0.047	0.711 (68.7)	–	845–1,036 (0.78) α-Pr	4^{51}							

Table 9.2 *(Continued)*

(1)	(2a)	(2b)	(3)	(4)	(5)	(6)	(7)	(8)	(9)	(10)	(11)	(12)
X	D^0 (10^{-4} m^2 s^{-1})	Q (eV) and (kJ/mole)	$D(T_m)$ (10^{-12} m^2 s^{-1})	T-range (K) ($\overline{T}/T_m$)	No. of data points	Material, purity	Experimental method	Remarks on the pp	Further remarks	Also studied	Figure	Reference
Cu	0.057	0.772 (74.5)	3,400	1,086–1,187 (0.94) β-Pr	8	pc 3N	^{64}Cu, vapour deposition; lathe	4 examples (very flat pp)			92.02	Dariel (1971) [92.04]
	0.084	0.785 (75.8)	–	927–1,059 (0.82) α-Pr	6							
Fe	4×10^{-3}	0.451 (43.5)	5,200	1,084–1,179 (0.94) β-Pr	6[51]	pc 3N	^{59}Fe, vapour deposition; lathe	1 example		Mn in Ce, Nd, Pr; Fe, Mn in Ce, Nd	92.04	Dariel (1975) [92.05]
	2.1×10^{-3}	0.399 (38.5)	–	888–1,057 (0.81) α-Pr	7[51]							
Ho	9.5×10^{-3}	1.141 (110.1)	16	1,084–1,177 (0.94) β-Pr	9[51]	pc 3N6	^{166}Ho, vapour deposition; lathe	No	*D(1,006 K) = 4.1×10^{-14} m^2 s^{-1}	Pr, In, La in Pr	92.05	Dariel (1969) [92.01]
	–	–	–	1,006 α-Pr	1[51]*							

In	0.096	1.253 (121.0)	55	1,075–1,198 (0.94) β-Pr	6^{51}	pc 3N6	^{114}In, vapour deposition; lathe	No	*D(1,039 K) = 3.0×10^{-13} m^2 s^{-1}	Pr, Ho, La in Pr	92.05	Dariel (1969) [92.01]
	–	–	–	1,039 α-Pr	1^{51}*							
La	0.018	1.115 (107.6)	39	1,081–1,191 (0.94) β-Pr	5^{51}	pc 3N6	^{140}La, vapour deposition; lathe	2 examples	*D(1,042 K) = 1.1×10^{-13} m^2 s^{-1}	Pr, Ho, In in Pr	92.05	Dariel (1969) [92.01]
	–	–	–	1,042 α-Pr	1^{51}*							
Mn	8.5×10^{-5}+	0.366+ (35.3)	250+	1,109–1,165 (0.94) β-Pr	3^{51}	pc 3N	^{54}Mn, vapour deposition[x]; lathe	1 example[x]	+Present fit to the depicted data [x]Simultaneous diffusion of Fe and Mn	Fe in Ce, Nd; Fe, Mn in Ce, Nd	92.04	Dariel (1975) [92.05]
	5.1×10^{-3}+	0.771+ (74.5)	–	929, 1,001 α-Pr	2^{51}							
Zn	0.63	1.171 (113.0)	800	1,095–1,195 (0.95) β-Pr	8	pc 3N7	^{65}Zn, vapour deposition; lathe	4 examples			92.03	Dariel (1970) [92.06]
	0.18	1.075 (103.8)	–	876–1,040 (0.80) α-Pr	6							

Table 9.3 Diffusion in neodymium, europium, gadolinium, erbium and ytterbium. (References, see page 332)

(1)	(2a)	(2b)	(3)	(4)	(5)	(6)	(7)	(8)	(9)	(10)	(11)	(12)
X	D^0 (10^{-4} m^2 s^{-1})	Q (eV) and (kJ/mole)	$D(T_m)$ (10^{-12} m^2 s^{-1})	T-range (K) ($\overline{T}/T_m$)	No. of data points	Material, purity	Experimental method	Remarks on the pp	Further remarks	Also studied	Figure	Reference
Fe in Nd	0.01	0.590 (56.9)	4,900	1,150–1,220 (0.92) β-Nd	6^{51}	pc 3N	^{59}Fe, vapour deposition; lathe	No		Mn in Nd, Ce, Pr; Fe, Mn in Ce, Pr	93.01	Dariel (1975) [93.01]
	4.6×10^{-3}	0.529 (51.1)	–	954–1,124 (0.81) α-Nd	7^{51}							
Mn in Nd	$(0.84)^+$	$(1.343)^+$ (129.7)	$(470)^+$	1,148, 1,182 β-Nd	2^{51}	pc 3N	^{54}Mn, vapour deposition^x; lathe	No	$^+$Present fit to the depicted data ^{x}Simultaneous diffusion of Fe and Mn	Fe in Nd, Ce, Pr; Fe, Mn in Ce, Pr	93.01	Dariel (1975) [93.01]
	$(4.2 \times 10^{-3})^+$	$(0.789)^+$ (76.2)	–	1,028, 1,073 α-Nd	2^{51}							
Eu in Eu	(1.0) 1.15^+	1.492 (144.0)	16.5^+	771–1,074 (0.84)	13 (10T)	pc 2N7	^{152}Eu, electroplated; lathe	2 examples (slight NSE)	$^+$Present approximation	Gd in Gd	93.02	Fromont (1977) [93.02]
Gd in Gd	(0.01) 0.011^+	1.418 (136.9)	34^+	1,549–1,580 (0.99) β-Gd	13 (12T)	pc 2N5	^{159}Gd, electroplated; lathe	3 examples	$^+$Present approximation	Eu in Eu	93.03	Fromont (1977) [93.02]

Er in Er	$\perp$ 4.51	3.134 (302.6)	0.71	1,475–1,685 (0.88)	10 (9 T)	sc 3N	^{169}Er, electroplated; grinder	Several examples		93.04	Spedding (1972) [93.03]
	// 3.71	3.124 (301.7)	0.62	1,475–1,659 (0.87)	8 (7 T)						
Au in Er	$\perp 2.06 \times 10^{-2}$	1.03 (99.4)		1,269–1,476 (0.76)	3[51]	sc 3N	^{168}Er; lathe	1 example (erfc-solution)	[+]Present fit to the depicted data	93.04	Dariel (1979) [93.04]
	// 4.45×10^{-3}[+]	0.66 (63.7)			3[51]						
Yb in Yb	0.12	1.253 (121.0)	21	996–1,076 (0.94) γ-Yb	10[51]	pc 3N	^{169}Yb, electroplated; grinder	No	[+]Present fit to the depicted data	93.05	Fromont (1974) [93.05]
	(0.034)	(1.520) (146.8)		813–983 (0.82)	6[51]						
	0.137[+]	1.625[+] (156.9)		α-Yb							
Yb in Yb	–	–	–	1,003–1,073 (0.95) γ-Yb	3	pc 3N	^{169}Yb, electroplated; grinder	No	a	$\Delta V/V_0 = 0.59$ –	Fromont (1975) [93.06]

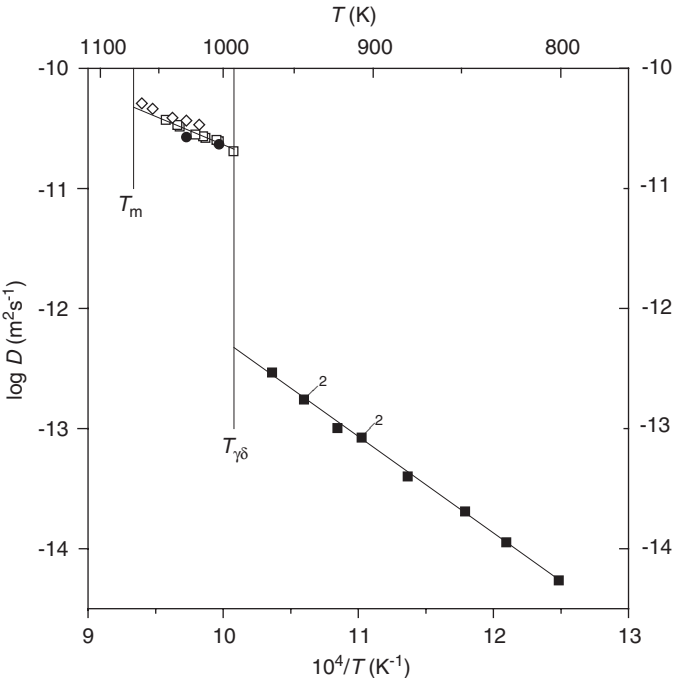

Fig. 91.01 Self-diffusion in cerium. □ (δ) and ■ (γ), Dariel [91.01]; ◇ (δ), Languille [91.02]; ● (δ), Languille [91.03]. Fitting line to δ-Ce according to [91.01].

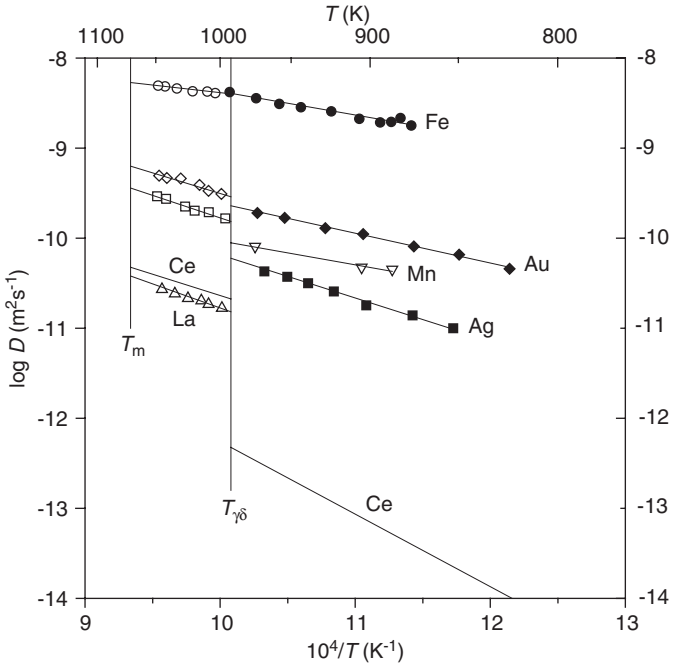

Fig. 91.02 Impurity diffusion in cerium. Ag in Ce: □ (δ) and ■ (γ), Dariel [91.05]; Au in Ce: ◇ (δ) and ◆ (γ), Dariel [91.05]; Fe in Ce: ○ (δ) and ● (γ), Dariel [91.08]; La in Ce: △ (δ) Dariel [91.09]; Mn in Ce: ▽ (γ) Dariel [91.08].

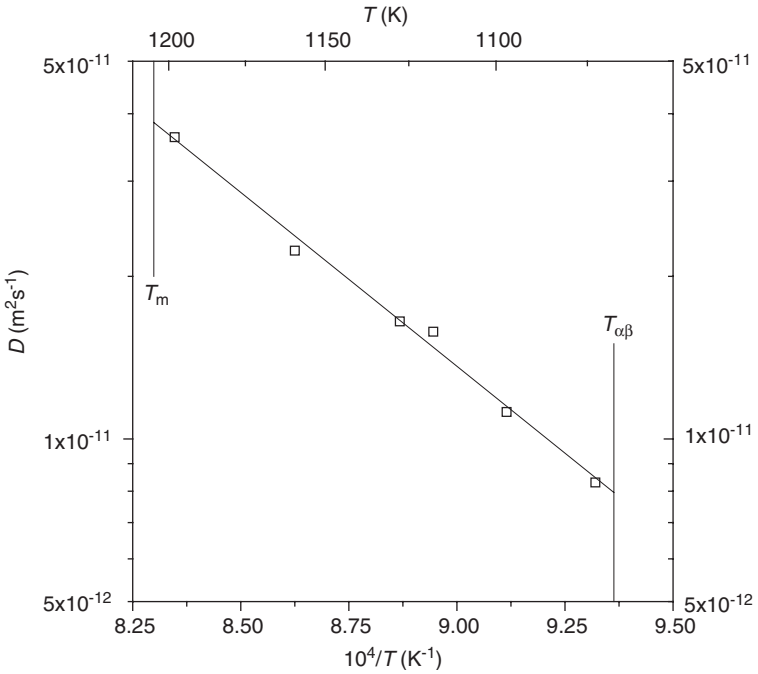

Fig. 92.01 Self-diffusion in β-praseodymium. □, Dariel [92.01].

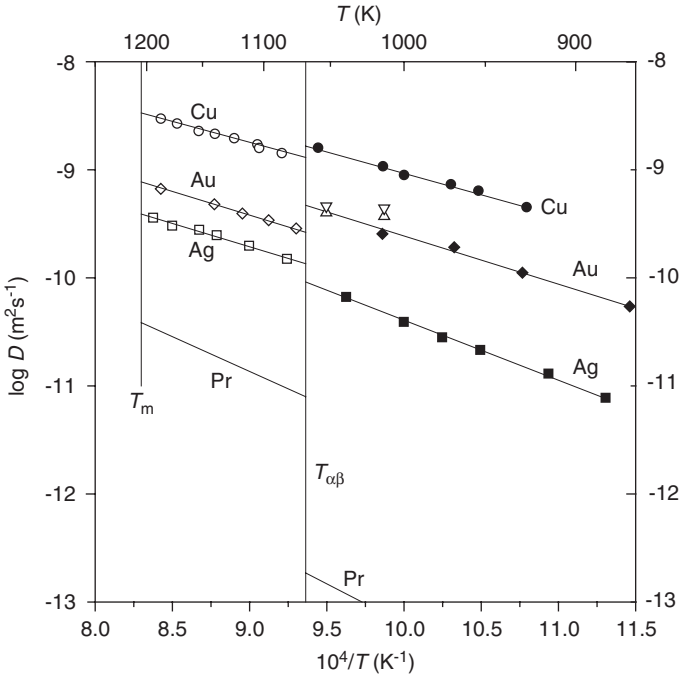

Fig. 92.02 Impurity diffusion in praseodymium, Ag in Pr: □ (β) and ■ (α), Dariel [92.02]; Au in Pr: ◇ (β) and ◆ (α), Dariel [92.02]; △ ($\perp$) and ▽ ($/\!/$), Dariel [92.03]; Cu in Pr: ○ (β) and ● (α), Dariel [92.04].

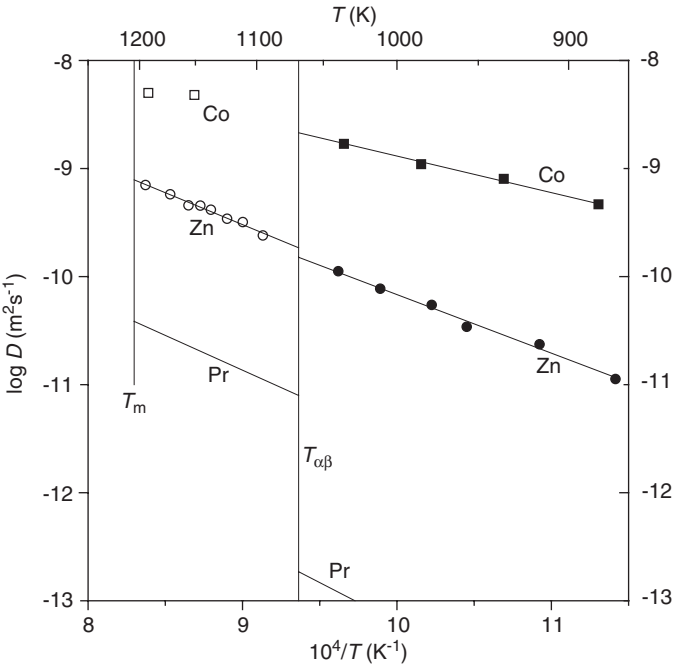

Fig. 92.03 Impurity diffusion in praseodymium. Co in Pr: □ (β) and ■ (α) Dariel [92.02]; Zn in Pr: ○ (β) and ● (α) Dariel [92.06].

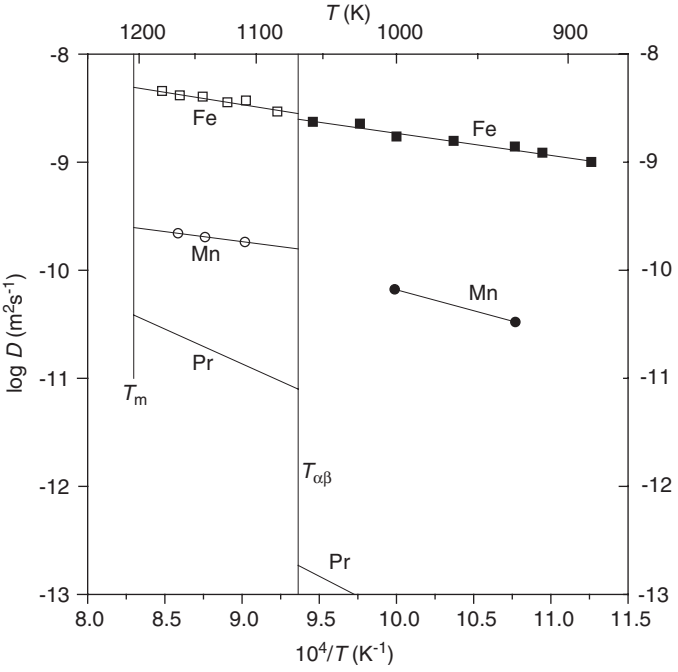

Fig. 92.04 Impurity diffusion in praseodymium. Fe in Pr: □ (β) and ■ (α) Dariel [92.05]; Mn in Pr: ○ (β) and ● (α) Dariel [92.05].

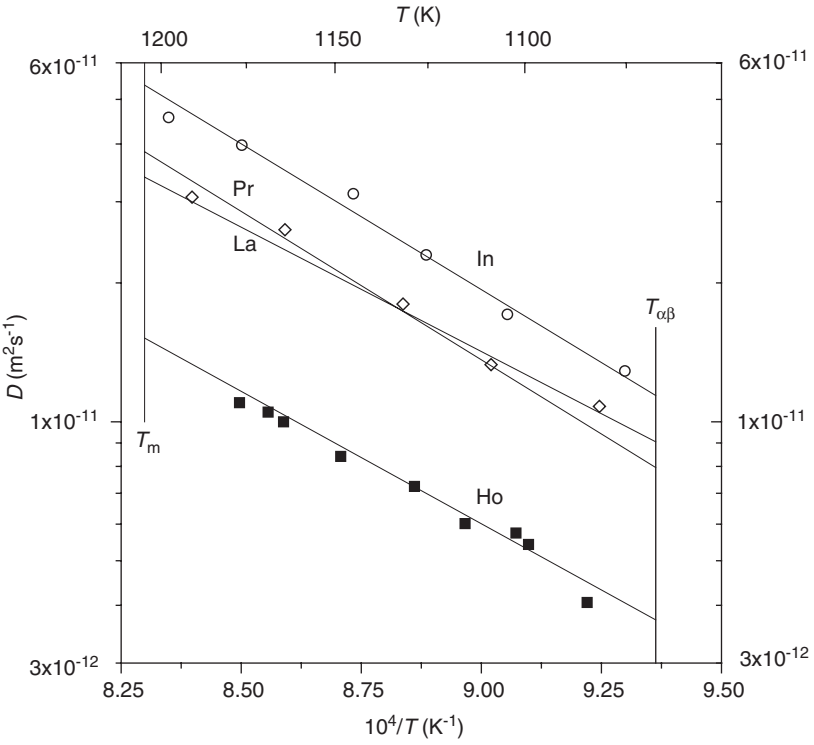

Fig. 92.05 Impurity diffusion in praseodymium. Ho in Pr: □ Dariel [92.01]; In in Pr: ○ Dariel [92.01]; La in Pr: ◇ Dariel [92.01].

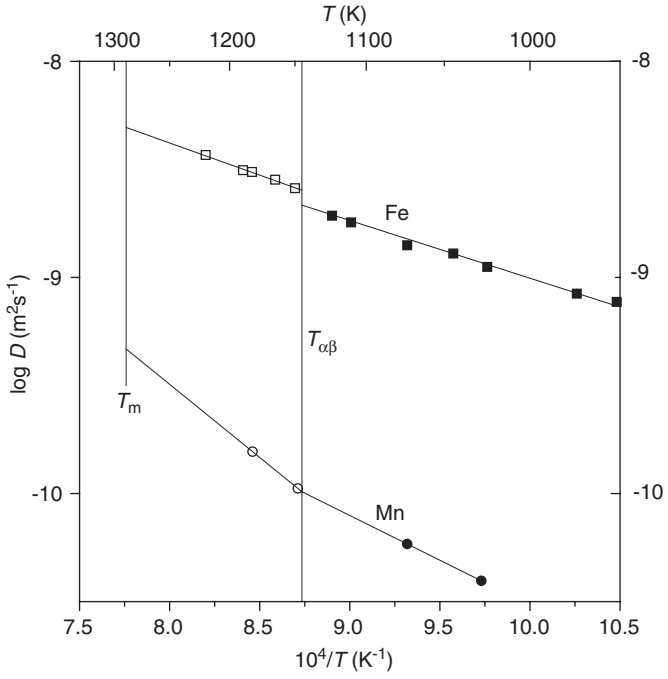

Fig. 93.01 Impurity diffusion in neodymium. Fe in Nd: □ (β) and ■ (α) Dariel [93.01]; Mn in Nd: ○ (β) and ● (α) Dariel [93.01].

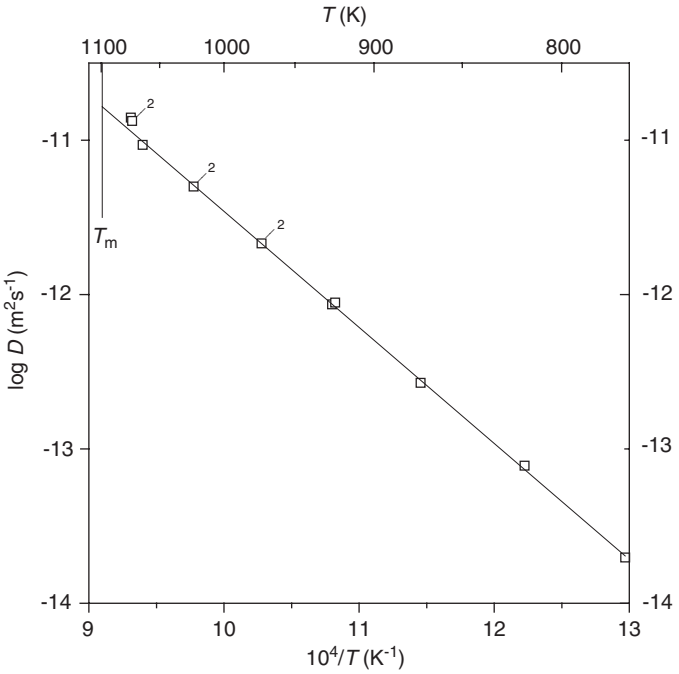

Fig. 93.02 Self-diffusion in europium. □, Fromont [93.02].

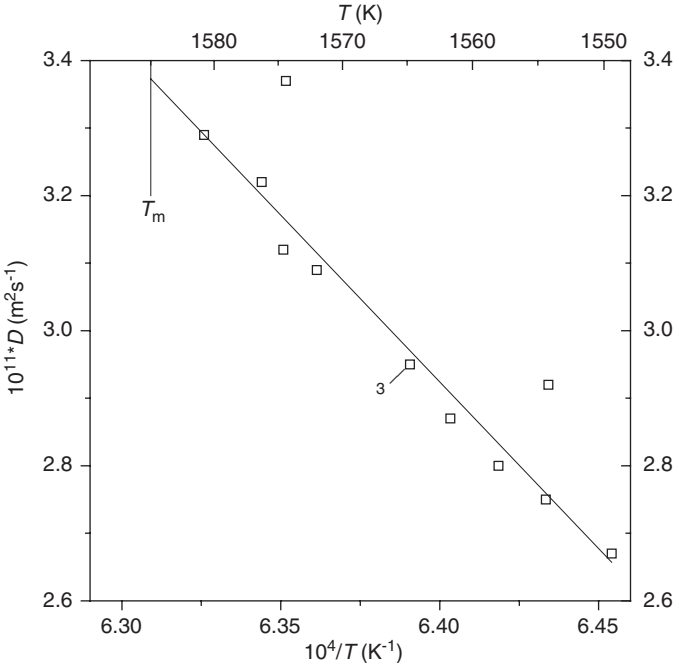

Fig. 93.03 Self-diffusion in gadolinium. □, Fromont [93.02].

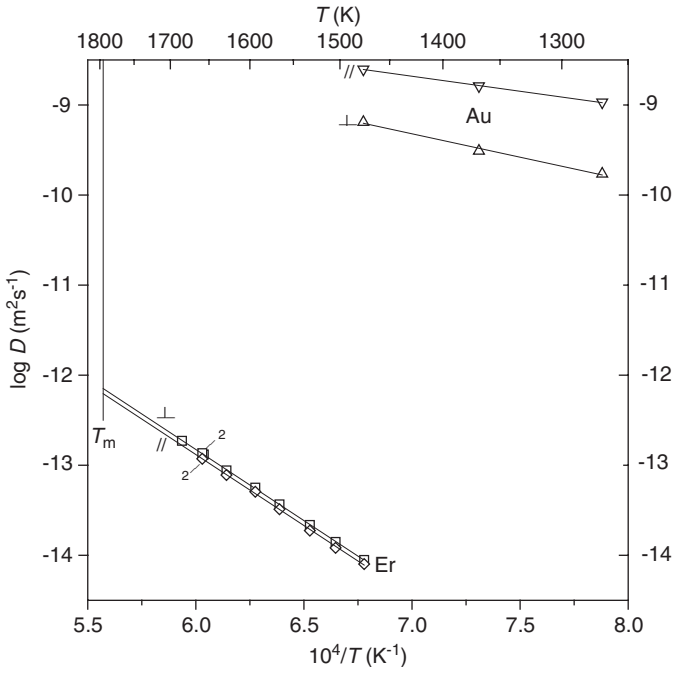

Fig. 93.04 Self-diffusion and impurity diffusion in erbium. Er in Er: □ and ◇, Spedding [93.03]; Au in Er: △ and ▽, Dariel [93.04].

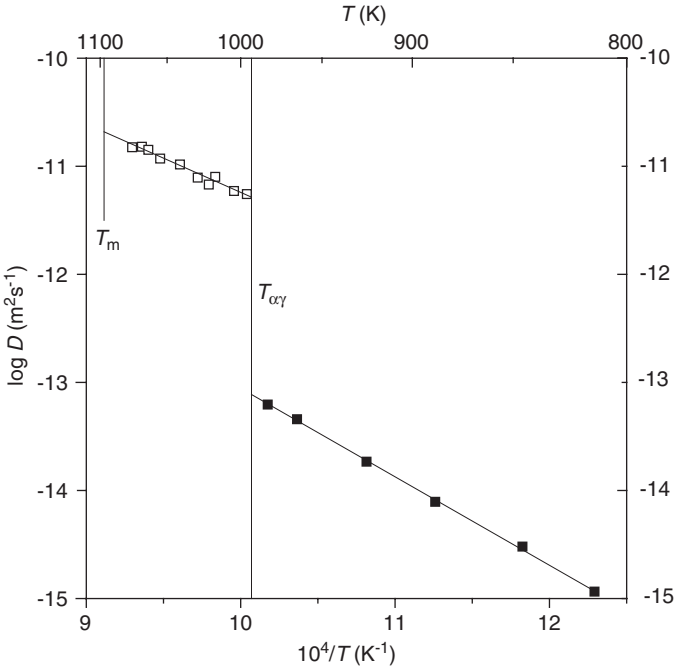

Fig. 93.05 Self-diffusion in ytterbium. □ (γ) and ■ (α), Fromont [93.05].

REFERENCES

References to Chapter 9.1

[91.01] M.P. Dariel, D. Dayan, A. Languille, Phys. Rev. B **4** (1971) 4348.
[91.02] A. Languille, M.P. Dariel, D. Calais, B. Coqblin, Mém. Sci. Rev. Métall. **70** (1973) 241.
[91.03] A. Languille, D. Calais, M. Fromont, J. Phys. Chem. Sol. **35** (1974) 1373.
[91.04] G. Marbach, M. Fromont, D. Calais, J. Phys. Chem. Sol. **37** (1976) 689.
[91.05] M.P. Dariel, D. Dayan, D. Calais, Phys. Stat. Sol. (a) **10** (1972) 113.
[91.06] W.N. Cathey, J.E. Murphy, J.R. Woodyard, Metall. Trans. A **4** (1973) 1463.
[91.07] G. Marbach, C. Charrissoux, C. Janot, *La Diffusion dans les Milieux Condensés – Théorie et Applications*, Proc. Colloque de Métallurgie, CEN Saclay, Vol. **1** (1976) 119.
[91.08] M.P. Dariel, Acta Metall. **23** (1975) 473.
[91.09] M.P. Dariel, Phil. Mag. **28** (1973) 915.

References to Chapter 9.2

[92.01] M.P. Dariel, G. Erez, G.M.J. Schmidt, Phil. Mag. **19** (1969) 1045.
[92.02] M.P. Dariel, G. Erez, G.M.J. Schmidt, J. Appl. Phys. **40** (1969) 2746.
[92.03] M.P. Dariel, O.D. McMasters, K.A. Gschneider, Phys. Stat. Sol. (a) **63** (1981) 329.
[92.04] M.P. Dariel, J. Appl. Phys. **42** (1971) 2251.
[92.05] M.P. Dariel, Acta Metall. **23** (1975) 473.
[92.06] M.P. Dariel, Phil. Mag. **22** (1970) 563.

References to Chapter 9.3

[93.01] M.P. Dariel, Acta Metall. **23** (1975) 473.
[93.02] M. Fromont, G. Marbach, J. Phys. Chem. Sol. **38** (1977) 27.
[93.03] F.H. Spedding, K. Shiba, J. Chem. Phys. **57** (1972) 612.
[93.04] M.P. Dariel, L. Kornblit, B.J. Beaudry, K.A. Gschneider, Phys. Rev. B **20** (1979) 3949.
[93.05] M. Fromont, A. Languille, D. Calais, J. Phys. Chem. Sol. **35** (1974) 1367.
[93.06] M. Fromont, J. Phys. Chem. Sol. **36** (1975) 1397.

CHAPTER 10

Self-Diffusion and Impurity Diffusion in Actinide Metals

Contents

Tables
10.1. Thorium (Th) 334
10.2. Uranium (U) 336
10.3. Plutonium (Pu) 339
Figures
Thorium 341
Uranium 343
Plutonium 346
References 348

For **protactinium** (Pa) and trans-uranium metals (except Pu) no data are available.

In bcc γ-U and ε-Pu abnormally high self-diffusivity is observed, similar to that in bcc β-Ti, β-Zr and β-Hf.

The orthorhombic α-U consists of corrugulated layers of atoms, with the layers parallel to the (010) plane and the corrugations parallel to the [100] axis. The interatomic distances in the corrugated planes are 0.276 and 0.285 nm, respectively, and 0.326 and 0.332 nm between the corrugated planes, respectively. This leads to a strong anisotropy of the diffusivity resulting in $D[100] \approx D[001] \gg D[010]$. Furthermore, the diffusivity in perfect single crystals is smaller than that in crystals with mosaic structure.

In Table 10.0 lattice structure, lattice constant, phase transition and melting temperature of actinide metals are listed.

Table 10.0 Lattice structure, lattice constant a, phase transition (T_{ij}) and melting temperature T_m

Metal	Th		U			Pu				
Phase	β	α	γ	β	α	ε	δ'	δ	γ	β
Structure	bcc	fcc	bcc	trig[1]	orh[2]	bcc	bct	fcc	orh[2]	mcl[3]
T_{ij} (K)	1,613		1,048	941		753	730	588	480	
T_m (K)	2,028		1,405				913			
a (nm)	0.416	0.508	0.347	[4]		0.364		0.464		

[1]trig = trigonal, [2]orh = orthorhombic, [3]mcl = monoclinic, [4]explanation in text.

Table 10.1 Diffusion in thorium (References, see page 348)

(1)	(2a)	(2b)	(3)	(4)	(5)	(6)	(7)	(8)	(9)	(10)	(11)	(12)
X	D^0 (10^{-4} m^2 s^{-1})	Q (eV) and (kJ/mole)	$D(T_m)$ (10^{-12} m^2 s^{-1})	T-range (K) ($\bar{T}/T_m$)	No. of data points	Material, purity	Experimental method	Remarks on the pp	Further remarks	Also studied	Figure	Reference
Self-diffusion												
Th	(395)	(3.105) (299.8)		998–1,140 (0.53)	8^{51}	pc ~2N8	^{228}Th, vapour deposition; non-destructive α-spectroscopy	No	$^{+}$Present fit to the depicted data	Pa, U in α-Th	101.01	Schmitz (1967) [101.01]
	1,300^{+}	3.22^{+} (311)	–	α-Th								
Impurity diffusion												
Co	(4×10^{-3}) $3.6 \times 10^{-3\ +}$	0.677 (65.3)	7,500^{+}	1,703–1,898 (0.89) β-Th	4	pc 3N5	Co; diffusion couple, Th/Th (0.057% Co); spark source mass spectroscopy	No	$^{+}$Present approximation	Fe, Ni in α-Th and β-Th; electrotransport	101.02	Weins (1979) [101.02]
	5×10^{-4}	0.572 (55.3)	–	1,238–1,613 (0.70) α-Th	6						–	
Co	7.4×10^{-3}	0.867 (83.7)	–	1,173–1,605 (0.68) α-Th	9	pc ~3N	Co; diffusion couple, Th/Th (0.05% Co); scanning laser mass spectroscopy	No			101.02	Axtell (1989) [101.03]
Fe	(4×10^{-3}) $4.3 \times 10^{-3+}$	0.742 (71.6)	6,200^{+}	1,703–1,898 (0.89) β-Th	4	pc 3N5	Fe; diffusion couple, Th/Th (0.038% Fe); spark source mass spectroscopy	No	$^{+}$Present approximation	Co, Ni in α-Th and β-Th; electrotransport	101.02	Weins (1979) [101.02]
	5×10^{-3}	0.837 (80.8)	–	1,238–1,613 (0.70) α-Th	6							
Hf	23^{+}	3.13^{+} (302)	38^{+}	1,693, 1,963 (0.90) β-Th	2*	pc^{61}	^{181}Hf; serial sectioning	All	$^{+}$Present calculation $^{*}D(1{,}693\,\mathrm{K}) = 1.09 \times 10^{-12}$, $D(1{,}963\,\mathrm{K}) = 2.09 \times 10^{-11}$ m^2 s^{-1}	Several impurities in γ-U	101.04	Rothman (1965) [101.04]
Mo	15.1	2.337 (216)		1,698–1,873 (0.88) β-Th	4	pc ~3N7	Mo; diffusion couple, Th/Th (0.02% Mo); scanning laser mass spectroscopy (Grube)	No		Re, W, Zr in β-Th; electrotransport	101.04	Schmidt (1984) [101.05]
Nb	0.50	2.090 (201.8)	320	1,643–1,933 (0.88) β-Th	4	pc ~3N7	Nb; diffusion couple, Th/Th (70 ppma Nb); spark source mass spectroscopy	No		Ta, V in β-Th; electrotransport	101.05	Schmidt (1978) [101.06]

Ni	(4×10^{-4}) 3.7×10^{-4} +	0.395 (38.1)		1,703–1,898 (0.89) β-Th	4*	pc 3N5	Ni; diffusion couple, Th/Th (0.038% Ni); spark source mass spectroscopy	No	+Present approximation; *Pronounced data scatter	Co, Fe in α-Th and β-Th; electrotransport	101.02 101.03	Weins (1979) [101.02]
	(4×10^{-3}) 3.7×10^{-3} +	0.807 (77.9)	–	1,238–1,613 (0.70) α-Th	6						
Pa	126	3.239 (312.8)	–	1,040–1,184 (0.55) α-Th	8^{51}	pc ~2N8	^{231}Pa, vapour deposition; non-destructive α-spectroscopy	No		Th, U in α-Th	101.01	Schmitz (1967) [101.01]
Re	4.04×10^{-3}	0.87 (84)	2,800	1,663–1,943 (0.89) β-Th	4	pc ~3N7	Re; diffusion couple, Th/Th (0.01% Re); scanning laser mass spectroscopy (Grube)	No		Mo, W, Zr in β-Th; electrotransport	101.05	Schmidt (1984) [101.05]
Ta	0.57	2.181 (210.6)	210	1,648–1,933 (0.88) β-Th	4	pc ~3N7	Ta; diffusion couple, Th/Th (30 ppma Ta); spark source mass spectroscopy	No		Nb, V in β-Th; electrotransport	101.05	Schmidt (1978) [101.06]
U	(2.21×10^{4}) 3,500+	(3.439) (332.0) 3.263+ (315)	– –	963–1,149 (0.52) α-Th	11^{51}	pc ~2N8	^{233}U, vapour deposition; non-destructive α-spectroscopy	No	+Present rough fit to the depicted data	Th, Pa in α-Th	101.01	Schmitz (1967) [101.01]
V	(0.019) 0.018+	1.344 (129.8)	820	1,653–1,939 (0.89) β-Th	4	pc ~3N7	V; diffusion couple, Th/Th (0.013% V); spark source mass spectroscopy	No	+Present approximation	Nb, Ta in β-Th; electrotransport	101.05	Schmidt (1978) [101.06]
W	(0.103) 0.108+	1.657 (160)		1,683–1,818 (0.86) β-Th	4	pc ~3N7	W; diffusion couple, Th/Th (0.01% W); scanning laser mass spectroscopy (Grube)	No	+Present approximation	Mo, Re, Zr in β-Th; electrotransport	101.04	Schmidt (1984) [101.05]
Zr	1.73×10^{4}	3.977 (384)		1,773, 1,873 (0.90) β-Th	2	pc ~3N7	Zr; diffusion couple, Th/Th (0.02% Zr); scanning laser mass spectroscopy (Grube)	No		Mo, Re, W in β-Th; electrotransport	–	Schmidt (1984) [101.05]

Table 10.2 Diffusion in uranium (References, see page 348)

(1)	(2a)	(2b)	(3)	(4)	(5)	(6)	(7)	(8)	(9)	(10)	(11)	(12)
X	D^0 (10^{-4} m^2 s^{-1})	Q (eV) and (kJ/mole)	$D(T_m)$ (10^{-12} m^2 s^{-1})	T-range (K) ($\overline{T}/T_m$)	No. of data points	Material, purity	Experimental method	Remarks on the pp	Further remarks	Also studied	Figure	Reference
Self-diffusion												
U	1.17×10^{-3}	1.154 (111.4)	8.5	1,073–1,323 (0.85) γ-U	4	pc[61] (0.1–0.3 mm)	^{233}U, vapour deposition; serial sectioning				102.01	Bochvar (1958) [102.01]
U	1.8×10^{-3}	1.193 (115.1)	9.5	1,073–1,313 (0.85) γ-U	6	pc ~2N8	^{235}U, diffusion couple of natural U and U enriched with 20% ^{235}U; residual α-activity	Several examples (probability plot)			102.01	Adda (1959) [102.02]
U	2.33×10^{-3}	1.236 (119.3)	8.6	1,077–1,343 (0.86) γ-U	5[51]	pc ~3N5	^{235}U (enriched to 93%), sputter deposition; lathe	All			102.01	Rothman (1960) [102.03]
	1.12×10^{-3x}	1.149[x] (111.0)	8.4	1,073–1,343	(15)				[x]Fit to the data of [102.01–102.03]			
U	0.0135	1.821 (175.9)	–	973–1,028 (0.71) β-U	4	pc[61]	^{234}U (enriched), diffusion couple of natural U and U enriched with ^{234}U; residual α-activity	No			102.01	Adda (1959) [102.04]
U	–	–	–	951–1,033 (0.71) β-U	5 (4T)	pc ~3N7	^{235}U, sputter and vapour deposition; lathe	All (non-linear in $\ln c - x^2$)	Marked data scatter		–	Rothman (1961) [102.05]
U	(2×10^{-3}) $1.8 \times 10^{-3+}$	1.735 (167.5)	–	853–923 (0.63) α-U	4	pc[61]	^{234}U; diffusion couple of natural U and U enriched with ^{234}U; residual α-activity	2 examples (probability plot)	[+]Present approximation		102.01	Adda (1962) [102.06]

U	–	–	–	898 α-U	3* (1 T)	sc[61] (mosaic structure)	^{235}U, vapour deposition; grinder	All	*D[100]=D[001] $= 1.95 \times 10^{-17}$ $m^2 s^{-1}$, $D[010] \ll D[100]$ (see introduction page)		102.01	Rothman (1962) [102.07]
U	–	–	–	913 α-U	8* (1 T)	sc pc (2–3 mm) ~3N	^{233}U, vapour deposition, electrolytical sectioning, residual α-activity, autoradiography	No	*Different orientations, D[001] $= 2.1 \times 10^{-17}$, $D[010] \leqslant 10^{-18} m^2 s^{-1}$ (see introduction page)		102.01	Bochvar (1965) [102.08]
U	9.3×10^{-3} ×	1.908 (184.2)	–	860, 926 α-U	9 (2T)	sc[61]*	^{235}U, vapour deposition; lathe and grinder	All (pronounced dislocation tails for D[010])	×Corrected value *Mosaic structure and perfect crystals; D[100] ≈ D[001] >> D[010] (see introduction page)		102.01	Rothman (1966) [102.09]
Impurity diffusion												
Au	4.86×10^{-3}	1.318 (127.3)	9.1	1,058–1,280 (0.83) γ-U	10 (5T)	pc 3N	Au[71], vapour deposition[73]; lathe	2 examples			102.02	Rothman (1961) [102.10]
Co	3.51×10^{-4}*	0.545* (52.6)		1,056–1,262 (0.82) γ-U	15 (8T)	pc 4N	^{60}Co, vapour deposition[73]; lathe	No	*Forced fit to the curved Arrhenius plot	Cr, Cu, Fe, Mn, Nb, Ni in γ-U; U in U(Co)	102.03	Peterson (1964) [102.11]
Co	0.015	1.190 (114.9)	–	965–1,036 (0.71) β-U	6	pc 3N8	^{60}Co, vapour deposition; lathe	3 examples		Cr in β-U	102.04	Dariel (1970) [102.12]
Cr	5.47×10^{-3}*	1.061* (102.4)		1,070–1,310 (0.85) γ-U	12 (7T)	pc 4N	^{51}Cr, vapour deposition; lathe	No	*Forced fit to the curved Arrhenius plot	Co, Cu, Fe, Mn, Nb, Ni in γ-U; U in U(Co)	102.03	Peterson (1964) [102.11]
Cr	–	–	–	1,021 β-U	1*	pc ~4N	^{51}Cr, vapour deposition; lathe	1 example	*D(1,021 K) $= 1.77 \times 10^{-13}$ $m^2 s^{-1}$	Fe in β-U	–	Rothman (1962) [102.13]
Cr	–	–	–	943–1,038 (0.70) β-U	10 (8T)	pc 3N8	^{51}Cr, vapour deposition[73]; lathe	2 examples	Extreme data scatter, possibly caused by anisotropic diffusivity; D values are ranging from $\sim 3 \times 10^{-14}$ to $\sim 2 \times 10^{-13}$ $m^2 s^{-1}$	Co in β-U	–	Dariel (1970) [102.12]

Table 10.2 *(Continued)*

(1)	(2a)	(2b)	(3)	(4)	(5)	(6)	(7)	(8)	(9)	(10)	(11)	(12)
X	D^0 (10^{-4} m^2 s^{-1})	Q (eV) and (kJ/mole)	$D(T_m)$ (10^{-12} m^2 s^{-1})	T-range (K) ($\overline{T}/T_m$)	No. of data points	Material, purity	Experimental method	Remarks on the pp	Further remarks	Also studied	Figure	Reference
Cu	1.96×10^{-3}*	1.043* (100.7)		1,060–1,310 (0.84) γ-U	14 (7T)	pc 4N	^{64}Cu, vapour deposition[73]; lathe	2 examples	*Forced fit to the curved Arrhenius plot	Co, Cr, Fe, Mn, Nb, Ni in γ-U; U in U(Co)	102.03	Peterson (1964) [102.11]
Fe	2.69×10^{-4}*	0.521* (52.9)		1,060–1,263 (0.83) γ-U	12 (6T)	pc 4N	^{59}Fe, vapour deposition[73]; lathe	No	*Forced fit to the curved Arrhenius plot	Co, Cr, Cu, Mn, Nb, Ni in γ-U; U in U(Co)	102.03	Peterson (1964) [102.11]
Fe	–	–	–	984, 1,033 β-U	4* (2T)	pc ~4N	^{59}Fe, vapour deposition; lathe	All	*D(984 K) $\approx 9 \times 10^{-13}$, D(1,033 K) $\approx 2.5 \times 10^{-12}$ m^2 s^{-1}	Cr in β-U	–	Rothman (1962) [102.13]
Fe	–	–	–	918 α-U	1*	pc[61]	Fe; D determined from precipitate dissolution	–	*D(918 K) $\approx 3 \times 10^{-14}$ m^2 s^{-1}		–	Stelly (1972) [102.14]
Mn	(1.81×10^{-4}) 2.14×10^{-4} +	(0.602) (58.1) 0.615+ (59.4)		1,060–1,212 (0.81) γ-U	6 (4T)	pc 4N	^{54}Mn, vapour deposition of Fe and n-irradiation, Fe(n,p)[73]; lathe	No	+Present approximation	Co, Cr, Cu, Fe, Nb, Ni in γ-U; U in U(Co)	102.03	Peterson (1964) [102.11]
Nb	0.0487	1.719 (166.0)	3.3	1,064–1,375 (0.87) γ-U	16 (8T)	pc 4N	^{95}Nb, dried-on from oxalate solution[73]; lathe	No		Co, Cr, Cu, Fe, Mn, Ni in γ-U; U in U(Co)	102.02	Peterson (1964) [102.11]
Ni	5.36×10^{-4}	0.679 (65.6)		1,060–1,312 (0.84) γ-U	14 (7T)	pc 4N	^{63}Ni, vapour deposition[73]; lathe	No		Co, Cr, Cu, Fe, Mn, Nb in γ-U; U in U(Co)	102.03	Peterson (1964) [102.11]
Pu	(1.7×10^{-8}) 1.7×10^{-8} +	(0.597) (57.7) 0.554+ (53.5)	–	683–813 (0.53) α-U	4	pc ~2N8	Pu; EPMA, U/U (17.5% Pu) (Matano, Hall)	No	+Present approximation		–	Dupuy (1965) [102.15]
Zr	(1.6×10^{-7})	(0.707) (68.2)		1,073–1,323 (0.85) γ-U	4	pc[61]	^{95}Zr; residual activity	No		U in β-Zr; U, Zr in U(Zr)	–	Fedorov (1968) [102.16]

Table 10.3 Diffusion in plutonium (References, see page 348)

(1)	(2a)	(2b)	(3)	(4)	(5)	(6)	(7)	(8)	(9)	(10)	(11)	(12)
X	D^0 (10^{-4} m^2 s^{-1})	Q (eV) and (kJ/mole)	$D(T_m)$ (10^{-12} m^2 s^{-1})	T-range (K) ($\bar{T}/T_m$)	No. of data points	Material, purity	Experimental method	Remarks on the pp	Further remarks	Also studied	Figure	Reference
Self-diffusion												
Pu	0.022	0.802 (77.5)	82	773–885 (0.91) ε-Pu	4	pc[61]	^{240}Pu, diffusion couple containing 1% and 8% ^{240}Pu; residual activity	All (probability plot)			103.01	Dupuy (1968) [103.01]
Pu	(0.003)* 0.005[x]	(0.681)* (65.7)		788–849 (0.90) ε-Pu	4	pc 3N	^{240}Pu, diffusion couple containing 0.94% and 9.4% ^{240}Pu; residual activity	All (probability plot)	*Erroneous thermal expansion correction; [x]Corrected value; [+]present fit to the not "corrected" D-values	$\Delta V/V_0 = -0.34$ (anomalous pressure dependence of D)	103.01	Cornet (1971) [103.02]
	3.75×10^{-3}[+]	0.681[+] (65.7)	65[+]									
Pu	(4.5×10^{-3})	(0.693) (66.9)		765–886 (0.90) ε-Pu	5	pc 3N	^{238}Pu, vapour deposition; grinder	1 example	[+]Present approximation		103.01	Wade (1978) [103.03]
	0.0122[+]	0.760[+] (73.4)	77[+]									
	(5.3×10^{32})	(6.10) (589)	–	730–750 (0.81) δ′-Pu	5			No			103.01	
Pu	4.5×10^{-3}	1.032 (99.7)	–	623–714 (0.73) δ-Pu	11[51] (7T)	pc[61]	^{238}Pu (enriched), diffusion couple; lathe	1 example (probability plot)			–	Tate (1964) [103.04]
Pu	(0.517) 0.50[+]	1.309 (126.4)	–	594–715 (0.72) δ-Pu	7	pc 3N	^{238}Pu, vapour deposition; grinder	1 example	[+]Present approximation	gb diffusion in γ-Pu and β-Pu (deduced from two linear branches in $\ln c - x^2$)	103.01	Wade (1978) [103.03]
	0.38	1.226 (118.4)	–	484–544 (0.56) γ-Pu	4			2 examples (gb tails)			103.01	
	(0.0169) 0.018[+]	1.119 (108.0)	–	409–454 (0.47) β-Pu	3						103.01	

Table 10.3 *(Continued)*

(1)	(2a)	(2b)	(3)	(4)	(5)	(6)	(7)	(8)	(9)	(10)	(11)	(12)
X	D^0 (10^{-4} m^2 s^{-1})	Q (eV) and (kJ/mole)	$D(T_m)$ (10^{-12} m^2 s^{-1})	T-range (K) ($\overline{T}/T_m$)	No. of data points	Material, purity	Experimental method	Remarks on the pp	Further remarks	Also studied	Figure	Reference
Impurity diffusion												
Ag	4.9×10^{-5}	0.416 (40.2)	26	772–884 (0.91) ε-Pu	4	pc[61]	^{110}Ag, vapour deposition; grinder	1 example[81]	Erroneous thermal expansion correction		103.02	Charissoux (1976) [103.05]
	–	–	–	695 δ-Pu	1[x]			No	[x]D(695 K) $= 1.0 \times 10^{-14}$ m^2 s^{-1} (not "corrected" D-value)		103.03	
Au	5.7×10^{-5}	0.447 (43.1)	19	788–887 (0.92) ε-Pu	4	pc[61]	^{198}Au, vapour deposition; grinder	1 example	Erroneous thermal expansion correction;		103.02	Charissoux (1976) [103.05]
	–	–	–	713 δ-Pu	1[x]			No	[x]D(713 K) $= 2.2 \times 10^{-14}$ m^2 s^{-1} (not "corrected" D-value)		103.03	
Co	(1.4×10^{-3}) $1.5 \times 10^{-3+}$	0.429 (41.5)	640	757–894 (0.90) ε-Pu	4	pc[61]	^{60}Co, vapour deposition; grinder	1 example	Erroneous thermal expansion correction [+]Present approximation		103.02	Charissoux (1975) [103.06]
Co	0.012	0.551 (53.2)	–	617–699 (0.72) δ-Pu	5	pc[61]	^{60}Co, vapour deposition; grinder	1 example[81]	Erroneous thermal expansion correction		103.03	Charissoux (1975) [103.07]
Cu	0.001*	0.533* (51.5)	110	753–853 (0.88) ε-Pu	5	pc[61]	Cu, diffusion couple (Matano)[x]		*$\tilde{D}$ extrapolated to $x = 0$; [x]Experimental data from [103.08]		103.02	Charissoux (1976) [103.05]

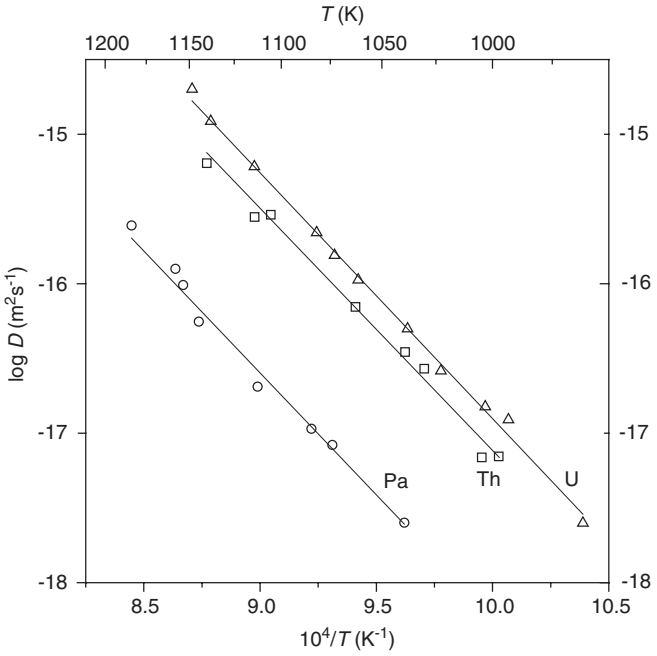

Fig. 101.01 Self-diffusion and impurity diffusion in α-thorium. Th in α-Th: □, Schmitz [101.01]; Pa in α-Th: ○, Schmitz [101.01]; U in α-Th: △, Schmitz [101.01].

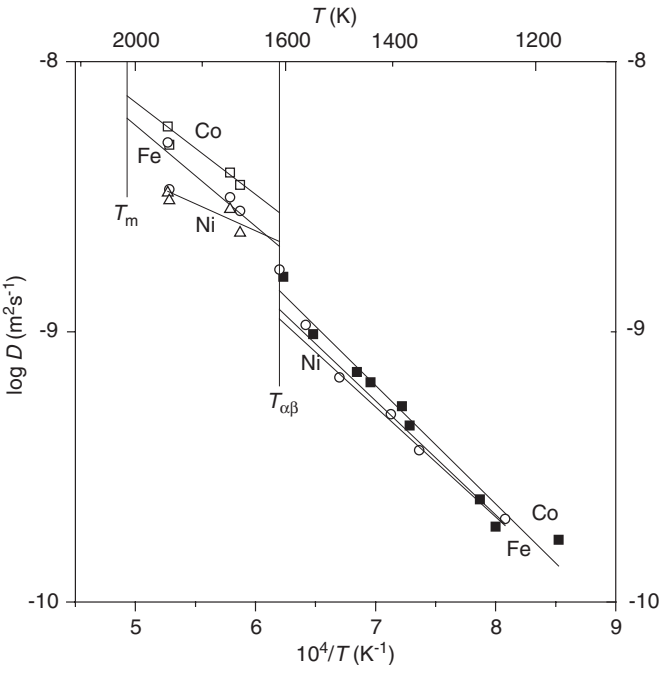

Fig. 101.02 Impurity diffusion in α- and β-thorium. Co in β-Th: □, Weins [101.02]; Fe in β-Th: ○, Weins [101.02]; Ni in β-Th: △, Weins [101.02]; Co in α-Th: ■, Axtell [101.03]; Fe in α-Th: ○, Weins [101.02]; Ni in α-Th: Weins [101.02] (only fitting line, see Fig. 101.03).

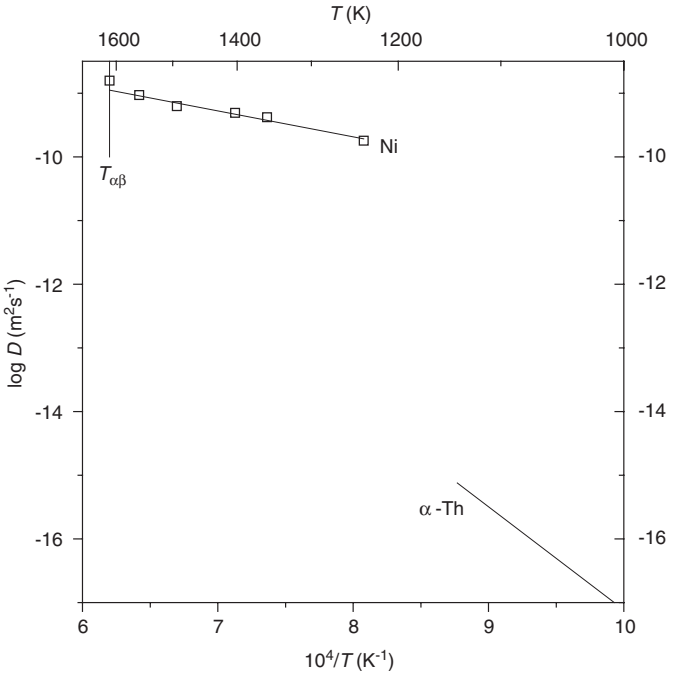

Fig. 101.03 Impurity diffusion in α-thorium. Ni: □, Weins [101.02].

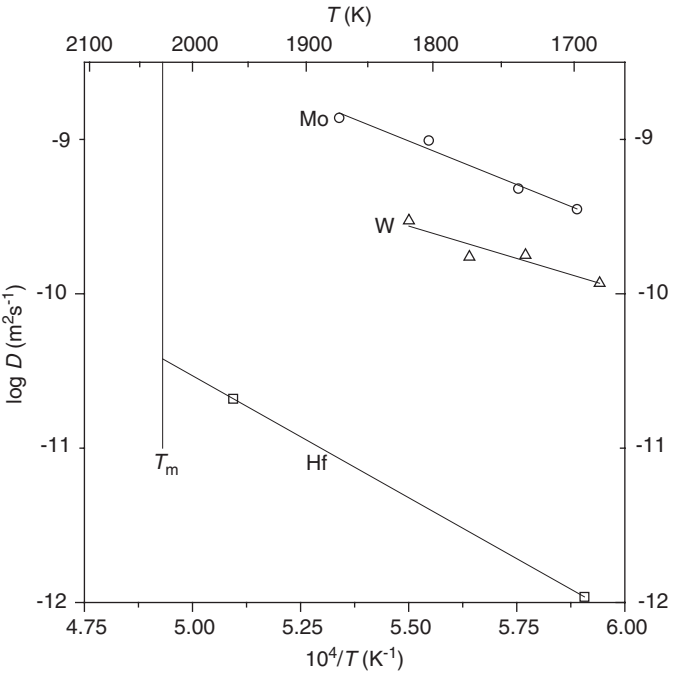

Fig. 101.04 Impurity diffusion in β-thorium. Hf: □, Rothman [101.04]; Mo: ○, Schmidt [101.05]; W: △, Schmidt [101.05]. No self-diffusion data available.

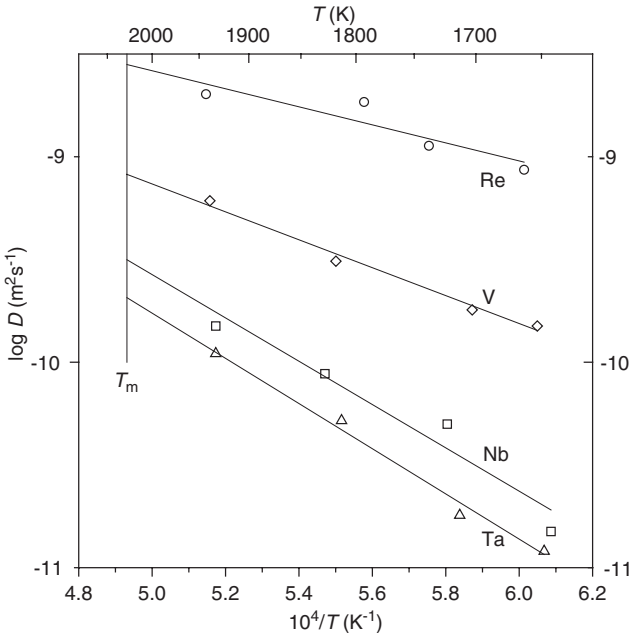

Fig. 101.05 Impurity diffusion in β-thorium. Nb: □, Schmidt [101.06]; Re: ○, Schmidt [101.05]; Ta: △, Schmidt [101.06]; V: ◇, Schmidt [101.06]. No self-diffusion data available.

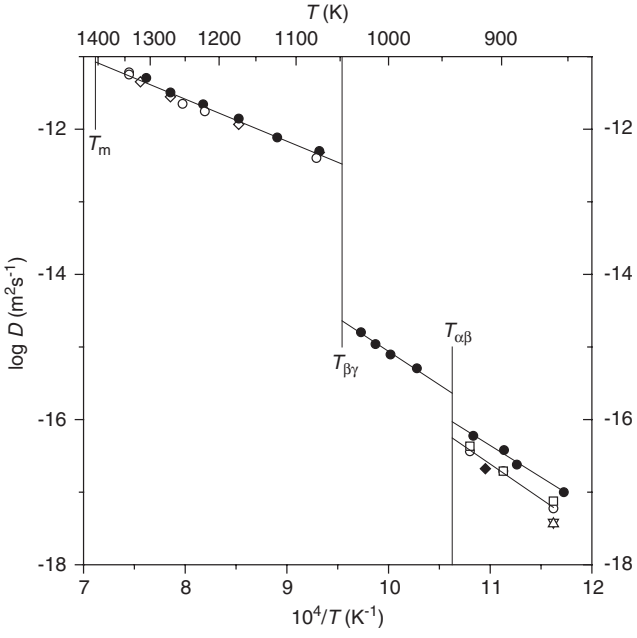

Fig. 102.01 Self-diffusion in uranium. U in γ-U: ◇, Bochvar [102.01]; ●, Adda [102.02]; ○, Rothman [102.03]. Fitting line using $D^0 = 1.12 \times 10^{-7} m^2 s^{-1}$, $Q = 1.149$ eV. U in β-U: ●, Adda [102.04]; U in α-U: ●, Adda [102.06] (polycrystals), in single crystals with mosaic structure: ○ [100], □ [001], in "perfect" single crystals: ▽ [100], △ [001], Rothman [102.07, 102.09]; ◆, Bochvar [102.08]. Fitting line for D[100] (mosaic structure) according to [102.09].

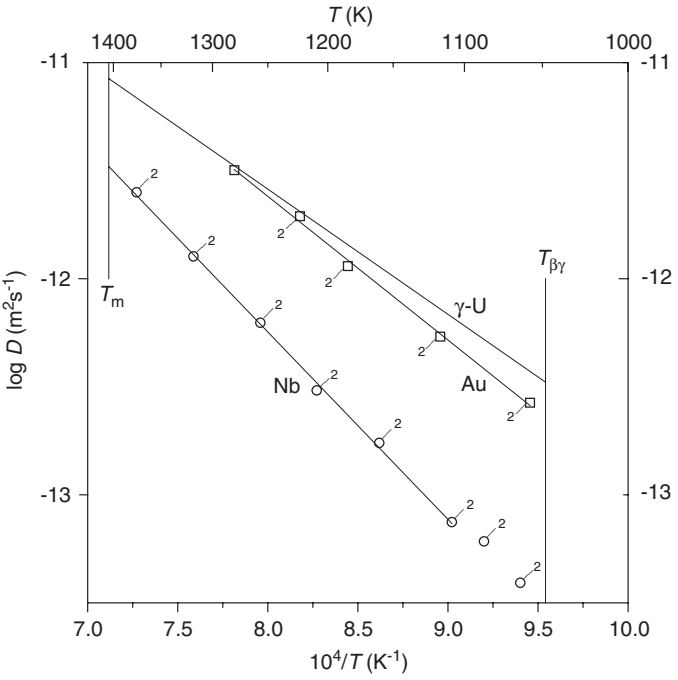

Fig. 102.02 Impurity diffusion in γ-uranium. Au in γ-U: □, Rothman [102.10]; Nb in γ-U: ○, Peterson [102.11].

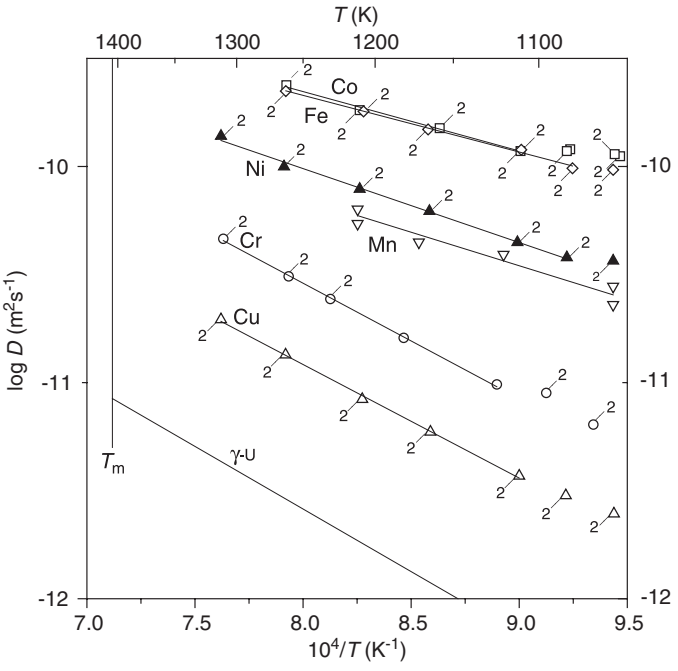

Fig. 102.03 Impurity diffusion in γ-uranium. Co in γ-U: □, Peterson [102.11]; Cr in γ-U: ○, Peterson [102.11]; Cu in γ-U: △, Peterson [102.11]; Fe in γ-U: ◇, Peterson [102.11]; Mn in γ-U: ▽, Peterson [102.11]; Ni in γ-U: ▲, Peterson [102.11].

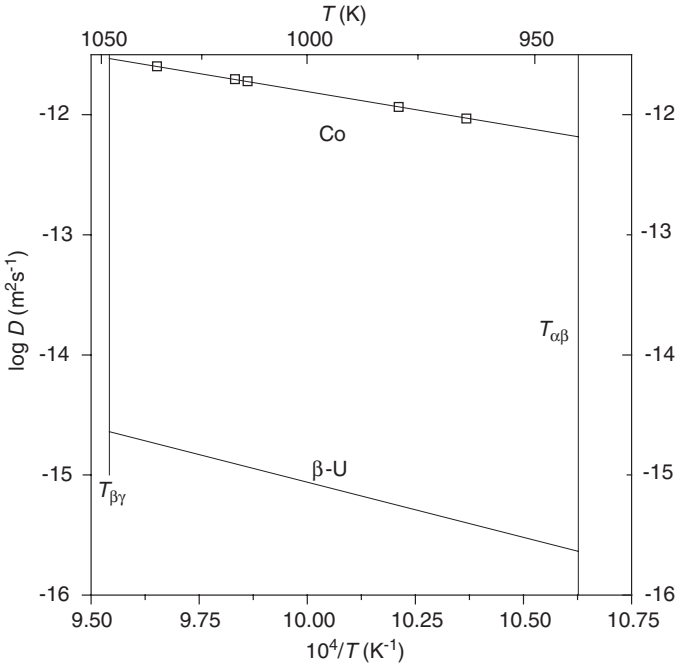

Fig. 102.04 Impurity diffusion in β-uranium. Co in β-U: □, Dariel [102.12].

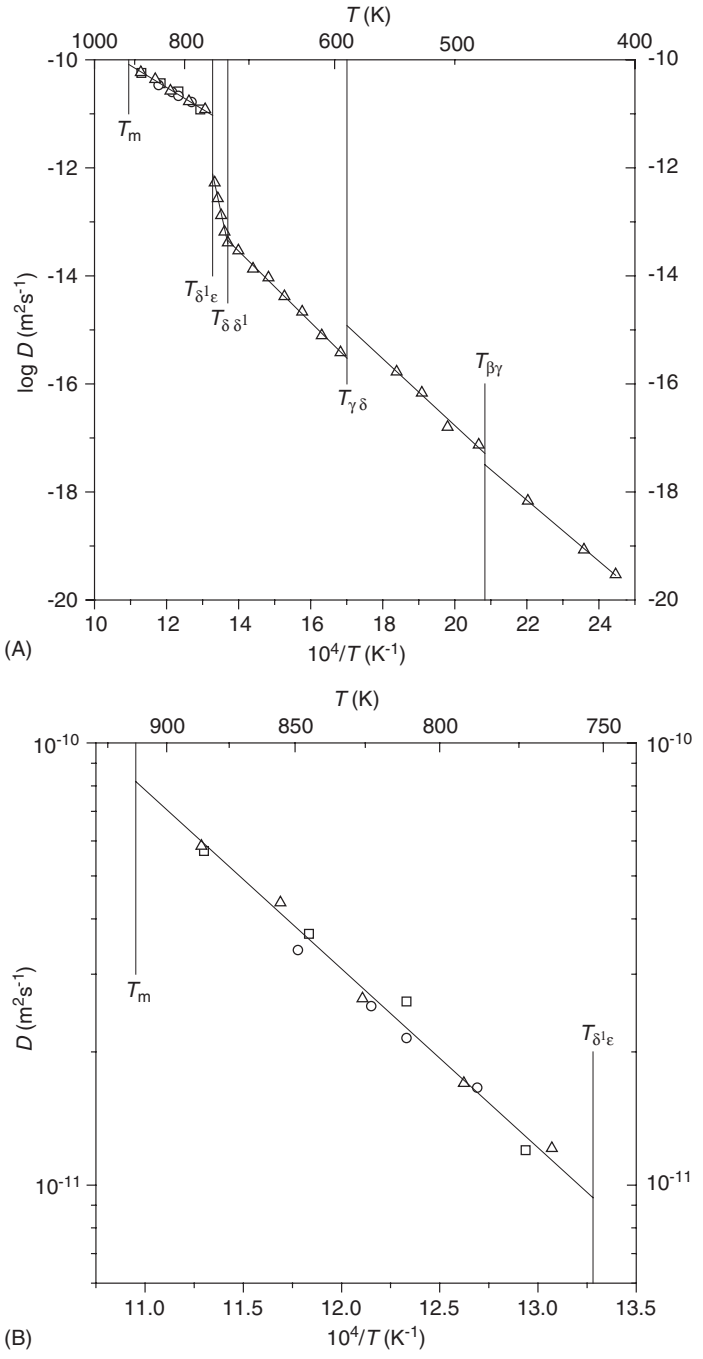

Fig. 103.01 (A) Self-diffusion in plutonium. Pu in ε-Pu: □, Dupuy [103.01]; ○, Cornet [103.02]; △, Wade [103.03]. Fitting line according to [103.01]. Pu in δ'-Pu, δ-Pu, γ-Pu, β-Pu: △, Wade [103.03]. (B) (Detail) Self-diffusion in plutonium. Pu in ε-Pu: □, Dupuy [103.01]; ○, Cornet [103.02]; △, Wade [103.03]. Fitting line according to [103.01].

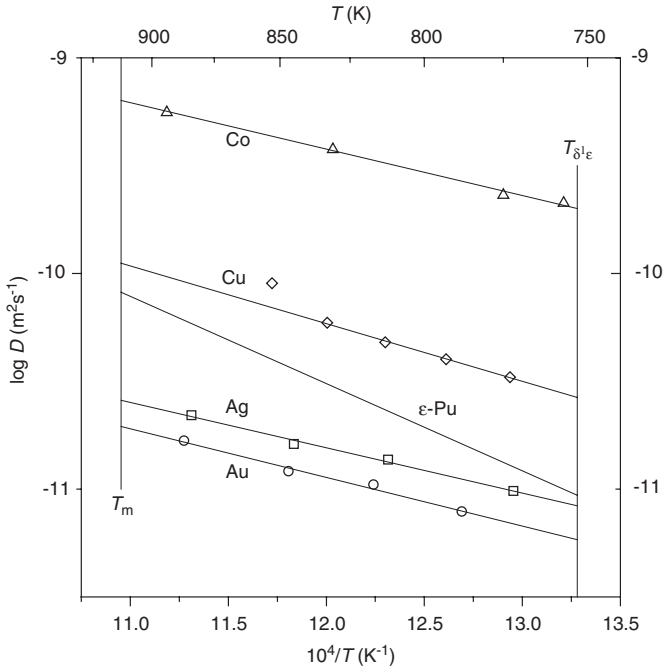

Fig. 103.02 Impurity diffusion in ε-plutonium. Ag in ε-Pu: □, Charissoux [103.05]; Au in ε-Pu: ○, Charissoux [103.05]; Co in ε-Pu: △, Charissoux [103.06]; Cu in ε-Pu: ◇, Charissoux [103.05].

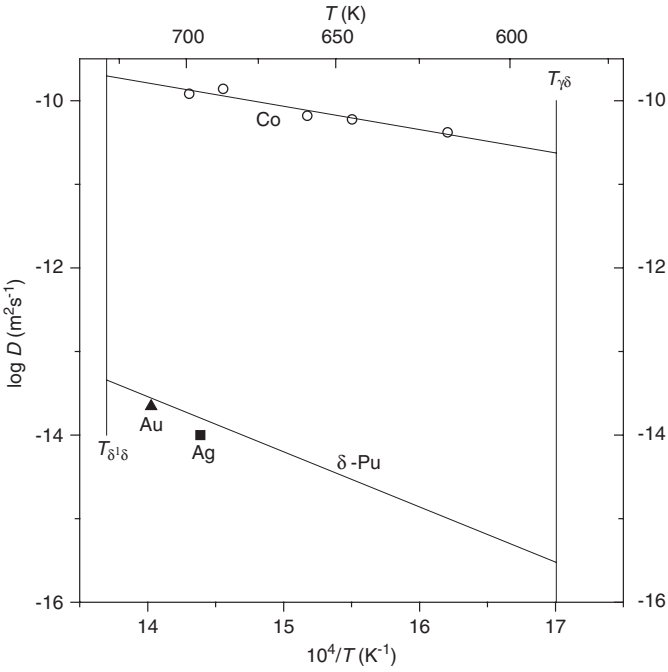

Fig. 103.03 Impurity diffusion in δ-plutonium. Ag in δ-Pu: ■, Charissoux [103.05]; Au in δ-Pu: ▲, Charissoux [103.05]; Co in δ-Pu: ○, Charissoux [103.07].

REFERENCES

References to Chapter 10.1

[101.01] F. Schmitz, M. Fock, J. Nucl. Mater. **21** (1967) 317.
[101.02] W.N. Weins, O.N. Carlson, J. Less-Common Met. **66** (1979) 99.
[101.03] S.C. Axtell, O.N. Carlson, Metall. Trans. A **20A** (1989) 2289.
[101.04] S.J. Rothman, N.L. Peterson, in: *Diffusion in Body-centred Cubic Metals*, Eds. J.A. Wheeler, F.R. Winslow, American Society for Metals, Metal Park, Ohio (1965), p. 183.
[101.05] F.A. Schmidt, M.S. Beck, D.K. Rehbein, R.J. Conzemius, O.N. Carlson, J. Electrochem. Soc. **131** (1984) 2169; see also I.C.I. Okafor, Acta Metall. **35** (1987) 759.
[101.06] F.A. Schmidt, R.J. Conzemius, O.N. Carlson, J. Less-Common Met. **59** (1978) 53.

References to Chapter 10.2

[102.01] A.A. Bochvar, V.G. Kuznetsova, V.S. Sergeev, in: *Proc. 2nd Intern. Conf. on the Peaceful Uses of Atomic Energy*, Geneva (1958), p. 68.
[102.02] Y. Adda, A. Kirianenko, J. Nucl. Mater. **1** (2), (1959) 120; see also C.R. Acad. Sc. Paris **247** (1958) 744.
[102.03] S.J. Rothman, L.T. Lloyd, A.L. Harkness, Trans. AIME **218** (1960) 605.
[102.04] Y. Adda, A. Kirianenko, C. Mairy, J. Nucl. Mater. **1** (3), (1959) 300.
[102.05] S.J. Rothman, J. Gray, J.P. Hughes, A.L. Harkness, J. Nucl. Mater. **3** (1961) 72.
[102.06] Y. Adda, A. Kirianenko, J. Nucl. Mater. **6** (1962) 130; see also C.R. Acad. Sc. Paris **253** (1961) 445.
[102.07] S.J. Rothman, J.J. Hines, J. Gray, A.L. Harkness, J. Appl. Phys. **33** (1962) 2113.
[102.08] A.A. Bochvar, V.G. Kuznetsova, V.S. Sergeev, F.P. Butra, Atomn. Energiya **18** (1965) 601; Sov. Atom. Energy, **18** (1965) 761 (English transl.).
[102.09] S.J. Rothman, B. Bastar, J.J. Hines, D. Rokop, Trans. AIME **236** (1966) 897.
[102.10] S.J. Rothman, J. Nucl. Mater. **3** (1961) 77.
[102.11] N.L. Peterson, S.J. Rothman, Phys. Rev. **136** (1964) A842.
[102.12] M.P. Dariel, M. Blumenfeld, G. Kimmel, J. Appl. Phys. **41** (1970) 1480.
[102.13] S.J. Rothman, N.L. Peterson, S.A. Moore, J. Nucl. Mater. **7** (1962) 212.
[102.14] M. Stelly, J.M. Servant, J. Nucl. Mater. **43** (1972) 269.
[102.15] M. Dupuy, D. Calais, Mém. Sci. Rev. Mét. **62** (1965) 721; see also C.R. Acad. Sc. Paris **260** (1965) 1412.
[102.16] G.B. Fedorov, E.A. Smirnov, F.I. Zhomov, Met. Metalloved. Chist. Met. (7) (1968) 116.

Further Investigations

γ-uranium

U [102.17] G.B. Fedorov, E.A. Smirnov, Met. Metalloved. Chist. Met. (6) (1967) 181.

β-uranium

U [102.18] G.B. Fedorov, E.A. Smirnov, S.S. Moiseenko, Met. Metalloved. Chist. Met. (7) (1968) 124.

α-uranium

U [102.19] G.B. Fedorov, E.A. Smirnov, F.I. Zhomov, Met. Metalloved. Chist. Met. (5) (1966) 92.

References to Chapter 10.3

[103.01] M. Dupuy, D. Calais, Trans. AIME **242** (1968) 1679; see also M. Dupuy, C.R. Acad. Sc. Paris **263C** (1966) 35.
[103.02] J.A. Cornet, J. Phys. Chem. Sol. **32** (1971) 1489.
[103.03] W.Z. Wade, D.W. Short, J.C. Walden, J.W. Magana, Metall. Trans. **9A** (1978) 965.

[103.04] R.E. Tate, E.M. Cramer, Trans. AIME **230** (1964) 639.
[103.05] Ch. Charissoux, D. Calais, J. Nucl. Mater. **61** (1976) 317.
[103.06] Ch. Charissoux, D. Calais, J. Nucl. Mater. **57** (1975) 45.
[103.07] Ch. Charissoux, D. Calais, G. Gallet, J. Phys. Chem. Sol. **36** (1975) 981.
[103.08] F. Lataillade, J. Després, B. Hocheid, *Plutonium and Other Actinides*, Nucl. Metall. **17** (1970) 144.